

# AGARD

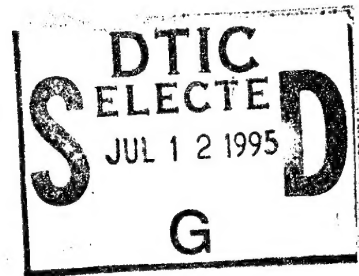
ADVISORY GROUP FOR AEROSPACE RESEARCH & DEVELOPMENT

7 RUE ANCELLE, 92200 NEUILLY-SUR-SEINE, FRANCE

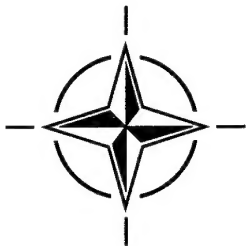
AGARD CONFERENCE PROCEEDINGS 561

## Space Systems Design and Development Testing

(les Essais dans la conception et  
le développement des systèmes spatiaux)



*Copies of papers presented at the Flight Vehicle Integration Panel Symposium,  
held in Cannes, France, from 3-6 October 1994.*



**NORTH ATLANTIC TREATY ORGANIZATION**

**DISTRIBUTION STATEMENT A**

Approved for public release;  
Distribution Unlimited

Published March 1995

*Distribution and Availability on Back Cover*

# AGARD

ADVISORY GROUP FOR AEROSPACE RESEARCH & DEVELOPMENT

7 RUE ANCELLE, 92200 NEUILLY-SUR-SEINE, FRANCE

## AGARD CONFERENCE PROCEEDINGS 561

### Space Systems Design and Development Testing

(les Essais dans la conception et  
le développement des systèmes spatiaux)

Copies of papers presented at the Flight Vehicle Integration Panel Symposium,  
held in Cannes, France, from 3-6 October 1994.



North Atlantic Treaty Organization  
*Organisation du Traité de l'Atlantique Nord*

|                      |                           |                                     |
|----------------------|---------------------------|-------------------------------------|
| Accession For        |                           |                                     |
| NTIS                 | CRA&I                     | <input checked="" type="checkbox"/> |
| DTIC                 | TAB                       | <input type="checkbox"/>            |
| Unannounced          |                           | <input type="checkbox"/>            |
| Justification _____  |                           |                                     |
| By _____             |                           |                                     |
| Distribution / _____ |                           |                                     |
| Availability Codes   |                           |                                     |
| Dist                 | Avail and / or<br>Special |                                     |
| A-1                  |                           |                                     |

19950705 036

DTIC QUALITY INSPECTED 5

# The Mission of AGARD

According to its Charter, the mission of AGARD is to bring together the leading personalities of the NATO nations in the fields of science and technology relating to aerospace for the following purposes:

- Recommending effective ways for the member nations to use their research and development capabilities for the common benefit of the NATO community;
- Providing scientific and technical advice and assistance to the Military Committee in the field of aerospace research and development (with particular regard to its military application);
- Continuously stimulating advances in the aerospace sciences relevant to strengthening the common defence posture;
- Improving the co-operation among member nations in aerospace research and development;
- Exchange of scientific and technical information;
- Providing assistance to member nations for the purpose of increasing their scientific and technical potential;
- Rendering scientific and technical assistance, as requested, to other NATO bodies and to member nations in connection with research and development problems in the aerospace field.

The highest authority within AGARD is the National Delegates Board consisting of officially appointed senior representatives from each member nation. The mission of AGARD is carried out through the Panels which are composed of experts appointed by the National Delegates, the Consultant and Exchange Programme and the Aerospace Applications Studies Programme. The results of AGARD work are reported to the member nations and the NATO Authorities through the AGARD series of publications of which this is one.

Participation in AGARD activities is by invitation only and is normally limited to citizens of the NATO nations.

The content of this publication has been reproduced  
directly from material supplied by AGARD or the authors.

Published March 1995

Copyright © AGARD 1995  
All Rights Reserved

ISBN 92-836-0014-2



*Printed by Canada Communication Group  
45 Sacré-Cœur Blvd., Hull (Québec), Canada K1A 0S7*

## Preface

In view of the importance of space capability to the fulfillment of future NATO requirements, the AGARD Flight Vehicle Integration Panel (FVP) has directed increased attention to space technology. The aim of the symposium reported in this document was to permit information exchange and discussion on the test aspects of space systems design and development, with emphasis on systems related to anticipated future NATO military needs such as, for example, quick response reconnaissance, surveillance, and communications.

The symposium began with two keynote papers addressing the military needs for space capabilities and the importance of adequate testing, and continued with six sessions on testing technologies and approaches. The six technical sessions, containing 28 papers in all, focused on: Testing Requirements and Practices; Flight Dynamics and Flexible/Deployable Structures; Systems Development and Evaluation, Simulation; Space Flight Experiments; and Test Facilities and Support.

## Préface

Considérant l'importance de la fonction spatiale pour la réalisation des futures objectifs de l'OTAN, le Panel AGARD de Conception intégrée des véhicules aérospatiaux (FVP), dirige son attention de plus en plus sur les technologies spatiales. L'objectif du symposium résumé dans ce document a été de permettre un échange d'informations et de discussions sur les aspects essais de la conception et du développement des systèmes spatiaux, en mettant l'accent sur les systèmes associés aux besoins militaires futurs prévisibles de l'OTAN, tels que la reconnaissance à réaction rapide, la surveillance et les communications.

Le symposium a commencé par deux discours d'ouverture, qui présentaient les besoins militaires en moyens spatiaux et l'importance de la réalisation d'essais adéquats, suivis de six sessions sur les technologies et les philosophies d'essais. Les six sessions techniques, comprenant 28 communications en tout, portaient sur les sujets suivants: les spécifications et les méthodes d'essais; la dynamique du vol et les structures flexibles/déployables; le développement et l'évaluation des systèmes; la simulation; les vols spatiaux expérimentaux; et les installations d'essais et le soutien technique.



# Flight Vehicle Integration Panel

**Chairman:** Professor L.M.B. da Costa CAMPOS  
Instituto Superior Tecnico  
Pavilhao de Maquinas  
1096 Lisboa Codex  
Lisbon, Portugal

## TECHNICAL PROGRAMME COMMITTEE

IGA J.-P. Marec  
Directeur pour les Applications  
aéronautiques — ONERA  
29, avenue de la Division Leclerc  
B.P. 72  
92322 Châtillon-sous-Bagneux  
France

Mr. J. Levine  
Director, Flight Programs Division  
Office of Advanced Concepts  
and Technology  
NASA Hq. (Mail Code CF)  
Washington, DC 20546-0001  
U.S.A.

## HOST NATION COORDINATOR

Mr. J.-P. Hémon  
AÉROSPATIALE  
Établissement de Cannes  
100, Boulevard du Midi  
B.P. 99  
06322 Cannes-La-Bocca Cedex  
France

## PANEL EXECUTIVE

J.B. WHEATLEY, LTC, USA

**Mail from Europe:**  
LTC J.B. WHEATLEY  
AGARD-OTAN/FVP  
7, rue Ancelle  
92200 Neuilly-sur-Seine  
France

**Mail from, USA and Canada:**  
AGARD-NATO/FVP  
PSC 116  
APO AE 09777

## Acknowledgements

The Flight Vehicle Integration Panel wishes to express its thanks to the National Authorities of France for the invitation to hold this meeting in their country as well as to AÉROSPATIALE for the facilities and personnel which made the meeting possible.

The Flight Vehicle Integration Panel also wishes to express its thanks to the Propulsion and Energetics Panel for its assistance in providing a Session Chairman, as well as to the Fluid Dynamics Panel for providing a Session Chairman and for presenting a paper at this Symposium.

# Contents

|  | Page      |
|--|-----------|
| <b>Preface/Préface</b>   | iii       |
| <b>Flight Vehicle Integration Panel</b>  | iv        |
| <b>Acknowledgements</b>  | v         |
|  | Reference |
| <b>Technical Evaluation Report</b><br>by G.G. Kayten   | T         |
| <b>Keynote Address 1</b><br>by Brigadier General S.F. Coglitore  | K1        |
| <b>Keynote Address 2</b><br>by IGA D. Estournet  | K2        |
| <b>An Overview of DOD Test Requirements for Launch and Space Systems</b><br>by C.J. Moening and S. Rubin   | 1         |
| <b>Tailoring Text Requirements for Application in Multinational Programmes</b><br>by P. Messidoro, M. Ballesio and E. Comandatore  | 2         |
| <b>Aérospatiale Satellites (Cannes Site) Integration and Test Center</b><br>by J.-F. Coroller and R. Macario   | 3         |
| <b>Expérience acquise par l'Aérospatiale dans le domaine de l'intégration de charges utiles optiques haute résolution</b><br>by J. Mendez and J.M. Leblanc                               | 4         |
| <b>Separation of Lifting Vehicles at Hypersonic Speed Wind Tunnel Tests and Flight Dynamics Simulation</b><br>by G. Sachs, W. Schoder and W. Kraus                                       | 5         |
| <b>Spacecraft Deployable Structure Testing</b><br>by R.D. Dotson   | 6         |
| <b>Active Structures for Vibration Suppression and Precision Pointing</b><br>by A. Preumont  | 7         |
| <b>Structural Verification of the Space Station Freedom Force Moment Sensor (FMS) Using Finite Element Modelling Techniques &amp; Qualification Testing</b><br>by B. Christie, B. Mackay | 8         |

|  |           |
|--|-----------|
| <b>Mastering the Effect of Microvibrations on the Performances of Reconnaissance Satellites</b><br>by D. Monteil, V. Guillaud and P. Laurens                                     | <b>9</b>  |
| <b>Aerothermodynamic Testing Requirements for Future Space Transportation Systems</b><br>by J.W. Paulson, Jr. and C.G. Miller, III   | <b>10</b> |
| <b>Test Aspects of Single Stage to Orbit Systems</b><br>by W.A. Gaubatz, D.R. Nowlan, M.G. Maras, J.A. Copper and K.A. Coleman   | <b>11</b> |
| <b>FADS, a Demonstrator for MilComSat AOCS</b><br>by M. Huddleston and P. Cope   | <b>12</b> |
| <b>Pegasus Air-Launched Space Booster Flight Test Program</b><br>by A.L. Elias and M.A. Knutson  | <b>13</b> |
| <b>S2000+ ou la conception préliminaire des systèmes spatiaux</b><br>by J.F. Gory  | <b>14</b> |
| <b>This paper was cancelled</b>  | <b>15</b> |
| <b>Spaceborne SAR Simulation Using Airborne Data</b><br>by J.-M. Boutry and J. Dupas   | <b>16</b> |
| <b>Use of Simulation Tools and Facilities for Rendez-Vous and Docking Missions</b><br>by J.B. Serrano-Martinez   | <b>17</b> |
| <b>Spacecraft Attitude and Orbit Control Systems Testing</b><br>by F.J. Sonnenschein, M. Schoonmade and T. Zwartbol  | <b>18</b> |
| <b>NASA Technology Flight Experiments Program</b><br>by S.L. Prusha, J. Levine and S.C. Russo  | <b>19</b> |
| <b>Technology Demonstration Experiments on STRV-1</b><br>by G.L. Wrenn and A.J. Sims   | <b>20</b> |
| <b>US In-Space Electric Propulsion Experiments</b><br>by J.F. Stocky, R. Vondra and A.M. Sutton  | <b>21</b> |
| <b>Shuttle Orbiter Experiments — Use of an Operational Vehicle for Advancement and Validation of Space Systems Design Technologies</b><br>by P.F. Holloway and D.A. Throckmorton | <b>22</b> |
| <b>Flight Testing Vehicles for Verification and Validation of Hypersonics Technology</b><br>by P.W. Sacher   | <b>23</b> |
| <b>Extension of the ESA Test Centre with HYDRA, a new Tool for Mechanical Testing</b><br>by P.W. Brinkmann   | <b>24</b> |
| <b>Essais de propulseurs à plasma stationnaire en ambiance spatiale simulée</b><br>by D. Valentian   | <b>25</b> |

|  |           |
|--|-----------|
| <b>Development of a Modal Testing Support System for Space-Based Radar Satellite Structures</b><br>by D.J. McTavish, G.B. Sincarsin and Y. Soucy | <b>26</b> |
| <b>A Preliminary Study of the Air Data Sensing Problem on a Re-entry Vehicle</b><br>by M. Borsi and E. Hettena                                   | <b>27</b> |
| <b>Hypersonic Aerodynamic/Aerothermal Test Facilities Available in Europe to Support Space Vehicle Design</b><br>by D. Vennemann                 | <b>28</b> |
| <b>Ground Testing and Simulation of Space Environment Hazards</b><br>by M. Roméro and J. Bourrieau   | <b>29</b> |

## TECHNICAL EVALUATION REPORT

by

Gerald G. Kayten  
4701 Willard Avenue  
Chevy Chase, MD 20815  
USA

### Background and Introduction

The AGARD Flight Vehicle Integration Panel (FVP) symposium on Space Systems Design and Development Testing was conducted October 3-6, 1994 in Cannes, France.

In the AGARD reorganization which established the FVP in early 1994, FVP absorbed the responsibilities of the Flight Mechanics Panel (FMP). FMP for many years had been a leader in aircraft testing and simulation and had recently been expanding its interests to incorporate space vehicle systems. In view of the apparent trend toward inter-dependent or collaborative development and operation of NATO assets including space systems, space topics related to integration and testing are likely to be addressed in future AGARD FVP activities.

This symposium was planned to discuss the test aspects of space systems design and development, with emphasis on types of systems related to anticipated NATO military needs, including launch vehicles, satellites and platforms, and entry vehicles. It was intended as a forerunner of increased AGARD space vehicle systems technology exchanges.

It is interesting to note that space systems testing was also a primary topic of discussion at three other meetings also held during October 1994 -- the Aerospace Testing Seminar in Manhattan Beach, CA, the International Test and Evaluation Association (ITEA) symposium in Baltimore, MD, and the annual International Telemetry Conference in San Diego, CA.

As listed in the Contents, the symposium papers covered acceptance and qualification testing requirements; testing for flight dynamics, space structures, and systems evaluation; simulation; in-space technology experiments;

existing and planned test and simulation facilities; and critical future facilities needs.

### Synopsis of Symposium Sessions

#### I -- KEYNOTE PAPERS

The two keynote addresses clearly established the importance of the symposium subject and its relevance to NATO military needs. Perhaps more importantly, the insights they presented provide a basis for extracting from the papers and discussions several questions and issues which may warrant further AGARD attention and possibly action.

The keynotes identified significant roles of space-based capabilities in missile warning, accurate navigation for sophisticated weapons and for infantry units, timely weather and environmental information, surveillance, and essential command and control communications. They stressed the growing importance of these military roles in future humanitarian and peacekeeping as well as wartime efforts. They also stressed the overriding necessity for cost reduction in military programs, particularly in space systems and space systems testing.

The cost-reduction pressures have led to harsh assessment of requirements and to difficult cost/capability tradeoffs. In addition, both keynote authors called attention to several trends that could greatly influence the manner in which future military space systems are developed and tested. Specifically, they predicted :

- increased military/civil cooperative development;
- increased use of commercial equipment, practices, and standards; and
- increased international cooperation in development, testing, and acquisition.

## II -- TESTING REQUIREMENTS AND PRACTICES

The overview of US Department of Defense acceptance and qualification test requirements (Paper 1) traced the history from the initial issuance in 1974 to the present MIL-STD-1540C version which is still in draft status. Compliance with the test standards both within the DOD and elsewhere has proven effective in increasing spacecraft reliability and reducing life-cycle costs. Revisions have broadened the applicability of the standards to include launch vehicles and upper stages, and have strengthened some requirements. At the same time, the latest version includes major changes designed to reduce testing costs where possible -- for example, guidelines for tailoring test requirements, removal of some acceptance tests, and expanded options for flight use of qualification items. In addition to MIL-STD-1540C, related documents such as MIL-STD-810D (Environmental Test Methods And Engineering Guidelines) and MIL-A-83577B (General Specification For Moving Mechanical Assemblies) also provide guidelines and standards for US military space vehicle, subsystem, and component testing.

The Alenia Spazio presentation on tailoring test requirements in multinational programs (Paper 2) revealed that some significant differences exist between US (DOD) and corresponding European testing standards such as ESA PSS-01-802. Although there are more areas of agreement than disagreement, the number of differences is appreciable, and requirements of both greater and less severity occur in each set of standards. It is therefore interesting to speculate on the economies that might be realized if agreement were to be reached on a large percentage of the less stringent requirements.

As illustrations of the facilities and capabilities needed to perform the required space systems testing, two presentations (Papers 3 and 4) described Aerospatiale's impressive new satellite integration and test center at Cannes and the experience and competence acquired in their testing of extremely high-resolution optical systems. The facilities discussion was effectively complemented by a visit of symposium attendees to the test center later in the week.

An additional paper incorporated in the session (Paper 29) summarized the various space envi-

ronment hazards to spacecraft, and discussed the experiments, simulations, and tests required to assure satisfactory space systems performance throughout the operational life. It pointed out that only recently has a working group been established within the International Standards Organization (ISO) to focus on the space environment.

The discussions in this session demonstrated that considerable effort and resources must be devoted to meeting customer testing standards and requirements for qualification and acceptance.

## III -- FLIGHT DYNAMICS AND FLEXIBLE/DEPLOYABLE STRUCTURES

This session was devoted to testing performed for flight dynamics and flexible/deployable structures. Paper 5 addressed the separation of lifting vehicles at hypersonic speeds -- for example, as in potential future two-stage space transportation systems. The simulations used in determining optimal separation and control techniques were based on hypersonic wind-tunnel test data -- a reminder that the success of future developments of this nature will be crucially dependent on the adequacy of hypersonic test facilities.

Three papers (6, 7, and 8) were directed at different facets of space structures testing. The first gave a comprehensive review of development and qualification testing of spacecraft deployable structures such as solar arrays, radiators, booms, doors, mirrors, or thermal shields. These structures and the moving mechanical assemblies that operate them must function under space conditions extremely difficult to represent in ground testing. Despite the innovative solutions and ingenious test hardware developed for testing purposes, deployable structures remain a major factor in the high cost of spacecraft testing.

Paper 7 presented a theoretical discussion of an active structures concept using piezoelectric technology, and described some associated laboratory testing and a test structure developed for a future in-orbit experiment to investigate the concept. It illustrated the wisdom of early preliminary experimentation during theory development as a baseline for subsequent verification testing.

Paper 8 reviewed the mathematical modeling and qualification testing employed to verify the Canadian Force Moment Sensor, a highly flexible structure developed for use in the Space Station Remote Manipulator System. It also described the techniques used in correlating test results with analytical predictions.

The final paper in this session addressed the analysis and testing methodologies used at MATRA Marconi Space for predicting and controlling the effects of microvibrations on the performance of very high resolution reconnaissance satellites. The paper reviewed the stability requirements for earth observation satellites, outlined the methodologies for analysis of vibration sources and effects, and described the analysis and testing performed at the component, subsystem and system levels to evaluate and improve satellite pointing performance.

#### IV -- SYSTEMS DEVELOPMENT AND EVALUATION

Coincidentally, three of the papers devoted to systems development and evaluation testing were related to future space transportation systems. The first, Paper 10, was a comprehensive dissertation on the ground-based (primarily wind-tunnel) test capabilities required to obtain the aerothermodynamic data essential for design and development of advanced fully or partly reusable launch vehicles. Although the major new challenge may be associated with hypersonic flight, the extensive testing required throughout the entire speed range was considered as well. The paper compared the needs against existing facilities and described a number of new facilities under consideration which would, if authorized and funded, fill the major gaps in current capability.

Papers 11 and 13 described two interesting flight test programs involving considerably different systems but with several features in common. Both involved unique vehicle concepts. Both were high-risk programs with limited funding, and for that reason neither enjoyed the thorough pre-flight data base and preparation that would characterize a full-scale development flight program. And despite the difficulties and some misadventures, both succeeded in accomplishing program objectives. The DC-X was an experimental one-third-scale version of a vertical-takeoff-and-landing single-stage-to-orbit vehicle. It

demonstrated concept feasibility, validated low-speed flight characteristics in and out of ground effect, and developed valuable information for use in full-scale development. Pegasus, a winged launch vehicle dropped from a carrier aircraft instead of launching vertically from the ground, was designed as an operational low-cost launcher. Its flight test program included successful delivery of several small payloads to orbit.

Paper 12 discussed an experimental program to evaluate attitude and orbit control system technologies for future UK military communication satellites. This Defence Research Agency effort, conducted jointly with industry, is focused on sensor technologies and control algorithms suitable for autonomous onboard capability independent of the ground support typically employed in civil systems.

CNES provided a presentation (Paper 14) on a computer-aided global approach to the definition of future space systems, including a "workbench" for integration of information from disparate sources and viewpoints. Although not evident in the paper, it is probably reasonable to assume that test data could be included in the information utilized.

#### V -- SIMULATION

Although the various programs reported throughout the meeting included significant simulation efforts, three papers devoted specifically to simulation were grouped in this session. One (Paper 16) described an ONERA effort in which side-looking airborne radar data were used to simulate spaceborne synthetic aperture radar (SAR) images. The simulated images are considered useful in the design of spaceborne SAR systems, and as aids in training image interpreters.

Paper 17 provided an excellent example of the use of simulation as a tool in development of a complex, dynamic system, and an equally excellent example of productive international cooperation in the planning and integration of a multi-element project. Although directed at rendezvous and docking for large systems such as space station complexes, it might also serve as a model for a similar study of cooperative simulation directed at potential future NATO military spacecraft systems.



In the final paper, NLR discussed overall development, test, and evaluation efforts on Attitude and Orbit Control Systems hardware and software, in which simulation played a major role — or, more accurately, roles. The presentation illustrated the variety of hardware and software simulation activities which are now vital integral elements of a typical space systems design and development program.

## VI -- SPACE FLIGHT EXPERIMENTS

This session covered the use of space vehicles as experimental facilities for testing or validating new technologies, or acquiring technical data not otherwise available. Paper 19 described NASA's Technology Flight Experiments Program, conducted to obtain research data, evaluate the operation of experimental mechanisms in the space environment, or validate concepts or hardware prior to application in future spacecraft. The experiments discussed as examples involved different degrees of technology maturity, and varied from basic research experiments to technology validation at the prototype system level.

A related paper from DRA Farnborough discussed the Space Technology Research Vehicles, two microsatellites placed in a geostationary transfer orbit in June 1994 to test a number of advanced technologies, with particular interest in the performance of carbon-PEEK structural components, a radiation-tolerant microprocessor, advanced solar panels, and a variety of experimental solar cells. The highly elliptical orbit permits radiation tolerance testing under exposure conditions considerably more hostile than those that would be encountered in subsequent operational applications.

A JPL/USAF presentation (Paper 21) reviewed NASA and Air Force ground-based and in-space electric propulsion experimental programs to validate low-power ion propulsion and high-power arcjet technologies. The experiments are intended to advance technology readiness for electric propulsion, which has the potential for significantly increased onboard propulsion efficiency for spacecraft functions such as station-keeping and repositioning.

Paper 22 presented the results of a series of experiments in which a specially instrumented Shuttle orbiter was utilized as a research vehicle to obtain valuable aerodynamic and aerothermal data throughout the entry flight regime.

The data made possible the resolution of uncertainties which had necessitated considerable conservatism in Shuttle design. The information has been helpful in orbiter performance enhancement efforts. However, the benefits should be much more apparent in the significant weight reductions, or increases in payload capability, that can now be achieved in design of advanced space transportation vehicles. In addition, the experiments impressively demonstrated that the use of operational or developmental vehicles for cost-effective flight research and technology development can be as valuable in space as it has been for many years in aeronautics.

The eventual need for validated hypersonic technology was the subject of the final paper (23), which convincingly advanced the argument that flight testing will be crucial to meeting that need with respect to future reusable space transportation systems involving hypersonic airbreathing propulsion. The paper outlined a study of alternative flight test vehicle concepts and configurations, and a proposal for international cooperation in a phased approach to flight testing leading to a future European Space Transportation System.

## VII -- TEST FACILITIES AND SUPPORT

The final session, devoted to test facilities and instrumentation, began with an ESTAC presentation on a major new addition to the environmental test center at Noordwijk. Presently under construction, the large 6-degree-of-freedom hydraulic shaker scheduled for initial operation in 1996 is intended for structural qualification of large Ariane-4 and Ariane-5 payloads. It will be capable of transient as well as sinusoidal testing.

Paper 25 described a vacuum chamber developed by SEP for Stationary Plasma Thruster (SPT) testing. The facility was modified from one originally used for the development of Field Emission and Xenon ion bombardment thrusters. The higher-thrust SPT testing needs required introduction of a much more powerful cryogenic pump to ensure maintenance of sufficiently low chamber pressure. A thrust balance was added, as well as a new Xenon feed system and beam diagnostic instrumentation. The facility will be used for engineering, qualification, and acceptance testing.

Another new facility under construction was described in a Canadian paper on development of a modal testing support system to deal with very large, very flexible structures which are incapable of supporting their own weight in a 1-g environment. The modal testing process is intended to provide an experimentally validated structural model for predicting structural dynamic behavior of, for example, space-based radar surveillance satellites.

An Alenia study provided the basis for a comprehensive review (Paper 27) of the entry vehicle air data sensing problem. Instrumentation difficulties and solutions throughout the large Mach number, angle of attack, pressure, and temperature extremes were discussed with respect to flight control system data requirements as well as post-flight analysis.

The final presentation (Paper 28) gave an overview of the five major European hypersonic wind tunnels identified by ESA as available facilities for spacecraft aerodynamic and aerothermal testing -- the ONERA S4 blow-down and F4 hot shot facilities in France, the Aachen TH2 shock tunnel and Gottingen High Enthalpy facility in Germany, and the Longshot piston gun tunnel at the Von Karman Institute in Belgium. Although these facilities are capable of good hypersonic research and are among the largest in the world, none of them would be considered adequate for the testing required in development of actual vehicle systems. In that sense, the situation in Europe is similar to the US picture presented in Paper 10.

## **Discussion**

The symposium papers and discussions provided a clear reminder that successful accomplishment of space missions requires major investment in testing, simulation, and experimentation, and in the associated facilities, test hardware and software, and expertise. The exchange of information in these areas was productive, competent, and timely and gave good evidence of mutually beneficial international cooperation in testing and in use of test and simulation facilities. It also called attention to several issues which need further consideration and which may present opportunities for important contributions by the AGARD FVP. These issues -- and particularly the vital issue of testing cost reduction -- are the primary focus of this discussion.

In responding to the demands for military space systems cost reduction, the cost of testing must be recognized as a major component. It is difficult to cite a definitive figure for the total cost of testing because of differences in bookkeeping systems among programs. But representative breakdowns indicate that testing can account for as much as 25-40 % of the total program recurring cost -- and an even higher percentage of the non-recurring cost if the test facilities are charged to the program. Developers may provide different estimates of testing cost, but there is total agreement that it must be reduced.

A major reason for the high cost has been that, because of the high cost of launch systems and spacecraft, and the harsh and uncertain operational environments, space system developers and buyers have been compelled to be extremely conservative in space systems verification testing. That conservatism has led to costly, prolonged, and possibly excessive testing -- but the data and the methodology needed to quantify the risk of deviating from traditional verification processes have simply not been available, and procuring agencies have been understandably reluctant to relax the requirements.

Nevertheless, with the increasingly austere funding limitations anticipated in future developments, it is clearly essential to develop new test approaches which are more cost-effective without compromising mission success.

Research is now in progress on methodologies for quantifying risks in specific mission concepts and verification programs. At the same time, methodologies and models are being developed to project mission success probability and identify areas where verification testing is most critical, by analysis of flight and test records on similar systems and subsystems. In addition, developers now usually integrate test personnel into system engineering teams at the very earliest stages of program development, allowing the team to achieve economies by establishing verification requirements based on risk and cost drivers identified during the conceptual design phase and refined as the program progresses.

These measures are significant steps toward economy. But much more aggressive action will be required to achieve the desired reductions in cost, and the test requirements im-

posed by the buyers constitute a major cost element.

The excellent presentations on testing standards indicate that significant progress is being made in this area toward reduction of high-cost customer-imposed testing requirements. Tailoring test requirements to specific program parameters and systems rather than general standards, qualification by similarity, rationalizing cycle and margin requirements, flight use of qualification test articles, and continued effort to identify and remove unproductive or unnecessary tests, are all positive, important steps toward reducing testing cost. Unfortunately, however, the data base required to achieve the full benefits of these and other new approaches still does not exist.

Testing standards are still evolving, and the Alenia Spazio and Aerospace comparisons disclosed some significant differences in philosophy in the USAF and European testing standards. Actually, efforts to develop international environmental testing procedures and standards have been ongoing for more than a decade among international partners, ad hoc testing groups, and NATO Standardization Agreement (STANAG) groups. But while both authors expressed a desire for increased harmony in the requirements, the lack of convincing data causes each party to rely on its own experience and prejudices, and makes it unlikely that either side will yield readily. In fact, similar differences continue to exist among various agencies and services within individual countries.

Clearly, resolution of differences in test standards, and reduction of dependence on overly conservative testing, are hampered by the lack of adequate data on which to base needed changes. In order to establish a fully rational basis for reduction of testing costs while maintaining a high degree of confidence in mission success, the development and testing communities will require ready access to a tremendous amount of engineering, flight, and test data, some of which exists but is not necessarily available to those who need it, and some of which still does not exist at all.

The necessary data base must include test results, failure information, and life-cycle performance histories accumulated from in-house development testing, formal qualification test programs, and operational experience for a

broad spectrum of components and subsystems. And the data must be in sufficient depth and detail so that, for example, "Qualification by Similarity" can be conducted with assurance that even the smallest differences in design, application, performance or environmental requirements, or manufacturing have been identified and accounted for. In the past, the handling and analysis of such vast amounts of data would have been an impossible task. But the power that now makes it possible for a computer to diagnose 100,000 alternative chess moves almost instantaneously and defeat an international chess champion should make it feasible to digest the technical data and evaluate the possible implications.

Several of the organizations represented at the 1994 Aerospace Testing Seminar are currently developing improved formats, procedures, and software for collection, storage, and computer-aided exchange of data on test results and on space flight failures and anomalies. These efforts may eventually be coordinated with international mechanisms such as the ISO's Standard for the Technical Exchange of Product Model Data (STEP), possibly with the assistance of the newly formed ISO space environment working group. However, involvement of the NATO community as a complementary data source might significantly accelerate and strengthen the process.

Even without the required data base, the commercial spacecraft world seems to be moving much more aggressively toward testing cost reduction than the military. The "smaller, faster, cheaper" theme is a very real and serious objective in commercial developments such as those now in progress for international communication systems, and some of those commercial developments may be closely related to future military products.

In one effort toward small satellite technology development, NASA in June 1994 placed two industry teams under contract to design, build, qualify, and launch two technology demonstration satellites, one within two years and the other within three. The technologies are quite advanced, the goal being to increase payload mass fraction by a factor of two or more. But an even more demanding challenge may be the requirement to reduce development time-to-flight from the current four or five years to one half that time, by using commercial rather than

government or military practices and standards.

The testing conducted in those developments will almost certainly be considerably abbreviated compared with conventional military programs. If they succeed, it will not necessarily mean that the identical approach would be suitable for military systems. However, it will challenge us to determine how far we might go in that direction without compromising mission success. The more rigorous approach to design and test requirements for military aircraft systems has long been based on the argument that military aircraft must operate in a far more hostile environment than civil aircraft. But this argument may not be as compelling with respect to military and civil space systems, both of which face similarly hostile launch and space environments.

Commercial spacecraft manufacturers are now exploring some significant departures from the traditional component, subassembly, subsystem testing progression and doing much of the testing only at the system level. They are also pursuing economies such as, for example, deemphasizing thermal cycling in favor of more prolonged testing at one high temperature determined to be critical.

In one of these programs, a communications system consisting of more than 60 individual satellites, the developer's philosophy is that the final testing on the first article should verify the manufacturing process -- and that once the manufacturing process is proven reliable, there is no need to test each of the other production satellites.

Some of these perhaps radical approaches may be entirely satisfactory for the particular applications. In a system employing large numbers of small, low-cost spacecraft, the risk of some losses may be an acceptable tradeoff for the higher cost of more conservative testing. Furthermore, it is not at all obvious that better testing would necessarily uncover all of the potential anomalies that may be encountered in flight. Analyses of space system in-flight failures have indicated that a large percentage could not have been detected in prior testing. And some commercial developers maintain it has never been proven that military spacecraft are actually more reliable than commercial spacecraft.

It remains to be seen whether and to what degree these commercial testing approaches may be applicable to military space systems development -- or even to military adaptations of commercial products. And it is certainly not recommended that any existing test standards be discarded without good justification. But whether it is decided to maintain or relax the conservatism in military and government verification testing, that decision (or those decisions in multinational cooperative programs) must be based on a solid data base which either justifies the relaxation or provides convincing defense against pressures for unwise corner-cutting.

If the FVP intends to include space systems testing among its responsibilities as part of an increased AGARD emphasis on future NATO military space needs, it would appear that the Panel should seriously consider the advisability of active participation in the effort to develop technical data which could serve as a basis for establishment or revision of military space systems testing standards.

In the discussions on testing requirements, it was observed that there are as yet no established standards for propulsion testing. It was also noted that, although several of the papers showed considerable software effort implicit in the test programs, and although the software literature contains ample references to software quality, testing and formal inspection, the documents specifically devoted to military space systems test requirements do not appear to include or make reference to software testing standards. In the new AGARD organization, propulsion and software may not be the province of this Panel. However, since both figure significantly in space system failure and cost histories, if the FVP does adopt space systems testing as a serious concern it may wish to at least examine the question of propulsion and software requirements in the test standards for military launch and space systems.

On the subject of test and simulation capabilities, the papers indicated that the facilities now in use and being developed or planned appear in general to be adequate for necessary testing in the immediate future, particularly if the trends in international cooperation continue. However, for the longer-range future -- at least with respect to the potential development of advanced systems such as air-breathing

transatmospheric vehicles -- the facilities, although presently supporting excellent hypersonic research, may be inadequate for aerothermodynamic and propulsion development testing. Further review of transatmospheric vehicle research and development testing needs could be a fruitful topic for consideration at a future symposium. The modes considered in such a review should of course include flight testing, which, as indicated in several of the symposium papers, remains an indispensable tool in aerospace research and development.

The papers also provided impressive evidence of the value of in-space flight experimentation relative to technology development and validation. That capability and the possibility of increased international cooperation appear well worth nurturing.

### **Conclusions and Recommendations**

Excellent capabilities, facilities, and technology for Space Systems Design and Development Testing exist within the NATO community, and continuing international cooperation greatly increases the value of these assets to the alliance.

Although the symposium topic was confined to testing and simulation, the papers actually covered a broad range of test activity extending from experimental verification of theoretical concepts to technology development and validation, in-house product development, and customer-specified qualification/acceptance testing. As in all areas of AGARD emphasis, technical exchange on these subjects is interesting and mutually beneficial. However, the spectrum of FVP concerns and responsibilities is quite broad, and future opportunities for meetings totally devoted to space systems testing -- or space technology -- may be necessarily limited. Consideration should be given to several alternatives, including more frequent resort to specialist meetings and integration of selected space topics in FVP aeronautical technology and flight testing symposia.

AGARD has been a leader in aeronautical flight testing technology for many years. The publications of its flight test working group provide valuable guidance and reference material for new flight test organizations and for the entire aeronautical testing community. Space systems testing has been maturing for three

decades without appreciable AGARD involvement, and the nature and extent of future FVP space-oriented activity has yet to be determined. However, several issues brought to light during the symposium and in this report suggest that the subject of military space systems qualification and acceptance testing should be of considerable concern to the Panel:

- the increasing importance of space to NATO military needs;
- the necessity to reduce all aspects of military systems cost, including testing;
- international, military, and commercial differences regarding test requirements;
- the possibility of military systems procurement based on commercial developments;
- the likelihood of multinational cooperation on military space systems; and
- the need for an improved data base to support resolution of differences in testing standards.

It is recommended that the FVP consider addressing the question of space system testing standards, with particular emphasis on cooperative data base development. A subcommittee, for example, could initially review the data needs, assess the value of an AGARD working group effort toward meeting the needs, and develop plans for conducting the effort and disseminating the results. The working group effort, if undertaken, would focus on components and systems directly applicable to perceived NATO military needs. It would not duplicate -- but could complement and benefit from -- similar data base efforts conducted elsewhere or for different purposes.

It is also recommended that the following subjects highlighted in the discussion be examined as potential topics for specialist meetings or other Panel actions:

- transatmospheric vehicle aerothermodynamic and propulsion testing needs, with emphasis on development testing and including consideration of appropriate flight research vehicles;
- increased international cooperation on in-space flight experimentation relative to technology development and validation; and
- international cooperative simulation of potential future NATO military space systems.

## **Bibliography**

In addition to the symposium papers and discussions with government and industry space systems development and testing personnel, the following relevant papers provided information useful in preparation of this report:

Harari ,O. : International Standardization of Environmental Testing for Space Programs. Proceedings of the ESA/ESTEC 2nd International Symposium on Environmental Testing for Space Programs, October 1993

Greenfield, M.A. and Vasekich, R.A. : NASA Spacecraft Hardware Verification. ITEA Journal, March/April 1994

Wong, K. : Qualification by Similarity Guidelines. Proceedings of the 15th Aerospace Testing Seminar, October 11-13, 1994

Harari, O. : Dynamic Tailoring Guidelines. Proceedings of the 15th Aerospace Testing Seminar, October 11-13, 1994

Kindl, M.R. : Software Quality and Testing: What DOD Can Learn from Commercial Practices. US Army Institute for Research in Management Information, Communications, and Computer Sciences (AIRMICS) 31 August 1992

Messidoro,P., Buratti, P., and Moreau ,D.: Verification Guidelines for ESA Spacecraft. Proceedings of the 15th Aerospace Testing Seminar, October 11-13, 1994



## PERSPECTIVES ON U.S. MILITARY SPACE SYSTEMS

Flight Vehicle Integration Panel Symposium  
on  
Space Systems Design and Development Testing  
Cannes, France 3 October 1994

Brigadier General Sebastian F. Coglitore  
Director, Space Programs (SAF/AQS)  
Room 4D330  
1060 Air Force Pentagon  
Washington, DC 20330-1060  
USA

As many of you know, the United States has a very robust space program. When we speak of space programs in the United States, many people tend to think of our civil space program through the National Aeronautics and Space Administration, or NASA, and conjure visions of Apollo 11 and the moon landing in 1969. We celebrate the twenty-fifth anniversary of that historic event just this year. Less recognized, however, is the role military space has played in the U.S. space program. Rather than a manned focus, our emphasis in the military space area has been on unmanned capabilities to enhance the warfighting effectiveness of U.S. and Allied forces.

Today, I would like to take a few minutes and discuss U.S. military space capabilities and what we are doing to ensure these capabilities are available to support national decision-makers and U.S. and Allied warfighting forces anywhere in the world.

### Overview

Space systems afford U.S. and Allied forces global reach and presence on an unprecedented scale through a mix of highly effective capabilities. I would like to briefly discuss the role of military space systems, my responsibilities in the acquisition area, the capabilities we currently have in space, and conclude by addressing some of the

driving forces affecting military space activities today.

### Value Of Space Systems

The value of space systems is measured by their ability to provide essential information and command and control for key decisionmakers and warfighting forces. They operate through the spectrum of conflict and enhance the effectiveness of warfighting operations. As a result we have grown to depend heavily on space systems as we have drawn back our forces from overseas yet seek to maintain a "Global Presence" in support of national interests worldwide.

### Demonstrated Value

Today, space-based military capabilities support the spectrum of military missions ranging from missile warning and navigation to environmental sensing and communications. Though effective throughout the Cold War era, our experience in Desert Storm illustrated just how effective these same military space systems could be in a conventional conflict. Our missile warning satellites served the international community in limiting the repercussions of theater ballistic missile attacks in the Gulf War and preserving the delicate coalition balance against Iraq. Navigation satellites provided unprecedented accuracies in the desert for

both sophisticated weapons systems like the F-16 and the backbone of our fighting forces -- the sometimes unheralded infantryman in the field. Environmental sensing systems enhanced the efficiency and accuracy of our fighter and bomber forces by providing very timely weather information for weapons load and target planning. And lastly, U.S. and Allied space-based communications systems provided the command and control backbone for deployed warfighting forces. Overall, a complex mix of new and older space capabilities directly supported the new joint and combined doctrines so critical to success on the modern battlefield. More than forty military satellites and supporting infrastructure ultimately supported coalition warfighting operations in Southwest Asia. Although our space capabilities proved effective, a clear lesson from Desert Storm was the need to emphasize and maximize the military utility of these systems. By and large, space was a new arena for our forces in the Gulf War, and our user terminals proved cumbersome and difficult to transport. In addition, we had not fully integrated space into our doctrine and warfighting plans. Since then, we have accelerated our acquisition of smaller, more transportable warning, navigation, weather and communications terminals to ensure information from these effective space capabilities gets to the people on the battlefield. We have also improved our space training and education. To that end, we established a Space Warfare Center to more fully train, integrate and exercise with space. I can say unequivocally, that space systems and their capabilities are more useful and more understood by more personnel in the military than ever before. In fact, these same people are the ones devising better ways to use the systems we have to greater effect. On the downside, we have also built a significant dependency on

space that will only grow in magnitude and complexity in the future. Consequently, we are pressed more than ever before to ensure these capabilities are retained, improved and replaced as necessary. This is the primary focus of my responsibilities in the space systems acquisition area.

### **Acquisition Responsibilities and Funding**

Our current space capabilities have evolved over time through a complex and extensive technology investment, research, development, and production process that traces its roots back to the initial U.S. commitment to space in the 1960's. U.S. civil and military space budgets reflect continuing support for space, and today, the U.S. Air Force military space budget is just over one-third the size of NASA's budget for civil space activities. Overall, from a military space perspective, there is a growing commitment to ensure space can be used to advantage by friends and allies and denied to adversaries.

### **Space Systems Overview**

With that space budget we are continuing to modernize our capabilities and plan for a future where use of space to support military operations will be as commonplace as the use of the skies or oceans today.

### **Warning**

Our infra-red missile warning system procured under the Defense Support Program served as a very effective strategic deterrent during the Cold War. And although successful at detecting the tactical class of ballistic missile we saw in Desert Storm, we are planning a new capability to better detect lower intensity infra-red signatures from a new class of short-range, theater ballistic missile we expect to proliferate within the next decade. Through a mix of consolidation of existing resources



in the near-term, and technology demonstration and an improved capability for the future, we will meet the growing threat of ballistic missile proliferation into the next century.

### **Milsatcom**

In the communications area, we have a robust mix of Ultra-High and Super-High Frequency satellites on-orbit that are the foundation of our military command and control structure. These satellites operate from very high altitudes to afford world-wide coverage for military operations. In February, we launched our first dedicated Extremely High Frequency system to augment our secure military communications infrastructure, and are currently testing its performance on-orbit. We are also in the process of improving our future mix of communications systems as we assess the best ways to replace aging satellites on-orbit in a budget constrained environment. Part of this assessment involves a careful look at where cooperation with commercial industry and international partners may play a more significant role than in the past. The International Military Satellite Communications or INMILSAT efforts are setting the stage for future international cooperation and we foresee substantial benefits from this new approach to space system development and acquisition.

### **Navigation**

We are also keeping pace in the navigation area with planned improvements to our Global Positioning System (GPS) to ensure the military utility of the system as well as serve a growing number of domestic and international users eager to exploit the accuracies provided by today's current capabilities. We are working closely with the civilian community to ensure

uninterrupted access to GPS, and we are accelerating the installation of receivers in our front line military aircraft by the end of the decade. More good news is, as we expected years ago, dramatic advances in technology and competition in the marketplace have already significantly reduced the cost of our military receivers by over 70 percent. On the satellite side, our plans include maintaining the existing constellation of satellites, providing an improvement by 1996, and pursuing a further improved spacecraft for launch after the turn of the century.

### **Environmental Sensing**

For environmental sensing, the United States has maintained a strong military capability since the 1960's, and an equally effective civil space program to monitor world-wide weather conditions. Budget realities and common requirements have refocused our attention on meeting civilian and military needs with a single family of satellites -- by converging both programs in a collaborative effort to maintain an effective and affordable national weather capability. This convergence process is currently underway and should be completed by the end of the year. Future procurements will be performed by an integrated program office, with the military responsible for acquisition and the civil space sector responsible for daily satellite ground control operations. On the user side, to provide a more mobile capability than the existing 12-ton terminals, light-weight, two-man transportable receivers are being acquired to meet Army and Air Force needs.

### **Space Surveillance Network**

During my earlier discussion I spoke of the unheralded nature of military space. Well, within the military space area, there are also unheralded elements -- one of which is the

surveillance area. Today, a large, complex mix of ground-based radar and optical sensors monitor and track over 7,000 space objects orbiting the earth via over 40,000 observations a day. A catalog of these observations is available to the world on INTERNET with monthly updates reported to the United Nations. Our observations tell us that space is becoming a busier place, and the importance of identifying and categorizing space objects is growing. More countries are going to space, and from a military perspective, we will need to continue strong involvement.

### **Space Surveillance Chart**

We also believe surveillance of objects in space and on earth can be better accomplished from space. To prove that, we are pursuing a technology demonstration effort involving launch of two satellites by 1998. We have high expectations, and look forward to a very successful demonstration to help us establish the baseline for an operational capability in the future.

### **Space Support**

As unheralded as space surveillance, yet tremendously important, are the capabilities we collectively categorize under "Space Support." These include space lift and satellite control. We have an extensive launch base and range infrastructure on the east and west coasts of the United States to ensure our space systems achieve orbit, and an equally effective network of satellite control and tracking stations to ensure they remain healthy and perform their missions.

### **Launch Vehicles**

We have a family of medium- and heavy-lift expendable launch vehicles to place these critical military satellites on-orbit. However, military dominance of the launch area has resulted in higher than normal costs

for completing this mission. Consequently, today we have sacrificed our share of the international space launch market to more cost effective competitors such as the European Space Agency and the very capable Ariane launch system. This is an area where we have plans to increase our competitiveness in the future.

### **Launch Programs**

Although we have a very successful launch history, we have never developed a dedicated space launch vehicle for satellite payloads. Today, our primary launch boosters are derivatives of liquid- and solid-fuel ballistic missiles from the 1960's, and we have an equally antiquated, costly and complex process of acquiring and launching these boosters. Although they have served us well, we have plans to build a dedicated family of launch vehicles to serve our military, civil and commercial launch needs into the next century.

We are working closely with NASA to establish the requirements for a joint effort to develop an evolved expendable launch vehicle to carry our medium-weight and heavier satellites to orbit as well as doing technology work on future reusable systems like a shuttle replacement. Fiscal reality and international competitiveness have combined to make cooperation between U.S. military and civil space programs an absolute necessity and we are making some good progress. President Clinton just released a new National Space Transportation Policy, and we are vigorously working on plans to implement its guidelines. DoD will be responsible for expendable launch vehicles, and NASA will be responsible for reusable, manned vehicles. In addition, the United States Air Force and NASA, supported by U.S. space launch industry, recently completed a

Launch Modernization Study which identified various options to reduce costs, improve responsiveness, and increase U.S. launch competitiveness in the world market. Consequently, we plan to maintain our current inventory of boosters until the next decade, when we will transition our satellite payloads to a new, improved family of boosters based on one of the options recommended in the modernization study.

### **Launch Infrastructure**

We are also improving our launch bases and ranges through a rigorous modernization program. Our launch infrastructure includes facilities for processing the launch boosters and satellite payloads, launch pads themselves, and launch range systems that monitor the launch process until the satellite payload is put into orbit. Over the next ten years, we will invest \$1 billion to automate and standardize our launch infrastructure to lower operating costs and improve logistics supportability. We are emphasizing exploitation of commercial products and standardized support through the existing DoD logistics system accordingly.

### **On-Orbit Control**

For satellite control -- what we refer to as "health and station keeping" of our satellites in space -- we have a very flexible, but somewhat costly network of ground stations to keep our satellites healthy on-orbit. This network of control centers and tracking stations has served both the U.S. military and civil space programs, as well as our Allies, since the 1960's by supporting over 60 U.S. and Allied satellites with over 110,000 satellite contacts per year. An average of twelve (12) contacts an hour every day of the year -- a capability unsurpassed by any nation in the world today. We are working to reduce the costs of operating this network with upgrades to

communications, more friendly computer software and increased automation of routine, repetitive satellite support functions.

### **Significant Issues Affecting Space**

Ensuring these space capabilities are ready when needed has always been a difficult task. With budget reductions, personnel cuts, reorganizations and closer scrutiny by our Congress, we are finding it more difficult than ever to maintain and improve our capabilities to meet a threat that is less clear and well-defined than several years ago. Consequently, we have taken steps to reduce costs by rigorously scrubbing our requirements and carefully assessing cost and capability trade-offs. In addition, we are increasing integration of commercial equipment, practices and standards into our systems, to take better advantage of technology and capabilities available in the commercial marketplace and reduce military uniqueness where practical.

The once robust space industrial base is restructuring itself to better meet the reduced military business base and is making progress in expanding its commercial space market. As an example, two of our leading U.S. space contractors, Martin-Marietta and Lockheed have announced a merger, and we have witnessed a dramatic reduction in the number of businesses willing to compete in the space marketplace. These are unprecedented changes, but some change is essential if the space industrial base is to remain viable.

Lastly, we are forging new relationships. At home, we are working more closely with the non-military or civil space sector. I have already mentioned our close ties to NASA in the launch area, however we are also seeking cooperative efforts in technology investment and cost sharing in common

capability development. Internationally, we are seeking new opportunities where they make sense from a cost and technology perspective.

### **Importance of Space to Future Missions**

Although demonstrated during Desert Storm, the importance of space to warfighting and non-warfighting operations is growing. Military personnel are looking to space to meet the more complex threats we will face in the future. Internationally, we have recognized that combined operations and coalition warfare will become the norm rather than the exception. Three years ago, no one could have predicted the unprecedented increase in multi-national cooperative efforts in peacemaking and peacekeeping we are witnessing today.

Space systems are on-station today in Bosnia, Rwanda, Iraq, and numerous other locations in support of United Nations missions. The role of the military in the eyes of the world is being redefined and we in space system acquisition are working hard to ensure space will continue to contribute to humanitarian and peacekeeping operations, as well as future warfighting efforts.

### **Space System Testing**

Through careful testing, we reduce the risk associated with bringing space capabilities to full operations. No one knows better than you in the audience today the risks and pitfalls of trying to develop, design, test and field military systems. Therefore, in line with the theme of your symposium, I would like to take the next few minutes and discuss how space systems fit into the testing area. We emphasize performance, reliability, size, and weight -- just like in the aircraft business, but we tend to focus on the unique

environment and stresses that space imposes on sensors, electronics, power systems, fuel systems and structures. Solar radiation, micro-meteorites, gravitational drag effects, and temperature are just some of the harsher realities which must be considered for operating in space.

To assess and compensate for these impediments, we have an aggressive Space Test Program to demonstrate new technologies and initial space capabilities before they are considered for integration on operational satellites. This program allows us to demonstrate new concepts and ideas, make development and design changes as necessary, and optimize performance for future implementation. The program makes use of any available space on just about any host satellite available, as well as some dedicated test platforms. Today, more than ever before, we are closely coordinating and linking these test and technology demonstrations to operational needs to ensure we maximize our return on these space flights. Our operational space command, representing the interests of the warfighting forces, is responsible for assessing and prioritizing these efforts, and they are doing a great job.

Today, there are over forty (40) separate technology projects on the books, some large, some small, but each one essential to maintaining our technological edge in space and the warfighting force multiplier effect of our military space capabilities. On average, it is taking between three and five years to get any one experiment on a test flight. We have averaged about eight (8) flights a year since 1990 and we hope to keep up that pace through the end of the decade. From a budget perspective, although we have seen some reductions in space test funding over the last few years,

we foresee continued strong support to fulfill our needs in the space test area into the next century.

### **Space Systems Flight Testing**

Like aircraft systems, to ensure they operate when needed, space systems go through a rigorous development, design integration and testing program. We make substantial investments in reliability and fault tolerant systems, as well as ground testing to ensure our systems, which can exceed \$1 billion for a combined booster and payload (such as the Milstar communications program) operate effectively once they are launched. This extensive test and integration process contributes to the high cost of our systems, accordingly. However, high investment costs in design and testing have routinely been more than offset by the longer lifetimes our satellites enjoy once they achieve their final orbits, and the operational flexibility afforded by their size and complexity.

Timelines for fabrication, factory integration testing, satellite and booster integration and on-orbit checkout vary significantly between systems based on a variety of factors such as maturity of the satellite design, launch and on-orbit support requirements, and operator experience. For example, GPS, a mature and reliable navigation system, and the new, highly complex Milstar communications system represent opposite ends of the spectrum of space systems. For Milstar, following the successful launch last February, we will spend about a year testing the basic satellite platform and communications payload! That is an extraordinary amount of time to spend testing a capability on-orbit before it is ready for full operations. For Milstar, we can expect some decrease in testing and checkout timelines as the processes become

more familiar and routine, however, the complexity of the satellite and communications payload will continue to warrant careful testing to ensure full operability to support life threatening warfighting operations. The less complex, and mature GPS test and checkout process is very rapid by comparison -- just over three weeks.

The space business as we know it today, is a complex and costly undertaking, but as we have seen from our experience in Desert Storm and elsewhere, the forces that take advantage of technology and can exploit space will be successful. They need reliable, immediate access to these capabilities, and we have additional initiatives underway to ensure space systems continue to meet the expectations of our warfighting forces.

### **Commercial Influence On Military Space**

As you might expect, military space system acquisition and operations are very technology intensive. At one time the military enjoyed a substantial position at the forefront of space technology in many areas. The military pushed civilian industry into many growing and lucrative business opportunities as a result. We have seen that position change in a very fundamental way over the last two decades. Today, civilian industry figures more heavily in our plans than ever before -- but in a leading role. For example, as you are aware, advances in computer technology are occurring at an incredible rate. Microprocessor speeds for table top computers are doubling and prices are halving at record pace. Discussions of the "information highway" abound in many symposiums and conferences like this one. We in the military have some very fundamental decisions to make regarding

how to best take advantage of these commercial advances.

We cannot fail to recognize the commercial marketplace is making many of our military capabilities technologically obsolete before we can complete the design review phase. That is one reason we are working so hard to make better use of commercially available capabilities and focusing on upward compatible systems based on commercial practices and standards. If we fail to do this, we will be relegated to the breakdown lane on the "information highway" as we will know it in the next century. Like it or not, the military is not in the drivers seat in many technology areas today, and we can expect this trend to continue. This phenomenon will affect not only space systems, but all terrestrially-based military systems as well. We foresee a change of focus for the future where we will continue to invest in military unique capabilities where appropriate, but rely on commercially available technology and components for the balance of our systems.

### **International Cooperation**

As we adjust our methods of acquiring and funding space systems, we will also seek new and better opportunities to bring new, less costly capabilities to our military forces. Unilateral efforts to acquire and sustain space capabilities are giving way to new ideas of affordability and cooperation. Similar in concept to our warfighting plans for coalition efforts, for the future we foresee significantly increased opportunities for international cooperation in space system acquisition.

As costs grow, we will seek new methods to cost share with our Allies where interests converge, and where needs can be satisfied with common solutions. Cooperative efforts

afford new opportunities to share the burdens of collective security, while also expanding the market for international cooperation across the spectrum of military and, where appropriate, commercial applications. For technology, we are simply outdistancing our capacity to unilaterally invest in our future. Consequently, we will also look for opportunities to benefit from international technological advances in lieu of seeking indigenous/domestic development.

We look to these cooperative efforts, not as radically new undertakings, but as a renewal and reinvigoration of international relationships in an era where, only through cooperation will we ensure we meet our own security needs and those of our Allies and friends.

### **Summary**

We face an uncertain world with more than its share of conflicts, but a world with many opportunities for progress in peaceful resolution of problems. Space will continue to play a pivotal role in both -- on any scale, and United States military space capabilities stand ready to fulfill continuing commitments worldwide.

Space capabilities improve the effectiveness of our terrestrial military forces and their use will continue to grow in importance accordingly. My goal in the space acquisition area is to ensure we provide U.S. and Allied warfighting forces with the space capabilities necessary to prosecute the full range of military operations anywhere in the world -- now and in the future.

## DEUXIÈME ALLOCUTION D'OUVERTURE du symposium AGARD

### sur les essais dans la conception et le développement des systèmes spatiaux

par l'Ingénieur général de l'armement Daniel Estournet  
Chef du Service technique des systèmes stratégiques et spatiaux  
(Délégation générale pour l'armement, Direction des missiles et de l'espace)

Ingénieur général D. Estournet  
DME ISTSS, 26, Boulevard Victor  
00460 Armées, France

Monsieur le Président, mon Général,  
Mesdames, Messieurs,

Il est évident que je ne vais pas vous dire des choses sur le fond très différentes de celles que le Général Coglitore vous a dites dans sa très intéressante synthèse d'introduction. Néanmoins, si j'en répète quelques-unes, ce sera à ma manière.

Je suis particulièrement heureux d'être ici parmi vous, car le thème de votre colloque *"les essais dans la conception et le développement des systèmes spatiaux"*, comme plus généralement le domaine spatial, me semble parfois quelque peu oublié, alors qu'il est très important, et d'ailleurs bien adapté à cette organisation scientifique et technique que constitue l'AGARD. Mais grâce aux efforts de M. Levine et de M. Marec, l'espace a commencé à constituer un véritable centre d'intérêt pour vos activités ; il faut continuer dans cette voie, et même renforcer cette tendance, croyez-moi.

Pour ce qui est des systèmes spatiaux militaires, leur importance était déjà grande depuis 20 ou 30 ans. Mais elle est devenue indiscutable depuis quelques années, en fait depuis qu'aux besoins de renseignement suscités par une confrontation stratégique bipolaire, forte et constante, se sont ajoutés ou substitués, dans un monde maintenant plus mouvant et plus dispersé, le besoin de gestion des crises et celui de surveillance liée à la prolifération – les deux n'étant, du reste, pas indépendants l'un de l'autre. L'expérience récente de la Guerre du Golfe a permis à tous de tirer des enseignements sur l'utilisation militaire de l'espace. Les uns ont pu recaler des estimations faites antérieurement de façon trop théorique ou dans des scénarios plus faciles, si l'on peut dire ; chez d'autres, les événements ont même, tout simplement, fait prendre conscience des opportunités que les techniques spatiales peuvent offrir au politique et à l'opérationnel, et aussi de leurs difficultés.

Pour sa part, la France a bien adapté sa logique de choix à ce changement géostratégique. Il est vrai qu'avant les années 90, et surtout jusqu'aux années 80, la France qui a fait acte majeur de présence dans l'espace civil n'a pas, pour des raisons de priorités financières entre autres, fait d'effort très important en matière d'espace militaire. En fait, depuis quelques

temps déjà, elle avait estimé à sa juste valeur ce pouvoir que procurent les systèmes spatiaux en matière d'orientation et de multiplication des forces, et qu'a rappelé le général Coglitore. Si bien que des programmes français ont été lancés avant 1990 : Syracuse 1, Hélios I. Mais les événements ont comme cristallisé cet intérêt et, dans son Livre Blanc sur la Défense comme dans sa loi de programmation militaire pour la période 1995-2000, le premier publié en mars 1994 et la seconde votée en juin 1994, la France donne une nette priorité à l'Espace militaire : elle estime devoir au minimum disposer de moyens spatiaux d'acquisition et de transmission de l'information, et bien entendu de lanceurs pour accéder à l'Espace. Elle bénéficie d'une industrie et d'une organisation étatique spatiale fortes, cette dernière d'ailleurs récemment rénovée et resserrée, avec la Délégation générale pour l'armement (DGA), l'Etat-major des armées (EMA) et le Centre national d'études spatiales (CNES), organisation supervisée par un Comité de l'espace présidé par les ministres tuteurs. Elle dispose déjà d'un système spatial de télécommunications militaires opérationnel : après Syracuse 1, c'est le système Syracuse 2 ; et elle disposera début 1995 du premier satellite militaire de reconnaissance : ce sera Hélios I.

Pour la suite, la France est bien décidée à accentuer cet effort. Dans le domaine des télécommunications spatiales militaires, on donnera un successeur à Syracuse 2. Dans celui de l'imagerie spatiale, le programme Hélios II est lancé pour ce qui est de l'optique, et un programme de radar spatial viendra bientôt le compléter. Dans le domaine de l'écoute électromagnétique, des études et expérimentations se poursuivent. Dans le domaine de l'alerte, toute une réflexion est entreprise. Dans le domaine de la surveillance de l'espace, un système probatoire est mis sur pied.

Mais la France ne peut ni ne doit poursuivre seule cet effort.

D'abord, l'espace militaire français ne demande qu'à s'europaniser. Il y a à cela des raisons économiques bien sûr, car l'accès à l'espace est coûteux. Mais il existe également des raisons politiques, car l'Europe est appelée à se doter de moyens spatiaux de surveillance des traités de désarmement et de moyens de renseignement permettant de mieux gérer les crises, voire les conflits ; or la France se doit d'y contribuer activement.



Ensuite, ou plutôt en même temps, d'autres raisons de ne pas travailler isolé dans ce domaine conduisent au-delà du seul cadre européen. Je citerai le souci d'assurer l'interopérabilité de la plupart des systèmes spatiaux avec les autres pays de l'OTAN. Je citerai aussi les enjeux politiques et économiques de dimension planétaire attachés à certaines applications, qui invitent à instaurer la plus large coopération internationale : je pense par exemple à l'alerte pour la défense aérienne élargie, ou aux moyens de cohérence comme la navigation et la météorologie.

Pour tous nos pays, il sera difficile, dans le contexte budgétaire actuel, de satisfaire tous les besoins opérationnels – par exemple, pour la France, ceux exprimés dans le Livre Blanc : il faut réduire les coûts des programmes d'armement. Les systèmes spatiaux, même s'ils sont particulièrement intéressants aujourd'hui, ne dérogent pas à la règle. Les pays à fort budget spatial voient celui-ci plutôt diminuer, les pays à budget spatial plus modeste ne voient pas celui-ci augmenter autant que les besoins le nécessiteraient. Pour rechercher des économies, plusieurs voies sont possibles, et la coopération internationale en est une, comme il a été rappelé. Mais l'utilisation de la synergie très forte qui existe entre les applications civiles et les applications militaires de l'espace en est une autre. Enfin, l'amélioration des méthodes de conception, de développement et de qualification, qui passent bien entendu par des innovations concernant les moyens de simulation et d'essais, en est une autre encore. Je suis sûr que l'AGARD, agence de l'OTAN au sein de laquelle sont représentés tant des "étatiques" que des "industriels", est consciente de ces enjeux.

Pour ce qui est de la France, comme vous le savez, le système Hélios est réalisé en coopération européenne. J'ajoute qu'une coopération est fortement recherchée pour tous les programmes spatiaux militaires futurs. On la favorise aussi pour les études actuelles, tant au niveau des technologies qu'à celui des systèmes. Quant à la synergie civilo-militaire, elle est également largement mise en œuvre dans le domaine spatial en France : la composante spatiale de Syracuse 2 est embarquée sur Télécom 2 aux côtés de la charge utile civile, le satellite Hélios 1 utilise la même plate-forme que le satellite civil Spot 4, et tous les moyens civils, qu'ils soient humains ou matériels, sont utilisés pour le développement des systèmes militaires, sans parler des services de lancement, pour lesquels il est bien connu que la France s'appuie, par principe, au travers de la filière Ariane, à la fois sur la coopération européenne et sur les moyens civils.

C'est dans ce contexte, à la fois de coopération internationale et de synergie civilo-militaire, que l'amélioration des méthodes de développement, de simulation et d'essais, qui constitue l'objet de ce colloque, doit être envisagée dans vos préoccupations à tous.

Il ne m'appartient pas – et vous me le pardonnerez sûrement car c'est à vous qu'il appartient – de montrer combien ce thème est intéressant par son contenu. Je me suis contenté de rappeler le cadre dans lequel il doit être traité, et qui, je pense, devrait le rendre encore plus attrayant à votre communauté professionnelle.

Néanmoins, je faillirais à mon devoir d'orateur introductif si j'omettais de dire que le domaine spatial est l'un de ceux pour lesquels les essais sont les plus importants. Voilà bien un domaine où l'on n'a pas de droit à l'erreur, et ce, quel que soit le type de système : les satellites, car aucune maintenance en vol n'est vraiment envisageable, les lanceurs, pour des raisons de coûts et de calendrier, sans parler des vols habités où des vies humaines sont en jeu. Il est donc essentiel de réaliser des essais très complets avant lancement, de simuler au mieux l'ambiance spatiale, et, plus que dans tout autre domaine sauf peut-être le domaine nucléaire, de tout contrôler et de tout prévoir.

Or – voyez comme le monde est mal fait ! – dans le domaine spatial, les moyens d'essais sont très coûteux. Par conséquent, la réduction des coûts des programmes spatiaux doit passer par une réduction des coûts de ces moyens d'essais. C'est ainsi qu'on cherchera à concevoir des moyens communs aux applications civiles et militaires, ou des moyens communs à d'autres applications non spatiales, ou bien à améliorer des moyens de simulation de façon à réduire les essais – dans la mesure où les simulations ne conduisent pas elles-mêmes à des coûts prohibitifs... –, ou bien à faire le maximum d'essais au sol, ou à utiliser des avions ou des fusées sondes lorsque des essais en vol sont nécessaires, ou encore à se servir de micro- ou minisatellites pour les technologies devant être validées en orbite, etc. Tous ces points seront abordés dans les différents panels de votre colloque.

Je viens de mentionner les moyens de simulation : la simulation revêt un caractère primordial lorsqu'on s'intéresse à l'espace et en particulier aux satellites. L'environnement spatial ne peut en effet pas être entièrement reconstitué au sol, mais partiellement et avec des moyens colossaux et coûteux (grandes chambres de test en vide thermique, etc.). La simulation prendra certainement une part croissante, comme dans toutes les applications, dans la conception et également dans le développement des systèmes spatiaux. Evidemment, elle devra être validée pour mériter toute confiance, et elle ne remplacera jamais complètement les séquences d'essais. Dès lors, toute la difficulté réside dans le dosage entre essais en vol, essais en ambiance simulée et simulations pures, et l'on peut parier, sans grand risque de se tromper, que ce dosage devra constamment être amélioré en coût/efficacité : voilà un axe de réflexion et d'effort particulièrement utile.



Quant à la coopération européenne et internationale en matière de moyens d'études et d'essais, on la retrouve bien entendu, et à la fois comme fin et comme moyen. En effet, d'un côté, la coopération ne pourra se trouver que renforcée par l'harmonisation des méthodes de conception et développement, des essais et moyens d'essais ; et d'un autre côté, la mise en commun de ces moyens évitera la duplication d'installations très coûteuses, notamment entre pays voisins.

La France dispose de nombreux moyens d'essais :

- pour les satellites : des moyens installés à Toulouse mais également ici-même, à Cannes, chez l'industriel Aérospatiale,
- pour les lanceurs : des moyens installés à Kourou, aux Mureaux, à Vernon, à Bordeaux ;
- à ces moyens spatiaux, il convient d'ajouter des moyens liés aux missiles, donc purement militaires, mais mis à la disposition des civils pour l'Espace quand cela est nécessaire (moyens installés sur certains des sites industriels déjà cités, ou au Centre d'Essais des Landes, ou sur le bâtiment d'essais et de mesures "Monge") ; ces moyens concernent essentiellement les lanceurs et les lancements compte tenu de la synergie avec les missiles ; aucun moyen spécifiquement militaire n'a en effet été développé pour les satellites militaires.

Au niveau européen, l'Agence spatiale européenne, ainsi que certains grands maîtres d'œuvre industriels européens, disposent de moyens intéressants.

Il importe aujourd'hui d'assurer une bonne coordination entre tous ces moyens et de les utiliser au mieux.

\*  
\* \*

En conclusion, je vous prie de ne pas me juger restrictif si je vous dis que c'est avant tout la diversité des moyens et des méthodes de réduction des coûts des programmes spatiaux militaires, que doivent montrer les nombreux sujets abordés dans ce colloque.

L'AGARD est un groupe *consultatif* : ce terme a son importance. Il recouvre l'influence que vos avis d'experts peuvent avoir sur les décideurs : tirez-en les conséquences. Un proverbe français dit qu'« on n'attrape pas les mouches avec du vinaigre » : ayez toujours présent à l'esprit que les décideurs sont friands de considérations qui vont dans le sens, à la fois :

- de l'économie et des diverses synergies et coopérations,
- et du maintien de l'indépendance ou de la souveraineté de chacun, car il est bien connu et constaté que l'espace a *valeur stratégique*.

Comme tous les énoncés de problèmes réels, celui-ci n'est pas exempt de contradictions apparentes ! mais vous êtes habitués au fait que tous les problèmes intéressants sont de cette nature.

Il s'agit de garantir le succès de l'Espace militaire pour l'ensemble de nos pays ; et pour moi, "succès", cela veut dire lancement effectif de programmes. Ainsi, malgré toutes les contraintes budgétaires et organisationnelles qui peuvent s'y opposer et qui sont étrangères aux considérations scientifiques et techniques, c'est tout le bonheur que je vous souhaite.

## AN OVERVIEW OF DOD TEST REQUIREMENTS FOR LAUNCH AND SPACE SYSTEMS

Mr. Charles J. Moening  
The Aerospace Corporation  
P.O. Box 92957, M4-899  
Los Angeles, CA 90009-2957

### ABSTRACT

MIL-STD-1540 Test Requirements For Space Vehicles was first issued in 1974. This Military Standard prepared by The Aerospace Corporation for the United States Air Force space programs has been a reference for defining test programs for most U. S. DOD space systems. The third revision, to be MIL-STD-1540C, was prepared over the last two years with a primary objective of including test requirements for launch vehicles and upper stages. This paper discusses the background and effectiveness in using earlier revisions of the Standard and summarizes the major changes incorporated in MIL-STD-1540C "Test Requirements for Launch, Upper Stages and Space Vehicles."

### 1. BACKGROUND

In the early 1970's the U.S. Air Force, supported by The Aerospace Corporation, conducted a review of testing practices being used in development of its satellites. This review was conducted as part of a broader critical examination of satellite design, development and manufacturing processes. The purpose was to identify improvements that could reduce the orbital failure rate of Air Force satellites. The review revealed a wide diversity of philosophy, methods and requirements. In some cases the lack of a lessons learned feedback process led to the same failures and failure modes being repeated on different programs. It was found that each Air Force satellite program developed its test requirements based on the particular experience of contractor, Aerospace, and Air Force personnel working on the program. In order to improve on this situation, work was initiated at Aerospace to document failures and the associated lessons learned that, if followed, would avoid repetition of failures. About the same time period, Lockheed Missile and Space Company (LMSC) developed a standard testing baseline to assure consistency and adequacy of their space vehicle testing which included certain Air Force programs.

With this background, Aerospace was directed to develop a military standard to establish a testing baseline for all Air Force space vehicles. MIL-STD-1540 "Test Requirements for Space Vehicles," was issued in 1974. To a large extent it was modeled after the LMSC document modified to incorporate experience and lessons learned from all other Air Force programs. The Standard defined test requirements starting at the unit (component or black box) level of assembly up to and including integrated system testing at the launch site. The general content is illustrated in Figure 1. Note that 1540 does not define test requirements for levels of assembly below units, i.e., for parts.

By the early 1980's, Aerospace had accumulated and documented sufficient lessons learned information to warrant a revision to 1540. MIL-STD-1540B was issued in 1982. Reference 1 summarizes the significant changes that were incorporated. Among the more subtle changes was the recommendation, stated in the forward of the Standard, that the unit test requirements be applied to launch vehicles as well as to satellites. The reasoning for this was that there was no standard for launch vehicles and the MIL-STD-1540B unit test requirements were based primarily on test objectives common to both satellite and launch vehicles. These objectives were 1) to demonstrate capability to survive launch and ascent environments and 2) to assure that workmanship defects were adequately screened from flight hardware.

In 1993 the decision was made to prepare MIL-STD-1540C. The decision was driven primarily by the need to have comprehensive test requirements for launch vehicles and upper stages. These were not explicitly defined in 1540B causing confusion in the DOD community regarding the extent to which the requirements were to be applied to launch vehicles and upper stages. A separate standard for testing of launch vehicles and upper stages was considered. This was rejected based on the reasoning that the entire complement of hardware dedicated to accomplishing a successful satellite mission should have comparable test requirements.

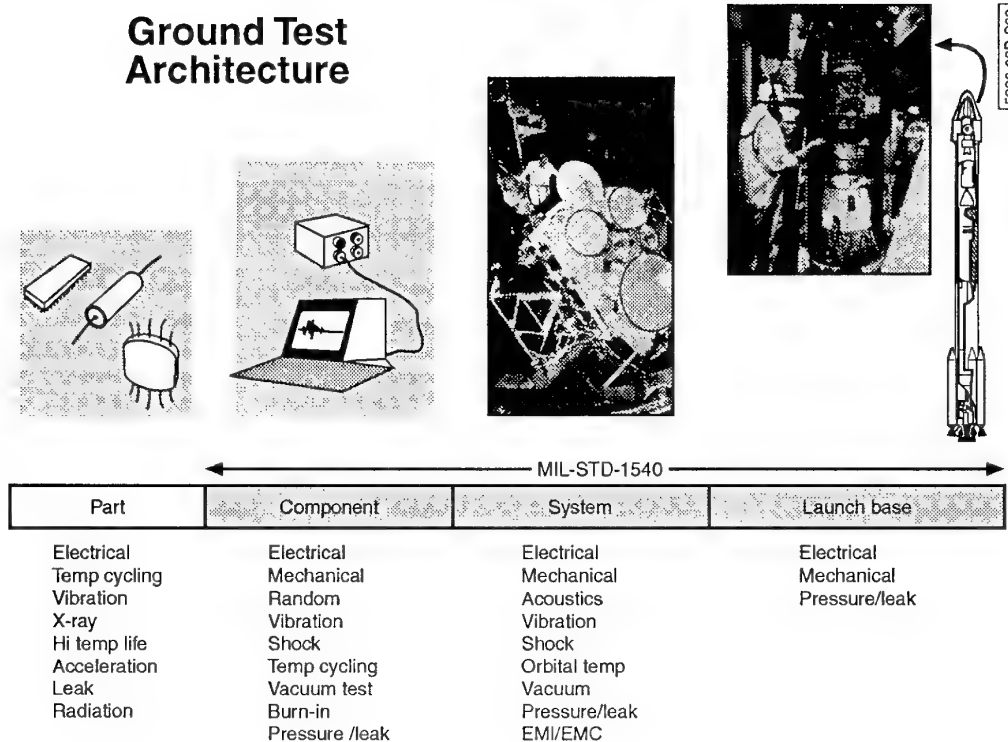


Figure 1. Scope of MIL-STD-1540

## 2. APPLICATION OF MIL-STD-1540A AND B

### 2.1 Application to Space Vehicle Programs

The application of 1540 across DOD space vehicle programs was done gradually to minimize cost increases. For example, it was generally not applied retroactively to existing programs. However, if an existing program procured a new unit or subsystem, the 1540 requirements often would be applied to the newly procured hardware. For new program starts, the intent was to apply 1540 by tailoring the requirements giving strong consideration to balancing cost versus risk. Thus low-risk programs such as those with large numbers of satellites, for example the Global Positioning System (GPS), tended to be more fully compliant than higher-risk one-of-a-kind programs. Figure 2 illustrates the range of compliance of a number of Air Force satellite programs as determined by their Test Thoroughness Index (TTI). Essentially the TTI is a measure of the

percent compliance with the aggregate of unit through system test requirements as defined in 1540 (Ref. 2). The TTI is determined by weighting and rating each individual test requirement depending on 1) its effectiveness in minimizing risk of flight failure and 2) how closely the test margins and other parameters meet the specified conditions of the Standard. As shown in Figure 2, compliance with MIL-STD-1540 for 12 satellite programs ranges from approximately 33% for the program with lowest compliance to a high of 94% for GPS. Program 12 (Fig. 2) with the lowest compliance was a one-of-a-kind program originated prior to the existence of the Standard and is shown for reference. Two commercial programs with TTIs in the range of 70 to 75% are also shown. Figure 2 also shows the TTI for risk classifications as defined in DOD HDBK-343 (Ref. 3). This document was prepared by Aerospace to be used as a guide in tailoring down the requirements of 1540 and other Military Standards for programs where higher risks were considered acceptable in order to reduce costs on one-of-a-kind programs.

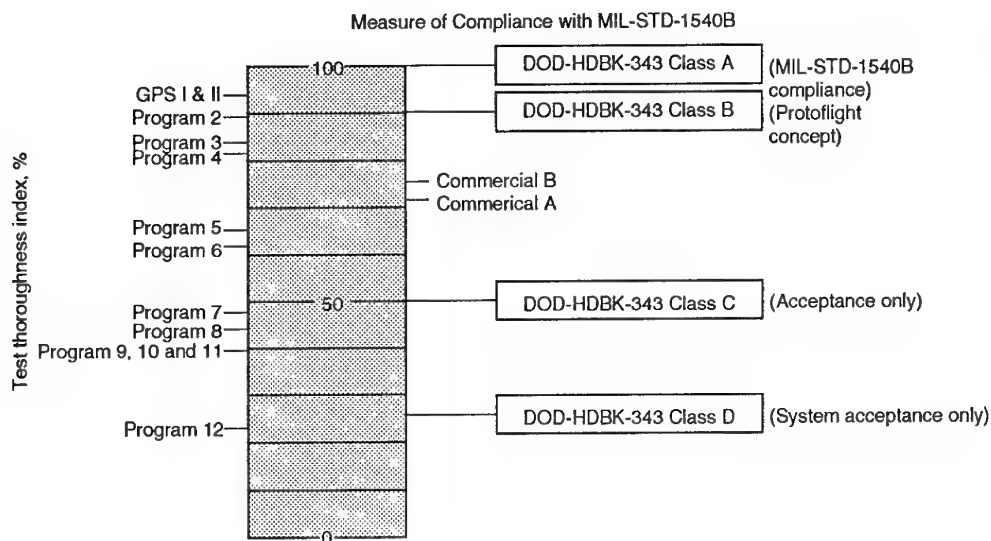


Figure 2. Test thoroughness index of various USAF and commercial satellites

## 2.2 Application to Launch Vehicle and Upper-Stage Vehicle Programs

The degree to which the Standard was applied to launch and upper stage vehicle programs varied even more widely and depended largely on the heritage of the program. For example, the Inertial Upper Stage (IUS) program was a totally new development with little heritage in the design or in hardware elements. In this case, 1540A was applied to the fullest extent, similar to the application to the GPS satellite program (Fig. 2). The application to the IUS is discussed in References 4 and 5. For launch vehicle programs such as Titan IV and its predecessor vehicles, which had a long history of heritage hardware, some of it dating from early Titan I and II Inter-Continental Ballistic Missiles (ICBMs), the Standard was applied as new contracting situations arose. The most notable example being in the mid 1980's after two catastrophic flight failures of Titan 34D. During the recovery-to-flight phase, a substantial upgrade of test requirements to those in 1540B was deemed necessary and accomplished by contract direction. As a result, much of the hardware was requalified and in some cases reacceptance tested to meet 1540B requirements. Similarly, the test requirements for Delta II and Atlas launch vehicle programs are being gradually upgraded to more closely comply with the Standard. The process of upgrading the test requirements for launch vehicles and upper stages

will continue for several more years, possibly at an accelerated pace with the release of MIL-STD-1540C.

## 2.3 Application to Non-DOD Programs

MIL-STD-1540 has also been used for reference or as a point of departure in establishing test requirements for many programs outside of the United States DOD community. These include NATO programs such as NATO-III and commercially developed launch vehicles in the U.S. such as Pegasus and Taurus. The Standard reportedly was used for the Chinese Long March launch vehicle. The Standard has been used in parts of the National Aeronautic and Space Administration (NASA) Space Station development. A review of the recent draft of European Space Agency (ESA) "Test Requirement Specification for Space Equipment," (Ref. 6), shows considerable similarity with requirements for components as defined in MIL-STD-1540B, suggesting it may have served as a reference for that document.

## 3. EFFECTIVENESS OF MIL-STD-1540 TEST REQUIREMENTS

The historical range of application of 1540 to space vehicle programs, as measured by the TTI, provided data with which to evaluate the value or effectiveness of the test requirements. A preliminary study was

conducted by Aerospace in the early 1980s to determine whether a correlation existed between the TTI and failures on orbit (Ref. 2). The approach taken was to determine the number of mission degrading orbital failures that occurred on each satellite and plot these versus the TTI. It was expected that, for a given TTI, the failure rate of a satellite would increase with its complexity as measured by the number of electronic piece parts contained. It was decided, therefore, to normalize the failures by the number of electronic piece parts (resistors, diodes, etc.) contained in the satellite.

The initial study to examine the correlation of TTI with orbital failure rate<sup>2</sup> showed that orbital failure rates were lower for those programs which had a higher degree of compliance with 1540 test requirements. Since that time, further work has been done to broaden the database by including more space vehicle programs, including a few commercial programs which do not use 1540. The results of this work appear in Figure 3, showing a clear trend of reduced early orbit flight failures with increasing test thoroughness. However, the study did not examine other aspects of the programs that could reduce orbital failure rate such as management oversight, development testing, and hardware maturity. In addition to this study, others have been performed at Aerospace to examine the costs of 1540 system level environmental tests, and the effect that these tests had on satellite reliability. The results provided insight into the cost benefits of testing<sup>7,8</sup>. These studies led to the conclusion that the benefit-to-cost ratios for individual system-level environmental tests varied from 5:1 to over 60:1 with a composite being in the range of 15 to 20:1. To state this another way, for each dollar spent on system level testing, a return of 15 to 20 dollars was realized in terms of reduced life-cycle costs. These studies proved and, to a certain extent, quantified, the value of system-level acoustic and thermal vacuum tests specified by 1540 for assembled satellites. Similar studies, although much more difficult, are also planned to quantify the value of the unit tests specified in 1540. The lack of such studies presented a problem to the authors of 1540C. This will be discussed later in this paper.

#### 4. OBJECTIVES OF MIL-STD-1540C

There were three basic objectives to be achieved in developing MIL-STD-1540C. These were 1) to broaden the scope to explicitly include test requirements for launch vehicles and upper stages, 2) to incorporate lessons learned from the use of 1540B, and 3) to reduce testing costs where possible. There also were certain ground rules

established that were deemed necessary to broaden industry support for the Standard. The ground rules were 1) provide industry the opportunity to review, comment and influence the content of the proposed Standard and 2) maintain the same general format used in previous versions of the Standard.

#### 5. MAJOR CHANGES FROM 1540B

The major changes from 1540B that were incorporated in the final 1540C consisted of the following:

- Add guidelines and contractual language for tailoring
- Broaden application to include launch vehicles and upper stages
- Remove unproductive aspects of acceptance tests
- Strengthen qualification tests
- Expand options for flight use of qualification items

These changes were based upon widespread government and industry reviews of drafts of 1540C. Several industry workshops to discuss early versions of the proposed Standards were held at Aerospace. These activities generated thousands of comments. The sources and distribution of written review comments are summarized in Figure 4. Each comment was reviewed and evaluated by the writing team consisting of seven senior members of the technical staff at Aerospace. A majority of the comments resulted in changes being made to alleviate or eliminate the reviewer's concern. Further explanation of the changes is provided in the following:

##### 5.1 Guidelines and Contractual Language for Tailoring

One of the strongest concerns expressed by both government and industry reviewers centered around the issue of tailoring for specific programs. Industry reviewer concerns usually stemmed from experiences where certain procuring agencies would sometimes not allow tailoring even when technically justified. On the other hand, experiences of some government reviewers was that contractors would avoid performing necessary tests because they were defined as "optional" in 1540B. These divergent views were accommodated in several ways as follows:

- a. Recommended contractual language and tailoring matrices were included for use by procuring agencies.

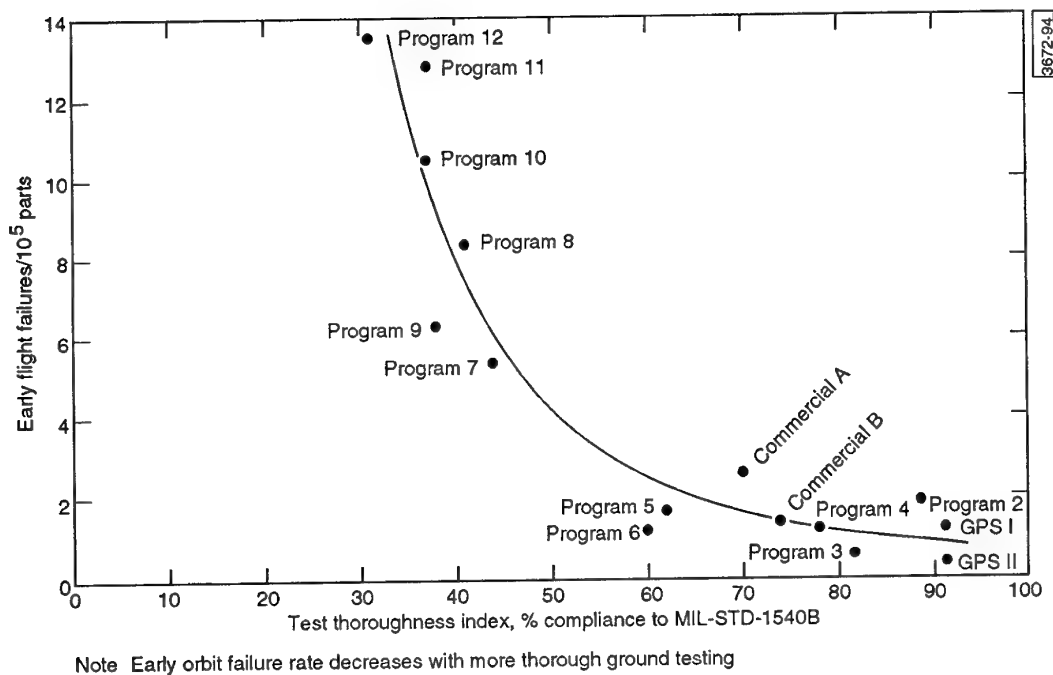


Figure 3. Orbital failures versus test thoroughness index of various USAF and commercial programs

| Total Industry Comments to Jan and Aug 93 Drafts = 1250   |                     |
|---|---------------------|
| Organization  | % of Total Comments |
| NASA (all centers including JPL)  | 17                  |
| MMC   | 13                  |
| Boeing  | 13                  |
| LMSC  | 11                  |
| TRW   | 10                  |
| Hughes  | 7                   |
| MDAC  | 7                   |
| USAF and Aerospace (Aug draft only)   | 7                   |
| General Dynamics  | 4                   |
| Others (RI, Thiokol, Fairchild, Litton Sandia, Aerojet, Honeywell, U.S. Navy, Alenia Spazio, Consultants) | 11                  |

Figure 4. MIL-STD-1540C draft review comments

- b. Self-tailoring was included in individual test requirements whenever possible. For example, unit thermal cycle tests can be tailored by trading temperature range for number of thermal cycles according to an algorithm provided.

- c. The words "shall," "should" and "may" were judiciously used in the Standard to indicate priority of requirements.
- d. The word "optional" was deleted from the test matrices. In place of this, tests previously defined as optional in 1540B are now defined as "other" tests. These are intended to be selectively changed to "required" based on technical and programmatic considerations for a particular program.

## 5.2 Broadened Application

As discussed earlier, one of the main reasons for revising the Standard was to incorporate test requirements for launch vehicles and upper stages. 1540C specifically identifies system and subsystem tests by vehicle category for launch, upper stage and space vehicles. These tests vary somewhat because certain tests for space vehicles are less applicable to launch vehicles. Unit test requirements are consistent and nearly the same for all vehicle categories. The reason is that unit tests are primarily intended to demonstrate basic workmanship and survival of launch and ascent environments, objectives common to all vehicle

categories. Industry reviews of 1540C drafts surfaced a mis-perception in parts of the launch vehicle community. The thinking was that space vehicle unit testing was more rigorous than needed for launch vehicles because of longer space vehicle mission durations. This view is not supported by Aerospace studies of unit failures on space vehicles which indicate that a high percentage of these failures occur as a result of the launch and ascent environments. Therefore, the differences in mission duration were not considered to be an overriding factor. Also, spacecraft and launch vehicle units need the same workmanship tests. Based on these reasons, it was concluded that comparable unit testing was appropriate and the Standard reflects this position.

### 5.3 Remove Unproductive Aspects of Acceptance Tests

As indicated earlier, one of the main objectives was to reduce test costs where possible, and 1540C accomplishes this in several ways. 1540B required that a qualification item be subjected to formal acceptance tests before entering its qualification test regimen. The intent of this was to enable the allocation of hardware defects into the categories of design and workmanship. Experience on Air Force programs is that, in practice, this was seldom accomplished. Therefore, 1540C no longer specifies that a formal acceptance test is required prior to performing qualification tests.

MIL-STD-1540B contained the acceptance test requirement for 300 hours of electrical burn-in, including 10 thermal cycles over an 85°C temperature range for electrical or electronic units. This was in addition to 8 thermal cycles required as part of a separate thermal cycle acceptance test. In 1540C, these two tests are combined into a single thermal cycling test of 12.5 cycles over a 105°C range with the burn-in reduced to 200 hours. Other changes made to reduce test costs included shortening the time required for each thermal or thermal vacuum cycle. A measure of how the typical unit thermal test costs are reduced from 1540B is provided in Tables 1 and 2. Shown in these tables are the estimated test time required by 1540C and 1540B for a typical electrical or electronics component. In all cases, the test time (and therefore cost) required by 1540C are equal to or less than required by 1540B. Most importantly, the recurring acceptance test costs are substantially reduced.

Industry review comments tended to be polarized regarding the necessity for thermal cycle acceptance tests for electrical or electronic units. A strong minority view was that thermal cycle tests are

unnecessary and could damage otherwise good hardware. Reviewers with this viewpoint generally believed that the number of thermal cycles could be reduced from 12.5 cycles down to 1 or 2 cycles. However, definitive engineering studies to support any particular position on the number of cycles needed for acceptance testing of launch or space vehicle hardware was not available. As mentioned

Table 1. Comparison of Unit Thermal Qualification Tests

| Tests   |       | Cycles   | $\Delta T$ (°C) | Test time (hr) |
|---------|-------|----------|-----------------|----------------|
| TV only | 1540C | 6        | 125             | 57             |
|         | 1540B | 3 + 1*   | 105             | 109            |
| TV/TC   | 1540C | 25/53.5  | 125             | 376            |
|         | 1540B | 24 + 18* | 105             | 76 + 300*      |

\* Addition due to acceptance test (not in 1540C)

Table 2. Comparison of Unit Thermal Acceptance Tests

| Tests   |       | Cycles     | $\Delta T$ (°C) | Test time (hr) |
|---------|-------|------------|-----------------|----------------|
| TV only | 1540C | 1 (2)      | 105             | 16             |
|         | 1540B | 1          | 85              | 27             |
| TV/TC   | 1540C | 4/8.5 (25) | 105             | 200            |
|         | 1540B | 18         | 85              | 300            |

( ) Maximum allowed including retest

earlier, the lack of unit test effectiveness studies presented a dilemma to the writing team. Essentially, the decision was to retain the equivalent thermal cycle tests specified in 1540B, but to allow tailoring. For tailoring, modification of the number of cycles (N) and temperature ranges ( $\Delta T$ ) is allowed using the following algorithm plotted in Figure 5.

$$N(\Delta T)^{1.4} = \text{constant}$$

Figure 5 also shows a reasonable degree of correlation with other military and industry requirements and compares these with MIL-STD-1540B and 1540C. The exponent of 1.4 was selected as a conservative value based on fatigue of solder data collected by Aerospace. Ten cycles at 125°C is the requirement in R&M 2000, an Air Force policy document for reliability and maintainability.

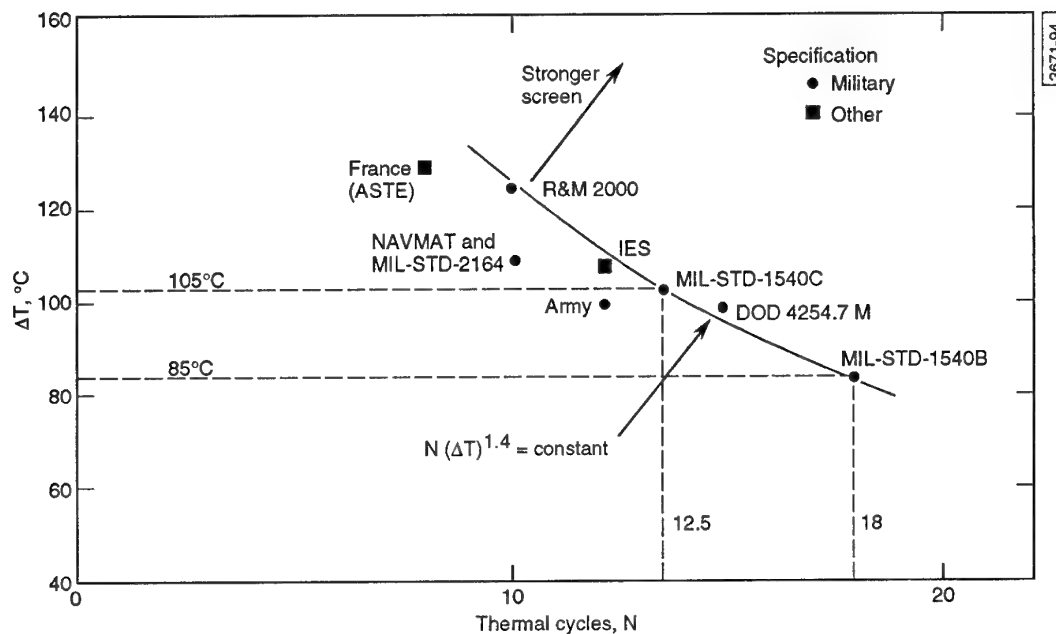


Figure 5. Comparison of thermal cycle acceptance test criteria

#### 5.4 Strengthen Qualification Tests

Qualification tests specified in 1540C were strengthened with the objective of reducing life cycle costs. Experience from many Air Force programs showed that very often hardware on a given program would be requalified at significant expense, usually for one of the following reasons:

- Repeated acceptance tests of a flight unit to resolve anomalies and workmanship failures would raise the question of whether sufficient fatigue life remained for flight. The qualification article of the unit in question would be requalified to prove that the flight unit was acceptable.
- Statistical variations in the flight environment would result in exceedances of predicted levels and sometimes even of qualification levels. The qualification unit would be subjected to additional testing.

To reduce the frequency of having to requalify hardware, 1540C established qualification requirements which address both the extreme expected flight environment and a maximum allowed amount of repeated acceptance testing. This applies to both thermal cycling and vibration tests. Also, the

statistical basis for shock, vibration and acoustic tests has been strengthened. 1540C specifies a P95/50 (not exceeded on at least 95% of flights, estimated with 50% confidence) level for acceptance, the same as 1540B. However, the qualification level is specified as P99/90 instead of a specific qualification margin. The P99/90 has been used for many years at Aerospace to assess adequate structural strength for dynamic loads. As a result of this statistical approach, as data from more flights are available, the margin between P95/50 and P99/90 can be reduced. The above changes are expected to reduce the amount of requalification needed on future programs.

#### 5.5 Expand Options for Flight Use of Qualification Items

For space vehicles, a common practice followed by military, NASA and commercial programs, where only a few flight systems are built, is to fly the qualification hardware. This qualification would generally be at reduced levels or durations or both. NASA commonly uses the term "Protoflight" for this approach. MIL-STD-1540B had a short section addressing "Flight Use of Qualification Equipment." In the revised Standard, this section has been expanded to provide the users with additional strategies that may be more cost effective



under certain conditions. 1540C contains a "Spares strategy," a "Protoqualification test strategy," and a "Flightproof test strategy." The latter strategy was not in 1540B. The different strategies are summarized as follows:

- Spares strategy
  - Full qualification at all assembly levels
  - Replace critical, nonredundant items for flight
  - Critical qualification items refurbished and reaccepted for use as spares
- Protoqualification test strategy
  - Combines qualification and acceptance for one flight item
  - Use half qualification margins and half qualification durations
  - Subsequent flight items acceptance tested
- Flightproof test strategy (new)
  - Combines qualification and acceptance for all flight items
  - Uses half qualification margins, full acceptance durations

The strategies involving the flight use of qualification equipment are only intended for use in space vehicle programs that have a very limited number of vehicles. These strategies do not apply to launch or upper stage vehicle programs or to space vehicle programs with large numbers of satellites because the short-term cost savings are generally outweighed by the long-term cost benefits achieved by a more rigorous qualification program.

## 6. FUTURE DOD TEST DOCUMENTATION

A major area not covered by MIL-STD-1540C is performance testing of propulsion equipment. In the early planning stages, consideration was given to including these, especially since 1540C was being broadened in scope to include launch vehicles. The decision was made to not include these propulsion test requirements in 1540C because it could not be completed in a timely fashion and a separate document seemed more appropriate. A Standard for performance testing of propulsion equipment is in the planning stage. 1540C does, however, apply to propulsion equipment for defining environmental test requirements.

MIL-HDBK-340 "Application Guidelines for MIL-STD-1540" will require revision to reflect the changes in content and scope of 1540C. Basically, this Handbook provides rationale and guidelines

for using 1540C. Since tailoring was a major issue in development of 1540C this will be more thoroughly addressed in the revised Handbook, along with other areas such as fatigue equivalence, statistics of environmental predictions, rationale for qualification by similarity, and guidance for hardware retesting.

## REFERENCES

1. Hamberg, O.; Graziadei, J. D.; Jepsen, L. L., "MIL-STD-1540B Revision Test Requirements for Space Vehicles" The Aerospace Corporation and USAF, Proceedings of the 9th Aerospace Testing Seminar - Institute of Environmental Sciences, October 1985.
2. Laube, R. B., "Methods to Assess the Success of Test Programs" The Aerospace Corporation, Proceedings of the 7th Aerospace Testing Seminar - Institute of Environmental Sciences, October 1982.
3. "Design, Construction, and Testing Requirements for One of a Kind Space Equipment" MIL-HDBK-343 (USAF), 1 February 1986.
4. McDaniel, H. M.; Hopkins, L. A., "Current Boeing Experience with MIL-STD-1540A Component Qualification Program" Boeing Aerospace Company, Proceedings of the 6th Aerospace Testing Seminar - Institute of Environmental Sciences, March 1981.
5. McDaniel, H. M.; Hopkins, L. A., "IUS Qualification and Acceptance Failure Data" Boeing Aerospace Company, Proceedings of the 7th Aerospace Testing Seminar - Institute of Environmental Sciences, October 1982.
6. "Test Requirements Specification for Space Equipment" ESA PSS-01-802 Draft 1, September 1993.
7. Hamberg, O.; Brackin, C. A.; Tosney, W. F., "Satellite Environmental Testing Cost Benefits" The Aerospace Corporation, Proceedings of the 12th Aerospace Testing Seminar - Institute of Environmental Sciences, March 1990.
8. Hamberg, O.; Tosney, W. F.; Brackin, C. A., "The Effectiveness and Cost Benefits of Satellite Environmental Acceptance Tests" The Aerospace Corporation, Proceedings of the International Symposium on Environmental Testing for Space Programmes ESTEC, Noordwijk, The Netherlands, June 1990.

# Tailoring Test Requirements for Application in Multinational Programmes

Piero Messidoro, Marino Ballesio, Emanuele Comandatore

Alenia Spazio S.p.A. - Turin Plant  
Corso Marche 41  
10146 Torino - Italy

## 1. SUMMARY

Participation in international cooperative programmes is giving rise to an interesting experience of test requirement tailoring to define mutually agreed specifications.

Significant differences, in particular between the European and US approach, have been pointed out in areas like: qualification/acceptance test philosophies, equipment and system thermal cycling, vibro-acoustic excitation and qualification test article quality standard.

The paper focuses on the experience gained in discussing the above points and suggests possible improvements towards an international standard for space testing.

## 2. INTRODUCTION

The recent evolution of space activities is towards international cooperation, see for example the new scenario of the space station "ALPHA". This project is involving as NASA partners the space organizations of different countries such as CSA (Canada), NASDA (Japan), ESA (Europe), ASI (Italy) and recently also RKA (Russia).

In the above international effort, namely with the Mini Pressurized Logistic Module and in several other programmes such as IRIS, Tethered Satellite, LAGEOS, SAX, etc., Alenia Spazio had the responsibility, through contracts of the Italian Space Agency (ASI), to design and develop space systems which represent the Italian contribution to the joint projects.

As part of this responsibility, also the verification and test activities were carried out following mutually agreed specifications.

The effort to tailor the applicable test requirements on the basis of the respective test practices represents one of the most significant experiences of these international cooperations.

In fact, different approaches in several areas have been identified as having important impacts on mission success and programme cost and planning.

In particular, starting from the most popular standards usually applicable to space projects, significant differences have been experienced in the following areas:

- test philosophies
- thermal cycling
- vibro-acoustic excitation
- qualification test article standard

The above aspects are discussed in detail herein and possible improvements are also suggested.

## 3. TEST PHILOSOPHIES

Concerning the Test Philosophies for equipment and system qualification and acceptance, the U.S. and European requirements are significantly different in certain areas as shown in Figures 1, 2, 3 and 4 (see following pages).

Fig. 1 compares the qualification test required by the European Space Agency (ESA) for different categories of equipment to be qualified for a generic space programme, as per ESA PSS-01-802 "Test Requirements Specification for Space Equipment" (Ref. 1), with the requirements for space vehicle components as per MIL-STD-1540C "Test Requirements for Booster, Upper Stage and space Vehicles" (Ref. 2).

Where discrepancies exist, they are highlighted and both versions are indicated as necessary.

Fig. 2 presents a similar comparison for the acceptance tests.

Figs. 3 and 4 respectively compare the qualification and acceptance tests for space vehicles as they are defined in the ESA PSS-01-801 "System Test Requirements for ESA Spacecraft" (Ref. 3) and again MIL-STD-1540C (Ref. 2).

On the basis of the multinational programme tailoring experience the following major considerations have been originated in view of an eventual harmonization of the standards :

| TEST                        | CAT. OF EQT    |                |                |                |                 |                |                |             |             |                |                 |                | NOTE                                |
|-----------------------------|----------------|----------------|----------------|----------------|-----------------|----------------|----------------|-------------|-------------|----------------|-----------------|----------------|-------------------------------------|
|                             | EL. EQUIPMENT  | ANTENNAS       | BATTERIES      | VALVES         | FLUID/PROP. EQ. | PRESS. VESSELS | THRUSTERS      | THERMAL EQ. | OPTICAL EQ. | MECHANICAL EQ. | MECH. MOV. ASS. | SOLAR ARRAYS   |                                     |
| FUNCT. & PERF. <sup>1</sup> | R              | R              | R              | R              | R               | R              | R              | R           | -           | R              | R               | R              | 1 - BEFORE AND AFTER ENV. TESTS     |
| THERMAL VACUUM              | R              | R              | R              | R              | R               | R              | R              | R           | O           | R/-            | R/-             | R/-            |                                     |
| THERMAL CYCLING             | R              | O              | R/O            | O              | O               | -              | O/-            | R           | O           | O              | R/O             | O              | 2 - ACOUSTIC OR VIBRATION           |
| VIBRATION                   | R              | R <sup>2</sup> | R              | R              | R               | R              | R              | R           | R           | R              | R               | R              |                                     |
| ACOUSTIC                    | -/O            | R <sup>2</sup> | -              | O              | -               | -              | -              | -           | O           | -              | O               | R              | 3 - ON SEALED PRESSURIZED EQUIPMENT |
| SHOCK                       | R              | O              | O              | O              | O               | O              | O              | O           | -           | -/O            | O               | O              |                                     |
| ACCELERATION                | R              | O              | O              | O/-            | -               | O              | -              | O           | -           | -/O            | O               | O              | 4 - IN-ORBIT ACTIVE EQUIPMENT       |
| HUMIDITY                    | O              | O              | O              | O              | O               | O              | O              | O           | O           | O              | O               | O              |                                     |
| PRESSURE                    | R <sup>3</sup> | -              | R <sup>3</sup> | R              | R               | R              | R              | -           | -           | -/R            | R               | R              | 3 - ON SEALED PRESSURIZED EQUIPMENT |
| LEAK                        | R <sup>3</sup> | -              | R <sup>3</sup> | R              | R               | R              | O              | O           | -           | -/R            | R               | R              |                                     |
| EMC/ESD                     | R              | O              | -              | R/-            | O/-             | -              | O/-            | -           | -           | -/O            | R               | R              | 4 - IN-ORBIT ACTIVE EQUIPMENT       |
| LIFE                        | O              | O              | O              | O              | O               | O/R            | O/R            | O           | O           | O              | O               | O              |                                     |
| MICROGRAVITY                | R <sup>4</sup> | -              | -              | R <sup>4</sup> | O/-             | -              | R <sup>4</sup> | -           | -           | -              | R <sup>4</sup>  | R <sup>4</sup> | 4 - IN-ORBIT ACTIVE EQUIPMENT       |
| BURN-IN                     | R              | O              | R              | R/-            | -               | -              | O              | -           | O           | -              | -               | -              |                                     |
| AUD. NOISE                  | O              | -              | -              | O              | O               | -              | O              | -           | O           | O              | O               | O              | 4 - IN-ORBIT ACTIVE EQUIPMENT       |
|                             | O              | -              | -              | O              | O               | -              | O              | -           | O           | O              | O               | O              |                                     |

R = REQUIRED    O = OPTIONAL    - = NO REQUIREMENT    ESA/MIL STD    ■ DISCREPANCIES

Fig. 1 - Equipment Qualification Test Requirements

• **Equipment Qualification (Fig. 1)**

- \* Solar Arrays should be clearly isolated as a category of equipment in line with the US approach
- \* Thermal vacuum should be "required" for Mechanical Moving Assemblies to cover tribology problems as per the European approach
- \* Thermal cycling should be "required" in line with European practice also for Batteries and Mechanical Moving Assemblies
- \* Shock and acceleration are strongly dependent on the mission and location inside the spacecraft and should be candidates for tailoring, then considered "optional" for all equipment
- \* Pressure and leak should be "required" for Mechanical Moving Assemblies as per MIL-STD if they contain sealed or pressurized equipment (note 2)
- \* EMC test should be "required" for valves as reflected in the European standard due to their electronic circuit
- \* Life test should be "required" as per US practice for pressure vessels and thrusters
- \* Microgravity test should be included as per European practice because it is mandatory for most of the scientific satellites and manned systems
- \* Burn-in test should not be included as per US practice, because performed at component level or combined with thermal cycling
- \* Audible noise test should be added in line with the European standard as "optional" for the equipment mounted inside manned systems.

• **Equipment Acceptance (Fig. 2)**

- \* Solar Arrays should be clearly isolated as a category of equipment in line with the US approach

| TEST                        | CAT. OF EQT    |                |                |        |                 |                |           |             |             |                |                 |              | NOTE                                |
|-----------------------------|----------------|----------------|----------------|--------|-----------------|----------------|-----------|-------------|-------------|----------------|-----------------|--------------|-------------------------------------|
|                             | EL. EQUIPMENT  | ANTENNAS       | BATTERIES      | VALVES | FLUID/PROP. EQ. | PRESS. VESSELS | THRUSTERS | THERMAL EQ. | OPTICAL EQ. | MECHANICAL EQ. | MECH. MOV. ASS. | SOLAR ARRAYS |                                     |
| FUNCT. & PERF. <sup>1</sup> | R              | R              | R              | R      | R               | R              | R         | R           | -           | R              | R               | R            | 1 - BEFORE AND AFTER ENV. TESTS     |
| THERMAL VACUUM              | R <sup>2</sup> | O              | R              | R      | R               | O              | R         | R           | O           | R              | R               | R            |                                     |
| THERMAL CYCLING             | R              | O              | O              | O      | O               | O/-            | O/-       | R           | O           | O              | O               | O            | 2 - ON HIGH POWER AND RF EQ.        |
| VIBRATION                   | R              | R <sup>3</sup> | O              | R      | O               | R              | R         | R           | R           | R              | R               | R            |                                     |
| ACOUSTIC                    | O              | R <sup>3</sup> | -              | -      | -               | -              | -         | -           | O           | -              | O/-             | O/-          | 3 - ACOUSTIC OR VIBRATION           |
| SHOCK                       | O/R            | -              | -              | -      | -               | -              | -         | O           | -           | -              | -               | -            |                                     |
| PRESSURE                    | -              | -              | R <sup>4</sup> | R      | R               | R              | O         | -           | -           | -              | -/O             | -            | 4 - ON SEALED PRESSURIZED EQUIPMENT |
| LEAK                        | R <sup>4</sup> | -              | R <sup>4</sup> | R      | R               | R              | O         | -           | -           | -              | -/R             | -            |                                     |
| BURN-IN                     | R              | -              | -              | O      | -               | O              | -         | -           | -           | -              | -               | -            | 4 - ON SEALED PRESSURIZED EQUIPMENT |
| WEAR-IN                     | -              | -              | -              | R      | -               | -              | R         | -           | -           | -              | R               | -            |                                     |
| MICROGRAVITY                | O              | -              | -              | O      | -               | O              | -         | -           | -           | -              | -               | -            | 4 - ON SEALED PRESSURIZED EQUIPMENT |
| AUD. NOISE                  | O              | -              | -              | O      | O               | O              | -         | -           | O           | O              | -               | -            |                                     |

R = REQUIRED    O = OPTIONAL    - = NO REQUIREMENT    ESA/MIL STD    ■ DISCREPANCIES

Fig. 2 - Equipment Acceptance Test Requirements

| TEST                        | SPACE VEHICLE  | NOTE                                    |
|-----------------------------|----------------|---|
| FUNCT. & PERF. <sup>1</sup> | R              | 1- INT. SYSTEM TEST & ISC               |
| EMC                         | R              |   |
| PYROSHOCK                   | -/R            | 2 - ACOUSTIC AND/OR VIBRATION           |
| ACOUSTIC                    | R <sup>2</sup> |   |
| VIBRATION                   | R              |   |
| PRESS./LEAKAGE              | R              | 3 - MAY BE COMBINED WITH THERMAL VACUUM |
| THERMAL CYCLE               | -/O            |   |
| THERMAL BALANCE             | R <sup>3</sup> |   |
| THERMAL VACUUM              | R              | 4 - COULD BE PART OF S/S QUAL.          |
| MODAL SURVEY                | R <sup>4</sup> |   |
| STATIC LOAD                 | R <sup>5</sup> | 5 - IF APPLICABLE                       |
| SPIN & DEPLOY.              | R <sup>6</sup> |   |
| PHYSICAL PROP.              | R <sup>7</sup> |   |
| ALIGNMENT                   | R <sup>8</sup> |   |
| MAGNETIC FIELD              | R <sup>9</sup> |   |

R = REQUIRED    O = OPTIONAL    - = NO REQ.    ESA/MIL-STD

Fig. 3 - Vehicle Qualification Test Requirements

- \* Shock should be candidate for tailoring (see above for qualification), so considered "optional" also for electronic equipment in line with the European approach
- \* Leak should be required for Mechanical Moving Assemblies as per MIL-STD if they contain sealed or pressurized equipment (note 3)
- \* Burn-in and Wear-in should not be indicated separately but should be combined with other tests like thermal cycling or functional and performance and in particular burn-in could be also carried out at component level
- \* Microgravity and Audible noise tests should be added in line with the European standard as "optional" (see above for qualification).
- **Vehicle Qualification (Fig. 3)**
  - \* Pyroshock test should be "required" as per the US standard at least to verify the separation with the launcher and activation of mechanisms

| TEST                        | SPACE VEHICLE  | NOTE                          |
|-----------------------------|----------------|-------------------------------|
| FUNCT. & PERF. <sup>1</sup> | R              | 1- INT. SYSTEM TEST & ISC     |
| EMC                         | O              |                               |
| PYROSHOCK                   | -/O            | 2 - ACOUSTIC AND/OR VIBRATION |
| ACOUSTIC                    | R <sup>2</sup> |                               |
| VIBRATION                   | R              |                               |
| PRESS./LEAKAGE              | R              |                               |
| THERMAL CYCLE               | -/O            |                               |
| THERMAL VACUUM              | R              | 3- IF APPLICABLE              |
| SPIN & DEPLOY.              | R <sup>3</sup> |                               |
| MASS PROPERTIES             | R              |                               |
| ALIGNMENT                   | R <sup>3</sup> |                               |
| MAGNETIC FIELD              | R <sup>3</sup> |                               |

R = REQUIRED    O = OPTIONAL    - = NO REQ.    ESA/MIL-STD

Fig. 4 - Vehicle Acceptance Test Requirements

- \* Thermal cycle should be indicated as "optional" considering the case of presence of thermal cycling acceptance test for screening purposes
- \* Physical properties and other specific tests included as "required" in line with the European standard.

#### • Vehicle Acceptance (Fig. 4)

- \* Pyroshock test should be indicated as "optional" in line with US practice taking into account the above considerations for qualification
- \* Thermal cycle could be considered "optional" for workmanship purposes.

#### 4. THERMAL CYCLING

Considering in detail the test requirements for equipment and system thermal cycling, the tendency in Europe with respect to the US is to be less severe in terms of number of cycles and to be dependent on the temperature range experienced during the mission. Actually this last is the prevalent industrial position much more than ESA's.

Normally at equipment level, 4 cycles in acceptance and 8 in qualification are required with the profile as shown in Fig. 5 (see following page - source Ref. 1).

The Delta T is derived from the flight predicted temperature with a margin of  $\pm 10^\circ\text{C}$  for qualification and  $\pm 5^\circ\text{C}$  for acceptance.

This proposal is based on statical investigation of European and American space programmes and on results of screening techniques on commercial electronic components.

It seems that the majority of workmanship defects at component level are discovered after a few cycles in acceptance (typically two), hence four cycles represents a margin to take into account the incidence of different Delta T's; finally eight cycles in qualification are a consequence of the above with proper qualification margins.

The US approach for equipment thermal cycling as reflected for instance in Ref. 2 (13 cycles in acceptance and 94 in qualification) but also in Ref. 4 (8 cycles in acceptance and 24 in qualification) is more severe and is based on a statistical basis which probably includes some programmes with higher reliability requirements.

The differences are so high and also the associated costs and risks are so significant that a dedicated harmonization effort seems unavoidable.

#### 5. VIBRO-ACOUSTIC EXCITATION

For the Vibro-acoustic excitations (i.e. shock, acoustic, sine/random vibrations), comparing again ESA standards of Refs. 1 and 3 with the US standard of Ref. 2 significant differences exist. In particular the qualification margins (with respect to the flight levels) and durations, the acceptance levels and durations, and the test tolerances are quite different.

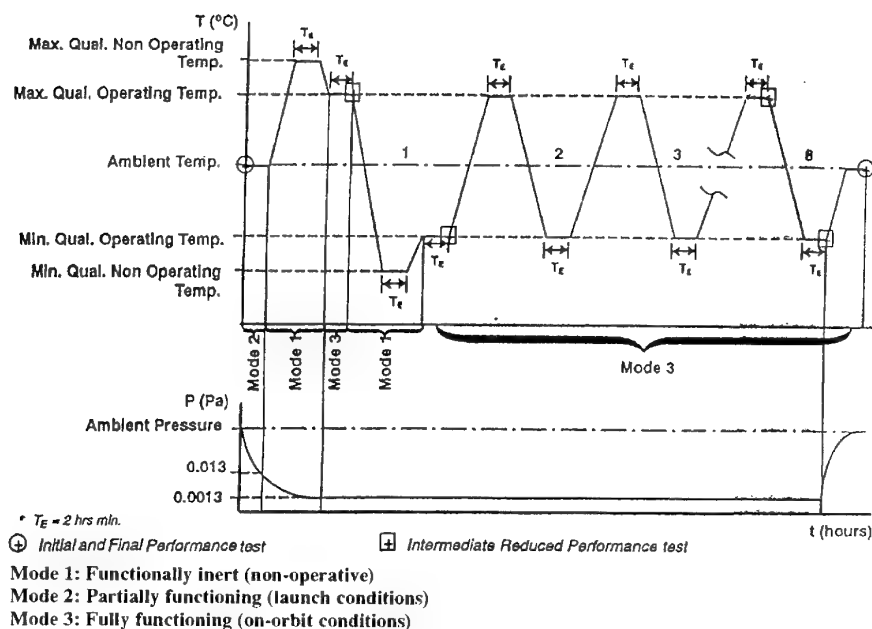


Fig. 5 - Equipment Thermal Cycling Profile In Europe

Fig. 6 shows the comparison for equipment and vehicle qualification, Fig. 7 shows the compared situation for acceptance and Fig. 8 for test tolerances.

On the basis of the multinational programme tailoring experience, the following major considerations have been originated in view of an eventual harmonization of the standard:

- \* a qualification margin of 3dB seems sufficiently justified for shock, acoustic and vibration testing
- \* acoustic durations of 2 min. in qualification and 1 min. acceptance seem adequate at both equipment and vehicle level (duration is obviously dependent on the number of missions)
- \* random durations of 2 min x axis in qualification and 1 min. x axis in acceptance seem adequate at both equipment and vehicle level
- \* sine duration of 2 oct/min for equipment qualification (1 sweep up and down) and for vehicle qualification (1 sweep only) are suggestable
- \*  $\pm 6\text{dB}$  for shock tolerances seem adequate in line with the European approach, the same seems suggestable for acoustic tolerances (i.e.  $\pm 3\text{dB}$  and  $\pm 1.5\text{dB}$  overall)
- \* the random vibration frequency tolerances of  $\pm 2\%$  as per the US standard seem more suitable
- \* the suggested tolerances for random Power Spectral Density are : from 20 to 500 Hz (25 Hz or narrower)  $\pm 3\text{dB}$ , fro 500 to 2000 Hz (50 Hz or narrower)  $\pm 3\text{dB}$ , overall grms  $\pm 1.5\text{dB}$

| TEST      | QUALIFICATION MARGIN   | DURATION  |
|-----------|--|---|
| SHOCK     | + 6dB (MIL 1540C)  | <i>Equipment:</i><br>3 shocks in both directions of 3 axes (MIL 1540C) (PSS 802)<br><i>Vehicle:</i><br>3 activations of ordnance (MIL 1540C)  |
| ACOUSTIC  | + 6dB (MIL 1540C) (PSS 802)<br>+ 3dB (PSS 801)   | <i>Equipment:</i><br>2 min (PSS 802)<br>3 min (MIL 1540C)<br><i>Vehicle:</i><br>2 min (MIL 1540C)   |
| VIBRATION | Sine and Random:<br>+ 6dB (MIL 1540C)<br>Std. spectra (PSS 802)<br>Random:<br>+ 3 dB (PSS 801) | <i>Equipment:</i><br>Random:<br>3 min x axis (MIL 1540C) (PSS 802)<br>2.5 min x axis (PSS 802)<br>Sine:<br>fatigue equivalent duration in flight of 15 s (MIL 1540C)<br>2 oct/min 1 sweep up and down (PSS 802)<br><i>Vehicle:</i><br>Random:<br>2 min x axis (MIL 1540C)<br>Sine:<br>2 oct/min (PSS 801) |

Fig. 6 - Comparison of Qualification Margins and Durations

| TEST             | ACCEPTANCE LEVEL  | DURATION  |
|------------------|---|---|
| <b>SHOCK</b>     | Maximum expected shock spectrum (MIL 1540C)   | <i>Equipment:</i><br>1 shocks in both directions of 3 axes (MIL 1540C)<br>1 shocks in both directions of 3 axes + random vibration (PSS 802)<br><i>Vehicle:</i><br>1 activation of ordnance (MIL 1540C) |
| <b>ACOUSTIC</b>  | Envelope of maximum expected acoustic spectrum (MIL 1540C)  | <i>Equipment:</i><br>1 min (PSS 802) (MIL 1540C)<br><i>Vehicle:</i><br>1 min (MIL 1540C) (PSS 801)  |
| <b>VIBRATION</b> | <i>Random:</i><br>Envelope of maximum expected spectrum and minimum spectrum (MIL 1540C)<br><i>Sine:</i><br>Maximum expected sine vibration environment (MIL 1540C)<br><i>Random (Equip.):</i><br>Std Acceptance Vibration Test (AVT) (PSS 802) | <i>Equipment:</i><br><i>Random:</i><br>1 min x axis (MIL 1540C)<br>2 min x axis (PSS 802)<br><i>Sine:</i><br>1 min x axis (MIL 1540C)<br><i>Vehicle:</i><br>Random and Sine: 1 min x axis (MIL 1540C)   |

Fig. 7 - Comparison of Acceptance Levels and Durations

## 6. QUALIFICATION TEST ARTICLE STANDARD

Theoretically, the qualification test philosophy requires a test article flight standard in order to fulfil the main qualification objective: demonstrate that the flight design satisfies the imposed requirements in environmental conditions more severe than the expected one.

Pratically deviations are accepted when they do not impact the success of the qualification campaign, typically the presence of simulators, instrumentation and test set-up adaptations.

The Alenia Spazio experience in the mentioned international joint ventures confirms the possibility to exploit successfully the use of Engineering Qualification Models as qualification test article.

These models are representative of the Flight Model to the necessary extent for the qualification purposes in form-fit-function but containing lower quality MIL Grade components instead of the flight standard HI-REL.

The components are procured from the same manufacturer, are built with the same design, materials and processes as the flight ones but with a less severe screening hence having reduced procurement time and cost.

| TEST  | DURATION   |
|---|--|
| <b>SHOCK</b><br>AMPLITUDE (Q = 10)<br>1/6 - OCTAVE BAND<br>CENTER FREQUENCY | $\pm 6$ dB with 30% of the spectrum values greater than the nominal test specification (PSS 802)<br>below 5000 Hz + 6dB/-3dB<br>above 5000 Hz + 9dB/-6dB<br>with 50% of the spectrum values greater than the nominal test specification (MIL 1540C)            |
| <b>DURATION</b>   | $\leq 20$ ms $\pm 1$ ms<br>> 20 ms $\pm 5\%$ (PSS 802)   |
| <b>ACOUSTIC</b><br>AMPLITUDE<br>1/3 - OCTAVE BAND<br>CENTER FREQUENCY       | $\pm 3$ dB overall $\pm 1.5$ dB (PSS 802)<br>31.5 to 40 Hz $\pm 5$ dB<br>50 to 2500 Hz $\pm 3$ dB<br>2500 to 10000 Hz + 3dB/-4dB<br>overall $\pm 1.5$ dB (MIL 1540C)   |
| <b>VIBRATION</b><br>FREQUENCY   | Random $\pm 2\%$ or 1 Hz which ever is greater<br>Sinus $\pm 5\%$ 10 Hz to 2000 Hz (PSS 802)<br>$\pm 2\%$ (MIL 1540C)  |
| <b>SINUSOIDAL AMPLITUDE</b>   | $\pm 10\%$ (MIL 1540C) (PSS 802)   |
| <b>RANDOM POWER SPECTRAL DENSITY</b>  | 20 to 500 Hz (25Hz or narrower) $\pm 3$ dB<br>500 to 2000 Hz (50Hz or narrower) $\pm 3$ dB<br>overall grms $\pm 10\%$ (PSS 802)<br><br>20 to 100 Hz (5Hz or narrower) $\pm 1.5$ dB<br>100 to 500 Hz (25Hz or narrower) $\pm 1.5$ dB<br>overall grms $\pm 1$ dB |

Fig. 8 - Comparison of Test Tolerances

The successfull development campaign and flight performances of projects using the above described approach, confirmed that the risks to have possible testing failures and non-conservative test behaviour are acceptable in front of the cost and schedule advantages.

In the light of the above considerations, it is Alenia Spazio's opinion that the relaxation of the quality standard requirement for qualification testing has to be investigated carefully.

## 7. CONCLUSIONS

Experiences from the participation in multinational space programmes demonstrated the need to tailor the applicable test requirements belonging to the different international standards.

Significant differences have been encountered and examples have been presented in this paper, together with the associated proposals of compromise, in areas like: qualification / acceptance test philosophies, thermal cycling, vibro-acoustic excitation and qualification test article quality standard.

In view of the future evolution of space activities towards international joint ventures (see for example the recent collaborations with the Russian organizations), and considering the need to optimize the effectiveness of space programmes in terms of cost and schedule, it seems opportune to start an international working group with the objective to harmonize the existing space testing standard.

## 8. REFERENCES

1. ESA PSS-01-802 - *Test Requirements Specification for Space Equipment*, draft 1 - September 1993
2. MIL-STD-1540C - *Test Requirements for Booster, upper stage and Space Vehicles*, draft - January 1993
3. ESA PSS-01-801 - *System Test Requirements for ESA Spacecraft*, draft 2 - September 1991
4. NASA SSP 41172 - *International Space Station ALPHA Qualification and Acceptance Environmental Test Requirements*, January 1994.

## AEROSPATIALE SATELLITES (CANNES SITE) INTEGRATION AND TEST CENTER

Macario Richard  
Mr Jean-François Coroller  
RF Department Manager  
Aerospatiale Espace et Défense  
Établissement de Cannes  
100 Blvd du Midi BP N099  
06322 Cannes la Bocca Cedex, France

### RESUME

Since October 1993, AEROSPATIALE uses the following extended integration and test facilities:

- a new large integration room
- a new space simulation chamber
- a RF simulation chamber (compact range type)

The aim of this presentation is to point out the technical characteristics of these new facilities and the advantages of the whole integration and test room center.

### SUMMARY CONCERNING THE MAIN TESTS NEEDED DURING SPACECRAFT INTEGRATION

A classic spacecraft integration sequence takes into account the following tests:

- Sine vibration test to simulate the vibrations induced on the spacecraft by the launcher
- Acoustic vibration test to simulate the acoustic constraints induced by the launcher
- Thermal vacuum test to test the working of equipments and mechanisms in space conditions
- Mass, centring and inertia measurements (MCI)
- Radiofrequency test on telecommunication satellites.

### CAPABILITY OF THE AEROSPATIALE TEST CENTER

- To integrate seven spacecrafts simultaneously
  - To integrate and test all spacecrafts compatible with AR4 and half AR5
  - To carry out all the environmental tests on CANNES site (except solar simulation)
  - To carry out the whole integration and test sequences without clean environmental breakdown
- The advantages to have all the facilities together and located in the same integration room are obviously:
1. a reduction of the risk on the spacecraft due to the fact that we have no packing and unpacking operation during all the integration sequence (it concerns mainly handling and contamination risks).
  2. a reduction of the time duration of the whole integration sequence for the same reasons as above.
  3. consequently a reduction of the cost.

### MAIN FEATURES OF THE INTEGRATION ROOM

#### General characteristics:

- Global surface: 2000 m<sup>2</sup>  
If necessary we have the capability to recover the area of the compact range room (about 300 m<sup>2</sup>) to do integration sequences
- Cleanliness class: 100 000. The parameters control and monitoring is centralised
- Accessibility to all the test facilities in cleanliness conditions
- Visitor gallery
- Travelling cranes in each integration room:
  - Maximal load : 7 tons
  - Height under hook : 10,5 m

### Facilities in this integration room:

- Shaker MB 220 type:
  - Max. force : 15000 DAN
  - Range frequency : (5Hz : 2000Hz)
- Acoustic chamber: Dimensions (6.3 x 5 x 8M)
  - Level maxi : 154 dB
  - Spectrum : 31.5 Hz ; 8000 Hz
- Inertia measurements SCHENK type
- Centring measurements SCHENK type
- Thermal vacuum chamber 70 M3:
  - Cylindrical horizontal axis
  - Dimensions: Ø 3,6 M ; L 4 M
- Thermal vacuum chamber 550 M3 (see details here after)
- Radio frequency simulation chamber (see details here after)
- Og deployment rail

### MAIN FEATURES OF THE SIMULATION SPACE CHAMBER

- Horizontal axis cylindrical chamber
- Vertical opening door stored above the chamber in opened position
- Available diameter: 7,5m. Available length: 8m
- Levelling device to control spacecraft horizontality during the test

#### ◆ Cold shroud:

The cold temperature is made by cold shrouds filled with boiling liquid nitrogen. The shroud is made of 8 individual zones. The shroud material is stainless steel. It is important to notice that with this concept we have only one cold temperature. It is ≤ 95 K with a thermal load of 105 KW

#### ◆ Heating device:

Performed by infrared lamps or rods (calrod type). Possibility to control up to 36 zones by using AC power supplies with a nominal power of 5 KW each and a maximal power of 7.5 KW each.

In addition the system has a set of DC power supplies including:

- 80 Gulton regulators with a maximal power of 150 W each.
- 33 power supplies 60 V, 9 Amps.

#### ◆ Vacuum:

- ≤ 10-6 mb with a leak of 0,15 mb.l/s inside the test volume.

#### ◆ Pumping device:

The breakdown of pumping device is:

- Two rough pumping channels with a speed of: 1250 + 5000 m<sup>3</sup>/hour
- Two turbomolecular pumps with a speed of 5000 l/s for the first one, and 2000 l/s for the other one
- Two Dynavac cryogenic pumps insulated by 2 Vat cryogenics valves. The speed of each pump is 50000 l/s.
- One 4,2 K static cryopump inside the test volume. The speed is about 100000 l/s and the autonomy between each He filling is 40 hours
- One nitrogen liquid cryopanel.



The maximal pumping speed measured in the test volume is 140000 l/s.

#### ◆ Control station:

The whole installation is monitored with 3 supervisors. Two HP 9000 (700 serial) computer stations control and monitor the whole parameters of each subsystem.

The system is fully redundant in case of failure of the computer or the network. If a PLC failure occurs, we can still monitor the parameters with the manual bay.

The system controls:

- Pumping device
- Cold shroud device (valves opening, shrouds temperatures)
- AC electric power supplies device
- DC electric power supplies device
- Nitrogen station (tank level, tank pressure...)
- Electric power delivery
- Water delivery (pressure, temp, flow rate...)
- Control gaz delivery (air, GN2...)
- Levelling device
- Computer and network system parameters.

In addition the leading procedure of the chamber is set in the computer to guide and to help the operators.

#### ◆ Data acquisition system:

The system is capable to acquire 2000 channels including 1500 thermocouples.

The scanning frequency can be rated from one scan per minute to sixty minutes with the full capacity. In addition the system is capable to scan simultaneously the 1500 thermocouples per minute and 40 thermocouples each 5 seconds to plot graphs in "real time".

The telemetry datas coming from the spacecraft can be collected on the DAS.

A specific processing software (Dynaworks) is used to sort the data.

### RADIOFREQUENCY SIMULATION CHAMBER

#### ◆ Test capabilities:

- EMC
- Antenna performance
- Telecommunication system performance

#### ◆ Shielding:

- Magnetic fields > 70 dB / 10 KHz - 10 GHz
- Electric fields > 70 dB / 1 KHz - 10 GHz  
> 100 dB / 1 MHz - 1 GHz

#### ◆ Reflectivity:

- < -35 dB above 1 GHz
- < -50 dB above 3 GHz
- (HYFRAL absorbers)

#### ◆ Compact range performance:

- Centre Quiet zone: 5,5(m) x 5(H) x 6(L)
- Scanned quiet zones (-4°/+7°): 3,5 x 3,5 x 6 (m)
- Plane wave deviations (max): +0,3 dB/+5°
- Gain accuracy  $\pm 0,25$  dB
- Sidelobe accuracy:  $\pm 1$  dB at -30 dB
- Cross polarization accuracy:  $\pm 2$  dB at -40 dB
- Frequency ranges:
  - 1.2 - 200 GHz (nominal performance)
- The positioner is installed on an air cushion dolly providing XY positioning at floor level
- The compact range is a DASA CCR model
- The Data acquisition system is based upon
- Scientific Atlanta 2095E with AZ/EL/AZ positioner (load up to 7T)
- Data treatment is done on separate sun computer.

#### ◆ Operations:

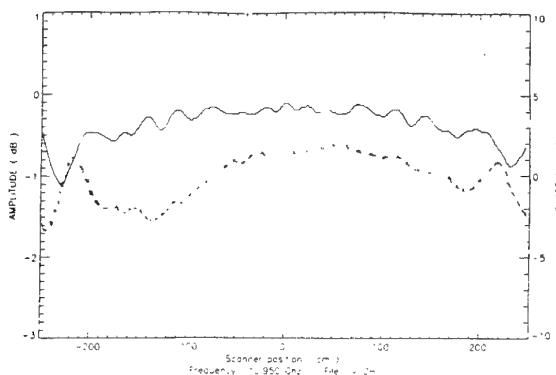
The compact range has demonstrated its full operational capabilities in C-band and Ku-band during INTELSAT 7 FM4 and FM5 testing.

For antennas (44 patterns measured à 8 frequencies) the test duration was 7 days (3 shifts).

The Payload end-to-end test duration (EIRP, G/T, Frequency Response, PIMP, spurious) was 15 days (3 shifts).

#### ◆ Compact Range Validation

The Compact Range has been aligned (feed position) using a large XY scanner (5 x 5 m with 0.15 mm planarity). A sample of reached plane wave quality is shown hereafter:



The final validation has been done by comparisons with Far Field test ranges measurements done at SS/LORAL and CNET La Turbie. The reference antennas were medium gain antennas (20/25 dBi) and high gain antennas (30/45 dBi), in both C-band and K4-band.

Test comparisons showed the following accuracies:

- Reproducibilities : < 0.1 dB (EOC)  
(over 8m width) < 0.5 dB (-30 dB levels)
- Gain :  $\pm 0.2$  dB
- Sidelobes (-30 dB) :  $\pm 1$  dB
- Xpol (-35 dB) :  $\pm 1$  dB
- Beam pointing :  $\pm 0.01^\circ$

By using the advanced Antenna pattern comparison software (developed by MARCH Microwave in Cooperation with AEROSPATIALE, and presented in AMTA 94 conference) the sidelobe/Xpol accuracies were found better than:

- 0.5 dB at -40 dB level.

#### ◆ Compact Range Description

##### 1. Compact range description

The CATR is a Compensated Compact Range model installed in a 36 m \* 12.5 m \* 12.5 m (L \* W \* H) shielded chamber room coated with absorbers.

This CATR consists of a two double curved reflector cross polar compensated system.

The spherical wave coming from the source produces through the compact range illuminator a local plane wave in a quiet zone surrounding the antenna under test.

The CATR is used in two different configurations:

- axial center quiet zone where the source is located in the focus point
- scanned quiet zone by excentering the source outside the focus.

The first configuration is generally preferred for antenna testing where optimized performances in term pointing accuracy are required.

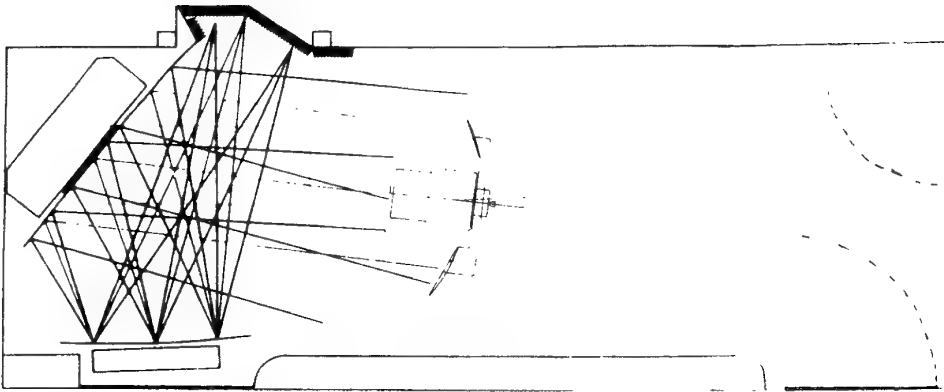
The second configuration is used for payload testing without moving the satellite laterally. Independent quiet zone are then generated around the respective satellite antenna.

These configurations allow to perform at system level antenna and payload testing of satellites up to 8 m width.

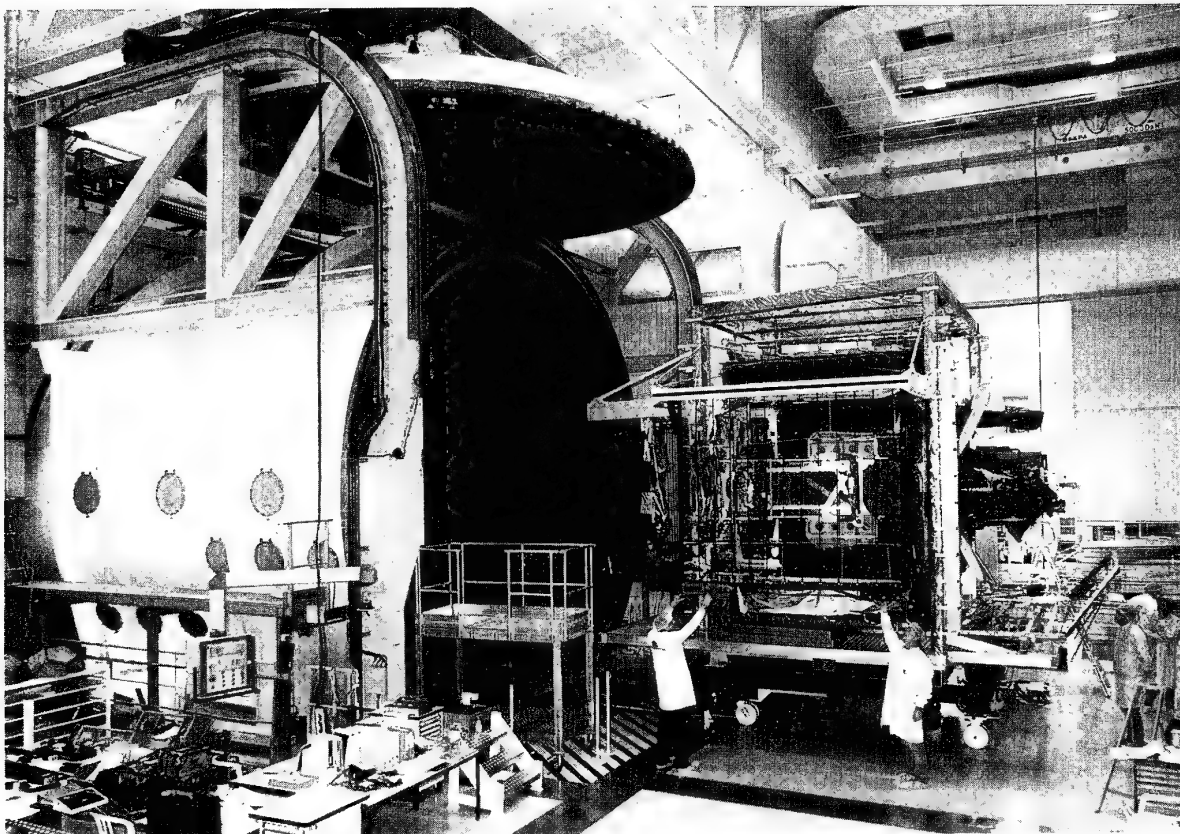
The CATR is associated to a three axis positioning system mounted on a air cushion dolly moving along a bar to locate the antenna in the test quiet zone.

For antenna testing, the acquisition system allows to perform simultaneously by switching up to four patterns measurements in two orthogonal polarizations for more than ten frequencies.

The CATR overall configuration is presented in figure hereafter.



The photograph below shows INTELSAT-7 FM4 under testing.



# EXPERIENCE ACQUISE PAR L'AEROSPATIALE DANS LE DOMAINE DE L'INTEGRATION DE CHARGES UTILES OPTIQUES HAUTE RESOLUTION.

J.MENDEZ & J.M.LEBLANC

AEROSPATIALE Espace et Défense - Etablissement de Cannes.  
100 Bld du midi - BP N099 - 06322 CANNES LA BOCCA CEDEX

## 0. MOTS CLES:

AEROSPATIALE / OPTIQUE / INTEGRATION /  
CONTROLE / ESSAIS / MOYENS.

## 1. INTRODUCTION:

Le sujet proposé concerne l'expérience acquise par l'AEROSPATIALE établissement de Cannes dans le domaine de l'intégration de charges utiles optiques.

Dans le cadre des activités relatives à l'observation spatiale, des investissements importants ont été réalisés à Cannes dans le but de pouvoir intégrer des instruments d'optique de très hautes performances.

L'objet de la communication proposée dans le cadre du symposium AGARD 1994 est de présenter les innovations qui ont été nécessaires pour assurer l'intégration et le contrôle des performances d'une charge utile haute résolution, tant au niveau des méthodes que des installations d'essais et des moyens sol développés spécifiquement. Nous ne traiterons pas des caractéristiques intrinsèques de cet instrument d'optique ni de sa mission.

## 2. UN UNIVERS TECHNIQUE NOUVEAU:

Un univers technique nouveau s'est présenté aux spécialistes de l'intégration, avec des contraintes très différentes de celles rencontrées pour l'intégration de satellites de télécommunication par exemple. Deux facteurs majeurs sont à la base de ces différences:

- les exigences très sévères de l'instrument, dans un domaine technique où les contraintes liées à l'optique sont draconiennes, ont conduit à la mise au point de méthode de mesures très sophistiquées étant donné la classe de précision demandée. Cela a nécessité le développement de moyens sol jamais réalisés jusque là, en terme de performances et de précision : de l'ordre du  $\mu\text{m}$  en mécanique et de quelques nanomètres en optique.
- les contraintes d'environnement ont quant à elles conduit au développement de moyens d'essais spécifiques de très haute technicité. Les conditions d'ambiance qui ont peu d'effet pour l'intégration des satellites de télécommunication, ont une influence prépondérante sur les opérations de réglage et de contrôle d'un instrument optique de cette classe de performances.

Les exigences de propreté ont eu des conséquences très importantes sur la conception des moyens d'une part et sur les conditions opérationnelles pour les équipes en charges de l'AIT (Assemblage Intégration Tests) d'autre part.

Ce sont ces deux aspects qui sont développés dans les chapitres suivants.

## 3. UNE NOUVELLE APPROCHE DANS LES METHODES D'INTEGRATION ET DE CONTROLE:

Les séquences AIT de la charge utile optique comprennent:

- les opérations de construction de la charge utile:

*opérations d'assemblage:* principalement mécaniques qui consistent à monter des sous-ensembles.

*opérations d'intégration:* assemblages, réglages, suivis de contrôle ou de tests (optiques, électriques, mécaniques...) permettant de s'assurer que l'ensemble constitué est compatible avec les performances finales recherchées.

- les opérations de tests:

*contrôles des performances* de la charge utile une fois les opérations d'assemblage et d'intégration terminées. Une partie de ces contrôles sont réalisés avant et après les essais d'environnement (mécaniques, thermiques, électriques) subis par la charge utile et lors de l'acceptation finale avant livraison.

Dans le présent chapitre nous aborderons en détail la phase de réglage de la partie optique du télescope, qui est une étape fondamentale, et le contrôle de la performance FTM (Fonction de Transfert de Modulation).

### 3.1. Intégration du collecteur de flux:

Pour un instrument d'optique l'une des phases d'intégration les plus critiques est le réglage des optiques. En effet la constitution du collecteur de flux est une étape majeure dans l'obtention finale des performances optiques et en particulier de la FTM. L'intégration du collecteur de flux se décompose en deux phases:

- une phase de réglage des optiques jusqu'à l'obtention du critère de succès.
- une phase de blocage qui consiste à figer mécaniquement les positions des optiques dans la monture.

Le réglage a nécessité d'adapter la mesure de front d'onde par interférométrie, bien connue des opticiens, aux contraintes liées à l'environnement. En effet l'instrument a été réglé dans des conditions proches de l'environnement opérationnel c'est à dire orbital. Les ambiances associées extrêmement sévères ont nécessité :

- de réaliser cette opération dans le vide pour s'affranchir des perturbations de l'air.
- de maintenir une ambiance thermique très stable pour diminuer au maximum les effets thermoélastiques de la structure mécanique et maîtriser la configuration d'essai dans son ensemble.
- d'amener et de maintenir la monture optique à un taux de désorption proche du taux en orbite, pour s'affranchir des contraintes hygro-élastiques.
- de compenser l'effet de la gravité lors du réglage.
- de minimiser les problèmes de micro-vibrations lors des mesures.

La mise au point de la mesure interférométrique par autocollimation utilisée lors du réglage, a nécessité une approche totalement nouvelle par rapport à l'expérience acquise sur des mesures réalisées à l'air et à température ambiante. Le principe consiste à positionner au mieux les optiques à régler puis à affiner le réglage par acquisitions successives de mesures de la surface d'onde vis à vis de critères d'optimisation définis préalablement. La configuration d'essai correspondante impose d'avoir un pilotage des moyens d'essais optiques de l'extérieur de la chambre à vide. En effet l'opération de réglage se fait en totalité au vide et donc sans possibilité pour les opérateurs d'intervenir directement soit sur le spécimen (optiques à régler) soit sur les moyens d'essais installés dans la chambre.

La mise au point de ce banc interférométrique, nécessaire lors du réglage et de la mesure finale après blocage, a donc demandé de mener des investigations très pointues. La condition de réussite des mesures effectuées a été la maîtrise de la configuration d'essais dans son ensemble. C'est l'un des grands enseignements tirés de ce programme.

### 3.1.1 Réglage du collecteur de flux:

Les différents composants optiques de l'instrument sont réalisés par la société REOSC. Avant leur livraison, ils sont contrôlés au niveau élémentaire puis au niveau sous-ensemble par mesure interférométrique de la surface d'onde. La qualité du sous-ensemble optique constitué est supérieur à quelques nanomètres.

L'opération de réglage du collecteur de flux lors de la séquence d'intégration à l'AEROSPATIALE, consiste à venir intégrer le sous-ensemble optique dans la structure de l'instrument de façon à optimiser la qualité de la surface d'onde.

Le principe du réglage consiste à optimiser la position de d'un miroir dans la structure de l'instrument, les autres éléments optiques ayant été préalablement installés, avec

des précisions résultants des tolérances de fabrication. Si ces derniers s'accommodent de tolérances assez larges de l'ordre de 0,1 mm, il n'en est pas de même pour le miroir à régler dont la position par rapport au correcteur doit être réglée et bloquée avec une précision de quelques microns et secondes d'arc pour atteindre la qualité de surface d'onde requise. La surface d'onde (SO) est mesurée par interférométrie en mettant le collecteur de flux en autocollimation devant un miroir plan selon la configuration montrée sur la figure 1.

L'onde de mesure, issue de l'onde de référence de l'interféromètre, entre dans le collecteur de flux du côté du plan focal, traverse l'instrument, se réfléchit sur le miroir plan d'autocollimation, repasse dans l'instrument pour venir interférer avec l'onde de référence.

La figure de frange obtenue est fonction des différences de formes entre l'onde de référence et l'onde de mesure qui a été déformée par son double passage dans l'instrument et sa réflexion sur le miroir d'autocollimation. On obtient donc la relation suivante :

$$SO_{brute} = 2 SO_{Collect.} + SO_{MPA}$$

d'où

$$SO_{collect.} = (SO_{brute} - SO_{MPA}) / 2$$

La figure de frange est très sensible aux effets de vibrations engendrant des déplacements des éléments optiques entre eux. La différence de marche maximale admissible est de  $\lambda / 4$  pendant la durée d'une acquisition de durée 1 à 20 ms. Ceci correspond à une stabilité de moins de 0,1  $\mu m$  à répartir entre 9 surfaces réfléchissantes. En l'absence de précaution particulière de filtrages de micro vibrations sismiques ces niveaux sont dépassés. Aussi l'ensemble du banc optique est-il suspendu sur des ressorts installés à l'intérieur de la chambre à vide.

La surface d'onde obtenue est mathématiquement transformée en une combinaison de formes indépendantes et caractéristiques des défauts optiques classiques (base de ZERNIKE). Cette décomposition est ensuite traitée par un logiciel d'optimisation optique (code V) dans lequel on a préalablement inscrit la combinaison optique de l'instrument avec les formes réelles, mesurées des miroirs.

A partir des mesures faites en 5 points du champ, le logiciel calcule quels sont les déplacements à appliquer au miroir pour atteindre la meilleure surface d'onde.

Ces mouvements sont ensuite effectués, le miroir étant à ce stade non solidaire de la structure mais tenu par un support motorisé 5 axes. Les déplacements et les orientations sont exécutés avec des précisions de 1 micron et de 1 seconde d'arc.

Le processus mesures / mouvement est itératif, le critère d'arrêt étant une évolution moyenne prédite par code V inférieure à une valeur limite correspondant aux performances recherchées.

Lors du réglage final, toutes ces opérations se déroulent au vide car la non uniformité de l'indice de l'air modifie le chemin optique des rayons de mesure d'une amplitude incompatible avec les précisions requises.

Les éléments perturbateurs propres aux différences sol/vol doivent être maîtrisés et ce à un niveau compatible avec les performances recherchées. Ces dernières se traduisent en stabilités géométriques de l'ordre de quelques microns.

Les principaux perturbateurs liés aux différences d'environnement entre intégration et utilisation avec leur seuil de tolérance sont :

- taux hydrique de la structure.
- température ambiante stabilisée.
- gradient interne instrument.
- gravité : compensations mécaniques ponctuelles par ressorts et contrepoids.

### 3.1.2 Blocage du collecteur de flux:

Lorsque la position optimale du miroir à régler est atteinte sa position par rapport à la structure de l'instrument, au droit des futurs points de liaison miroir/structure, est enregistrée via des capteurs capacitifs d'une précision inférieure au micron.

Le blocage du miroir sur la structure est réalisé par injection de colle dans des éléments de liaisons périphériques. L'opération d'injection, qui est critique, est effectuée manuellement dans les conditions ambiantes, ce qui nécessite l'ouverture de la chambre à vide et engendre des perturbations thermo-élastiques non négligeables. C'est pourquoi au moment de l'injection et pendant la polymérisation de la colle, la position du miroir par rapport à la structure est contrôlée via les capteurs capacitifs et le support motorisé 5 axes de façon à reproduire après blocage la position du miroir enregistrée à la fin du réglage sous vide. Les tolérances allouées au blocage sont de l'ordre de quelques  $\mu\text{m}$  pour les translations et secondes d'arc pour les rotations. Après blocage, la surface d'onde doit être d'une part optimale et d'autre part représentative de la surface d'onde qui sera obtenue en orbite.

Le collecteur de flux ainsi obtenu, la "partie optique" de la charge utile est constituée, la position du plan focal est connue par rapport au référentiel de la structure.

### 3.2. Mesure de la FTM:

L'opération d'intégration suivante consiste à intégrer le sous ensemble de détection de la charge utile. Cette séquence n'est pas abordée dans ce document. Le présent chapitre traite uniquement de la méthode de contrôle de la FTM utilisée à la fois lors de l'intégration du sous-ensemble de détection et lors du contrôle final de la charge utile.

Le contrôle final des performances optiques et en particulier de la spécification de FTM a été effectué après tous les essais d'environnement, par mesures globales sur l'instrument complet. Cette séquence d'essai est très importante sur le plan de la validation de la charge utile car elle permet de garantir le respect des spécifications

avant livraison. La configuration d'essai correspondante (voir figure 2) se déroule dans la chambre à vide utilisée pour les mêmes raisons que celles évoquées lors du réglage du collecteur de flux.

Pour réaliser ce contrôle, la méthode retenue consiste à imager au foyer de la charge utile des mires crénaux placées au foyer d'un collimateur. Ce moyen sol optique a pour fonction de générer une image réglée à l'infini devant la charge utile. Les mires sont fixées sur la source et leur déplacement est piloté de l'extérieur de la chambre à vide. Au cours de la mesure, la mire défile pas à pas au foyer du collimateur, le signal détecté  $I$  étant enregistré sur quelques pixels voisins. Au cours de l'acquisition la mire est statique. La connaissance de  $I_{\text{max}}$  et  $I_{\text{min}}$  permet de déterminer la FTC (Fonction de Transfert de Contraste) par la relation:

$$\text{FTC} = (I_{\text{max}} - I_{\text{min}}) / (I_{\text{max}} + I_{\text{min}} - 2I_0)$$

où  $I_0$  est le signal d'obscurité.

La FTM est ensuite déterminée mathématiquement par la somme de plusieurs FTC par série de Fourier limitée aux premiers termes:

$$\text{FTM}(v) = \pi/4 ( \text{FTC}(v) +/ - \text{FTC}(3v)/3 +/ - \text{FTC}(5v)/5 +/ - \dots )$$

Le signe des harmoniques dépend du rapport entre la fréquence spatiale mesurée et la fréquence de coupure du détecteur.

La mise au point de ces mesures nécessite une mise en oeuvre complexe et contraignante:

**Complexe** car elle fait intervenir des moyens sol critiques tel que le collimateur équipé de la source. La caractérisation de ce moyen, dont les performances optiques sont meilleures que celles du télescope, nécessite à elle seule une configuration de mesure interférométrique quasiment aussi complexe que celle utilisée pour le contrôle optique du télescope effectué avant intégration de la détection.

**Contraignante** car elle impose aux moyens une fiabilité élevée. La disponibilité de ceux-ci doit être maximale lors de la séquence de mesure. En effet une défaillance majeure d'un des moyens nécessitant l'intervention dans la chambre à vide, remettrait en cause la séquence avec des impacts importants sur les délais et les coûts.

Le point important qui constitue l'innovation par rapport aux mesures optiques classiques est l'adaptation et la maîtrise de ces contrôles dans des conditions opérationnelles draconiennes, avec l'utilisation de moyens d'essais complexes.

## 4. DES MOYENS D'ESSAIS SPECIFIQUES DE TRES HAUTE TECHNICITE.

Sur le plan industriel, la maîtrise de l'environnement thermique, hydrique, micro vibratoire, a imposé la réalisation de moyens d'essais et de moyens sol de très haute technicité.

#### 4.1 Moyens d'essais.

Parmi les moyens d'essai les plus critiques figure la chambre à vide développée spécifiquement pour ce programme. Les principales caractéristiques de ce moyen d'essai sont:

$\Phi$  utile= 5 m  
 L'utile= 7m  
 Vide primaire et secondaire=  $10^{-5}$  mb

Elle fait partie d'un complexe d'essai de 700 m<sup>2</sup> et est situé dans un environnement classe 100, pour répondre aux exigences sévères de propreté. En effet pour éviter tous risques de pollution non admissible des optiques, les différentes opérations d'intégration ont été effectuées en classe 100.

Cette chambre permet d'effectuer les mesures optiques dans les environnements spécifiés. Equipée d'un banc optique, conçu pour filtrer les micro vibrations, elle est régulée en température à  $\pm 0,25^\circ\text{C}$  permet de réaliser les mesures optiques sous vide primaire, et secondaire. Le banc optique a un rôle important, notamment lors des mesures interférométriques au cours desquelles le critère de stabilité impose une différence de marche entre l'onde de référence et l'onde de mesure inférieure à  $\lambda/4$ . La conception du banc a nécessité une approche globale prenant en compte les moyens sol et la charge utile positionnés directement sur celui-ci, les besoins liés à la précision de mesure et les contraintes liés à l'environnement (excitations extérieures). Les caractéristiques dimensionnelles de ce banc ont augmenté la criticité du développement et sa mise au point.

Ce moyen est utilisable pour l'AIT des futures charges utiles optiques haute résolution. Il confère à l'AEROSPATIALE un complexe d'essai important et un savoir faire dans le développement et la maîtrise opérationnelle d'un tel moyen.

#### 4.1 Moyens sol.

Les contraintes liées aux ambiances lors de la mise en oeuvre, avec la nécessité d'essais au vide et le travail en classe 100, ont eu un impact considérable sur la spécification des moyens sol intervenant dans les configurations d'essais.

Parmi les moyens sol développés, les plus critiques sur le plan technique, développement et mise au point, ont été les Moyens Sol Optiques. Comme nous l'avons vu dans les chapitres précédents des Moyens Sol Optiques, d'une complexité parfois analogue à celle de l'instrument lui-même avec certaines performances supérieures, ont dû être développés pour l'intégration et le contrôle.

Les exigences optiques spécifiées ont conduit à réaliser des Moyens spécifiques, aucun moyen classique ne répondant au besoin.

A titre d'exemple la déformation admissible des surfaces optiques de ces Moyens Sol Optiques et leur stabilité dans le temps s'expriment en nanomètres, pour le Miroir Plan d'Autocollimation et le collimateur. L'exigence sur la connaissance de la surface d'onde est quand à elle supérieure, ce qui impose un plan de métrologie et de calibration très sophistiqué.

A ces exigences optiques très sévères s'ajoutent les contraintes mécaniques qui en découlent. En effet une optique seule n'existe pas sans structure porteuse. Mécaniquement la conception de ces moyens, et en particulier celle du collimateur, a été d'une difficulté technique majeure. Les exigences de stabilité en cours d'utilisation, la maîtrise mécanique en excentrement et en tilt ont été les problèmes les plus critiques à résoudre.

Ces moyens de contrôle optiques comme le miroir plan d'autocollimation et le collimateur, sont fixés sur des supports mécaniques dont la fonction est de les supporter et de les positionner en fonction de la zone du plan focal instrument qui est analysée. La résolution de ces supports, dont la masse est proche de la tonne, est de l'ordre de la seconde d'arc pour les rotations. Le dispositif de réglage du miroir a quand à lui des exigences de l'ordre du  $\mu\text{m}$  pour les translations et de la seconde d'arc pour l'orientation en tilt. La classe de précision de ces moyens est d'un ordre supérieur à ceux développés communément à l'AEROSPATIALE pour des moyens sol, et on peut dire que les limites technologiques ont quasiment été atteintes.

De plus lors des mesures sous vide ces moyens sont pilotés de l'extérieur de la chambre à vide, sans possibilité d'intervention en cas de panne, ce qui impose une fiabilité opérationnelle très élevée.

L'enseignement majeur qui peut être tiré de ce programme est la nécessité de développer ce type de moyen en ayant une approche globale de la configuration d'essai d'une part et une démarche analogue à celle d'un matériel de vol d'autre part.

#### 5. UNE NOUVELLE PHILOSOPHIE DU METIER D'INTEGRATEUR.

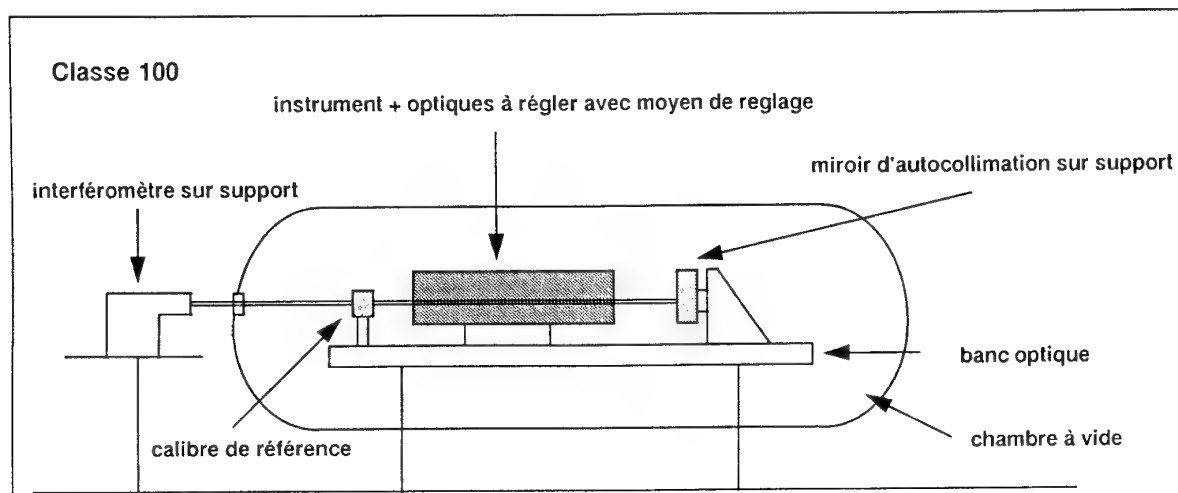
Il a été nécessaire d'adopter une nouvelle philosophie du métier d'intégrateur. Pour les séquences AIT critiques que nous avons évoquées dans les paragraphes précédents, la maîtrise de la configuration dans sa globalité est un élément essentiel pour l'obtention des performances de la charge utile optique. Il est indispensable d'avoir une "approche système AIT" dès les phases de conception de l'instrument en cohérence avec l'ingénierie et en prenant en compte les contraintes liées à l'environnement dans lequel est intégré et testé l'instrument. Ce point est capital car conditionne la réussite de l'opération d'intégration et l'obtention des performances (voir figure 3). L'objectif est de définir très tôt les méthodes qui seront utilisées, les bilans d'erreur associés, pour garantir la cohérence technique des différents moyens sol et maîtriser leurs développements.

Sur le plan humain, les méthodes de travail ont été régies par les contraintes de propreté très sévères et extrêmement difficiles à gérer car remettant en cause beaucoup d'acquis et demandant une organisation adaptée.

## 6. CONCLUSION:

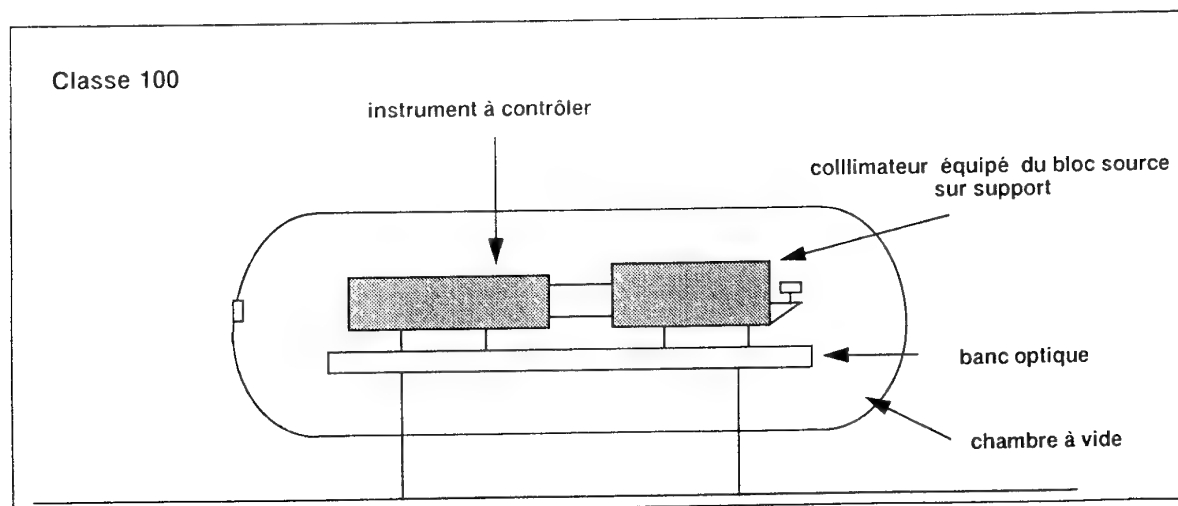
Une nouvelle approche du métier d'intégrateur, un investissement important dans des moyens d'essais de très haute technicité, une expérience technique et humaine d'une richesse exceptionnelle, un acquis de compétence dans un domaine de pointe, tels sont les enseignements que l'on peut tirer de tels du programmes.

Un atout indispensable pour se préparer et maîtriser l'intégration des charges utiles optiques du futur.



Nb : tous les moyens sont pilotés de l'extérieur de la chambre à vide

**Fig 1 - Configuration de réglage des optiques**



Nb : tous les moyens sont pilotés de l'extérieur de la chambre à vide

**Fig 2 - Configuration de controle**

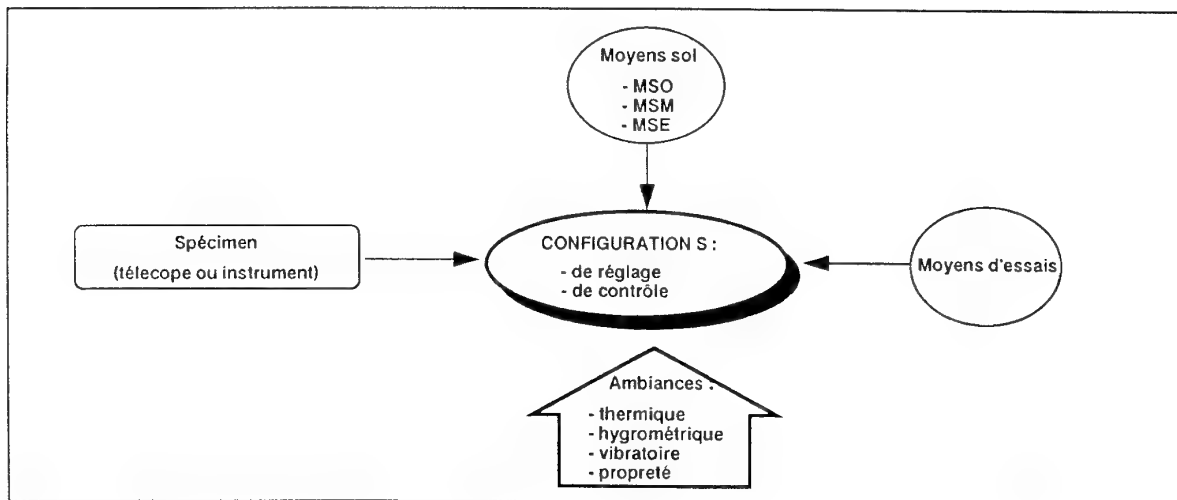


Fig 3 - Approche globale AIT



# SEPARATION OF LIFTING VEHICLES AT HYPERSONIC SPEED

## WIND TUNNEL TESTS AND FLIGHT DYNAMICS SIMULATION

G. SACHS\*  
W. SCHODER\*\*

*Technische Universität München  
Arcisstr. 21, 80290 Munich, Germany*

and

W. KRAUS\*\*\*

*Deutsche Aerospace AG  
81663 Munich, Germany*

### 1 Summary

Several topics of the separation maneuver of two-stage hypersonic vehicles are considered. Results will be presented which have been obtained from wind tunnel tests of the separation maneuver and related investigations on flight dynamics. In test facilities of DLR (Cologne), the aerodynamics characteristics of a two-stage space transportation system were investigated. The test campaign was focused on aerodynamic interference effects which exist when the two stages are in close proximity. The results of the wind tunnel tests provide a detailed data base for flight mechanics investigations. Numerical simulation of flight dynamics based on a well founded aerodynamics model is an appropriate technique to investigate such a highly dynamic maneuver. Control of both vehicles for achieving an optimal motion of the system is investigated. In addition, adequate stability and control characteristics from a piloting point of view are considered. Particular emphasis is put on a robust control technique. This is because robust control is an adequate means for dealing with a system which shows great changes. During close proximity of the first and orbital stages, system changes are due to the separation maneuver itself because of aerodynamic interference effects.

|                |   |
|----------------|---|
| $K_0$          | collision avoidance factor  |
| $K_{q,\alpha}$ | controller coefficients   |
| $n_z$          | load factor in z-axis direction   |
| $q$            | pitch rate  |
| $\alpha$       | angle of attack   |
| $\delta_T$     | thrust setting  |
| $\delta_e$     | pitch control deflection angle  |
| $\Delta$       | denoting separation variable,<br>e.g. $\Delta\epsilon$ relative pitch angle |
| $\omega_n$     | natural frequency   |
| $\zeta$        | damping coefficient   |

#### subscripts

|      |                                  |
|------|----------------------------------|
| 1    | first stage                      |
| 2    | orbital stage                    |
| rel  | at release moment                |
| rear | at the rear of the orbital stage |

### 2 Nomenclature

|       |                             |
|-------|-----------------------------|
| A     | coefficient matrix          |
| B     | matrix for control inputs   |
| $C_m$ | pitching moment coefficient |
| $C_D$ | drag coefficient            |
| $C_L$ | lift coefficient            |
| J     | performance criterion       |

\*Prof. Dr.-Ing. G. Sachs, Director,  
Institute of Flight Mechanics and Control.

\*\*Dipl.-Ing. W. Schoder, Research Assistant.

\*\*\*Dipl.-Ing. W. Kraus, Head Aerodynamics.

### 3 Introduction

A promising concept for future space transportation vehicles is a two-stage lifting system like the German Sänger, Refs. 1, 2. The two stages are equipped with wings. The first stage is propelled by an airbreathing propulsion system (turbo/ramjet combination) and the orbital stage uses rockets. The separation which takes place at hypersonic speed is an important flight maneuver posing new and challenging problems.

It is the purpose of this paper to present results of wind tunnel tests of the separation maneuver and related investigations on flight dynamics. Numerical simulation of flight dynamics based on a well founded aerodynamics model is an appropriate technique to investigate the highly dynamic separation maneuver. Particular emphasis is placed on aerodynamic interference effects which exist when the two stages are in close proximity.

A detailed experimental and numerical analysis of the highly intricate flowfield at staging can be found in Refs. 3, 4.

Experience concerning the separation of lifting vehicles has been gained primarily at subsonic speed, Ref. 6. Separating at supersonic speed showed great problems, Ref. 7. No experience is available for the separation of lifting and airbreathing vehicles at hypersonic speed.

## 4 Basic Problem Description

The overall separation maneuver may be decomposed into three phases each of which shows specific characteristics. During these phases, various problems rapidly changing exist and several goals have to be achieved. For initiating the separation maneuver, a pull-up is conducted. Problems related to this phase concern the achievement of a starting condition favorable for releasing the orbital stage. During or after pull-up, the orbital stage is extended to a position suitable for release. The problems investigated here are related to trimming the vehicles and to load factor control for achieving forces admissible for the interstage attachment with the use of which the orbital stage is extended, Ref. 8. After releasing the orbital stage, the main goal based on safety considerations is to achieve a certain distance between the two vehicles as quickly as possible. Control of both vehicles is concerned with achieving an optimal motion of the system during the overall separation maneuver such that its flight performance is maximized. Another problem area is the rotational motion of the orbital stage immediately after release. This is because the rear of the orbital stage may move towards the first stage by an improper rotation control for increasing angle of attack. It will be shown how a hazardous situation can be avoided with practically no performance penalty by including a safety requirement in the optimization of the separation maneuver.

## 5 Wind Tunnel Tests

The first part of the paper deals with aerodynamics and wind tunnel testing of a two-stage lifting configuration. Aerodynamics effects play a major role during the separation maneuver, when the first and the orbital stage are in close proximity. For this reason a test campaign was planned and conducted by MBB and performed in test facilities of DLR, Cologne, Refs. 3, 5. The windtunnel tests were performed at Mach 6.0. The tests were aimed at investigating the flowfield between the two separating stages at hypersonic speed.

For the wind tunnel tests a titanium model (size 1:160) was manufactured. A sketch of the model is shown in Fig. 1. Some problems related to the small size of the models will be considered. Since it is not possible to simulate the full function of the turbo-/ramjet-intake, the powerplant area of the first stage is omitted (except sidewalls). An exact bookkeeping method was applied to combine the measured aerodynamics values with the powerplant datasets. It was not possible to perform pressure measurements on wings and fins. So, two different balances for the first and the orbital stages had to be adjusted.

Another item is the Reynolds number of the wind tunnel tests ( $Re = 3.4 \cdot 10^6$ ). This differs from the values of a realistic configuration ( $Re = 3 \cdot 10^8$ ).

The longitudinal behavior of the two stages was investigated by varying the following parameters:

- angle of attack of first stage ( $\alpha_1$ )
- relative pitch angle between both stages ( $\Delta\epsilon$ )
- vertical distance between both stages ( $\Delta z_{\text{rear}}$ ).

Major results of the test campaign are as follows:

There are strong aerodynamic interference effects when the two stages are in close proximity. During the separation reflecting shocks occur between the first and the orbital stage. Schlieren pictures show that the main impacts concerning the aerodynamics of the first stage are due to the impingement of the bow shock of the orbital stage. On the other hand strong effects on the orbital stage result from the flowfield around the first stage and the first reflection of the bow shock (Fig. 2).

The position of the shocks is a function of speed, angle of attack, distance and relative pitch angle between the two stages. As a consequence, substantial changes in aerodynamic forces and moments exist during the separation maneuver.

In Fig. 3 lift and pitching moment coefficients of the first stage are shown as a function of angle of attack for several distances  $\Delta z_{\text{rear}}$  of the first stage. Lift of the first stage is basically a linear function of angle of attack. It is decreased when the orbital stage is in close proximity. Pitching moment characteristics presented in Fig. 3 show that reducing the vertical distance leads to an additional nose-up moment when compared with an interference free condition.

In Fig. 4 the related curves for the orbital stage are presented. It can be seen that the lift as well as the pitching moment are non-linear functions of angle of attack. Lift of the orbital stage is considerably increased when the two stages are in close proximity and angle of attack is small.

These results show that there are some important characteristics of the aerodynamic interference effect with regard to the separation maneuver. Lift decrease of the first stage and lift increase of the orbital stage represent a force characteristic which is favorable for the separation of the two stages. More complex is the influence on the aerodynamic pitching moments of the two stages. The pitching moments of both stages show varying dependencies with regard to the relative position of the two separating vehicles.

Further investigations were concerned with control effectiveness. The results show that flap efficiency has strongly non-linear characteristics. This represents a major point regarding control of both stages during the separation maneuver as it is considered in a later part of this paper.

## 6 Model for Flight Dynamics Investigation

The mathematical model for describing longitudinal dynamics of both stages can be formulated as three systems of coupled equations, Ref. 8:

- Absolute motion of the first stage
- Relative motion between first and orbital stages
- Forces and moments at interstage attachment connecting both stages

Flight dynamics simulation of the separation maneuver includes results described in the first part of the paper. Based on the addressed wind tunnel investigations and on CFD results, a realistic modelling for flight dynamics investigations is developed. Particular emphasis is placed on aerodynamic interference effects on flight dynamics.

For modelling aerodynamics including interference effects, the following relations are applied

$$\begin{aligned} C_{L1} &= C_{L1}(\alpha_1, \Delta\epsilon, \Delta z, \delta_{e1}), \\ C_{D1} &= C_{D1}(\alpha_1, \Delta\epsilon, \Delta z, \delta_{e1}), \\ C_{m1} &= C_{m1}(\alpha_1, q_1, \Delta\epsilon, \Delta z, \delta_{e1}), \\ C_{L2} &= C_{L2}(\alpha_1, \Delta\epsilon, \Delta z, \delta_{e2}), \\ C_{D2} &= C_{D2}(\alpha_1, \Delta\epsilon, \Delta z, \delta_{e2}), \\ C_{m2} &= C_{m2}(\alpha_1, q_2, \Delta\epsilon, \Delta z, \delta_{e2}). \end{aligned}$$

Aerodynamic interference effects are expressed as a function of the distance and the relative pitch angle between both stages. The dependence of aerodynamic forces and moments on Mach number can be ignored for the present problem because Mach number changes during the separation maneuver which is rather short are negligible.

Thrust is expressed as

$$T_1 = \delta_{T1} T_{1\max}(h, Ma, \alpha_1), \quad T_2 = \delta_{T2} T_{2\max}$$

## 7 Optimal Separation

An important precondition before release of the orbital stage is that the relative acceleration between the two stages must be greater than zero:

$$\Delta\dot{w} > 0.$$

The two decisive parameters to influence the relative acceleration are the relative pitch angle  $\Delta\epsilon_{rel}$  and the load factor of the first stage  $n_{z1}$ .

The flight phase immediately following release of the orbital stage is intended for achieving a safe distance between the two stages as quickly as possible.

For a safe separation maneuver, a collision must be avoided after the mechanical links are disconnected. A critical point concerns the relative motion of the rear of the orbital stage and the adjacent part of the first stage. To prevent both vehicles from approaching each other, a collision avoidance criterion  $Ko = \Delta\dot{w}_{rear}/\Delta\dot{w}$  is introduced. The factor  $Ko$  can be used to describe the motion of the rear of the orbital stage in relation to the surface of the first stage. The rear of the orbital stage does not move towards the first stage when  $Ko \geq 0$ . By applying an appropriate bound  $Ko_{min}$ , the separation motion can be controlled such that a hazardous approach of the rear of the orbital stage can be avoided.

The performance of the separation maneuver after release is maximized by applying an optimal control technique,

with realistic constraints imposed. A performance criterion has been defined for maximizing the translational displacement between the centers of gravity of both vehicles within a prescribed time interval:

$$J = \Delta z(T).$$

State and control variables during the separation maneuver are subject to the following constraints:

$$\begin{aligned} \text{First Stage:} \quad & (\alpha_1)_{min} \leq \alpha_1 \\ & (\delta_{e1})_{min} \leq \delta_{e1} \leq (\delta_{e1})_{max} \\ \text{Orbital Stage:} \quad & \alpha_2 \leq (\alpha_2)_{max} \\ & Ko_{min} \leq Ko \\ & (\Delta z)_{min} \leq \Delta z_{ign} \\ & (\delta_{e2})_{min} \leq \delta_{e2} \leq (\delta_{e2})_{max} \end{aligned}$$

In Fig. 5, a separation maneuver without a constraint concerning rotation of both vehicles is shown. As may be seen, the rear of the orbital stage initially moves towards the first stage (i.e.,  $\Delta z_{rear}$ ), although the centers of gravity separate in a way which can be considered as sufficient (i.e.,  $\Delta z$ ). Additionally, Fig. 5 shows a separation maneuver significantly improved in regard to the movement of the rear of the orbital stage  $\Delta z_{rear}$ . The improved control can be achieved when considering a constraint of  $Ko_{min} = 0.5$ .

The maximum displacement achievable after  $T = 5$  sec is shown in Fig. 6 as a function of the limit  $Ko_{min}$  of the collision avoidance factor. The region of positive  $Ko_{min}$  values is of particular interest. This is because it indicates a motion where both stages do not approach each other at any instant during the separation phase. Negative values indicate a motion where the rear of the orbital stage initially moves towards the first stage. The examples shown in Fig. 5 are marked by  $\square$ . From the results presented in Fig. 6 it follows that safety considerations concerning the avoidance of an adverse rotational motion result in a small degradation in the achievable distance (small positive  $Ko_{min}$  values).

Furthermore, it is shown that the angle of attack limit of the first stage  $(\alpha_1)_{min}$  has a significant effect. By contrast, the relative pitch angle at release as given by  $\Delta\epsilon_{rel}$  has a comparatively small effect. This may be of importance for the mechanical support which is used for extending the orbital stage and for appropriately positioning it for release.

In Fig. 7, the relative motion of the vehicles is shown for different types of thrust control. As may be seen, the relative motion in longitudinal direction may be effectively controlled by an appropriate thrust setting for the orbital stage (with the orbital maneuvering system engines OMS used for the orbital stage). Fig. 7 also illustrates the maximum displacement possible in forward and rearward direction (at constant thrust setting of first stage). A further result concerns the vertical displacement between both stages. The vertical separation does not depend much on thrust control. The main contribution to vertical displacement is due to control of aerodynamic lift.

During the separation phase described, the rocket engine of the orbital stage is ignited at a suitable time which may be chosen such that plume impingement on the first stage is avoided. In this case, a certain distance  $\Delta z_{min}$  between both stages must be reached before the engines can be ignited. After ignition, a time interval of some 4 sec is

required before the rocket engine achieves full thrust. For this reason the main engine has no significant influence on the vertical displacement.

## 8 Robust Control Application

After release of the orbital stage the flight dynamics behavior of both vehicles undergo significant changes, which are due to aerodynamic interference effects. There may be parameter uncertainties as regards a precise knowledge of the aerodynamic effects. Robust control is a technique which is capable of coping with substantial changes of forces and moments.

An additional topic dealt with concerns inherent aerodynamic instability of the vehicles. The control system must remove this instability and provide a stability level and also damping properties acceptable from a flying qualities point of view. For this purpose, a stability augmentation system is required.

The control system considered is of the type "Alpha Command". This system features a feedback of angle of attack and pitch rate to the pitch control surface. Precise control of angle of attack is required for two reasons. One point is performance of the engine intake which shows a strong dependence on angle of attack. The other point is that performance and safety of the separation maneuver are significantly influenced by angle of attack of first stage (Fig. 6).

Short period dynamics of the two stages are considered to be of primary importance during the separation maneuver. For dealing with this problem, a simplified system model is applied which is representative for short period dynamics. It may be written as

$$\dot{\mathbf{x}} = \mathbf{A}\mathbf{x} + \mathbf{B}\mathbf{u}$$

Before release of the orbital stage, the dynamics of the system can be described with the use of a state vector  $\mathbf{x}$  consisting of two elements  $[\alpha_1, q_1]^T$  denoting variables of the first stage. It can be controlled by the pitch control deflection  $\mathbf{u} = [\delta_{e1}]$ . The elements of the 2x2 coefficient matrix  $\mathbf{A}$  describe the characteristics of the overall system consisting of the first and orbital stages including their changes during the positioning procedure.

After release of the orbital stage, short period dynamics of both stages moving separately are considered. In this case, the state vector consists of four elements  $\mathbf{x} = [\alpha_1, q_1, \alpha_2, q_2]^T$ . The control vector now reads  $\mathbf{u} = [\delta_{e1}, \delta_{e2}]^T$ . Accordingly,  $\mathbf{A}$  is now a 4x4 matrix which accounts for the separate but coupled motion of both vehicles. The forces and moments of the first and the orbital stages are coupled after release because of aerodynamic interference effects. This is illustrated in Fig. 8 which shows the coupling of the equations in a signal diagram form. The equations are strongly influenced by these interference effects which are functions of the vertical distance  $\Delta z$  and the relative pitch angle  $\Delta \epsilon$ . Fig. 9 shows an example which is representative for the interference effects on force and pitching moment characteristics. In this Figure, the changes of the lift coefficients due to interference effects are represented by a grey region for each stage.

A required damping and frequency combination can be achieved by an appropriate set of controller coefficients. Reference is made to flying qualities requirements such as Refs. 9, 10. Characteristics which may be adequate from a flying qualities point of view can be expressed by an admissible pole region as shown in Fig. 10. Thus, the admissible region of  $\zeta$  and  $\omega_n$  correspond to an equivalent region of  $K_\alpha$  and  $K_q$ . This is also shown in Fig. 10. The assignment of required dynamics characteristics to an admissible region of controller coefficients is provided by a parameter space method.

One problem in selecting an appropriate control system are large plant parameter variations which significantly change the dynamic behavior of the two stages. The pull-up maneuver shows large load factor changes ranging from one boundary to the other, i.e. from  $(n_z)_{\min}$  to  $(n_z)_{\max}$ . The positioning procedure of the orbital stage after pull-up results in additional parameter changes because of increasing the distance between both stages and, thus, altering aerodynamic interference effects.

To take these uncertainties into account, the dynamics of the systems are evaluated at several characteristic flight conditions during the separation maneuver (Table 1). The gains  $K_\alpha$  and  $K_q$  are controller coefficients which can be used for achieving required dynamics characteristics during the separation maneuver. To get a fixed-gain controller for the whole separation maneuver, the above pole assignment is repeated for all flight conditions described in Table 1, each resulting in an admissible region for the controller coefficients. Then, the admissible regions for all flight conditions are superimposed. The intersection results in a region of controller coefficients which can stabilize the vehicles at all investigated flight conditions. This straight forward technique to find coefficients for a fixed-gain controller is called "Multi-Model-Approach", Ref. 11.

As may be seen in Figs. 11 and 12, the resulting admissible regions provide some freedom for selecting controller coefficients. This may be used for taking additional control design requirements into account.

For a highly dynamic system, the approach described above may be considered an approximation since the reference conditions represent what may be called frozen points of the trajectory. Therefore, simulation of the nonlinear equations has been used to show that the controllers yield a good performance of the systems.

## 9 Conclusions

The separation maneuver of two-stage hypersonic lifting vehicles poses new and challenging problems in the fields of aerodynamics and flight mechanics.

Wind tunnel tests were performed at DLR facilities in Cologne, with emphasis placed on aerodynamic interference effects at Mach 6.0. The investigations show that the lift increase for the orbital stage and the lift decrease of the first stage represent a force characteristic which is favorable for the separation maneuver. The interference effect concerning the pitching moment shows varying dependencies with regard to the relative position of the two separating vehicles. This may cause problems in controlling the two stages during the separation maneuver.

The flight dynamics investigations are concerned with two further issues. One is related to the safety of the relative motion of both vehicles after release of the orbital stage. The other issue addresses robust control for stabilizing the vehicles which show inherent aerodynamic instability and large parameter variations during the separation maneuver.

For the motion after release of the orbital stage, it is necessary to achieve a safe separation and a quick translational displacement. An optimal control technique is used to reach this goal without a significant performance penalty. A collision avoidance factor is introduced which can be used for describing appropriate motion characteristics.

A robust control technique is applied for stabilizing the vehicles in the phase before and after separation. It is shown that such a technique is capable of providing sufficient stability and damping for vehicles which show large parameter changes caused by dividing the overall system into two subsystems as well as by strong interference effects. In addition, the robust control technique is used to remove the inherent instability of the basic vehicles.

## 10 References

### Literatur

- [1] Högenauer, E., "Raumtransporter," *Zeitschrift für Flugwissenschaft und Weltraumforschung*, pp. 309-316, 1987.
- [2] Koelle, D. E., Kuczera, H., "SÄNGER Space Transportation System - Progress Report 1990," *IAF-90-175*, 1990.
- [3] Esch, H.: Kraftmessungen zur Stufentrennung am MBB-Sängerkonzept im Überschall, *IB-39113-90 C 08*, Köln, 1990.
- [4] Schröder, W., Hartmann, G.: Analysis of Inviscid and Viscous Hypersonic Flows past a Two-Stage Spacecraft, *Journal of Spacecraft and Rockets*, Vol. 30, No. 1, 1993, pp. 8-13.
- [5] Gottmann, T., Cucinelli, G., "Experimental Results in Aerodynamic Stability and Control of a TSTO Configuration" *AGARD-CP-514*, 1992.
- [6] Wilhite, A.W., "Analysis of Separation of Space Shuttle Orbiter from a Large Transport Airplane," *NASA TM X-3492*, 1977.
- [7] Crickmore, P.F., "Lockheed SR-71 Blackbird" *Oxcart and the A-12* pp. 33-35.
- [8] Sachs, G., Schoder, W., "Optimal Separation of Lifting Vehicles in Hypersonic Flight," *AIAA Guidance, Navigation and Control Conference Proceedings*, pp. 529-536, 1991.
- [9] MIL-F-8785C - "Flying Qualities of Piloted Airplanes," 1980.
- [10] MIL-STD-1797 - "Flying Qualities of Piloted Vehicles," 1987.
- [11] Ackermann, J., "Robuste Regelung", Berlin, Heidelberg, New York: Springer-Verlag, 1993.

| Flight Condition |   |  | Configuration   |
|------------------|---|--|---|
| 1                | $V_1$<br>$h_1$<br>$n_{z1}$<br>$\Delta z$<br>$\Delta \epsilon$           | 2056 m/s<br>31 km<br>1<br>4.067 m<br>-1.5°                               | First stage with retracted orbital stage (cruise configuration)     |
| 2                | $V_1$<br>$h_1$<br>$n_{z1}$<br>$\Delta z$<br>$\Delta \epsilon$           | 2056 m/s<br>31 km<br>( $n_{z1}$ ) <sub>max</sub><br>4.067 m<br>-1.5°     | First stage with maximal admissible load factor (pull-up)           |
| 3                | $V_1$<br>$h_1$<br>$\alpha_1$<br>$\Delta z$<br>$\Delta \epsilon$         | 2035 m/s<br>34.3 km<br>( $\alpha_1$ ) <sub>min</sub><br>4.067 m<br>-1.5° | First stage with retracted orbital stage (beginning of positioning) |
| 4                | $V_1$<br>$h_1$<br>$\alpha_1$<br>$\Delta z$<br>$\Delta \epsilon$         | 2035 m/s<br>34.3 km<br>( $\alpha_1$ ) <sub>min</sub><br>6.067 m<br>1.0°  | First stage with extended orbital stage (end of positioning)        |
| 5                | $V_{1,2}$<br>$h_{1,2}$<br>$\alpha_1$<br>$\Delta z$<br>$\Delta \epsilon$ | 2035 m/s<br>34.3 km<br>( $\alpha_1$ ) <sub>min</sub><br>6.067 m<br>1.0°  | First and orbital stages at release                                 |
| 6                | $V_{1,2}$<br>$h_{1,2}$<br>$\alpha_1$<br>$\Delta z$<br>$\Delta \epsilon$ | 2035 m/s<br>34.3 km<br>( $\alpha_1$ ) <sub>min</sub><br>8.067 m<br>2.2°  | First and orbital stages after separation ( $Ko_{min} = 0.9$ )      |
| 7                | $V_{1,2}$<br>$h_{1,2}$<br>$\alpha_1$<br>$\Delta z$<br>$\Delta \epsilon$ | 2035 m/s<br>34.3 km<br>( $\alpha_1$ ) <sub>min</sub><br>10.067 m<br>4.6° | First and orbital stages after separation ( $Ko_{min} = 0.9$ )      |
| 8                | $V_{1,2}$<br>$h_{1,2}$<br>$\alpha_1$<br>$\Delta z$<br>$\Delta \epsilon$ | 2035 m/s<br>34.3 km<br>( $\alpha_1$ ) <sub>min</sub><br>100 m<br>12.0°   | First and orbital stages after separation (no interference)         |

Table 1 Reference flight configurations

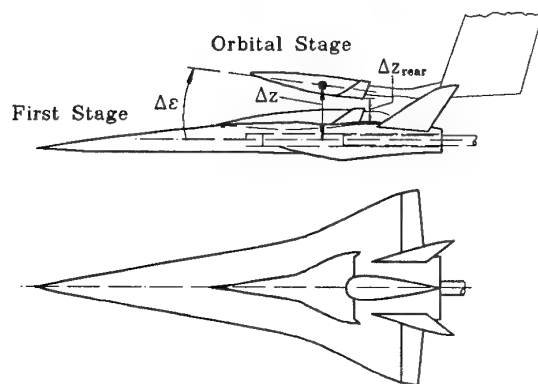


Fig. 1 Sketch of windtunnel model and measurement equipment

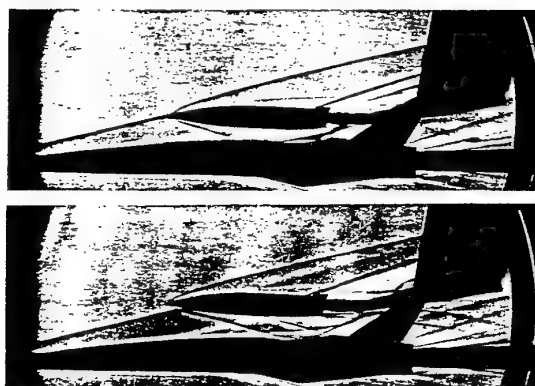


Fig. 2 Schlieren pictures at Mach 6.0

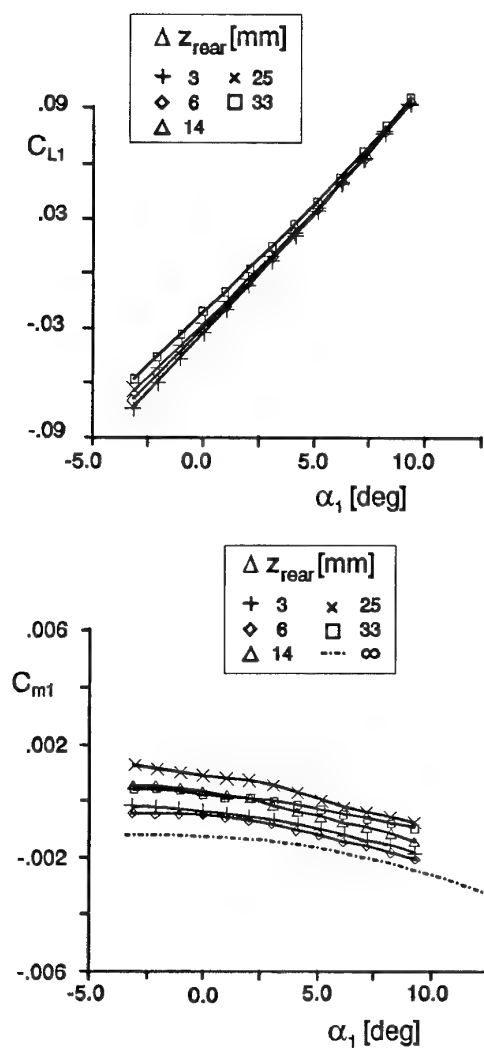


Fig. 3 Influence of interference effects on lift and pitching moment of first stage,  $\Delta\epsilon = 2^\circ$

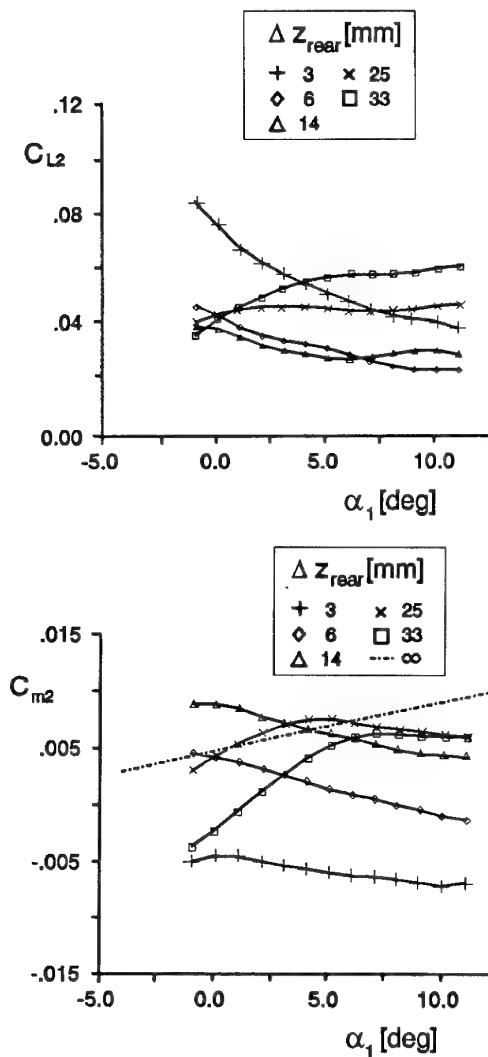


Fig. 4 Influence of interference effects on lift and pitching moment of orbital stage,  $\Delta\epsilon = 2^\circ$

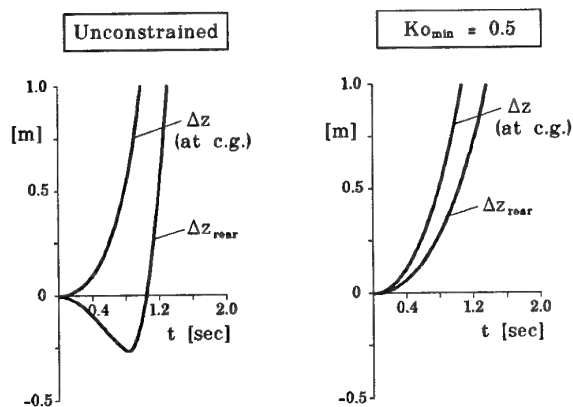


Fig. 5 Relative motion during the initial phase of optimized separation maneuver (beginning with zero at release)

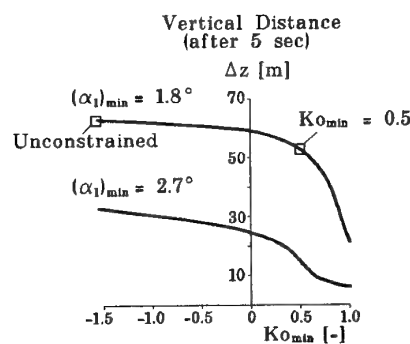


Fig. 6 Maximized distance between centers of gravity of both stages (relative pitch angle at release  $\Delta\epsilon_{rel} = 1^\circ$ )

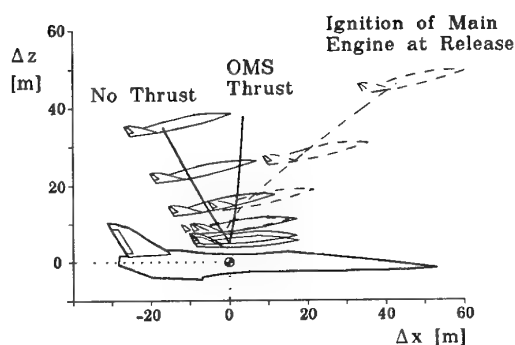


Fig. 7 Effect of thrust control on longitudinal separation ( $\delta_{T1} = 1$ )

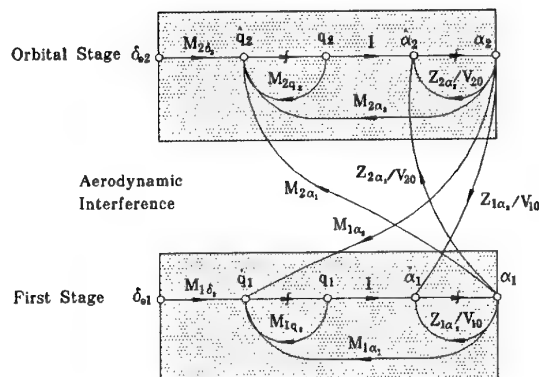


Fig. 8 Coupled linearized equations of motion for both stages after release

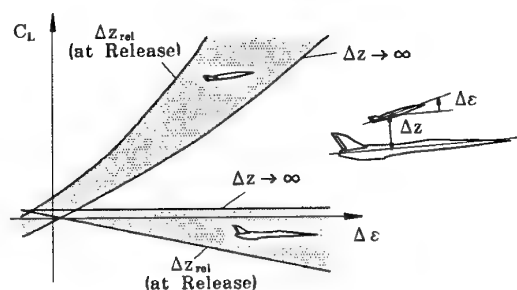


Fig. 9 Interference effects for lift coefficients ( $\alpha_1$  constant)

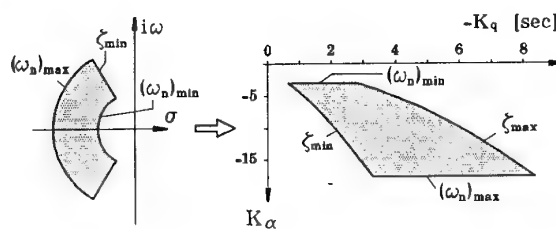


Fig. 10 Required stability characteristics and related controller coefficients  
 $\zeta_{min} = 0.35$ ,  $\zeta_{max} = 1.30$ ,  
 $(\omega_n)_{min} = 2$  rad/sec,  $(\omega_n)_{max} = 5$  rad/sec

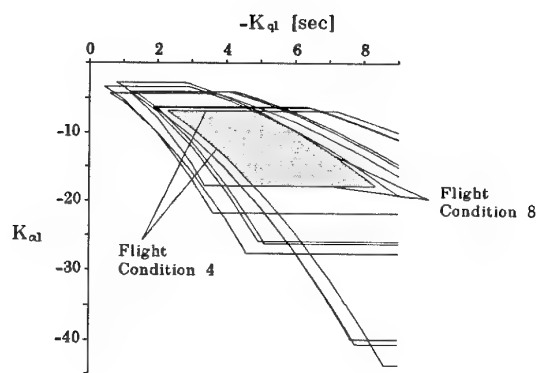


Fig. 11 Intersection of admissible regions for the controller coefficients of first stage

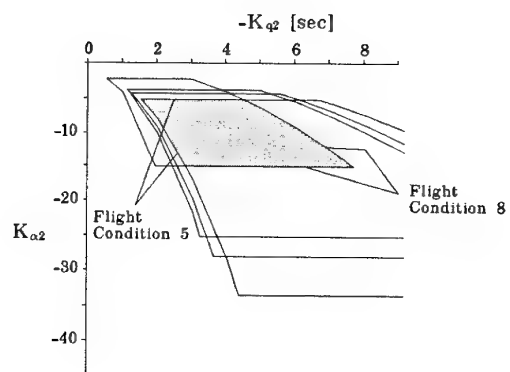


Fig. 12 Intersection of admissible regions for the controller coefficients of orbital stage



## SPACECRAFT DEPLOYABLE STRUCTURE TESTING

Dr. Ronald D. Dotson  
 Manager of Structural Dynamics  
 Space Systems Division  
 Lockheed Missiles and Space Co., Inc.  
 B150, O/74-03, 1111 Lockheed Way  
 Sunnyvale, CA 94089  
 USA

SUMMARY

This paper describes test programs that develop and qualify spacecraft deployable structures. Spacecraft deployable structures (examples are solar arrays, antennas and booms) are typically a combination of moving mechanical assemblies (examples are joints, latches and gimbals) and structural elements. Moving mechanical assemblies contain numerous potential sources of nonlinearities, such as freeplay, friction and hysteresis in joints and sliding surfaces. Also, larger deployables have low natural frequencies when deployed and may have large area to weight ratios. These subsystems can be significantly affected by gravity, air, humidity and other "ground based effects". This paper discusses how to address these concerns for deployable structures testing when simulating the desired environments and demonstrating functionality.

INTRODUCTION

Spacecraft deployable structures combine complexities of moving mechanical assemblies with structures of varying size, stiffness and complexity. These structures, stowed for ascent, deploy and may operate in different orientations and rates once deployed. Additionally, they may be retractable and/or separable. To properly test these systems on the ground with their varied configurations while exposed to simulations of their different environments can be a challenge.

Testing and maintenance costs are a major element of the life cycle costs of most space programs. Unlike aircraft programs, where the testing and maintenance costs occur primarily during operational use, the test costs for space vehicles are primarily incurred prior to space operations. Test costs may represent a sizable percentage of life cycle costs for high reliability, long-life, small quantity space vehicles. Testing of deployables represent a sizable percentage of most spacecraft testing.

Deployable spacecraft structures must be designed, analyzed and tested to cover a wide range of conditions.

These structures must:

- Exist and perform in different configurations
- Move reliably between different configurations
- Function so as to not adversely interfere with the integrity and performance of other parts of the system
- Survive the trip from factory to space (and in some instances back again)
- Deploy and operate in a space environment characterized by vacuum, weightlessness and extreme thermal conditions.

Many factors, including minimum weight, stowage volume allowances, stay out zones for payload sensors, and system and sensor performance budgets constrain the design. However, the cost and ability to test, as well as to predict through analysis and test, are design considerations as well.

Examples of deployable spacecraft structures [1] are solar arrays, radiators, antennas, booms, doors, segmented mirrors, thermal shields and even portions of the main body of some spacecraft. These types of structures normally include moving mechanical assemblies (MMA's). Examples of MMA's are

bearings, gimbals, latches, motors, clutches, springs, actuators and dampers. The structure, mechanisms and any equipment mounted outside the deployable's attachment interface to the main vehicle body defines the deployable structure for purposes of this paper.

History in testing and flight has provided lessons to be learned. Table 1 shows a brief list of some of the known failures for deployable structures in flight. Some have resulted in complete mission failure and some only in temporary, intermittent or permanent reduction in mission performance. Interactions with the system through ground control, or in some instances manned flight interactions, eliminated or improved some of the problems. For example, problems with jitter and loss of lock on stars for pointing was discovered on the Hubble Space Telescope when the vehicle entered and exited the earth's shadow. Analysis and test, including flight tests, helped narrow the problem source to solar array vibration caused by rapid thermal gradient changes. In flight control excitation was used to improve modal information on the arrays. Then the spacecraft control system algorithms were modified from ground control and performance problems reduced significantly.

Each failure provides insight into mistakes made or further improvements needed in test, design and analysis. In retrospect, many of the problems listed could have been prevented by better design practices or procedures within the scope of current test technology. Some, such as the cold welding problem with the Galileo high gain antenna, could indicate possible test procedure changes and facilities needs. In the case of the Galileo antenna failure, combinations of ground vibration testing and vibrations during ground transportation is suspected to have worn away the lubricant on the ball and socket surfaces [24]. In flight in the vacuum of space, enough vibration occurred to create galling which in turn lead to cold welding in the vacuum. This effect in turn prevented the antenna deployment. Design changes and materials selection could prevent this from happening. However, this experience could also point to a need to do vibration testing within thermal vacuum chambers for some classes of deployable systems.

Also, there have been many more discoveries of problems during ground testing. Every spacecraft contractor has a long list of lessons learned [2,3] and design problem discoveries resulting from their tests and flights. Conferences and proceedings such as the Aerospace Mechanisms Symposia and the Structures, Structural Dynamics and Materials Conferences have discussed many lessons learned.

Although elaborate and exhaustive testing is performed on most deployables, many times simple and avoidable problems cause failures. Snags caused by a thermal blanket not on during the right test, wires not properly held down, or a bolt with a slightly larger head put on at the last moment prior to flight are all examples of real in-flight failures.

Ground based testing is performed when possible, since testing on the ground is generally more cost and schedule effective than flight testing. Those characteristics of the earth, ascent and space environments that are important to replicate for proper testing will depend on the deployable design and application. The goal is to simulate environmental characteristics and

proper loading. Thermal vacuum chambers, acoustic chambers, shake tables, special test fixtures and other facilities and support equipment are used to approximate the environments for design qualification and to help prove functionality.

Tests are conducted on deployable structures to cover ascent, deployment and on-orbit operations and possibly for retractions, descents, reparability, separability, and landings. They may also have to operate outside earth and earth orbit related environments for activities in lunar, planetary and solar system environments. This paper addresses approaches and issues related to testing of deployable structures that remain attached to earth orbiting unmanned satellites. However, much of what is presented applies to man tended and interplanetary spacecraft.

#### TESTING STANDARDS AND GUIDELINES

Guidelines and standards for testing of space vehicles and their subsystems and components [4,5] have been established by numerous U.S. government agencies, such as the U.S. Air Force and various NASA centers, as well as commercial contractors. Differences that may occur are usually based on tailoring to specific classes of satellites, payloads, booster systems, performance priorities and each company or agency's experience base.

One common standard is detailed in MIL-STD -1540C (USAF). This standard establishes the environmental and structural ground testing requirements of booster vehicles, upper-stage vehicles, space vehicles and their associated subsystems and components. However, as is stated in the document, it is usually an accepted fact that "these test requirements should be tailored to each program after considering test item design complexity, design margins, vulnerabilities, technology state of the art, in-process controls, mission criticality, life cycle costs, number of vehicles involved, and acceptable risk". The USAF military specification MIL-A-83577B, General Specification For Assemblies, Moving Mechanical, For Space and Launch Vehicles, sets forth the general requirements for the design, manufacture, quality control and testing of moving mechanical assemblies to be used on space and launch vehicles. MIL -STD-810D, Environmental Test Methods and Engineering Guidelines, provides guidelines for conducting environmental engineering tasks to tailor environmental tests to end item equipment applications as well as providing test methods for determining the effects of natural and induced environments on equipment used in military applications.

#### TEST SEQUENCE AND CONTENT

Tests for static loads, vibration, acoustics, shock, pressure, vacuum, radiation, acceleration, electromagnetic compatibility and temperature extremes and cycles are generally performed. These tests assess the effects on materials, mechanisms and structure for deployables. Functional testing is typically performed after each environmental exposure to verify no adverse effects on the deployable from the specific environment. The sequence of development, qualification and acceptance testing is performed at the component, assembly and system levels. The philosophy is to set test levels and schedules to catch problems at the lowest level of assembly possible.

Whether or not the test is required or optional depends on factors such as:

- Level of assembly(component, subsystem, system)
- Type of test(functional, thermal vacuum, sine vibration, other test)
- Configuration( stowed, deploying, deployed)
- Type of design application(antenna, solar array, MMA)

The Military Standards referenced above give recommendations on which tests to consider required and which to consider optional. The preferred order of the tests is one that simulates the actual sequence seen in operation. Figure 1 is an example.

It is up to the engineer to use a combination of analysis and development testing to assess air, thermal and gravity influences on the design functionality. This assessment will be important to determining environmental requirements, suspension system needs and design, orientation to the gravity vector during test and other possible considerations.

In addition to design verification tests, there are analysis model verification tests. Examples are modal and thermal balance tests used to verify structural dynamic and thermal models, respectively. Other tests such as mass properties tests and spin balancing of spinning spacecraft may require special attention to account for air, aerodynamic force, thermal and gravity induced distortions effects on deployables.

#### FUNCTIONAL TESTS

If feasible, mechanical function testing is always done at the subsystem or system level. It may only be done in selected circumstances at the component level. Since hot and cold temperature is normally a stressing condition for deployable function, functional tests at all levels of assembly are performed under these conditions. In cases where it is not feasible or practical to perform a system level test at extreme temperatures, adequate confidence may be gained through information developed from extreme temperature testing at the component and subsystem levels.

For systems with multiple deployables, the sequence of deployments performed on the ground is the same as that which occurs in flight. If the satellite is spinning at a significant rate during deployment then that rate is duplicated either with the actual satellite spinning or on a centrifuge used to simulate the proper forces.

At the subsystem or system level a complete functional test using the actual release devices and allowing the deployable to go from actual release to lock-in is an important demonstration. No matter what level of assembly is used to perform the comprehensive test, a limited mechanical function test is done on the flight deployable. The limited function test typically consists of a manual demonstration of proper release and initial motion. Sometimes the deployable is moved through its full motion, with support when necessary. This end item limited function test helps to verify that there are no final build interferences from such things as thermal blankets, wiring harnesses or other sources. Also, at the launch site, it is a common practice, when possible, to demonstrate at least first motion following manual release prior to installing any final release devices, such as pyrotechnic devices.

#### MODAL TEST

Analytical models are used to reduce and configure test requirements. Modal tests are used to verify these analytical dynamic models.

Some stowed deployable systems have frequencies above significant amplification frequencies associated with ascent excitation and response. This might be, for example, above 50 Hz for a Titan launched system. For these types of deployables, large load factors tend to be used for design. Here a simple tap or twang test to verify that its stowed frequency is indeed above the required level will generally suffice. When the system level modal test is performed, measurements can be made on the

deployable or its dynamic simulator to insure the as installed frequency is still sufficiently high.

Some deployed structures aren't large enough to have an influence on the vehicle performance. If their dynamic characteristics aren't a major factor in their own performance, then a twang or tap test may also suffice.

For large and low frequency deployed or stowed deployables, the system level modal test is usually preceded with accurate modal tests of the assembly. This test is usually done hard mounted, unless the local flexibility with the spacecraft is important. If so, the local flexibility of the spacecraft main body is simulated or the deployable is mounted to a representative S/C structure for the test.

If the deployed structure needs support to offset gravity influences, a need exists for support schemes which have minimal interaction with the specimen. Gravity off load devices are discussed in the section, gravitational considerations.

For ambient environment modal testing of large area light weight stowed structures with relatively small clearances between adjacent large area surfaces, the air pumping effect can be significant in affecting the modes. For example, a modal test was performed on a 10.4 x 3.7 m honey comb panel solar array folded at it's center line with a 3.8 cm clearance between the panel. What would have been a 22 Hz frequency tenth mode in a vacuum was a 7 Hz frequency first mode in ambient conditions. Methods for analytically accounting for this air effect have been developed from more approximate methods [6] to more accurate methods using fluid finite elements. If model verification is needed for the space environment, stowed or deployed, testing in full or partial vacuum may be required.

Some deployables, such as large area flexible solar arrays whose blankets get their stiffness from tension, can not be tested fully deployed in one piece on the ground. Both gravity and air effects can be significant. This has lead to in flight modal tests such as was performed on the Solar Array Flight Experiment attached to the space shuttle.

There are numerous techniques for performing modal tests. An extensive comparison [7] of different techniques performed on the Galileo spacecraft. Because deployables tend to have nonlinearities, one of the best techniques for modal testing of deployables and for finding and identifying nonlinearities is the sine sweep with sine dwell with single or multiple shakers. The sweep is done from below and above in frequency and at different amplitudes to help discover any nonlinear behavior.

Large deployables can have nonlinearities or complex dynamic characteristics. Modal testing the spacecraft system with these deployables attached can lead to difficulties correlating models with modal results. As such, many times, the major deployables are represented with simple mass simulators during the prime structure modal test to allow easier correlation. The deployables are tested by themselves and their correlated models analytically combined with the rest of the system to obtain system modes.

#### STATIC TEST

The static test is used to verify that the design meets structural integrity requirements under loads. The applied loading conditions are typically conservative combinations which bound numerous dynamic and static events. Since it is not always possible to generate the worst case loading for all parts of the structure, stress analysis is used to assess the areas with least margin of safety to properly define the test loads. In the

stowed configuration the static loading normally envelope ascent loads from dynamic events such as lift off and engine shutdown response transients.

Deployed structures on spacecraft with significant on-orbit loading may also be subjected to static loads tests to represent or envelope those events. Reboost acceleration loads, maneuver or docking events, and thruster plume forces are examples of events which may create critical loadings. For some deployables the deployment event with its lockup loads are design drivers for much of the deployable structure and mechanisms, in which case the actual functional deployment tests could provide load qualification. Stiffness information can be obtained from the static test to help in model improvements and verifications.

For some types of deployables point loads from actuators cannot properly represent or bound the critical loading considerations. For these a centrifuge test may be more applicable. This is the case, for example, where prevention of slippage in folded membrane solar arrays in their stowed position must be demonstrated. Gradients of acceleration loads due to variation with distance from the centrifuge rotation axis must be taken into account.

The static test can be overly conservative for alignment assessment in classes of precision deployable structures that have hysteresis or shifts in joints and latches. Hysteresis or other misalignment sources can be a function of load time duration, as well as magnitude. Static hysteresis is typically higher than dynamic in that the dynamic cycling of the loads generally will leave smaller residual misalignments. So if the dominate loads do come from vibratory dynamic loadings it is best to do dynamic loading. But if static loading is done, it is perceptive to cycle the static loads in the tests in a manner representative of the dynamic loading peaks.

#### ACOUSTIC TEST

Acoustic tests are especially important for stowed large area light weight deployables such as solar arrays, radiators and solid surface antennas. Acoustically induced stresses in solar cells and loads and responses induced in mechanisms and electronics mounted on or in the vicinity of these types of deployables can be design drivers for those items. For predictions of acoustic response and for model to test correlation, the air pumping effects can be significant for air between large area close surfaces and should be accounted for in the modeling [8].

#### VIBRATION TEST

Random vibration testing is almost always performed on the stowed configuration for components and assemblies. Sine vibration is usually performed at component levels and for other levels if the spacecraft flies on a booster with a sine type environment. Component level sine testing is especially important to perform if a system level sine test is planned. Since sine tests can be overly conservative, load or response limiting to not exceed design loads is usually done. Performing sine testing at lower levels of assembly also provides knowledge of when to limit the sine test inputs at higher levels of assembly.

#### SHOCK TEST

Most deployable structures contain release devices which produce shock. Also the lockup event for deployment can produce a shock type input. Shock inputs from the rest of the vehicle such as shroud or S/C booster interface separations can also be significant. Although there are concerns about

brinelling of gear surfaces and bearings, shock is mostly a problem for electronics. It is important to verify the ability of the deployable to withstand the shock from all sources on the S/C booster combination. Additionally, it is important to measure the shock from the deployable's own separation devices as it might affect other parts of the spacecraft. New classes of release devices using paraffin, nitinol and other materials to release or pull pins are producing lower shock inputs. With more experience and design improvement, it may become an acceptable practice to eliminate shock tests for inputs from these low shock devices.

### THERMAL TEST

The thermal vacuum deployment test is one of the most perceptive of tests for revealing problems with manufacture, assembly or design of deployables. Additionally, it is the environment which creates challenges to operations during and after deployment. The colder temperatures and thermal gradients affect the friction in joints, bearings, and other interfaces. It creates larger damping and resistance coming from wiring and thermal protection blankets. Special pull away heaters and cooling shrouds are designed, if necessary, to create the proper temperature and gradients in the MMA portions of the deployable structures for functional deployment tests. At the vehicle level, a thermal balance test, which augments and validates the detailed thermal analysis, is usually combined with thermal vacuum. Pass criteria depend not only on survival and operation of each equipment within specified temperature limits, but also on correlation of the test results with theoretical thermal models.

### ACCELERATED LIFE TEST

For deployables with significant duty cycles over long life, such as solar array gimbals, accelerated life testing is necessary and performed normally in a thermal vacuum environment. Life tests for systems with wet lubrication systems are difficult to accelerate since changes in speed changes the character of the lubrication regime. The lubrication film is also time and gravity vector sensitive for storage considerations with creep and degradation a factor. Another area of study and concern is the different effects one g versus zero g has on debris accumulation in bearing areas.

### GRAVITATIONAL CONSIDERATIONS

For small light compact deployables or mechanisms the earth's gravity is normally secondary to vacuum and thermal effects. These types of systems may not require special gravity off load devices.

Small compact mechanisms such as gearboxes can sustain the one g environment without damage but their performance may be degraded by additional friction forces generated in bearings and other moving components. In all cases of this nature at least one test should be performed with a one g off load to evaluate its effect on performance. If the load relief does not provide a significant improvement in performance, then tests may be performed in one g without off loading with reasonable confidence that the results will be realistic.

However, there are many situations adversely affecting the deployment or operational dynamics which may require gravity off loading during deployment or deployed state testing. Bearing friction or binding of pivots due to loads or large deflections may be excessive. Flexible and rigid body motions out of the horizontal plane can add or subtract potential and kinetic energy. Modal properties may change for the lower frequency systems. The gravity induced loads may be too large for structural integrity. For all of these and other reasons,

emphasis must be placed on the design of special support structure to make the gravity influence on these types of systems acceptable.

Depending on the characteristics of the design, different classes of suspension systems can be used to support the devices for the deployment event. Some of the more common support devices are shown in Table 2.

For deployment testing, the type of support device used depends on the planarity of the deployment trajectories and the degree of coupling of the flexible body dynamics in the various degrees of freedom. For many planar solar arrays, for example, deployment with the plane of the arrays vertical can be performed with the panels supported from an overhead track [9]. These fixtures must be designed to minimize inertia and friction effects as seen by the test specimen. For very large flexible systems, servo controls of movable fixtures becomes a necessity.

Research and development efforts have recently focused on suspension systems needed for supporting large space structures in ground testing for study of on orbit dynamics and control. The fundamental modes of this class of structures, many of which are deployables, are typically quite low in frequency. The SAFE array flown on the shuttle, for example, had a fundamental cantilevered bending mode of 0.04 Hz. Fundamental frequencies of 0.1 to 2 Hz are common in various classes of these systems.

A general rule of thumb is to have a minimum factor of 5 and preferably a factor of 10 separation between the specimen fundamental mode frequency and the suspension effective frequency. This would mean, for example, that a suspension system with a 0.1 Hz "mode of suspension" could be used to support a system with a 1 Hz fundamental. However, there are other dynamic interaction effects, such as added inertia and damping, from the suspension that must be addressed as well.

Pendulum cables have been used extensively for structures which have uncoupled planar modes and can be meaningfully tested in the horizontal plane. For low frequency structures the height from which the cable is hung must be large, which limits the available facilities. For example, to attain a pendulum frequency of 0.1 Hz requires a height of 25 m.

For structures where horizontal plane testing is not appropriate, suspension systems are needed which will have minimal interaction in studying control-structure interaction or during modal testing. The suspension devices must be distributed to unload joints and reduce gravity induced loads and stiffness changes in the test article. The stiffness, inertia and damping forces from the suspension system should have minimal influence on the dynamic properties of the test article. The main emphasis in the past has been to develop low stiffness while being able to support the specimen weight. Inertia and damping effects from the suspension can be equally important. An example pointed out in reference 10 is the use of helium filled balloons to support the test article. While vertical stiffness is small the mass added can never be less than 16% of the supported mass. Also, the balloon system is difficult to properly model in attempts to try to remove its influence analytically from dynamic test results.

Even with this "soft suspension" approach, many suspension systems have higher frequency modes that can couple or interfere with the validity of the modes of the system being tested. For this reason, it is desirable to understand the effects of the suspension through analysis and test of the suspension system itself. Many of these systems can have their own dynamic characteristics readily modified to help reduce coupling effects.

Two types of devices which allow minimally restrained dynamics in all directions have recently been studied by NASA [11] for use in suspending low frequency structures. They were initially designed to accommodate a range of 20 to 135 Kg each, provide suspension frequencies of about 0.1 Hz and allow vertical travel on the order of 7.5 cm. One is a passive device called the zero-spring-rate mechanism (ZSRM) [12]. The other is a hybrid pneumatic/electromagnetic active device referred to as P/ESD [13]. The P/ESD device has recently been extended to support 227 Kg with a vertical frequency of 0.1 to 0.2 Hz, a breakaway friction under 1 gram, a stroke of 15 cm and an inertia addition of 2.7 Kg-m [10].

For modal testing of some systems, an approach which helps alleviate interaction of the suspension system is to attach at the nodal points of the particular mode being sought.

For systems where ground testing is not practical or needs validation, aircraft flying zero gravity parabolic flight paths are often used. This is also a way to validate ground test suspension systems by comparing air flight with ground test results. Aircraft such as the NASA Johnson Space Center KC 135 turbojet transport KC 135 (test section is 2x3x18 m) and the French Centre National d'Etudes Spatiales Caravelle 6R (test section is 2x3x12 m) can provide 25 to 30 second time intervals of acceleration environments of 0.01 to 0.1 g for about 40 events per flight. The size of the specimen being tested may limit the actual free float times to less than the 25 seconds because of impacts with sides of the test section. For example, a 2 meter truss might experience 6 to 12 seconds of free-float time before encountering part of the cabin structure. Additionally, unless it can sustain 2 g's vertical acceleration without damage, it will have to be supported quickly upon pull-up in the flight trajectory. Numerous systems have been tested on these aircraft [14,15].

#### AERODYNAMIC CONSIDERATIONS

Aerodynamic forces created by the structures movement during the deployment functional tests can be significant for large area, light weight deployables. This effect sometimes must be reduced to acceptable levels through use of vacuum chambers, helium tents, replacement of panels with open frameworks or other means.

For some spinning satellites the forces created by air on deployables such as solar arrays can affect the proper balancing and determination of the mass properties. To save the cost of using vacuum chambers, techniques such as use of helium tents to reduce gas loading and to allow hands on operations through the covering are being assessed [16].

#### INERTIAL CONSIDERATIONS

Representative inertia properties are important to simulate proper dynamics and loads. To simplify functional tests of deployables with small flexible body effects, inertia simulators are sometimes used. These simulators are usually driven through a high ratio gear train to allow compact and light masses or inertia to be driven. This can allow a compact and automated test setup and allow placement in smaller environmental chambers.

If the deployment or retraction is sufficiently slow and inertial forces created by motions of the base of the deployable are small, inertia effects may become second order compared to damping in ascertaining the functionality of the design. Hence, if gravity adversely interacts with the deployment of the actual system, mass that is involved with non structural weight can be removed to lessen the effect of gravity. For example, in

one case retractions of a flexible solar array with membrane mounted solar cells failed during zero g parabolic maneuvers in an aircraft. The solar cells and kapton membrane were replaced with a light membrane for ground based studies and the retraction mechanisms redesigned. Once everything was working properly, the real array panels were reflown in the aircraft and successfully retracted [17].

#### DAMPING CONSIDERATIONS

In order to control rates of deployment for systems which use stored energy from springs or deformed structures, discrete dampers are used. Damping from these devices can be set based on the needs of the deployment.

On the other hand inherent damping of both stowed and deployed structure is difficult to determine. This damping is sensitive to environment, amplitude of motions, type of modal test excitation used and other effects. In the stowed configuration, modal testing is normally performed in ambient conditions. Although practices do vary, seldom is damping from the modal test used directly in the ascent loads and response analyses. On occasions where modal damping in critical modes is less than 1%, a lower value is used. But, normally 1% critical, or an established schedule based on experience, is used for the spacecraft or major assembly modes for ascent loads analysis.

Most deployables have joints and interfaces which contribute significantly to the damping. Damping, which may be nonlinear in orbit anyway, is influenced in these classes of structures in ground testing by air, gravity, temperature and other factors. Inherent damping is probably the characteristic of a deployable structure most difficult to determine, model and control. The normal approach is to try to set or determine a lower bound on damping and design to that value where necessary. This of course depends on whether or not use of a lowest value is conservative. For satellites with high precision mission needs or with large low frequency deployables, the modal characteristics, including damping, drives much of the control system design. Higher damping tends to help control system design and improve on orbit performance. Figure 2 shows modal damping properties in the first mode of a deployable solar array boom. The damping characteristics are representative of many deployable truss booms. They demonstrate very low damping at very low displacements and velocities and the damping transitions to much higher value at higher displacement and velocity values. This particular boom was used on a precision satellite. For assessing structural integrity of the boom for significant maneuver loads a 1% critical damping value was used because the motion levels were sufficiently high. However, for control system design and on orbit performance evaluations, the levels of allowed array motion necessitated use of 0.2% critical damping.

Advances in developing and understanding damping treatments, such as viscoelastics, has helped improve the ability to obtain more damping and to model the damping. Shape memory alloys, with thermally or strain induced hysteresis, active actuation of smart materials, and magnetic devices have generated advancements in damping technology. Use of this damping technology is starting to offer opportunities to add (or actively adapt), model and test for damping and its nonlinear properties.

#### PERFORMANCE TESTS

Tests are performed to assess the operational performance of a spacecraft when feasible. Examples of performance issues are pointing, jitter or those resulting from reflector or mirror surface changes. The deployables may operate and

induce responses in the spacecraft/deployable combination or operations within the spacecraft can excite the deployable dynamics which then can affect the spacecraft performance. In addition the dynamics created by the space environment, such as rapid thermal changes, can excite the deployables and affect the performance.

One performance issue of interest are thermally induced responses of deployables as they enter and exit the earth's shadow. From earlier days when the Transit satellite gravity gradient booms caused wobble in this navigational satellite to more recently when the Hubble Space Telescope solar arrays caused pointing and jitter disturbances, this rapid thermal gradient change has caused problems. These problems normally occur in appendages that have low frequency modes. Many of these flexible deployables are difficult to test as a complete system on the ground because of gravity effects and thermal vacuum chamber size limitations. Much attention has been focused on designing to prevent thermal snap issues through use of low coefficient of thermal expansion materials, active and passive damping and thermal control techniques. For deployables where it is not possible to test as a whole, such as large solar arrays to be used on precision spacecraft, testing to determine structural/thermal properties may be performed on elements of the design. These properties are used in analysis, along with verified dynamic/thermal models, to predict the deployable and system response to thermally induced response issues.

Rotating and maneuvering antennas, tracking of the sun by solar arrays and numerous other activities and on board disturbances can cause operational performance issues and must be addressed by analysis and test combinations. The total system with deployables can not be always be operated with good simulation because of gravity and seismic influences, or facility size restrictions. For these situations, alternate approaches are sometimes used such as exciting the spacecraft without deployables at the deployable spacecraft interface. The forces and moments used for exiting the system are developed from bench and subsystem tests on the drive mechanisms and actual deployable or its dynamic simulation.

#### FLIGHT TESTS

Space flight tests of deployables are performed for different reasons. Some structures can't be supported in one g in such a way as to give confidence that its dynamic characteristics are known well enough under on orbit environmental influences to predict on orbit performance. Another reason is to prove a successful deployment where size or complexity doesn't allow adequate ground based testing. Other reasons might be to use flight to prove that certain ground based approaches are working and can be applied to a broad category of similar structures. Anomalies in flight might dictate special tests to assess the probable cause and solutions. The Solar Array Flight Experiment (SAFE) in part was performed to study the deployment and deployed dynamics of a large low frequency solar array [18,17]. The Middeck Active Controls Experiment (MACE) [19] is currently planned to fly in 1995 to study not only advanced control algorithms for a 2 Hz main body with multiple slewing payloads but also for comparisons to see if new advanced ground based levitation systems can properly off load gravitational effects. The Hubble Space Telescope was having undesirable disturbances coming from its solar arrays responding to rapid thermal gradient buildups at entry and exit from the earth shadow. To help track down and understand the cause and explore possible solutions, a dynamic test was run on the vehicle in orbit. The reaction wheel torque was shaped to

best excite the fundamental modes and the gyro outputs were used to determine modal frequency and shape information.

#### COMBINING ANALYSIS AND TEST

Advancements in analytical tools combined with testing can improve the confidence and decrease risk in complex testing situations where ground base testing may not be feasible or cost effective to completely cover all issues. One approach is to test segments or pieces of a complete structure and then combine the models analytically to predict the all up system characteristics and performance. Another is to use dynamic scale models for tests and demonstrate the ability to predict and then use those analytical techniques for the full scale system. References 20 and 21 discuss activities in scale model work addressing large space structures issues.

Another approach is to demonstrate the ability to accurately predict in the influence of the test environment and then use analysis to cover the effects of the differences between test and space environments. An example of this approach is the use of recent improvements in multiple/flexible body dynamics analysis software and methods. These tools, along with faster computers, have allowed complex deployment problems to be solved with reasonable accuracy at reasonable cost and schedule. Reference 23 discusses some of these multibody dynamics tools.

Analysis and test on a 5.7 x 5.3m Wrap-Rib antenna illustrates the ability of new multibody dynamic methods and software to accurately predict very complex system motions and loads. This analysis ability decreases the risk of not having a test in zero g, or with gravity off loading, by using a combination of analysis and test in a one g environment. This elliptical parabolic reflector is comprised of 16 curved ribs of eight different lengths with C section cross section aluminum ribs used to form the foundation for a mesh surface. The ribs store strain energy when wrapped around a cylindrical hub with their C section flattening. The flattened C section ribs initially start deploying almost simultaneously, pulling the mesh out when doors holding them spring open. Each rib has a locking hinge at its base so that when it rotates around where the rib base is perpendicular to the hub then that hinge locks. The ribs, being of different lengths, bunch up and contact each other during deployment. Only when mesh is in tension does its stiffness restrain the ribs. When the ribs lock up, their deployment energy is partially absorbed by a two stage crushable honeycomb load absorber at the hub of the antenna. The analytical problem, which was solved with a code called DYNACON [22] (not commercially available), is highly nonlinear and computationally intensive, taking about 3 hours of CRAY YMP CPU run time for the coverage of 4 seconds of the deployment event. The antenna design prevents use of any kind of suspension system to the ribs to offset gravity during its deployment in a vacuum chamber. Bench tests, for input to the analysis, measured properties such as stiffness versus displacement or load for the ribs, mesh, load absorber and other components.

Figure 3 shows a comparison with test that resulted from the multibody deployment analysis for loads at the base of the boom supporting the antenna. Good comparisons between analysis and test with gravity effects modeled were obtained. With this comparison, the decision was made that analysis of the zero g environment event could be accepted for loads and response determination without the cost of a flight test.

#### TECHNOLOGY IMPROVEMENTS

There are numerous technology improvements that could make testing of deployables simpler and less costly, taking the designs



more robust. One of the more exciting and promising is the breadth of possible applications of smart materials. Designs with shape memory alloys to replace hinges, joints and gimbals will be simpler, more linear or predictable and more robust. Actuators used for reconfiguring and reorienting deployables can be made from smart materials. This approach can allow controlled deployments without dampers and other devices. Various low shock release devices using paraffin or shape memory materials reduce loads and can remove the need to test for some shock events.

Smart materials, such as piezoceramics, provide sensing for health monitoring to allow integrated measurements from ground through life in orbit. Active controls and smart materials can be applied to levitation devices to reduce interaction between the supports and the specimen for one g testing. Smart actuation, both static and dynamic built into the deployable design, can be used to modify properties, such as modal characteristics and to remove nonlinearities. This will allow tests to only show results within bounds on characteristics rather than having to have accurate test results. The active and adaptive devices will adapt the system to the desired characteristics. Precision structures especially will benefit from this approach. Smart materials will allow damping larger than inherent damping on many of the classes of structures. This approach will make prediction and test correlation easier and damping values assumed for design less conservative.

Miniaturization of electronics is also making promising strides in directions of benefit to testing and performance. Sensors which can measure acceleration, stress, temperature, pressure and other characteristics along with the necessary electronics, software and memory are being placed on small silicon chips. This will not only allow wide spread, lightweight inexpensive sensing, but will benefit data gathering without burdening the specimen with significant additional mass. Test consoles for electronics test and for structural/mechanism test are benefiting from the advances in computers and software. This results in lower cost and greater versatility in test consoles. The consoles and supporting software allow easy adaptation to the particular test requirements. Faster computers and improved analysis methods are allowing faster test assessments and model correlation to occur, allowing test configurations to spend less time in the test labs.

#### FUTURE DIRECTIONS

The increased commercialization of space will undoubtedly change the way testing is performed. There will be greater emphasis on cost and schedule. The prevailing perception seems to be that analysis is cheaper than testing and it may be worth taking the higher risk of doing less testing. Development tests will be reduced and greater reliance placed on modeling and simulations. There will be fewer projects with qualification test units, with qualification test philosophies such as protoflight being adopted.

Advances in miniaturization in payloads and sensors and the high cost of booster systems will create an ability and a pressure for many applications to design smaller lighter spacecraft that fly on smaller boosters. Packing lighter satellites into smaller volumes or placing multiple spacecraft on larger boosters will create less real estate for packaging. With these smaller lighter systems with tighter packaging there may occur more deployable structures with more joints and interfaces. And even though the deployables may be smaller in size they will still be designed to as low an allowable weight as possible leading again to design and testing issues with low frequency appendages.

Large space structures, such as the Space Station Freedom, will require testing of large deployables. Many of these systems cannot be tested as one piece on the ground. Space flight experiments, scale model tests, testing pieces and interfaces and combining analytically, and other approaches will be used to gain confidence in the reliability and functionality of these large systems.

#### REFERENCES

1. Mikulas, Jr., M.M. and Thomson, M., "State of the Art and Technology Needs for Large Space Structures, Chapter 3, Vol. 1, Flight-Vehicle Materials, Structures, and Dynamics-Assessment and Future Directions, 1993.
2. Hinkle, K. (Contact), "Spacecraft Deployable Appendages", Goddard Space Flight Center, Engineering Directorate, May 1992.
3. Gibb, J., "MILSTAR's Flexible -Substrate Solar Array-Lessons Learned", 26th Aerospace Mechanisms Symposium, May 13-15, 1992, pp. 35-243.
4. Peterson, L.H. and Guthrie, F. E., "A Comparison of Environmental Results on a NASA and SAMSO Program", Proceedings of the 3rd Aerospace Testing Seminar, The Institute of Environmental Sciences, The Aerospace Corp., Los Angeles, CA, 1976.
5. Carrier, J. A. and Pedretti, C. D., "A Comparison Between Testing Methods, MIL-STD-1540A, NASA and Commercial", Proceedings of the 3rd Aerospace Testing Seminar, The Institute of Environmental Sciences, The Aerospace Corp., Los Angeles, CA., 1976.
6. Pinson, L.D., "Inertial Effect of Air Between Two Vibrating Plates in Close Proximity", Aerospace Technical Memorandum ATM 79(4403-01)-25, Aerospace Corporation, June 27, 1979.
7. Wada, B. K., "Structural Qualification of Large Spacecraft", AGARD Conference Proceedings No. 397, Mechanical Qualification of Large Flexible Spacecraft Structures, Sept. 9-13, 1985.
8. Wijker, J.J., "Acoustic Effects on the Dynamics of Lightweight Structures", AGARD Conference Proceedings No. 397 on Mechanical Qualification of Large Flexible Spacecraft Structures, Sept. 9-13, 1985.
9. Chung, D.T., "Deployment/Retraction Ground Testing Of a Large Flexible Solar Array", 16th Aerospace Mechanisms Symposium Proceedings, NASA Conference publication 2221, May 13-14, 1982, pp. 249-262.
10. Kienholz, D.A., "Defying Gravity with Active Test Article Suspension Systems", Sound and Vibration, April 1994.
11. Cooley, V.M. and Giunta, A.A., "Laboratory Evaluation of Two Advanced Suspension Devices for Ground Vibration Testing of Large Space Structures", Presented at the 33rd Structures, Structural Dynamics and Materials Conference(part 1), Dallas, TX, April 13-15, 1992.
12. Gold, R., Friedman, I., Reed III, W. and Hallauer W.L., "Suspension Systems For Ground Testing of Large Space Structures", NASA Contractor Report 4325, Oct. 1990.
13. Kienholz, D.A., Crawley, E.F. and Harvey, T.J., "Very Low Frequency Suspension Systems for Dynamic Testing", Proceedings of the 30th Structures, Structural Dynamics and Materials Conference (part 1), Mobile AL, April 3-5, 1989, pp. 327-336.
14. Chung, D.T. and Young, L.E., "Zero Gravity Testing of Flexible Solar Arrays", 15th Aerospace Mechanisms Symposium, May 14-15, 1981, pp. 115-136.
15. Swanson, A. D., Yuen, W. and Pearson, J., "Zero-Gravity Dynamics of Space Structures in Parabolic Aircraft Flight", First Joint US/Japan Conference on Adaptive Structures, Nov. 13-15, 1990, Maui, Hawaii, pp. 952-965.
16. Boynton, R., Bell, R. and Wiener, K., "Using Helium to Predict the Mass Properties of an Object in the Vacuum of

- Space", Paper No. 2024, 50th Annual Conference of the Society of Allied Weight Engineers, Inc., May 1991.
17. Elms, R.V. and Young, L.E., "SEP Solar Array Development Testing", Proceedings of the 14th Intersociety Energy Conversion Engineering Conference, Boston, Mass., Aug. 5-10, 1979, pp. 1273-1277.
  18. Elms, R.V., Hill, H.C. and Young, L.E., "Solar Array Shuttle Flight Experiment- Hardware Development and Testing", 16th IEEE Photovoltaic Specialists Conference, 1982, pp. 25-30.
  19. Miller, D., Sepe, R., Saarmaa, E. and Crawley, E., "The Middeck Active Control Experiment(MACE)," Fifth NASA/DOD Control Structure Interaction Technical Conference, Lake Tahoe, NV, March, 1992.
  20. Kvaternik, R.G. and Hanks, B.R., "Research on the Structural Dynamics Verification of Flexible Spacecraft", NASA Langley Research Center, Hampton, Va.
  21. Gronet, M.J., Crawley, E., and Allen, B.R., "Design, Analysis and Testing of a Hybrid Scale Structural Model of a Space Station, 30th Structures, Structural Dynamics and Materials Conference, Mobile, AL., April 1989.
  22. Banerjee, A. K., "Block Diagonal Equations for Multibody Elastodynamics with Geometric Stiffness and Constraints", Journal of Guidance, Control and Dynamics, Vol. 16, No. 6, Nov.-Dec. 1993, pp. 1092-1100.
  23. Haug, E.J., "Dynamics of Articulated Structures", Flight Vehicle Materials, Structures and Dynamics, Assessment and Future Directions, Structural Dynamics and Aeroelasticity, Vol. 5, 1993, pp. 45.
  24. Johnson, M.R., "The Galileo High Gain Antenna Anomaly", 28th Aerospace Mechanisms Symposium, May 18-20, 1994, pp.359-377.



**MOVING MECHANICAL ASSEMBLY FAILURES**

| <b>Program</b>                  | <b>Problem</b>  | <b>Cause</b>   |
|---------------------------------|---|--|
| Program 461(1964)               | Solar array failed to deploy fully  | Mishandling during stowage   |
| STP 67-2(OV2-5)<br>#(1968)      | Solar array booms<br>failed to deploy fully   | Field modification problem   |
| 777(1970)                       | Omni-antenna latch broke during spin-up   | Attitude control instability   |
| Program A(1971)                 | Antenna failed to deploy fully  | Wire harness binding   |
| Program B(1971)                 | Solar array deployed late   | Silicon rubber sticking  |
| STP 71-5(1972)                  | Boom not deployed   | Dynamic clearance problem  |
| SKYLAB(1973)                    | Solar array failed<br>to deploy   | Interference with cabling<br>or thermal blankets                       |
| Transit (1975)                  | Solar array failed<br>to fully deploy<br>;cable hung up   | Anomalous flat trajectory<br>caused high heating rates                 |
| VIKING(1975)                    | Sampling arm failed to deploy   | Debris in gear train   |
| STP 74-1<br>(SOLRAD)(1976)      | Solar panel failed to deploy  | Release mechanism binding  |
| DMSP-F-1(1976)                  | Solar array failed to deploy fully  | Excessive wire harness stiffness                                       |
| DMSP-F-2(1977)                  | Solar array delayed release   | Friction Welding   |
| Voyager 2(1977)                 | (1) Science boom failed to fully deploy<br>(2) Scan platform gearbox seized<br>(3) Magnetometer boom Misalignment | (1) Microswitch failed<br>(2) Lubricant failure<br>(3) Unknown         |
| SEASAT(1978)                    | Spacecraft power<br>failed  | Slip ring debris between<br>power and ground rings                     |
| APPLE(1981)                     | Solar Array failed to deploy  | Failure of deployment device   |
| DE(1981)                        | Sensing antenna failed to deploy  | Unknown  |
| INSAT1(1982)                    | Solar sail failed to deploy   | Unknown  |
| ERBS(1984)                      | Solar array failed to deploy  | Thermal binding  |
| GLOMR(1985)                     | Spacecraft failed to<br>separate from orbiter   | Canister door did not<br>open fully                                    |
| VUE(1988)                       | Telescope failed to<br>rotate about azimuth   | Inadequate torque margin<br>on azimuth caging arm                      |
| GALILEO(1989)                   | High gain antenna failed to deploy  | Cold welding in ball and socket joint                                  |
| GALILEO(1989)                   | Instrument cover jettisoned late  | Thermal binding  |
| MAGELLAN(1989)                  | Solar array failed to latch at end of travel  | Microswitch misadjusted  |
| MACSAT(1990)                    | Gravity-gradient boom failed to deploy  | Inadequate force margin  |
| CRRES(1990)                     | Magnetometer boom<br>failed to fully orient   | Interference between thermal blanket<br>velcro and wiring harness      |
| ULYSSES(1990)                   | Spin stabilized<br>spacecraft wobbles   | Antenna boom thermal distortion<br>caused S/C center-of-gravity offset |
| Hubble Space<br>Telescope(1990) | Solar array deployment<br>booms oscillate as S/C<br>goes from shade to sun  | Thermal gradient across<br>boom diameter                               |
| ANIK E2(1991)                   | C-band antenna did not fully deploy   | Thermal blanket interference   |
| Unknown                         | Sampling arm failed to<br>deploy  | Screw backed out and<br>wedged against housing                         |

TABLE 1

(Courtesy of Aerospace Co., Inc.)

## Common devices to support vertical motion:

- Counter weights ( weights, chains ( with lines and pulleys))
- Springs ( linear, negator, and variations with different orientations to get zero spring rate)
- Walking beams
- Balance beams
- Buoyancy ( gases (balloon), liquid(underneath))
- Active electromagnetic/pneumatic devices

## Common devices to support horizontal motion:

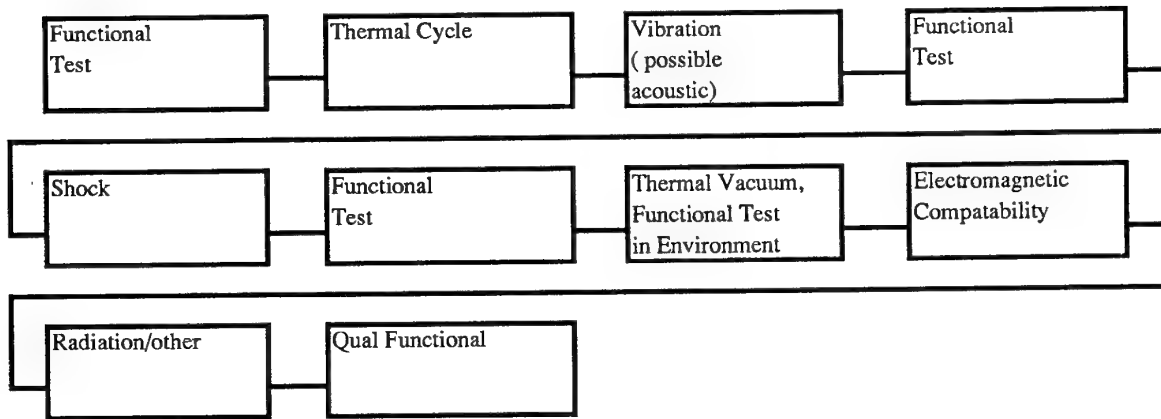
- Low Friction rollers (some with active feedback) and surfaces
- Magnetic
- Flotation (Gases in balloons, liquid float tanks, air cushions)
- Mobiles
- Pendulums (simple, trapezoidal, conical, conical with compression hold off beam)

## Which ones to use are affected by considerations such as:

- which environment does it need to be tested in (vacuum, thermal)
- can it be supported from above or below
- what parasitic stiffness, inertial and damping forces are allowed
- are multiple supports needed and can they be accommodated
- safety of specimen
- cost/schedule
- accessibility
- volume and height of facilities
- range of displacements required
- degrees of freedom of deployment ( i.e. are movements 3 dimensions needed)

Table 2. Suspension Devices for Test Support in 1 g

### Example Qualification Flow for Components/Assemblies



### Example Vehicle Qualification Test Flow

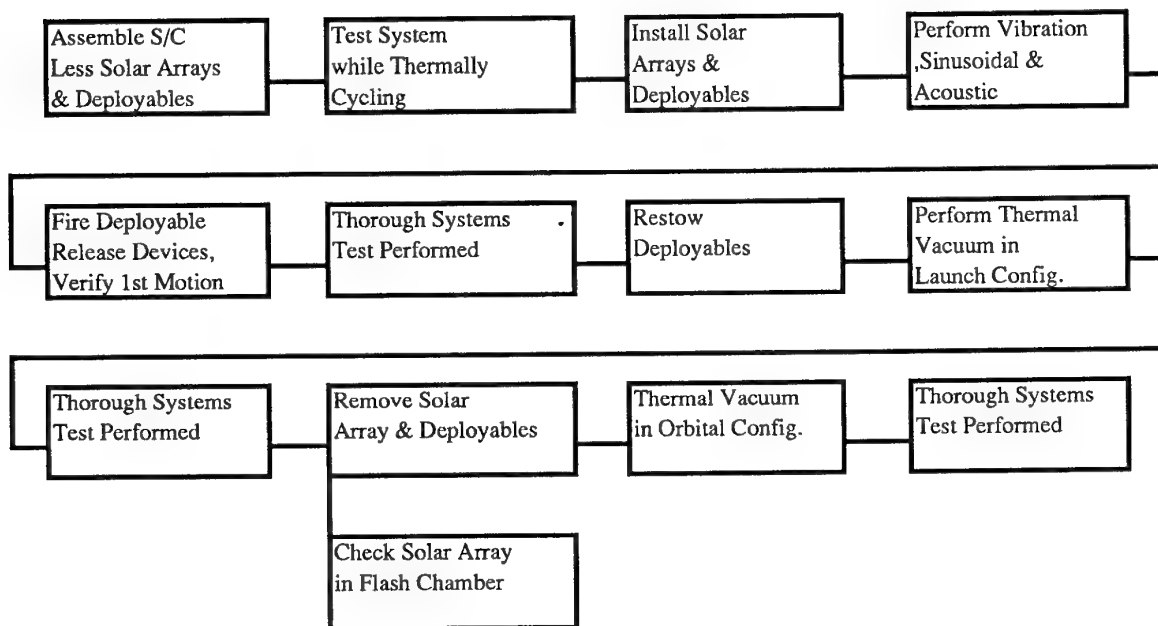


Figure 1

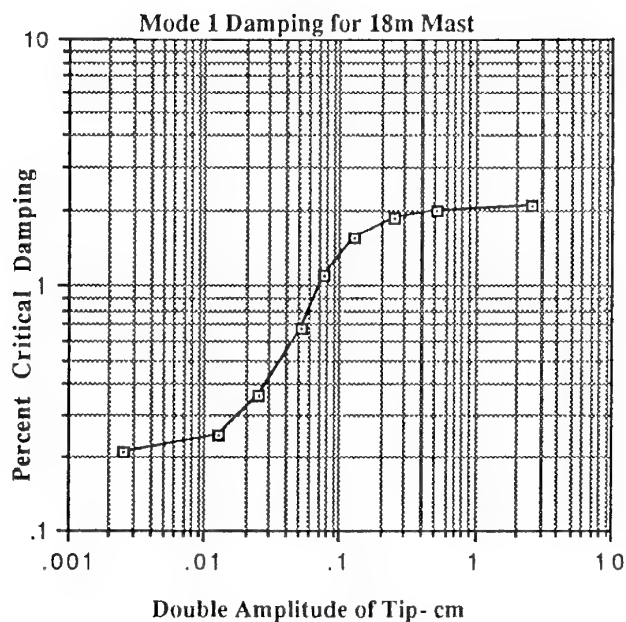
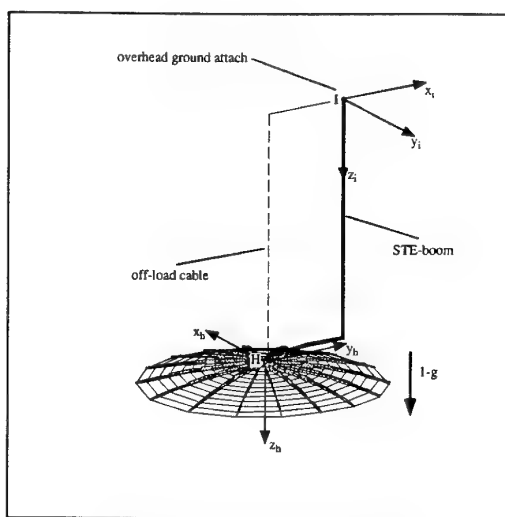
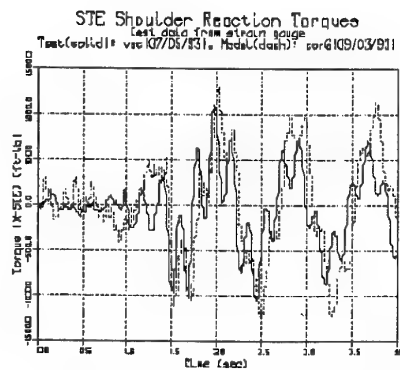
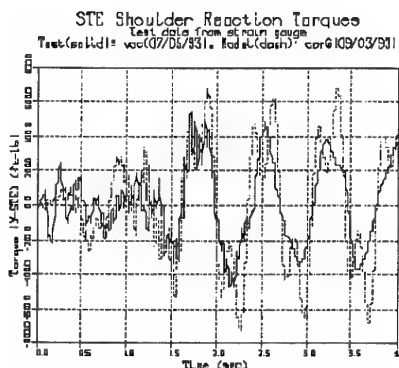
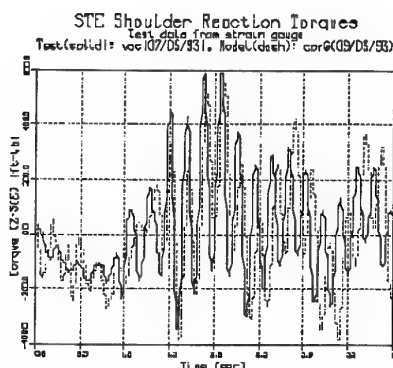


Figure 2



Flight Reflector Test Model

STE Boom Reaction Torque Comparison  
(Interface x-direction)STE Boom Reaction Torque Comparison  
(Interface y-direction)STE Boom Reaction Torque Comparison  
(Interface z-direction)

Comparison of Bending Moments at Boom Shoulder - Deployment Test vs Analysis

Figure 3

# Active Structures for Vibration Suppression and Precision Pointing

Professor André Preumont  
 Université Libre de Bruxelles  
 Prof. of Mechanical Eng. & Robotics  
 Serv. construct. mécaniques, CP165,  
 50, avenue Franklin Roosevelt  
 1050 Bruxelles  
 Belgium

## Abstract

This paper describes the work performed at *ULB* for the development of active structures for space applications, using the piezoelectric technology. The control strategy involves two embedded control loops. The inner loop consists of a decentralized active damping using colocated actuator-sensor pairs and control schemes with guaranteed stability properties. The outer loop consists of a pointing or position control using non-colocated actuators and sensors. Two examples of active damping are presented: a truss with linear actuators and a plate with piezo strips. Next, a position control is developed for the truss. The control law is derived from the *frequency-shaped LQG* methodology, using a simplified model of the actively damped structure; the bandwidth of the control system includes the first two flexible modes of the structure. It is demonstrated that the active damping improves substantially the performance and the robustness of the position control loop, inside and outside its bandwidth.

## 1 Introduction

The spacecrafts are subjected to a variety of thermal, static and dynamic perturbations. The former, of very low frequency, arise from the time varying exposure to the sun during the orbit, while the dynamic loading is produced by attitude control rotating wheels or thrusters, antenna pointing mechanisms, pumps, changes of configuration of the solar pannels or other pointing instruments. Dynamic loads may also result from human activity, the docking of other spa-

cecrafts, or unexpected phenomena like the thermoelastic instability recently observed on the solar pannels of the Hubble space telescope.

In spite of these perturbations, it is essential to maintain the pointing or the shape of the instruments with very high accuracy (e.g. the line of sight of an optical communication terminal or of an antenna, the shape of the primary mirror of a telescope).

Because of the wide variety of perturbations, the ever more stringent operating specifications in terms of bandwidth and pointing error, one can anticipate that active structural control will play a major role in future space technology.

On the other hand, the thermal environment in space may induce substantial changes in the stiffness properties of the flexible appendages of the spacecrafts. This results in large parametric variations which are difficult to predict (ground tests of large structures are often impossible) and which must be accommodated by the control system.

Robust control is difficult to achieve, particularly when the pole-zero pattern is subject to major changes (e.g. pole-zero flipping [1]). The situation is substantially more comfortable if the actuator and sensor are *colocated*, because in this case, the poles and zeros (of an undamped structure) alternate on the imaginary axis [1,2]. This useful property is used whenever possible, in particular for active damping.

The robust control of a lightly damped flexible structure is best achieved by a mixture of active damping and model-based control. This approach is often referred to as *HAC/LAC* (*high authority control / low authority control*) [3]. The control system consists of two loops as shown in Fig.1. The inner loop uses a set of co-

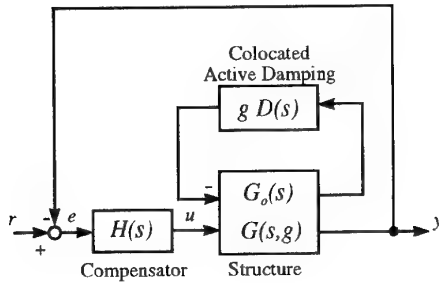


Figure 1: Dual loop position control.

located actuator-sensor pairs for decentralized active damping with guaranteed stability properties; the outer loop uses a model of the actively damped structure. This approach has the following advantages:

- The active damping extends outside the bandwidth of the control system and reduces the settling time of the modes which are outside the bandwidth.
- The active damping makes it easier to stabilize in gain the modes outside the bandwidth of the outer loop (improved gain margin).
- The damping of the modes within the controller bandwidth makes them more robust to the parametric uncertainty (improved phase margin).

## 2 Active damping

### 2.1 Generalities

As already stressed in the introduction, the use of colocated actuators and sensors leads to an alternating pole/zero pattern, on the imaginary axis if the structure is undamped, or slightly in the left half plane if the structure is lightly damped. Thanks to this property, a number of active damping schemes with guaranteed stability have been developed and successfully tested with various types of actuators and sensors (e.g. [4-8]). They can be implemented in a decentralized manner, with each actuator interacting only

with the colocated sensor. In this case, the control system consists of independent *SISO* loops, whose stability can be readily established from the root locus of

$$g D(s) G_0(s) \quad (1)$$

where  $G_0(s)$  is the structure transfer function between the actuator and the colocated sensor,  $D(s)$  is that of the active damping scheme, and  $g$  is the scalar gain.

For practical implementation purposes, however, one should be careful that  $D(s)G_0(s)$  has enough roll-off at high frequency, to accommodate the actuator and power amplifier dynamics and the inevitable phase lag due to sampling. This implies that some roll-off should appear in  $D(s)$  if there is a feedthrough component in  $G_0(s)$  (which often occurs in colocated systems). Nearly colocated systems may sometimes be preferable to strictly colocated ones, to suppress the feedthrough component in  $G_0(s)$  while preserving the interlacing property in the frequency band where the active damping is significant.

It is also important to note that guaranteed stability does not imply guaranteed performance of the control system. Good performance requires the proper sizing and location of the actuators and sensors, to achieve good controllability and observability. This will be reflected by well separated poles and zeros of the open loop system, leading to wide loops in the root locus plot (Fig.3).

### 2.2 Truss structure

Consider a truss structure where active members have been substituted to some of the bars (Fig.2). If the stiffness of the active members is chosen to match that of the bars they replace, the structural properties of the system (natural frequencies, mode shapes) remain almost unaffected. Each active member consists of a linear piezoelectric actuator colocated with a force sensor. The input of the system is the piezoelectric extension  $\delta$  which, if one neglects the hysteresis of the piezoelectric material, is proportional to the applied voltage. The structural response can be evaluated by treating the piezoelectric extension  $\delta$  as an equivalent piezoelectric force (as for thermal deformations):

$$p = K_a \delta \quad (2)$$

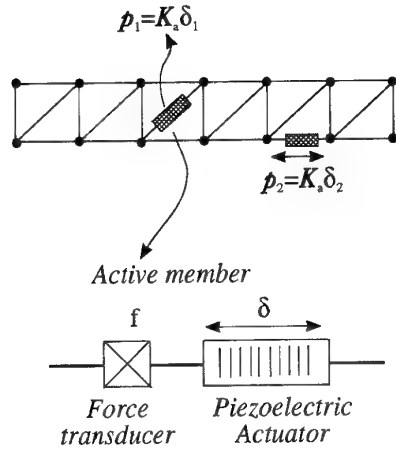


Figure 2: Truss structure with active members consisting of a linear piezoelectric actuator and a force transducer.

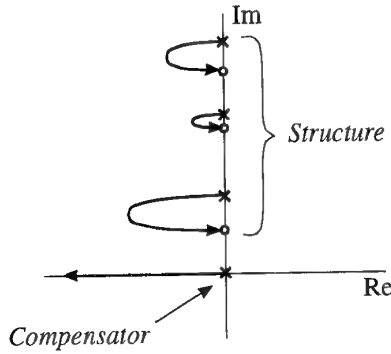


Figure 3: Integral force feedback.

where  $K_a$  is the stiffness of the active member.

The equation of motion of the undamped system is

$$M\ddot{x} + Kx = Bp \quad (3)$$

where  $B$  is the influence matrix of the active bar (its elements are the directional cosines of the active member). The output force is proportional to the elastic extension of the active member, equal to the total extension  $B^T x$  minus the piezoelectric extension  $\delta$ .

$$f = K_a(B^T x - \delta) \quad (4)$$

The fact that the same matrix  $B$  appears in Equ.(3) and (4) is due to colocation.

In the *SISO* case,  $f$  and  $\delta$  are scalar quantities and it can be shown [7] that the open loop

transfer function of the undamped structure can be expanded as

$$G_0(s) = \frac{F(s)}{\delta(s)} = K_a \left\{ \sum_{i=1}^n \frac{\nu_i}{(1 + s^2/\omega_i^2)} - 1 \right\} \quad (5)$$

where the sum includes all the modes. The residues  $\nu_i \geq 0$  are the *modal fraction of strain energy in the active element*. Note that

(i)  $\nu_i$  can be regarded as an index of control authority on the various modes of the structure (they are readily available from finite element programs).

(ii) Truncating the modal expansion in Equ.(5) may lead to a substantial error on the location of the zeros of  $G_0(s)$  (and therefore on the estimation of the performance of the closed loop system). To avoid that, one must include the static contribution of the high frequency modes:  $G_0(s) \simeq$

$$K_a \left\{ \sum_{i=1}^m \frac{\nu_i}{(1 + s^2/\omega_i^2)} + \sum_{i=m+1}^n \nu_i - 1 \right\} \quad (6)$$

It is not difficult to establish from the above equations that

$$\sum_{i=1}^n \nu_i = \frac{K_a}{K^*} \quad (7)$$

where  $K^* = (B^T K^{-1} B)^{-1}$  is the stiffness of the structure seen from the active element. From this result, one can evaluate the contribution of the high frequency modes to Equ.(6) without knowing their  $\nu_i$ .

Notice that  $G_0(s)$  does have a feedthrough component, which requires some roll-off in the active damping scheme  $D(s)$ . It can be readily seen from the root locus plot that the compensator

$$D(s) = -\frac{1}{sK_a} \quad (8)$$

is always stable. For small gains, it can be shown [7] that the modal damping ratio is approximately

$$\xi_i = \frac{g\nu_i}{2\omega_i} \quad (9)$$

In practice, it is advisable to move slightly the pole of the compensator along the negative real

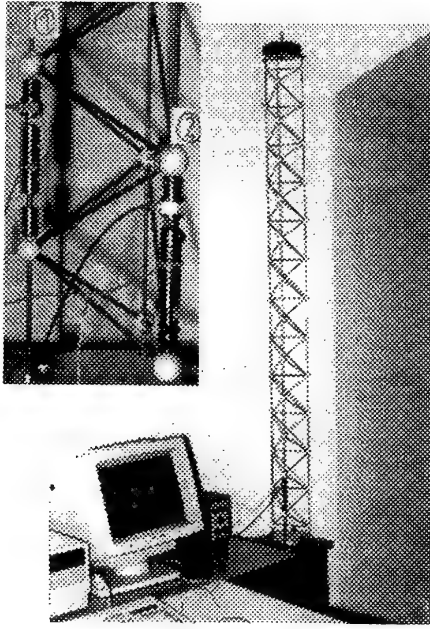


Figure 4: Test structure.

axis; this does not affect the general shape of the root locus but avoids saturation which often occurs with integral control.

The foregoing control scheme has been applied to a 12 bay vertical truss of 1.7 m long (Fig.4), clamped at its base and provided with a tip mass of 2 kg. The lowest bay is provided with two active members. The first four natural frequencies are  $f_1 = 8.8\text{Hz}$ ,  $f_2 = 10.5\text{Hz}$ ,  $f_3 = 58.1\text{Hz}$  and  $f_4 = 88.3\text{Hz}$  (notice the gap between  $f_2$  and  $f_3$ ). The dynamics of the force transducers can be considered as perfect at  $f_1$  and above (at lower frequencies they behave as high-pass filters). With this arrangement, a damping ratio larger than 0.10 has been obtained for the first mode of the structure [7]. By nature, the integral force feedback is less efficient for the high frequency modes.

### 2.3 Plate structure

Piezoceramics can also be used for actuators and sensors on beam, plate and shell structures (e.g.[4,8-12]). The dynamic modelling of the coupled system must include the effect of the ceramics on the mass and stiffness distribution and the piezoelectric effect. The former can be

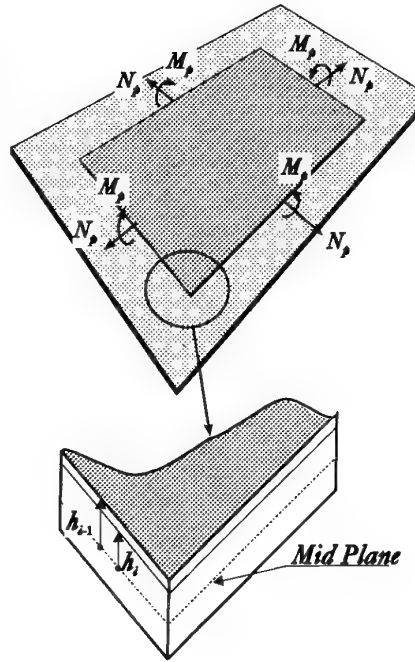


Figure 5: Equivalent piezoelectric loads.

obtained by considering the coupled system as a multi-layer composite material. The application of a voltage  $V$  to the actuator can be represented by equivalent piezoelectric loads as indicated in Fig.5. Assuming the piezoelectric constants isotropic in the plane ( $d_{32} = d_{31}$ ), these loads are given by

$$N_p = \frac{E_p}{1 - \nu_p} d_{31} V \quad (10)$$

$$M_p = \frac{E_p}{1 - \nu_p} \cdot \frac{h_i + h_{i-1}}{2} \cdot d_{31} V \quad (11)$$

where  $h_{i-1}$  and  $h_i$  are the distances of the two electrodes to the mid-plane and  $E_p$  and  $\nu_p$  are the Young modulus and Poisson's ratio of the piezoceramics.

Similarly, assuming that the electrodes of the sensor are connected to a charge amplifier as indicated in Fig.6, the output voltage is given by



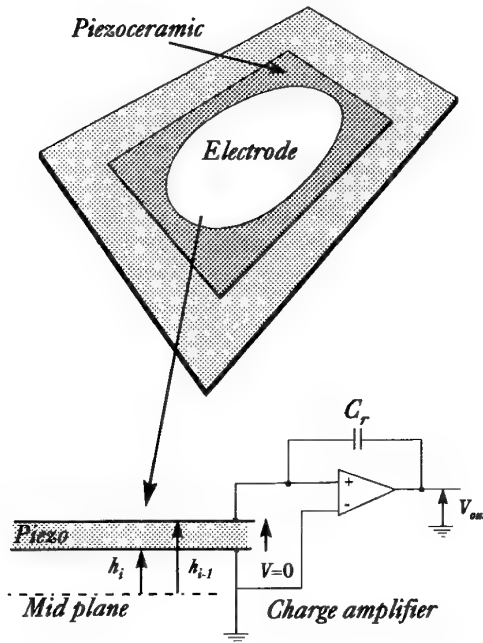


Figure 6: Sensor configuration.

$$V_{out} = \frac{d_{31}}{C_r} \frac{E_p}{1 - \nu_p} \left\{ \int_{\mathcal{E}} (\varepsilon_x^0 + \varepsilon_y^0) dS + \frac{h_i + h_{i-1}}{2} \int_{\mathcal{E}} (k_x + k_y) dS \right\} \quad (12)$$

where  $\varepsilon_x^0$  and  $\varepsilon_y^0$  are the strains of the mid-plane and  $k_x$  and  $k_y$  are the curvatures. The first integral represents the contribution from the membrane strains while the second one is due to bending. The integrals extend over the electrode (the part of the piezo not covered by the electrode does not contribute to the signal).

The foregoing approach is well suited to a finite element implementation. This allows, in principle, to predict the open loop transfer functions of any structure covered by piezoceramics with electrodes of arbitrary shape. Our experience is that it works well for configurations involving non-colocated actuators and sensors. However, when the actuator and the sensor are nearly colocated (e.g. on each side of the plate, or side

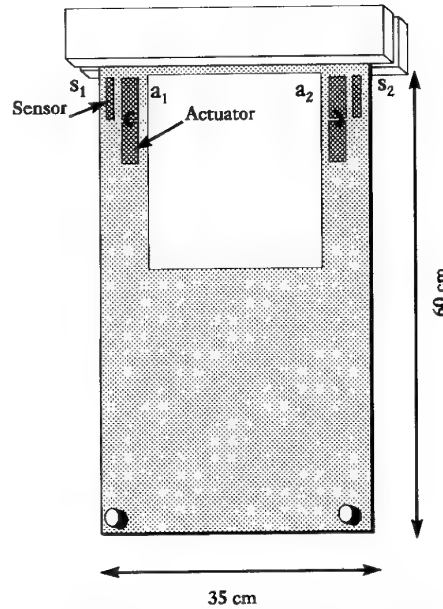


Figure 7: Test structure for the in-orbit experiment.

by side), the feedthrough component is dominated by local effects and the exact location of the zeros is difficult to predict.

The test structure has been developed in preparation of a future in-orbit experiment, in the framework of ESA's Technology Demonstration Program (TDP). The flight model is due to fly in a *GAS* container located on the Shuttle bay, during 1995. The laboratory demonstration model consists of a 0.5mm thick rectangular cantilever steel plate with a large rectangular hole, hanging from the top and provided with lumped masses of 150gr at the bottom corners. The actuators and sensors, made of 0.25mm thick PZT strips, are located as indicated in Fig.7. This very flexible system has a considerable geometric stiffness, which makes it very sensitive to gravity effects. The observed natural frequencies in the lab are  $f_1 = 0.89Hz$  (bending),  $f_2 = 2.33Hz$  (torsion) and  $f_3 = 5.44Hz$  (second bending), and the structural damping is  $\xi \simeq 0.003$ . The predicted natural frequencies in a zero-gravity environment are  $f_1 = 0.509Hz$ ,  $f_2 = 2.156Hz$  and  $f_3 = 5.37$ . As for the truss structure, the active damping has been implemented in a decentralized manner, each sensor interacting on-

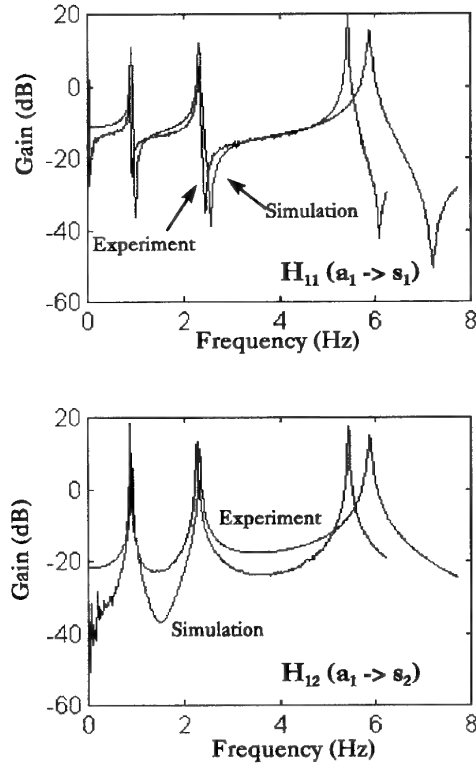


Figure 8: Comparison of predicted and experimental transfer functions.

ly with its nearly colocated actuator; the same compensator is used for both sides.

Figure 8 shows the transfer functions  $a_1 \rightarrow s_1$  and  $a_1 \rightarrow s_2$ ; both numerical and experimental results are displayed. As expected, the colocated transfer function  $H_{11}$  reveals alternating poles and zeros with no roll-off at high frequency [some roll-off is therefore necessary in the compensator  $D(s)$ ]. The error at low frequency is due to the high-pass dynamics of the sensor. The mathematical model tends to overestimate the spacing between the poles and zeros.

The control strategy adopted is the *Positive Position Feedback (PPF)* [4]. The compensator consists of a set of second order filters tuned on the  $n_c$  modes to be controlled:

$$D(s) = \sum_{i=1}^{n_c} g_i \frac{\omega_i^2}{s^2 + 2\xi_i \omega_i s + \omega_i^2} \quad (13)$$

The filter parameters  $g_i$ ,  $\omega_i$  and  $\xi_i$  are tuned to achieve the desired performance in the

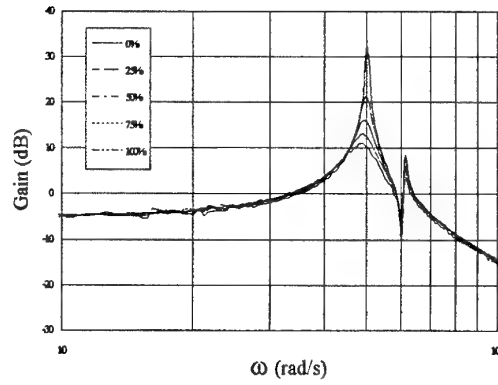


Figure 9: Transfer function  $G(\omega, g)$ .

targeted modes (the first two in this study). When a strong feedthrough component results in very close pole-zero pairs, the performance of the compensator depends critically on the filter frequency and the closed loop poles become more sensitive to parameter uncertainties. This raises an interesting question for the in-orbit experiment: the compensator parameters, tuned from an inaccurate zero-gravity model of the structure, may turn out to be ineffective during flight.

With the foregoing arrangement, a damping ratio larger than 0.10 has been obtained for the two targeted modes.

### 3 Position control

In the first part of this paper, we have discussed the active damping using colocated actuator-sensor pairs and control schemes with guaranteed stability properties; this is often referred to as *LAC* control. We now turn to the *HAC* control, namely model-based control with non-colocated actuators and sensors.

To illustrate this, the truss structure of Fig.4 was equipped with a one channel laser interferometer measuring the tip displacement  $y$  along one coordinate axis. The objective was to design a control system for  $y$ , using as input one of the piezo actuators already used for active damping. The targeted bandwidth was  $\omega_c=100$

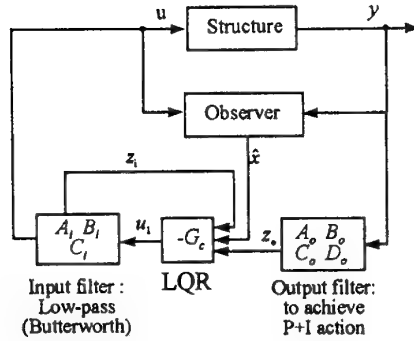


Figure 10: Principle of the frequency-shaped LQG.

rad/sec (above the second mode).

The transfer function  $G(\omega, g)$  between the input voltage to the actuator and the tip displacement  $y$  is shown in Fig.9 for various values of the gain  $g$  of the active damping. One observes that the active damping works very much like passive damping, affecting only the frequency range near the natural frequencies. We also observe that the second mode does not affect substantially the amplitude of  $G(\omega, g)$  and that the phase lag associated with the pole at  $f_2$  is compensated by the phase lead of a zero at a frequency slightly lower than  $f_2$ . From this observation, we concluded that mode 2, which is close to mode 1, would be phase stabilized with mode 1; as a result, the compensator design was based on a model of the first mode alone.

The compensator should be designed in such a way that the lightly damped high frequency dynamics remains stable (spillover [14]) and, in order to compensate the thermal perturbations and avoid steady-state errors, it is desirable that it exhibits some integral action at low frequency.

### 3.1 Compensator design

The standard LQG is not well suited to the above requirements, because the quadratic performance index puts equal weights on all frequencies. The design objectives require larger weights on the control at high frequency, to avoid spillo-

ver, and larger weights on the states at low frequency, to achieve integral action. Both of these features can be achieved by the *frequency-shaped LQG* [15]. The penalty on the high frequency components of the control  $u$  is obtained by passing the control through a low-pass filter (second order Butterworth filter in this case). Similarly, the  $P + I$  action is achieved by passing the output  $y$  through a first order system (Fig.10). The complete system is governed by the following equations:

- *Structure*

$$\dot{x} = Ax + Bu \quad (14)$$

$$y = Cx + Du \quad (15)$$

- *Output filter (P+I)*

$$\dot{z}_0 = A_0 z_0 + B_0 y \quad (16)$$

$$y_0 = C_0 z_0 + D_0 y \quad (17)$$

- *Input filter (low-pass)*

$$\dot{z}_i = A_i z_i + B_i u_1 \quad (18)$$

$$u = C_i z_i \quad (19)$$

These equations can be combined together as

$$\dot{x}^* = A^* x^* + B^* u_1 \quad (20)$$

$$y_0 = C^* x^* \quad (21)$$

with the augmented state vector

$$x^* = (x^T, z_i^T, z_0^T)^T$$

and the notations

$$A^* = \begin{pmatrix} A & BC_i & 0 \\ 0 & A_i & 0 \\ B_0 C & B_0 DC_i & A_0 \end{pmatrix} \quad (22)$$

$$B^* = \begin{pmatrix} 0 \\ B_i \\ 0 \end{pmatrix} \quad (23)$$

$$C^* = (D_0 C, D_0 DC_i, C_0) \quad (24)$$

The state feedback  $-G_c x^*$  is obtained by solving the LQR problem for the augmented system with the quadratic performance index

$$E[y_0^T y_0 + \rho u_1^T u_1] \quad (25)$$

Notice that, since the input and output filter equations are solved in the computer, the states  $z_i$  and  $z_0$  are known; only the states  $x$  of the structure (two in this case) must be reconstructed with an observer.

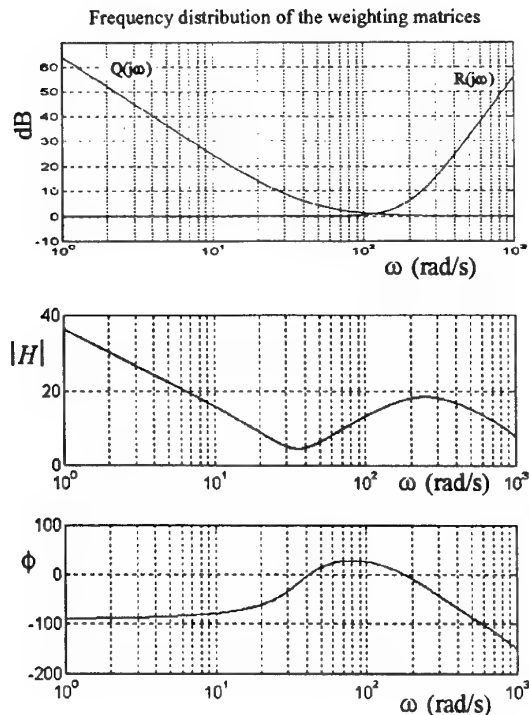


Figure 11: Frequency distribution of the weights in the  $LQG$  and Bode plots of the compensator.

### 3.2 Results

The compensator has been designed with the foregoing methodology. As already mentioned, the reduced model of the structure includes only the first flexible mode; the output filter is a first order equation with feedthrough to achieve  $P+I$  action, and the low-pass input filter consists of a second order Butterworth filter. The observer was designed as a Kalman filter with appropriate distribution of the noise intensity. The frequency distribution of the weights resulting from the input and output filters is shown in Fig.11. The large penalty  $Q(\omega)$  on the states at low frequency corresponds to the integral action and the large penalty  $R(\omega)$  on the control at high frequency aims at reducing spillover. The Bode plot of the compensator,  $H(\omega)$ , is also shown in Fig.11. The compensator behaves like an integrator at low frequency, provides some phase lead in the vicinity of the flexible mode and near crosso-

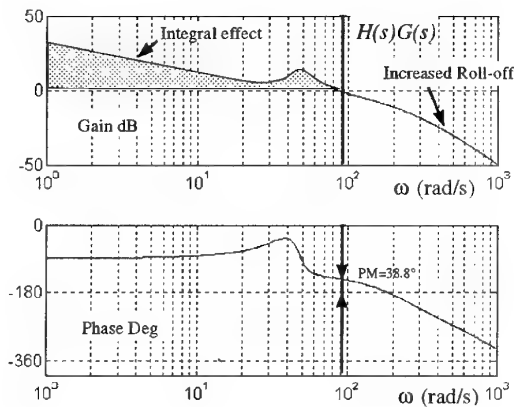


Figure 12: Bode plot for the one mode model,  $H(\omega)G(\omega, g)$ .

ver, and increased roll-off at high frequency. The open loop transfer function of the control system is shown in Fig.12. The bandwidth is 100 rad/s and the phase margin  $PM = 38.8^\circ$ .

The effect of this compensator on the actual structure can be assessed from Fig.13. As expected, the second flexible mode does not cause any trouble, because it is protected by a zero. On the other hand, we observe several peaks corresponding to higher frequency modes in the roll-off region; their stability can be assessed from the Nyquist plot also represented in Fig.13. From the Nyquist plot, we conclude that the first peak exceeding 1 in the roll-off region of the Bode plot (noted 1 in Fig.13) is indeed stable (it corresponds to the wide loop in the right side of the Nyquist plot). The second peak in the roll-off region (noted 2) is slightly unstable for the nominal gain of the compensator; some reduction of the gain is necessary to achieve stability (small loop near -1 in the Nyquist plot). This reduces the bandwidth to about 70 rad/s. The potentially unstable mode corresponds to a local mode of the support of the mirror for the displacement measurement system. This mode is not actively damped; the situation could be improved by a redesign of the support for more stiffness and more damping (e.g. passive damping locally applied).

The above controller has been implemented digitally on a  $DSP$  processor. Figure 14 compa-

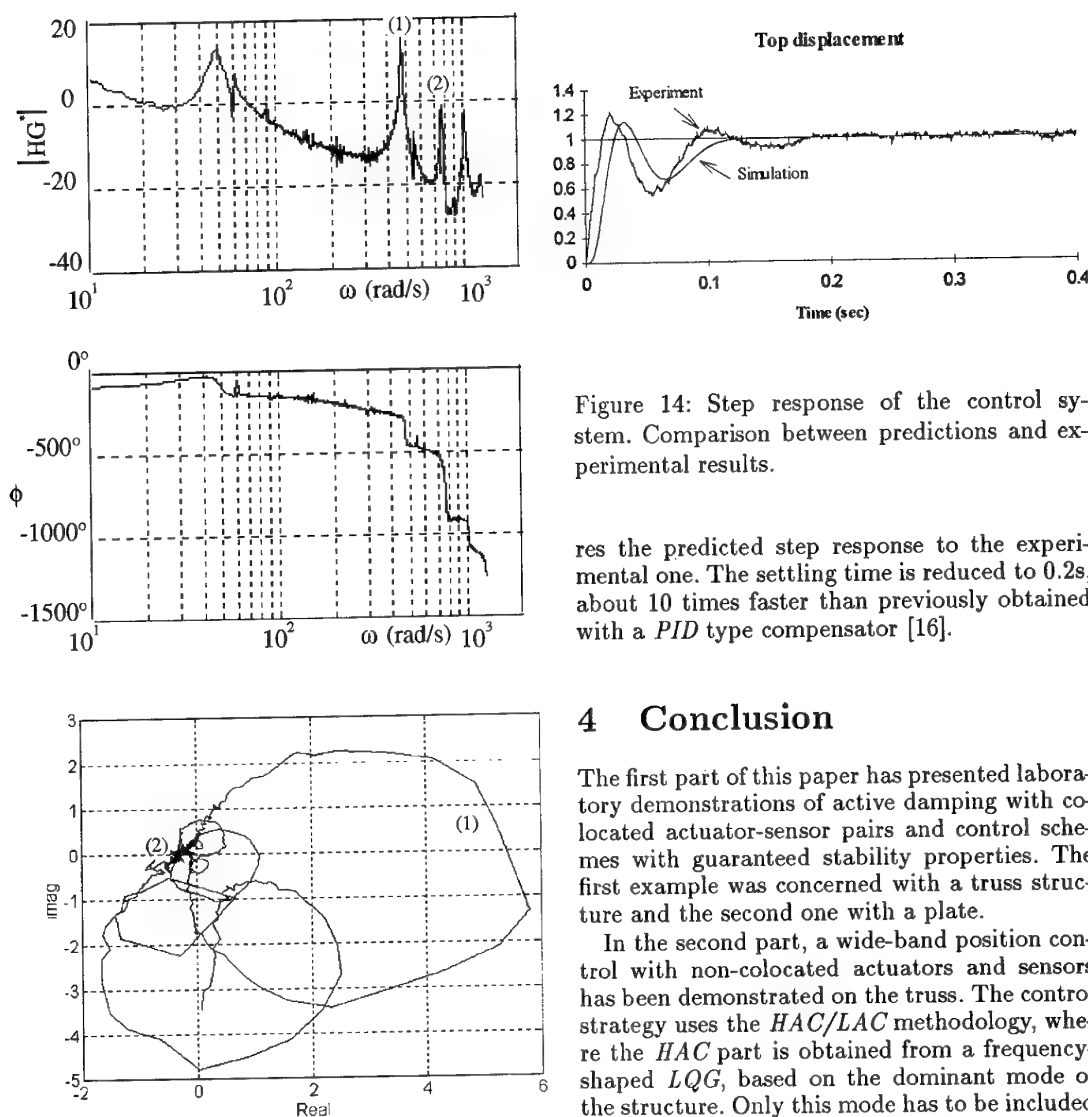


Figure 13: Bode plot of the actual control system  $H(\omega)G^*(\omega)$  and smoothed Nyquist plot demonstrating the stability.

Figure 14: Step response of the control system. Comparison between predictions and experimental results.

res the predicted step response to the experimental one. The settling time is reduced to 0.2s, about 10 times faster than previously obtained with a *PID* type compensator [16].

## 4 Conclusion

The first part of this paper has presented laboratory demonstrations of active damping with collocated actuator-sensor pairs and control schemes with guaranteed stability properties. The first example was concerned with a truss structure and the second one with a plate.

In the second part, a wide-band position control with non-collocated actuators and sensors has been demonstrated on the truss. The control strategy uses the *HAC/LAC* methodology, where the *HAC* part is obtained from a frequency-shaped *LQG*, based on the dominant mode of the structure. Only this mode has to be included in the state observer. The control system has no steady state error, and its bandwidth includes the first two flexible modes of the structure.

## References

- [1] R.H. CANNON & D.E. ROSENTHAL (1984) Experiment in Control of Flexible Structures with Noncolo-

- cated Sensors and Actuators. *AIAA Journal of Guidance*, Vol. 7, No 5, Sept-Oct., 546-553.
- [2] W.B.GEVARTER (1970) Basic Relations for control of Flexible Vehicles. *AIAA Journal*, Vol.8, No 4, April, 666-672.
  - [3] E.K.PARSONS (1989) An Experiment Demonstrating Pointing Control on a Flexible Structure, *IEEE Control Systems Magazine*, April, pp.79-86.
  - [4] J.L.FANSON & T.K.CAUGHEY (1990) Positive Position Feedback Control for Large Space Structures. *AIAA Journal*, Vol.28, No 4, April, 717-724.
  - [5] E.SIM & S.W.LEE (1991) Active Vibration Control of Flexible Structures with Acceleration or Combined Feedback. *SDM Conference*, Long-Beach, AIAA paper 91-1015-CP
  - [6] A.PREUMONT, N.LOIX, D.MALAISE & O.LECRENIER (1993) Active Damping of Optical Test Benches with Acceleration Feedback. *Machine Vibration*, Vol.2, pp.119-124.
  - [7] A.PREUMONT, J.P.DUFOUR & Ch.MALEKIAN (1992) Active Damping by a Local Force Feedback with Piezoelectric Actuators. *AIAA J. of Guidance*, Vol 15, No 2, March-April, 390-395.
  - [8] R.L.FORWARD (1981) Electronic damping of orthogonal bending modes in a cylindrical mast - Experiment. *AIAA J. of Spacecraft*, Vol.18, No 1, Jan.-Feb., 11-17.
  - [9] E.F.CRAWLEY & J.de LUIS (1987) Use of piezoelectric actuators as elements of intelligent structures. *AIAA Journal*, Vol.25, No 10, 1373-1385.
  - [10] C.-K.LEE, W.-W.CHIANG & T.C.O'SULLIVAN (1989) Piezoelectric modal sensors and actuators achieving critical active damping on a cantilever plate. *SDM Conference*, AIAA paper 89-1390-CP.
  - [11] E.F.CRAWLEY & K.B.LAZARUS (1989) Induced strain actuation of isotropic and anisotropic plates. *SDM Conference*, AIAA paper 89-1326-CP.
  - [12] S.HANAGUD, M.W.OBAL & A.J.CALISE (1992) Optimal vibration control by use of piezoceramic sensors and actuators. *AIAA J. of Guidance and Control*, Vol.15, No 5, Sep.-Oct., 1199-1206.
  - [13] IEEE Standard on Piezoelectricity. (ANSI/IEEE Std 176-1987)
  - [14] M.J.BALAS (1978) Active control of flexible systems. *J. of Optimization Theory and Applications*, Vol.25, No 3, 415-436.
  - [15] N.K.GUPTA (1980) Frequency-Shaped Cost Functionals: Extension of Linear Quadratic Gaussian Design Methods, *AIAA J. of Guidance and Control*, Vol.3, No 6, Nov-Dec, 529-535.
  - [16] A.PREUMONT, C.MALEKIAN & N.LOIX (1992) Joint Compensation of Static, Thermal and Dynamic Perturbations of a Truss Structure. *MOVIC-1*, Yokohama, September.

## Structural Verification of the Space Station Freedom Force Moment Sensor (FMS) Using Finite Element Modelling Techniques & Qualification Testing

B. Christie  
B. MacKay  
CAL Corporation  
1050 Morrison Drive, Ottawa  
Ontario, Canada K2H 8K7

### Summary

The design and development of the Canadian Force Moment Sensor (FMS) for use on the Space Station Remote Manipulator System (SSRMS) involved structural verification of strength, stiffness and life capabilities. The FMS, which is comprised of a primary structure - the sensor ring unit (SRU) and an electronics unit (EU), is used to detect on-orbit, operational forces and moments by measuring strain across six complexly shaped flexural members (struts). To achieve the required sensitivity, the struts must maintain a relatively high degree of flexibility which makes them more susceptible to the severe, repetitive loading environments experienced during the launch and on-orbit phases.

The structural verification of the FMS system was demonstrated by structural analyses and qualification testing. The structural analyses included detailed finite element modelling of the FMS-SRU which examined strength margins, stiffness characteristics and fracture susceptibility. The Qualification Test Program supported the finite element modelling and included strength and stiffness testing using special test equipment (STE) in addition to the standard environmental tests. This paper describes the mathematical modelling and testing which was used to verify the structural performance of the FMS, and the techniques used in correlating test results with the predictions.

### Introduction

The major challenge involved in designing and developing a force moment sensor for use in a space application was satisfying two diametrically opposed sets of design requirements imposed by the launch and operational phases. The FMS, which is used to detect on-orbit, operational forces and moments by measuring strain across flexural members (struts), requires a relatively high degree of flexibility to achieve the required sensitivity. At the same time, the struts must be rugged enough to withstand the severe, repetitive loading environments experienced during the launch and on-orbit phases. Surviving high launch loads while maintaining an adequate measurement sensitivity required a highly analytical approach and involved extensive optimization in developing the design.

Structural verification of the FMS system was achieved in stages over the course of the engineering model (EM) and qualification model (QM) phases. Correlation of the EM finite element model (FEM) predictions with the EM test results was performed to validate and refine modelling

techniques. Discrepancies between the EM test results and the initial EM FEM predictions indicated that a more rigorous approach was required. Further refinement of the FEM modelling techniques was performed through correlation of the QM FEM predictions with QM test results at the component and system level. Verification of the overall system level FMS stiffness and strength is performed through system level testing of the QM. Life capabilities of the FMS were verified by fracture analysis and NDE inspection techniques.

This paper presents the SSRMS FMS system and describes the process involved in performing structural verification. The paper also includes a description of the mathematical modelling techniques and testing used in verifying the FMS structural performance. The methodologies presented in this paper can be used in those applications requiring a high degree of structural characterization.

### FMS Performance Requirements Summary

As noted previously, the FMS must withstand severe launch loading environments while maintaining an ability to measure extremely small forces and moments. Launch loads range up to 6900 times the required measurement resolution levels; the FMS measurement sensors must be capable of measuring deflections as small as 0.2  $\mu\text{in}$ . A summary of the significant SSRMS FMS functional performance requirements is given in Table 1.

The FMS stiffness requirements are:

Bending:  $\geq 5.02 \times 10^7$  in-lb/rad  
Torsion:  $\geq 4.44 \times 10^7$  in-lb/rad

The FMS strength requirements dictate that the unit shall maintain structural integrity under all operating or non-operating environments. A positive margin of safety is required for the worst case loading condition using the following factors of safety:

Yield Factors of Safety:

1.1 (On-orbit); 1.0 (Launch and Landing)

Ultimate Factors of Safety:

1.5 (On-orbit); 1.4 (Launch and Landing)

The FMS must be shown to be capable of surviving all pre-launch, launch and on-orbit structural and thermal environments for a minimum of 30 years.

**Table 1 SSRMS FMS Functional Performance Requirements**

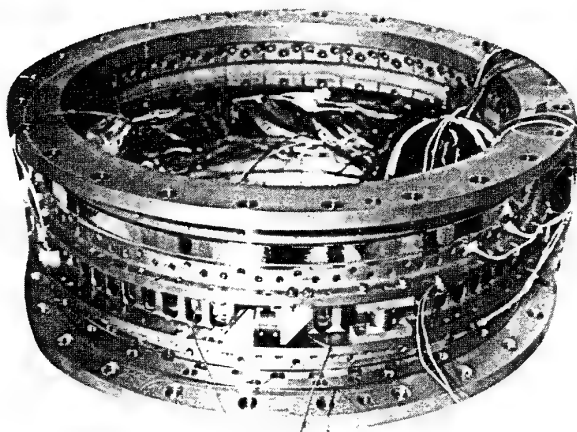
| Load Type       | Measurement                       | On-orbit Limit | Launch                          |
|-----------------|-----------------------------------|----------------|---------------------------------|
| Moment (in-lbs) | 3600 Max<br>17.6 Min (see note 4) | 44880          | Torsion: 35336<br>Moment: 82244 |
| Force (lbs)     | 100 Max<br>1.1 Min (see note 4)   | 360            | Axial: 4592<br>Shear: 2287      |

**Table 1 SSRMS FMS Functional Performance Requirements (Cont'd)****Notes:**

1. Moment load types include bending and torsion unless otherwise specified.
2. Force load types include shear and force unless otherwise specified.
3. Load Measurement Accuracies (Isothermal Environment)  
Moment:  $\pm 12$  in-lbs or  $\pm 3\%$  whichever is greater  
Force:  $\pm 1.5$  lbs or  $\pm 4\%$  whichever is greater
4. Load Measurement Resolution: Moment:  $\pm 17.6$  in-lbs; Force:  $\pm 1.1$  lbs

**Design Description****a. Engineering Model**

The EM FMS consists of four primary units - two interface rings, G-10 thermal isolators and the sensor ring unit (SRU) as shown in Figure 1, and the electronics unit (EU).

**Figure 1 EM FMS Layout**

The first of two primary design features of the EM FMS is that the unit conveys SSRMS arm loads through itself as uniformly as possible to allow accurate resolution of forces and moments. Capacitive sensors measure displacements within the SRU which are converted to displacements using look-up tables. The interface rings

are made of aluminum alloy 7075 T73 and are located on the ends of the FMS. They consist of flat flanges that couple the FMS to the SSRMS. Twenty-four bolts at each end provide a uniform solid connection. The SRU is the central load bearing flexure region between the interfaces. The SRU, also of aluminum alloy 7075 T73, utilizes 64 slender struts evenly spaced around the circumference to maximize the flexibility of this region while maintaining strength and stability.

The second major design feature of the FMS was the thermally isolated SRU. The SRU is heated to maintain a constant temperature that is higher than its operating environment to minimize any thermal gradients that would alter the sensor readings. The G-10 isolators minimize the power requirement for heating the SRU. The isolators also serve as the means of physically connecting the SRU to the interface rings. The EU resides within the SRU and performs all the sensor data manipulation.

**b. Qualification Model**

Changes in the FMS design requirements necessitated the incorporation of an orbital replaceable unit (ORU) interface, a mate/demate mechanism for electrical connectors, a curvic coupling on the remaining L-flange interface, and changes in envelope. The QM FMS is comprised of one primary structure - the sensor ring unit (SRU) as shown in Figure 2, and an electronics unit (EU).

The SRU is an aluminum structure which is machined from a die forging of aluminum alloy 7075 T73 using conventional machining as well as electro-discharge machining (EDM). An integral, unibody design eliminates thermal contact resistances from the assembly, thereby minimizing thermal distortion and hysteresis effects.

On-orbit, operational forces and moments are detected by measuring the strain across the struts. The strut region is comprised of six complexly shaped struts which are located at  $55^0$ ,  $55^0$  and  $70^0$  intervals around the circumference of the SRU as shown in Figures 3 and 4. Stiffened bulkheads are located on each side of these struts to isolate any irregular, external perturbations. A straight load path has been maintained along the length of the FMS unit in order to minimize the effects of offset moments.



Figure 2 QM FMS Layout

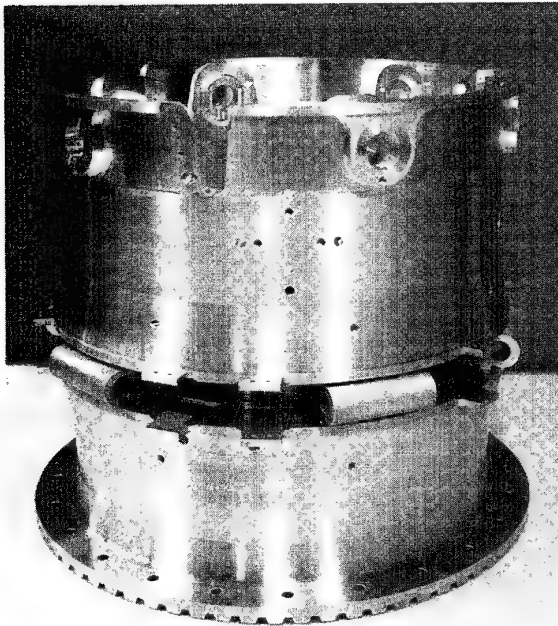
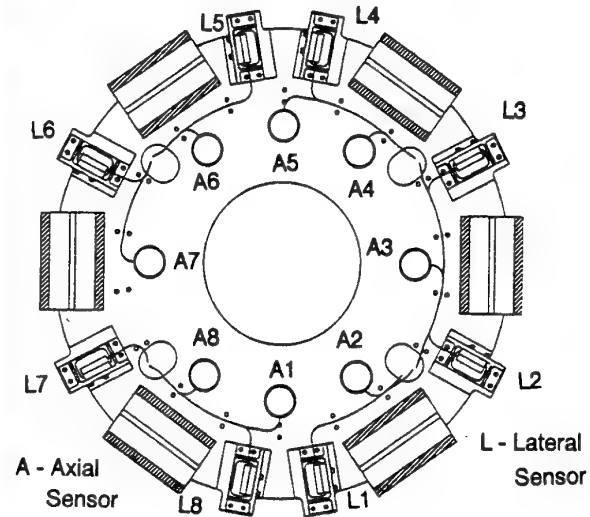
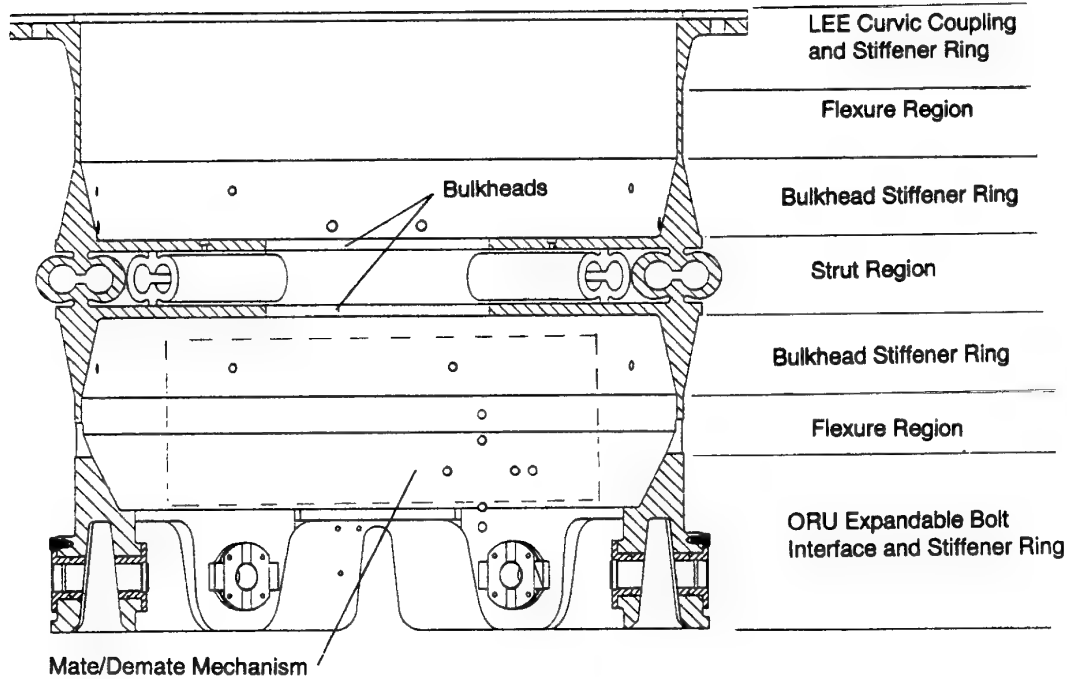


Figure 3 FMS Strut &amp; Sensor Locations



Strains across these two stiffened bulkheads are measured using capacitive sensors which are mounted to the bulkheads in the locations shown in Figure 3. The sensor ring structure, sensor mounting brackets and sensor assemblies are thermally self-compensating towards bulk temperature changes; the 0.015 inch sensor gap alone requires correction for changes under bulk temperature changes by  $dT \cdot L_{gap} \cdot CTE_{aluminum}$ . Tangential and axial sensor outputs are digitized, converted to displacements

Figure 4 FMS Sensor Ring Structure



using look-up tables, corrected for temperature and then used to calculate forces and moments through a calibration matrix.

Operating loads are reacted at the SSRMS roll joint interface through six expandable bolts as shown in Figure 4. The latching end effector (LEE) interface transmits operating loads to the FMS through a bolted curvic coupling flange. Both FMS interfaces have continuous stiffener rings which tend to minimize FMS interface disturbances caused by interface misalignments, thermal distortion and induced moments caused by offset load paths. The centrally located strut region is further isolated from interface effects through the presence of flexure regions located between the central bulkhead stiffeners and the interface stiffener rings. The central bulkheads, in addition to acting as sensor mounting interfaces, are used in isolating ovaling effects.

The FMS sensor ring structure is shown in Figure 4.

### Structural Verification of the FMS

#### a. Engineering Model

##### a1. Introduction

A NASTRAN FEM was created during the EM project phase in order to assess the developing design's viability as it progressed. The basic philosophy behind the initial FE analyses was that a rudimentary model would be accurate enough to predict the general characteristics of the structure. The intent was to use the FEM to determine the reaction of the SRU to externally applied forces, thermal distortions, and any other external perturbations (e.g. misalignment or warping at the external interfaces). These characteristics would then be confirmed in subsequent testing. The structural analyses were not considered to require an extraordinary level of detail. In particular, localized deflections due to warping at the interface, and distortions due to thermal gradients were not considered. This approach assumed that uniform distribution of the load bearing members and heating of the SRU precluded the need for detailed analysis of these effects.

##### a2. EM FEM Description

The EM design is significantly different from the QM and flight models (FM). The FEM consists of rings of QUAD4 elements representing the interface flanges, the SRU, and the G-10 fiberglass thermal isolators (See Figure 5). The model consisted of 600 shell and rigid elements (QUAD4 and RBE2) and 600 nodes. Sensor displacements were computed as the difference in displacements of pairs of GRID points on the two sensor flanges in the model.

The EM models are considerably less complex than the models of the QM and FM.

##### a3. EM System Level Testing

The EM testing consisted of performance and stiffness tests. The performance results were obtained through the use of a test rig which applied known forces and moments through a lever and arm system as shown in Figure 6.

These tests occurred inside a thermally stable environment. The FMS would be loaded with a number of input load combinations and the sensor outputs would be

used to produce a calibration matrix. This matrix allowed loads to be determined from sensor inputs.

**Figure 5 SSRMS FMS EM Finite Element Model**

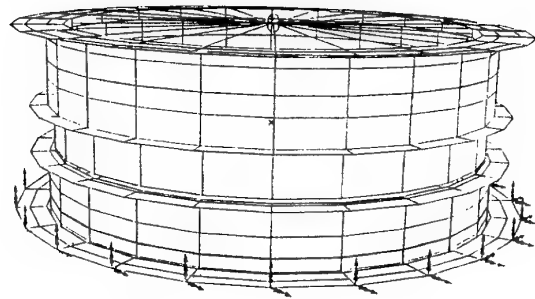
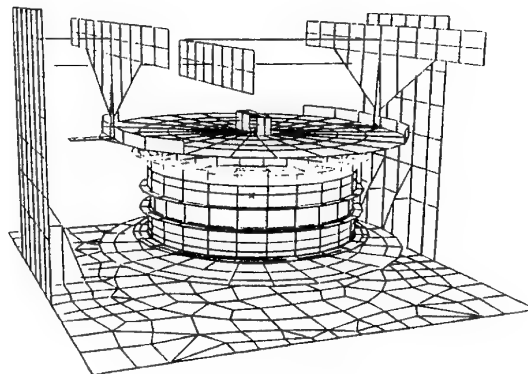


**Figure 6 EM Calibration Test Rig**



Stiffness tests were performed using a combination of modal analysis and theodolite measurements. The theodolite measurements were used to find the torsional stiffness of the FMS by applying a torque with the calibration rig. The difference in the alignment mirror positions after applying the loads indicated how far the FMS had deflected in rotation. Modal analysis involved attaching a large mass beam to one interface of the FMS and restraining the opposite interface to a fixed test platform. Accelerometers attached to the SRU and the beam measured responses to impulses on the beam.

Impulses were input to excite either the torsional or the bending modes. The resulting natural frequencies were then used to determine the SRU stiffness.

#### a4. EM FEM Validation

EM FEM validation was achieved by correlation of predictions with the following test results:

- Modal Test (Bending & Torsion)
- Theodolite measurements (Torsion)
- Load Testing (Axial)

The EM testing indicated that the FMS was a precision instrument that was highly influenced by all external structural and thermal perturbations. One observation that was made was that the mesh density in the strut region was too low. As a result, the EM FEM was refined using a combination of detailed NASTRAN cyclic symmetry models and refined EM FEMs as described in the following section.

#### a5. EM Post Testing FEM Refinement

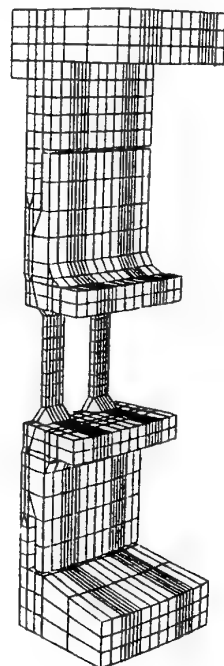
Comparisons of test results versus the initial predicted FEM values indicated that there were significant discrepancies. The FMS sensor responses under test conditions and some of the structural stiffness values were very much in error. Further analyses determined that these discrepancies were a result of inadequately addressing the FMS boundary conditions.

The sensor responses produced by the test rig were incorrect not only in magnitude but sometimes in sign as well. It was discovered after modeling the test rig which hadn't been done before, that it was very flexible relative to the SRU. In addition, the design of the loading mechanisms had introduced significant warping loads that impaired the performance of the test rig. The detailed model of the SRU in the test rig (Figure 6) accurately replicated the test results that were obtained, as shown in Table 2. This discovery led to the successful redesign of the test rig with much more attention being paid to the analysis detail.

Subsequent investigation into the origin of the structural and thermal test result errors indicated that the resolution of the SRU model was too low, particularly in the region of the load bearing struts. This discovery led to the development of cyclic symmetry models that contained a large amount of detail while only modeling a small fractional slice of the axially symmetric structure Fig. 7. The cyclic symmetry model results correlated well with the test results (see Table 2).

Figure 7

#### EM Cyclic Symmetry FEM



#### b. Qualification Model

##### b1. Introduction

The experiences gained in the verification of the EM led to a change in philosophy with respect to the QM structural analysis. The EM indicated the FMS was a precision instrument that was highly influenced by external structural and thermal effects. The QM analysis was therefore initiated on the premise that no FE modeling methods would be used untested, that some form of verification of every analysis step would be performed. Several of the more significant modeling features are described below.

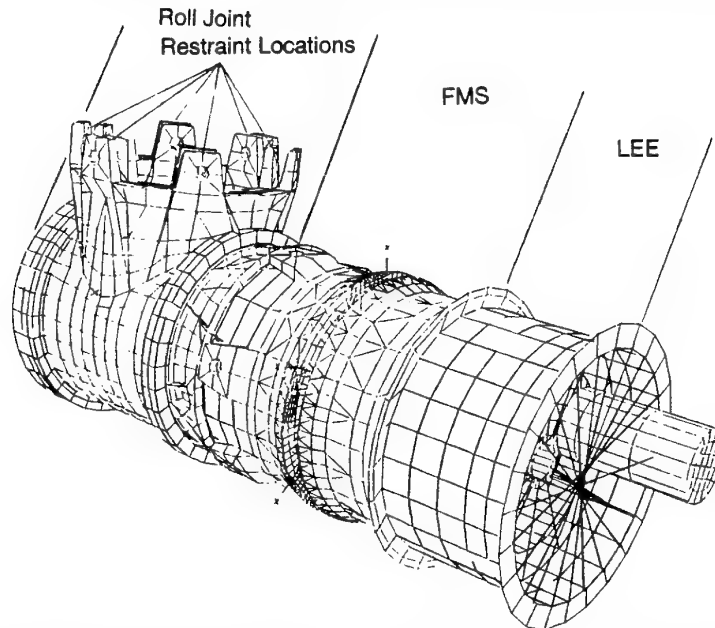
##### b2. QM FEM Description

To analyze the FMS behaviour as accurately as possible, the roll joint, the FMS, and the latching end effector (LEE) were integrated together in a coupled NASTRAN FEM as shown in Figure 8.

Table 2 Comparison of Refined FEM & Tested Stiffness Values

| Load Case | Prediction vs Test Error (%) | Prediction Method                             | FEM                                |
|-----------|------------------------------|---|------------------------------------|
| Bending   | 16                           | modal analysis (FEM)                          | Refined EM                         |
| Torsion   | 18<br>6.3                    | modal analysis (FEM)<br>static analysis (FEM) | Cyclic symmetry<br>Cyclic symmetry |
| Axial     | 3.2                          | static analysis (FEM)                         | Refined EM                         |

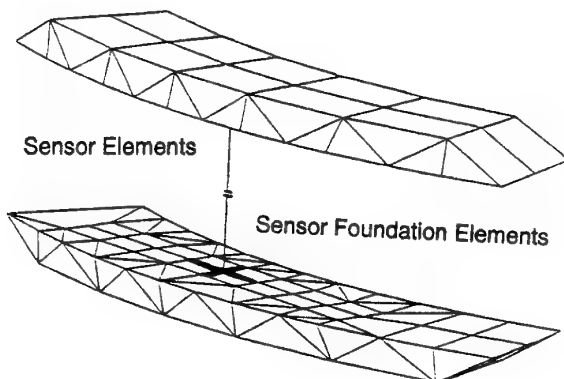
**Figure 8 SSRMS FMS QM Finite Element Model**



Due to the size and complexity of the roll joint, the roll joint FEM was reduced to DMIG cards (direct matrix injection at GRID points) using a NASTRAN direct matrix abstraction programming (DMAP) sequence. The resulting roll joint model includes 12 interface GRID points - six at the FMS expandable bolt interface and six fixed restraint locations as shown in Figure 8. This reduction allows the roll joint to interact with the FMS but has no facility for recovering displacement or stresses within the roll joint itself. This format allows for extremely rapid and accurate execution of the roll joint, since local displacements and stresses in the roll joint are not a primary concern. This approach maintains accurate 'global' stiffness characteristics of the roll joint when it is coupled to the FMS.

For the purposes of accurately determining performance values at the sensor locations, vertical BAR elements are attached to the bulkhead element plane to represent the sensor bodies and brackets as shown in Figure 9.

**Figure 9 FMS Sensor Bar Elements**



In the plane of the bulkhead, each vertical sensor BAR element has a foundation of four additional BAR elements to simulate the effect of the sensors' mounting footprints. These elements average out the localized bending over a small area of the bulkhead and convey this average movement to the sensor BAR. These foundation elements are very flexible and cannot impart any significant loading to the FMS structure. Multi-point constraint equations link the ends of the sensor gaps to a measurement GRID placed in the middle of each sensor gap. The difference in movement of the gap nodes become the actual displacements of the measurement nodes.

The integrated model was divided into multiple superelements for efficient execution of such a large model. Dividing a large model into superelements allows for more rapid solution of models where results for sections of the model are not required. As well, execution can be performed piecemeal for the individual superelements. Subsequent modifications to the model are also easier to manage when superelements are used.

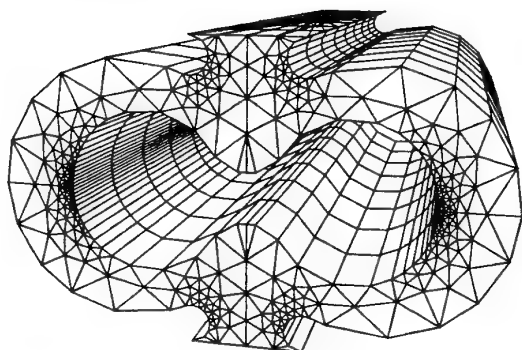
The LEE portion of the model is contained within one superelement which is comprised of 550 shell and rigid elements (QUAD4, TRIA3 AND RBE2) and 555 nodes. Output is not requested for this superelement.

The FMS SRU structure, excluding the struts but including the DMIG'd roll joint model are included in one superelement. The FMS portion of this superelement is comprised of 3100 beam, shell, solid and rigid elements (BAR, QUAD4, TRIA3, HEXA, PENTA, TETRA, RBE2 and RBE3) and a total of 3200 nodes.

The six struts are modelled by creating one highly detailed strut model which is then linked to the SRU structure as a primary superelement, similar to the ones described above. The remaining five struts are geometrically congruent with the first one; this property allowed the use of NASTRAN secondary superelements (images). These image superelements take their physical characteristics from the one primary strut model and are mapped into the remaining strut locations. The SRU superelement behaves as though

there are six struts modelled. Displacement and stress results of the image struts are mapped back to the primary strut for the purposes of post-processing the analyses. The primary strut, shown in Figure 10, is comprised of 3700 solid and rigid elements (PENTA and RBE2) and 2700 nodes. The remaining five image struts utilize 54 nodes each.

**Figure 10 FMS Strut Superelement**



To allow mapping of the FMS temperature response to the FEM to analyze thermal distortion, the superelement format is replaced with a single large model. To speed execution of the model, the solid element struts were replaced with representative stiffness shell element versions. Since thermal distortion stresses were found to be much smaller than launch stresses, the lack of a detailed mesh was considered acceptable for the thermal distortion model.

External loads are applied to the FMS FEM at a central GRID point located at the end of the LEE model furthest from the FMS (+Z direction). The central GRID is attached to the LEE by RBE2 rigid elements.

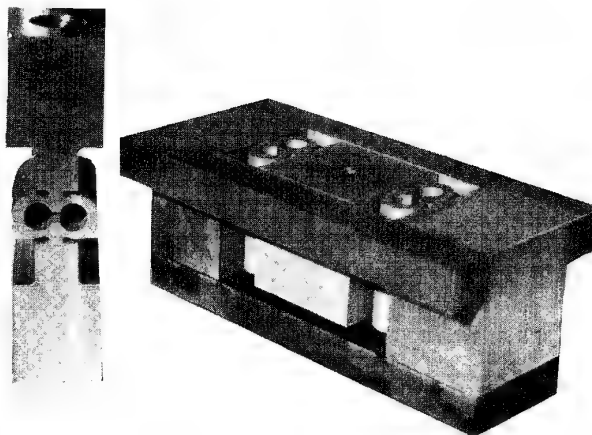
### **b3. QM Component Level Testing**

The QM component level testing included both stiffness and strength testing of the FMS strut as described below.

### **Stiffness Testing**

Stiffness testing was performed on two strut configurations as shown in Figure 11. The first, a single strut, was used to measure the axial stiffness, while the second which was comprised of two struts linked at the roots was used in measuring shear stiffness.

**Figure 11 Strut Load Test Specimens**



The axial and shear tests were performed on an Instron load test machine which recorded crosshead displacement and plotted it against the load cell readings. As a backup, manual measurements were made using a vernier caliper in the axial test and a dial indicator in the shear test.

The results of the QM strut stiffness testing is given in Table 3.

### **Strength Testing**

The QM strut strength testing was performed using the same test specimens and test setup used in the strut stiffness testing.

The results of the QM strut strength testing is given in Table 4.

**Table 3 QM Strut Stiffness Test Results**

| Load Case | FEM Predict (lb/in) | Stiffness Test (lb/in) | FEM vs Test (%) |
|-----------|---------------------|------------------------|-----------------|
| Axial     | $6.575 \times 10^5$ | $5.525 \times 10^5$    | -16             |
| Shear     | $1.958 \times 10^6$ | $1.613 \times 10^6$    | -17.6           |

**Table 4 QM Strut Strength Test Results**

| Load Case | FEM Predict (kg)        | Strength Test (kg)                    | FEM vs Test (%) |
|-----------|-------------------------|---------------------------------------|-----------------|
| Axial     | 3720 Yield              | 3900 Yield<br>7600 Ultimate           | 4.8             |
| Shear     | 6495 Yield (see Note 1) | Yield (see Note 2)<br>>10000 Ultimate | >54.0 *         |

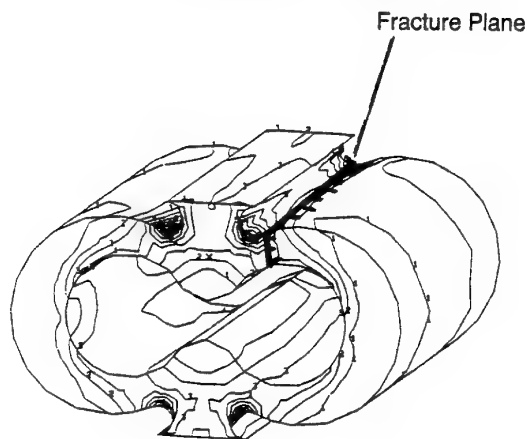
**Notes:**

1. FEM predicts very localized initial yield on the internal strut radii; this yielding has negligible effect on stiffness.
2. Yield point was not discernible from test results.

The fracture of the axial test strut occurred at 7600 kg, while the shear test struts withstood the maximum load capacity of the testing machine (10000 kg). The FEM predicted that only a very small volume of material will yield under 10000 kg of shear load for the given shear test configuration.

During the course of these static load tests, the automated test results were found to be erroneous. As a result, the backup measurements were used to obtain the results given above. Given the experimental error inherent with this technique, the difference between the FEM predictions and the test results agree within the accuracy of the test for the axial test (1.4 % once corrections are made). The shear test however gave results that agreed with FEM predictions at best within 11% once corrections had been made for experimental error. However, these corrections do not fully account for boundary condition effects peculiar to this test setup.

The location of the fracture of the axial test specimen is shown in Figure 12.

**Figure 12 FMS QM Strut Stress Profile & Axial Test Fracture Plane**

The stress profiles given in Figure 12 have shown that the most highly stressed region is the internal strut radii. While local yielding may begin at these locations, failure of the strut does not necessarily occur at the internal radii. Since the stresses shown are determined from a linear analysis, they do not accurately reflect the non-linear

yielding behaviour at such high load levels. Therefore, failure may occur elsewhere in the structure of the strut as demonstrated by the strut strength testing.

**b 4. QM Material Testing**

Material strength testing performed on samples taken from the aluminum forgings have shown the forging strength to be greater than 56.5 ksi and 68.6 ksi for yield and ultimate respectively. This value compares favourably with the published values taken from the Metallic Materials and Elements for Aerospace Vehicle Structures, MIL-HDBK-5E (56 ksi yield, 66 ultimate). Since all material allowables were taken from this reference, it is clear that there is adequate margin built-in to the material properties.

**b 5. QM Life Verification**

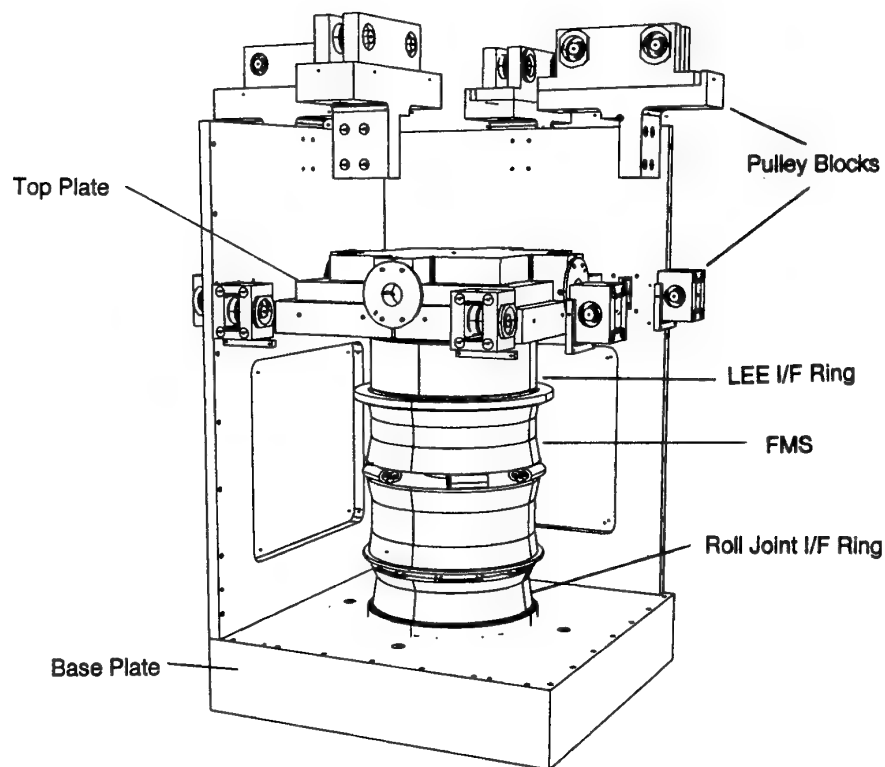
The FMS life was verified by performing a fracture analysis and NDE inspection of the FMS structure to determine the size and extent of cracks. The fracture analysis included safe life and fail safe analyses which were performed using the NASA Flagro crack growth analysis software. The safe life analysis was performed on the most highly stressed region of the FMS SRU - the six, centrally located struts. The load spectra used included the test program, launch and landing and on-orbit load cases. The test program included stiffness and strength testing as well as vibration testing. Calibration testing, ground handling operations and transportation environments were considered negligible due to the low loading levels present in each (Note that the FMS is shock mounted during transportation).

The fail safe analysis used a similar approach and load spectra but used stress levels generated when one half of the most highly loaded strut was cut

In both analyses, Flagro examined crack growth using initial surface cracks which corresponded to standard NDE crack sizes for liquid penetrant. The crack case used was a 2D surface crack in a finite width plate (surface crack type SC01). This model, which is used in situations where a plate is subjected to a combined axial force and bending moment, closely represents the outer leg of the FMS struts. Since stress concentrations were present on surfaces of the internal radii of the struts, the worst case corresponded to the minimum depth of crack as defined by the standard Flagro values. The load levels were calculated by integrating stress levels around the elliptical initial crack tip when it was located in the highest stress field.

The safe life analysis results have shown the FMS structure to be capable of withstanding over four service lifetimes including 30 years of on-orbit operational life.

Figure 13 QM Calibration Test Rig



The fail safe analysis has determined that the FMS SRU is unable to survive four complete service lifetimes with a severed strut. As a result, the FMS structure is deemed Fracture Critical. This necessitates that the FMS structure undergo rigorous nondestructive inspection to assess initial cracks and flaws that may be present.

#### b6. QM System Level Testing

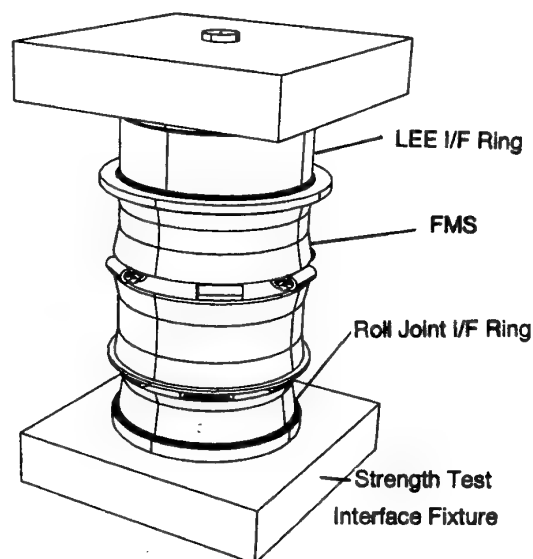
System level testing is comprised of performance, stiffness, and strength tests. The performance and stiffness tests will be performed in a special test rig (Figure 13) while the strength test will utilize a separate test setup (Figure 14).

The test rig will be used to calibrate the FMS. Calibration loading will also determine the structure's stiffnesses. The test rig will also simulate FMS operation under thermal loading. The design of this test rig parallels that of the SRU itself. The SRU model is incorporated into the test rig model. The test rig is designed to load the FMS in an accurate and repeatable way. The design of this rig paid special attention to the fact that the FMS can sense small non-uniformities in its loading conditions. The analysis of the test rig coupled to the FMS predicts how the FMS will behave under test conditions. Once an accurate correlation is determined in this setup, the analysis can then be used to determine how the FMS will behave under service conditions.

The strength test is used to determine whether the FMS can sustain a proof load of 33000 lbs. This value was

determined from the launch loads analysis. The peak launch level loading stress produced by a multi-axis force and moment load combination is simulated in test with an axial load. This axial load will be applied with a hydraulic press with the FMS in the configuration shown in Fig. 14.

Figure 14 QM FMS Strength Test Setup



### QM Stiffness Testing

The QM stiffness testing will be performed on the FMS assembly using representative interface plates and a special calibration test rig as shown in Figure 13.

### QM Strength Testing

The QM strength test will utilize the same interface plates used in stiffness testing. Loads will be applied against the interface plates to levels determined in FEM performance analyses for the worst case launch loads combination. Structural analysis has determined that the combination of axial forces and bending moments constitute the worst load case. This load combination applies predominantly axial loads to the most highly stressed strut as evidenced by the stress profiles shown previously. Therefore, the strength test applies equivalent axial loads such that each strut is loaded to the maximum stress levels. The results of

the test will be a pass or fail based on the structural integrity of the unit after the test which will be determined by a complete physical inspection. The lack of permanent deformation in the struts or elsewhere in the structure is considered a successful test.

### b 7. QM FEM Validation

Based on the EM test results which determined that the FMS was extremely sensitive to interface effects and mesh densities, numerous modelling features were incorporated to improve the accuracy and functionality of the model. The QM FEM was validated using a series of test models and/or independent means which isolated and examined specific aspects of the structural model independently from the full FMS model. The agreement between the QM FEM and these models or alternative validation means are given in Table 6.

**Table 6 Strut FEM Results Compared to Independent Checks**

| Load Case  | FEM vs Independent Means of Verification of FMS Stiffness (%) |             |             |             |
|------------|---|-------------|-------------|-------------|
|            | Hand Calcs  | FE Model #1 | FE Model #2 | FE Model #3 |
| Tangential | 2.3   |             |             |             |
| Axial      |   | 4.4         | 4.8         | 9.1/3.0 *   |

\* Corrected stiffness (see paragraph below)

FE Models #1 and #2 are representative BAR and CBEND models of the strut outline (see Figure 15). FE Model #3 is a model of the end face of the strut made with TRIA3 elements (see Figure 15).

FE model #3 depicts the strut geometry very accurately but cannot account for Poissons effect (the full model used is not allowed to strain along the length of the strut). The Poisson effect would stiffen FE model #3 by approximately 12%. This would put the result within 3%

of the full model. With this correction, the table shows that the FEM strut model stiffness values agree closely with those of the check methods.

Using the validated FEM strut model stiffness values, the stiffness interactions of the six struts together in the FMS structure were predicted using manual calculations. These values were compared to the FEM predictions as shown in Table 7.

**Figure 15 FEM Test Models**

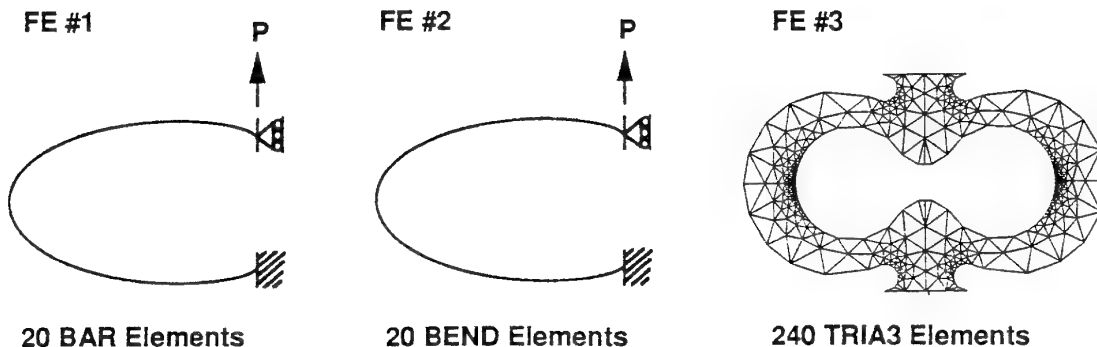




**Table 7 QM FMS FEM Results vs. Manual Predictions**

| Load Case | FEM vs Calc Error (%) | Load Case | FEM vs Calc Error (%) |
|-----------|-----------------------|-----------|-----------------------|
| FX        | 10.6                  | MX        | 25.6                  |
| FY        | 14.0                  | MY        | 8.0                   |
| FZ        | 4.5                   | MZ        | 13.3                  |

QM FEM validation was also performed by correlation of FEM predictions with QM testing (described in the following sections).

### **Conclusions**

The FMS was found to be very sensitive to changes in its environment. In particular, the operational boundary conditions are different from those of the test conditions and had to be analyzed separately. This required a major portion of the structural analysis effort to be devoted to examining the sensitivity to boundary conditions.

The FMS structural verification was performed in stages starting with the lowest levels of detail and progressing to the system level. Initially, tests were performed on materials and components. FEM modelling techniques were checked and correlated to test models and independent manual calculations as well as to component/subsystem test results.

Having established confidence in FMS components and subsystems, system level structural verification was achieved through FEM analyses which was correlated to system level test results. Every step of the structural verification required that inputs to a subsequent stage be as accurate as possible. For this reason, every analysis method is correlated to another method or to tests or to both whenever possible.

# MASTERING THE EFFECT OF MICROVIBRATIONS ON THE PERFORMANCES OF RECONNAISSANCE SATELLITES

D. MONTEIL  
V. GUILLAUD  
Ph. LAURENS

MATRA MARCONI SPACE FRANCE  
31, rue des Cosmonautes, 31077 TOULOUSE CEDEX - FRANCE  
Phone : (33).61.39.61.39 - Télex : 530980F - Fax : (33).61.39.73.78

## 1. SUMMARY

Since a few years, the development of very high resolution observation satellites inevitably leads to microdynamic problems. The quality of the images produced by reconnaissance satellites imposes that they observe stringent line-of-sight stability requirements. The aims of this paper are to present the methodologies used at MATRA MARCONI SPACE (MMS) and to show the importance of tests in the prediction and verification logic.

In the first part, stability requirements for reconnaissance satellites are reviewed. Constraints issued from new signal processing technologies are presented. In the second part, microvibration sources, their propagation throughout the satellite and their effects on the line-of-sight (LOS) are detailed. The prediction and verification logic is described in the third part. It is based on an intimate combination of analyses and tests at equipment, subsystem and satellite levels : the proposed approach for microdynamics is similar to thermal and mechanical processes using hierarchical specifications, tests, analyses and interface control documents. Finally several examples of microdynamic tests performed at MMS on reconnaissance satellites are presented to illustrate their major contributions to high frequency pointing requirements demonstration.

The work presented in this paper was performed in the frame of projects under CNES contracts.

## 2. NEW STABILITY REQUIREMENTS FOR EARTH OBSERVATION SATELLITES

Earth observation satellites like SPOT or HELIOS, universe observation satellites like the Hubble Space Telescope, or laser inter-satellite link terminals like SILEX require high accuracy pointing and stringent line-of-sight stability. For 10  $\mu$ rd required for LANDSAT and SPOT1, less than 1 or 0.1  $\mu$ rd are now necessary (Ref. [1]) for SPOT new generations, HST or SILEX (Fig. 2/1). In the particular case of reconnaissance satellite, the requirements are expressed in terms of :

- length alteration limitation in order to measure and identify precisely objects on earth,
- temporal registration constraints in order to observe evolution and movement on the ground by comparison of images,
- spatial registration constraints when several lines of pixels issued from the same instrument or from different instruments located on the satellite have to be connected,
- modulation transfer function to prevent blurring which damage resolution.

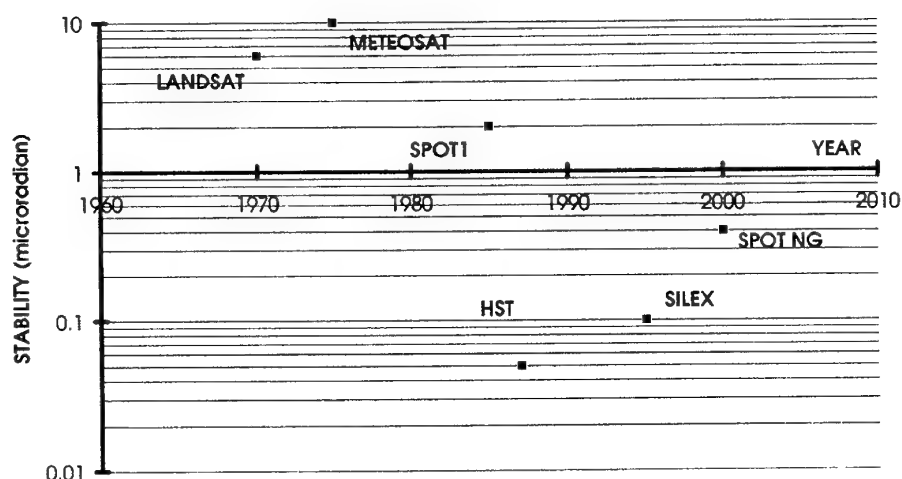


FIGURE 2/1 : Stability requirements evolution

These requirements become more and more stringent with the use of new technologies like Time Delay and Integration (TDI). TDI is a signal-processing technique (Ref. [2]) in which individual input signals pass through separate delay lines and are subsequently combined by an adder into a single output signal. By scanning the image across a linear array of detectors, each image point is sampled many times. Variations in the noise and responsivity of the detectors are averaged out by adding all of the output signals together, but the major drawback of this mode is the high accuracy synchronization needed between time delay and scan rate to prevent blurring.

Mastering microvibrations on satellites becomes more and more a necessity to assure ultimate pointing accuracy in a wide frequency range.

### 3. MICROVIBRATIONS : SOURCES AND EFFECTS

Spacecraft internal disturbances cover the whole frequency range up to several hundred hertz. The spacecraft Attitude and Orbit Control System (AOCS) can attenuate low frequency disturbances (typically below 1Hz), but is not able to control higher frequency ones.

In a spacecraft, there is a lot of microvibrations sources. Stationary or transient forces and torques are produced by actuators or equipments such as :

- reaction and momentum wheels used to control or modify the attitude of the satellite,
- magnetic tape recorders used in orbit to store the instrument data,
- mechanical coolers used to cool down to cryogenic temperatures the focal plane of an instrument. A pair of coolers can be back-to-back synchronised to reduce the disturbances produced by the moving masses,
- pointing mechanisms such as solar array drive mechanisms or oblique viewing mirrors,
- thrusters used to control the orbit at regular intervals,
- electrical relays or propulsion subsystem latch valves.

The disturbances are propagated throughout the satellite structure up to optical elements and may have a significant impact when a sine disturbance is in coincidence with a structural resonance (Ref. [6]). Vibrations of mirrors, dioptries and focal plane induce line-of-sight instability which must be studied from the beginning of satellite development.

### 4. PREDICTION AND VERIFICATION LOGIC

The prediction and verification logic presented hereafter is issued from the experience acquired by MATRA MARCONI SPACE on the SPOT4, HELIOS 1, SOHO and SILEX programs. It relies on a number of analyses and tests, implemented in a progressive manner from equipment level to system level, along the development cycle of the satellite or instrument program. This approach strongly relies on the experience and in-orbit performance of existing satellites.

#### 4.1. METHODOLOGY FOR MICROVIBRATION ANALYSIS

The methodology for microvibrations analysis is described on Figure 4.1/1 (Ref. [6]). It involves the following steps :

- identification, characterisation, modelling of disturbances sources ;
- structure and optics modelling of the spacecraft/instrument using finite element analysis ;
- calculation of dynamic transfer functions between each disturbance degree-of-freedom (i) and each response degree-of-freedom (j) ;
- in the frequency domain for steady state disturbances, or in the time domain for transients, calculation of the microvibration levels on critical response nodes (e.g. line-of-sight degrees-of-freedom) ;
- when necessary, specific treatments such as filtering, sampling/aliasing, control-loop rejection.

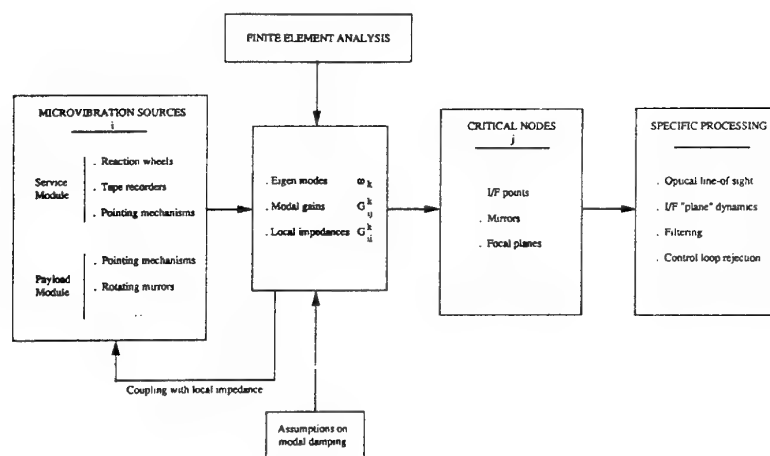


FIGURE 4.1/1 : Microvibration Performance Analysis

## 4.2. MICROVIBRATION TESTS

On-ground microvibration testing is an essential element to assess the performance of sensitive space systems. Roughly speaking, microvibration tests can be separated into three main families, with complementary objectives (Ref. [11]).

- Characterisation of equipment (in particular disturbing equipment) is the first main application of microvibration testing. For elementary tests, this characterisation consists in the measurement of disturbances (i.e. forces and torques at the interface, measured on a dynamometric table) induced by the equipment on the structure (Fig. 4.2/1). More complex tests can be performed, providing also information on the internal behaviour of the equipment itself (current in a stepper motor, rotor displacements in a reaction wheel, ...). The results of these measurements can either be used directly as input data for microvibration analyses, or as validation elements for a dynamic model of the equipment.

- "Low level" modal identification of structures is also an important field of interest for microvibration testing. These tests consist in measuring the acceleration response on different points of the structure, when excited by a calibrated force (usually below 1 N). The acceleration-to-force transfer functions provide data for an experimental modal analysis; they can also be directly used as input data for microvibration analyses.

- System tests at satellite level finally allow verification of prediction analyses by directly measuring its performances (Refs. [3], [5]). At satellite level, such tests are performed by measuring the behaviour of sensitive payload instruments (line-of-sight rotations ideally, linear accelerations of some constitutive elements of the line-of-sight more frequently) while the main disturbing pieces of equipment are successively operated. The solutions worked out to ensure a good representativeness of on-ground microdynamic tests are further discussed in section 5.2.

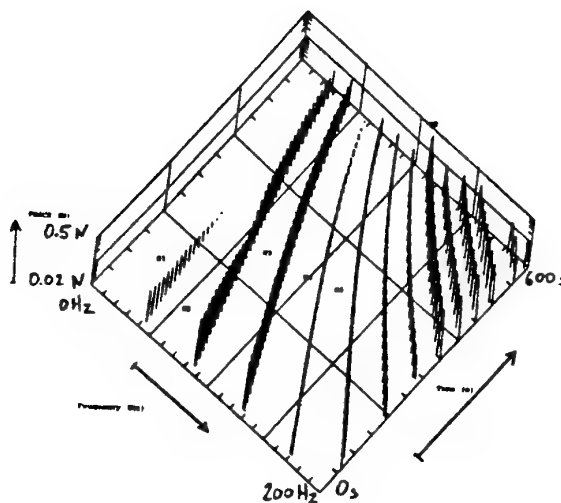


FIGURE 4.2/1 : Disturbance Forces of a SPOT4 Reaction Wheel (waterfall representation)  
The harmonic forces are clearly identified. Their amplitude increases with the wheel rotation rate.

### 4.3. HELIOS II MICROVIBRATION VERIFICATION LOGIC

The verification logic for high frequency performances of the HELIOS II satellite is based on an intimate combination of analyses and tests. A large number of analyses and tests are scheduled at various stages of the project :

- Equipment level
  - . mathematical models of disturbance sources and associated isolators, coupled models,
  - . tests dedicated to single or coupled element characterisation, and validation of the mathematical models.
- Subsystem level
  - . Finite Element Model of the instrument, including LOS motion resulting from the motion of the optical elements. Specific tests at instrument level to validate and improve modelling,
  - . Finite Element Model of the platform,
- Satellite level
  - . Elaboration of the satellite model by a combination of equipment mathematical models and Finite Element Models,
  - . Prediction of satellite performances (see section 4.1),
  - . Measure of transfer functions and experimental modal analysis on the satellite structural model to improve and validate the finite element model,
  - . System verification on the satellite flight model. Measurement of optical elements motions during disturbance sources operation.

The purpose of the early tests and analyses as the hardware design and development progress is to evaluate more and more precisely the satellite pointing performances, to identify any hardware that could be a potential threat and make appropriate design modifications early in the program, so that costly changes at later stages can be avoided.

This microvibration prediction and verification logic relies on a structured and hierarchical approach, similar to that of thermal and mechanical activities :

- specification from satellite to equipment level,
- analyses, validation of models by specific tests at each level, models transmitted from equipment to satellite level,
- final performance demonstration at satellite level (analyses using a complete model and system satellite tests),
- introduction of Dynamical Interface Control Documents to manage the interfaces between the different levels.

## 5. EXAMPLES OF MICRODYNAMICS TESTS

### 5.1. HISTORY OF MICRODYNAMICS TESTING AT MMS

An overview of the most significant microdynamics tests performed at MMS over the last few years is provided in Table 5.1/1.

| TYPE OF TEST                                       | TEST IDENTIFICATION        | DATE  |
|--|----------------------------|-------|
| Microdynamic Tests at equipment level              | EUROSTAR Momentum Wheel    | 88    |
|  | Reaction Wheel SPOT Mark 2 | 91/94 |
|  | Reaction Wheel on Isolator | 92    |
|  | Lavotchkin damping devices | 93    |
|  | Reaction Wheel SOHO        | 93/94 |
|  | MCV Mechanism SPOT 4       | 92/93 |
|  | MCV Mechanism SPOT 3       | 93    |
|  | CPA Mechanism SILEX        | 94    |
|  | Freezer-Cooler COLUMBUS    | 94    |
|  | Tape recorder SOHO         | 94    |
| Microvibration Tests on substructures              | HELIOS Telescope Mount     | 91    |
|  | SILEX Optical Assembly     | 93    |
|  | SILEX Mobile Part          | 93    |
|  | MAROTS Structure           | 92/93 |
| Microvibration Tests on satellites and instruments | INMARSAT 2 PFM             | 89    |
|  | TELECOM 2 PV1, MV2         | 91    |
|  | SPOT 3 MV                  | 91    |
|  | HELIOS MSTH                | 92    |
|  | SPOT 4 P1, PV              | 93/94 |
|  | SILEX STM, MQV             | 93/94 |

TABLE 5.1/1 : Microdynamics Testing at MMS

### 5.2. REPRESENTATIVENESS OF MICRODYNAMICS TESTS

Microdynamics tests are dedicated to study the behaviour of a system in orbit conditions ; ideally they should be performed also in such conditions. For example, a verification test at satellite level should feature on a free-free structure, in vacuum, in zero gravity... Solutions have been worked out, that allow to simulate in-orbit conditions with a good accuracy (Ref. [11]) :

#### \* *Environmental disturbances*

Most microvibration tests are performed at night, on seismic floors. In addition, air-conditioning, laminar flows (if any) and lights are turned off during measurement sequences. This ensures a reduction of external mechanical and acoustic noise (by minimisation of human activity, traffic, etc... and seismic noise filtering with low cut-off frequency). Very low noise electronics are used for signal conditioning, amplification and acquisition. A particular care is also taken to realize a "safe" electrical test configuration, in order to avoid EMC problems.

#### \* *Configuration of the test specimen*

- A "quasi free-free" configuration can be achieved using low frequency suspension devices : soft sling suspension for satellite's microvibration tests ; low frequency springs for SILEX tests... Such devices also isolate further the test specimen from external mechanical disturbances.
- On ground, it is often impossible to deploy flexible appendages such as solar arrays, large antenna reflectors (on telecommunication satellites), masts .... However, since most of their modal mass is in the low frequency range, these appendages do not affect the dynamic behaviour of the structure in the frequency range of interest for microdynamics (typically above 5 Hz). In turn, they are not integrated on the test specimen, with no impact on the test representativeness.

### **\* Gravity effects on equipments**

The behaviour of some equipments can be strongly affected by gravity (magnetic bearing wheels, unbalanced pointing systems...). In some cases, they can even not be operated under 1g. Therefore dedicated anti-gravity devices must be designed; the most currently used are based on low-frequency suspensions that are adjusted to compensate the weight effects. These solutions are generally preferred to solutions using a counterweight: no added mass, tuning capability, low added stiffness and damping - consequently minimum interaction with the test specimen.

### **\* Air effects on high frequency dynamics**

Air effects were investigated by analysis and test in the frame of the ESA R&D study Prediction of High Frequency Low Level Vibration (Ref. [8]). The results illustrated how added mass and added damping could affect the structural response, typically above 250 Hz. They also showed that most of these effects can be eliminated by placing the test specimen under a helium tent (Refs. [9], [10]). Since it is often impossible to perform microdynamics tests in vacuum (especially when large structures with suspension devices are involved), this alternative solution is used when high frequencies have to be investigated. If for any reason the test cannot be performed under the helium tent, "rule-of-thumb" margins (derived from past experience) must be applied above 250 Hz to the results obtained in air.

### **\* Effects of test instrumentation**

The test instrumentation itself may affect the dynamic behaviour of the test specimen: mass is added to the specimen (sensors); stiffness and damping are added (wires). This can be a real problem, especially on light weight structures. No standard solution is readily available; it is rather a case of "engineering feeling" and experience: a correct trade-off in terms of instrumentation must be reached (mass vs. sensitivity, quantity vs. quality of information, find the "right" location and a correct wiring). The ultimate solution is to include the additional mass due to the microvibration sensors in the Finite Element Model of the test specimen and to use this model for correlation.

These problems of on-ground representativeness - and their associated solutions - are illustrated in the next sections, which develop some significant examples of microdynamics tests performed recently at MMS.

## **5.3. TEST ON SPOT REACTION WHEELS**

The SPOT 4 Reaction Wheels are 40 Nms magnetic bearing wheels, developed by AEROSPATIALE (RRPM, for "Roues de Réaction à Palier Magnétique"). They have been identified through preliminary analyses as a possible major disturbance source, and a particular effort has been made to improve the knowledge of this equipment. In this frame, a series of dedicated characterisation tests have been performed on the three SPOT 4 Flight Models to quantify the disturbances applied to the structure by the wheels in rotation.

### **\* Aims of the test**

The aim of the test was to measure the 6-axis interface forces and torques generated by the wheels, rotor in rotation, and to quantify their variation versus the wheel rotation speed. Emphasis was set on the characterisation of the spectral contents of the disturbance source.

### **\* Test configuration and representativeness**

The three flight models were (successively) rigidly mounted on a 6-axis Kistler dynamometric platform (rotation axis vertical). This platform is designed to measure the interface forces with an accuracy of 1 milli-N. It is integrated inside a vacuum chamber, itself mounted on a massive seismic concrete block - isolated from the ground by a low cut-off frequency spring system. The calibration of the test set-up has shown that accurate measurements were ensured in a bandwidth between 2 Hz and 250 Hz (at least). Inside this bandwidth, the representativeness of the test configuration is correct: the wheel is in vacuum (then no unwanted aerodynamics effects can occur), and the gravity effects on the disturbance generation process remain limited.

### **\* Test instrumentation**

The eight charge signals delivered by the four piezoelectric force transducers were amplified by very low noise Brüel & Kjaer charge amplifiers. Data digitalisation and real-time processing was performed by a Hewlett-Packard front-end (with 16 active channels); they were stored on a Hewlett-Packard 9000 workstation. The Software was the IDEAS test package (developed by SDRC), also used for post-processing of the test data.

### **\* Measurement sequences**

Taking into account the need for characterisation of the disturbances in the whole operational range of rotor velocity, the following method was used:

- Run-up with full motor torque up to the maximum operational rotation speed ( $\approx 40$  Hz).
- Run down at zero motor torque; the rotor speed decreases due to internal friction. During the run-down (duration  $\approx 25$  minutes), the eight Kistler force channels were recorded in the time domain, with a sampling frequency of 512 Hz; the tachopulse signal was also recorded (reference for angular velocity).

Due to the low level of friction, the rotor speed decreases very slowly; over a short period of time (1 or 2 seconds), it is justified to consider this speed as constant. The run-down phase can thus be processed as a "series of quasi-steady states" of the wheel: this principle is exactly similar to that on which is based the experimental modal analysis by "sweep sine" excitation. The post-processing performed at MMS was the following:

- Calculation of the 6-axis torque at the interface of the wheel (time domain).
- Series of spectra vs. time all along the run-down phase ("waterfall" representation).
- Identification and tracking of the main harmonics, as a function of the rotor velocity.

This method is particularly well adapted to microdynamics tests involving a reaction or momentum wheel. It allows a comprehensive characterisation of the disturbance through one unique test sequence.

### \* Typical results

An example of spectra in "waterfall" representation is given for the radial force on Figure 5.3/1 ("radial" means in the plane perpendicular to the rotation axis) over a run-down phase. This plot shows the harmonic contents of the disturbance, which can be interpreted as the "image" of geometric imperfections of the position detection ring (used as reference for the active radial control). The

frequency of the harmonics decreases in time, following the decrease of the rotation velocity.

A typical result for the axial force (parallel to the rotation axis) is also provided on Figure 5.3/2. This plot shows the level of the axial force harmonics vs. the wheel rotation frequency. The peaks correspond to the coincidence between the harmonics excitations and the axial resonance frequency of the magnetic bearing ( $\approx 18$  Hz).

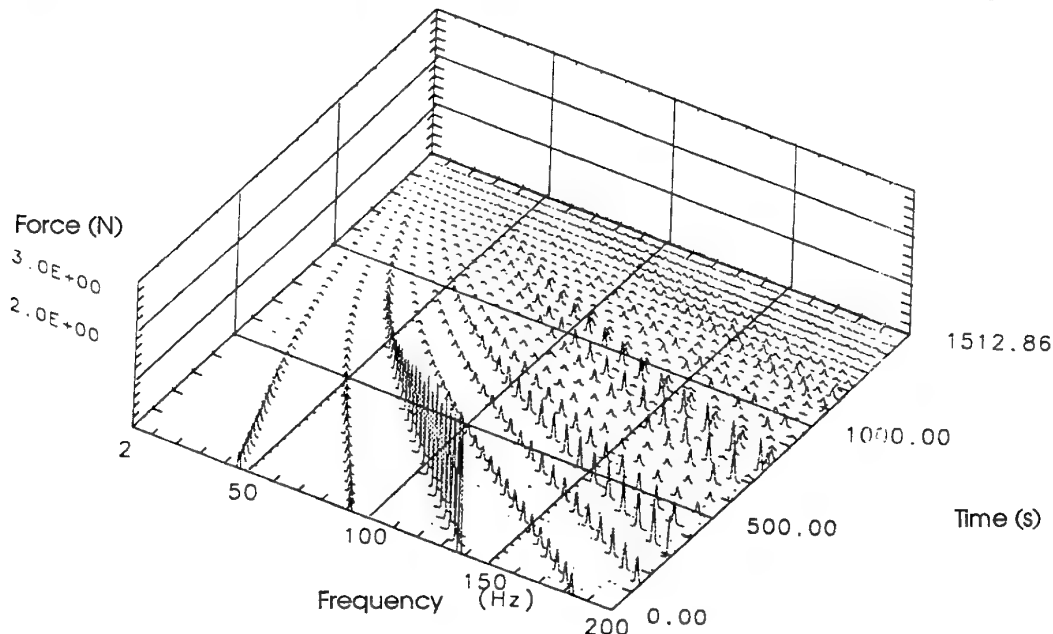


Figure 5.3/1 : Radial Disturbances Force on a SPOT Reaction Wheel

*This "waterfall" series of disturbance spectra illustrates the evolution of the harmonic content as the rotor speed decreases. These experimental data were obtained on a SPOT magnetic bearing Reaction Wheel, mounted on a Kistler 6-axes dynamometric platform.*

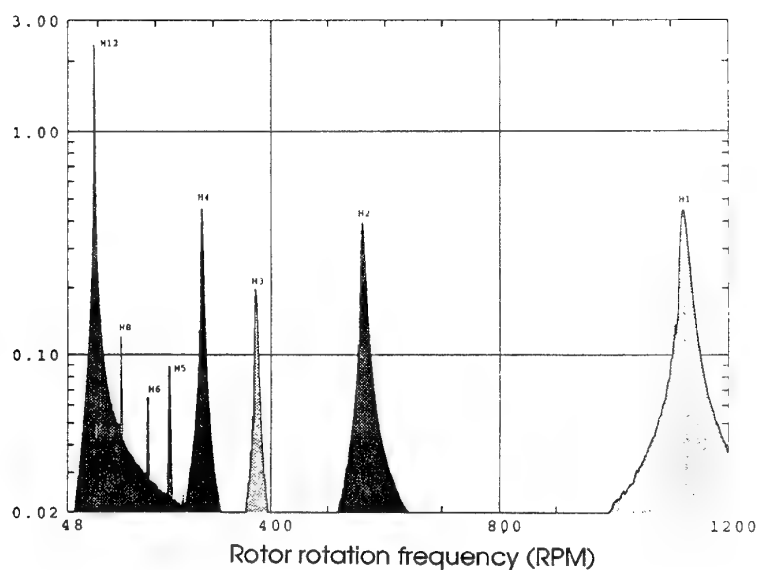


Figure 5.3/2 : Axial Disturbance Force on a SPOT Reaction Wheel

*This figure shows the amplitude of the axial force vs. rotor rotation frequency. The peaks correspond to the excitations by the successive harmonics of the axial resonance of the magnetic bearing.*

#### 5.4. TEST ON HELIOS I TELESCOPE MOUNT

In orbital configuration, the HELIOS I telescope is linked to the platform by a flexible isostatic mount made of three titanium blades to filter interface deformations. A test on this mount was performed at MMS in January 91.

##### \* Aims of the test

The main objectives of this test were :

- to measure the frequencies of the first modes introduced by the flexible mount and to compare with Finite Element Model predictions,
- to measure the damping ratios of these modes for very low excitation levels and to evaluate their sensitivity to the level of excitation,
- to compare the damping factors for two hanging configurations, and to evaluate the effect of the wiring between the telescope and the platform.

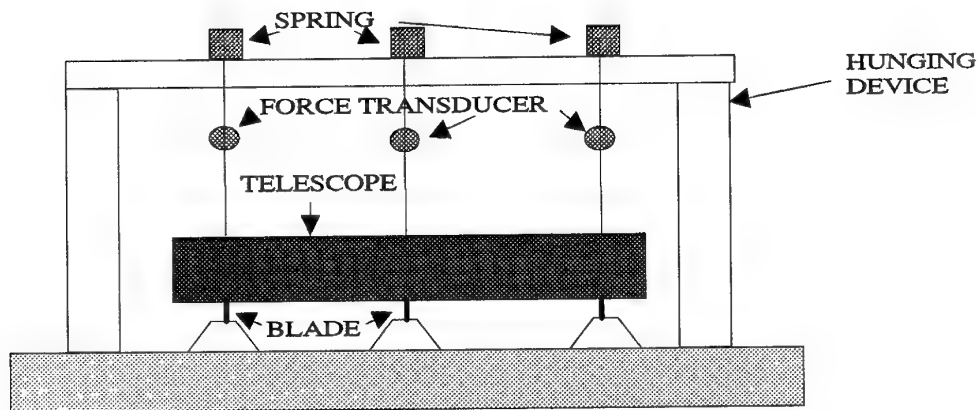


FIGURE 5.4/1 : Test Set-up on HELIOS 1 telescope mount

##### \* Test configuration and representativeness

The test was performed with the Identification Model (structurally representative) of the telescope mount and a telescope mock-up representative of mass but only partially for center of gravity and inertia. Two configurations were used. In the first one, the mock-up was hung by three suspension devices (low frequency springs) to compensate gravity, to place the telescope in orbital configuration and thus avoid static constraints in the blades (Fig. 5.4/1). In the second configuration, gravity was not compensated, and springs under the 3 blades were used to place the telescope in orbital configuration. In addition, to limit external disturbances, tests were performed at night, air-conditionning and light turned off. Some "high level" tests were performed in the day-time.

##### \* Test instrumentation

The test instrumentation was based on 7 very high sensitivity piezoelectric accelerometers (Endevco 7707), 1 servo-accelerometer (Sundstrand QA2000), 2 inertial angular displacement sensors (Systron-Donner 8301F) to measure microvibrations, and 3 force transducers to monitor the forces introduced by the anti-gravity device. An electrodynamic shaker (Brüel and Kjaer 4810) fitted with a force sensor (Brüel and Kjaer 8201) was used to generate calibrated excitations. Data were stored on a magnetic tape recorder (RACAL - 14 channels) and monitored on a Hewlett-Packard 9000 workstation.

##### \* Measurement sequences

After a complete characterization of seismic noise effects and anti-gravity system, two measurement sequences were performed :



- measurement of accelerations and angular displacements of the telescope hung by the anti-gravity system for different excitation levels. Excitations were applied along several telescope axes, for different types of excitation (random, sine) and force level (from 0.01 N to 2 N),
- a subset of these measurements was performed again without the anti-gravity system.

Finally, effects of additional wires between the telescope and the platform were measured during specific test sequences.

#### **\* Typical results**

Very clean transfer functions have been obtained between 8 and 40 Hz (range of first mount modes frequencies) except for very low levels of excitation. Due to the poor representativeness of center of gravity position, inertia and not modeled blades local interface stiffness, differences on modes frequencies (20 %) were observed between measurements and analysis results. Damping ratios were estimated with three methods : modal analysis, width of the response curve at the "half power point" ( $\xi = \Delta\omega/2\omega_n$ ), and by comparison with typical response plots drawn for different modal damping factors. Measurements have shown a very small sensitivity to the excitation level, no effect of static constraint in the blades (anti-gravity system use or not) and a limited increase of damping (15%) in the presence of wires.

Test results were finally introduced into the mathematical model to improve the prediction of line-of-sight stability.

### **5.5. TEST ON HELIOS I STRUCTURAL MODEL**

Low level modal identification of structures can be illustrated by the test performed on the HELIOS I structural model at MMS in February 1992.

#### **\* Aims of the test**

The essential aims of this test were the following :

- measure precisely the modal characteristics of the first main satellite modes to reduce uncertainty on frequencies, damping factors and modal shapes,
- measure transfer functions between the disturbance sources (reaction wheels, magnetic tape recorders) and the line-of-sight, and compare them with predictions issued from finite element analysis.

#### **\* Test configuration and representativeness**

The test was performed on the satellite structural model, fully representative of mechanical and dynamical behaviour of the flight model. The satellite was hanged by four textile soft slings and a 0-gravity system (three springs between the telescope and a whiplike tree) was developed to place the telescope in orbital configuration. This "quasi free-free" configuration allows the satellite to have a behaviour very close to the orbital one. Like other microvibration tests, this test was performed at night in a clean room, air-conditioning and lights turned off.

#### **\* Test instrumentation**

A similar instrumentation to the telescope mount test described in section 5.4 was used during this campaign. The number of accelerometers was increased up to twenty-two in order to identify modal shapes and to elaborate final LOS motion resulting from the motion of each degree-of-freedom of the optical elements (mirrors, focal plane).

#### **\* Measurement sequences**

Transfer functions for different levels of excitation were measured between the calibrated force generated by the dynamic shaker and the acceleration responses over the structure, and especially on optical elements.

An additional sequence with modified accelerometers location was added to characterize the effects of the satellite suspension device and the 0-gravity telescope system.

#### **\* Typical results**

Modal analysis was performed by CNES to identify modes characteristics (frequency, damping factor and shape) and a comparison between measured transfer functions and predictions issued from a finite element analysis was performed.

For the first modes (below 42 Hz), a disturbing coupling effect was identified between the satellite and the two 0-gravity systems making the correlation between analysis results and test measurements difficult. Modal analysis has shown a very good reproducibility of frequencies and an increase of damping factors for high levels of excitation (fig. 5.5/1). Between 42 Hz and 120 Hz, only transmissibility levels were compared because of the great number of modes in this frequency band.

### **5.6. SYSTEM LEVEL TEST ON SPOT4/SILEX**

A test was performed at MMS in December 1993 on the SPOT 4 satellite (structural representative model), with its SILEX payload (Structural and Thermal Model). By the complexity of its realisation, it is a very typical example of what can be done in the frame of system level microdynamics testing.

#### **\* Aims of the test**

The essential aims of this test were the following :

- Assess the validity of the SPOT 4 Finite Element Model and identify the modal damping factors on the main structural modes, for very low excitation levels.
- Verify the modal coupling between the SPOT 4 satellite and the SILEX terminal.
- Verify the effects of dynamical coupling between the disturbing equipments and the structure (forces generated by some equipments are affected by the dynamical impedance of the structure).
- Verify the effects of the main in-orbit disturbance sources on measurement points "as close as possible" to the constitutive elements of the SPOT4 and SILEX Lines-of-Sight, in the case of the test configuration : SILEX in canonical position, balanced Oblique Viewing Mirrors...

| FREQUENCY<br>(Hz) | DAMPING RATIO<br>(%) |
|-------------------|----------------------|
| 22.5              | $0.4 < \xi < 1.1$    |
| 27.6              | $0.3 < \xi < 0.6$    |
| 29.2              | $0.4 < \xi < 1.3$    |
| 31 and 32         | $0.4 < \xi < 0.9$    |

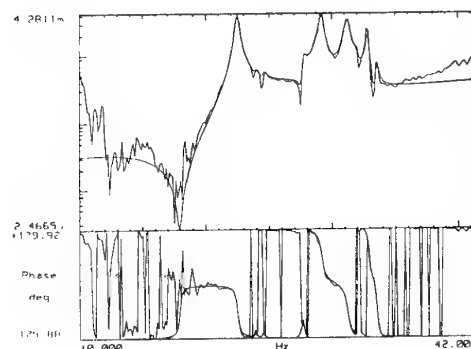


FIGURE 5.5/1 : Experimental modal analysis - Frequencies and damping factors

#### \* Test configuration and representativeness

The test configuration (Fig. 5.6/1) has been defined to ensure a good representativeness of the specimen, in application of the general methodology presented in Section 5.2. The satellite was hung by a dedicated suspension device (four textile soft slings, held by a whipple tree under the overhead rail) ensuring low frequency decoupling and minimum added mass. The Mobile Part of SILEX was also hung by its own anti-gravity system (MGSE based on low frequency springs). A correct tuning of these two suspensions was necessary to reach an acceptable alignment of the system.

As recommended in Section 5.2, this test was performed at night, air-conditioning and lights turned off in the clean room during the measurement sequences.

According to the complexity of the test specimen, it was not possible to use the helium tent to reduce the effects of air at high frequency. Anyway the behaviour of the structure above 250 Hz was not the essential concern for this test; the limitation of representativeness due to air was found acceptable, considering that "rule-of-thumb" margins would be applied to correct the measurements in this frequency domain.

Some additional limitations were due to effects of gravity on the Magnetic Bearing Reaction Wheels (however found acceptable in the range of wheel spin rate for the SPOT4 mission, i.e. below 400 rpm) and on the Oblique Viewing Mirrors: these mirrors are unbalanced in orbit configuration, but have to be balanced for on-ground operation.

#### \* Test instrumentation

The test instrumentation was based on 40 very high sensitivity piezoelectric accelerometers (Endevco, Wilcoxon) for sub-micro g measurements. Very low noise charge amplifiers were used (Brüel & Kjaer, Kistler), powered by internal batteries to limit interaction with the external AC supply. Data digitalization and realtime

processing were performed by a 40-channel Hewlett-Packard front-end; they were stored on a Hewlett-Packard 9000 workstation. The Software was the IDEAS test package (developed by SDRC), also used for post-processing of the test data.

An electrodynamic shaker was used for the test sequences dedicated to modal analysis. This shaker, fitted with a force sensor (Brüel & Kjaer), is able to deliver low level forces (1 N, 0.1 N and below) in a bandwidth between 10 Hz and 2 kHz. It is particularly well fitted to modal analysis in the microvibration domain.

#### \* Measurement sequences

Two different types of measurement sequences were performed during this test, with complementary objectives:

- Transfer functions measurement: these sequences were dedicated to the modal characterization of SPOT4/SILEX. Transfer functions were measured between the calibrated force generated by the dynamic shaker and the acceleration responses over the structure. Excitations were applied on several points and along several spacecraft axes, so as to obtain a comprehensive data set for experimental modal identification.
- Measurement of accelerations induced by the in-orbit disturbance sources: pointing stability performance of the system was evaluated by operating the main on-board disturbance sources, and by measuring their induced accelerations near the sensitive payloads. The equipments operated during these sequences were the three Magnetic Bearing Reaction Wheels, one Tape Recorder, two gyroscopes (high speed rotating mechanisms), one Oblique Viewing Mirror of the SPOT 4 instruments ("full step" stepping motor), the elevation motor of SILEX Coarse Pointing Assembly ("microstep" stepping motor) and one PHL50 electrical relay (single-event mechanism).

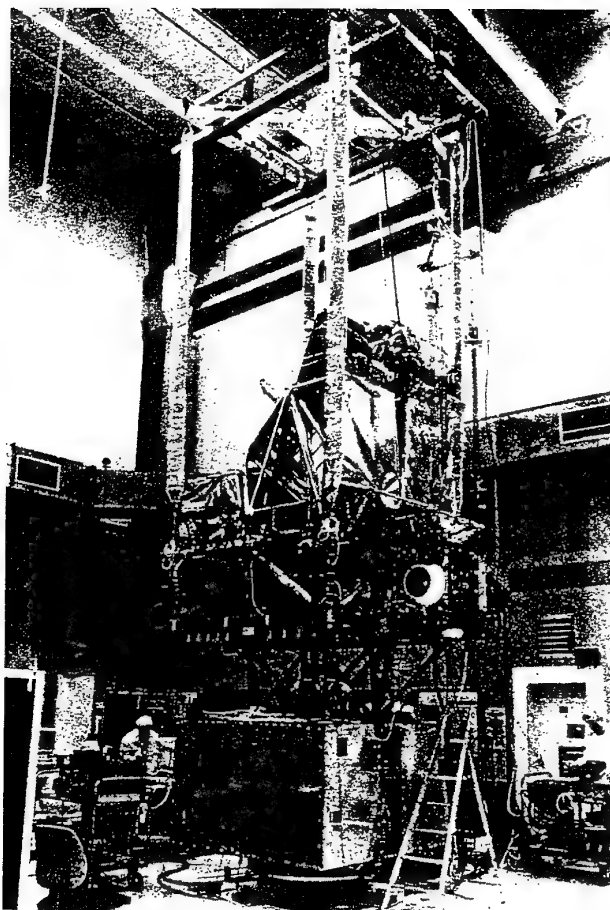


FIGURE 5.6/1 : SPOT4/SILEX microvibration test set-up

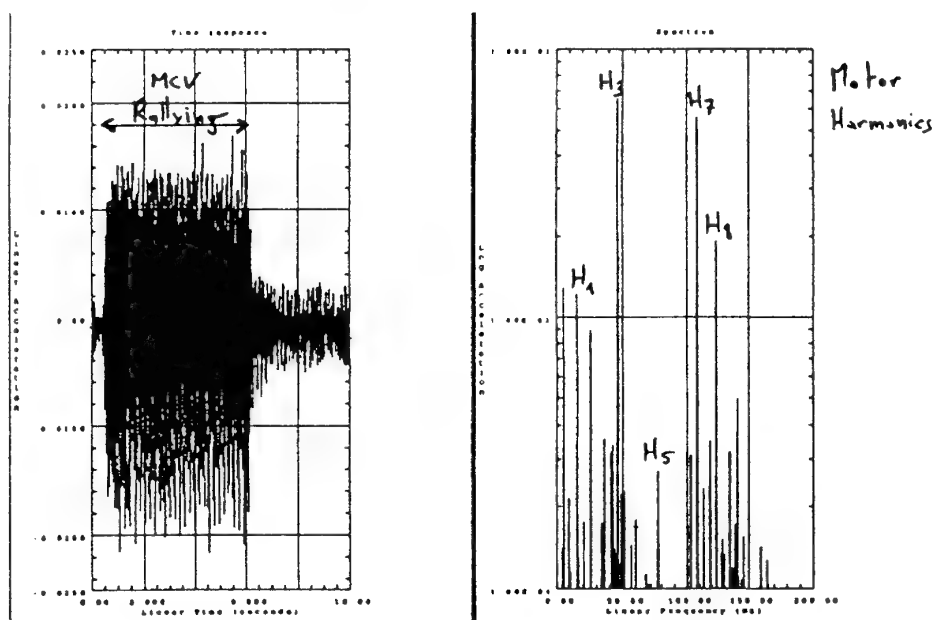


FIGURE 5.6/2 : Signature of a SPOT 4 MCV as seen by SILEX

### \* Typical results

Very clean transfer functions have been obtained especially between 20 Hz and 800 Hz. Interesting results have already been obtained concerning the equipments/structure dynamic coupling. Figure 5.6/2 illustrates the effect on SILEX of a rallying motion commanded to a SPOT4 Oblique Viewing Mirror (time history and frequency domain plots) : this very clean response signal shows only spectral lines corresponding to well known frequencies (expected from analysis) : harmonics of the 16 Hz motor switch frequency, plus some subharmonic lines due to well identified non linear effects on the motor.

The comprehensive analysis of this very rich and complex test is still under progress at MMS.

## 6. CONCLUSION

Mastering microvibrations on satellites is a key issue for future reconnaissance satellites requiring ultimate pointing accuracy in a wide frequency range. The objective of this paper was to present the methodologies used at MATRA MARCONI SPACE for the prediction and verification of microvibrations.

Stability requirements have been reviewed in the first part of the paper, whereas microvibration sources and effects are described in the second part. In the third part, the presented logic for microvibration prediction and verification has shown the combination of analyses and tests at equipment, subsystem and satellite level to demonstrate satellite performances. Finally, a set of tests performed at MMS has been described to illustrate the importance of testing to master high frequency pointing stability performances.

The thorough understanding of high frequency spacecraft dynamics, disturbance signatures and coupling effects between the disturbance sources and the spacecraft structure, acquired by MATRA MARCONI SPACE in the frame of on-going spacecraft developments, has already allowed to propose design improvements such as structural design optimization or disturbance source minimization.

In parallel, a comprehensive R&D programme has been initiated in the early 90's to identify and test innovative techniques and technologies to master microvibrations for future very high pointing accuracy missions (Ref. [12]). In particular, passive and active vibration isolation and damping concepts are currently investigated to proof-of-concept level, for application to observatory and reconnaissance satellites.

## 7. ACKNOWLEDGEMENTS

The work presented in this paper has been performed in the frame of CNES contracts (HELIOS and SPOT4 satellites). The authors wish to thank MMS and CNES

engineers involved in these studies for the many fruitful discussions and their helpful contributions.

## 8. REFERENCES

- [1] In-orbit microvibrations, JM. Bétermier, F. Mercier, M. Pircher, DGA, Sciences et Défense 92.
- [2] TDI Improves Scanned Imaging Systems, L. Hudson, Laser Focus World, February 1992.
- [3] Influence of Microvibrations on Spacecraft Performances, N. Jourdon, V. Guillaud, International Conference on Spacecraft Structures and Mechanical Testing, Noordwijk, The Netherlands, April 1991.
- [4] An overview of CNES's Microdynamic Research Activities and Rationale in order to Prepare New Missions Requiring Very Accurate Stabilization, JM. Bétermier, First International Symposium on Space Microdynamics and Accurate Control, Nice, France, December 1992.
- [5] Microvibration Tests on Satellites : Lessons Learned from the SPOT 3 Experiment, JM. Bétermier, M.C. Charneau, N. Jourdon, V. Guillaud, First International Symposium on Space Microdynamics and Accurate Control, Nice, France, December 1992.
- [6] Line-of-Sight Jitter Analysis of SILEX Optical Terminals, P. Camarasa, V. Pascal, A. Capitaine, V. Guillaud, E. Desplats, 2nd International Conference on the Dynamics and Control of Structures in Space, Cranfield, UK, September 1993.
- [7] Improvement for Interpretation of Structural Dynamics Calculation using Effective Parameters for Subsystems, T. Berthelon, A. Capitaine, International Conference on Spacecraft Structures and Mechanical Testing, Noordwijk, The Netherlands, April 1991.
- [8] Prediction of High Frequency Low Level Vibration, ESA contract 9787/92/NL/PP (SC), October 1991.
- [9] Prediction of High Frequency Low Level Vibration, N. Jourdon, YM. Lefèvre, First International Symposium on Space Microdynamics and Accurate Control, Nice, France, December 1992.
- [10] Test and Vibroacoustic Predictions of Microvibrations Transmission in Space Structures, N. Jourdon, YM. Lefèvre, C. Clerc, DG. Eaton, 44th International Astronautical Congress, Graz, Austria, October 1993.
- [11] Microdynamics Tests at MMS, Ph. Laurens, V. Guillaud, 2nd ESA International Conference on Spacecraft GNC Systems, Noordwijk, The Netherlands, April 1994.
- [12] Mastering Microvibrations for High Pointing Accuracy Systems, V. Guillaud, C. Champetier, A. Capitaine, YM. Lefèvre, 2nd ESA International Conference on Spacecraft GNC Systems, Noordwijk, The Netherlands, April 94.

## AEROTHERMODYNAMIC TESTING REQUIREMENTS FOR FUTURE SPACE TRANSPORTATION SYSTEMS

John W. Paulson, Jr. & Charles G. Miller, III  
Aerothermodynamics Branch/Gas Dynamics Division  
NASA Langley Research Center  
Hampton, VA 23681-0001, USA

### SUMMARY

Aerothermodynamics, encompassing aerodynamics, aero-heating, and fluid dynamic and physical processes, is the genesis for the design and development of advanced space transportation vehicles. It provides crucial information to other disciplines involved in the development process such as structures, materials, propulsion, and avionics. Sources of aerothermodynamic information include ground-based facilities, Computational Fluid Dynamic (CFD) and engineering computer codes, and flight experiments. Utilization of this triad is required to provide the optimum aerothermodynamic design to safely satisfy mission requirements while reducing undue design conservatism, risk, and cost. This paper discusses the role of ground-based facilities in the design of future space transportation system concepts. Testing methodology is addressed, including the iterative approach often required for the assessment and optimization of configurations from an aerothermodynamic perspective. The influence of vehicle shape and the transition from parametric studies for optimization to benchmark studies for final design and establishment of the flight data book is discussed. Future aerothermodynamic testing requirements including the need for new facilities are also presented.

### LIST OF SYMBOLS

|                   |   |
|-------------------|---|
| $C_h$             | heat transfer coefficient                               |
| $C_L$             | lift coefficient  |
| $C_l$             | rolling moment coefficient                              |
| $C_m$             | pitching moment coefficient                             |
| $C_n$             | yawing moment coefficient                               |
| $C_p$             | pressure coefficient                                    |
| $C_Y$             | side force coefficient                                  |
| $L/D$             | lift to drag ratio                                      |
| $M$ or $M_\infty$ | Mach number   |
| $P_0$             | stagnation pressure, psi                                |
| $Re$              | Reynolds number   |
| $Re_{\infty,L}$   | length Reynolds number                                  |
| $T_0$             | stagnation temperature                                  |
| $T_w/T_{aw}$      | ratio of wall temperature to adiabatic wall temperature |
| $\alpha$          | angle of attack, deg                                    |

|                  |                            |
|------------------|----------------------------|
| $\gamma$         | ratio of specific heats    |
| $\delta_{flap}$  | flap deflection, deg       |
| $Pt/\rho_\infty$ | normal shock density ratio |

### INTRODUCTION

#### Future Space Transportation System Concepts

The Access to Space Study (Reference 1) is a recently completed review of the launch vehicle needs of the United States of America carried out by an interagency group with members from the National Aeronautics and Space Administration (NASA), the Department of Defense (DOD), and the Department of Transportation (DOT). This study evaluated several options for launch vehicles which could provide a more economical access to space than the current Space Shuttle. The first option was to continue flying the Shuttle system until the year 2030 while improving its performance and reducing operational costs. The second was to fly the Shuttle to the year 2005 while making the transition to a new system based on current technology, expendable launch vehicles (ELV) and a Personnel Launch System (PLS) and a Cargo Delivery and Return Vehicle (CDRV). Configurations being studied for this system range from lifting bodies capable of horizontal, runway landings to ballistic shapes. Finally, the third option was to use advanced or "leapfrog" technology to develop a fully reusable vehicle to replace the orbiter in 2008.

From a large matrix of concepts in option 3, the field was narrowed to three. The first is a winged single stage-to-orbit rocket (SSTO-R) powered vehicle that would takeoff vertically and glide back for a runway landing. This concept is under study and development at NASA Langley Research Center (LaRC) and is presently referred to as Single Stage Vehicle (SSV)-001. This study of a winged configuration serves as the foundation for a potential subscale flight demonstration vehicle referred to as the X-2000. A vertical launch and landing concept (e.g., McDonnell Douglas DC-Y) was also examined as a SSTO-R candidate. The second is a supersonic-hypersonic airbreathing SSTO concept that employs small rockets at a flight Mach number of approximately 15 to achieve orbit. This concept, which minimizes the need to carry on-board supplies of liquid oxygen by using ramjet and scramjet engines burning hydrogen mixed with atmospheric air, would takeoff and land horizontally. It represents a derivative of the USA National Aero-Space Plane (NASP) X-30. As a follow-on to the NASP program, HySTP (Hypersonic System Technology Program) is intended to demonstrate the viability of scramjet propulsion at high hypersonic Mach numbers. Finally, the third is a runway-based, two stage-to-orbit (TSTO) concept whereby a large mothership powered by advanced ramjets and rockets carries an orbiter aloft for launch. The orbiter may be rocket or airbreathing/rocket powered and may be carried above or below the mothership. This concept involves separation of the orbiter from the mothership at supersonic or hypersonic conditions and both vehicles return for a

horizontal landing. A precursor to this concept is Germany's Saenger (reference 2).

The depth and breadth of these studies cover a wide range (Figure 1), with some concepts represented by paper studies and others developed to sufficient maturity to warrant construction of hardware. Following an extensive review of the three options considered in the Access to Space Study, the third option involving utilization of advanced, or "leapfrog", technology was deemed the preferred approach. Of the various concepts considered in this option, the SSTO-R vertical takeoff/horizontal landing vehicle was judged to be the most viable for the time frame considered (i.e., operational by the year 2008).

Also, other studies include concepts designed to provide low cost launch of relatively small payloads such as communication satellites and explorer-type spacecraft (e.g., 500 to 1500 lbs) into low Earth orbit (LEO). Included in these Small Payload to Orbit Vehicle (SPOV) concepts are partially reusable configurations. After separation on ascent at hypersonic conditions, the first stage would enter and land horizontally. Such concepts incorporate rocket and airbreathing propulsion systems. Not to be overlooked are planetary transportation systems and probes such as the Pathfinder and Mars Environmental Survey (MESUR). The Mission from Planet Earth program includes the development of relatively small probes which enter planetary atmospheres at high velocities. Research in this area is dictated by an unknown schedule for future space exploration.

This paper will discuss the role of aerothermodynamics for the design of future space transportation system concepts as well as, scope and sources. Testing methodology will be addressed, including the iterative approach often required for the assessment and optimization of configurations from an aerothermodynamic perspective (Figure 2). The influence of vehicle shape (i.e., different challenges associated with very slender compared to quite blunt configurations) and the transition from parametric studies for optimization to benchmark studies for final design and establishment of the flight data book are discussed. Future aerothermodynamic testing requirements are examined, including the design and fabrication of test articles, advances in measurement techniques, enhancements to existing ground-based facilities and/or the need for new facilities.

## **ROLE OF AEROTHERMODYNAMICS**

### **Definition**

Aerothermodynamics is defined herein as encompassing three disciplines: (1) aerodynamics, involving forces, moments, and pressure loads on the vehicle across the speed range from take-off to orbit, beyond Earth orbit, and entry to landing (e.g., Mach 0.1 to 40); (2) aero-heating, which includes convective and radiative heat-transfer rates over a configuration at flight conditions; and (3) fluid dynamic and physical processes which involve complex flow phenomena from the free molecular to the continuum regimes (e.g., boundary-layer/shear-layer transition to turbulence,

shock/shock interactions, shock impingement, flow separation and reattachment, etc.) and processes associated with high temperature gases (e.g., chemical reactions, transport processes, radiation, coupled relaxation and/or excitation processes, thermodynamic nonequilibrium, gas-surface interactions, etc.). Designers of aerospace vehicles are primarily concerned with the aerodynamic performance, stability and control and vehicle surface characteristics such as aerodynamic pressure and heating loads. Fluid dynamic and physical processes are closely coupled to aerodynamics and aero-heating and provide explanations for phenomena observed at the surface by understanding the flowfield about the vehicle. This three-part definition of aerothermodynamics is applied across the subsonic-to-hypersonic speed regimes for the full spectrum of aerospace vehicle configurations.

### **Scope**

Efficient aerothermodynamic design is vitally important for all aerospace vehicles and depends on vehicle shape and size, as well as velocity, attitude, altitude, and atmospheric composition. Fundamental flow phenomena may have a major influence on the aerodynamics or aero-heating depending primarily, but not exclusively, on the vehicle shape, flow conditions, and attitude. For example, boundary-layer transition may be of critical importance for a slender body at hypersonic conditions but may be of secondary interest for a blunt, nonablating body. Real-gas effects may be important for blunt-body design, but of less consequence for design of slender bodies except in the leading edge regions and around deflected control surfaces. Thus, the expertise developed for the Mercury, Gemini, Apollo, Viking, Aeroassist Flight Experiment (AFE), and other programs involving blunt bodies, may not be directly applicable to the design of more slender hypersonic bodies. Within the extremes of these vehicle shapes are what are commonly referred to as moderately blunt bodies. Examples of moderate blunt bodies are the Shuttle Orbiter and candidate lifting body PLS and winged SSTO/TSTO concepts, which enter the Earth atmosphere at relatively high incidence. Since various shapes represent different challenges to the aerothermodynamic experimental and computational communities, it is important to maintain a balanced program for the full spectrum of shapes projected for future needs.

### **Sources**

The three sources of aerothermodynamic information are: (1) ground-based facilities, (2) computational fluid dynamic (CFD) computer codes and/or engineering codes and (3) flight experiments.

Ground-based facilities provide the fundamental information for flight. As is well recognized, duplication of all flight conditions is not possible and experimental aerothermodynamicists resort to the simulation of important flight parameters, such as Mach number, Reynolds number, and ratio of specific heats for subsonic to high hypersonic conditions and to the duplication of certain aspects of a flight condition (primarily velocity and the product of density and a characteristic length). Although no one facility can provide all of the aerothermodynamic information required for the

design of a vehicle, the combination of several facilities using various test gases (e.g., air/nitrogen and lighter and heavier gases) can simulate a major portion of the flight trajectory. The success enjoyed by the Apollo, Shuttle Orbiter, and other hypersonic flight programs, for which the vast majority of the aerothermodynamic data used in the design of the vehicle originated from ground-based facilities, is indicative of the applicability and importance of ground-based experimentation. Ground-based facilities such as subsonic, transonic, supersonic and hypersonic wind tunnels represent a tried and proven approach for providing aerothermodynamic information. As noted previously, wind tunnels provided the vast majority of aerothermodynamic information for the Shuttle Orbiter and the highly successful first flight (STS-1) of the orbiter, without the benefit of a hypersonic subscale or prototype flight vehicle, clearly demonstrated the validity of this approach.

Although CFD capabilities were not sufficiently mature in the late 1960's and early to mid 1970's to contribute substantially to the aerothermodynamic assessment of shuttle orbiter concepts studied in that time frame, significant advances have been made in CFD, particularly in the last decade. CFD is now in a position to contribute significantly to the aerothermodynamic design of the next generation of advanced aerospace vehicles and can significantly complement information from ground-based facilities. Validated CFD may be used to predict surface and flow field conditions for the full-scale vehicle at atmospheric conditions (i.e., density, temperature and molecular weight) for points along the flight trajectory. The highest confidence in any ground or flight data set occurs when results obtained by experimental and computational methods are in full agreement.

Flight experiments represent the third source of aerothermodynamic information and are quite costly. These experiments are generally performed with sufficient instrumentation to measure local phenomena (e.g., catalytic versus noncatalytic heating at hypervelocity conditions), but are not sufficiently instrumented to accurately model global phenomena such as laminar to turbulent boundary layer transition. In addition, they require considerable time and cost to perform.

Along with the researchers and facilities of the experimental community, another critical program requirement is the supporting infrastructure. This infrastructure consists of highly skilled model designers, precision model makers, facility engineers and technicians, instrumentation specialists, computer scientists, and system analysts for enhancing existing capabilities and applying new, advanced computer capabilities to acquire, reduce and store huge volumes of data. The infrastructure for experimental aerothermodynamics is often overlooked in specifying program requirements but is absolutely essential for success.

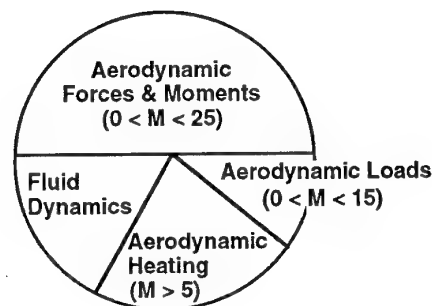
The present aerothermodynamic community of personnel and facilities is only a fraction of what it was in the 1950's and 1960's. However, advances in testing techniques and CFD should provide a significantly improved aerothermodynamic

capability, whereby much more can be achieved in less time with less manpower.

## **TESTING METHODOLOGY**

### **Balance of Testing Requirements**

In all likelihood, future crewed aerospace vehicles, will be fully, or nearly fully, reusable. Most concepts presently under study that include return to Earth capability have sufficient lift-to-drag (L/D) capability for conventional, horizontal landing upon return from orbit. Relatively high hypersonic L/D is required for high range and cross range to provide flexibility in landing sites, and may be achieved using lifting or asymmetric slender bodies. Higher values of L/D may be provided by winged vehicles. For conventional, horizontal landing, subsonic values of L/D of about 5 are desired and may be provided by lifting bodies with fins and by winged vehicles. Naturally, sufficient values of L/D must be achieved for vehicles using horizontal takeoff (e.g., those using airbreathing propulsion). For these horizontal takeoff and/or landing vehicles, extensive ground-based testing over the Mach number range from 0 to 25 is required to assess and to optimize takeoff, ascent to orbit, reentry, approach, and landing aerodynamic characteristics. From the perspective of the designers of such vehicles, the approximate balance between aerodynamic forces and moments, aerodynamic loads, aerodynamic heating, and fluid dynamic testing is shown in the following figure:



### **Iterate to Closure**

The design of the vehicle usually begins with a screening of the various concepts, whereby the aerodynamic characteristics of each concept are examined via testing across the subsonic to hypersonic regime. Parallel tests in hypersonic wind tunnels to determine aerodynamic heating characteristics, particularly the identification of regions of high heating. The vehicle field is generally narrowed to a single configuration. As the aerolines and required control surfaces begin to evolve towards an optimum flying concept, aerodynamic performance characteristics, aerodynamic loads and aerodynamic heating are measured in wind tunnels and predicted by CFD/engineering codes. Surface pressure distributions are measured/predicted across the speed regime

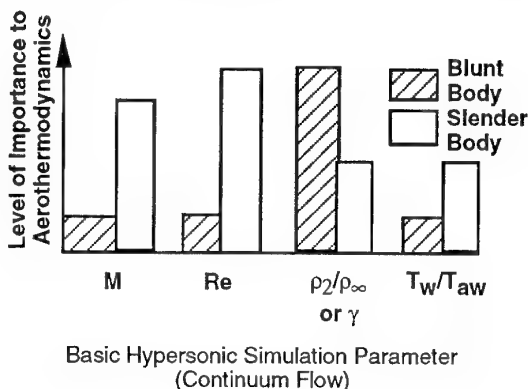


to determine loads on the vehicle during ascent and descent and particularly for abort trajectories. Testing and the running of CFD/engineering codes are performed to determine if fluid dynamic phenomena such as shock/shock interactions, separated/reattached flows, real-gas and rarefied flow effects, etc. will have a first or second order influence on aerothermodynamic characteristics. Findings of the aerodynamicists and aerothermodynamicists reveal what is expected to occur on the surface of the vehicle during flight and are complemented by the findings of the fluid dynamicists who generally examine local surface phenomena in more detail and also provide insight as to the nature of the flow field about the vehicle which produces the observed surface conditions. Knowledge of flow field properties (thermodynamic, kinetic (velocity), and atomic/molecular composition) provides an understanding of surface conditions, thereby often resolving anomalies that may occur, and are necessary for the calibration of fluid physics and chemistry models used in CFD computer codes.

### Effect of Vehicle Shape

As the approach to generating aerodynamic and aero-heating information is developed, an important factor to be considered in ground-based testing is the basic shape of the aerospace vehicle concept(s), since the shape dictates which simulation parameters will dominate. From a hypersonic perspective, the test approach for a very slender configuration will be quite different from that for a blunt configuration. For example, a hypersonic airbreathing (i.e., scramjet) vehicle will be slender and fly at low incidence during the high dynamic pressure ascent flight trajectory. For a slender shape and low incidence, the flowfield about the vehicle will be principally supersonic/hypersonic. The effects of compressibility (Mach number), viscosity (Reynolds number), gas properties (e.g., ratio of specific heats), and thermal driver potential (ratio of wall-to-adiabatic wall temperatures) are all expected to be important; that is, to have a first order influence on aerothermodynamic characteristics. Of particular importance is the state of the boundary layer (i.e., whether the boundary layer is laminar, transitional, and/or turbulent) which will determine the level of control effectiveness as well as heating. Because of the small shock inclinations associated with slender bodies at small incidence, finite-rate chemistry effects on aerodynamics (e.g., variation in center of pressure) and aero-heating (e.g., thermochemical nonequilibrium heating including surface catalytic effects) are usually second order except in local regions of flow stagnation and/or shock/shock interactions. On the other end of the shape spectrum, the flow over the forebody of a very blunt configuration is principally subsonic becoming supersonic as it expands around the corners. For very blunt shapes the most important hypersonic simulation parameter for aerodynamics is the density ratio across the normal portion of the bow shock for continuum flow. In the continuum flow regime, Mach number effects for Mach numbers in excess of five are generally negligible (Mach number independence principal) as are viscous effects on the forebody where the boundary layer is quite thin. The detachment distance of the bow shock from the forebody surface and the location of the sonic line separating the subsonic flow and supersonic flow regions are a strong

function of the density ratio and the influence of density ratio on these parameters may have a first order influence on the aerothermodynamic characteristics. The density ratio is a function of the gas ratio of specific heats ( $\gamma$ ) before and after the shock. With very high velocity the gas can dissociate through the shock and  $\gamma$  will be much lower than that found in undissociated air. These effects for blunt and slender configurations are summarized in the figure at the top of the following page. Winged vehicles and lifting body concepts may exhibit slender body or blunt body hypersonic characteristics during entry, depending primarily on the angle of attack.



### Parametric to Benchmark Process

Most concepts of advanced aerospace vehicles are presently developed via systems analysis studies whereby the various components (e.g., propulsion system, tankage, crew compartment, etc.) are sized, weighed and packaged. Aerodynamic characteristics for the vehicle are estimated using relatively simple engineering codes. Having developed a concept that satisfies mission requirements, the aerolines are provided to the experimental aerothermodynamic community for assessment of aerodynamic and aero-heating performance. As noted previously, the mission requirements will have a major impact on the shape of the proposed vehicle, and the shape has a major impact on the approach to ground-based testing.

As an example, consider a single stage to orbit rocket powered vehicle that would be launched vertically and land horizontally (SSTO-R VT/HL). To minimize weight, an SSTO-R VT/HL concept emerging from a systems analysis study may simply resemble a relatively small wing attached to a large cylindrical tank. Beginning with this "minimum weight" concept, tests in ground-based facilities are initiated. At the NASA Langley Research Center, the study to assess aerodynamic/aero-heating characteristics of the proposed concept begins with the formulation of the approach and the construction of wood or aluminum models (typically about 24 inches in length) having a family of removable control surfaces with different deflections. Since the purpose of the first series of tests is to provide a quick look at aerodynamic characteristics, handwork of the model surface is held to a



minimum to expedite the fabrication process and keep costs down. The first tests performed are generally at subsonic conditions to assess landing characteristics. Forces and moments are measured for various stages of configuration buildup (i.e., fuselage only, fuselage with wing, with canards, with vertical tail, etc.) over a range of attitude (i.e., angles of attack and sideslip) and control surface deflections. If these measurements reveal that the aerodynamic characteristics are unacceptable for approach and landing, an iterative process is initiated whereby the experimentalists, often in concert with the system analysts, modify the aerolines of the concept to achieve the desired characteristics. Unfortunately, such modifications generally correspond to additional weight to the vehicle thereby compromising the results of the system analysis study; that is, as weight is added, a domino effect occurs throughout the various components of the vehicle. For example, another rocket engine may be required, thereby requiring modifications to most components of the vehicle. Aerolines are modified, and the concept is retested until acceptable subsonic aerodynamic characteristics are achieved.

Next, wooden or aluminum models, generally about half as large as the first series of models tested at subsonic conditions, are tested in the LaRC 22-Inch Mach 15/20 Helium Tunnel. By using helium as the flow medium, the test gas does not have to be heated to avoid liquefaction during the expansion process via a diverging nozzle (i.e., helium may be expanded to freestream Mach numbers of approximately 28 without requiring heating to prevent liquefaction); thus, wooden or plastic models constructed quickly and inexpensively may be tested in this facility without damage. Other advantages of using helium are that large values of freestream Reynolds number may be obtained at high hypersonic Mach numbers (the highest Mach number and Reynolds number simulation capability in the USA is provided by the LaRC Helium tunnel) and the flow conditions are well known since the test gas behaves ideally. The primary disadvantage is the higher than air ratio of specific heats for helium. Forces and moments are measured at Mach 15 and/or 20 over a wide range of Reynolds number, attitudes and control surface deflections. Corresponding thermal mappings are measured on ceramic models using phosphor and/or infrared emission thermography with the helium heated via an electrical heater. Changes are made to the aerolines, if required, to achieve the desired hypersonic aerodynamic/aero-heating characteristics. If these changes are extensive, additional tests are performed at subsonic conditions to ensure landing characteristics have not been compromised. These tests, beginning with the initial subsonic tests, represent the first phase of the screening process. Such a screening process may be performed for a number of proposed SSTO-R concepts in parallel and in series.

Having refined the aerolines to provide acceptable aerodynamic performance at the extremes of the Mach number spectrum (i.e., "bounding the problem" at Mach 0.1 and 20), precision stainless steel force and moment and pressure models are fabricated as are corresponding ceramic models for global heating measurements. These models are tested in several hypersonic wind tunnels at LaRC to assess aerodynamic and aero-heating characteristics and in the LaRC Unitary Plan Wind Tunnel to assess aerodynamic

characteristics for ascent and descent attitudes at Mach 1.6 to 4.6. Tests at hypersonic conditions involve using the LaRC 20-Inch Mach 6 Air, 31-Inch Mach 10 Air, and 20-Inch Mach 17 Nitrogen Tunnels, and perhaps most importantly, the 20-Inch Mach 6 CF<sub>4</sub> Tunnel. As noted previously, using a heavy gas such as CF<sub>4</sub> provides an accurate simulation of real gas effects on aerodynamic characteristics. Such effects are expected to be first order for a concept having surface curvatures that produces a significant region of flow expansion such as the aft portion of the shuttle orbiter windward surface. Depending upon facility availability, tests are also performed at transonic conditions, again for ascent and descent attitudes. Testing is continued in this second phase until closure is achieved on aerolines that provide: (1) the optimum aerodynamic performance across the subsonic to hypersonic speed regime; (2) acceptable pressure and heating loads during the entire flight trajectory; and (3) volumetric efficiency for effective packaging of the required components.

Once these criteria have been satisfied, benchmark testing is initiated in well-calibrated, high flow quality, ground-based facilities using precision, highly instrumented models. Highly accurate measurements of aerodynamic forces and moments, detailed surface pressure, and detailed, discrete heat transfer measurements are required in this final phase. Emphasis is on accuracy and creditability of the data, as these data will be used for final vehicle design and to develop the aerodynamic flight data book. From a hypersonic testing perspective, benchmark aerothermodynamic measurements are expected to be performed in a number of facilities, including those at the LaRC, Tunnel 9 at the Naval Surface Warfare Center (NSWC), Tunnels B and C at the Air Force Arnold Engineering Development Center (AEDC), and shock tunnels at Calspan, Buffalo, New York and/or Calspan University at Buffalo Research Center (CUBRC). Tests are performed during this phase to determine the performance of the reaction control system (RCS), to simulate propulsion during ascent, to examine aerodynamic performance during abort maneuvers, and so forth to complete the flight data book. It is during this phase of ground-based testing that predictions of aerothermodynamic characteristics via CFD computer codes provide a significant contribution. Having been calibrated against wind tunnel data, CFD codes are applied at flight conditions, which cannot be properly simulated in the wind tunnels.

## TESTING REQUIREMENTS

### Preface

The primary intent of the preceding sections was to provide background information concerning future space transportation vehicles under study by NASA, the role of aerothermodynamics as the genesis for the design and development of such vehicles, sources of aerothermodynamic information and their interaction, and the required testing methodology for parametric studies to optimize performance data book. The remaining portion of this report will be devoted to the process used at the NASA Langley Research Center to

develop/ assess/optimize aerothermodynamic characteristics of proposed advanced aerospace vehicle concepts via ground-based testing. As discussed previously, a triad consisting of systems analysis, CFD and engineering computer codes, and ground-based testing is used at Langley to develop such vehicles. The final sections will address the ground-based testing portion of this triad. (References 3 and 4) The process, evolved over the last three decades, relies on a strong in-house infrastructure consisting of engineer/scientist and technician personnel, ground-based facilities, test article or model design, fabrication, and instrumentation, and diagnostics. Each component of this infrastructure will be addressed (Figure 3).

Simply stated, future aerothermodynamic testing requires that studies be performed faster, cheaper, and better with significantly fewer resources, particularly personnel. Excellent progress has been made towards accomplishing these goals in recent years, but much remains to be done. Of paramount importance is the interaction of the experimental and computational aerothermodynamic communities. The highest level of confidence in predicting the flight performance of an aerospace vehicle is achieved when ground-based data extrapolated to flight conditions and CFD computer code predictions for actual flight conditions are in excellent agreement. The pace at which the development of aerothermodynamic technology via tests in ground-based facilities and CFD computer code predictions can be applied is very important. Both need to be productive not only in a timely manner but also in essentially the same time frame. This requirement places great demands on the testing community to perform studies faster, with no sacrifice in quality and also pressures the CFD community to perform rapid grid generation and calculations without losing accuracy.

### Personnel

The most important resource for the development of aerothermodynamic information for advanced aerospace vehicles is, naturally, personnel. Knowledge of aerodynamics (i.e., forces and moments and aero-loads) across the subsonic-to-hypersonic speed regime, aero-heating, and complex fluid dynamic and high temperature flow phenomena is required. At Langley, the same engineers/scientists perform subsonic, transonic, supersonic, and hypersonic aerodynamic testing, as opposed to different personnel testing (i.e., specializing) in each speed regime. This approach provides continuity which is vitally important, particularly since iterations are generally required to optimize aerodynamic performance across the speed regime. Working closely with the aerodynamicists are engineers/scientists performing aero-heating studies for a range of hypersonic conditions. Regions of high heating are identified and, if deemed unacceptable, modifications are made to the vehicle aerolines, attitude and perhaps the trajectory to reduce heating loads without jeopardizing the aerodynamic performance. Teams of experimentalists examining concepts are, by design, generally small, consisting of 3 to 6 members. (Smaller teams have been observed to function more efficiently and effectively than larger teams.) Experience is a critical ingredient in the makeup of the teams. Senior engineers/scientists having

experience with the Mercury/Gemini/Apollo, shuttle orbiter, Viking, etc. programs are teamed with highly educated and motivated junior engineers/scientists. This mix of junior and senior personnel encourages the transfer of corporate knowledge and unites the savvy of senior personnel with the "can-do-attitude" of junior personnel.

Principal investigators for a study are supported by facility engineers and technicians, data acquisition and instrumentation specialists, model makers, and so forth. Communication among personnel is enhanced via proximity, as most or all of the supporting cast are located at the Center and readily accessible.

### Test Articles

Often overlooked, but a major factor in ground-based testing, is the design, fabrication, and instrumentation of models. To be cheaper and faster, future wind tunnel models must minimize or avoid costly and time consuming design. Aerolines developed during system analysis studies or developed for incorporation into CFD computer codes are transferred to numerical cutting (NC) machines by compatible software. NC machines are then used to machine a precision model, with close interaction between the machinists and the researchers. This approach was used successfully in the NASP program, whereby aerolines describing the consortium developed vehicle (referred to as configuration 201) were transferred to the NASA Langley Research Center, loaded onto numerical cutting machines, and models fabricated in an extremely fast-paced manner without formal model design. High fidelity, configuration buildup, stainless steel models were fabricated for force and moment and for pressure testing and ceramic models made for thermal mapping studies. These models were constructed, tested and the data reduced, analyzed, and disseminated within a matter of months.

Typically, formal model design requires several months to complete depending on model complexity. The extremely fast pace of model design, fabrication, and testing demonstrated for the NASP program can, in reality, be maintained only for relatively short periods of time which require very high center priority. However, the methods and procedures developed can be, and are applied to the "normal, day-to-day" experimental programs with significant savings in time and cost of producing quality test results.

Casting of metallic models can have a major impact on fabrication time and cost. With the development of the stereolithography (SLA) processes, high quality patterns may be manufactured in a short time once the model surface geometry is known. These patterns are used to build molds which in turn are used to quickly cast the metallic model. If high precision is required, the model may be cast slightly oversized, and then final machining is performed. This approach minimizes wasted material and time compared to traditional machining methods where blocks of a metal are machined down to final shape.

Most thermal-mapping study models are made of a ceramic and constructed using a mold usually made from high-fidelity metallic force and moment models. However, SLA patterns

and molds are also used to cast ceramic models. These models, after being fired, are tested to provide global qualitative and quantitative thermal mappings via direct infrared and/or phosphor thermography. Because models can be made quickly and inexpensively, thermal-mapping tests for a given configuration may be performed during the same test series as the force and moment tests. Thus, the designer of a proposed hypersonic flight vehicle is provided in a very timely manner both aerodynamic and aero-heating data for trade studies.

### Measurement Techniques

Measurement techniques which are routinely employed in the supersonic and hypersonic wind tunnels at Langley are discussed in this section. The most commonly performed studies involve the measurement of aerodynamic forces and moments on models. Next are aero-heating studies, which may utilize qualitative measurements of surface temperature-time histories with thermal mapping techniques or quantitative global measurements with thermography and/or discrete gages to provide more accurate values of heat-transfer rate. Measurements of model surface-pressure distributions are also performed frequently. In all types of studies, flow-visualization techniques are used to provide information on shock locations and boundary-layer characteristics, such as separation and reattachment. Presently, flowfield surveys within the shock layer/ boundary layer of models may be performed with probes in all facilities and nonintrusive flowfield measurements may be performed at Mach 6 in air using the Rayleigh scattering and/or planar laser induced fluorescence (PLIF) techniques.

### Forces and Moments

A large inventory (approximately 60) of internal strain-gage balances that cover a wide range of maximum design loads and sensitivities for blunt, high-drag models and for slender, high-lift models is maintained at Langley. Most balances are six component (normal, axial, and side forces and pitch, yaw, and roll moments) and are water cooled. These balances, generally less than one inch in diameter and five or six inches in length, are very accurate with uncertainties of less than 0.5 percent.

### Pressure

Pressure distributions on the relatively small-scale models tested in the hypersonic tunnels (Figure 4) are measured with electronically scanned pressure (ESP) silicon sensors while limited measurements may be made with high-volume, multirange, variable-capacitance diaphragm-type transducers. The trend since the early 1980s has been toward the ESP systems because of the advantages that they offer over other types of pressure-measurement systems. For example, ESP modules typically contain 32 or 48 sensors and yet are comparable to the size of a pack of cigarettes; furthermore, they combine internal multiplexing and amplification to provide scanning at high data rates. In some cases, the module can be mounted inside the model, in the strut, or at its base to reduce the response time by minimizing tubing length

between the model pressure orifice and the sensor. An integral, pneumatically controlled mechanism allows the sensors to be rapidly calibrated on-line. The ESP sensors have been used in the Langley hypersonic wind tunnels to accurately measure pressure levels ranging from 50 to 0.05 psi.

Recent experimental work in a laboratory setting has shown promise for obtaining simultaneous luminescence barography and thermography results in hypersonic air wind tunnels. The work uses a two-color imaging system and adsorbed dye luminescence on silica ceramic test models (Reference 5). In trial applications, it was found that an adsorbed perylene dye on slip-cast silica was pressure (oxygen) sensitive and reusable to relatively high temperatures ( $\sim 150^\circ\text{C}$ ). Adsorbed dye luminescence was excited by blue light (460nm) or long-wave ultraviolet (UV)(365nm). Visible emission was found to be green-red with color depending on absorbed film thickness and temperature. Surface pressures and temperatures were determined from emission brightness and green-to-red color-ratio measurements.

### Qualitative Heat Transfer

Thermal-mapping studies (Figure 5) have gained increased use because they provide a rapid, relatively inexpensive determination of qualitative heating characteristics on models of various shapes and complexity. Four techniques have been used over the last 5 years, or so: phase-change paint, thermographic phosphors, liquid crystals, and infrared emission. However, recent developments in phosphor thermography have revolutionize aero-heating studies and the use of phase change paints and liquid crystals at Langley has stopped. In addition, the high quality infrared (IR) measurements can be made using charge coupled device (CCD) cameras without having to apply coatings to the models.

### Quantitative Heat Transfer

The technique used for global quantitative heat transfer measurements at Langley is phosphor thermography. The phosphor material is applied to the model and is illuminated by ultraviolet light that excites electrons; during their subsequent relaxation to lower energy levels, these electrons emit visible radiation that is temperature dependent, and the amount of radiation may be used to determine local temperatures. Advantages of this technique over the phase-change-paint technique are that the model does not have to be recoated after a run, and that temperatures are measured continuously everywhere on the surface, as opposed to along a melt line (isotherm). The relative intensity two-color system that has been developed at Langley by Gregory M. Buck (Reference 6) is independent of the optical path and essentially provides most of the aero-heating data generated. Several systems have been assembled and may be moved from facility to facility without requiring a lengthy setup and calibration. Data acquisition and reduction techniques developed by N. Ronald Merski provide both qualitative and quantitative heating to the researcher shortly after a test.

Primarily because of the relatively small model sizes, discrete heat-transfer gages are seldom used. Instead, heating distributions are generally measured using the thin-film resistance thermometer technique (Figure 6) originally developed for use in impulse-type facilities. To fabricate thin-film gages, thin-film elements of palladium or platinum, about 1000 Å thick, are sputtered, vapor deposited, or painted onto the highly (optically) polished surface of a substrate. The most commonly used substrate materials are quartz, pyrex, and MACOR, a machinable glass ceramic, and particular attention must be paid to the dimensions of the substrate for use in conventional-type hypersonic wind tunnels. As with the thin-skin technique, thin-film models are rapidly inserted into the flow, and the voltage across each gage is monitored as the gage resistance changes with temperature. From a previously performed calibration of gage resistance with temperature, the surface temperature-time history is determined, which thereby yields the heat-transfer rate. Thin-film gages are also used to study boundary-layer stability wave motion and transition. However, there is one important disadvantage of thin-film gages--they are not very durable. This is a primary reason that flow filters have been placed upstream of the test section in most of the hypersonic tunnels at LaRC.

The thin-skin transient calorimeter technique is also used, but not to the extent of the thin-film technique. For this technique, the rate of heat storage in the model skin is inferred from temperature-time histories measured with thermocouples attached to the inside surface of the skin. A transient is obtained by rapidly injecting the model from a shielded position (where it was maintained isothermally near room temperature) into the test flow. Because thin-skin models are durable, this technique may be preferred when the flow in a tunnel is known to be dirty. Also, thin-skin models can generally be fabricated and instrumented more readily and less expensively than thin-film models.

#### Flow Visualization

Included in the category of flow-visualization techniques are shadowgraph, schlieren systems, interferometry systems vapor screens, electron-beam flowfield visualization, and surface oil flow. For the latter technique, smooth, dark-color models are sprayed with a mixture of oils of various viscosities mixed with white artist pigment and then injected rapidly into the flow. Movement of the oil is photographed while the model is in the flow, thereby qualitatively revealing surface streamline patterns--that is, the direction of the flow adjacent to the surface, including lines of separation and reattachment. Fluorescent chrysene may also be mixed with the oil and illuminated with ultraviolet light to visualize the surface-flow pattern.

The schlieren method is one of the most frequently applied optical visualization systems in wind tunnels, since it combines a relatively simple optical arrangement with a high degree of resolution (Figure 7). Parallel light is passed through the test section, and an image of the light source is focused in the plane of a knife edge. At high Mach numbers, schlieren quality may be poorer because of the low density levels and density gradients. However, the use of high

density charge coupled device (CCD) cameras which allow image enhancement has improved the results significantly. An alternate technique is to induce fluorescent flow visualization using an electron gun, thereby revealing the shock structure and characteristics of the flow field.

#### Flow-Field Surveys

Generally, a single probe or small survey rake is traversed normal to the model surface outward through the boundary layer and shock layer. Probes must be made as small as possible to minimize interference effects close to the surface. For pressure measurements, the speed of the probe or rake must account for system response. Because of the small probe dimensions, the lag times may be long, and reasonably long tunnel run times are required. A miniature (outside diameter of 0.013 inch), water-cooled total-pressure probe was recently designed, fabricated, and tested at Langley that provided fast response and yet eliminated probe interference effects close to the model surface. (Reference 7)

An active effort to develop nonintrusive diagnostics for the tunnels of the Hypersonic Facilities Complex (HFC) occurred during the 1960s and 1970s, but the momentum was diverted to other areas with the decline in interest in hypersonics. Now, there is renewed interest in such diagnostics. Recently, Rayleigh scattering and planer laser induced fluorescence (PLIF) systems have shown promise for obtaining quantitative flowfield measurements in the 15-Inch Mach 6 High Temperature Tunnel.

#### Data Acquisition/Recording System

Although hypersonic wind tunnels that remained operational in the late 1970s and early 1980s did not receive a high priority for facility upgrades, advances were achieved nevertheless, particularly in the area of data acquisition. Stand-alone, as opposed to large centralized, data acquisition systems (DAS) have been introduced into all of Langley's hypersonic facilities. The heart of these systems is a 256-channel, 16-bit, amplifier per channel, analog-to-digital (A/D) system that is interfaced to a computer through a pacing unit and real-time clock, thereby allowing different sampling rates to be used during a run. These A/D systems have programmable, as opposed to plug-in, amplifiers and filters for each channel. Advances in desktop-computer capabilities allow complete data reduction to be performed between tests. These systems are complemented by mass storage systems, high-speed printers, and calibration standards.

#### Ground-Based Facilities

The ground based facilities used for experimental aerothermodynamic studies at LaRC run the gamut from low speed wind tunnels for takeoff, approach, and landing aerodynamic studies to conventional-type hypersonic blow down-to-vacuum wind tunnels and an expansion tube for generating hypersonic/hypervelocity real gas flows. Starting at the low speed end of the spectrum, several examples of available facilities will be discussed with emphasis on the requirements for obtaining quality data.

As previously mentioned, aerothermodynamics covers a wide range of Mach number. The low-speed end of the flight envelop for space transportation vehicles is obviously for takeoff, subsonic maneuvering, approach, and landing. First order effects on configuration aerodynamics, stability and control effectiveness, and ground effects can be obtained using relatively inexpensive, rapidly constructed models in a number of low-speed wind tunnels. One such facility often used in the first phase of a screening or assessment study is the Vigyan Research Associates 3-by-4 Foot Low Speed Tunnel located very close to the Center. This small facility provides a freestream dynamic pressure up to about  $50 \text{ lb/ft}^2$  at a unit Reynolds number of about  $1.5 \times 10^6/\text{ft}$ . The length of slender and moderately blunt models is generally around 24 inches, corresponding to a Reynolds number based on length of about  $3 \times 10^6$ . With proper boundary-layer transition strips applied to the model surface, this Reynolds number is sufficient to study first-order effects. Models are generally constructed of aluminum, wood or fiber glass, and are relatively inexpensive. Any similar facility would be expected to provide equally good results.

A specific example of the usefulness of the "bound the problem" approach mentioned previously is the results obtained early in the access to space option 3 testing (Figure 8). A single-stage vehicle configuration which was generated by a systems analysis study using engineering codes was tested subsonically and found to be unflyable. Changes in the configuration forebody geometry and wing planform were performed by a senior researcher to provide acceptable subsonic aerodynamics. However, this iteration on the aerolines had an effect on the high-speed characteristics. The point is, however, if the low speed tests had not been conducted early in the design cycle, a potential show stopping problem might not have been discovered in a timely fashion.

For "benchmarking" of low-speed characteristics, larger precision models are tested to ensure maximum model detail and the highest possible test Reynolds number. At LaRC, this requires the use of the 14-by 22-Foot Subsonic Tunnel where the freestream dynamic pressure can reach  $140 \text{ lb/ft}^2$  with a unit Reynolds number of about  $2.2 \times 10^6/\text{ft}$ . For a model length on the order of 9-10 feet, length Reynolds numbers of about  $20 \times 10^6$  are possible. This tunnel is also equipped with a model support system which allows easy ground effects testing if that is a requirement. These large models, while certainly more expensive than 2-foot models, can still be fabricated out of aluminum and fiber glass for relatively low cost.

An alternative approach is to use smaller precision models and test in the Low Turbulence Pressure Tunnel (LTPT) where a significant range of Reynolds number is available. Tests are conducted over a range of Reynolds numbers until no further effects are noted and then testing continues at the appropriate high Reynolds number.

If high Reynolds numbers approaching flight are required then testing must be conducted in facilities like the 40-by 80-Foot Tunnel or the 12-Foot Pressure Tunnel at the Ames

Research Center or the 5-Meter Tunnel of the Royal Aeronautical Establishment at Farnborough, England. The cost of the models for these facilities is quite large since the physical size is large in the 40-by 80-Foot Tunnel and the aerodynamic loads are high in pressure tunnels. The high loads will generally require an all steel model. The nearly full scale models that can be installed in the 40-by 80-Foot Tunnel can cost millions of dollars. However, since high Reynolds number is generally needed only for accurate performance (i.e., L/D) and subsonic performance is generally not an issue for this class of vehicles, testing of very high cost models in order to obtain very high Reynolds number data should not be a major factor in the development of space transportation system vehicles.

Transonic/supersonic testing generally requires testing in multiple facilities as very few, if any, can cover the Mach number range from 0.8 or 0.9 to 4 or 5. There are several quality transonic and supersonic wind tunnels around the United States and the world where tunnel time can be obtained depending on schedules and program priority. At LaRC the transonic facilities are the 8-Foot Transonic Tunnel, the 16-Foot Transonic Tunnel and the National Transonic Facility (NTF). The NTF is a pressure tunnel for high Reynolds number testing in air and a cryogenic tunnel for very high Reynolds number testing in nitrogen. Supersonic testing is performed in the Unitary Plan Wind Tunnel. This facility has two separate test sections providing overlapping Mach number ranges of 1.6 to 2.8 and 2.5 to 4.6. However, two complete model installations are required to obtain data from Mach 1.6 to 4.6.

The same models can be tested in both transonic and supersonic facilities to reduce the cost of model construction. Conventional design and fabrication techniques provide stainless steel models capable of withstanding the aerodynamic loads imposed by these testing conditions. However, this will not be the case if testing in the NTF is required. Model design and fabrication techniques for the cryogenic environment of the NTF are quite stringent and the cost of models is considerably more than for other facilities.

Since these vehicles tend to spend little time in the transonic/supersonic Mach number range, accelerating rapidly at low angles of attack on ascent and decelerating rapidly at moderate angles of attack on descent, accurate performance data are not generally required, eliminating the need for testing at very high Reynolds numbers in the NTF. Basic aerodynamics, stability and control characteristics to ensure "flyability" are the main driver for testing in this Mach number range. An example of the need for testing in this range is the Langley HL-20 configuration which had good hypersonic and acceptable low speed aerodynamics. However, the HL-20 trimmed at negative angle of attack in the low supersonic range (Figure 9) which would clearly not be an acceptable flight condition. This information led to a configuration change which not only solved the supersonic problem but also improved the subsonic characteristics. However, the new hypersonic characteristics, especially in the presence of real gas effects have not been determined at this writing and could be of concern.

The airbreathing class of launch vehicles can present a different set of problems in this speed range. Obviously, the basic aerodynamics, stability and control characteristics must be known. Since this vehicle class is thrust limited at low speeds, accurate performance estimates are necessary in order to ensure positive thrust minus drag in this region. The inclusion of propulsion effects, on top of high Reynolds number, may be necessary in order to provide confidence that these vehicles can actually accelerate to supersonic and then hypersonic speeds. This can significantly increase the model cost and testing complexity but may well be the critical design points for airbreathing concepts from an aerodynamic perspective.

Space transportation vehicles spend most of their flight time in the hypersonic speed range, either at low angles of attack while accelerating during ascent or at high angles of attack while decelerating during entry. While basic aerodynamics stability and control are needed to ensure "flyability" aero-heating may become a paramount concern to ensure the "survivability" of the vehicle. These two requirements can be at odds with one another if, for example, a large control deflection required for hypersonic trim corresponds to the control surface being too hot to survive the entry (Figure 10).

Conventional hypersonic testing is conducted at LaRC in blow down to vacuum wind tunnels, at Mach numbers from 6 to 20, using a variety of test gases depending on the simulation parameters being examined. One pair of tunnels, the 20-Inch Mach 6 Air and CF<sub>4</sub> Tunnels, is unique in that Mach number and Reynolds number can be held constant while the test gas ratio of specific heats is changed from 1.4 to 1.22 to simulate the low gamma present in a dissociated "real gas." As mentioned, gamma is of critical importance in blunt and moderately blunt configuration testing and can be important in regions of high expansion such as forward of the body flap on the Space Shuttle. This combination of HFC tunnels makes "across the Mach number" testing very easy as the same model and support sting can be designed to fit in all the facilities, eliminating concerns of model to model fidelity and interference effects from different support hardware.

Except for testing in helium, these tunnels all require steel or ceramic models to handle the high stagnation temperatures involved with ground based hypersonic flows. However, because of the relatively small size of these tunnels, model costs are not high, but extensive pressure or heat-transfer measurement instrumentation can significantly increase model cost.

## **GROUND-BASED TESTING CAPABILITIES**

### **Existing Facilities**

There currently exist a number of facilities (Reference 8) that can provide data for assessment and design of future space transportation systems, however, there are limitations in some areas. An assessment of ground-based testing capability readily available to the Aerothermodynamics Branch will be

discussed in the following section beginning with low speed tunnels and ending with those in the hypersonic speed range.

### **Subsonic**

While there are several subsonic tunnels at LaRC and around the country, there is a real shortage of good quality facilities for conducting inexpensive, parametric testing in a timely fashion at more than the lowest of Mach numbers. The former 7-by 10-Foot Tunnel at LaRC was such a facility where models of reasonable size (3-4 feet in length) could be tested up to about Mach 0.8. With the shutdown of that facility in 1993, the options at LaRC are somewhat limited to small low speed tunnels such as the Vigyan Research Associates 3-by 4-Foot Tunnel or the 14-by 22-Foot Subsonic Tunnel, the latter being heavily booked, so that occupancy time can be a problem. The LaRC Low Turbulence Pressure Tunnel (LTPT) can be used to address potential high Reynolds number effects but it is in fact a two-dimensional tunnel not normally configured for three-dimensional testing. Because of the major effort needed to make the conversion to three-dimensions and the current heavy test schedule, the aerothermodynamics program can only be provided a month or so of tunnel time every couple of years. However, examples such as the previously mentioned low speed problems with the original single stage vehicle concepts and the significant adverse ground effects on the National Aero-Space Plane configurations attest to the need for low speed testing of aerospace vehicle concepts. Shortcomings notwithstanding, a great deal of the potential low speed problems for advanced space transportation system concepts can be adequately addressed with the facilities currently in hand.

### **Transonic**

This is not the case at LaRC for transonic Mach numbers. With the projected closure of the 8-Foot Transonic Tunnel, LaRC will be left with the 16-Foot Transonic Tunnel, a heavily scheduled propulsion and component integration facility, and the National Transonic Facility, a very expensive tunnel from an operation and model construction point of view. Neither of these facilities are amenable to the smaller parametric type of models needed during the initial screening and analysis phases of a configuration development program. While there are transonic facilities around the country that can provide quality aerodynamic information, occupancy time is expensive and high schedule priority may be difficult to obtain. The bottom line is that the aerothermodynamics program is fast losing the capability to perform a quick assessment of the transonic characteristics of a vehicle concept. The one serious deficiency in the data set for the NASP concepts was at transonic speeds because even that fast-paced, high priority program seemed unable to obtain transonic tunnel time.

### **Supersonic**

The picture is a bit brighter in the supersonic Mach numbers. The LaRC Unitary Plan Wind Tunnel is a good facility for parametric testing from Mach 1.6 to 4.6 in that the same model and sting hardware can be tested at all Mach numbers.



Larger scale models for UPWT can be tested in the lower speed facilities and smaller scale models can be tested in the higher Mach number facilities for potential savings in model fabrication cost. Another LaRC facility that is in the process of being calibrated prior to re-activation is the 20-Inch Supersonic Wind Tunnel (SWT). This tunnel will be ideal for the parametric screening process, once it is operational, as it is sized perfectly to accept models from the hypersonic facilities. While there are other supersonic tunnels which also provide excellent capabilities, as with the transonic facilities, they are relatively expensive and difficult to schedule. The importance of supersonic testing was shown in the HL-20 program where a potential major problem was uncovered in the low supersonic speed range and configuration changes were made which not only corrected the supersonic trim problem but also improved the low speed characteristics for improved landing performance. A negative aspect of testing in UPWT is the somewhat restrictive limit on Reynolds number which could be a problem for some configurations, particularly if performance results are required.

As a summary of low speed (less than Mach 5) facilities, it can be said that LaRC and the nation are in reasonably good shape to address the subsonic and supersonic Mach number ranges with a possible shortcoming in the transonic range.

#### Hypersonic

The set of facilities at LaRC known as the Aerothermodynamic Facilities Complex (AFC) provides a wide range of basic hypersonic simulation parameters (i.e., Mach number from 6 to 20, Reynolds number from 0.01 to  $40 \times 10^6/\text{ft}$ , normal shock density ratio from 4 to 12, and wall-to-total temperature ratio from 0.15 to unity) and offers a unique opportunity to obtain hypersonic aerothermodynamics at one location (Figure 11). Models can be sized for testing in all facilities to provide the widest range of simulation parameters (Figure 12), at the lowest possible cost, within a reasonable time frame. These tunnels have undergone an extensive series of upgrades and improvements over the past five or six years to enhance the flow quality, testing capability, and productivity (Figure 13). When combined with the existing infrastructure at LaRC, quality high speed aerodynamics and aero-heating information have been generated in a very short time frame as evidenced by the assessment of the NASP 201 configuration in 1991.

One of the important capabilities at LaRC is the ability to simulate the large density ratio or low ratio of specific heats ( $\gamma$ ) found in a real gas by testing in a heavy gas, such as  $\text{CF}_4$  with a molecular weight of 88. The 20-Inch Mach 6  $\text{CF}_4$  Tunnel is unique and has shown its worth by demonstrating the cause of the Space Shuttle Orbiter pitchup anomaly to be real gas expansion effects just forward of the body flap. This expansion to lower pressures than would be found with an ideal gas is due to the low values of the ratio of specific heats experienced within the Orbiter windward shock layer during entry. The values in the shock layer are very nearly duplicated in the 20-Inch Mach 6  $\text{CF}_4$  Tunnel. Comparing results from the 20-Inch Mach 6  $\text{CF}_4$  and Air

Tunnels (Figures 14 and 15) allows all parameters to be held constant except  $\gamma$  which is 1.22 in  $\text{CF}_4$  and 1.4 in Air. Thus, the only effect should be the low  $\gamma$  aspect of the real gas. This orbiter result (Figure 16), backed up by CFD calculations at flight conditions, as well as AFE blunt body results (Figure 17), yields high confidence that real gas effects can accurately be predicted using this testing technique.

While the AFC offers an excellent capability for parametric testing, there certainly are some limitations. The first is the lack of high Reynolds number at high hypersonic Mach numbers in air. The exception is the capability provided by the helium tunnel, where very high Reynolds numbers are provided but at the expense of higher than air values of  $\gamma$ . Although the 31-Inch Mach 10 Tunnel (Figure 18) provides near flight values of Reynolds number based on length for a NASP vehicle on descent, it is a factor of 20 to 30 deficient for ascent. There are larger and/or higher Reynolds number hypersonic facilities available in the country that produce extremely high quality data. However, as with the lower speed facilities their cost of operation is very high. Consequently they are generally not used in the screening/initial analysis phase of a study but rather in the benchmarking phase. A second deficiency is the lack of rarefied flow testing capability, which presently is a national problem since there are no active, hypersonic, heated, low-density tunnels in operation. A third deficiency to be noted is the lack of hypersonic-hypervelocity (high enthalpy) testing capability. However, it should be noted that although operation of the Langley Expansion Tube was terminated in 1982, it was moved to Long Island, New York and is currently operated for NASA by the General Applied Science Laboratory (GASL) and is referred to as NASA Hypulse at GASL. Hypulse has contributed to a number of aero-heating studies being performed in the AFC and for which an extension to the real (dissociated)-gas regime was desired. Since the test gas for the expansion tube is arbitrary, tests at velocities in excess of 17,000 ft/sec in air, nitrogen and helium may be performed. Hypulse is the only facility known to this writer capable of testing highly instrumented models at hypersonic-hypervelocity conditions for which the air or nitrogen free stream flow is believed to be essentially undissociated and in thermochemical equilibrium. The last deficiency to be noted is the lack of large scale testing capability with low freestream disturbances and a relatively high Mach number (i.e., a Mach 8 or 10 quiet tunnel). This capability is required for detailed boundary layer transition studies and LaRC is currently working the problem but without a real operational capability to date.

As a summary of the hypersonic testing capability at LaRC, the AFC provides a unique opportunity for obtaining hypersonic data over a wide range of simulation parameters in a cost effective, timely fashion. The HFC is doing what it was designed to do. There are some limitation, but when additional data are needed there a quality tunnels around the country that can provide the information.

## New Facilities

Currently, there are no plans to build additional conventional-type, nonlow-disturbance hypersonic wind tunnels at Langley. The major emphasis in hypersonic facility construction at Langley in the 1990's may be for low-disturbance tunnels. The techniques and requirements for the design and fabrication of low-disturbance hypersonic wind tunnels have, to a large part, been developed. Such facilities will be essential for calibrating/validating boundary-layer stability and transition prediction codes for the speed range applicable to hypersonic aircraft of the twenty-first century. With the current level of interest in hypersonics, the likelihood of major new facilities is very remote. However, the following discussion details the facilities that would be needed in the future to complete the aerothermodynamics testing facilities.

Langley is considering a large-scale (24-inch diameter), piston-driven expansion tube and expansion tunnel as a candidate for proposed future facilities. This facility, as with any facility advancing the state-of-the-art, would require considerable research prior to performing a preliminary engineering design. An important phase of this research would be the incorporation of a piston-driven mode to the NASA Hypulse facility at the General Applied Science Laboratory to serve as a pilot facility. (Hypulse is a conventional-type expansion tube having a 6-inch diameter.) The primary purpose for a large-scale expansion tube is the generation of hypersonic-hypervelocity undissociated air flows for airbreathing propulsion studies with relatively large test articles. Although amenable for aero-heating studies, the run times for this proposed facility are expected to be too short for meaningful aerodynamic studies.

In response to the testing limitations mentioned in the previous section, Langley is considering the proposal of the Hypersonic-Hypervelocity Facilities Complex (HHFC). The HHFC would: (1) contribute to aerodynamic/aero-heating/fluid dynamic studies for Earth and planetary flight (i.e., arbitrary test gas); (2) be based on existing technology; (3) be relatively inexpensive to operate in terms of hardware, expendables, and required personnel; (4) fit nicely into the Langley infrastructure providing "matches" in capability with the 31-Inch Mach 10 and 20-Inch Mach 17 Nitrogen Tunnels (for sanity checks), and (5) be amenable for a major CoF project.

The focus of the HHFC would be a conventional-type (as opposed to combustion driver or piston driver), high pressure, long run time shock tunnel modeled after the Large Energy National Shock Tunnel (LENS) at the Calspan/ University at Buffalo Research Center (CUBRC, Reference 9). This shock tunnel would be used to perform hypersonic aerodynamic, aerothermodynamic and fluid dynamic studies for a wide range of Reynolds number, including values at Mach 10 that exceed the present Langley capability by a factor of 20, or so. A family of axisymmetric, contoured nozzles would be fabricated to provide uniform flow from Mach 6 to 20 in air or nitrogen and Mach 10 to 12 in CO<sub>2</sub>. The test section would be designed for maximum optical access and for maximum access to models and instrumentation.

The shock tunnel would be designed such that the downstream portion of the driven tube and the nozzle could be rapidly replaced by a cylindrical section having the same diameter as the driven tube. Provision would be provided for installation of a secondary diaphragm and a plug would be inserted into the driver section to reduce its volume. Thus, for relatively little additional expense, the shock tunnel could be converted into an expansion tube which would utilize the peripheral equipment including signal conditioning, data acquisition, and optical systems at the test section. This expansion tube would be larger than Hypulse, capable of the same range of velocities (approximately 15,000 to 23,000 fps) and most importantly would incorporate a system to protect the model from the high pressure, contaminated post-run flow. Because the shock tube/expansion tube would require an excellent vacuum system, it was proposed to improve this vacuum system for the purpose of installing a rarefied-flow facility. Although expected to contribute to aerothermodynamic and fluid dynamic studies, the primary emphasis would be on aerodynamics. This rarefied-flow facility would be designed for heated air or nitrogen at Mach 20. Thus, HHFC represents three facilities in one, with each facility eliminating a deficiency in test capability at Langley.

An ultra-high performance, ground-based, aerodynamic/aerothermodynamic hypervelocity facility referred to as the Advanced Hypervelocity Aerophysics Facility (AHAF, Reference 10) has been proposed by LaRC. AHAF would provide the capability to duplicate flight velocities from 10,000 to 40,000 ft/sec in atmospheres matching those of Earth and other planets with heavily instrumented, large-scale models and full-scale aerospace vehicle components such as nose tips. The emphasis is on size--sufficient model size to contain a large number of onboard sensors, signal conditioning, amplification, filtering and analog-to-digital conversion. Data would be transmitted by telemeter during flight, and perhaps stored via a flight recorder that would be recovered and played back. Models would be sufficiently large to provide relatively thick shock layers, boundary layers, and shear layers amenable to off-board optical diagnostics to obtain detailed flowfield surveys. The capability to examine boundary-layer transition and real-gas phenomena over a wide range of duplication parameters in the continuum and noncontinuum regimes would become a reality with AHAF. Unfortunately, advances in launcher technology have not progressed to the point where a launcher capable of firing an 18 to 24 inch diameter model/sabot at 20,000 fps could be designed and constructed with an acceptable level of confidence. Thus, it has not been possible to proceed with the preliminary design of AHAF.

## SUMMARY REMARKS

This paper has described the need for experimental aerothermodynamic studies of advanced space transportation systems. Aerothermodynamics is the genesis of the design process and has been defined in a threefold manner; (1) aerodynamics from Mach 0 to 40 to include both takeoff and landing of advanced concepts as well as entry into the atmospheres of the Earth or other planets; (2) aero-heating at



whatever Mach number may be of concern; 3) fluids and/or physics to describe the detailed flow field around a vehicle and its influence on surface conditions. This includes such complex phenomena as real-gas effects, boundary-layer/shock layer interactions and boundary-layer transition. The process by which the assessment and analysis of advanced concepts is carried out was discussed. Low subsonic testing coupled to hypersonic testing is undertaken to initially "bound the problem." This will give an idea of potential problems at the extremes of the flight conditions that may require early configuration changes. These iterative configuration changes are worked in concert with the system analysis specialist to ensure that changes do not preclude a viable airframe concept and vice versa that a structural system does not preclude viable aerothermodynamics. The mature iterations on a configuration design are then tested over the complete Mach number range to ensure "flyability" or acceptable aerodynamics and "survivability" or acceptable aero-heating. Depending on the level of the design effort final benchmarking of the aerothermodynamics prior to flight may be required.

A description has been provided of the facilities required to provide data that can be used in an assessment and analysis of an advanced space transportation system concept from low speed to extreme hypersonic velocities. An assessment of the capability has indicated that LaRC and the country are in good shape to carry out this design process except possibly in the transonic and the extreme hypervelocity speed ranges. It has also been noted that facilities exist, coupled with computational fluid dynamics, which can provide the benchmarking required prior to flight. This final step is quite expensive and is not taken until a very mature design has evolved.

A solid infrastructure which can bring all aspects of personnel, facilities, model design and fabrication, instrumentation and testing techniques to bear on a given problem is highly desirable. This infrastructure is in place at LaRC, and a coupling with a strong systems analysis capability, will provide a significant capability to deliver future space transportation system designs.

## REFERENCES

1. "Access to Space, Advanced Technology Team Final Report", Vol. 1: Executive Summary, July 1993.
2. Koelle, D. E. and Kuczera, H., "Sanger Space Transportation System Progress Report 1989", Paper No. IAF-89-217, 40th Congress of the International Astronautical Federation (IAF), Torremolinos, Spain, October 1989.
3. Miller, C. G., "Langley Hypersonic Aerodynamic/Aerothermodynamic Testing Capabilities - Present and Future", AIAA Paper No. 90-1376, June 1990.
4. Miller, C. G., III, "Hypersonic Aerodynamic/Aerothermodynamic Testing Capabilities at Langley Research Center", AIAA Paper No. 92-3937, July 1992.
5. Buck, G. M., "Simultaneous Luminescence Pressure and Temperature Measurements on Dyed Ceramic Models for Hypersonic Wind Tunnels", AIAA Paper No. 94-2482, June 1994.
6. Buck, G. M., "Surface Temperature/Heat Transfer Measurement Using a Quantitative Phosphor Thermography System", AIAA 91-0064, 1991.
7. Ashby, G. C., Jr., "Miniaturized Compact Water-Cooled Pitot-Pressure Probe for Flow-Field Surveys in Hypersonic Wind Tunnels", ISA 34th International Instrumentation Symposium, 1988.
8. Penaranda, Frank E. and Freda, M. Shannon, Aeronautical Facilities Catalogue, Vol. 1, "Wind Tunnels", NASA RP-1132, 1985.
9. Holden, M. S., "Large Energy National Shock Tunnel (LENS): Description and Capabilities", Calspan/University at Buffalo Research Center (CUBRC) brochure, 1990.
10. Witcofski, R. D., et al., "An Advanced Hypervelocity Aerophysics Facility: A Ground-Based Flight-Test Range", AIAA 91-0296, 1991.

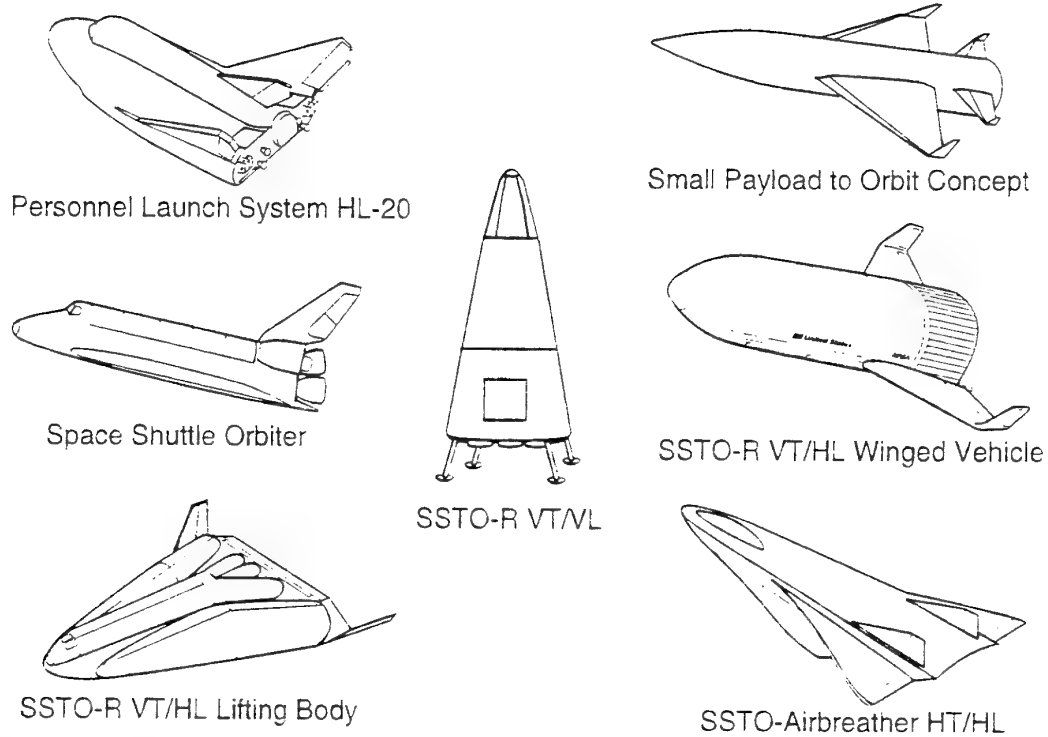


Figure 1. Sketch of future space transportation concepts.

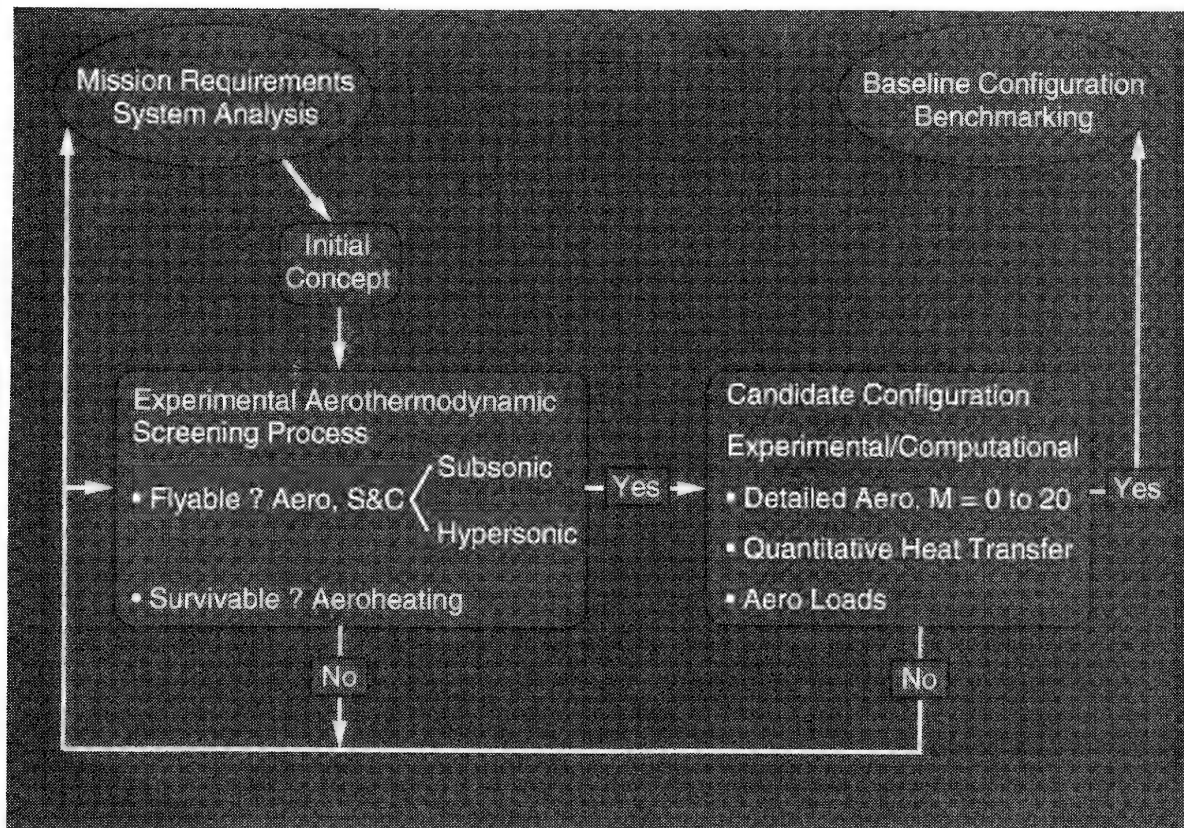


Figure 2. Flow chart of process for the development of space transportation vehicle concepts.

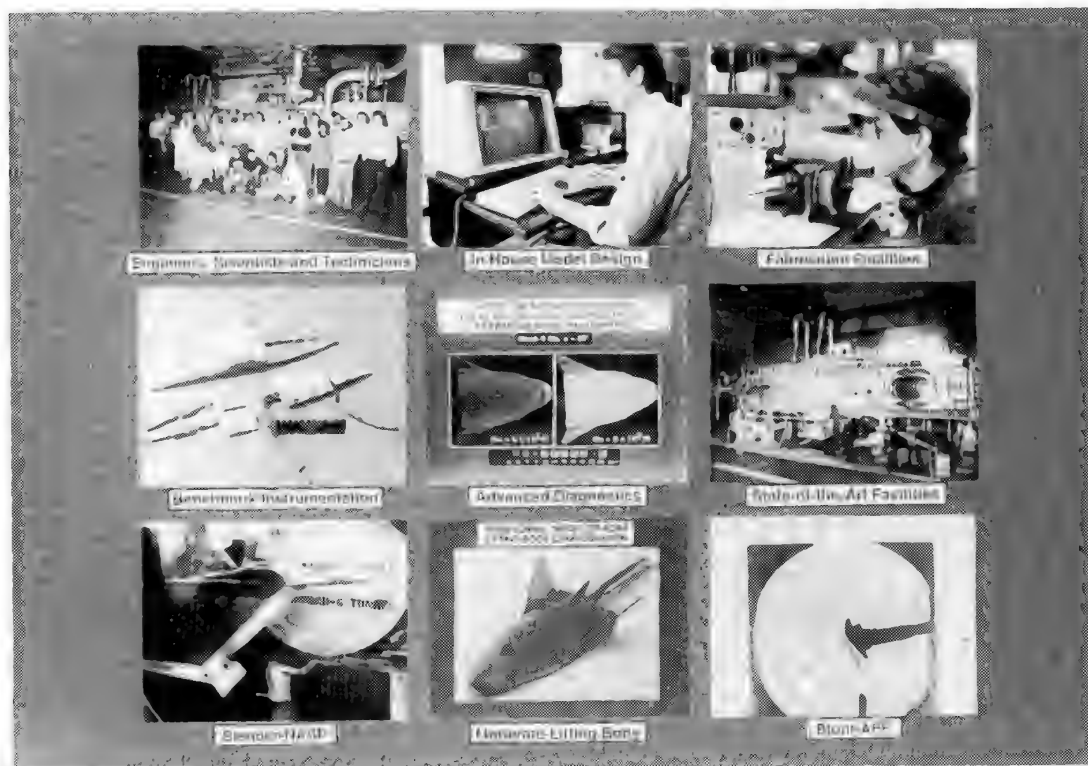


Figure 3. Aerothermodynamic infrastructure at Langley Research Center.

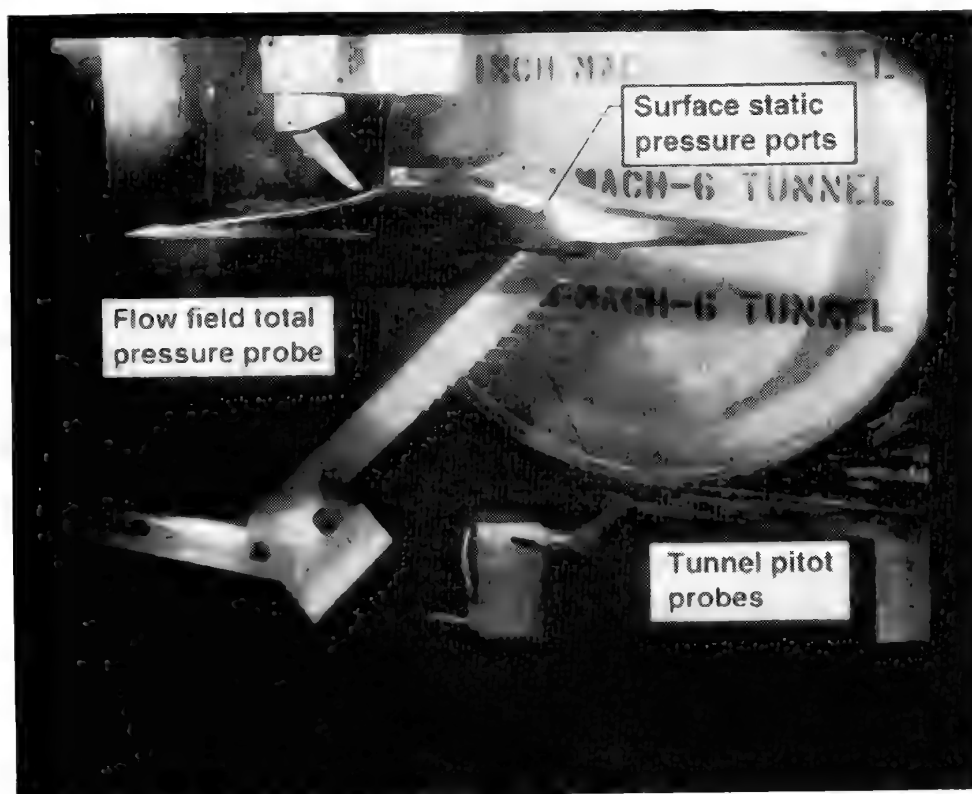


Figure 4. Photograph of surface pressure model installed in the LaRC 20-Inch Mach 6 Tunnel.

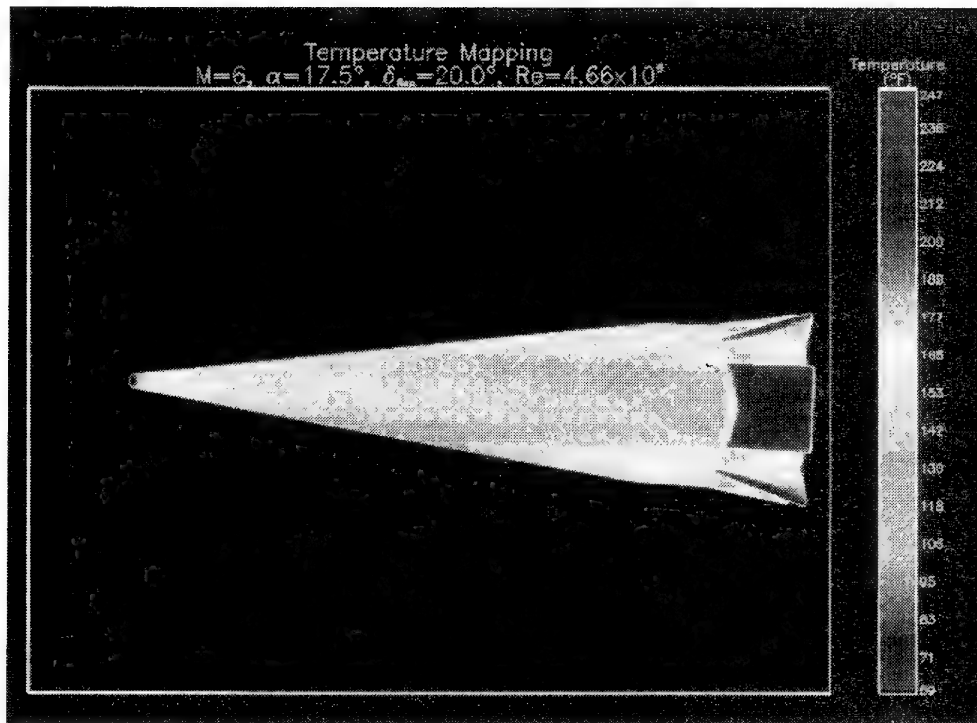


Figure 5. Surface temperature, thermal mapping, image obtained using thermographic phosphor system.

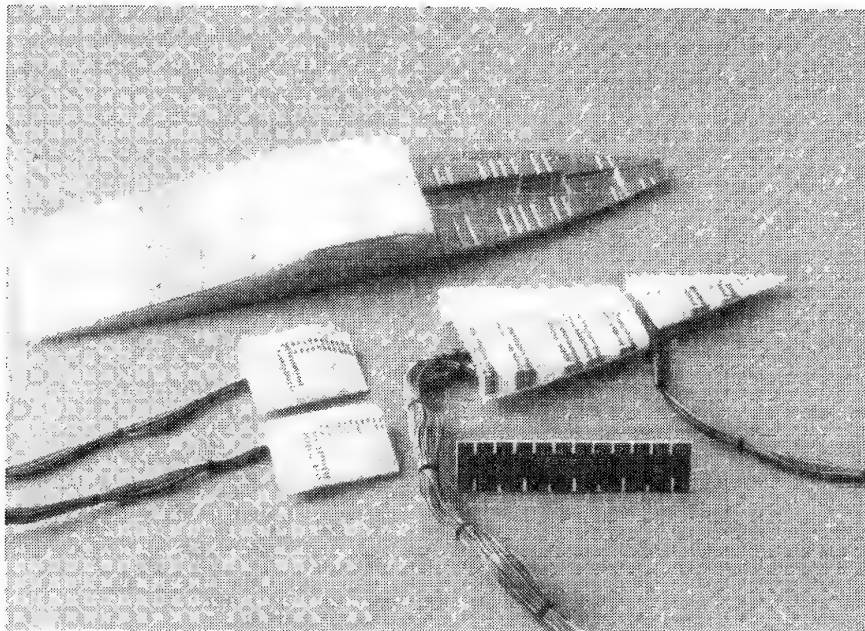
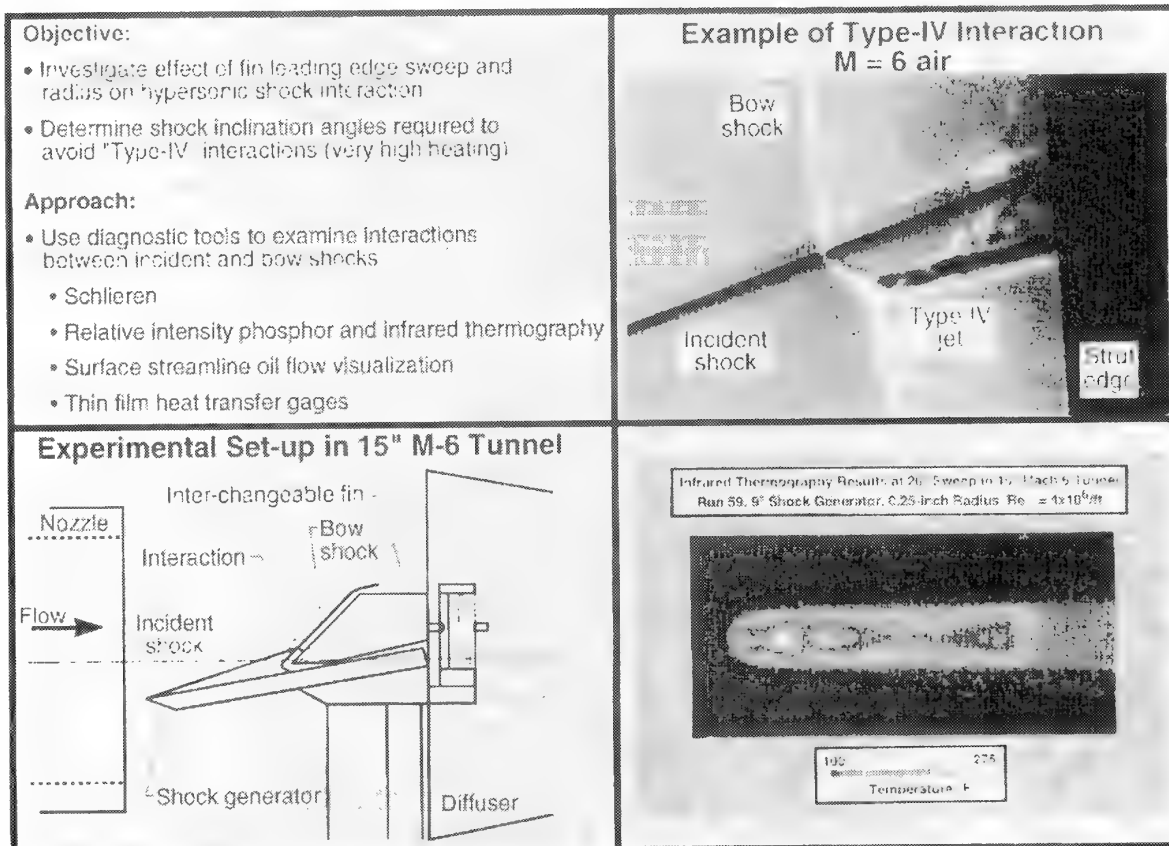
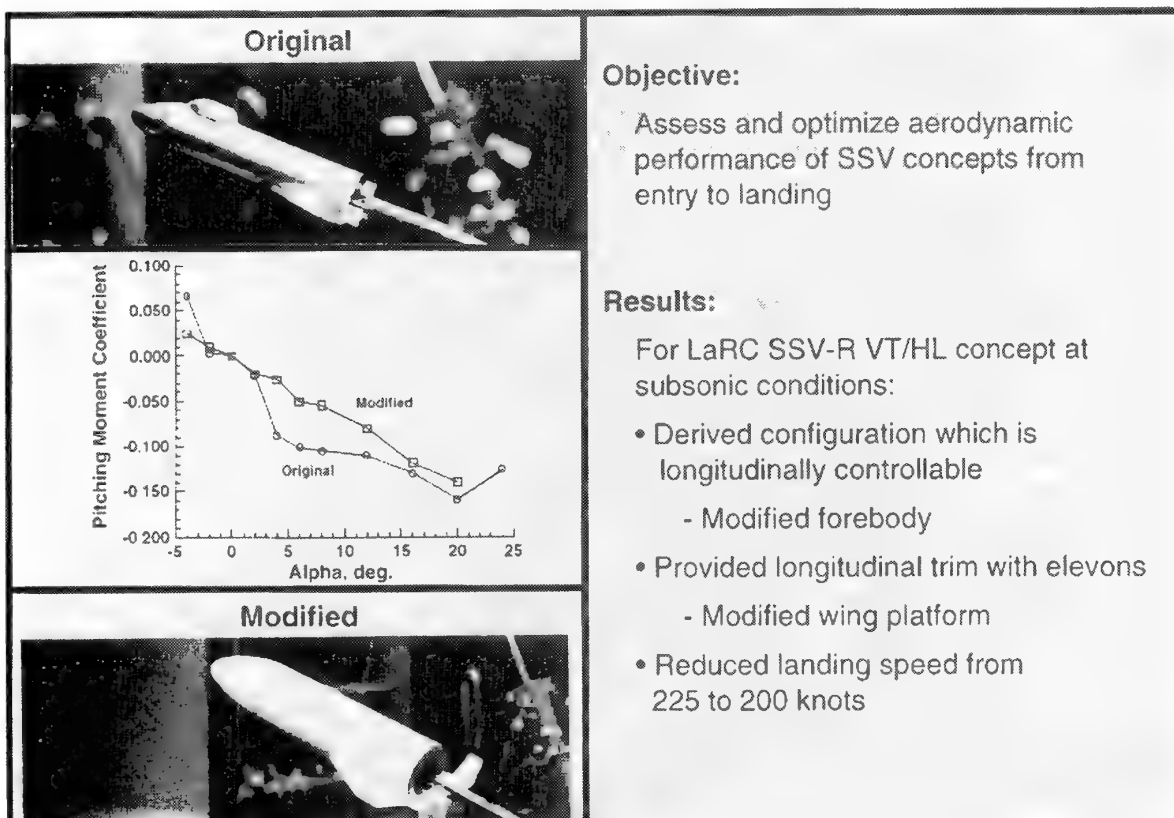


Figure 6. Thin film surface temperature gages on MACOR model.



**Figure 7. Shock/shock interaction study using schlieren system, thermographic phosphor, and infrared temperature measurements as well as thin film gages.**



**Figure 8. Single stage vehicle VT/HL low speed aerodynamic investigation.**



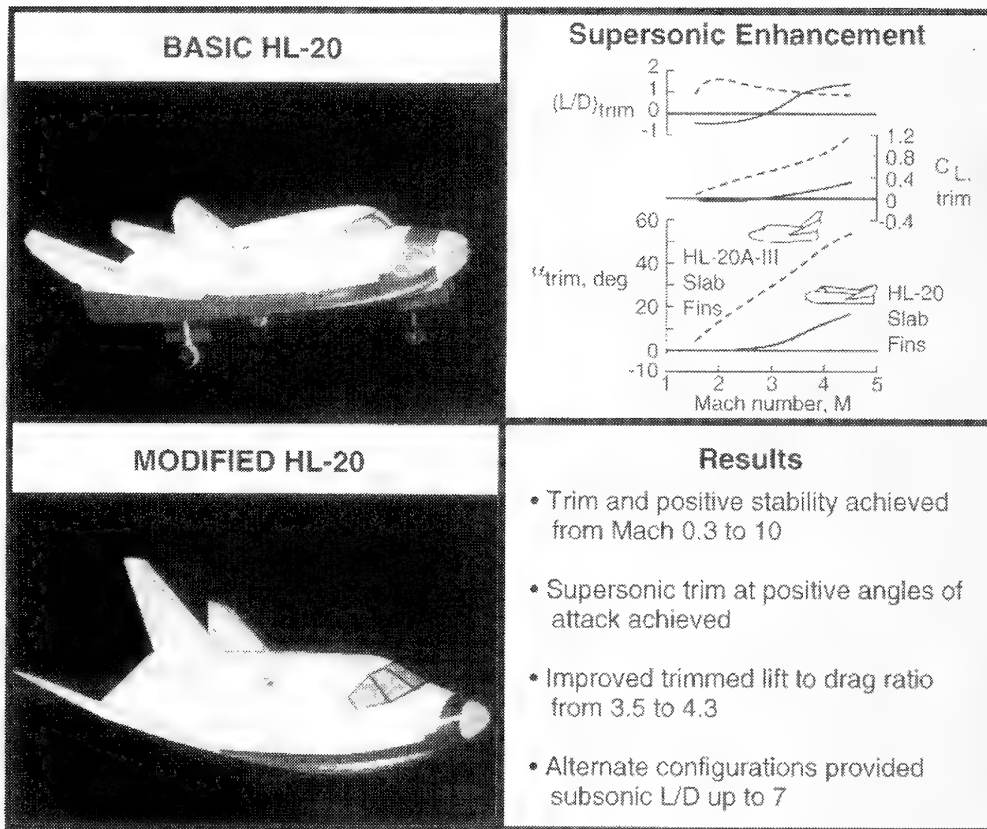


Figure 9. HL-20 lifting body supersonic aerodynamics investigation.

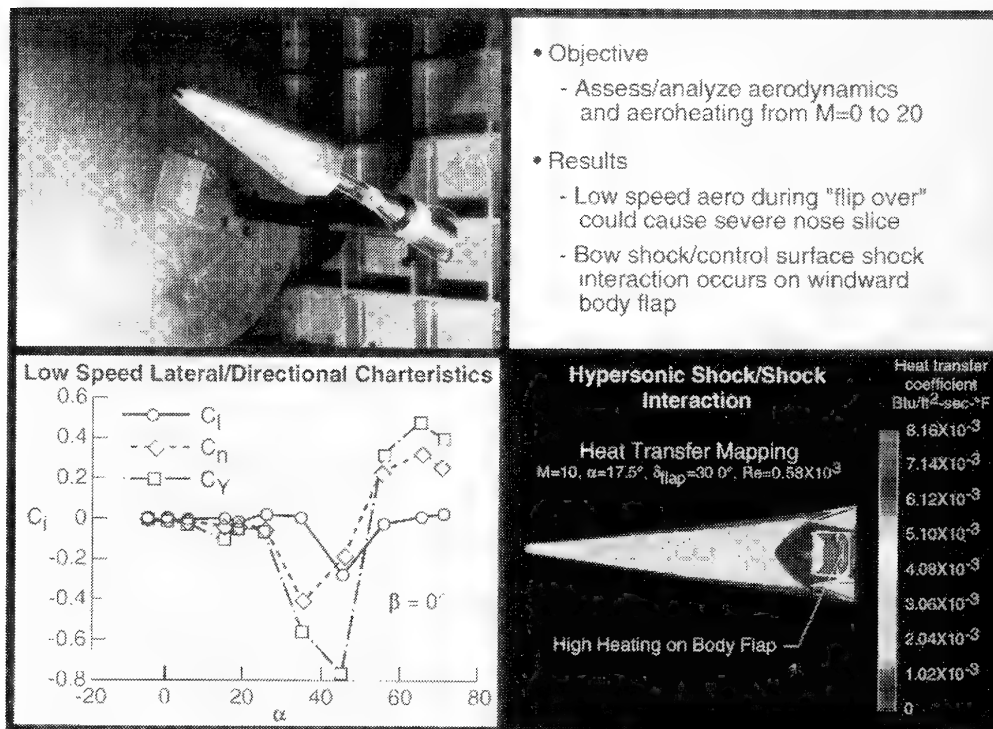


Figure 10. Single stage vehicle VT/VT low speed aerodynamics and hypersonic aero-heating investigation.

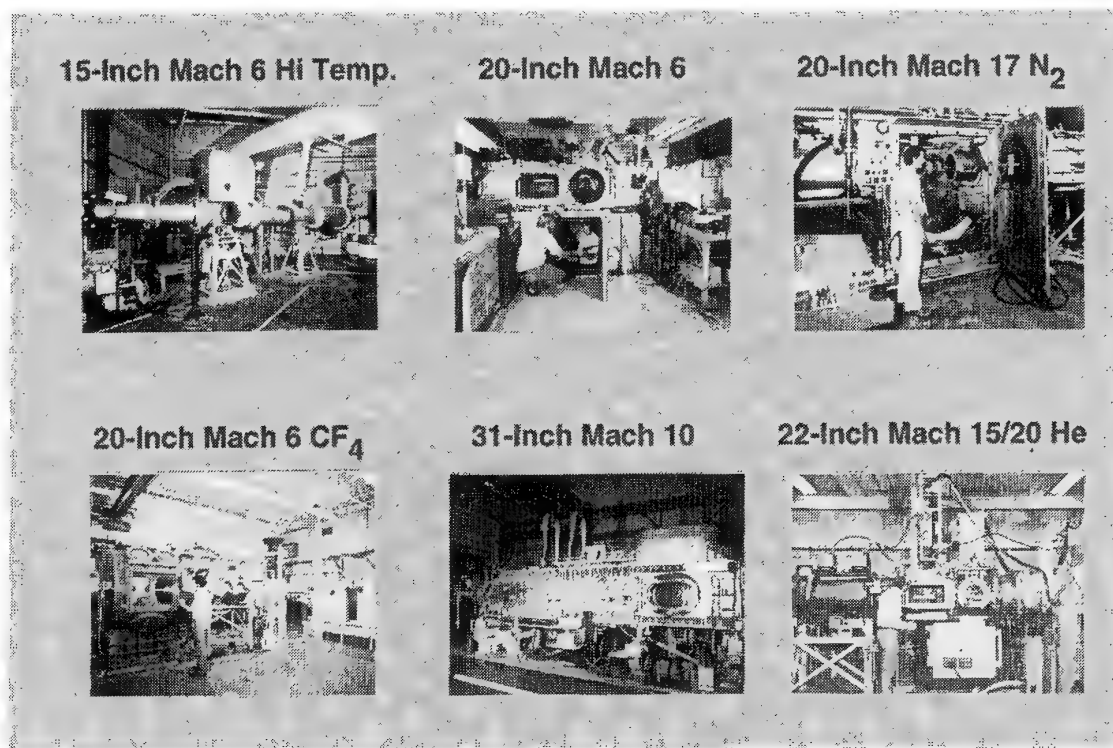


Figure 11. The Langley Research Center Aerothermodynamics Facilities Complex.

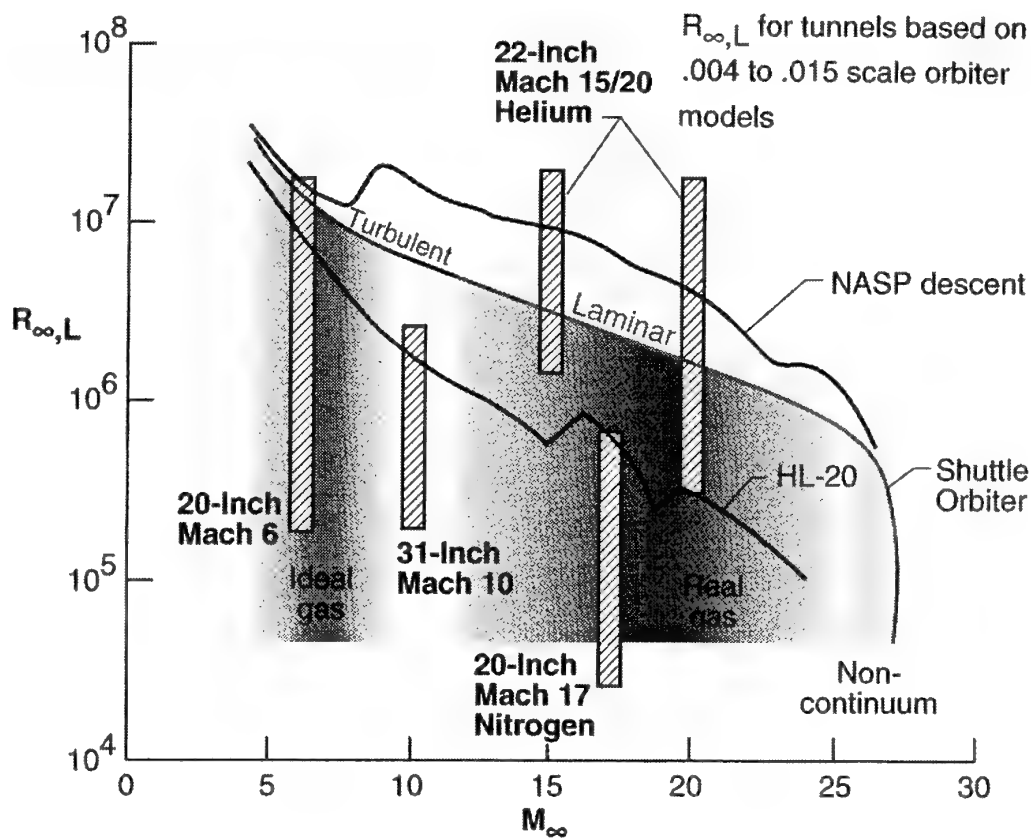


Figure 12. Mach number and Reynolds number simulation capability of the Aerothermodynamics Facilities Complex.

**Objectives:**

Enhance flow quality, testing capability, and productivity of HFC facilities for studies of advanced aerospace vehicle concepts.

**Recent Upgrades and Modifications**

| Mods.         | 15" M-6 Air | 31" M-10 Air | 20" M-6 CF <sub>4</sub> | 22" M-20 He | 20" M-17 N <sub>2</sub> |
|---------------|-------------|--------------|-------------------------|-------------|-------------------------|
| Nozzle        | X           | X            | X                       | X           | X                       |
| Filter        | O           | X            | X                       | O           |                         |
| FFSP/Pitot    |             | X            | X                       | X           | X                       |
| Test Section  | O           |              | X                       | X           | X                       |
| Model Inject. | O           |              | X                       | X           |                         |
| Hi Pressure   | X           |              |                         |             | X                       |
| Vacuum        | X           | X            |                         | O           | X                       |
| Data Acq.     | X           | X            | X                       | X           | X                       |

X Complete

O Underway - funding approved

**Achievements for HFC Facilities**

- Flow quality
  - State-of-the-art nozzle contours
  - Solid particle filters (5 microns)
- Testing capability
  - 3 axis flow field survey probes (FFSP)
  - High accuracy model position ( $\alpha$ ,  $\beta$ )
  - New data acquisition systems common in all facilities
- Productivity and reliability
  - High pressure systems
  - Vacuum systems

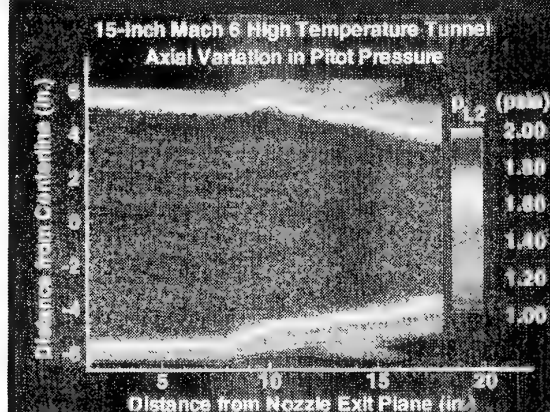


Figure 13. Aerothermodynamics Facilities Complex improvements and upgrades.

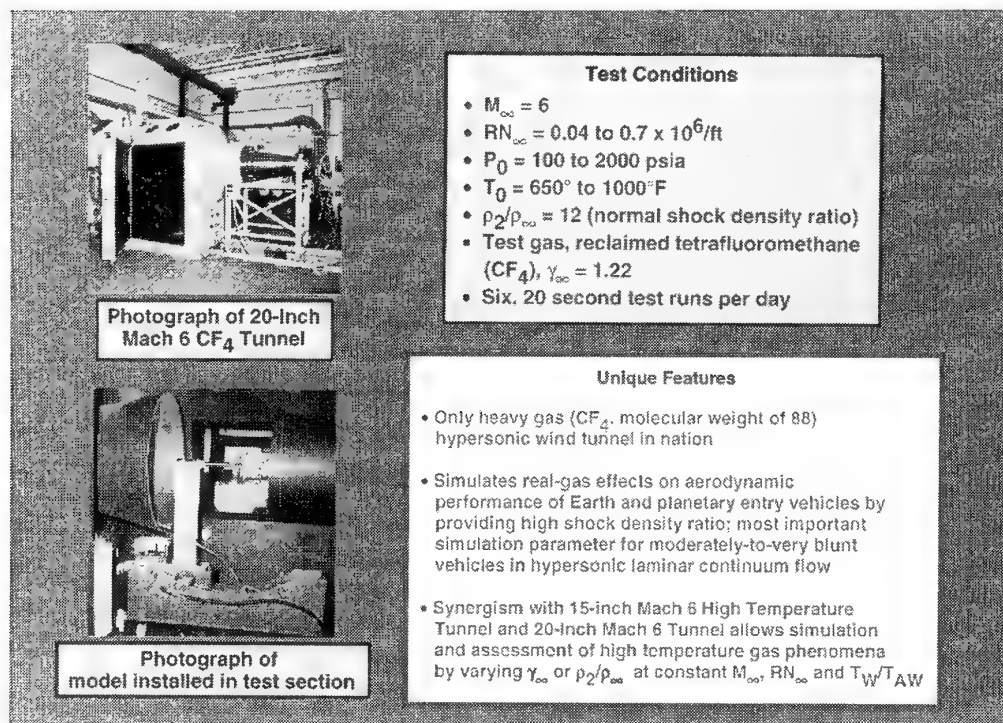


Figure 14. The LaRC 20-Inch Mach 6 CF<sub>4</sub> Tunnel.



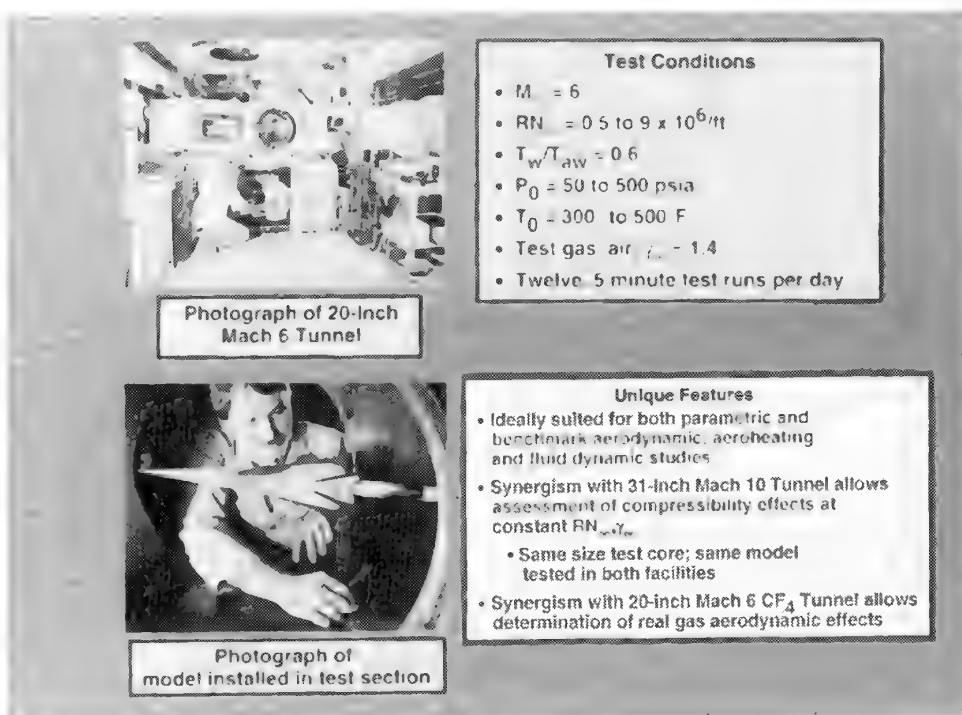


Figure 15. The LaRC 20-Inch Mach 6 Air Tunnel.

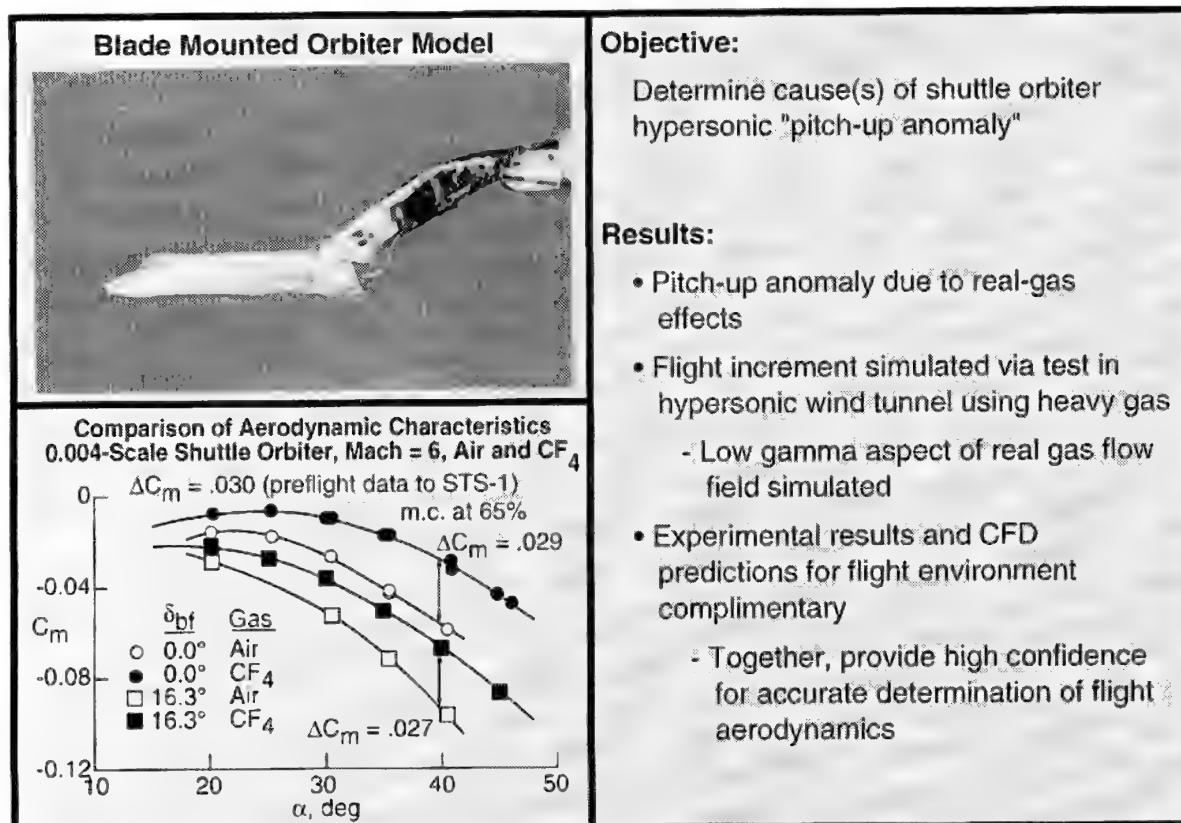


Figure 16. Real gas simulation results for the Space Shuttle Orbiter.

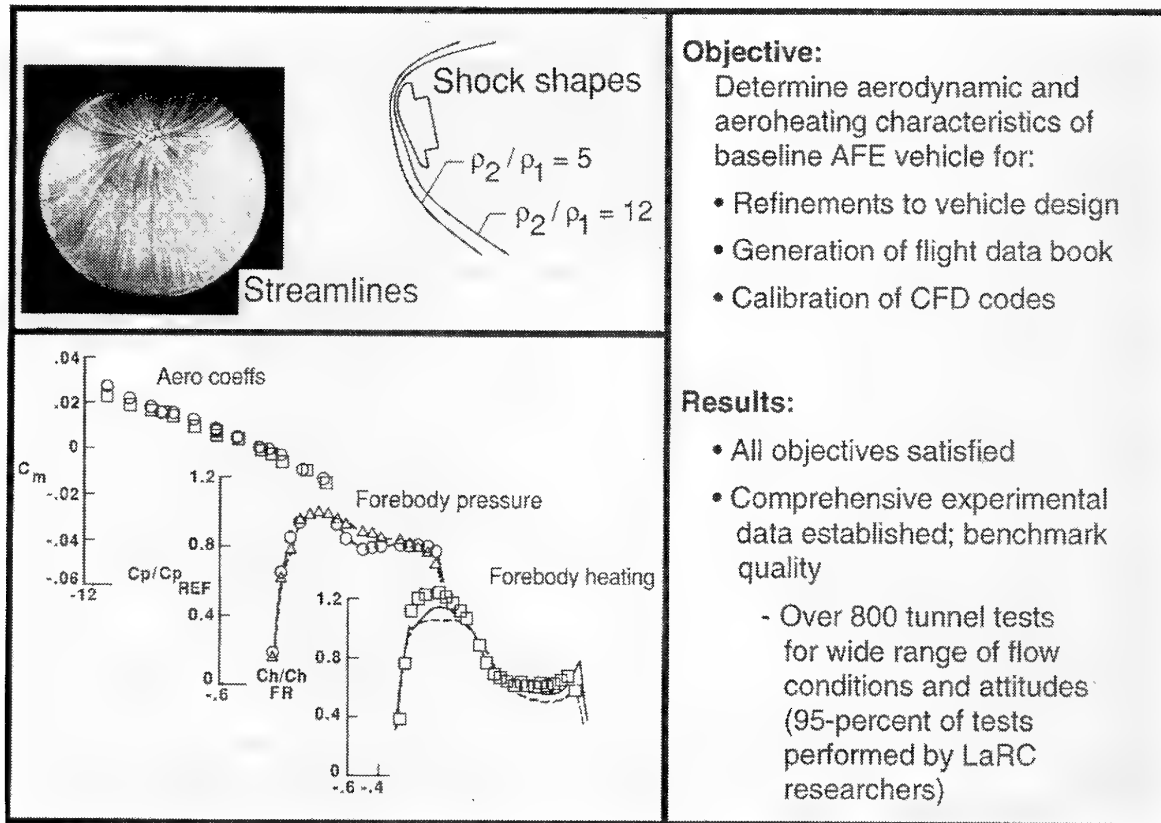


Figure 17. Real gas simulation results for the aero-assisted flight experiment configuration.

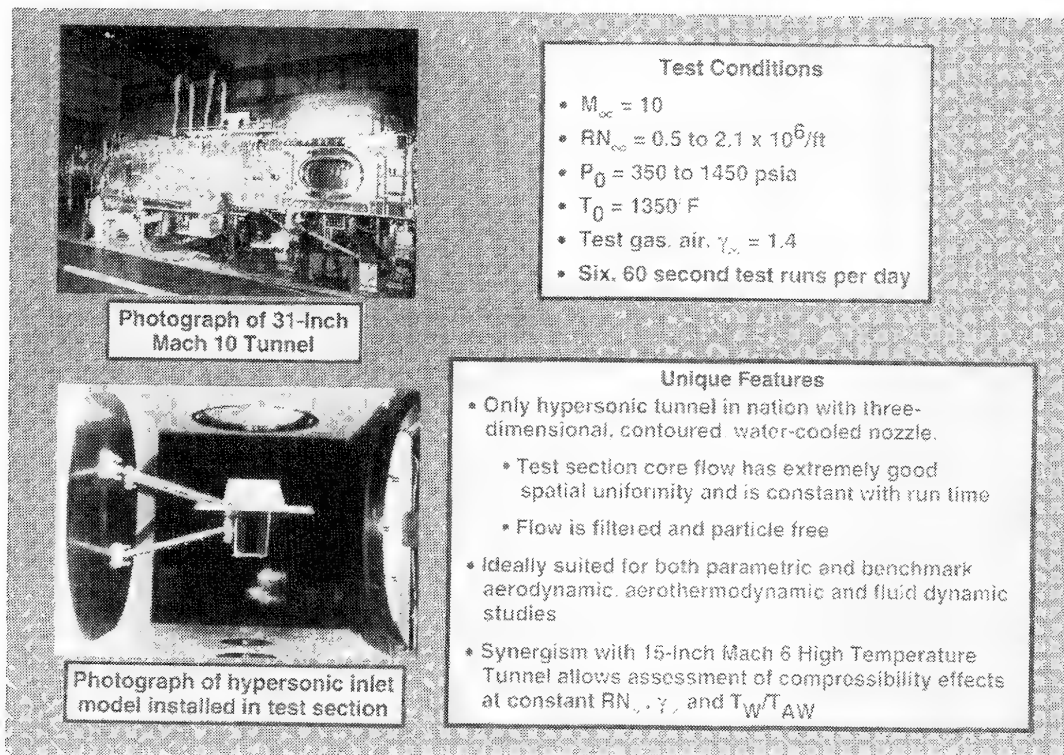


Figure 18. The LaRC 31-Inch Mach 10 Tunnel.

## Test Aspects of Single Stage to Orbit Systems

Dr. William A. Gaubatz  
Daniel R. Nowlan  
Matthew G. Maras  
John A. Copper  
McDonnell Douglas Aerospace  
Huntington Beach, CA

Ms Kate A. Coleman  
Coleman Science & Research  
701 West Cavalcade  
Andover, Kansas 67002-8737  
USA

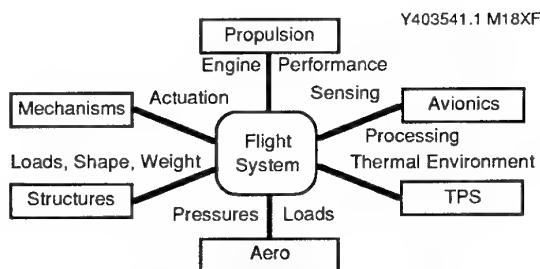
The McDonnell Douglas Delta Clipper Team recently completed the initial flight testing of a one third scale version of an operational single stage to orbit vehicle. The Delta Clipper Experimental, DC-X, is a 14 meter tall, totally reusable, liquid hydrogen/liquid oxygen fueled test vehicle, powered by four P&W RL-10A5 rocket engines. It has a totally autonomous on board flight control and mission control systems; flight test mission requirements are simply added through software to the mission controller. The DC-X is designed to explore and validate the low speed flight qualities of a vertical take-off and vertical landing spacecraft and its flight characteristics closely duplicate those predicted for the full scale DC-1 vehicle. The DC-1 vehicle would be capable of routinely flying people and/or cargo to and from space and would have a lift capacity for carrying 12 metric tons to low earth orbit.

One of the unique features of the DC-X development was the use of the CASE (Computer Aided Software Engineering) tools which reduced the development time for the software by at least a factor of three and the cost by a factor of ten. This enabled the development work for the aerodynamics and controls to be extended and control algorithms to be routinely updated based on results of hardware in the loop simulations, on going wind tunnel testing, ground and flight testing.

The flight test program was carried out in a series of flight envelope expansion tests similar to the approach used for aircraft testing. Ramp testing started at the NASA White Sands Test Facility and included full duration engine firings to exercise and validate all control functions for both engine and aero control systems. Flight tests started with short duration (60 second) flights in which the DC-X took-off vertically to an altitude of several hundred meters, hovered, translated across approximately 110 meters and descended vertically to land on a flat concrete pad. These tests validated key aero and control characteristics associated with ground effects as well as validating overall control effectiveness and total system performance. Subsequent flight tests followed similar flight profiles except to altitudes of several thousand meters to validate the aerodynamics and controllability at

higher dynamic pressures during the base first descent. Tests were carried out in the presence of ground winds and winds aloft to validate controllability. The final test series is designed to prove out the rotation maneuver which is used to reorient the vehicle from a nose first attitude, used to fly back from space, to a base first attitude which is used to land.

This 30 month program was carried out under the sponsorship of the Ballistic Missile Defense Organization; Major Jess Sponable was the Program Manager.



**There is no substitute for the realism of a flight vehicle**

**Figure 1. Flight Vehicle Forces Technology/Subsystem Integration.**

The DC-X flight test article provides an integrated system testbed. It has been used to validate subsystem and flight dynamic characteristics at the system level. While it's true that each subsystem can be tested and validated under non-flight test conditions, their relative effectiveness and interaction at the system level is best demonstrated by actually flying the vehicle.

Development of the flight control system for DC-X involved integration of various aspects of the vehicle subsystems. The propulsion system engine performance was validated for the first time with the flight article, first during static fire testing, then during actual flight tests. Differential throttle control was evaluated and engine performance database enhanced during the flight test program.

The hydraulic actuation of the main engine gimbals provided an excellent opportunity to evaluate response requirements for a vertical take-off/vertical landing vehicle since attitude control was maintained essential through thrust vector control (TVC) of the main engines.

Vehicle structural elements play an important part in defining flight characteristic boundaries, related to loads and weight. Shape obviously effects the aerodynamics flight characteristics in terms of loads and pressures.

The thermal environment must be assessed and appropriate measures taken to minimize heat transfer to the core vehicle. Of particular concern on DC-X was the base area heating associated with vertical take-off and more importantly powered landing. Baseplate, landing gear and engine bell mounting designs all were effected by thermal considerations, which also drive the flight envelopes considered for vertical landing.

Obviously the avionics also play a very important part in the flight test and subsystem control aspects of the vehicle. Sensor/effector relationships, command/control paths and flight dynamics all play an important part in the flight test vehicle design.

As individual elements these subsystems and technologies all provide a moderate level of maturity, however when integrated onto a vehicle such as the DC-X, for the purpose of flight testing a level of "realism" is introduced that focuses the designers to consider issues at a system level.

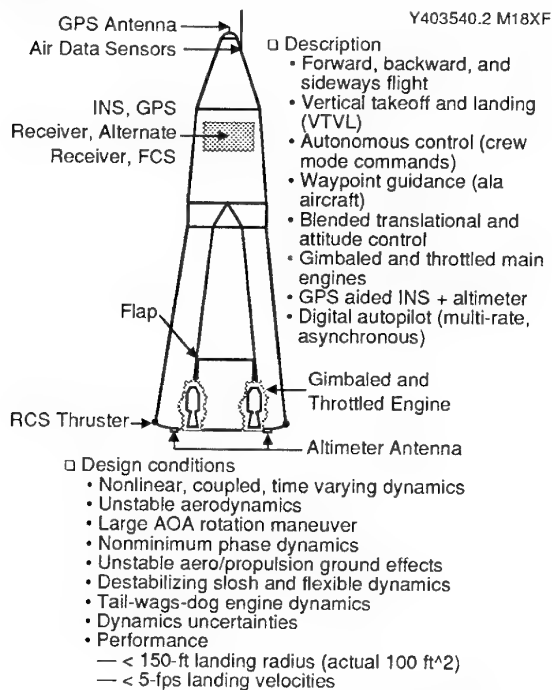


**Figure 2. DC-X Test Bed Validates Key Subsonic Delta Clipper Flight Controls Performance Issues.**

DC-X is a unique vehicle from a flight test standpoint. It has the capability to flight forward (nose first), backward, and sideways, which allows for a vertical take-off, vertical landing flight system. All flights are autonomous, no ground control intervention from the Flight Operation Control Center crew is required for nominal flight conditions. Waypoint guidance, similar to that used on most commercial airliners today, is used to pre-define the flight trajectories. The flight control software is database controlled. This database can be changed, via uplink commands to reflect the flight crews desired mission plans. The Autopilot is completely digital, and integrates commands, controls and sensor data at many different computational rates (up to 6 different rates of operation). This additional complexity was added in order to accommodate a wide range of off-the-shelf avionics components, again demonstrating great flexibility in the system design. Navigation is performed autonomously on-board using a GPS aided INS (Honeywell H770 INS off the F-15 military aircraft), coupled with a Radar Altimeter which provides accurate height above ground data for landing purposes.

DC-X as a flight test article requires consideration of the following design conditions: (a) nonlinear, coupled, time varying dynamics, (b) unstable aerodynamics (valid for all modes of flight), (c) large angle of attack rotation maneuvers (required to re-orient the vehicle prior to vertical landing), (d) nonminimum phase dynamics associated with guiding the vehicle in translation or sideways motion, (e) unstable aero/propulsion ground effects (the plume interaction with the ground and the vehicle during landing, coupled with the gimbal effects to maintain commanded attitude, result in an unstable flight condition, which must be accounted for in the control system design. Note: flight testing has been the most effective and reliable means for quantifying the interactive forces and moments in this flight regime), (f) destabilizing slosh and flex-body dynamics (characteristics that are typically vehicle specific, but which must never the less be accounted for), (g) tail-wags-dog engine dynamics (coupling effect of engine/gimbal inertias versus the vehicle inertia), (h) dynamics uncertainties (with limited wind tunnel data available, particularly in the low-speed, subsonic regions, flight tests have been the only way to evaluate aerodynamic and coupled dynamic uncertainties), (i) landing performance is critical (DC-X has a 100 ft square landing surface and must land with < 5 ft/sec horizontal and vertical landing velocities for all flight conditions).

The picture identifies the major avionics and effector locations on the vehicle. From top to bottom, the GPS antenna is located in the nose cap. This provides sufficient satellite coverage for ascent, portions of the descent and all of the landing phases of operations. The vehicle is equipped with a full air data system including measurements of dynamic pressure, alpha and beta angles of attack.

The avionics system bay is mounted in the forward aeroshell area, just above the LO2 tank. It contains the INS

(inertial navigation system), GPS Receiver (P(Y) Code accuracy), Radar Altimeter (RALT) Receiver (note the antennas are installed on the baseplate), a set of redundant accelerometers and rate gyros for controls purposes and the flight computer. The base of the vehicle contains the main control system effectors including the throttleable main engines (4x Pratt & Whitney RL10-5A, LOX/LH2 fueled), gimbals for thrust vector control (2 per engine), flaps (5 total, one on each side, with one side having a split flap to accommodate aerodynamic role control) for aero control surfaces, and the Aerojet GH2/GO2 reaction control system.

Y403547.1 M18XF

#### Vehicle Management System

- GPS aided INS + Altimeter
- Horizontal Position Errors  $\leq 10$  m ( $1\sigma$ )
- Altitude Error  $\leq 3$  ft +  $1\%$  ( $1\sigma$ )
- Velocity Errors  $\leq 0.35$  m/s ( $1\sigma$ )
- 32-Bit Architecture, Ada Compiler
- Throughput  $\sim 4.4$  Mips (DAIS mix)
- Memory = 256K (EPROM), 128K (RAM)
- Computation Rates - 100/s

#### Instrumentation

- Air Data (Qbar, AOT, AOSS)
- LVDTs (Engine, Flap), Pc

#### Main Engines

- Four RL10A-5 Engines (LH<sub>2</sub>/LO<sub>2</sub>)
- Thrust = 13,694 lb/3331 lb (3500 ft)
- Thrust Throttleability = 4.1 to 3.4
- Isp = 346 sec/288 sec (3500 ft)
- Control Valve Response = 0.7 to 1.0 Hz

#### Main Engine Gimbal Actuation System

- Two Hydraulic Actuators per Engine
- Maximum Deflection  $\geq 8$  deg
- Maximum Rate  $\geq 30$  deg/s
- Average Rate Cap.  $\geq 9$  deg/s
- 10-Hz Response Time ( $\zeta = 0.3$ )

#### Flap Actuation System

- One Hydraulic Actuator per Flap
- Maximum Deflection  $\geq 30$  deg
- Maximum Rate  $\geq 20$  deg/s
- Average Rate Cap.  $\geq 10$  deg/s
- 10-Hz Response Time ( $\zeta = 0.3$ )
- Windward Load Cap.  $\geq 4340$  lb

#### Reaction Control System

- 4 Thrusters (GH<sub>2</sub>/GO<sub>2</sub>)
- Thrust Level = 431 lb (4000 ft)
- MIB = 50 lb-sec, Isp = 320 sec (vac)
- Total Impulse  $\sim 29,000$  lb-sec

**Figure 3. Flight Control Requirements Established Early in the Program.**

This chart defines some of the key control system requirements, which were defined very early in the program in order to support hardware development and system performance evaluations. Many of these requirements have been validated at the subsystem level during component, subsystem and/or vehicle testing prior to flight, however complete system level verification and checkout can only be assessed as the flight envelope is expanded during flight testing.

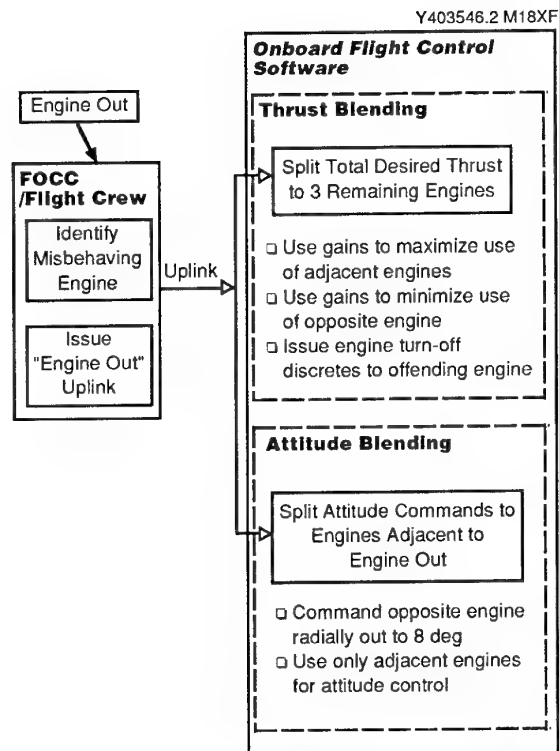


**Figure 4. DC-X Incorporates On-Board Engine Out Response Algorithms**

Like most commercial aircraft flying today, DC-X has the capability to respond to an engine out and either continue the mission as defined as part of its pre-defined flight plan or initiate a series of procedures to burn off excess propellants and land vertically from the point where the anomaly occurred (this capability is part of a module identified as Autoland/Autoclimb, which can also be initiated by the flight crew from the FOCC). Since all engine health data is available to the flight crew in the Flight Operations Control Center, they have the capability to access engine performance and issue, via RF uplink, a command to shut down an engine and continue the mission on the remaining 3. The on-board flight control software has the capability of responding in two ways. The total thrust desired is allocated to the remaining 3 operational engines. Gains are adjusted to "balance" adjacent and opposite engines. Attitude control is then allocated to the adjacent engines, and the opposite engine is splayed out to 8 degrees. This splay command provides additional control stability, particularly during the landing phase, analogous to the attempt to stabilize a table that's lost one of its legs.

This engine out capability is consistent with the whole operational concept of a re-usable single stage to orbit vehicle or a commercial airliner, when an engine failure occurs the system must be capable of bringing back the vehicle and payload intact to the launch site.

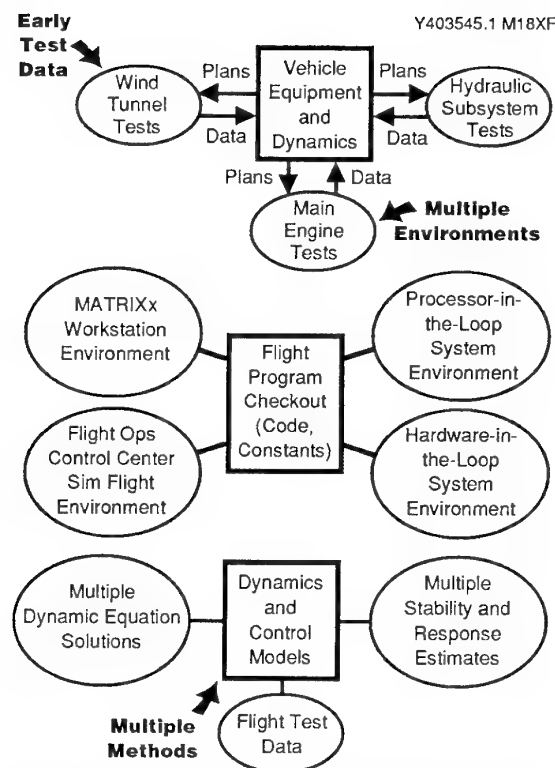


**Figure 5. Simulation Validation Techniques Enhance Flight Control Quality.**

As part of the validation process for the DC-X flight test program many steps were taken to develop detailed simulations and analysis tools which could be used to verify design requirements prior to committing the vehicle to flight testing. "Early" (early is used here as a relative term since many subsystem tests were occurring in parallel with system integration and test activities) testing (wind tunnel, main engine and hydraulic subsystem tests) produced a performance database which was used to develop the core of a 6 degree of freedom simulation model. This core was designated as the Vehicle Equipment and Dynamics Model. It was used to iterate on many of the early subsystem tests to refine additional tests required to fully characterize performance.

The guidance, navigation and controls design (algorithm development) was supported by multiple sets of dynamic equation solutions developed over the years, and included different methodologies as well. The product of this activity is the GN&C design which is enhanced by flight test data.

The Flight program, consisting of source code and the mission constant database is validated in multiple environments, all interrelated and all capable of supporting design upgrades, quickly in order to maximize launch system availability. Key point to make here is that this validation system (methods and test environment) are essential to the risk management approach for any flight test program. In addition the validation process for any particular flight test

mission must be flexible and responsive to changes in the design as a result of test data (component, subsystem or flight). As an example, flight test data is available from the test site (FOCC) within minutes of the completion of a test. This data is incorporated into the validation test database and comparison plots are generated automatically at that point for designers and test evaluators. In addition, a 3D visualization tool has been developed which allows us to "playback" flight tests, using flight telemetry data, immediately after a flight is completed. The buildup of this capability for the DC-X program is key to maintaining the quality and success of the flight test program.

#### SSRT DC-X Low Hover Test No. 2 Y403544.2 M18XF

Flight Controls Telemetry Calculated Pitch Attitude Error

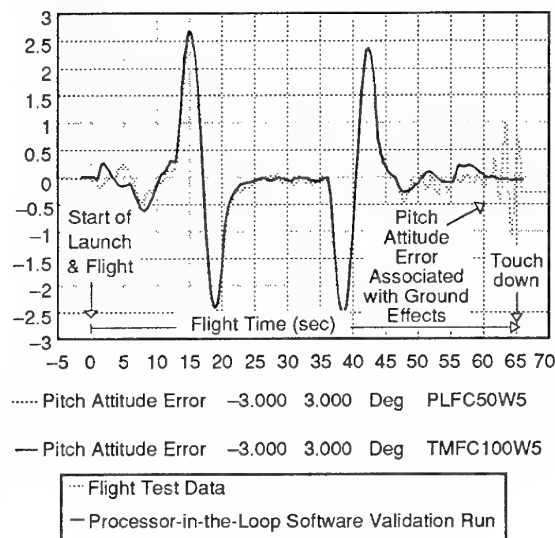


**Figure 6. Flight Critical Simulation Parameters Match Flight Test Data.**

As mentioned above, a validation test database is maintained for each flight test. Included in this database are traces of telemetry data produced as a result of design simulation & Software validation test cases. This data is overlaid against actual flight data as part of the post-flight performance assessment. This chart shows one of the key flight control related parameters, pitch attitude error, from the second flight test (designated Low Hover Flight Test #2). The particular parameter, calculated as part of the flight control algorithms, provides insight into the attitude control autopilot and the servo loops associated with gimballing of the main engines. The traces are essentially an exact match with the exception of the final few seconds of the mission related with the final phases of landing. The flight test data reveals an instability associated with ground effects (discussed earlier), which is accounted for in the controls design in the frequency domain analysis, but which is not modeled in the 6 degree of freedom model used to generate these validation runs.

| Y403543.2 M18XF |                    |                                  |                                |                 |                        |
|-----------------|--------------------|----------------------------------|--------------------------------|-----------------|------------------------|
|                 | Miss Distance (ft) | V <sub>Horizontal</sub> (ft/sec) | V <sub>Vertical</sub> (ft/sec) | Tip Angle (deg) | Wp Surface Angle (deg) |
| Requirement     | < 150              | < 5                              | 2<Vv<5                         | < 2             | < 8                    |
| FT No. 1        | 3.6                | 0.5                              | 3.6                            | 0.36            | <2.0                   |
| FT No. 2        | 5.2                | 0.5                              | 3.7                            | 0.92            | <5.1                   |
| FT No. 3        | 4.3                | 0.4                              | 3.7                            | 0.75            | <5.2                   |
| FT No. 4        | 30                 | 0.4                              | 3.5                            | 0.17            | <3.6                   |
| FT No. 5        | N/A                | 0.64                             | 4.0                            | 0.78            | <3.4                   |

**Figure 7. Vertical Landing Flight Test Performance Has Been Outstanding.**

This is a summary chart contrasting the landing phase performance requirements against actual data taken from the first three flight tests of DC-X. Note: one indication of the vernier vertical control capability we have experienced is that on flight tests #2 and 3 the control system vertical velocity during landing was "re-set" to 3.8 ft/sec, and 3.7 was achieved. In general landing velocities, which have a significant impact on landing gear load capability have been excellent (less is better, horizontally and the ability to accurately control vertical descent rates for a powered vertical lander is critical for thermal as well as attitude control purposes).

| Y403542.2 M18XF      |          |            |         |                |   |
|----------------------|----------|------------|---------|----------------|---|
| Date                 | Alt (ft) | Qbar (psf) | V (fps) | Flt Time (sec) | Comments  |
| 8/18/93              | 150      | 1.2/0.6    | 35/23   | 59             | □ Verified FC system functionality  |
| 9/11/93              | 300      | 3.0/1.1    | 55/33   | 66             | □ Ascent/landing mods, second GE sample   |
| 9/30/93              | 1200     | 15/5       | 120/75  | 72             | □ 180-deg roll, Cx and 90-deg Cn aero data  |
| 6/20/94              | 2850     | 15/5       | 120/75  | 135            | □ Full Wp load, long flt time, RALT aiding low Q/AOA sweep (0 deg to 70 deg)          |
| 6/27/94 <sup>1</sup> | 4350     | 20/10      | 145/100 | 1359           | □ Fast turnaround, curved ascent laterally to 1200 ft, higher Q Cx and 90-deg Cn data |
| TBD                  | 8000     | 30/20      | 175/140 | 145            | □ Alternate pad, higher Q/AOA sweep, RCS roll control, GPS aiding                     |
| TBD                  | 8000     | 30/20      | 175/140 | 145            | □ Alternate pad, low Q gimbal rotation  |
| TBD                  | 9500     | 80/40      | 280/200 | 155            | □ Low AOA/high Q gimbal/flap control  |
| TBD                  | 8500     | 100/55     | 315/235 | 150            | □ Alternate pad, low Q aero rotation  |
| TBD                  | 8500     | 120/65     | 350/250 | 150            | □ Alternate pad, nominal Q aero rotation  |

<sup>1</sup>Note: Autoland was issued 17 sec into Flight No. 5, not all flight dynamics were achieved, resumption of flight testing would pick up at this point

**Figure 8. A Ten Flight Test Program is Planned.**

DC-X has completed five flight tests to date (7/94). Flight test times have ranged from 59 to 135 seconds covering altitudes from 150 ft to 2850 ft. The majority of the test objectives identified for the low hover test series have been completed, including demonstration of three of the four major flight phases, ascent, translation and landing. The remaining flight phase is rotation. The flight test program planned for would include demonstration of the remaining flight phase through a series on incremental flight tests. The remaining objectives would include resolution of aero/control issues related to peak normal forces and pitching moments, asymmetric vortex shedding and axial force/hot gas effects. All of these issues will help to reduce the uncertainties in the wind tunnel and subsonic aero data. Additional testing would also provide a means to validate previous subsonic tunnel and flight data, and would allow the operational concept of a rapid turnaround to be demonstrated.

Flight testing of the DC-X resumed in May, 1994 after approximately a 8 month delay associated with securing additional funding for the program. Within a month the vehicle and all ground systems were brought out of storage conditions, verified to be fully operational, and several static tests were performed on the launch mount, within a 2 week time frame, to specifically confirm engine start transient performance and verify system readiness to fly. Two additional flight tests have been completed since this reactivation, with the two occurring within 7 days (actually 6 days and one day off for the flight & ground crew), validating the 7 day turnaround program objective. In addition, planning for next flight had been completed and it was scheduled to occur 3 days following Flight #5.

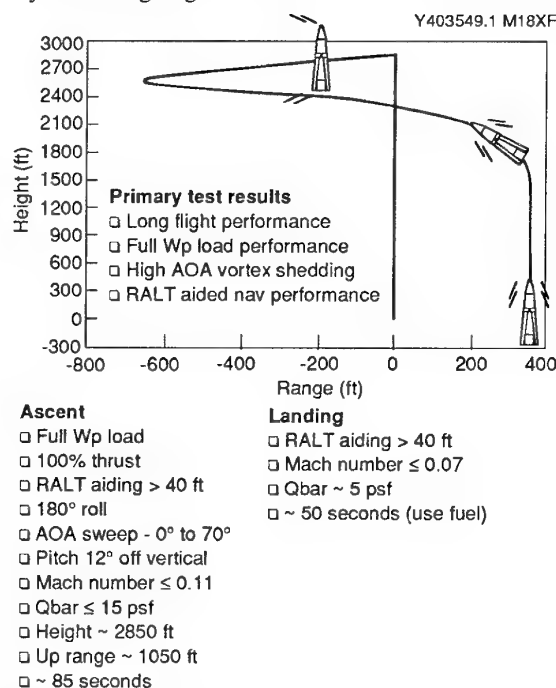


**Figure 9. Flight Test #4 Provides High AOA AVS and RALT Aided Nav Data.**



Flight testing resumed on 6/20/94 with Flight Test #4. This test featured several firsts for the program including (a) a full propellant load for flight, (b) full, 100% thrust commanded on ascent, (c) a flight time twice as long as previous flights, (d) a doubling in altitude from Flight #3, (e) 3 times as far up range (to 1050 ft), (f) and saw total heat loads 2 or more times higher due to longer flight time coupled with flight dynamics. Flight #4 was considered the first in a series of envelope expansion tests leading up to a rotation demonstration.

There were several specific test objectives for Flight #4 which dealt with aerodynamic and control issues. An angle of attack (AOA) sweep over a range from 0 to 70 degrees was performed to begin testing for asymmetric vortex shedding (AVS) in flight. This phenomena has been observed in several wind tunnel tests, and was one of the primary reasons for adding the strakes seen running vertically down the forward aeroshell.

Flight #4 also was the first flight to implement Radar Altimeter (RALT) aiding of the vertical navigation channel. The flight control software was modified subsequent to Flight #3 to allow RALT data inputs, above 40 ft to be processed by the onboard "processed altitude Kalman Filter" which in turn produces an altitude estimate used in the guidance algorithms. Previous flight test data provided the confidence to incorporate the RALT as the primary altitude measurement aid for this critical flight function.

The extended flight time did have an impact on landing accuracy summarized previously (note: the vehicle landed 3.8 ft to the west and 29.8 ft to the north of center, and the dispersion is within the specified drift error on the unaided INS). Since this and all previous flights relied entirely on the INS for navigation accuracy (unaided), drift performance plays a significant role in landing accuracy. On the first 3 flights navigation errors associated with INS drift were less than 5 feet, reflecting exceptional quality of the INS, and guidance and control software. This type of performance for shorter duration flights also provided the opportunity to characterize the RALT and GPS systems prior to incorporating them into the flight system.

Flight Test #5 occurred on 6/27/94, as mentioned above only 6 working days after Flight #4. This test was to featured (a) a constant angle of attack on ascent of ~15 degrees in order to expand the aerodynamic flight test database, (b) ascent & descent mach numbers were designed to be in the Mach = 0.1 range in order to reduce existing nose forward and base forward  $C_x$  uncertainties, (c) a side translation was planned, with the vehicle oriented near vertical in order to reduce peak  $C_n$  uncertainties, (d) a flap effectiveness demonstration was scheduled for ascent phase, (e) and descent dynamic pressure was designed to increase providing additional base first control information, (f) and finally this flight was to have been the first to demonstrate GPS/INS navigation aiding.

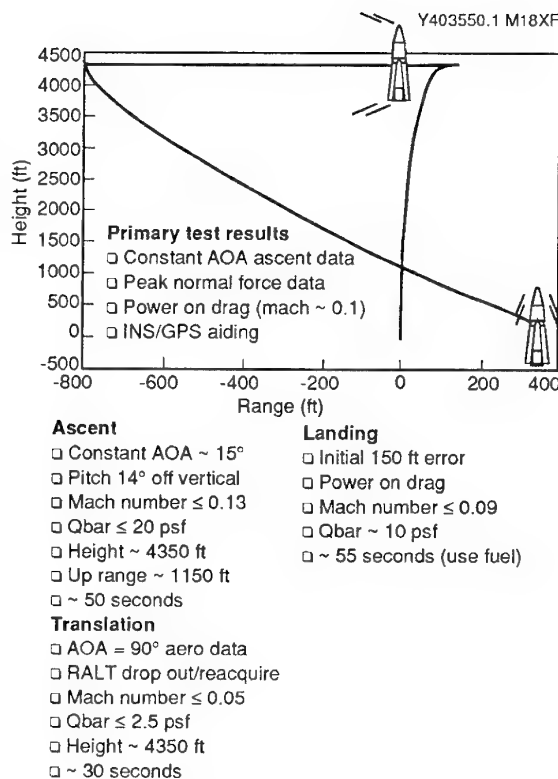


**Figure 10. Flight Test #5 Provides Constant AOA Ascent, Peak  $C_n$  and Power On Drag Data.**

During pre-flight operations an anomaly occurred resulting in a detonation of the chill-down propellants which free flow away from the vehicle on the current design. This detonation resulted in an overpressure which in turn damaged the aeroshell, and also separated the nose cap from the forward aeroshell. Since damage was limited to the aeroshell structure, no on-board flight critical systems were effected and the system was allowed to transition into the flight mode of operation. The flight continued on track, with all flight critical subsystems operational, even though visually ground video was picking up debris in the form of aeroshell sections peeling away from the vehicle. At 17.6 seconds into the flight the Flight Crew issued the Autoland uplink command. Issuance of Autoland ended the flap demonstration prematurely (flaps were commanded shut at that point) and resulted in another first time event for the flight control software.

Autoland was developed with the following primary guidelines in mind: (1) minimize differences from the nominal landing performance, (2) minimize perturbations imparted on the vehicle to land ("be gentle"), (3) assume the vehicle is in a controlled state (this limited the details of fault detection and isolation logic). With these guidelines in mind the Autoland flight performance was a complete success. At the time the command was issued the vehicle happened to be within a few feet (horizontally uprange) of the center of the



landing pad. East velocity was -42 feet per second (fps) and north velocity was -8.5 fps (note that Autoland looks to minimize side velocities to a range  $\pm 15$  fps prior to initiating nominal landing phase processing). The vehicle was at 1170 ft above ground level, traveling at 127 fps, and accelerating at  $5 \text{ ft/sec}^2$ . The landing gears are deployed at the time the Autoland command is issued.

At 34 seconds into flight the vertical velocity passed through 0 fps, with the vehicle at 2580 feet. Vertical descent velocity peaked at -110 fps, steadying to -100 fps at around 45 seconds into the flight. DC-X touched down at 77.6 seconds into Flight #5, on the unprepared desert floor. Landing subphase dynamics were very similar to a normal landing with a constant vertical landing velocity of  $\sim 4$  fps and a tip angle  $< 1.0$  degs.

A couple of significant observations regarding this first Autoland flight test include the following:

- (1) This was the first flight test with a planned early ascent pitch maneuver. This maneuver put the vehicle well away from the launch mount and minimized concern or potential for Autoland bringing the vehicle down on GSE equipment.
  - (2) The Flight Control SW does not currently rely on the GPS or air data sensors (they are not flight critical items). Both were lost when the nose cap and pullaway connector separated from the vehicle.
  - (3) Autoland establishes its own deceleration schedule, based upon estimated weight. The vehicle landed about 5000 lbs heavier than normal.
  - (4) Landing guidance is designed to effectively minimize the landing gear side loads via nulling lateral velocities at the expense of tip angle. The landing gear struts maintained their integrity despite the unprepared landing surface touchdown.
  - (5) A significant flight software change was made prior to Flight #5 which included transition from fixed to dynamic gain scheduling. This upgrade provided additional robustness to handle anomalies similar to the one that occurred.
  - (6) Autoland lateral velocity limits were reduced which resulted in a shorter Flight #5 time by at least 8 seconds. Its imperative to reduce flight time during anomalous conditions such as those incurred on this flight.
  - (7) Powered vertical landers have a distinct advantage in dealing with ascent aborts. They don't require aerodynamics/aero loads to stay up, and can burn off propellant if necessary in hover mode.
- Post-landing processing occurred without incident, the vehicle was returned to the launch mount the same day, and has subsequently been transported back to the assembly area at McDonnell Douglas Aerospace - West in Huntington Beach, California for detailed inspection and repair.

DC-X provides a breakthrough in flight testing. Because it has throttled propulsive control, it can have full vehicle control even at zero speeds. This capability translates to no lower bound on controllable vehicle velocities and rotation rates, which means there is lots of flexibility in setting flight test conditions to match desired conditions to scale for larger vehicles.

# FADS, a Demonstrator for MilComSat AOCS

by Martin HUDDLESTON, DRA, Farnborough, Hants, GU146TD, UK &

Paul COPE, MMS, Portsmouth, Hants, PO35PH, UK

© British Crown Copyright, 1994/DRA<sup>1</sup>

## 1. Introduction

This project covers the attitude & orbit control systems (AOCS) research programme being carried out as part of the MOD applied research programme for AD CIS(OR)1.

### 1.1 Project summary

The project programme is to evaluate the candidate sensor technologies and control algorithms, such as Kalman filters, which may be applied to future UK military ComSats. The specific needs of military satellites for robust and threat-resistant control are not offered by current civil technologies which normally use vulnerable earth sensors or RF pointing which is vulnerable to deception. The programme is also to investigate ways of reducing control system complexity and improvements in attitude control precision by enabling structural modes to be controlled.

The project examines the most promising attitude control system technologies required to support such future communications payloads. User requirements indicate a need for improved threat resistance and for narrower spot beams, and the programme supports this perceived need by the use of improved sensors and control algorithms. Improved pointing on civil ComSats is normally by means of ground RF measurements to form a closed loop control system with the spacecraft. For threat reasons this method is unsuitable for military ComSats, and on-board sensors are therefore used. The use of Silicon array star or earth sensors are the most promising, and the sensor programme is to concentrate on these. Limited development and available civil sensors will be considered.

Experimental work is based on demonstrating and evaluating real hardware-in-the-loop on an existing air bearing experimental rig. This offers the closest simulation of real flight performance that can be obtained.

The programme will develop the Filtered Attitude Determination System (FADS) rig to be fully

representative of a MilSatCom satellite, threat-resistant AOCS solution, employing Silicon array star and earth sensors. Both the BAe Mosaic Earth Sensor (MES, developed by BAe and ESA funds) and Marconi Versatile Star Sensor (VSS, developed by MMS and MOD funds) technologies show considerable potential as attitude sensors. The VSS and MES capabilities will be evaluated on the FADS rig.

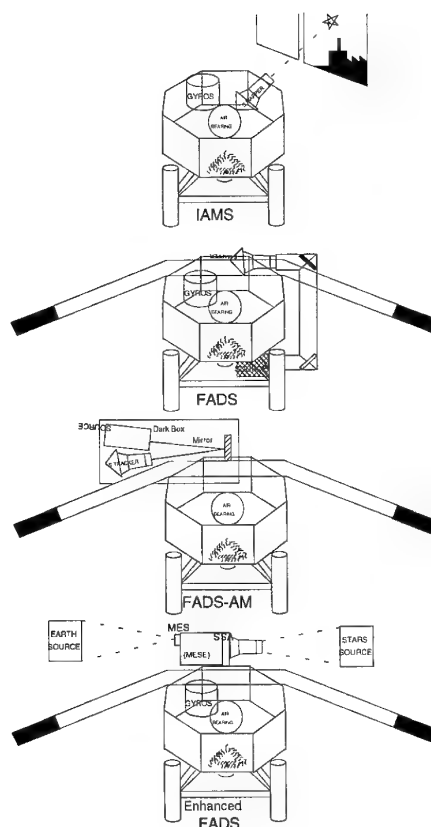


Fig.1: FADS History in Sketches

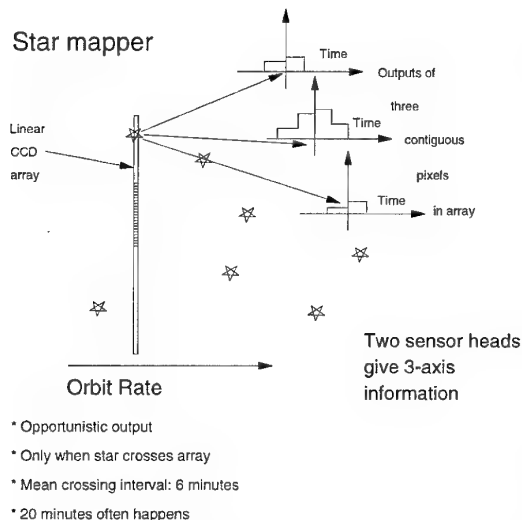
### 1.2 History of FADS demonstrations

The first figure shows, in sketch form, the evolution of the FADS hardware from its earliest days.

<sup>1</sup> Reproduced with the permission of the Controller of Her Britannic Majesty's Stationery Office

The equipment now known as the FADS demonstrator began life in 1977 as the IAMS test rig at RAE. It was planned to control a three-axis air bearing to be space stable by the use of inertial sensors (hence Inertial Attitude Measurement System) and then to mount a star mapper on this laboratory platform looking through an optical window to track the night sky. Before the project had been completed a policy change dictated that industry should be involved and a joint team of British Aerospace (Filton), Ferranti (Edinburgh) and Marconi (Portsmouth) embarked on the programme, now retitled FADS due to the use of Kalman filter elements in the attitude state estimator.

RAE Space Dept. (now DRA(F)) wrote the design specification for a demonstrator based on these principles which had the objective of providing guidance to a low orbit earth observation platform with an accuracy well in excess of the capabilities of current earth sensors, then around 40 arcseconds rms. Initial studies showed that the HIG/starmapper combination was potentially capable of 2 arcseconds rms accuracy (some 5m resolution from 500Km altitude).



Demonstrating such accuracies in the laboratory requires some care and it was quickly established that the small, light payload on the air bearing would be inordinately susceptible to laboratory air currents at this level of accuracy. The moment of inertia in the two most important axes, pitch and roll, was therefore increased to the order of 200Kg<sup>m</sup><sup>2</sup> by the addition of a mass-loaded boom some 5m long fitted with draught-shielding cuffs. This served to reduce the "plant noise" component due to the laboratory air currents to a level compatible with the theoretical accuracy.

The gyro pack used was supplied by Ferranti and contained four type 125 gyros, a derivative of an original Kearfott design built under licence. The gyro electronics were built by Ferranti and provided a digital angle output with an 1sb level of 0.09 arcseconds (450nrad).

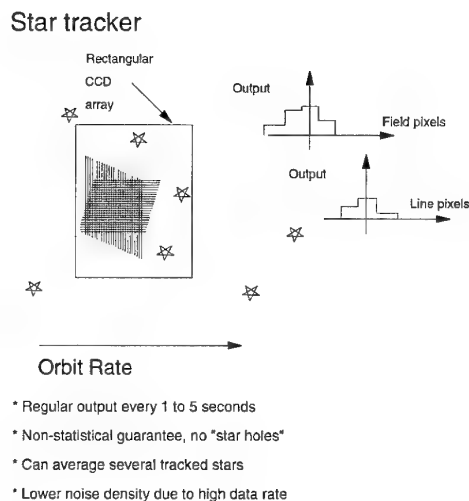


Fig.2: Comparison between Star Mapping & Star Tracking

The starmapper used was developed by Marconi to breadboard level and then under contract from the RAE to engineered standard and used a 2048-element linear CCD array. Two coordinates were extracted from each star passed by the field of view (FoV), one derived from the actual crossing time and the other derived from the distribution of the light among the adjacent pixels where the array was illuminated. The sensitivity was such that a usable star was crossed every 6 minutes on average in low earth orbit (LEO).

The interconnection of these equipments and with the estimation and control electronics was the first application of the ESTeC MACS bus designed for the

interconnection of spacecraft Modular Attitude Control Systems (MACS).

This demonstrator was ready for use at Portsmouth during the spring of 1984 and showed the full expected accuracy of 2 arcseconds rms to numerous visiting parties from MoD, DTI and ESA. Marconi then undertook a short study showing, by the use of a vacuum chamber test rig, that the combination of star mapper correction with cold gas thruster drive prediction alone could achieve 5 arcseconds rms without benefit of gyros. However, the loop was insufficiently robust for use during station-keeping.

The availability of 2-dimensional CCD arrays then led to the possibility of their use as star trackers giving 2 orders of magnitude higher data rate than a star mapper. This is illustrated in Fig.2. The no-gyros configuration with a star mapper was explored as a FADS Application Mission and proved to be both accurate and robust.

The further work to develop an engineered model of the 2-D star tracker (versatile star sensor or VSS) was then undertaken. The VSS/AOC processor used a MIL-1750 processor and the ADA Language. The demonstrator was re-installed at DRA(F) to facilitate further demonstrations.

At this stage a feasibility study into future extensions of the use of the FADS rig was carried out. One objective of this study was to characterise the residual level of plant noise and to draw conclusions regarding the sphere of applicability of the FADS rig in its present form as a demonstrator. It was found that, for example, the rig would be usable at all current and foreseeable levels of communication satellite pointing stability and this has led to its application as an AOCs demonstrator for MilComSats. Fig. 3 is a summary chart from this study and Fig.4 shows the measured disturbance spectrum in comparison with other sources of attitude disturbance and measurement error.

### 1.3 The Enhancement of FADS

The main objective of the current work is to allow comparison and evaluation of the VSS stellar sensing and the Mosaic Earth Sensor (MES) albedo sensing equipments developed by MMS for MilComSat use in comparison with the infra-red earth sensors (IRES) used

exclusively hitherto for ComSat guidance. Fig. 5 shows an outline of the new FADS configuration. The comparison of the sensors involves exploring the limitations on the rapid control action required to avoid depointing outages during station-keeping operations due to the presence of infrequent or noisy data from the sensors.

The presence of significant and ever-increasing levels of flexibility, complicating the spacecraft dynamic response, puts additional burdens on the sensor performance due to the need for increased response bandwidth to extend the mode-damping capability of the control loops.

The opportunity offered by this design update is also being used to improve the versatility of the facility by the introduction of ISI's proprietary "System Build" graphics interface suite and its adjuncts, X-math and Interactive Animation (IA). The relations between the components of this comprehensive software tool are shown in Fig.6. The control processor will, in future, be a powerful Texas TMS320 DSP running compiled C-code which has itself been generated automatically from inputs provided by the DRA users in block diagram and transfer function form using the System Build graphics input interface.

ISI's X-math adjunct allows each block diagram or transfer function change to be analysed by frequency response, root locus or transient response methods whilst the IA facility provides real-time control, parameter variation and display capabilities to assist in parameter optimisation and subsequent demonstration.

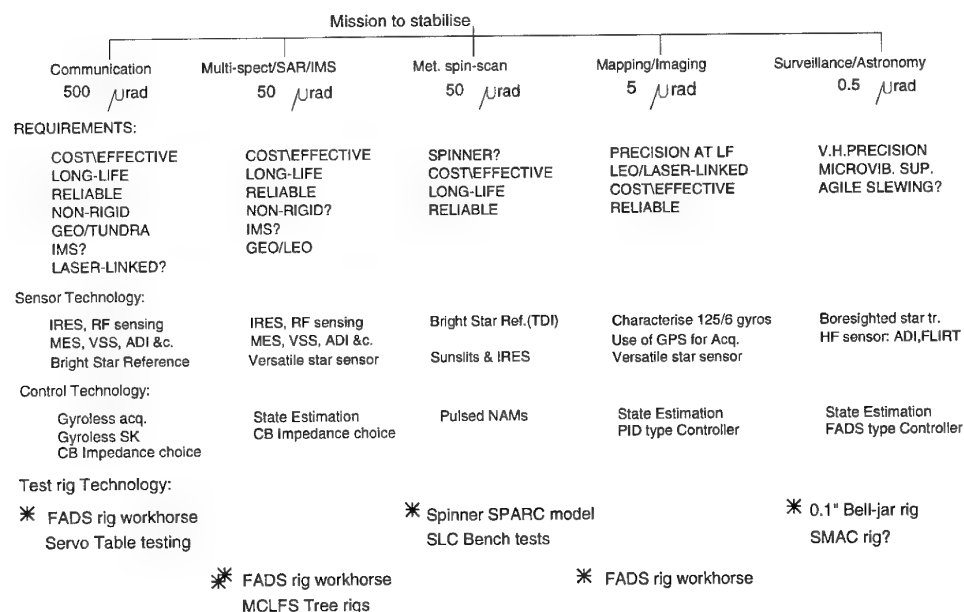


Fig.3: Summary chart showing Suitability of Test Rigs for Missions

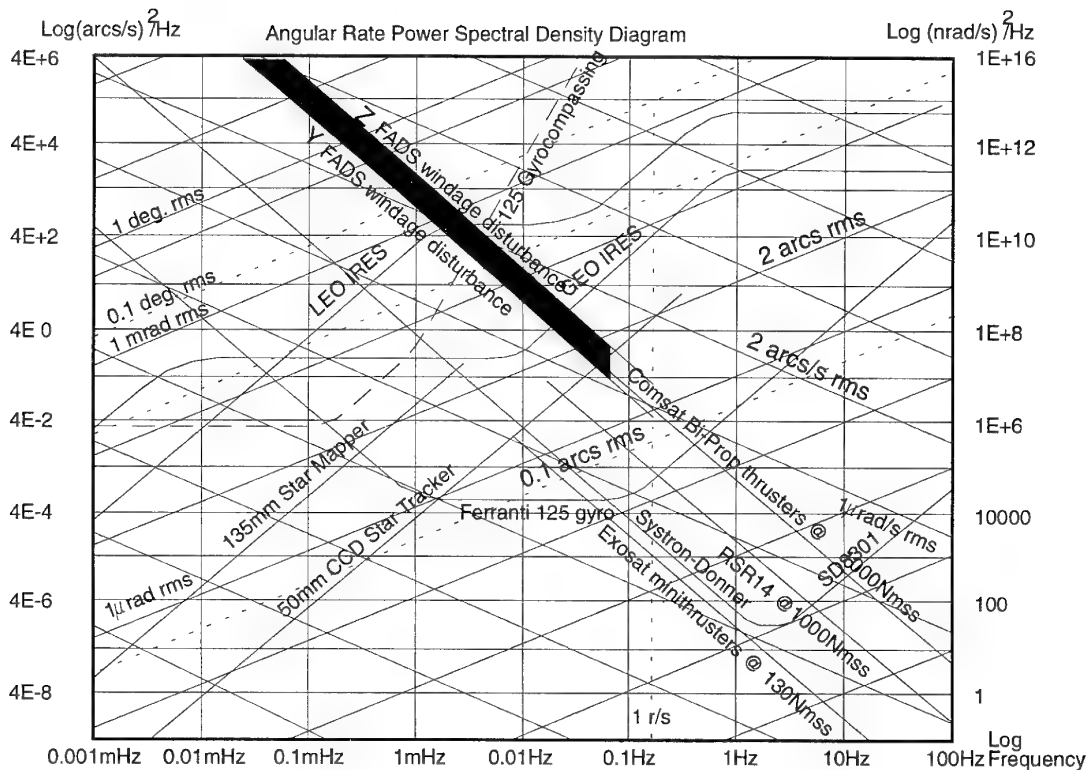


Fig.4: Angular Rate PSD Dg. showing FADS Windage &c.

## 2. The Mosaic Earth Sensor

This sensor, developed under Company, ESTeC and DRA funding at the Stevenage facility, makes use of a large area optical detector array to detect an earth image produced by a small lens using visible scattered sunlight or "albedo" radiation (See Fig.7). The parallel processing array has sufficient power to enable the real-time recognition of the precisely semi-circular earth limb in the presence of the more irregular terminator (shadow edge) or of the sun in the lenses FoV. Additionally, the large area array has sufficient dynamic range so that, with some change in integration time, the sensor may be made to operate even on the scattered light around the earth rim during solar eclipse by the earth. An early flight opportunity is to be sought to verify the operation of this sensor which promises higher accuracy and faster response than traditional IRES sensors in normal circumstances as well as much improved hardness to ground-based laser interference.

## 3. The Versatile Star Sensor

This sensor was brought to breadboard stage under company funding and has been engineered under RAE

funding with a view to its incorporation in the FADS

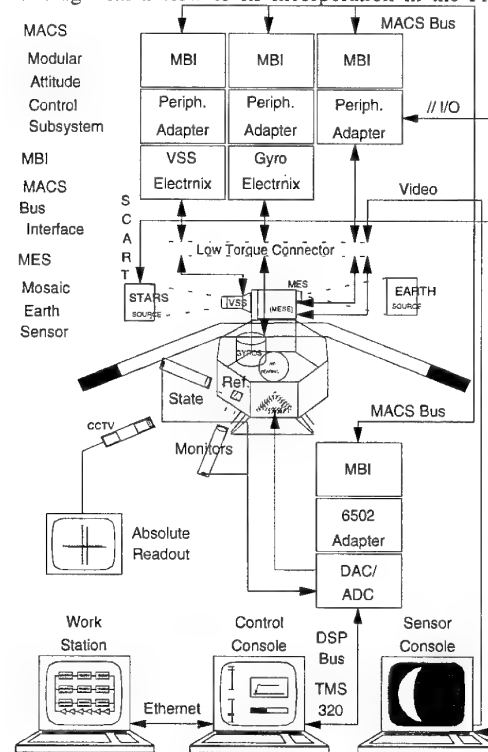


Fig.5: Enhanced FADS Demonstrator

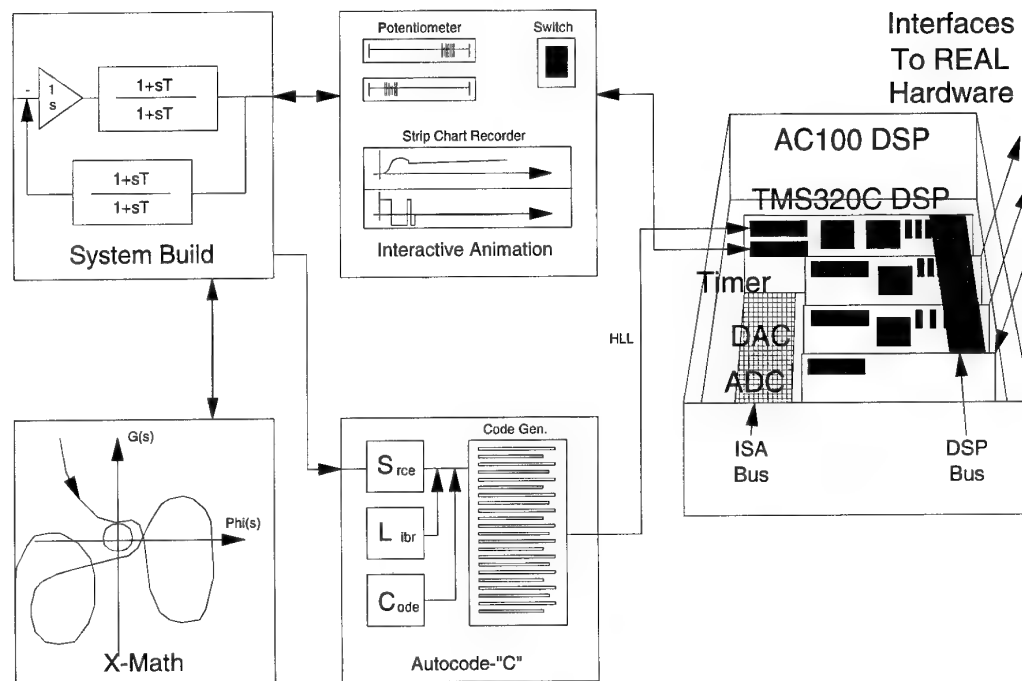


Fig.6: Main Features of ISI's System Build/AC-100 Suite

demonstrator (See Fig.8). During the demonstration of FADS in the MilComSat application mission the breadboard model of the sensor was used with a single star as target, sometimes moving, sometimes stationary.

the need for initialisation altogether by providing autonomous star pattern recognition.

#### 4. Spacecraft flexible dynamics representation

The fundamental flexure frequency of the inertia bar of the facility is in excess of 3Hz and the overtone modes which could cause sensor rotation lie at much higher frequencies and are well damped due to the riveted construction of the main structure. Thus the facility itself can effectively be regarded as a rigid body for all normal control loop bandwidths.

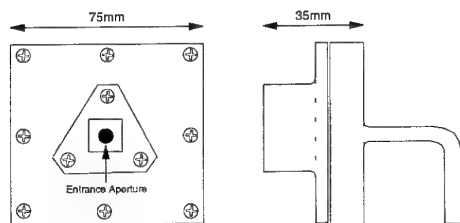


Fig.7: Outline of Head Unit of MES

For the new demonstration the engineered model of the sensor is to be used and the target is now to take the form of a complete and moving star field, down to magnitude 7, displayed on an S-VGA raster using a fine grey-scale to minimise pixel quantisation effects. This sensor is to be mounted with an outward-looking FoV on the spacecraft which would not include any ground-based interference source. Furthermore sun eclipse, if anything, assists the operation of the VSS.

The intelligence for this sensor is based on the use of a MIL-1750 processor, manufactured within the Company, and programmed in the ADA language.

Currently the following of the stored star map requires attitude initialisation but much work has been carried out within the company to demonstrate that alternative software combined with a wider sensor FoV could avoid

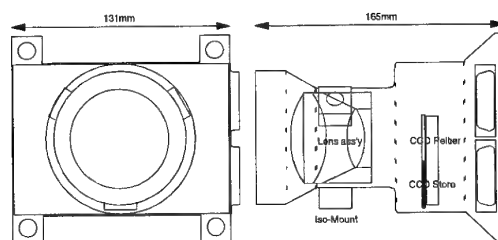


Fig.8: Outline of Head Unit of VSS

The flexibility modelling process to be used equates this rigid body behaviour with the centre body behaviour of the normal ComSat arrangement where the sensors and actuators are effectively co-located. Fig.9 illustrates the method to be used. The thruster torque levels (simulated by moving coil actuators) are adjusted to obtain this equivalence in terms of thruster-induced centrebody acceleration. The flexibility model in the TMS320 then "factors" the additional inertia effect seen at lower and

lower frequencies as each modal inertia becomes coupled in to the centrebody until, below the fundamental modal frequency, the inertia has effectively risen to the total inertia including the static effect of all the flexible appendages.

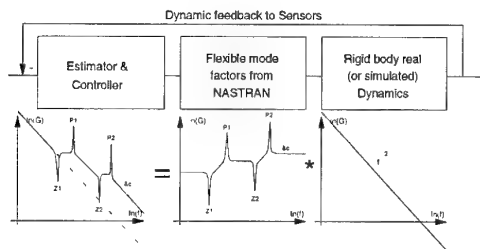


Fig.9: Principle of "Series" type of Flexure Model

In demonstrating the impact of flexibility on station-keeping behaviour it is quite possible, using the IA facility, to "switch off" the flexible behaviour. Switching off, however, involves a conscious choice between removing the flexibility by removing the flexible appendages leaving only the small centre body (pulling the wings off the insect!) or by imagining the appendages to be transformed, magically, into infinitely rigid material. In the latter case the control laws are hardly likely to be robust against the huge loss of high frequency response in the dynamics.

Due to the DSP origin of the flexibility factor it is possible to choose any "Q" value for the modes up to infinity. Olympus in-flight measurements have shown Q values up to 500.

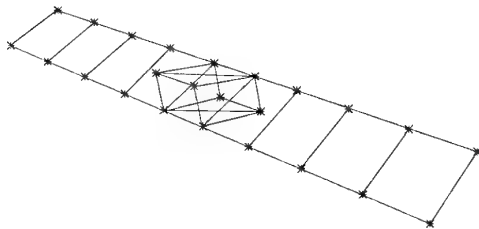


Fig.10: Simple Satellite Model

The modal structure to be used initially has been derived from a NASTRAN analysis of a simple satellite model (See Fig.10) with a restricted number of nodes but including sufficient asymmetry to ensure heavy intercoupling between roll and yaw (oblique solar array angle) and light intercoupling between U-modes and centrebody rotation (asymmetry between panels due to manufacturing tolerances). No non-linearity due to deployment hinge backlash has been included currently although the effects of such imperfections and the remedial measures envisaged could well be explored using FADS at a subsequent stage.

The full simulation diagram System Build representation at one level of hierarchy above the transfer function

blocks is shown in Fig.11. The key blocks in this diagram are the estimation and control blocks, the other blocks all contribute in various ways to providing the dynamic and demonstration environment for the key blocks.

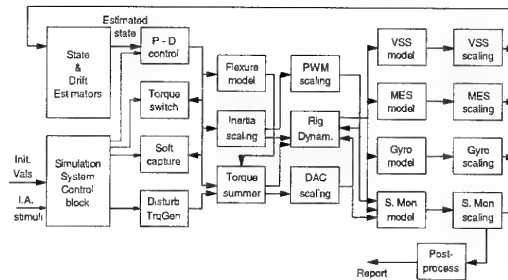


Fig.11: Next to Top Hierarchy of FADS SysBld

## 5. Attitude Estimation & Control

One of the main applications foreseen by DRA for the updated FADS demonstrator is the testing and optimisation of estimation and control algorithms for MilComSat and other applications. However, the contractor has been asked to include typical, if not optimised, algorithms to perform these functions as a baseline for comparison and some care has gone into the selection of suitable approaches.

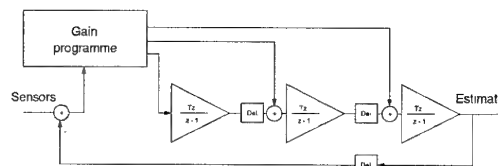


Fig.12: System Build State Estimator

The attitude estimation (See Fig.12) uses a predictor/corrector approach with the prediction based on the centrebody inertia so that the flexibility effects appear as external disturbances. The optical sensor data are then used for correction. A third-order estimator is used in order to generate disturbance acceleration estimates as well as angle and rate estimates. When station-keeping is initiated the correction gains are increased right up to the dead-beat observer condition at the iteration rate in use (~5Hz) so as to obtain fast response at the expense of high actuation noise. After the actual NSSK burn is completed a gain programme is applied to reduce the correction effect progressively by nearly two orders of magnitude so that the sensor noise becomes heavily filtered allowing the thruster actuations to settle to a classical statically-disturbed limit-cycle behaviour ready for a later transition to solar sailing control for normal operation (not simulated). The gain programme is chosen to be slow enough not to "freeze in" transient errors and to allow plenty of time for propellant swirl to decay whilst avoiding the unnecessary prolongation of noisy thruster behaviour.

The controller (See Fig.13) is designed to make use of the positivity principle to ensure robustness in the face of a wide range of flexibility parameters. It operates in a pulse-width modulation fashion to nullify any angular rate observed by the estimator within each iteration cycle. This ensures that the energy in every flexibility mode is dissipated by the continual removal of rotational energy in the coupled centrebody. Positional control is added to this basic rate-nulling behaviour by the addition of a weak position term which becomes fully effective only below the bandwidth of the fundamental flexible mode. Large torque errors are prevented by feeding forward torque corrections based on the estimates generated in the 3rd order estimator. This avoids the need for integral control and the associated "negativity".

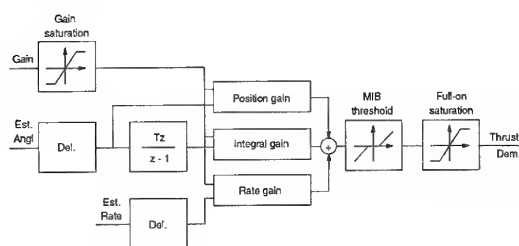


Fig.13: System Build Controller

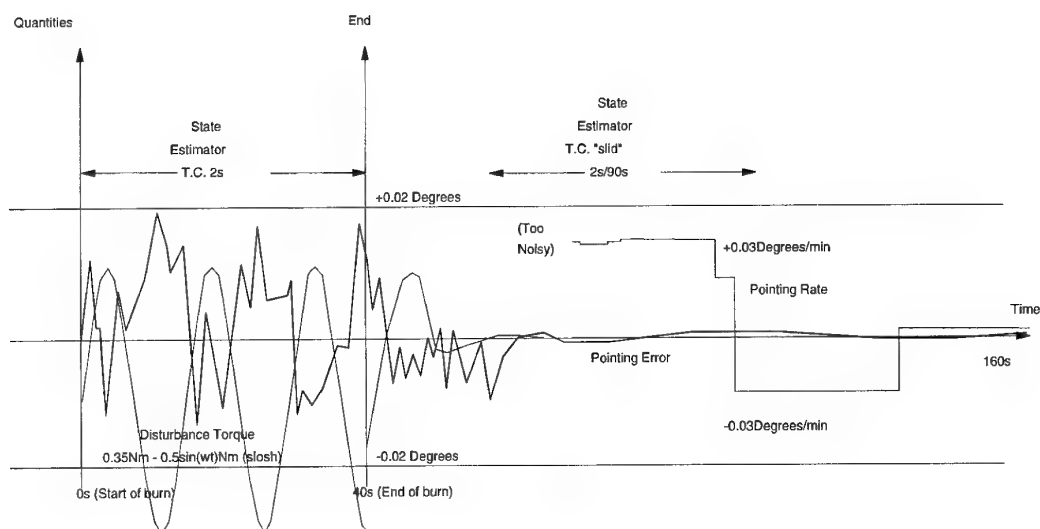


Fig.14: Tracing of NSSK result

## 6. Conclusion, - Expected performance

The work has reached a sufficient state of completion for the anticipated behaviour to have been predicted using the MatrixX facility in the ISI software. Typical station-keeping behaviour results are shown in Fig.14.

Under the particular circumstances of this simulation pointing outages beyond  $0.02^\circ$  are avoided, however, this achievement is highly dependent upon the actual choices for intangibles like sloshing behaviour and swirl after burn as well as CM evolution, plume impingement &c. which all complicate the behaviour. Investigation of the parametric effect of such features on communication outage, if any, will be the subject of DRA investigations using the facility during 1995 and beyond.



## Pegasus Air-Launched Space Booster Flight Test Program

**Antonio L. Elias**  
Senior Vice-President, Special Projects Group  
Orbital Sciences Corporation  
21700 Atlantic Boulevard  
Dulles, VA 22166  
USA

**Martin A. Knutson**  
Director of Flight Operations  
NASA Ames Research Center

### 1. SUMMARY

Pegasus is a satellite-launching space rocket dropped from a B-52 carrier aircraft instead of launching vertically from a ground pad. Its three-year, privately-funded accelerated development was carried out under a demanding design-to-nonrecurring-cost methodology, which imposed unique requirements on its flight test program, such as: the decision not to drop an inert model from the carrier aircraft; the number and type of captive and free-flight tests; the extent of envelope exploration; and the decision to combine test and operational orbital flights. The authors believe that Pegasus may be the first vehicle where constraints in the number and type of flight tests to be carried out actually influenced the design of the vehicle. During the period November 1989 to February of 1990 a total of three captive flight tests were conducted, starting with a flutter clearing flight and culminating in a complete drop rehearsal. Starting on April 5, 1990, two combination test/operational flights were conducted. A unique aspect of the program was the degree of involvement of flight test personnel in the early design of the vehicle and, conversely, of the design team in flight testing and early flight operations. Various lessons learned as a result of this process are discussed throughout this paper.

### 2. INTRODUCTION

Pegasus is a satellite-launching space rocket designed and privately developed by Orbital Sciences Corporation (OSC) with technical support from NASA Ames Research Center's Dryden Flight Research Facility (now NASA Dryden Flight Research Center). It is dropped from a carrier aircraft instead of launching vertically from a ground pad. OSC selected the air-launched technique to reduce the system's recurring and non-recurring costs by reducing the size of the resulting rocket, eliminating the need for a ground launch pad, and limiting the number of people needed to work in the proximity of the vehicle especially during launch operations<sup>1</sup>. Additional advantages would be the simplification of range safety problems, reduction of weather-related delays, ability to launch from different ranges without multiple facilities, and enlargement of the practical launch azimuth limits. This air-launch technique, however, posed some unique problems, such as the choice and modification of a carrier aircraft, man-rating the system prior to launch from the carrier aircraft, safe recovery from aborted launches, testing of the mated and free-flight configurations, and remote (over ocean) flight test operations.

Early trade-off studies compared the benefits of launching Pegasus from a small, high speed, high altitude platform (such as the Lockheed SR-71) versus launching from a larger, subsonic platform (such as the Lockheed C-141). The studies concluded that a large subsonic platform was necessary to achieve the minimum desired payload of 200 kg (440 lb) to low earth orbit. NASA's NB-52B-008 was identified as the only suitable platform available at the time<sup>2</sup>.

While privately funded, the Pegasus program had as an early customer the Defense Advanced Research Projects Agency (DARPA- now ARPA) which agreed to become an anchor customer for, and support the first test flights in exchange for launching a number of experimental, low cost government satellites at approximately \$6M for a dedicated flight. In the summer of 1987, OSC approached the Dryden Flight Research Facility with a request to use the U.S. Government-owned, NASA operated NB-52B-008 mothership aircraft to launch a small three-stage, all-solid orbital booster, subsequently named Pegasus. The B-52, popularly known as "008", had been previously used during the NASA/USAF X-15 supersonic research aircraft program and was then in use to support a USAF F-111 escape pod parachute requalification program. After evaluating the request, Dryden's management agreed to sign an agreement with DARPA that made the B-52 mothership as well as technical support for design, qualification, and flight testing available to the OSC Pegasus program.

### 3. BRIEF DESCRIPTION OF VEHICLE

As shown in Figure 1, Pegasus is a three-stage, solid propellant rocket with a basic 1.27m (50 inch) diameter. A 6.7m (22 ft) span, 45° sweepback delta wing with an 8° truncated double wedge profile provides the lift necessary to control the trajectory during the early portion of the flight. Stage separation is accomplished by linear shaped charges: two during Stage 1/Stage 2 separation, and one for Stage 2/Stage 3 separation. The third stage contains the inertially-based avionics and electrical power system as well as the cold gaseous nitrogen Reaction Control System (RCS) for exoatmospheric attitude control during unpowered flight. Pitch and Yaw is controlled by nozzle Thrust Vector Control (TVC) during Stage 2 and Stage 3 powered flight. Endoatmospheric attitude control during Stage 1 flight is via three all-flying electromechanically actuated tail fins.

<sup>1</sup> While monitored from the ground, the entire flight operations are carried out by three of the four crewmembers on board the mothership: pilot, co-pilot and Launch Panel Operator (LPO).

<sup>2</sup> In 1993, a Lockheed L-1011 was procured and modified to carry and launch Pegasus-class rockets.

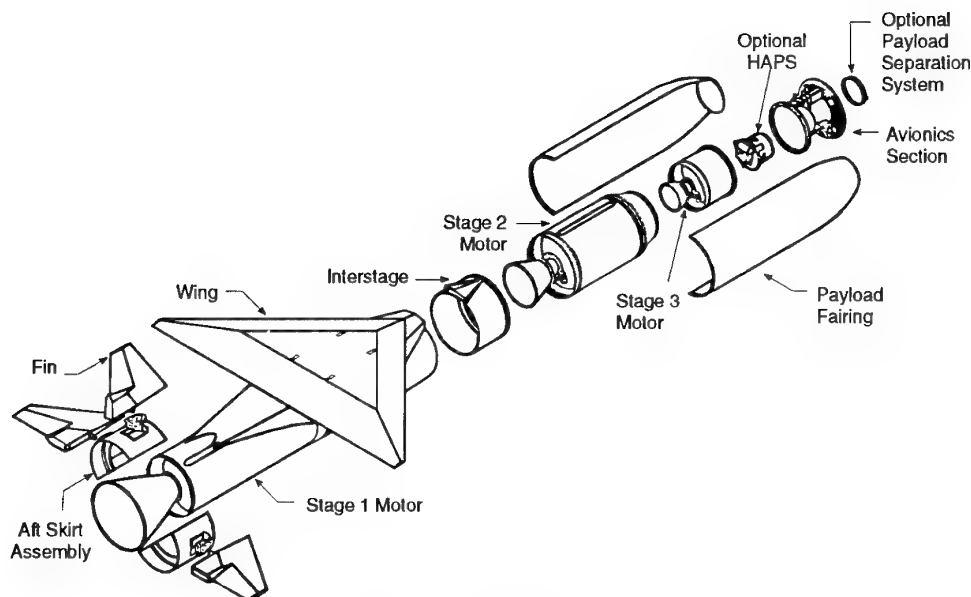


Figure 1. Pegasus Vehicle

#### 4. OBJECTIVES OF FLIGHT TEST PROGRAM

The Pegasus flight test program took into consideration some unusual technical and managerial characteristics of the program. Pegasus used three brand-new solid rocket motor stages; these motors, designed and built by Hercules Aerospace, were based on existing technology, including the propellant, the fiber/epoxy matrix system, internal insulation and throat and nozzle materials and design. While the size, Maximum Expected Operating Pressure (MEOP), temperatures, case, bond and propellant stresses and other design parameters were well within the Hercules Aerospace experience envelope, the 1.27m (Stages 1 and 2) and 0.97m (Stage 3) tooling, throats (including flex-seals) and nozzles were all new designs. Also new was the large integrally-wound metal saddle used to distribute the captive carry and wing aerodynamic loads into the Stage 1 motor case structure<sup>3</sup>. Stage 1/2 separation was accomplished by means of two Linear Shaped Charges (LSC). The first LSC cut the Stage 1 motor skirt at the Stage 2 nozzle exit plane station to insure snag-free stage separation. This was the first application of an LSC to cut graphite material directly. The second cut, performed simultaneously with Stage 2 motor ignition, cut the aluminum Stage 1/Stage 2 field joint ring, allowing separation of the 30 Kg (60 Lb) interstage.

The vehicle and its flight dynamics (shown in Figure 2) are unconventional: a 19 Tm (42,000 lb) high-thrust (2.8 g's) lifting configuration with a wing loading of approximately 14,000 Pa (290 psf), or about twice that of a high-performance jet fighter. More significantly, the flight operations involved presented a combination of aeronautical and space problems: a precise point in space and time had to be reached by the carrier aircraft at the maximum possible airspeed and altitude; range safety constraints limited the acceptable drop point "box", while orbital trajectory

constraints dictated the time and launch azimuth window<sup>4</sup>. Uniquely for a space vehicle, it reaches two environmental extremes (low temperature and vibroacoustics) before its launch<sup>5</sup>; while this offers the opportunity to return to base if these extremes affect either the launcher's equipment or the payload, there was no experiential data base to predict their levels before the flight test program<sup>6</sup>.

A classical aeronautical test range (NASA-Dryden) was responsible for carrier aircraft safety, while a classical space test range (USAF Western Test Range) was responsible for public safety. For these reasons, thorough testing of the captive carry and pre-drop procedures was a significant objective of the flight test program. A final factor was, the use of an older, existing carrier aircraft and structural attachment (wing pylon) with limited design and test data available, particularly in the area of fatigue and crack propagation.

On the other hand, it was deemed acceptable to modify the design to simplify the test program; for example, the basic vehicle telemetry system was sized to provide all of the low-bandwidth data that would be required for development and flight test, above and beyond the capability expected to be required for operational flights. Another design decision related to flight testing was the increased design safety margins on all elements of the system considered "man-rated" from a ground and flight operations point

<sup>3</sup> While the Short Range Attack Missile (SRAM) had a similar-design saddle, there was an almost order of magnitude increase in size, weights and loads between the single-stage SRAM and the three-stage Pegasus.

<sup>4</sup> In brief, Right Ascension of the Ascending Node (RAAN) dictates the drop time, while inclination dictates the launch azimuth.

<sup>5</sup> Lowest equipment temperature is reached just before drop, after prolonged captive carry at altitude; maximum vibroacoustic levels are encountered during the takeoff roll under max aircraft engine thrust.

<sup>6</sup> Ambient temperature in the launcher's equipment bay depended on both inflow leakage of boundary layer air and its ram compression temperature rise as well as leakage outflow of inside air - all hard to model.

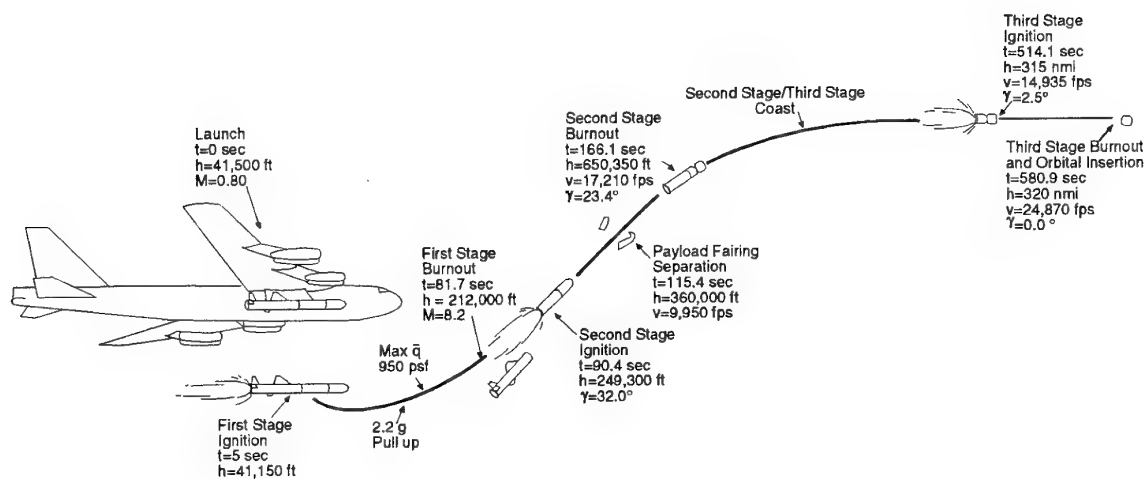


Figure 2. Typical (F1) Pegasus Flight Profile.

of view: pressure vessels, motor cases and captive carry structural items were designed to higher safety margins than are normally the case for expendable launch vehicles, and the ensuing performance penalty deemed economically acceptable.<sup>7</sup>

Programatically, the Pegasus development was characterized by being privately sponsored with government support in the form of unique facilities and equipment (B-52, test ranges). Personal safety, both with regards to project personnel as well as the general public, and protection of project and public property was an overarching requirement of the program, and no compromises or extraordinary risks were accepted.

Classical space Flight Termination Systems (FTS) and processes were used, with the only modifications being those associated with the unique manned aircraft part of the operations.<sup>8</sup>

As part of the U.S. Government support for the project, NASA and the USAF became responsible for safety before and after the drop, respectively; OSC, on the other hand, was solely responsible for mission success and performance. Therefore, OSC was able to make program risk decisions based on economic considerations alone, unencumbered by government regulations, tradition, or political considerations. These included the decision to predict aerodynamic characteristics by analytical and numerical methods only, a single static firing test per motor, limitation of the orbital test flights to two, and the acceptability of payloads on these flights. However, it was deemed that the risks incurred by this trade of flight tests vs. ground test and additional analysis were acceptable in light of the program schedule and cost reduction they provided.

## 5. FLIGHT TEST OVERVIEW

As the Pegasus Flight test was to be accomplished at an aircraft flight research facility, a much simpler and shorter flight test plan was derived than one would have expected to implement at a space flight facility. While OSC's concerns were overall mission performance, risk management, and the associated costs, NASA DFRF's concerns were limited to the rocket motor ground safety issues and having no harm befall the B-52 and its crew. Additional simplification relative to conventional space hardware practices was the use of aircraft based safety, reliability, and quality assurance (SR and QA) doctrine and practices.

In order to minimize the number of captive carry flight tests required, it was decided to build a flight weight, fully functional prototype with inert propellant.<sup>9</sup> By matching the exact mass and structural dynamics of the flight vehicle, and by having the subsystems fully functional, the captive-carry flight tests would be identical to an operational flight up to the instant of drop, but without the risks associated with live propellant. With the planned availability of this inert vehicle, the original flight test plan was evolved and consisted of a flight envelope clearance flight ("Inert 1"), a full mission profile (up to drop point), dress rehearsal ("Inert 2"), and six test/operational orbital flights ("F1 through F6"). Note that a drop of an inert test vehicle prior to the first live shot was not planned. Although this type of test was considered by some as required to verify that the drop maneuver was safe from the standpoint of the (manned) mothership, after much debate it was accepted by all parties involved that due to the nature of the solid propellant used<sup>10</sup>, the only credible risk to the mothership would be physical damage due to recontact. Thus,

<sup>7</sup> For example, the motor cases were designed with a 1.25 (ultimate) safety factor vs. the industry standard of 1.1.

<sup>8</sup> For example, the FTS was armed only after confirmed separation from the carrier aircraft; at the same time, engine ignition was inhibited by the same FTS Safe and Arm devices, making engine ignition impossible until after FTS arming.

<sup>9</sup> Basically the same formulation as the real propellant with the Ammonium Perchlorate (AP) oxidizer replaced by an inert material of similar physical and mass properties.

<sup>10</sup> 69% AP, 19% 20μ grain size Al fuel, Hydroxyl Terminated Polybutadiene (HTPB) binder, with traces of plasticizer, crosslinker, cure catalyst, AP bonding agent and anti-oxidant.

the risk would be the same from dropping a full weight "inert" as from a "live" vehicle.

As the Pegasus design finalized and hardware was being manufactured, the greatest flight test concern became flight envelope clearance for the B-52 with the Pegasus mounted on the right inboard pylon. As a result of the need for a pylon "interface", the center of gravity of a mated Pegasus would be one meter lower than previously experienced with vehicles carried by the B-52. Thus, a potential pendulum effect regarding the mated Pegasus became the focus of flutter analyses and flight test and flight envelope clearance for aeroelastic instabilities.

Although analysis had determined that sufficient margins existed to initially clear the aircraft/rocket combination to speeds up to 460 Km/h (250 knots) and altitudes below 3 Km (10,000 ft), the heightened concern regarding structural dynamic response dictated that a high speed taxi test be added to the test plan prior to first flight. This would act as a final "sanity" check of the combined structural dynamics<sup>11</sup> and also would verify the operation of the wideband instrumentation prior to committing to an actual flight.

Due to the aforementioned and other situations that occurred, the actual flight test program flown consisted of one high speed taxi test, one flight envelope clearance flight, two mission profile flights, and only two orbital flights (the system was declared operational after the second orbital flight). One of the authors (Martin A. Knutson) was the NASA Site Manager at Dryden, and ultimately responsible for flight and ground safety, while the other (Antonio L. Elias) was Launch Panel Operator (LPO) on the B-52, as well as the vehicle's chief designer and ultimately responsible for the vehicle's performance.

## 6. HIGH-SPEED TAXI AND CAPTIVE FLIGHT TESTS

The high-speed taxi and first inert flight (I1) took place on November 1989. Pegasus avionics (including the Inertial Navigation System, INS) were powered and initialized as on an actual orbital flight. Flight-like checklists were used to evaluate timelines and crew workload. Hook loads during the high-speed taxi were well within predictions, clearing the B-52/Pegasus combination for its first takeoff.

Initial altitude/airspeed clearance was to 3 Km (10,000 ft) and 220 KCAS (Mach 0.4). At this altitude, elevator, rudder and aileron pulses were applied by the project pilot. Instrumentation was used to determine the actual amplitude of the control pulse applied. The structural response was observed by 6 accelerometers on the B-52, 6 on the Pegasus vehicle and 9 strain gages on the hook and pylon adapter. Responses were observed on the ground in real time via wide-band strip chart recorders and Fast Fourier Transform (FFT) analyzers. Flight conditions were also monitored from the ground. Thermal instrumentation was used to determine the temperature at altitude of the various Pegasus avionics components.

After the first set of pulses it became apparent that the structural response to aileron (roll) inputs was negligible, and it was decided to eliminate further aileron pulses from the test. At each altitude/speed point, the stimulus/response ratio and response fundamental frequency was compared against predetermined

criteria before the B-52 was cleared to the next flight envelope point. Figure 3 shows the sequence of test points followed.

There were two anomalies observed during this test: first, significant portions of the spray-on Thermal Protection System (TPS) coating debonded from the graphite skin and separated from the vehicle; the areas affected are depicted in Figure 4. It was later determined that the particular sequence of protection materials used was undesirable both from the thermal protection as well as from the mechanical integrity standpoints. Successive vehicles and flights used a new TPS material and process, and the problem was never re-encountered.

The second anomaly involved noise between the Pegasus avionics and the LPO console on board the B-52; while the telemetry data was displayed without problems on the ground, the LPO display suffered from numerous dropouts. This signaled the beginning of a tedious process of protecting the Pegasus/B-52 data link from the high electrical noise environment of the B-52. This problem was not entirely cleared until the first orbital test flight.

The second inert flight (I2) was conducted on December 15, 1989. Whereas the first flight was entirely conducted over the Edwards, CA Air Force Base restricted area, Inert 2 replicated the flight path, timeline and procedures to be used during the first orbital flight (Figure 5).

A particular feature of this test flight is that the separation sense wires used to initiate the Pegasus flight sequence were routed to a switch on the LPO console, allowing the LPO to "fool" the rocket into believing it had separated. This was used to initiate the flight sequence and allow observation by telemetry of the behavior of the rocket's avionics. A test flight sequence was used for this purpose.

Voice, tracking and telemetry data was successfully handed off from a direct link in the Edwards area to the Western Test Range (Vandenberg Air Force Base). About 5 minutes before the simulated drop, the LPO lost its telemetry display, and the rest of the flight was handled from the ground control room at the NASA Dryden Flight Research Center<sup>12</sup>. Another anomaly discovered during this test was an improper software decoding of the baro-altimeter encoder used to aid the B-52's inertial navigation system, resulting in an incorrect navigational state being transmitted to the INS on the rocket. A final test was the actuation of the Pegasus fin's thermal batteries in order to verify the fin actuator performance, battery lifetime and contingency fin re-locking.

It was also noted during this test that the mission timelines resulted in excessive crew workload during the last two minutes before drop. It was then decided to perform a third inert test flight (I3), also a full "dress rehearsal" involving the Western Test Range. The third inert flight took place on January 30, 1990. Again, the fins were powered up, and the test sequenced to rehearse a complete mission. The only significant anomaly was the initialization of both the B-52 and Pegasus IMU's to an *eastern* instead of western longitude, resulting in flawless operation of the system in a "mirror image" of the actual trajectory.

## 7. ORBITAL TEST FLIGHTS

The initial test plan provided for two or more test flights without actual payloads. However, it was deemed appropriate to seek

<sup>11</sup> Analysis had predicted that high-speed taxi and braking where significant vibration and dynamic structural loads drivers.

<sup>12</sup> Loss of LPO display was a planned-for contingency.

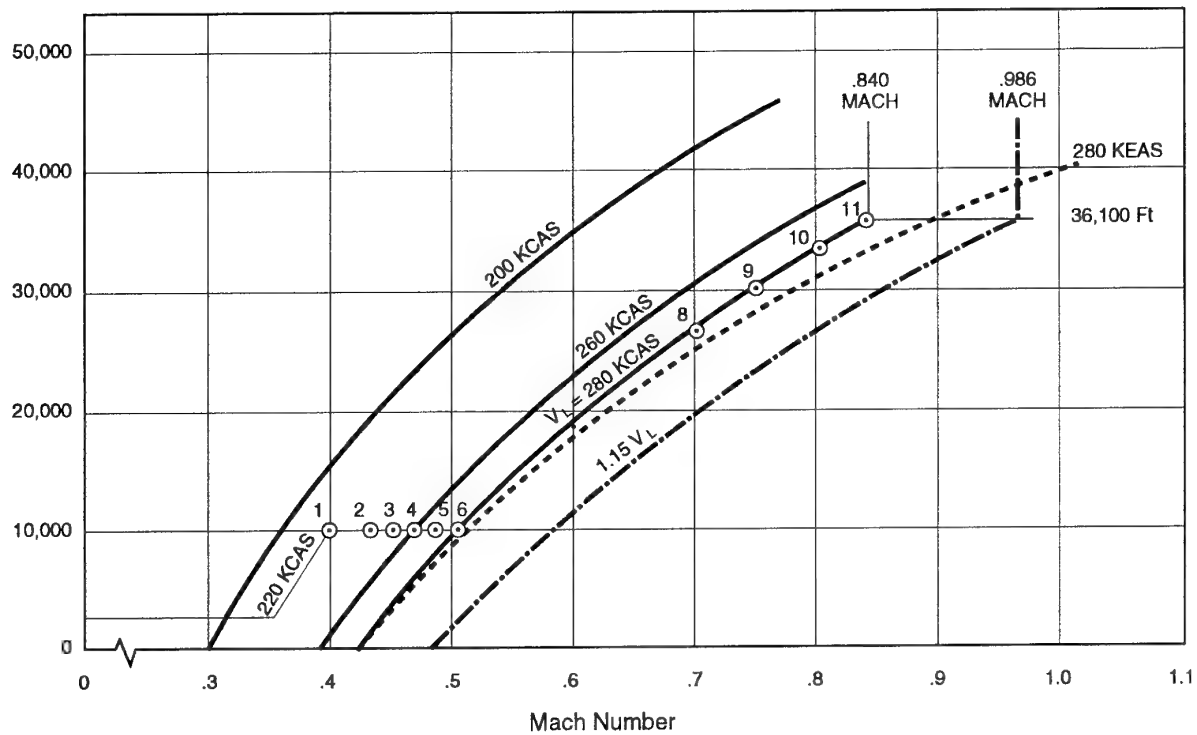


Figure 3. Flutter Clearance Flight Test Envelope Stops.

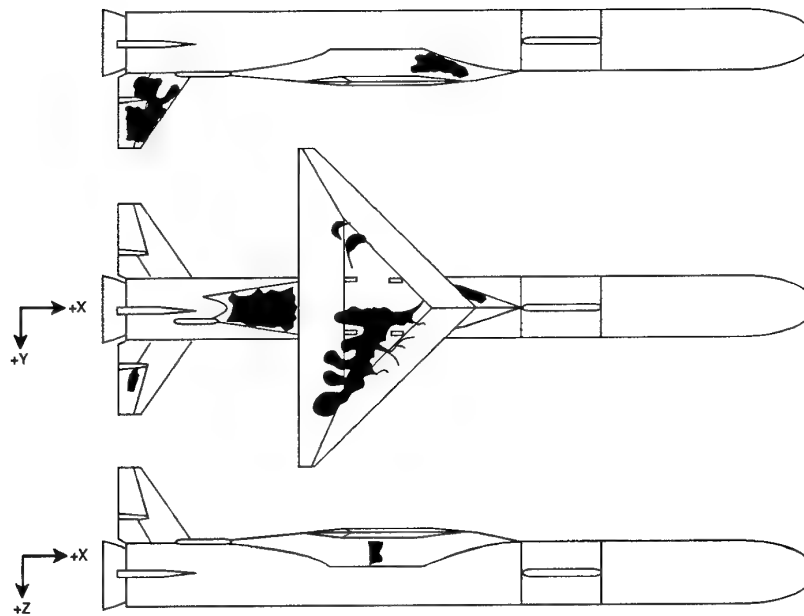


Figure 4. Schematic of TPS Damage After Flutter Clearance Flight.

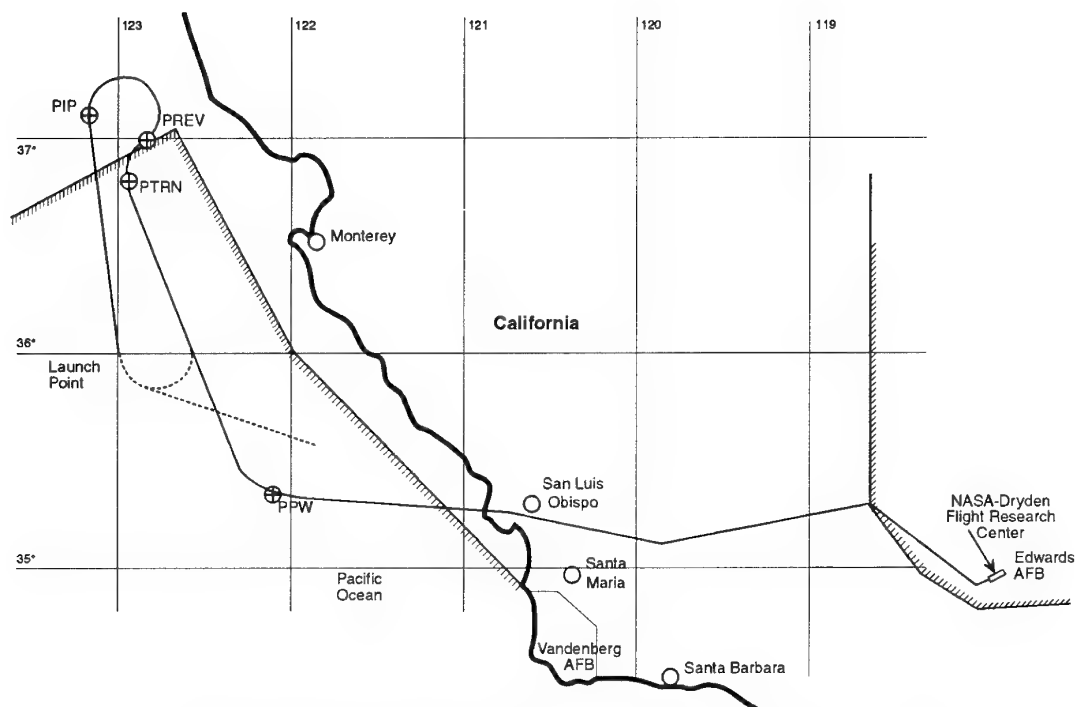


Figure 5. Ground Track for Inert Flight 2 and 3, and Orbital Test Flights 1 and 2.

high-risk orbital payloads that would not normally not have had a chance to be launched and offer them a ride on the test flights. For the first orbital test flight (F1), NASA Goddard Space Flight Center assembled an inosperic chemical release payload that could not have been flown on the main Combined Release and Radiation Experiment Satellite (CRRES) flight in spring of 1990 (because of an incompatibility in the orbital inclination). DARPA also contributed the Small Experimental Communications Satellite (SECS) developed for the U.S. Navy. An unexpected result of this decision was that the very first Pegasus orbital flight had an extremely tight launch time constraint<sup>13</sup>. While the Goddard Payload (dubbed "PEGSAT") had an 18 minute launch window, our desire to be able to recycle the launch once in case of a missed attempt resulted in a three minute primary launch window and a three minute contingency launch window.

Table 1 shows the F1 target orbital parameters vs. the achieved ones. Because of the lack of extensive simulated-altitude ground test firings of the third stage, the orbital error was expected to be dominated by the uncertainty of the third stage's total delivered impulse. However, the main cause for the lower Semi-major axis (320 nm vs. 360 nm) was lower than predicted Stage 1 and Stage 2 total impulse, which was only slightly compensated by a higher than predicted Stage 3 total impulse. Stage 1 reconstructed flight impulse was 0.23% lower, Stage 2 1.28% lower, and Stage 3 0.15% higher than predicted. These variations were well within the expected uncertainty given the single ground static firing and was part of the known program risk budget for the first flight<sup>14</sup>.

The majority of the eccentricity difference, however, was due to a software error in the IMU navigation algorithm which was corrected and verified during successive flights. This error assumed a near-earth (constant-radius) geometry in the kinematics of the integration from velocity to position and was a consequence of the heritage of the IMU's navigation software (naval torpedo), and affected position only, not velocity, as illustrated in Figure 6. Additional anomalies discovered during this flight were two different small autopilot-structural coupling oscillations, one during Stage 1 and one during Stage 2 powered flight.

Perhaps the most significant test result of Flight 1 was the verification of the Stage 1/Stage 2 separation dynamics. After the first of the two separation cuts described earlier, Stage 1 becomes aerodynamically unstable, and there was concern that this instability might induce a tipoff on the upper portion of the stack, or, even

| Parameter   | Desired Value      | Achieved Value     |
|-------------|--------------------|--------------------|
| Apogee      | 740 Km<br>(400 nm) | 685 Km<br>(370 nm) |
| Perigee     | 592 Km<br>(320 nm) | 500 Km<br>(270 nm) |
| Inclination | 94.0°              | 94.15°             |

Table 1. Orbital Test Flight 1 Results.

<sup>13</sup> Indeed, no subsequent Pegasus flight has had a tighter launch time constraint.

<sup>14</sup> Subsequent flight performance predictions incorporated actual motor performance data from the early flights.

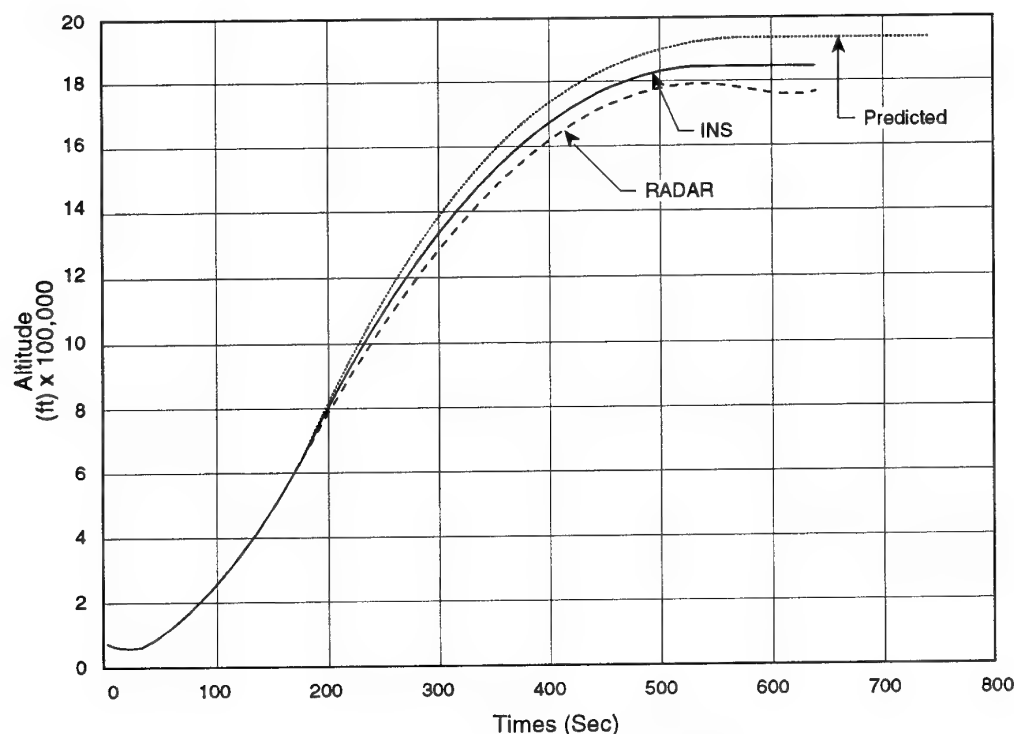


Figure 6. INS Anomaly During Orbital Test Flight 1.

recontact. This concern was the reason for the two-step stage separation scheme adopted. On the other hand, there was a design defect in the fin rocket motors that remained uncovered during flight 1 and was only discovered on subsequent flights, although a-posteriori analysis of the flight 1 data indicated it had occurred during this flight. This design effect caused catastrophic failure of the fin rockets at ignition, rendering them ineffective. Failure to detect this anomaly during Flight 1 was in part caused by the incorrect assumption that the fin rockets were necessary for vehicle stability during the end of the Stage 1 burn, and therefore the stability observed implied that they had worked.

This test flight also verified the payload environment during flight, indicating that both vibration as well as pyro shock levels had been significantly overpredicted. Structural static loads were also slightly overpredicted even when accounting for the actual trajectory flown.

Flight 2 took place on July 17, 1991 at 36° North, 122.99° West and 13.7 Km (45,000 ft) altitude. Pegasus release occurred 29 minutes into a 46 minute window at a Mach number of 0.82 and a true heading of 172.3°. A significant feature of this flight was the use of a hydrazine fourth stage integrated with the avionics bay and referred to as the Precision Injection Kit (PIK)<sup>15</sup>. The purpose of the PIK was to supplement the Stage 3 burn to achieve an elliptical transfer orbit as well as circularize the orbit at the apogee of the transfer orbit. Optimization of this maneuver required the basic booster to fly a very depressed trajectory (i.e. at a higher dynamic pressure) than Flight 1<sup>16</sup>. The payload con-

sisted of seven identical DARPA Microsatellites on an OSC-built carriage structure. Both the IMU software bug as well as the two autopilot oscillations identified during Flight 1 had been corrected and did not reoccur in any subsequent flight. However, three new and major anomalies occurred during this test flight.

First, the initial Stage 1/Stage 2 separation cut did not completely sever all the carbon fibers in the Stage 1 skirt, leaving a "hinge" that, when combined with the force of the separation springs, caused Stage 1 and the upper stack to "jackknife" together, as shown in Figure 7. Reconstruction of the events by dynamic simulation of the observable motion, illustrated in Figure 8, shows that, in this movement, the upper stack longitudinal axis was as far as 120° away from its intended attitude. Three seconds after the command to fire the first separation cut, the second stage ignites simultaneously with the second (aluminum-cutting) separation cut. At this point, the upper stack separates accelerating rapidly away from Stage 1. Using Thrust Vector Control authority, the autopilot commanded a yaw and pitch back to the intended flight attitude, which was acquired after about 13 seconds. The Yaw channel was saturated during the first 1.2 seconds of second stage burn, while the pitch channel was saturated for about 2.5 seconds. We have no knowledge of any launch vehicle having recovered from such an extreme attitude deviation.

A consequence of this extreme attitude deviation was the loss of about 135 m/s (445 ft/s) of velocity increment due to the large component of thrust normal to the trajectory during that period.

<sup>15</sup> Later renamed Hydrazine Auxiliary Propulsion System (HAPS). The nomenclature PIK and HAPS is interchangeable.

<sup>16</sup> Indeed, this has been, to date, the highest dynamic pressure Pegasus flight.

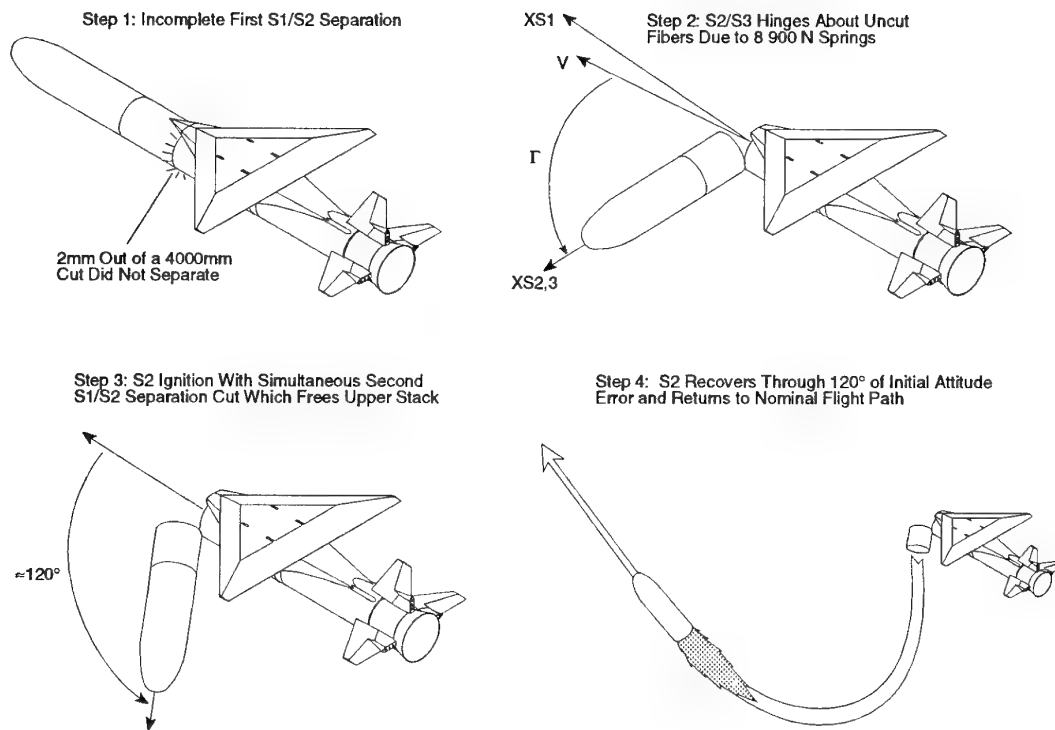


Figure 7. Pictorial Depiction of S1/S2 Separation Anomaly During Orbital Test Flight 2.

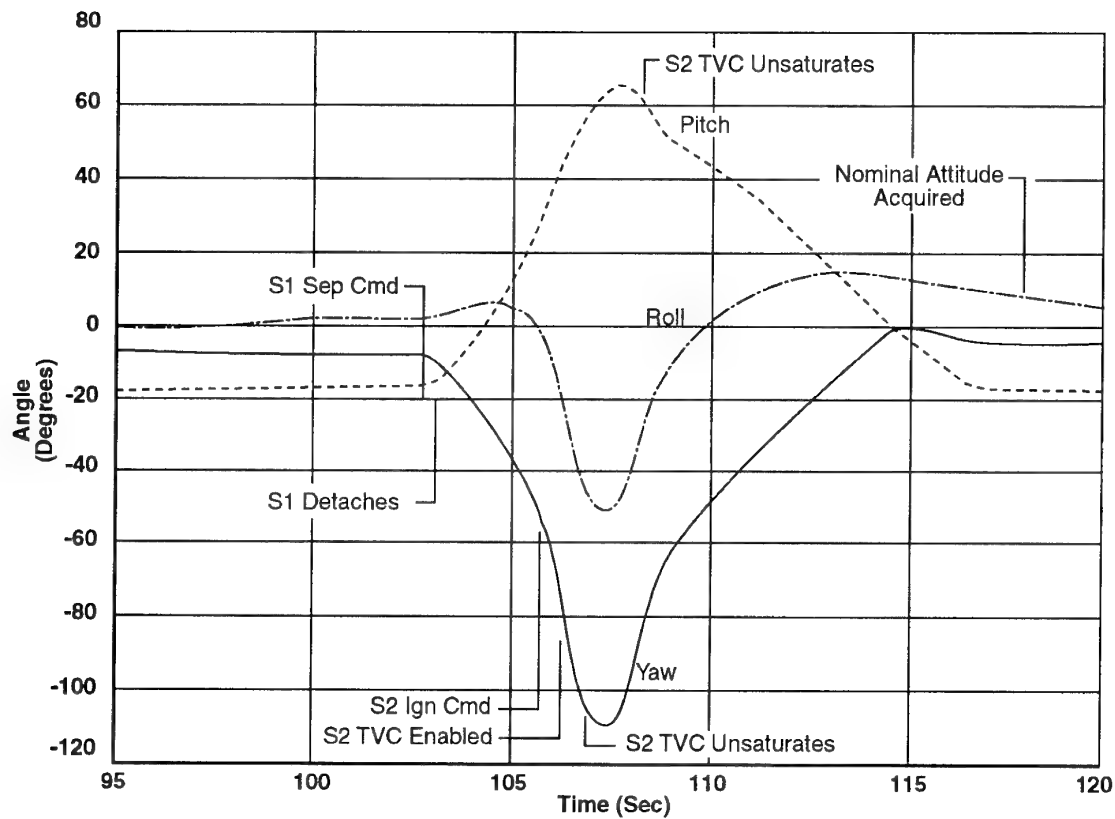


Figure 8. Attitude Traces During S1/S2 Separation Anomaly.



Had the original PIK burn schedule been kept, the resulting orbit would have been highly eccentric, with an endoatmospheric perigee. However, the guidance system was programmed to override the planned target transfer orbit apogee in extreme low energy cases to achieve lower altitudes, but more circular, orbits, resulting in the final orbital state summarized in Table 2.

| Parameter   | Desired Value      | Achieved Value     |
|-------------|--------------------|--------------------|
| Apogee      | 720 Km<br>(389 nm) | 454 Km<br>(245 nm) |
| Perigee     | 720 Km<br>(389 nm) | 356 Km<br>(192 nm) |
| Inclination | 82.0°              | 82.0°              |

Table 2. Orbital Test Flight 2 Results.

The cause of this anomaly was subsequently traced to a combination of improper design and improper installation of the detonation block for the first separation cut which resulted in fratricidal damage to the end of the linear shape charge before the charge itself detonated at that end, resulting in a minute (1 to 2 mm) strand of graphite being left uncut.

The second anomaly observed during F2 was an abnormal opening of the fairing that covers both Stage 3 and the payload during atmospheric flight. In brief, one half of the fairing failed to open completely during initial fairing deployment, resulting in the cold gas RCS jets on that side impinging temporarily on the hung fairing half, causing a unique "Reverse RCS polarity" effect. This effect ended at Stage 2/Stage 3 separation, since the fairing is attached to the Stage 2 front skirt<sup>17</sup>. The cause of this anomaly was subsequently traced to the dislodgment of one of the fairing deployment actuator ball-end joints from its mating hemispherical socket due to a design defect.

The final anomaly was the discovery from acceleration data that the nine small 850 N (190 lbf) thrust level solid motors installed

at the base of the fins to supplement fin aerodynamic control authority at the end of Stage 1 burn did not operate properly. A short, large thrust transient was detected at the time of their ignition, but no additional acceleration was measured during their 19 seconds nominal burn time. It was subsequently discovered that the weather seal caps had been installed with an improperly strong adhesive, causing the aft end of the motors to rupture at ignition due to overpressure, and that this also happened during Flight 1.

While the most spectacular result of Flight 2 was the achievement of orbit under what would have normally been considered fatal attitude conditions as a result of the Stage 1/2 separation anomaly, Flight 2's most important results, in addition to the first flight test of the PIK, were: validation of the performance models adjusted from the Flight 1 data; verification of the resolution of the design deficiencies uncovered during Flight 1 and verification of the vehicle's ability to fly at the high-dynamic-pressure boundary of its flight envelope.

## 8. CONCLUSIONS AND RECOMMENDATIONS

The Pegasus flight test program was considerably condensed and abbreviated for schedule and cost reasons; nevertheless, it provided essential data to identify and correct design deficiencies at a fraction of the cost and time of additional ground test and analysis. Part of this effectiveness was due to the program's willingness to accept reasonable risks during the first few flights.

Some of this positive evaluation is due to the fact that both test flights, as well as the next four Pegasus flights did achieve useful orbits. By comparison, the first Pegasus XL flight, on June 29, 1994, ended in failure due to improper autopilot gains caused by imperfect knowledge of attitude aerodynamics.

It must be emphasized, however, that the level of risk of these two programs was approximately the same, i.e. the original ("short") Pegasus could equally have experienced a flight failure during its test program. While all reasonable precautions for personnel safety and test success must be taken, it is important to resist the temptation to strive for a "zero-risk" flight test program for political or other reasons; indeed, if all risk is removed from the program before test flying, the principal purpose for flight testing ceases to exist.

<sup>17</sup> The angle of opening of the fairing was sufficient to allow Stage 3 and the payload to separate without contacting the stuck fairing half.

# S2000+ ou la conception préliminaire des systèmes spatiaux

J. F. GORY

Centre National d'Etudes Spatiales  
18, avenue Edouard Belin  
31055 Toulouse Cedex France

## 1. SUMMARY/RESUME

As in all other industries, the space industry is evolving in three primary areas : technology, costs and socio-organisational approaches.

A project conducted in CNES aims to revise the definition of future space systems with the introduction of global methods and computer-aided tools. One of the main goals is the definition and the development of a Workbench for missions and space systems design. It will be composed of a certain number of design and simulation tools dealing with unique and coherent information shared between different viewpoints.

Operated in CNES, this computer-based Workbench will focus on the early stages of projects but will also treat first order or "simplified" models which are managed daily during the projects' life span, in accordance with the detailed models from industry.

## 2. INTRODUCTION

Avec le développement continu des technologies, les systèmes qui seront conçus dans les dix prochaines années différeront sensiblement de ceux produits aujourd'hui, tant de par leurs caractéristiques de définition que par les méthodes de conception et de développement mises en oeuvre.

Ce fait est confirmé un peu plus chaque jour dans de nombreux domaines. Que l'on prenne des exemples dans l'informatique (calcul parallèle, intelligence artificielle, logique floue, etc.) ou dans l'électronique (capacité mémoire de 4 Mbits par chip aujourd'hui et 1 Gbit en 2000), cette tendance irréversible s'accélère au point que l'on peut même parler de révolution.

La compétitivité va au-delà de la fourniture d'un produit au meilleur rapport qualité/prix et passe maintenant par la mise à disposition du produit le plus évolué, de haute qualité et conçu au plus vite.

Les deux aspects développement technologique et compétition économique sont liés. Une des principales observations dans ce domaine réside dans le temps d'obsolescence qui diminue pour tous les produits. Dans l'industrie spatiale, il a été estimé que, sur une période d'une dizaine d'années, la durée séparant la date de début de conception de la date à laquelle le système n'est plus compétitif est passée de 12 à 6 ans environ (figure 1).

Pour le CNES, cela signifie dans les dix ans à venir :

- améliorer notre capacité de proposition face à nos clients en prenant en compte les dernières technologies et en innovant en terme d'architecture,
- maintenir et renforcer notre compétence dans la gestion du développement de systèmes spatiaux, de complexité croissante, qui nous sont confiés. En particulier, cela recouvre l'aptitude à spécifier au plus juste les tâches confiées aux maîtres d'oeuvre.
- optimiser au mieux les ressources budgétaires et ainsi augmenter la compétitivité du secteur spatial.

Pour faire face à ce défi, de nouvelles méthodes d'optimisation doivent être développées. Ces méthodes doivent être mises en oeuvre non seulement pour prendre en compte les nouvelles technologies mais aussi pour établir des compromis globaux incluant les performances les coûts et la sûreté de fonctionnement, tout au long du cycle de vie des projets.

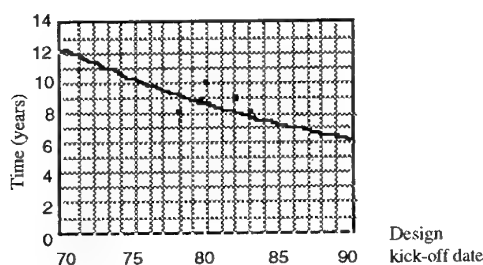


Figure 1. Évolution du temps d'obsolescence des systèmes spatiaux

## 3. CADRE DE LA CONCEPTION PRÉLIMINAIRE

### 3.1 Contenu des phases 0 et A

Le contenu des phases préliminaires est standardisé dans l'industrie aérospatiale européenne par les recommandations édictées par le BNAE (BNAE 1991). Les pratiques à la NASA sont tout à fait similaires avec les phases correspondantes dites pré-A et A (Fragomeni et al. 1993). Par ailleurs, des groupes de travail ont été constitués en interne, avec le support de la DGA pour évaluer l'intérêt des approches développées par le Département de la Défense américain (CAL 90), (DoD 92).

Les entrées d'une phase 0 ou pré-A sont constituées des demandes et des souhaits du client. Pendant cette première phase, les objectifs de la mission sont identifiés, les besoins, spécifications et contraintes sont estimés. Des concepts alternatifs pour la mission et des architectures (lanceur, orbite, plate forme satellite, charge utile, segment sol, communication et opérations) sont identifiés et les ressources nécessaires sont évaluées grossièrement. La spécification de mission est alors générée.

L'objectif technique de la phase A est de prouver la faisabilité du service et de faire des estimations préliminaires des performances attendues. Une ou plusieurs architectures sont proposées, accompagnées d'un planning des ressources affiné et d'un plan de développement de développement des technologies nécessaires. Les spécifications système sont alors définies.

### 3.2 Approche traditionnelle

La décomposition traditionnelle d'un système spatial en sous-systèmes fut introduite par la NASA dès le début des années soixante et correspondait à l'état des technologies de cette époque. Chaque sous-système est fait d'un ensemble

d'équipements matériels et/ou logiciels et concourt à l'optimisation d'un ensemble soit bord soit sol (traitement bord, contrôle d'attitude, structure, chaîne de puissance etc.). Des métiers spécialisés sont apparus dans chacun de ces domaines et des organisations puissantes et performantes se sont mises en place. Mais malheureusement ces métiers ont eu tendance à se démarquer les uns des autres, parfois de façon très radicale. Chaque domaine s'est doté de ses propres méthodes et outils, parfois très sophistiqués, mais les ingénieurs système qui gèrent les interfaces et les compromis globaux travaillent généralement sur de l'information "papier".

Aussi, à l'intérieur d'une organisation matricielle classique, l'interaction entre ingénieurs sous-systèmes appartenant à des structures métiers et ingénieurs projets appartenant à des structures projets est relativement faible. Ceci est particulièrement vrai pour la conception préliminaire lorsqu'on met en oeuvre les outils d'analyse des sous-systèmes. Peu de configurations différentes peuvent être étudiées et il est généralement difficile de prendre en compte des besoins qui évoluent dans le temps.

### 3.3 Besoins généraux et perspectives

L'émergence de nouvelles technologies amène à considérer les systèmes dans leur globalité. Ainsi un système spatial doit être perçu comme un ensemble constitué par un ou plusieurs satellites associés aux segments sol utilisateurs et opérations. La conception du système recouvre la conception simultanée de la mission, du produit et du projet. Les activités de conception d'un système spatial sont clairement identifiées à l'intérieur du cycle de vie. Sa définition évolue selon des versions successives gérées en configuration. Pendant les phases préliminaires, le processus créatif, mené par des experts, est essentiellement mental. Dans les phases aval de la définition, les différents domaines techniques mettent en oeuvre des outils très sophistiqués mais généralement incompatibles. Les activités d'ingénierie système recouvrent les aspects configuration, documentation, gestion des coûts et délais, sous la responsabilité du chef de projet, alors que les tâches de définition technique sont conduites par les spécialistes sous-systèmes. L'analyse fonctionnelle est souvent utilisée pour la conception du logiciel (méthodes IDEF0), la conception détaillée de matériels mais rarement pour les activités de conception globale.

Les besoins suivants ont été recueillis auprès des concepteurs système du CNES :

- un système d'information global devrait intégrer des informations techniques du produit et du projet,
- des capacités de simulations devraient fournir des représentations virtuelles du système et de son comportement,
- des canevas de conception devraient décrire des processus type de tâches de conception, mais aussi des aspects gestion et soutien logistique.

Un système d'information global pour la conception en phase préliminaire doit être différencié d'un outil de gestion de documents et de modèles : le but d'un tel système n'est pas de stocker et de gérer des sortes de "photographies" du système spatial à des moments précis de la définition (points clé, revues, versions) mais de fournir à n'importe quel moment toute l'information nécessaire à l'équipe de conception. A propos de la cohérence des informations manipulées en conception, il faut d'ailleurs considérer deux phases importantes dans la vie d'un projet. Pendant les phases préliminaires, les concepteurs ont besoin de différentes représentations, chaque représentation étant globalement cohérente. Mais deux représentations

différentes peuvent se trouver partiellement et momentanément incohérentes car se rapportant à des hypothèses ou des états de définitions différents. Par contre, dans les phases aval, la définition et les architectures sont rigoureusement déterminées et toutes les informations sont absolument cohérentes pour l'ensemble des personnes impliquées dans le développement. Enfin, des mécanismes particuliers doivent être prévus pour transmettre l'information depuis les phases préliminaires vers les maîtres d'oeuvres

### 3.4 Projet S2000+

Le projet S2000+ a proposé deux concepts intégrés à l'horizon de l'an 2000 :

- le développement d'un environnement de conception constitué d'outils de conception, de capacités de gestion d'information et de simulation,
- la mise en place d'un observatoire des technologies émergentes.

La figure 2 montre les principales étapes d'une approche fonctionnelle de la démarche de conception. Elle ne couvre que les aspects conception préliminaire et l'on voit que le processus de conception interagit avec deux sources d'information :

- des informations relatives aux projets du passé, les experts travaillant souvent par analogie dans les phases préliminaires,
- des bases de données d'équipements disponibles "sur étagère", c'est-à-dire d'équipements ayant déjà volé ou d'équipements virtuels dimensionnés techniquement et économiquement et qui comportent de nouvelles technologies.

Ces équipements virtuels doivent être conçus par les spécialistes sous-systèmes, qui enrichiront donc les bases de données, alors que les ingénieurs systèmes étudieront les impacts de l'introduction des nouvelles technologies sur les architectures, tant d'un point de vue technique qu'économique.

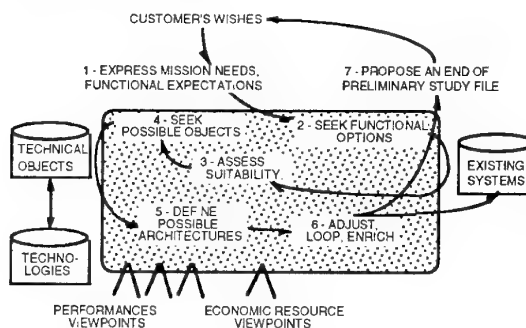


Figure 2. Vers l'Environnement de Conception et l'Observatoire des Technologies proposés par S2000+

Une première étape de S2000+ est destinée à démontrer la faisabilité du projet en dotant progressivement le CNES d'une nouvelle approche pour la conception des systèmes spatiaux en phase préliminaire. Le développement d'un environnement d'aide à la conception est proposé sous le terme " Environnement Coopératif de Conception de Missions et Avant-projets de Systèmes Spatiaux".

Cette proposition résulte des deux faits suivants :

- dans les activités du secteur spatial, le CNES représente généralement le client et a besoin de représentations globale du système,
- les performances du produit et les coûts/délais du projet sont pratiquement déterminés par cette phase.

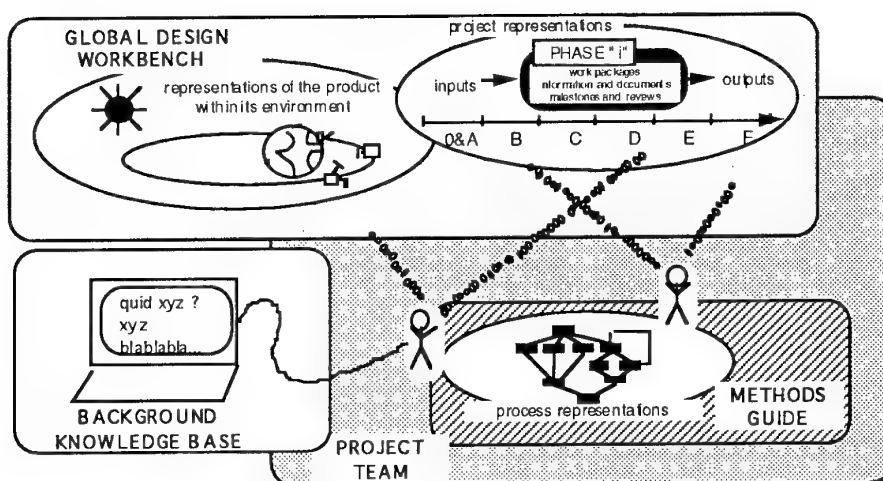


Figure 3. Environnement Coopératif de Conception Préliminaire

#### 4. ENVIRONNEMENT COOPÉRATIF DE CONCEPTION PRÉLIMINAIRE

##### 4.1 Composants de l'Environnement

Un tel environnement pour la conception de mission et d'avant-projets de systèmes spatiaux comporte au moins (figure 3) :

- des ingénieurs système très motivés capables de concevoir par eux-mêmes des systèmes spatiaux à un niveau de détail correspondant à une phase de faisabilité. Ces ingénieurs sont organisés en équipes intégrées.
- un Guide Méthodologique fournissant des démarches type de conception,
- une Mémoire Technique de Conception fournissant notamment toutes sortes d'informations sur les projets du passé,
- un ensemble d'outils dénommé "Atelier d'Aide à la Conception Globale", qui gère les informations caractérisant le système spatial, son environnement et le projet et qui fournit une aide pour les activités de conception et de simulation.

##### 4.2 De nouveaux profils de concepteurs

L'approche traditionnelle par sous-systèmes a produit des résultats remarquables mais certains problèmes demeurent. D'abord, trop de métiers sont impliqués au cours des phases

de faisabilité et la communication entre concepteurs en est rendue difficile. Par ailleurs les technologies ont évoluées et certains compromis ne peuvent plus être considérés comme par le passé. Pour prendre un seul exemple, les progrès réalisés pour le traitement des informations à bord des satellites font que le partage du traitement de l'information entre le bord et le sol évolue rapidement. C'est la raison pour laquelle nous proposons de considérer les équipes intervenant dans les phases de faisabilité non en terme d'ingénieurs sous-systèmes travaillant à distance avec les ingénieurs systèmes mais en terme d'un nombre minimal de "concepteurs globaux" travaillant en groupe (Green 89). Chaque concepteur global a la responsabilité de la conception d'une fonction bord et sol appelée "thème fonctionnel", comme indiqué dans la partie droite de la figure 4.

L'animateur de l'équipe gère les activités de l'équipe de conception conformément aux principes de l'ingénierie concourante (Mc Afee 92). Il fournit les premières allocations pour les fonctions, régle les analyses, gère les configurations et intervient le cas échéant lors des conflits entre thèmes

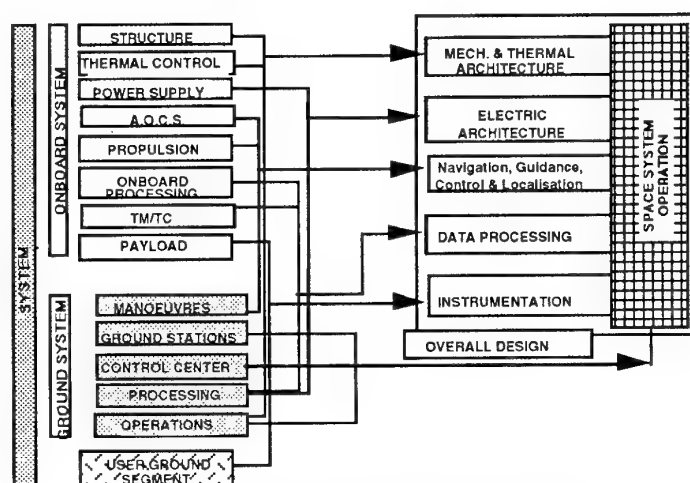


Figure 4. Sous-systèmes et thèmes fonctionnels

#### 4.3 Guide méthodologique

A tout moment du projet, ce guide doit permettre de répondre aux questions : quelles tâches? qui? pour qui? pourquoi? avec quelles informations? etc.

Différentes sources fournissent des éléments de réponses à ces questions :

- standards de gestion de projet,
- pratiques des ingénieurs systèmes,
- analyse des processus techniques.

Une première étude conduite sur les études de faisabilité à la NASA/USA (Wert 92), à l'ESA/Europe et au CNES/France a recensé cinq étapes successives, avec pour chacune des informations et des outils de conception typiques.

#### 4.4 Mémoire Technique de Conception

Toutes sortes d'informations doivent être mises à disposition des équipes projet depuis les publications à grande diffusion (magazines, actes de conférences, ...) jusqu'aux connaissances des experts "maison" à propos de leur connaissances des projets passés. Une telle activité ne peut être organisée uniquement qu'à l'échelle de l'entreprise et notre but est seulement d'identifier les types d'informations pertinentes pour la conception préliminaire, les localiser au CNES et proposer le développement de prototypes.

### 5. ATELIER DE CONCEPTION GLOBALE

#### 5.1 Intégration des outils contre intégration des informations

Une tentative d'intégration des outils fut développée sur une période de plusieurs mois : il est en effet possible d'"interconnecter" des méthodes de conception pour certains thèmes fonctionnels traitant de problèmes voisins. On peut prendre l'exemple de l'architecture mécanique et thermique et de l'architecture électrique : les deux métiers interprètent clairement des données communes et des outils logiciels existent déjà pour optimiser globalement des éléments tels les générateurs solaires. Cela devient vite difficile d'y intégrer les dimensionnements d'orbite ou des analyses économiques : un vocabulaire identique recouvre souvent des représentations différentes d'un même objet.

La généralisation de l'approche de conception par intégration des outils existants fut alors abandonnée au profit d'une intégration par les données et plus généralement par les informations. Tous les concepteurs d'une équipe d'avant-projet devront accéder à l'information commune à travers un interface utilisateur unique. A travers cet interface, les concepteurs auront à leur disposition des outils d'intérêt général : PAO, manipulation graphique d'information, gestion documentaire, interrogation de bases de données et accès réseau. Durant les analyses successives, les échanges d'informations seront stockées sur support informatique.

#### 5.2 Architecture de l'Atelier

L'Atelier est situé dans un environnement constitué du client, du cycle de vie du programme (revues, points clé, standards), les ingénieurs sous-systèmes et leurs moyens, ainsi que les maîtres d'oeuvre qui réaliseront les phases de définition (phase B & C).

Les concepteurs vont optimiser le système avec l'aide de l'Atelier mais ce dernier ne comporte aucune capacité de conception automatique. Toutes les décisions de conception sont donc prises par l'équipe de concepteurs. Sa principale production demeure la documentation de fin de phase A qui est nécessitée pour la décision de démarrage de la phase B.

Toutes les informations à partager dans l'équipe et qui concernent tous les aspects d'une phase préliminaire sont gérées par l'Atelier. Un certain nombre de "représentations" supportent l'organisation des informations concernant la mission, le produit et le projet (figure 5).

Ce sont en fait des modèles supportés par des graphes et contenant toutes les informations algébriques et textuelles relevant d'une phase de faisabilité. Cela inclue donc des spécifications, des descriptions de solutions techniques et des estimations des ressources nécessaires.

Différents types de liens sont appliqués sur ces informations en terme de liens de correspondance et de dépendance. Pour définir ces liens, les concepteurs sont assistés par des techniques d'analyse syntaxique.

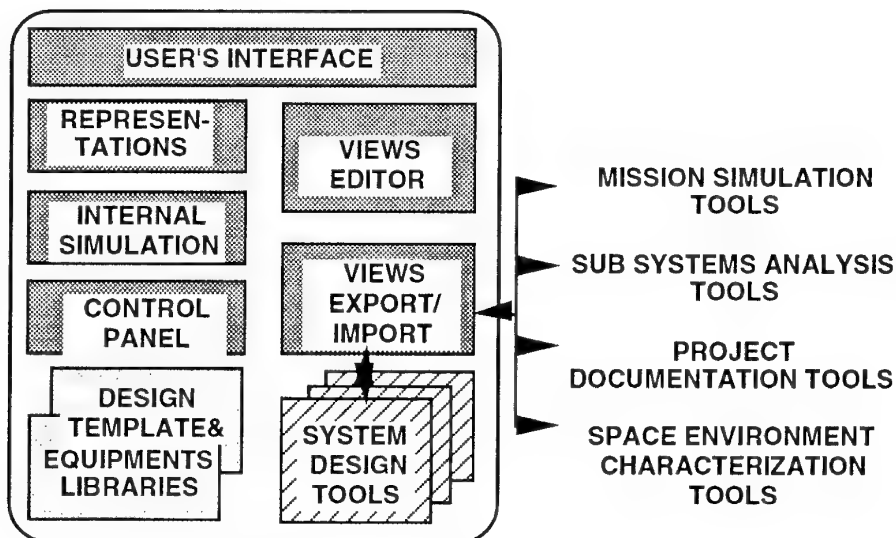


Figure 5. Architecture de l'Atelier

Les informations sont consultables directement par l'utilisateur ou manipulées à l'aide d'un système de vues et points de vue. Elles sont extraites vers les concepteurs pour être analysées ou bien vers des outils pour être traitées.

Plusieurs mécanismes sont directement implantés dans l'Atelier pour manipuler l'information à des fins de calcul et de simulation élémentaire.

Par exemple, il paraît très intéressant de tenir à jour en permanence et pour chaque configuration tous les paramètres caractérisant les principales performances du système. (masse, puissance électrique consommée, coûts,...) et ses caractéristiques techniques (centre de gravité, inertie, flux thermiques incidents, ...).

Des outils spécifiques sont mis en oeuvre par les concepteurs système pour traiter l'information lors des étapes de conception. Ces outils permettent de mener les premières estimations du système et du projet : il s'agit d'outils d'ingénierie système et d'outils originaux d'aide à la conception.

Plusieurs scénarii doivent être étudiés en parallèle et il faut donc gérer plusieurs configurations et ensemble d'hypothèses.

Le processus de conception progresse d'une étape lorsqu'un concepteur extrait des données du système d'information (import), réalise une analyse de type purement "mentale" ou assistée par des outils (outils d'aide à la conception), puis enrichit les informations du système (export). A chaque interaction majeure avec le système d'information ou lors d'une situation conflictuelle, le concepteur rend compte et interagit avec l'animateur de l'équipe et les autres concepteurs. Un tableau de bord fournit à l'équipe un certain nombre d'indicateurs caractérisant l'état d'avancement du projet :

- les différentes configurations en cours d'étude,
- une liste d'hypothèses pour chaque configuration,
- un liste des conflits détectés,
- l'historique du processus de conception.

Une bibliothèque dédiée à la réutilisation de constituants de systèmes spatiaux permet aux concepteurs de se référer à des équipements sol et bord disponibles "sur étagère". Les premiers catalogues disponibles concernent des équipements pour les Petits Satellites pour lesquels une philosophie ligne de produits a été clairement identifiée. Des éléments de mission décrivent des solutions à des problèmes type : choix d'orbites, configuration lanceurs, architectures satellites, disponibilité stations sol, etc. De telles bibliothèques seront établies et maintenues avec le concours des spécialistes sous-systèmes.

L'éditeur de vues sera connecté par un mécanisme d'import/export vers les outils associés à l'Atelier et des outils externes. Des informations seront en effet transférées vers l'environnement des concepteurs d'avant-projet avec :

- les outils sous-système,
- les simulations mission (qualité image pour l'observation de la terre par exemple),
- la description de l'environnement naturel (radiations, gravitation,...) et artificiel (lanceur, réglementation,...) d'un système spatial,
- la documentation gérée par le contrôle projet à partir de la phase B.

### 5.3 Représentations

L'équipe de conception doit pouvoir gérer les informations communes grâce à un ensemble ouvert de représentations à base de graphes. Cinq graphes ont été définis (Keller 92) :

- un graphe fonctionnel,
- un graphe de spécifications,
- un graphe de décomposition physique;
- un graphe "produit" qui fournit toutes les fournitures effectives au projet incluant celles du modèle de vol mais aussi toutes les fournitures intermédiaires (telles qu'un banc de mesure associé au test d'un équipement embarqué),
- un graphe des tâches au sens WBS.

Des objets sont placés à chaque noeud des graphes et des liens verticaux sont utilisés pour l'héritage de propriétés. Comme indiqué précédemment à propos des tâches de conception préliminaire, toutes ces représentations ne doivent pas être absolument cohérentes. Le processus de conception pouvant alors diverger, il doit être canalisé par la définition de liens horizontaux, inter-graphes, appliqués aux divers objets des représentations. Ces liens que nous appelons "prescriptions" sont définies manuellement par le concepteur, avec une assistance du système d'information.

Un premier prototype élémentaire de ce système a été développé en 1992 en utilisant une boîte à outils du commerce s'appuyant sur le langage Le\_Lisp et qui supporte les représentations objets et la théorie des graphes (figure 6). Il avait pour but de prouver la faisabilité d'un certain nombre des concepts précédents concernant la possibilité de gérer des informations avec les graphes, d'effectuer directement des calculs et des simulations simples et de réaliser une maquette des éléments d'interface utilisateur. Par ailleurs, un tel prototype permet d'une part de clarifier nos besoins et d'autre part d'évaluer avec plus de perspicacité les outils qui apparaissent sur le marché.

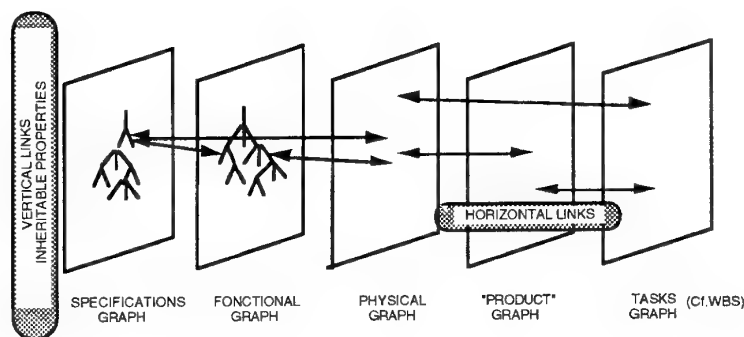


Figure 6. Les cinq graphes de base pour une étude de faisabilité

#### 5.4 Outils d'aide à la conception

Les ingénieurs système ont également besoin de concevoir par eux-mêmes au cours des phases préliminaires.

Ces activités impliquent des activités d'ingénierie spécifiques du spatial et des outils originaux sont nécessaires et doivent donc être développés.

Ils sont fournis et maintenus par des concepteurs spécialistes sous-systèmes dans les domaines suivants :

- calculs d'orbite et contrôle d'attitude et d'orbite,
- architecture électrique,
- opérations,
- traitement des informations bord et sol,
- architecture mécanique et thermique.

Certains outils ont déjà été développés pour les compromis d'architecture électrique et les simulations d'analyse de mission. Par exemple, à partir de la description des puissances électriques nécessaires à bord et du profil d'orbite, l'architecte électrique peut définir des bilans d'énergie du satellite et les caractéristiques des équipements de la chaîne électrique. (générateur solaire, batteries, électronique de puissance, câblage, etc.). Au niveau des architectures, il choisit une ébauche d'architecture parmi des architectures type incluant des équipements réutilisables. Les autres outils sont développés de la même façon dans la perspective de la conception préliminaire menée par des concepteurs systèmes mettant en oeuvre des modèles simplifiés via des interfaces conviviaux.

#### 5.5 Outils d'ingénierie système

De nombreux outils génériques de conception et de simulation sont maintenant disponibles sur le marché et ce serait un non-sens que de ne pas en tenir compte.

Aussi nous avons décidé d'évaluer systématiquement tous les outils potentiellement intéressants.

Nous avons pu ainsi acquérir de l'outillage dans les quatre domaines suivants :

- la simulation globale avec MATRIX-x,
- la réalisation et la gestion du Cahier des Charges Préliminaire avec CDCF-Produit,
- la gestion des spécifications avec DOORS,
- l'analyse fonctionnelle avec RELIASEP ou ASA+.

MATRIX-x est un outil très général pour la simulation. Le système modélisé est décomposé en une hiérarchie de "blocs", chaque bloc élémentaire étant décrit par des entrées, des sorties et une fonction de transfert. Nous simulons actuellement de cette façon pour les mini-satellites les effets combinés du freinage atmosphérique sur la thermique, la puissance électrique et le contrôle d'attitude.

CDCF\_Produit supporte une méthode d'analyse de la valeur pour la gestion du CdCF et DOORS peut récupérer le CdCF ainsi créé pour éclater sur des graphes les besoins clients et les développer en spécifications système.

Les spécifications en phase préliminaire des deux projets DORIS et AGHF ont été ainsi réorganisées.

Le choix final entre RELIASEP et ASA+, tous deux utilisés sur des projets spatiaux, n'est pas encore intervenu à ce jour. RELIASEP, développé par SEP a été mis en oeuvre sur le projet MARS 94 alors qu'ASA+ l'a été sur des segments sol, à dominante informatique et sur HERMES. Ces deux outils d'analyse fonctionnelle permettent divers types d'approches sûreté de fonctionnement. Avec RELIASEP, il est possible de gérer les AMDEC alors qu'avec ASA+ on peut simuler les comportements vis-à-vis d'états normaux et anormaux des composants du système.

Si l'utilisation de tels outils par des concepteurs peut se révéler d'un intérêt certain, leur mise en oeuvre passe par un certain "habillage". Par exemple, il s'est avéré indispensable de penser dans MATRIX-x réutilisation de composants de simulation. De la même façon, il semble opportun de disposer au début d'un projet de canevas pour l'analyse fonctionnelle et l'écriture de spécifications.

Enfin, une autre façon de sensibiliser et d'attirer les ingénieurs système vers l'outillage de conception est de leur offrir la meilleure offre technologique pour l'informatique de bureau en terme de simplicité d'utilisation, de convivialité et d'adéquation au travail en groupe. Avec une solution axée sur un réseau MacIntosh, cela fut très facile à démontrer et ceci sans pratiquement aucun effort d'apprentissage.

#### 5.6 Développement d'un prototype préliminaire de l'Atelier

Certains des outils précédents peuvent être interfacés, connectés ou encapsulés selon les informations qu'ils véhiculent et aussi en fonction des contraintes techniques.

Par exemple, des informations peuvent être extraites des blocs diagrammes MATRIX-x pour fournir des données aux attributs du graphe de décomposition physique de l'Atelier. De la même façon, le graphe de spécification de l'atelier pourrait provenir directement d'un graphe DOORS.

Une nouvelle spécification est actuellement en cours de réalisation pour le développement d'un second prototype de l'Atelier, conformément à la figure 8.

Toutes les manipulations des concepteurs système seront réalisées sous un seul interface utilisateur. A partir d'information provenant des modèles de conception et d'ingénierie, les graphes seront créés de façon itérative et mis à jour pas à pas. Un éditeur de vues gèrera ces informations vers les concepteurs et vers les outils.

Plusieurs bilans typiques du niveau système seront tenus à jour (masse, puissances électriques, coûts, ...) et des capacités de simulation seront introduites (centre de gravité, inertie, flux thermiques, bilan de liaison,...)

Le système sera également doté d'un gestionnaire de configuration capable de gérer des jeux d'hypothèses.

Des bases de données d'équipements réutilisables et des solutions type pour les éléments de mission seront proposés pour les petits satellites.

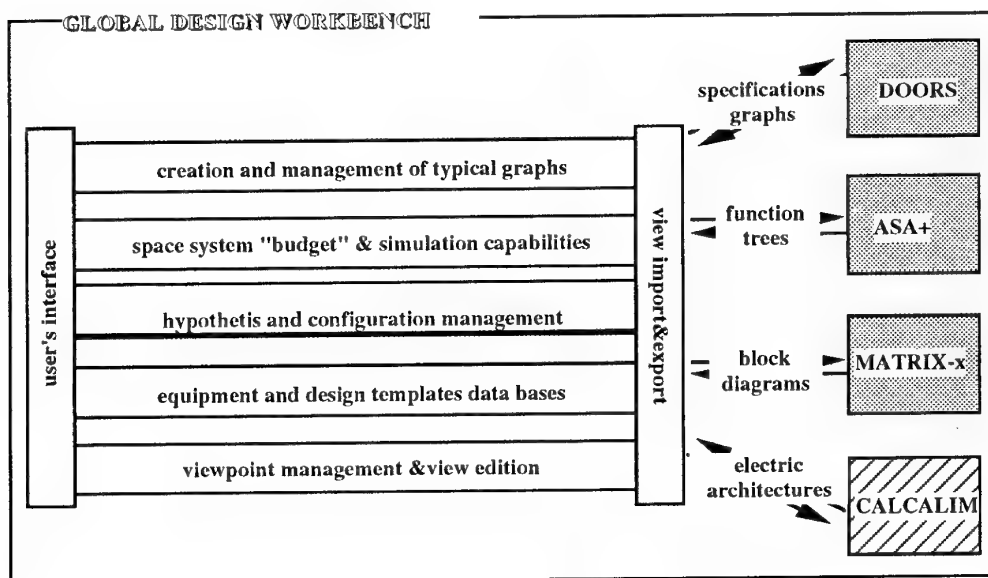


Figure 8. Prototype de l'Atelier

## 6. CONCLUSION

Les personnes impliquées dans les phases préliminaires des projets spatiaux manipulent, d'une part, de nombreuses informations à caractère ingénierie système sur le besoin, le produit, le projet et, d'autre part, des outils de conception et de simulation peu compatibles. Ces outils sont en général mis en oeuvre par des spécialistes sous-systèmes et les modèles résultants sont compartimentés et incapables de communiquer entre eux.

En fait, pendant ces phases préliminaires, de petites équipes originales devraient travailler suivant les principes de l'Ingénierie Simultanée. En mettant en oeuvre les nouvelles technologies informatiques, nous pouvons démontrer la faisabilité d'approches de conception intégrant la gestion d'information de type ingénierie système et des capacités de conception et de simulation.

Les difficultés d'ordre socio-organisationnelles apparaissent parfois plus fortes que les problèmes d'ordre purement techniques et il faut convaincre les concepteurs système des bienfaits de notre approche. La mise à disposition pragmatique d'outils et le développement de prototypes même partiels, apparaissent comme un moyen essentiel pour illustrer des concepts qui présentés oralement ou sur papier soulèvent scepticisme ou pire incrédulité.

## REMERCIEMENTS

Je tiens à remercier tous ceux que nous avons rencontrés pour leurs commentaires et leurs suggestions. En particulier, je tiens à remercier particulièrement toutes les personnes du CNES qui apportent leur contribution à ce projet.

## RÉFÉRENCES

- (BNAE 91) BNAE - *La spécification de management de programme* - RG Aéro 000 40 - June 1991
- (CALS 90) DoD - *CALS Program Implementation Guide - MIL-HDBK-59A* - Sept. 1990
- (DoD 92) DoD - *Systems engineering* - MIL STD 499B - May 1992
- (Fragomeni 93) Fragomeni A.D. & al - *The NASA SEPIT Life Cycle* - NCOSE 1993
- (Green 89) Green T.L. & al - *The Designer of the 90's : a Live Demonstration* - NASA CP 3031 -1989
- (Keller 92) Keller Pierre - *Vues de conception* - Symposium La conception en 2000 et au-delà- Strasbourg - Nov. 1992
- (McAfee 92) McAfee N. - *Concurrent Engineering: Toward Enterprise Integration* - ILCE Initiatives - June 1992
- (Wertz 92) Wertz J.R. and Larson W.J. - *Space Mission Analysis and Design* - Space Technology Library - 2nd edition 1992



## SPACEBORNE SAR SIMULATION USING AIRBORNE DATA

J.-M. Boutry, J. Dupas  
Direction des Etudes de Synthèse  
Office National d'Etudes et de Recherches Aérospatiales  
B.P. 72 92322 Chatillon cedex, France

### ABSTRACT

The synthetic aperture technique, together with a procedure to make up wide band pulses, enables to achieve high resolution bidimensional images of the ground with a side-looking airborne radar system. With some kinds of transpositions, such images, gathered during an airborne campaign, are significant of results in a space-based context.

### 1 INTRODUCTION

The design of spaceborne imaging SAR's<sup>1</sup> requires calibrated data to determine optimum sensor parameters with respect to the system missions : choice of frequency, polarization, ground resolution...

Numerical simulations provide large data bases at low costs and make it easy to vary many parameters. Nevertheless, due to the surface scatter complexity (such as multiple paths, ground penetration...), it is difficult to simulate in a realistic way every object or background inside a given radar scene. Furthermore, source experimental data are needed for numerical simulations, in order to take into account the true radar signature of the objects.

These reasons justify the need to gather images using airborne SAR. The paper is dedicated to the characteristics of such sensors, as compared to spaceborne ones. After a brief review of the main principles of the SAR technique, the various transpositions from an airborne to a spaceborne context will be emphasized and discussed. Eventually, an example performed with the ONERA French experimental radar system will be shown.

<sup>1</sup> SAR: Synthetic Aperture Radar

### 2 SAR PRINCIPLES

SAR processing is a technique which enables to increase the resolution of coherent imaging radars, using the Doppler effect due to the motion of the radar system platform. In the particular case of a side-looking radar, this technique, combined with any method to make a fine slant range discrimination, leads to a bidimensional image fitting an almost orthogonal grid of the ground surface.

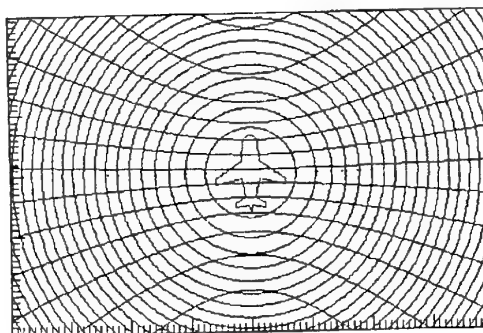


*figure 1: lines of equi-distance  
and equi-doppler*

#### 2.1 Conventional radars versus SAR

In order to produce an image, a conventional radar is not efficient because the resolution is determined by the beam footprint on the ground which can be rather wide, thus giving a poor image, unless a very narrow beam width is used at the expense of an unrealistic large antenna. The solution to this problem is the synthetic aperture technique which enables to increase the resolution of a radar by simulating an antenna wider than the real one.

The size of this synthetic antenna is given by the displacement of the radar system along a determined track. The ultimate resolution that can be obtained is then only limited by the entire time the scatterer is within the footprint and is equal to half the size of the aerial. Actually, the cross-range resolution is no

longer directly related to the real aperture, but to the length of the fictive antenna. Thus, even a relatively small antenna enables a good resolution through this technique.

## 2.2 Overview of the cross-range processing

Inside the radar footprint on the ground, the different scattering centres are separated thanks to their differential Doppler frequencies. This is done by integrating the echoes of the illuminated targets. The discrimination is all the more fine that the integration time is long and, thus, the Doppler filter bank is narrow. According to the integration time used, we'll speak about a focused or unfocused radar signal processing.

When all the echoes from a single scatterer are taken into account as long as it is illuminated by the beam, we'll obtain the ultimate cross-range resolution. This calls for a lot of caution, such as the compensation of the Doppler evolution of every scattering centre, so as not to mix different centres which will then be distinguished through a stable differential Doppler frequency.

When only a poorer resolution is required, an unfocused processing may be reliable. The integration time is reduced so that the Doppler signal has a frequency which does not sweep from one Doppler filter to another during this time. Then, the above-mentioned evolution doesn't need to be compensated.

## 2.3 Motion compensation

As it has been mentioned before, some effects due to the platform displacement need to be compensated if a very high resolution is required: Doppler evolution, range walk and range curvature (due to the fact that the distance between the radar and a scattering centre varies during the illumination time)....

It is true even when the platform has experienced a very stable flight. If it is not the case, other corrections must be taken into account, such as changes in the velocity of the aircraft, accelerations, vibrations..., which can bring about some defocusing effects, increase the peak and integrated sidelobe levels, therefore degrading the contrast and distort the image.

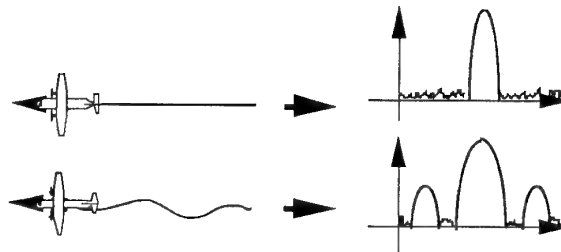


*figure 2: perturbations in the motion of the platform and their effects*

## 2.4 Slant-range processing

The slant-range resolution obtained with the real pulse width of the transmitted waveform must often be increased in order to have an homogeneous image in both dimensions. It is inversely proportional to the transmitted bandwidth.

The solution consists in transmitting a wide "spread" band instead of a very short pulse which would bring about some problems related to average power limitation and, thus, to signal to noise ratio. A technique commonly used is pulse compression with linear frequency modulation. Alternative solutions are phase coding or stepped frequency waveforms.

# 3 TRANSPOSITION

The SAR technique operates quite well and is currently used in many airborne radar systems. The data so obtained may be meaningful for studies of spaceborne imaging radars, provided that several transposition rules are fulfilled. This issue is addressed in the next parts.

## 3.1 Radar frequency and polarization

The experimental sensor must operate in the frequency bands and polarizations which are expected to be used for spaceborne sensors, as these are driving parameters for the resulting radar signature of the objects. In particular, the frequency bands will be chosen among L, S, C and X.

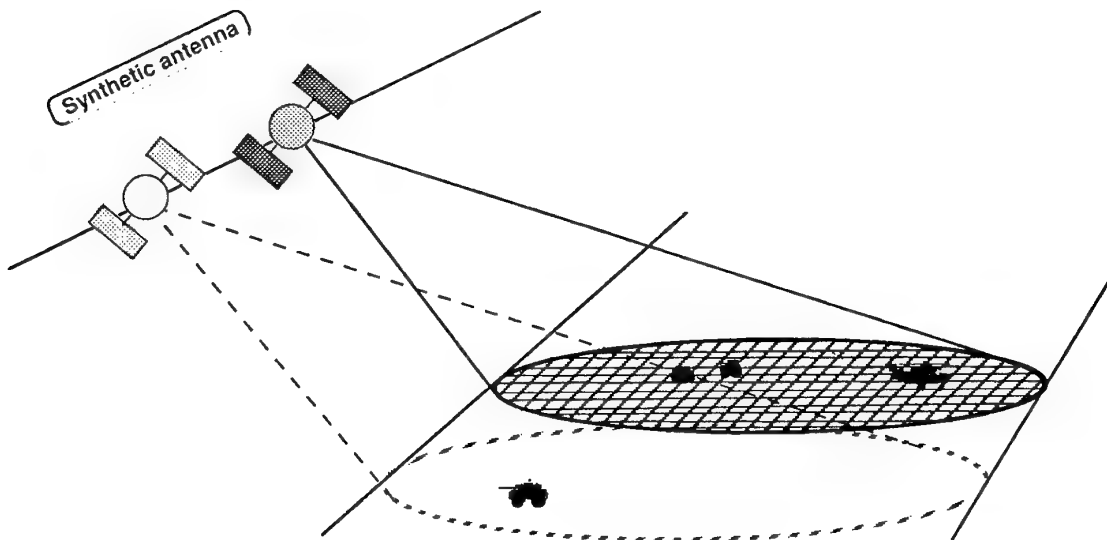


figure 3 : Configuration of a space-based SAR

### 3.2 Ground resolution

The next parameter to be analysed is ground resolution. As it has been highlighted above, the main interest of SAR is to achieve cross-range resolution which is not directly related to the real aperture of the antenna. The cross-range resolution is given by :

$$(1) \quad \text{Res} = \lambda R / 2 V T_i$$

where :

$\text{Res}$  : cross-range resolution  
 $\lambda$  : wavelength  
 $R$  : range  
 $V$  : forward velocity of the platform (satellite or aircraft)  
 $T_i$  : integration time

$(V T_i)$  is the forward displacement of the radar during the integration time, which can be seen as a "synthetic antenna" length (see figure 3).

$T_i$  is limited by the duration of illumination of a given object. Its maximum value is given by :

$$(2) \quad T_{i\_max} = R \tan(\theta) / V$$

where :

$\theta$  : real antenna beam aperture

This leads to a best cross-range resolution given by :

$$(3) \quad \text{Res}_{min} = \lambda / 2 \tan(\theta)$$

The aperture of the antenna is related to its physical length by :

$$(4) \quad \tan(\theta) = \lambda / d$$

where :

$d$  : antenna length

Finally :

$$(5) \quad \text{Res}_{min} = d / 2$$

This fundamental characteristic makes it possible to design spaceborne imaging radars with an acceptable resolution. This can even be improved by using so-called "spotlight" techniques. The same technique may be applied with an airborne system in order to get the same resolution.

Along the other dimension (ground-range), the resolution of spaceborne imaging radars is achieved through pulse compression techniques. The same resolution with an airborne sensor will be achieved by simply using the same transmitted signal bandwidth.

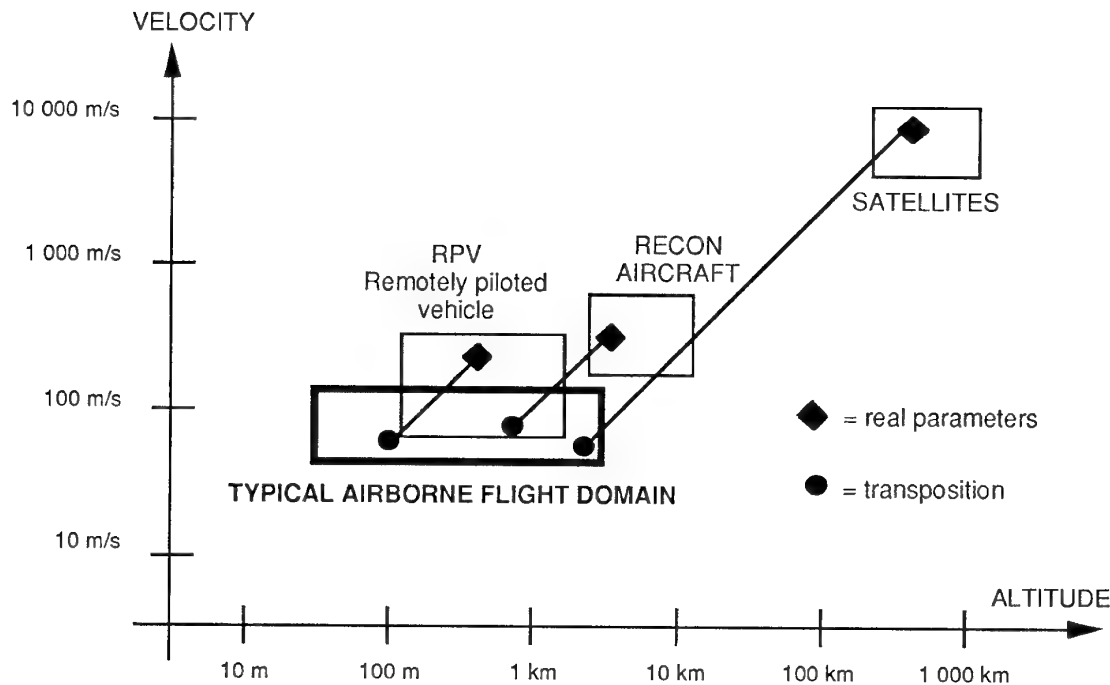


figure 4 : Transposition rules preserving the integration time

### 3.3 Integration time

As mentioned above, the cross-range resolution of a SAR space-based sensor is obtained through integrating the received signal over a matched time length, ranging from a few tenths of a second to a few seconds. In some cases, when observing non stationary objects (for example sea surface), it may be important to maintain the same integration time (or at least the same order of magnitude) in an airborne simulation for a given cross-range resolution. The integration time is :

$$(6) \quad T_i = \lambda R / 2 V \text{ Res}$$

Therefore, to fulfil this condition, the airborne sensor must operate under conditions reproducing the ratio (Range / Velocity) of the satellite's orbit, as illustrated on figure 4.

### 3.4 Sensitivity

In a SAR image, the noise level is measured by an equivalent reflectivity ("Noise Equivalent  $\sigma_0$ "). This parameter depends on the power budget and can be simulated in airborne SAR images by two means :

- tuning of the average transmitted power to compensate for the differences of

antenna gain and range between airborne and spaceborne sensors.

- coherent addition of noise to raw data or to images.

### 3.5 Image size and incidence angle

In case of a spaceborne SAR, power budget considerations lead to limit range and therefore to produce images with low incidence angles (off-nadir). The limitation of flight altitude of an airborne SAR makes it difficult to get large swath images combined with low incidence angles, which may appear as a limitation for airborne simulations. As a matter of fact, this problem can be solved by mosaicking techniques, which consist in processing data coming from multiple passes along parallel routes, in order to build large swath images (figure 5). This type of process relies on high precision navigation data, such as those provided by GPS in differential mode.

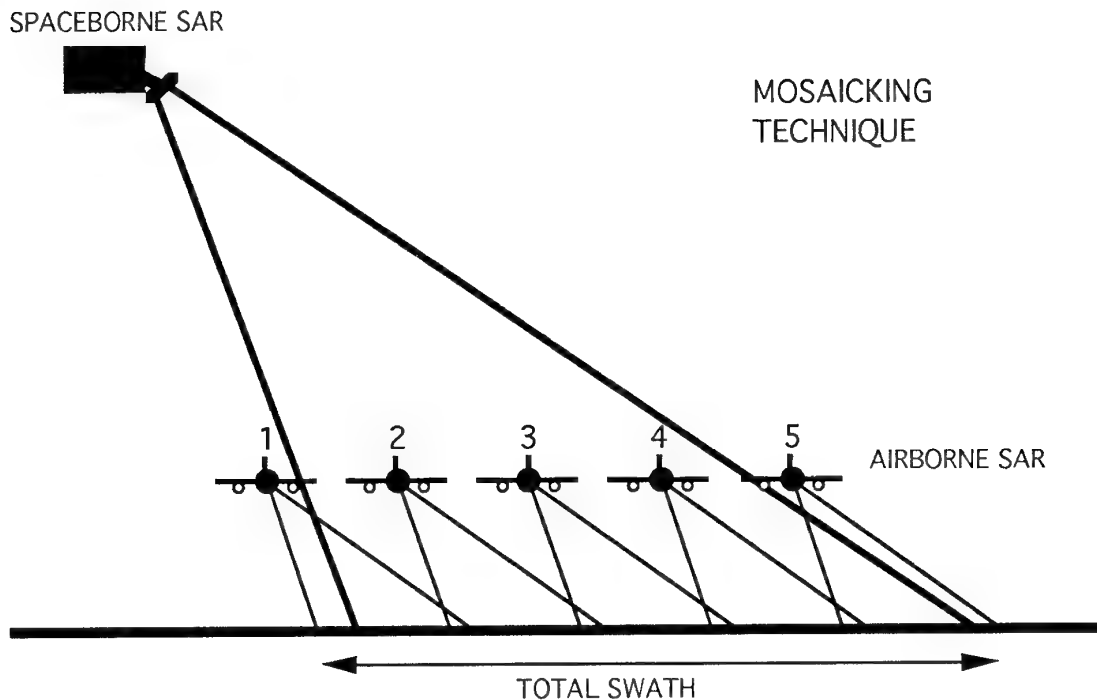


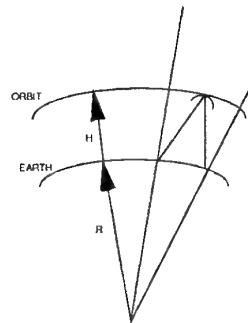
figure 5: Mosaicking technique preserving image size and incidence angle

### 3.6 Specific aspects for a space-based radar

The choice of a determined orbit and the mode to make up the synthetic aperture have direct consequences on the processing of the radar echoes, because some distortions and perturbations will appear. Some examples are given below.

**Range-processing:** in addition to the above-mentioned range effects, such as range curvature and walk, one should take into account the shape and the rotation of the Earth, the eccentricity of the orbit, the "squint" angle induced by the Earth motion together with the platform motion.

**Cross-range processing:** concerning the cross-range effects, the Doppler evolution of the scatterers and, thus, the mathematical expression of the matched filtering will be affected by the particular geometry in the satellite-based context. In addition to this, one should notice that a space-based SAR has also a slight "spotlight" effect due to the behaviour of the satellite on its orbit.



**Cartography:** topographic distortions can be quite important with a space-based SAR when the swath is large. The shape of the Earth must then be taken into account.

### 3.7 Summary

The following table about transpositions sums up the different aspects that have been emphasized. As we can see, some parameters can be directly implemented, others must be derived to simulate a space-based configuration from an airborne one.

| PARAMETER              | TRANSPOSITION   |
|------------------------|---|
| Frequency              | direct restitution  |
| Polarization           | direct restitution  |
| Incidence angle        | direct restitution  |
| Image size             | restitution through the mosaicking technique<br>which moreover preserves the mean incidence angle   |
| Range resolution       | direct restitution<br>- same pulse width (real pulse)<br>- same band-width(synthetic pulse)   |
| Cross-range resolution | direct restitution by fitted coherent integration time  |
| Integration time       | same velocity to distance ratio (figure n°4)  |
| Antennas apertures     | -> swath  |
| Transmit power         | direct restitution is not necessary<br>(signal to noise ratio must be preserved)  |
| Waveform               | direct restitution or transposition preserving the principal parameters<br>(resolutions, ambiguities)   |
| Sensitivity            | -tuning of the average transmitted power to compensate the differences of<br>antenna gain and range<br>- coherent addition of noise to raw data or images |

*figure 6 : Summary of the different transpositions of parameters*

## 4 EXAMPLES

This review is illustrated by examples coming from RAMSES, which is an experimental multi-band radar based on a TRANSALL C160 aircraft. It has the capability to provide SAR images in multiple configurations, including ones dedicated to space-based radar simulation.

### 4.1 The RAMSES airborne system

This system, developed by ONERA under fundings from French MOD, is operated on board a TRANSALL C160 aircraft of the Brétigny Flight Test Center (CEV).

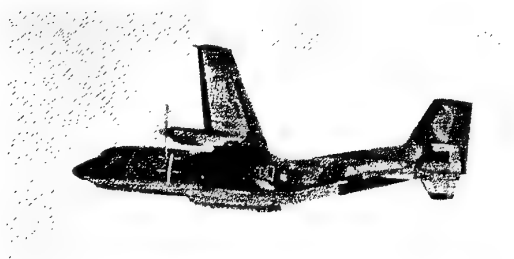


*figure 7: TRANSALL in SLAR configuration*

It has the capability of analyzing the effect of various parameters such as frequency, polarization, incidence, resolution,... in the field of air-to-ground radar applications. These applications include SAR imaging for various purposes such as surveillance, detection of targets, map-matching, remote sensing....

The system consists of several radar RF sections operating over a wide range of frequency bands (L, C, X, Ku, Ka, W and S to come). They are connected with common modules for waveform generation and data acquisition and storage. Two RF sections can be operated simultaneously. All the equipments are fully programmable in order to vary the radar configurations. The data are stored on-board, together with auxiliary data coming from video cameras and navigation sensors. The images are obtained through off-line processing of the data.

| frequency band<br>parameter<br>GHz | L<br>1 - 2 | S<br>2 - 4 | C<br>4 - 8 | X<br>8 - 12        | Ku<br>12 - 18      | Ka<br>26 - 40 | W<br>75 - 110          |
|------------------------------------|------------|------------|------------|--------------------|--------------------|---------------|------------------------|
| Bandwidth (MHz)                    | 200        | 300        | 300        | 300                | 300                | 500           | 500                    |
| Power stage                        | SSA        | SSA        | SSA        | TWT                | TWT                | TWT           | EIA                    |
| Power (W) - CW                     | 100        | 150        | 20         | 200                | 200                | 100           | 50                     |
| Antennas                           | array      | array      | horn       | horn               | horn               | horn          | horn                   |
| Elevation aperture                 | 23°        | 30°        | 13°        | 15°                | 13°                | 5°<br>20°     | 3°<br>5°<br>10°<br>20° |
| Azimuth aperture                   | 16°        | 10°        | 6.5°       | 15°                | 13°                | 5°<br>20°     | 3°<br>5°<br>10°<br>20° |
| Transmitted polarization           | V or H*    | V or H*    | V          | V or H*<br>L or R* | V or H*<br>L or R* | L or R        | L or R                 |
| Received polarizations             | V,H        | V,H        | V          | V,H<br>L,R         | V,H<br>L,R         | L,R           | L,R                    |

\* Pulse to pulse switching  
SSA: Solid State Amplifier

TWT: Travelling Wave Tube

EIA: Extended Interaction Amplifier

figure 8 : Main characteristics of the RF assemblies of RAMSES radar system

#### 4.2 Examples of results

Two examples, corresponding to the same site of Salon-de-Provence in France, are shown here. The first one has been obtained in L band. The four terms of polarization are available although only one is shown here. The second one in X band with two terms of polarization.

Concerning the L band images, the characteristics of the geometric configuration and the waveform are given in the following table :

|                   |                    |
|-------------------|--------------------|
| Configuration     | : SLAR             |
| Velocity          | : 80 m/s           |
| Ground height     | : 2590 m (8500 ft) |
| Mean incidence    | : 45°              |
| Polarization      | : HH+HV+VV+VH      |
| Waveform          | : chirp            |
| Reception         | : de-ramp          |
| Transm. bandwidth | : 80 MHz           |

The SAR processing of these data leads to images having the following characteristics :

|                     |        |
|---------------------|--------|
| Single pass swath   | : 1 km |
| Multi pass swath    | : 6 km |
| Length              | : 9 km |
| Ground-range resol. | : 5 m  |
| Azimuth resolution  | : 5 m  |
| Pixel spacing       | : 4 m  |
| Number of looks     | : 8    |

Concerning the X band images, the geometry and the waveforms are described above:

|                   |                    |
|-------------------|--------------------|
| Configuration     | : SLAR             |
| Velocity          | : 80 m/s           |
| Ground height     | : 2590 m (8500 ft) |
| Mean incidence    | : 45°              |
| Polarization      | : HH+HV            |
| Waveform          | : chirp            |
| Reception         | : de-ramp          |
| Transm. bandwidth | : 160 MHz          |

The resulting SAR images have the following features:

|                     |         |
|---------------------|---------|
| Single pass swath   | : 1 km  |
| Multi pass swath    | : 6 km  |
| Length              | : 9 km  |
| Ground-range resol. | : 2,5 m |
| Azimuth resolution  | : 2,5 m |
| Pixel spacing       | : 2 m   |
| Number of looks     | : 8     |

These images have been obtained by means of the mosaicking technique. For instance, the L band multi-swath image has been assembled with seven single-swath images.

The incidence angle is nearly constant over the whole swath, and representative of some space-based radar configurations.

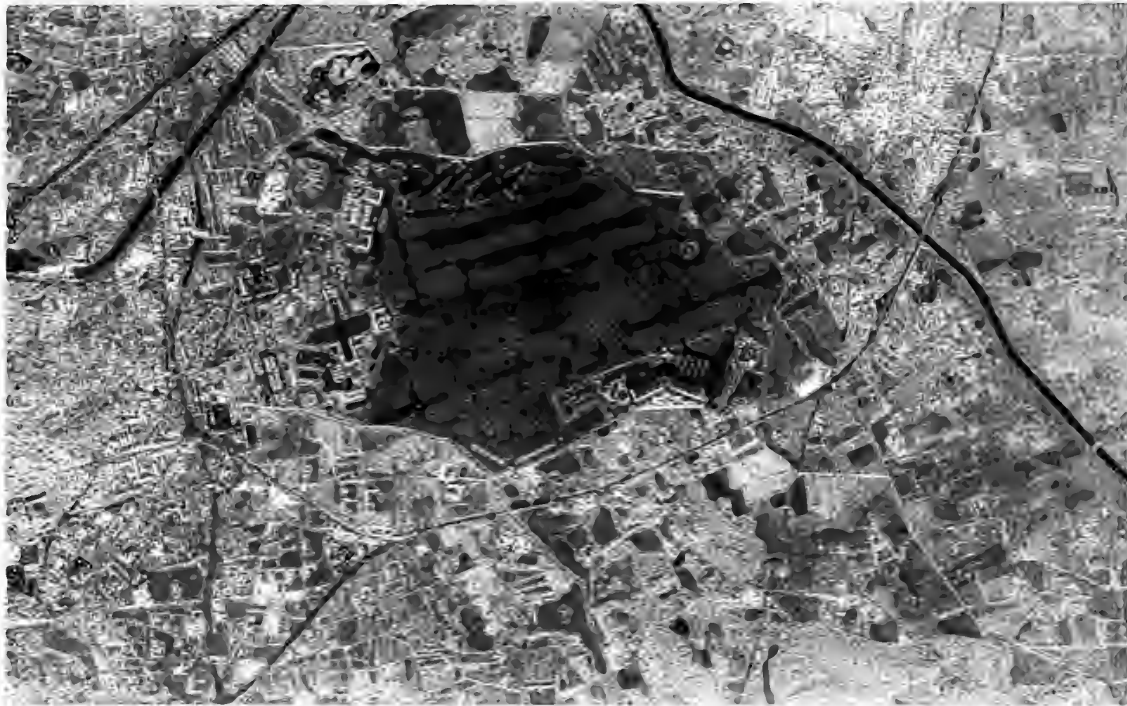


*figure 9 : RAMSES SAR image of Salon-de-Provence - L band*



*figure 10 : RAMSES SAR image of Salon-de-Provence - X band*



## CONCLUSIONS

It has been shown that airborne SAR data can be used to simulate space-based SAR images, either directly or after some kind of reprocessing. Some transposition conditions have to be fulfilled.

These images may be useful for studying the design of spaceborne systems. They are also suitable for training photo-interpreters.

## ACKNOWLEDGEMENT

The development of RAMSES is funded by several directorates of DGA (Délégation Générale pour l'Armement). In particular, spaceborne SAR related studies are supported by the Directorate for Missiles and Space (DME, Direction des Missiles et de l'Espace).

## REFERENCES

- [1] J.-M. Boutry, D. Le Coz et J.-P. Bruyant, 'Instrumentation embarquée de la station expérimentale RAMSES', L'Onde Electrique Vol.74-N°1, pp 1 à 7, Janvier 1994.
- [2] High resolution radar.  
D.R. Wehner (Editions Artech House).
- [3] Space-based radar handbook.  
Leopold J. Cantafio (éditions Artech House).
- [4] A discussion of digital processing in synthetic aperture radar.  
John C. Kirk (Raytheon Company).  
IEEE Transactions on Aerospace and Electronics Systems, vol AES-11, n°3, mai 75.
- [5] Concepts for high resolution space based SAR/ISAR systems.  
C. Bösswetter, A. P. Wolfram, T. K. Pike (MBB Space Systems Group) & J. M. Hermer (Thomson-CSF).  
Agard Conference Proceedings n°459, mai 89.
- [6] A theory of squinted synthetic aperture radar.  
M. R. Vant & G. E. Haslam.
- [7] A signal processing view of strip-mapping synthetic aperture radar.  
David C. Munson & Robert L. Visentin.  
IEEE transactions on acoustics, speech and signal processing, vol. 37, n°12, december 89.
- [8] Conceptual design of satellite SAR.  
R.K. Raney (Canada Centre for Remote Sensing, Ottawa, Canada).  
Proceedings of IGARSS'84 Symposium, august 84.
- [9] Spaceborne synthetic aperture imaging radars: applications, techniques and technology.  
Charles Elachi, T. Bicknell, Rolando L. Jordan & Chialin Wu.  
Proceedings of the IEEE, vol.70, n°10, october 82.
- [10] Modeling and a correlation algorithm for spaceborne SAR signals.  
Chialin Wu (IEEE Member) & Michael Jin (Jet Propulsion Laboratory).  
IEEE transactions on aerospace and electronic systems, vol. AES-18, n°5, september 82.
- [11] SAR digital image-formation processing.  
Dale A. Ausherman (Environmental Research Institute of Michigan).  
SPIE vol. 528, 1985.

# Use of Simulation Tools and Facilities for Rendez-Vous and Docking Missions

J.B. Serrano-Martínez

GMV, S.A.

Isaac Newton, 11 (PTM)  
28760 Tres Cantos-Madrid  
Spain

## 1. SUMMARY

This paper presents a methodology for the use of simulation tools and facilities for the different phases of a Rendezvous and Docking (RVD) project. The methodology is developed trying to minimize development risks and planning shifts. Emphasis is placed on the elements which are unique on the RVD systems, namely, the Guidance, Navigation and Control subsystem, the on-board operations and the docking mechanism assembly.

Such a methodology is based on the reuse of existing simulation tools and facilities in Europe. The Automatic Rendezvous and Capture Demonstration Mission (ARC) is taken as example of RVD project. The rationale of the proposed methodology is presented including: the role of simulators during the different phases of the RVD project (namely, development, verification, execution and post flight phases), the identification of the simulation requirements derived from the foreseen application and the particularities of the RVD systems, the review of existing simulation tools and facilities in Europe and the analysis of their applicability for the ARC project including the identification and analysis of the required upgrades and adaptations on the reused simulators and the required characteristics of the non-existing simulators.

## 2. INTRODUCTION

### 2.1 Background

The study of automatic Rendezvous and Docking (RVD) and the development of the associated technology had been initiated in Europe in the beginning of the eighties in expectation of future European Space programs including mating of two or more spacecraft. Within these technology programs a number of simulation tools and facilities for development support and performance verification had been identified and their development had been started.

With the Columbus and Hermes programs emerging in the mid of eighties Europe had for the first time space projects requiring Rendezvous and Docking and in particular, requiring and automatic RVD capability. After the definition of the mission scenarios, the spacecraft concepts and the RVD strategies of Hermes and the Columbus Free Flyer, ESA initiated a RVD-Proof-of-Concept program to support the Hermes and Columbus RVD developments. Within this program the majority of technological items, tools and facilities developed in Europe had to be integrated in order to develop and demonstrate on breadboard level the design and performance of a complete RVD onboard system.

On the other hand, the planned evolution of the in-orbit infrastructure in the coming years is towards the implementation of space stations, either man tended or permanently manned, in low Earth orbit. On the CIS side, MIR is currently flying and might be upgraded as MIR 2. On the US side, the SSF should be operational before 2000. On the European side a pressurized laboratory, attached to the SSF (Columbus APM) should be operational before 2000, and an European Space Station in the years 2005-2010 is part of the long term plans (EMSI). In addition, the Hermes project will undergo a reorientation period for a redefinition of the objectives of the spaceplane in the frame of a cooperation with Russia: obviously, the spaceplane mission will be defined in the context of rendezvous with

European or Russian space stations at the horizon of beginning of next century. Such manned IOI requires an adequate space transportation system that is capable to perform rendezvous and capture. Following the trends of both European and American Space activities, it can be anticipated that the effort will promote automatic rendezvous and capture techniques, even for manned vehicles.

Due to that, an after evaluation of the possibilities of a RVD demonstration in the first half of 1992, the joint ESA/NASA working group recommended to both NASA and ESA managements to undertake a joint ESA/NASA Automatic Rendezvous and Capture (ARC) demonstration mission in the time frame of 1996/1997. A low cost ARC project was been finally approved for a 1997 flight.

### 2.2 The Automatic Rendezvous and Capture Demonstration Mission

The general objective of the ARC demonstration mission is to ensure the availability of an automatic rendezvous and capture (docking or berthing) capability in order to reduce the risks of future space projects. This objective translates, among others, into the following detailed objectives:

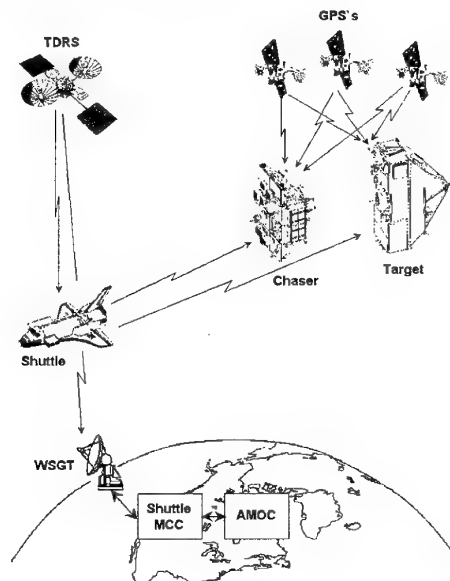


Figure 1: Elements involved in the ARC Mission.

- Demonstrate a number of generic manoeuvres required for approaches and departures in V-bar and R-bar directions and for achievement of docking and berthing conditions.
- Demonstrate safety of automated rendezvous, proximity and capture operations including recovery from anomalous situations.

- Acquire expertise, knowledge and skills necessary to develop an operational ARC system.
- Demonstrate on ground and in orbit availability of relevant ARC technology.
- Demonstrate functional and performance capabilities of the elements and the ARC system.
- Establish and validate testbeds and test procedures for use in future projects.
- Contribute to the interoperability of rendezvous operations between vehicles of different space powers.

The mission is to be implemented in a system which includes a set of elements shown in figure 1: chaser and target are based on the DASA Spas family.

The mission will be broken down in various phases including those properly related to the RV itself (ARC operations) and those necessary for the launch, delivery, retrieval, reentry and landing supported by the Shuttle (non ARC operations). ARC operations are further decomposed in three major phases: initial separation being under ESA responsibility (phase 1) basically demonstrating separation and R-bar approaches, RV operations under NASA responsibility (phase 2) and additional RV operations under ESA responsibility involving V-bar approaches as well as for demonstrating the passive safety concept.

The chaser includes a set of equipments and algorithms (called *modules*) necessary for performing the RV operations. They are grouped in the so called ESA and NASA "ARC packages". The ESA package includes a GPS receiver, two different Rendezvous Sensors (RVS), the docking mechanism (called spacecraft attachment mechanism, SAM) and flight software implementing the different Mission and Vehicle Management (MVM) functions as well as the Guidance, Navigation and Control (GNC) functions. Modes are defined as a set of individual *modules* and required equipments which describe the overall GNC functioning and associated FDI procedures to reach certain objectives during a defined part of the mission (e.g. forced approach from 1000 to 100 m). Those modes necessary for performing the RV operations are managed by the Phase and Mode Management (PMM) software. Whereas the management of the on-board resources is performed by the vehicle configuration management (VCM) software. Finally, the High Level FDIR software is in charge of the detection and identification of failures and the corresponding recovery at mission level. PMM, VCM and HL-FDIR are grouped into the MVM software.

In addition to that, a Ground Operator Assistant System (GOAS) will be on-ground for mission monitoring and for having an additional level of FDIR redundancy to increase the probability of mission success.

### 2.3 Military applications of the Rendezvous and Docking technologies

The investigation of the different technologies (including the use of simulation tools and facilities) which are specific for Rendezvous and Docking missions is very important due to the wide range of military applications which might be foreseen for such kind of missions. Some examples would be

- the servicing of friend orbiting spacecraft and/or space stations either by manned or by unmanned vehicles,
- the retrieval of friend orbiting spacecraft (e.g., for either in-orbit -in case of manned missions- or on-ground repair of friend vehicles),
- the capture and retrieval of unfriend orbiting spacecraft,
- the destruction of unfriend orbiting spacecraft by mechanical means, by disconnecting elements and/or systems or by locating any destructive system on the spacecraft.

In all those applications, the target vehicle will be rendezvoused, approached and berthed and/or docked by the chaser. Subsequent separation of the chaser from the target is required in case of in-orbit servicing missions (either with or without retrieval of the spacecraft). In all the cases the target might be assumed as passive (namely, it does not perform any maneuver for supporting the RVD operations): the chaser is the active element. However, there is a clear difference between the involvement of a friend or an unfriend target. In case of a friend target, in general, it might be considered as a cooperative space-

craft. That means, it might mount

- a pattern for being used by the Rendezvous Sensor on the chaser in order to ensure appropriate relative navigation for short distances
- a GPS receiver and the target might transmit the relevant data for being used in the chaser for performing a GPS based relative navigation for medium and large distances,
- an appropriate half of the docking mechanism, ...

On the other hand, an unfriend target will not be cooperative. This implies quite unique and challenging characteristics for the corresponding RVD mission:

- the docking and/or berthing mechanism should be quite different from the previous one (i.e., mechanism with two halves one on the chaser and the other on the target),
- the relative navigation should rely neither on information provided by the target nor on elements mounted on it. Hence, the relative navigation should be based on passive optical or radar means (the former one being preferred in order to reduce the probability of being detected by the target). For large distances, only relative position (and eventually velocity) would be required whereas for short distances relative attitude is needed, hence complex image processing techniques (including target shape identification techniques, image correlation techniques, ...) will be used,
- the relative guidance and control might deal with quite specific characteristics in order to meet unique requirements for ensuring the success of the mission (e.g., if the chaser is detected by the target, it may try to perform avoidance maneuvers).

## 3. IDENTIFICATION OF ARC PROJECT SIMULATORS REQUIREMENTS

### 3.1 Role of RVD simulators for the ARC project

#### 3.1.1 Development and Verification Phases

The design and implementation of a complete RVD system is a complex activity in which any error or mistake during the early system design phases may have a very severe cost and schedule impact on the overall project. Such errors can be avoided by using an appropriate method for the design and the development of the complete system. Furthermore, the verification should not be considered as a single act at the end of the development but a continuous process from concept definition to flight acceptance in order to control the risk at each step of the system development.

The selected development and verification logic consists of splitting the process into five major phases as follows

- *System definition*: from the mission objectives and requirements the mission scenario is stated, an appropriate RVD strategy is selected and the overall system is defined.
- *System design and subsystem definition*: once the system definition is complete, the detailed system concept is developed and the system components, namely subsystems, are defined according to the system derived specifications.

The feasibility of the system design (in accordance with the requirements of the system) should be ensured. This is performed by non-real-time simulations in closed loop with modelling of equipments, environmental effects, preliminary representative operation software and related interfaces with the rest of the system. Real-time software simulations in closed loop are needed in order to start covering the real-time aspect where it appears critical.

- *Subsystem design, function definition and design and element definition*: detailed concepts are developed for the identified subsystems and a detailed design (leading to specifications on the components) is performed. The subsystem components (in terms of functions and elements) are further defined and designed.

The feasibility of the designs should be proofed in order to minimize the development risks. This can be done in three steps: first, by performing non-real-time simulations using

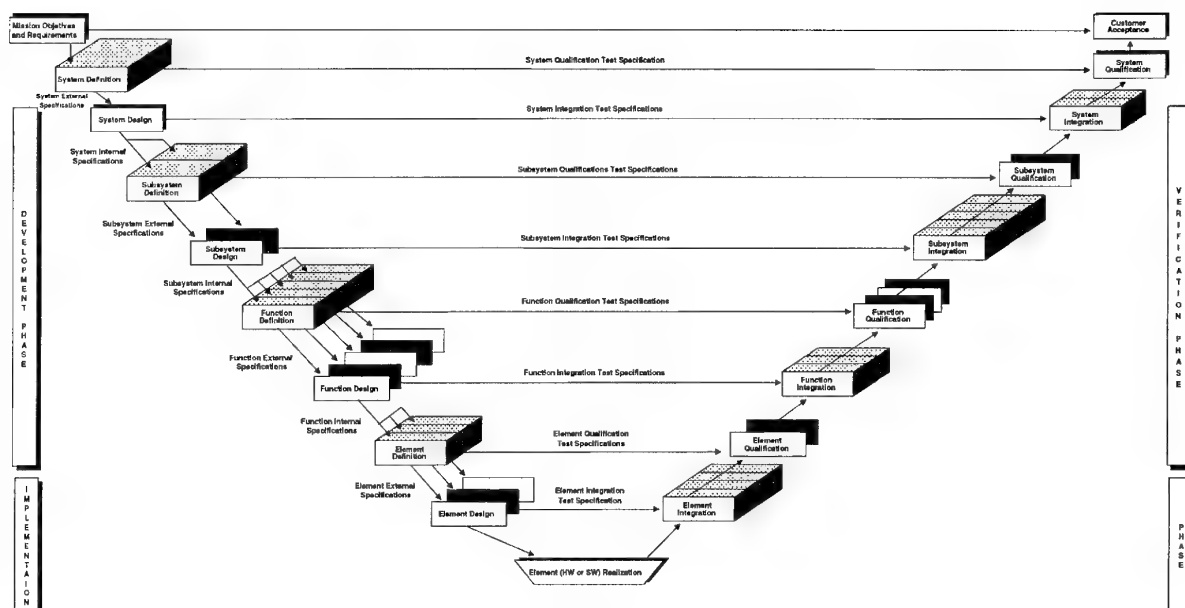


Figure 2: Development and Verification logic of a RVD system.

coarse modelling, second, by running non-real-time simulations in closed-loop with modelling of equipments and environmental effects, third, with preliminary real-time software simulations in closed loop in order to start covering the real-time aspect and identify potential problem areas considered as critical.

- **Element design and implementation:** the different RVD elements which constitute the overall system are designed, developed and integrated.
- **System verification:** the elements are verified, functions and subsystems are integrated and verified and the overall system is integrated. Specifications stated during the design and development phase are checked. The following steps should be performed at three different levels.

At element level: verification of the element design with respect to induced and naturally occurring environment loads and basic performance characteristics.

At subsystem and function level: first, checking of the correctness of the interfaces between functions or elements (as applicable), second, verification of applicable specifications using non-real-time and real-time simulations with sophisticated modellizations and using prototype software, then, validation of the subsystem or function using real time operational software in closed-loop, real-time processor, hardware busses and real equipment (electrical stimuli generators might be necessary).

At system level: first, checking of the correctness of the interfaces between subsystems, second, verification of system specifications using non-real-time and real-time simulations with sophisticated modellizations and using prototype software, then, validation of the system using real-time operational software in closed-loop, real-time processor, hardware busses and real equipment (electrical stimuli generators might be necessary) and, finally, the verification of the operations including man-in-the-loop aspects, automatic sequencing of modes and interaction with the communication system, ...

Although these five phases should nominally be performed in sequence, it turns out that some iterations may be required for the final specification of the whole RVD system. Interactions between levels should take into account the following aspects: any modification at a certain level will have a direct impact on the lower level, it has to be checked that any component

(namely, subsystem, function or element) modification at a certain level is fully consistent with the parallel developments for the other components and it has to be checked that any modification at a certain level meets the specifications imposed from the upper level.

### 3.1.2 Execution Phase

In addition to that and during the execution phase of the mission, a/some simulation tool/tools is/are required by the Ground Operator Assistant System in order to perform detailed investigations on onboard processes as well as to validate commands by simulating their effects. The required simulation tool/tools has/have to be able to be fed in an automatic fashion with the current situation of the chaser and target and also with proposed commands in such a way that a prediction of the mission evolution could be simulated and therefore the current situation and/or the commands assessed.

The simulation tool/tools is/are not planned to be used running continuously in real time in parallel to the mission but only as requested by the operator getting the initial conditions from the TM, and allowing the introduction of any possible modification (e.g., a planned command) which the operator wants to assess.

### 3.1.3 Post flight Phase

One of the major objectives of the ARC Demonstration mission is to establish and validate test beds and test procedures that could validate future RVD system prior to flight. Hence, the ground simulation tools use for the previous phases of the mission shall be verified and calibrated with the flight data obtained after mission completion, in order to complete the establishment of the test beds and test procedures for utilization on future automated rendezvous and capture systems. That purpose will be achieved by performing tasks for

- comparing the pre flight mission simulations with the simulation run in parallel with the mission itself,
- re-running the actual mission profile on the simulation tools using updated data such as actual initial spacecraft state vector, actual sensor performances, actual satellites stability performances and characteristics, actual flight conditions (including environmental conditions, illumination conditions), ...
- re-running fully representative portions of the actual mission on the simulation facilities with hardware-in-the-loop using updated data such as actual initial spacecraft state vector, actual sensor (if no associated hardware is

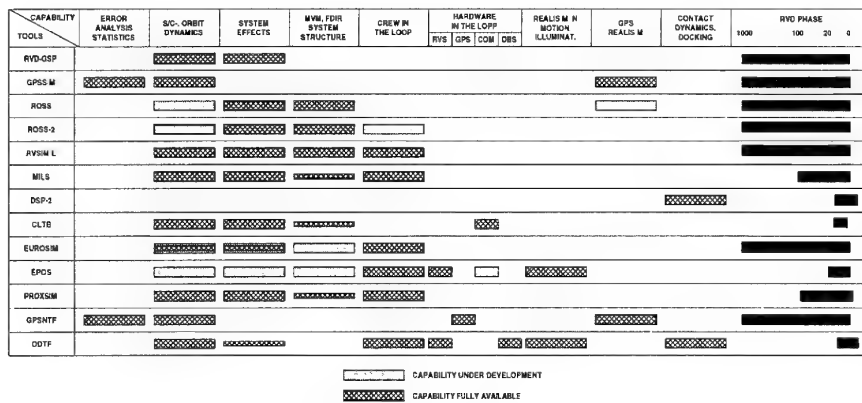


Figure 3: Capabilities of the European RVD simulator.

used) performances, actual satellites stability performances and characteristics, actual flight conditions (including environmental conditions, illumination -Sun, parasitic reflections, ...- conditions), ...

- comparing the re-run simulation results with those obtained during the mission and assessing the accuracy achieved with the simulation tools and facilities and assessing their adequacy for future automated rendezvous and docking projects (e.g., ATV).

### 3.2 ARC Project simulators requirements

The tools and facilities required for the development, verification, execution and post flight phases of the ARC project might be grouped into five major categories

- *Non real time software simulation tools*: which are oriented to the analysis of the features which do not need real-time investigations (e.g., feasibility analyses, GNC performance analyses, MVM concept analyses, ...).

The level of detail of those simulation tools depends on the activities to be supported and the level of definition of the on-board system: in case very detailed analyses are required, the high fidelity models of the dynamics, kinematics and environment and for the equipments might be required in addition to that, a detailed design of the on-board system should be used (the influence of the on-board system design on the results might be equal or higher than the simulation models). That means, such analyses should be performed after having enough information on the required data, that is, they should be made after the completion of the on-board system design.

On the other hand, preliminary analyses might be enough for performing a first iteration on the mission design and analysis and for starting the design of the on-board system: tools implementing medium or low fidelity models and processes (e.g., on-board algorithms) might be used. Different tools might be used: simple tools based on the computation of the nominal or reference trajectory and associated characteristics, low/medium complexity tools implementing general purposes models and either generic on-board algorithms or particular algorithms used as examples of on-board algorithms which associated parameters are adapted to the ARC mission or medium/high complexity tools implementing general purpose models and either generic or particular algorithms used as examples of on-board algorithms which associated parameters are adapted to the ARC mission.

- *Real time software simulation tools*: which are required for performing investigations of transient effects during critical phases of the mission, of the impact of the operational software characteristics on the GNC and MVM performances, for the verification of the design of the on-board software and for the verification of the GOAS design.

In addition to that, these simulators will be used for the validation of the high fidelity simulation models during the post flight analysis phase of the project performances of the complete on-board system (or elements of such a system) for the GPS based phases of the mission.

- *Real equipment facilities*: which integrate real equipment and operational software. Electrical stimuli generators are used for exciting the corresponding equipment. High fidelity models, real-time capabilities and hardware-in-the-loop (namely, on-board computer, GPS receiver and RVS) are required.

These facilities will be used for the verification of the GPS receiver performances, for the verification of the design of the GPS based navigation function with real hardware-in-the-loop and for the verification of the performances of the complete on-board system (or elements of such a system) for the GPS based phases of the mission. They will be validated during the postflight analysis phase of the project.

- *Kinematical facilities*: which provide realistic relative motion (kinematics) between chaser and target. Realistic illumination conditions are ensured in order to investigate the RV sensor characteristics. High fidelity models, real-time capabilities and hardware-in-the-loop (namely, on-board computer and RVS) are required.

These facilities will be used for the verification of the RVS performances, for the verification of the design of the RVS based navigation function with real hardware-in-the-loop and for the verification of the performances of the complete on-board system (or elements of such a system) for the RVS based phases of the mission. They will be also validated during the postflight analysis phase of the project.

- *Dynamical facilities*: which provide realistic contact loads between the two halves of the docking mechanism using realistic relative kinematics between them (i.e., a dynamical facility is a kinematical one which, in addition, allows investigations on the loads occurring during docking). Real-time capabilities and high fidelity models are required. Realistic illumination might be available.

These facilities are required for the verification of the SAM. They will be also validated during the postflight analysis phase of the project.

## 4. REVIEW OF AVAILABLE SIMULATORS FOR RVD ACTIVITIES

### 4.1 General

The RVD simulation tools and facilities which are available in Europe have been reviewed in order to identify which of those might be reused for the ARC project. Simulators falling into five major categories have been identified: non-real time software simulation tools (RVD-GSP, GPSSIM, DSP-2, ROSS-1, RVSIMIL and MILS), real time software simulation tools

(ROSS-2, EUROSIM and PROXSIM), real equipment facilities which integrate real equipment (electrical stimuli generators are used for exciting the corresponding equipment) and operational software (GPSLAB/GNSS TBF, CLTB, EUROSIM and EPOS), kinematic facilities which provide realistic relative motion (kinematics) between chaser and target (EPOS) and dynamic facilities which provide realistic contact loads between the two halves of the docking mechanism using realistic relative kinematics between them (DDTF).

The major capabilities of those simulators are summarized in Figure 3. Simulators with the Man-in-the-loop (MIL) capabilities (RVSIMIL, MILS) are not included because no MIL capabilities are foreseen for the ARC mission.

## 4.2 RVD-GSP: RVD Guidance Simulation Program

The RVD Guidance Simulation Program is a general purpose tool for designing concepts, evaluating performances and defining requirements in RVD scenarios and missions, control laws and RV equipment. The software structure is designed around the Dynamics and Control Analysis Package (DCAP, release 3). Its output is in the form of ASCII files and time plots.

The RVD-GSP models control modes (a large library of GNC algorithms is available), RV equipment for attitude and position estimation, sensors, actuators, spacecraft dynamics and kinematics including external perturbations, internal dynamic effects, occultation and blinding due to Earth and Sun and orbit constellations (e.g., GPS). It simulates all phases from homing transfer to final translation and docking or berthing for nominal approach, nominal withdrawal from target spacecraft and contingency operations. And, furthermore, it enables to tune, change, delete and/or add GNC equipments and/or algorithms.

## 4.3 GPSSIM: GPS Navigation Simulator

The GPS Navigation Simulator is a highly modular and flexible software simulator for analyzing the performances of a GPS based navigation function for Low Earth Orbit missions: the performances of the absolute GPS navigation as well as those of the relative GPS navigation might be assessed. High fidelity models for the spacecraft orbital dynamics (GEM-10, Jacchia-Roberts atmospheric model, third body perturbations, ...), GPS constellation and GPS receiver are available; in addition, state-of-the-art GPS based navigation algorithms are implemented.

Attitude evolution is not simulated: it is assumed to be a fixed input to the program. Guidance and control functions might be implemented by the user in the dummy modules.

## 4.4 DSP-2: Docking Simulation Program

The Docking Simulation Program is an upgraded contact detection and handling package which can be interfaced with different generic dynamic simulation programs (e.g., DCAP) for simulating the dynamic processes during docking between two spacecraft (see Figure 4): the dynamic simulator integrates the equations of motion and at each time step provides DSP-2 with the system configuration in terms of state vector, then, DSP-2 establishes if there is any contact between the elements and in such a case returns the contact forces to the dynamics simulator. In summary, the general purpose dynamics simulator is in charge of modelling the spacecraft (flexibilities, sloshing,...) and orbit conditions, integrating the equations of motion, computing the relative kinematics and introducing torques, forces and deformations in the desired locations; whereas DSP-2 is in charge of modelling the docking system, identifying the contact points, computing the contact forces and processing the docking outputs.

The major characteristics of the DSP-2 are the following: flexibility in the definition of the configuration to be simulated (the user describes, at input level, the number and identification of elements and the number, dimensions and connections of components in each element), capability to produce large number of simulation runs, finding ways (architectures, models, algorithms) to overcome some computational heaviness deriving from peculiarities of the docking simulation problem (discontinuities and high frequencies at contact) combined with

the use of general purpose dynamics simulators and an easy interface with the user (user intervention is possible at different levels such as definition of configuration and of all needed data, definition of interfaces between DSP-2 and the dynamic simulation package, output management and optimization of contact research).

One of the most important problems found during docking simulation activities is the reliability of the results, not only in terms of code correctness, but mainly of validation of implemented models. The contact force model is the most troublesome, in particular when considering flexibilities in the system (attenuation system, structural elasticity of the mechanism itself and of its connection to the spacecraft). The problem could be overcome by using DSP-2 because it has been cross validated with a physical simulation bench (DDTF, section 4.11) by simulating and testing the same cases.

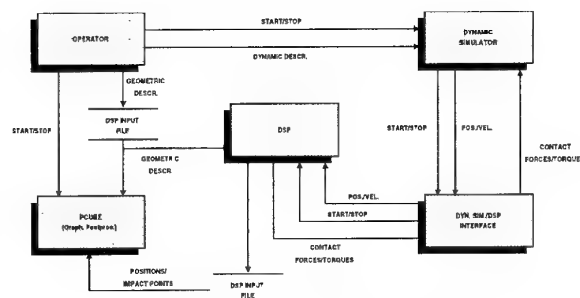


Figure 4: Docking Simulation Program.

## 4.5 ROSS: Rendezvous On-board System Simulator

The Rendezvous On-board System Simulator simulates the on-board system controlling the automatic approach for several scenarios including the full on-board system structure modelling (using the Hermes guidelines) and prototype RV-control software. Spacecraft, orbit dynamics and perturbations, orbit constellation, GPS space segment and communications are modelled with high fidelity. It has the capability of building a wide range of RVD scenarios by constructing different strategies in terms of GNC modes using existing equipment and GNC, FDI and MVM algorithms.

ROSS is a virtual simulator of a physical simulator configuring three computers (namely, simulator computer, system computer and GNC computer), the memories of the two on-board computers, all data channels, the Real Time Bus (RTB) and all equipment (sensors and actuators). It consists of (Figure 5)

- The simulation system which hosts a distributed virtual operating system (VOS) which offers specific sets of system services to the software located on the three computers. The VOS is actually not a self contained operating system, but a small system software layer between the application software and the actual operating system. Its purpose is to keep the application software independent of the underlying hardware and system software configuration, and to be able to change the configuration without affecting the application software. All access to any of the data lines can be done only via VOS service calls (both on-board computers can, of course, directly access the database contained in its own local memory).
- A simulation computer which simulates the on-board and on-ground environment to the on-board computers. It allows to operate and control the simulation system via an operator interface that serves both the simulator operator and, possibly, several mission operators. The simulator computer is connected to the on-board computers via dedicated lines (it is assumed that it has remote access to the local memories of the two on-board computers): a TC channel for telecommand input to the System Computer, a TM channel for output of all telemetry data output of the System Computer and a RTB simulation line for the RTB



data transfer for those equipments that are simulated on the Simulation Computer, namely, actuators (such that chaser and target biliquid and cold gas thrusters, chaser docking/berthing actuator and chaser and target reaction wheels) and sensors (namely, inertial reference assembly, star sensor, Sun sensor, Earth sensor, GPS receiver, rendezvous sensor and proximity sensor). Detailed target (including target attitude control) and chaser dynamics are simulated. The following effects are considered:  $J_2$ , gravity gradient, magnetic torques, air drag, flexible appendages, plume impingement and liquid sloshing.

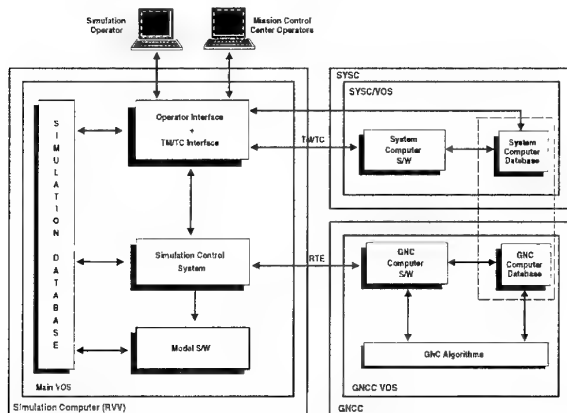


Figure 5: Rendezvous On-board System Simulator.

- The on-board software which is distributed in two on-board computers, the System Computer (SYSC) and the GNC Computer (GNCC). Each of the on-board computers has direct access to a database contained in its local memory (each database holds all global data maintained by the respective computer). The on-board computers are connected via a bi-directional bus that allows exchange of data packets in both directions.

The System Computer performs the activities related to the High Level Failure Detection, Isolation and Recovery, Phase and Mode Management, TC/TM and Vehicle Configuration Management. On the other hand, the GNC Computer performs the Guidance, Navigation and Control and Low Level FDI algorithms management and the Real Time Bus Interface: the GNC Computer is connected to the Real-Time Bus which interfaces to a number of equipments (sensors, actuators); part (or all) of the equipments may be physically available to the RTB, and another part (or all) may be simulated on the Simulation Computer (the actual configuration of physical and simulated equipments is maintained by VOS and transparent to the application software).

An upgrade of ROSS is now under development: it will run in real time and will enable some manual modes for intervention in the GNC loop and MVM functions (concepts for human operator intervention could be analyzed).

#### 4.6 CLTB: Closed-Loop Test Bench

The Closed-Loop Test Bench is an equipment-in-the-loop simulator for the real-time closed-loop testing with a GNC processor (e.g., AGCP) and systems busses (e.g., OBDH and MACS) hardware and the control mode (including both GNC and MVM algorithms) for the last part of the approach (from 20 m to 0) coded in Ada.

The facility software consists mainly in three parts: the application software to be executed on the GNC processor, the system services software located in the GNC processor and test work station located RV control environment software. The RV control environment software is in-line with the corresponding of ROSS, but quite simplified due to the fact that only few GNC modes are implemented. This software implements spacecraft dynamics and equipment modelling, high level FDIR (for the

analysis and recovery of failures detected and isolated in the on-board processor and for the functional failures) and postprocessing capabilities.

#### 4.7 GPSLAB and GNSS TBF: GPS Navigation Test Facilities

The GPS Navigation Laboratory is a test bench which is designed to support the testing of GPS receivers and related navigation algorithms by simulating, with a high degree of fidelity, the information provided by the GPS receiver during a space mission. The GPSLAB consists of (Figure 6) a DEC/VAX station running a software which models the motion of the GPS satellites and that of the user space vehicle and which computes the relative motion between each GPS satellite and the user spacecraft. The relative motion data are downloaded in real time to the GPS multichannel signal simulator (which implements multipath and selective availability effects) via an IEEE interface to generate the corresponding GPS like signals (the simulator is able to generate up to ten different GPS signals). The output of the simulator is connected to the low noise amplifier through a 4.3 m cable and then to one of the inputs of the GPS receiver. In between, an attenuator allows to select the desired signal to noise ratio.

The control of the GPSLAB is performed through the VAX station. The facility operates in three modes: during an initial preprocessing mode all aspects of the scenario are defined by the operator and the models are run to calculate the real-time GPS signal generation control data, during the run-time mode, the corresponding GPS satellite signals are generated in real-time from the pre-processed data and the receiver output is obtained. Such output is optionally logged and displayed on the operators screen and, finally, the third mode deals with the post-processing of the receiver output data.

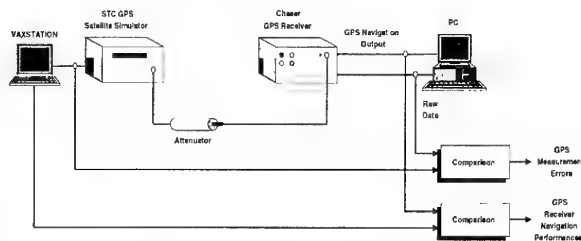


Figure 6: GPS Navigation Laboratory.

An upgraded version of the GPS Navigation Laboratory is under development by ESA. This is the GNSS Test Bed Facility (GNSS TBF). It will consist of a GNSS Simulator (GPS, GLONASS, 2nd generation GNSS, etc) and necessary means to produce simulated RF outputs which feed the receivers being connected, the user equipment (mainly GPS/GLONASS receivers, ground sensors -i.e., simulated GPS reference stations, etc- and on-board sensors as required), the user simulator (for the specific vehicle simulation), the control computer which is in charge of controlling the overall simulation scenario and the on-board computer (implementing on-board algorithms).

#### 4.8 EUROSIM

The Simulator to achieve rendezvous (EUROSIM-STAR) is a high quality animation graphic interaction simulator running in real-time and simulating Hermes/MTFF RVD. It has been used for the development, analysis and validation of Man Machine Interface (MMI) for RVD and it might be used for the investigation of RVD MIL concept issues. It is now being integrated in the EUROSIM simulator environment at ESTEC. STAR models the Hermes/MTFF scenario, simplified on-board system, simplified spacecraft and orbit dynamics and perturbations, automatic mode, pilot in GNC loop for manual state update and manual control and high quality MMI.

In addition to that, a EUROSIM based RVD system test bench (EUROSIM-RVDSTB) is being developed. Its main objective is to allow the testing of the on-board software, hence, an on-board system (including both MVM and GNC) based on the RVD-

POC developments is going to be implemented. Furthermore, the on-board software in the EUROSIM environment will be such that it could be ported to an on-board computer with minimum changes (if any change is required, no doubt of the validity of the tests results should arise).

In order to perform the development and verification tests of the on-board system, the EUROSIM based simulator should provide a complete environment. Hence, a RVD environment should be implemented. Such part of EUROSIM is being implemented allowing: the replacement of standard software models or equipment or perturbations by user provided models, the replacement of simulation software models of chaser and/or target equipment by actual hardware, the implementation of actual on-board computer hardware, the replacement of software parts of the environment by stimuli with the RVD environment driving the stimuli generators, and the modification of chaser/target messages and the implementation of the chaser TM/TC required for connection with target and ground.

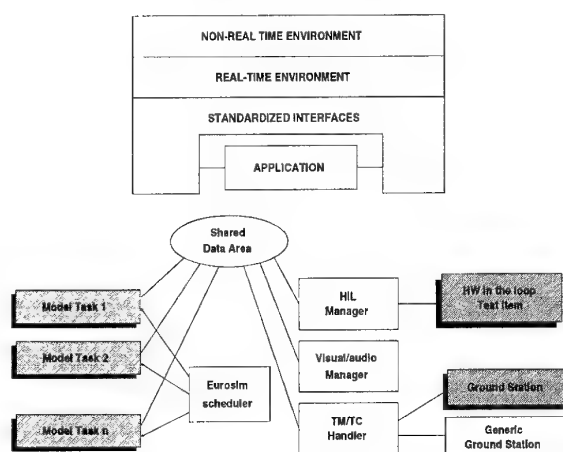


Figure 7: Eurosim simulation shell.

What will be hereafter referred to as EUROSIM is the ESA provided simulation shell (Figure 7) to which the necessary software implementing models and test items, including operational software (i.e., implementing on-board algorithms) and hardware (including onboard equipment, Ground Operator Assistant System workstations, ...) must be inserted so as to create a rendezvous and docking simulation environment: it includes models of all items and features which are not the test item. The major advantage of such an environment is that the models are developed in modular software blocks and that the interfaces between the various simulator and the model S/W blocks are standardized. Two main environments are supported in EUROSIM:

- **Development environment:** in this environment, Eurosim compatible simulation models are produced, together with their interfaces and specific configuration information (TM/TC, HIL, ...). Eurosim does not provide for modelling tools like MatrixX, but has the capability to include the source code generated by such tools into the simulation S/W. Eurosim supports development of simulation models in C, Fortran 77 and Ada, with the support of the configuration control function.
- **Execution environment:** this provides for real-time execution of the models and execution of the surrounding tools and utilities (simulation control, data logging, visual/audio output, HIL manager). Eurosim relies on well-proven technologies for real-time cyclic execution of tasks based on priority assignments and non-degrading priority thread scheduling scheme, together with shared memory.

#### 4.9 EPOS: European Proximity Simulator

The European Proximity Operations Simulator (EPOS) is a test bed comprising hardware motion facility which has been designed to serve as a verification/validation tool for the RVD

flight dynamics during the critical last meter approach (25 meters). EPOS provides the capability of real time and real size simulation of the closed loop controller S/C dynamic motion with sensor and controller hardware in the loop (RVS hardware, GNC computer hardware and the associated RV control software). It provides full scale simulation of the flight up to the point of contact between the chaser and target under real motion (chaser 6DoF, target 3DoF) and illumination conditions in real time.

EPOS consists of five major subsystems (Figure 8): the Dynamic Motion Subsystem (DMS) which corresponds to the chaser spacecraft and performs the chaser attitude motion and the relative translational motion, the Target Mount (TMO) which represents the target spacecraft and performs the target attitude motion, the Illumination Subsystem (ILS) which illuminates the target patterns seen by the sensor to simulate the sun illumination effects if the sun is behind the chaser, the Direct Sun Illuminator (DSI) which illuminates the sensor aperture to simulate the sun in the sensor field of view (i.e., the sun is close to the target) and the Data Processing System (DPS) which has to perform real-time control of the DMS and system logs and to provide interfaces to the motion system operator (which controls the DMS) and the test operator, which runs the simulation and test control computer, STC, and operates the sensor hardware (furthermore, it has to interface with the sensor processors and to log the sensor output data and select EPOS performance data).

Data flow control within the EPOS STC at simulation run time is controlled by the test control (TC) part of the software and is based on a central data structure also called the datapool. This data structure contains, among others, all data which are externally accessible, i.e. which are displayed to and modified by the test operator or which are transferred between the various interfaces.

The dynamics of the spacecraft performing the rendezvous are generated by the Model Software Package (MSW). This software package implements the evaluation of the relative spacecraft states in the EPOS required space coordinates (CLW frame) compatible with the MSC input requirements. Also the information of the in-orbit dynamics is used to compute the responses of the various spacecraft equipment not implemented as hardware test items but the output of which is required by the GNC software.

In its standard configuration EPOS provides model software, so that in principle the user need not take care of it. This MSW provides a set of standard equipment models as well as the models of the relevant in-orbit dynamics. It can therefore be used during very early phases of rendezvous hardware development at equipment test level to close the loop via simplified control laws.

Besides the use of the EPOS MSW the user has also the option of providing his own model software. In this case the user MSW has to conform to a limited set of interfacing rules and must support the simulator state transitions. Furthermore, the logic of EPOS hardware and software interface handling has been made identical, then, EPOS can also accommodate user MSW running on dedicated user computers.

The accommodation options for the GNC software are comparable. The capacity of the EPOS DPS has been specified such that it can be implemented as software test item without having a readily developed on-board computer available. Using the same interface principle as above there is no difficulty in a later stage of the development to replace this software test item when the on-board computer becomes available and can be attached to the spacecraft bus.

EPOS is still under development reaching its operational phase not before 1995, the current configuration is considered to act as a prototype facility (this refers to the hardware as well as to the software). The final EPOS configuration will comprise realistic motion, using a dynamic model including plume impingement, differential air drag, fuel sloshing, etc, dynamic illumination of the docking scene and of the sensor, realistic real-size target mock-up (including target patterns), interface to a real on-board computer with the RV control software (MVM and GNC algorithms), real optical RVS and cameras and



simulated actuators.

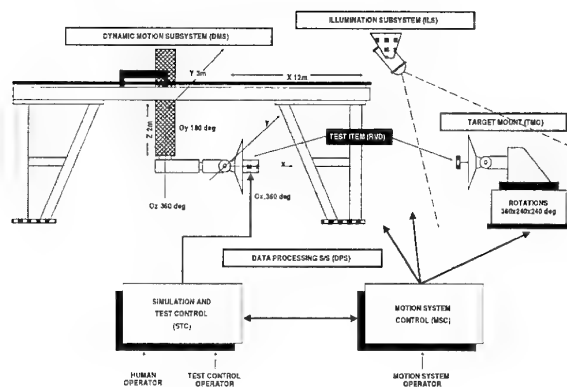


Figure 8: European Proximity Operations Simulator.

#### 4.10 PROXSIM: Proximity Operations Simulator

PROXSIM is a software simulator with high fidelity real time graphic animation (including shadowing and lighting effects, 3D and animation at 5 Hz) and simplified MMI. The environment modelling includes for orbital dynamics and perturbations the use of the Clohessy-Wiltshire equations of motion, air drag and mask effects, gravity gradient and plume interactions. On the other hand, the spacecraft modelling includes the simulation of masses, flexibilities, inertias, fuel sloshing, thruster control IMU and rendezvous sensor. A simplified on-board system is used. The simulator can be used with automatic or manual modes with pilot in the loop for supervisory or manual (1 to 6 DoF) control.

#### 4.11 DDTF: Docking Dynamics Test Facility

The Docking Dynamics Test Facility is a physical simulation bench which represents with high fidelity the relative 6DoF motion between the docking interfaces of two rendezvousing spacecraft. This 6DoF relative motion is basically performed by accommodating the docking interface of one of the spacecraft on a six axes table driven by six electrical screw-jacks. The other spacecraft interface is fixed in the laboratory frame. When necessary, the translational capability along the docking axis can be increased by using an additional translational device for the former spacecraft motion along this axis. In addition, the relative attitude capability can also be increased by a two axes rotating device implemented on the second spacecraft side. Consequently, up to 9 DoF are to be driven.

RVS, video camera, docking mechanism (including electronics), target pattern and hand controllers hardware can be used in the DDTF. Such hardware as well as the dedicated DDTF hardware (namely, 6 DoF and 2 DoF tables, screw-jacks and force transducers) is driven by a dedicated real-time computer architecture basically consisting of a 68020 workstation, an array processor (AP) for the dynamics and kinematics computation, and a Gould 32/67 computer in charge of the AP software development and providing all the necessary utilities and peripherals (plotters, storage capability, etc).

The facility software is in charge of simulating the in-orbit behavior and managing all the algorithms required to drive the DDTF. Its architecture basically allows to perform the computation of the forces and torques applied on the two spacecraft at contact deduced from the force transducers outputs, the simulation of the spacecraft dynamics, with possible features such as sloshing, flexible modes, thruster management and maneuver implementation, control laws, ... the simulation of sensors such as gyros and accelerometers, the simulation of the environment composed of orbital perturbations such as first order Clohessy-Wiltshire dynamical model, plume effects and constant perturbations for the differential drag effects, the management of the six (6) to nine (9) electromechanical axes in order to perform the relative motion, and the laboratory 1 g effect compensation, when necessary.

## 5. ARC PROJECT SIMULATORS PHILOSOPHY

### 5.1 ARC project simulators utilization

The ARC project simulators philosophy is defined by the utilization of the different simulators and by the characteristics of such simulators. Different simulators are planned to be used during the development, verification, flight and postflight phases of the project (see Table 1) as detailed in the following.

Simulators will be used during the *development phase* of the project in order to perform the mission design and analysis (i.e., computation of fuel and time budgets) as well as to support the design and analysis (conceptual and performance) of the GPS based and RVS based navigation functions, guidance and control functions, MVM functions, GOAS functions, GPS receiver (in particular the characterization of the associated errors), RVS (in particular the analysis of the dynamic errors due to the relative motion between chaser and target, illumination of the target pattern and specular reflections or Sun in the FOV and the derivation of an appropriate simulation model) and SAM. Once the different elements have been designed, different simulators will support the verification of the corresponding designs in non-real time as well as in real time and, for the verification of the navigation functions, with hardware (i.e., GPS receiver and RVS) in the loop.

Simulators will be used during the *verification phase* of the project in order to support the verification of the functionalities, interfaces and performances of the different specific RVD elements which conform the on-board system including GPS receiver, RVS, flight software, GOAS and SAM. Equipment verification will be carried out for the GPS receiver, RVS and SAM, whereas the flight software verification will include verification before and after its implementation on the on-board computer. On-board subsystem verification will include the verification with all the elements in the loop as detailed in the summary table.

During the *execution phase* of the project, simulators will be used for the analysis of the telecommands to be uplinked (including the analysis of the replanning strategies if required) as well as for the verification of such telecommands.

The *post-flight activities* to be supported by simulators will encompass the validation of the high fidelity simulation models of the spacecraft dynamics, kinematics and environment (DKE), of the spacecraft sensors (including GPS receiver, RVS, star tracker and gyros) and actuators (cold gas system and attachment mechanism) as well as validation of the different facilities used (i.e., GNSS TBF, EPOS and DDTF) including the stimulation models (e.g., the RF signal simulator for GPS and the RVS stimulator) and the motion and dynamic capabilities.

Details on the simulators referred in Table 1 are provided in the next section.

### 5.2 ARC project simulators

#### 5.2.1 GPSSIM

This simulator might be used as it is (see section 4.3) for the analysis and design of the GPS based navigation function. Analysis of the complete GNC using such a simulator would require the implementation of the associated guidance and control algorithms in the dummy modules.

An alternative approach is not to use this simulator but reuse some pieces (e.g., user spacecraft dynamics, kinematics and environment, GPS constellation, GPS observables generation) for the construction of the ISI environment based RV Design Simulator (section 5.2.4).

#### 5.2.2 RVD-GSP

This simulator might be used as it is (section 4.2) for the performance analysis of the GNC with simplified models for the simulation. The parameters of such a models should be adjusted to the ARC mission.

| ACTIVITY            |                | GPS            | Flight Software            | RVS            | GOAS                    | SAM   |
|---------------------|----------------|----------------|----------------------------|----------------|-------------------------|-------|
| Design and Analysis |                | Specific Tools | GNCSIM (GPSSIM, GSP, ROSS) | Specific Tools | General Purpose Tools   | DSP-2 |
| Design Verification | No Real Time   | --             | GNCSIM (ROSS)              | --             | ROSS                    | DSP-2 |
|                     | Real Time      | --             | RVSim (if available)       | --             | TM/TCSim (if available) | --    |
|                     | HW-in-the-loop | --             | GPSLAB                     | --             | --                      | --    |
| Verification        | Real Time      | --             | RVSim                      | --             | TM/TCSim                | --    |
|                     | HW-in-the-loop | GPSLAB         | SGSE                       | EPOS           | Target and Chaser SGSE  | DDTF  |
|                     |                | --             | GNSS TBF/SGSE              | --             |                         |       |
|                     |                | --             | EPOS/SGSE                  | --             |                         |       |
|                     |                | --             | GNSS TBF/SGSE              | --             | GNSS TBF/SGSE           |       |
| Execution           | Real Time      | --             | --                         | --             | TM/TCSim                | --    |

|                                  |                | Star Tracker  | Gyros | Thrusters | GPS      | RVS   | DKE           | SAM   |
|----------------------------------|----------------|---------------|-------|-----------|----------|-------|---------------|-------|
| Postflight models validation     | Real Time      | RVSim         | RVSim | RVSim     | RVSim    | RVSim | RVSim & DSP-2 | DSP-2 |
| Postflight facilities validation | HW-in-the-loop | --            | --    | --        | GNSS TBF | EPOS  | --            | DDTF  |
|                                  | HW-in-the-loop | GNSS TBF/SGSE |       |           |          | --    | GNSS TBF/SGSE | --    |
|                                  |                | EPOS/SGSE     |       |           |          | --    | EPOS/SGSE     | --    |
|                                  |                | --            | --    | --        | --       | --    | DDTF          |       |

Table 1: Summary of simulators utilization for the ARC project.

Important upgrades of this simulation tool (e.g., higher complexity models) are not worthwhile due to the fact that the GNCSIM tool (section 5.2.4) will override GSP with higher fidelity models.

### 5.2.3 DSP-2

This simulator might be used as it is (section 4.4) for the performance analysis of the spacecraft attachment mechanism. The existing simulation models and parameters should be adjusted to the ARC mission.

No major upgrades are planned. The use of this simulator might be preferred to some other existing simulator due to the fact that it has been cross validated with a physical simulation bench (DDTF) by simulating and testing the same cases.

### 5.2.4 RV Design Simulator (GNCSIM)

It has been proposed to use the ISI (Integrated Systems, Inc.) product family as basic environment for the analysis and design of the ARC on-board system: namely, MATRIX<sub>x</sub> and SystemBuild<sup>TM</sup> will be used as development environment. Apart from the software development cost saving and off-the-shelf capabilities, some other advantages of using this environment can be summarized as follows

- non-linear models developed in SystemBuild<sup>TM</sup> are extremely useful for system simulation purposes. These models may be simulated, with the simulation results sent to the MATRIX<sub>x</sub> database. In this way, simulation results may be analyzed, displayed, and compared in the same way as any other data. Nonlinear models, however, cannot be used directly with the linear design and analysis tools which are available through linear systems theory and control design. SystemBuild<sup>TM</sup> solves this problem by generating equivalent linear models from nonlinear SystemBuild<sup>TM</sup> block diagrams. Operating points, input values, and perturbation parameters can be specified, resulting in an extremely flexible linearization capability. Linearized models can then be analyzed using any of the linear techniques available with the MATRIX<sub>x</sub> linear systems tools (or with the advanced extension modules such as the Control Design one),
- tools are available in the Digital Signal Processing module of MATRIX<sub>x</sub> to perform frequency response calculations for nonlinear, hybrid, and even multirate systems. These tools automatically simulate the SystemBuild<sup>TM</sup> model, exiting the modes of interest, and determine the frequency response based upon the input/output data. In this way, no inaccuracies are introduced through linearization or resampling of the model,

- SystemBuild<sup>TM</sup> is designed to integrate easily into an existing simulation environment: existing models and components can be incorporated directly into SystemBuild<sup>TM</sup> through the User Code Block (UCB) interface. With the UCB, such a software can be added to the SystemBuild<sup>TM</sup> library providing the capability for extremely accurate models. These blocks are then treated the same as any other element in the standard SystemBuild<sup>TM</sup> library.

Therefore, the simulator to be utilized for the analysis and design activities (named GNCSIM) will be based and integrated in such an environment. Due to the characteristics of the ISI based environment two major basic strategies might be followed for the simulation of the spacecraft dynamics, kinematics and environment and spacecraft equipment (i.e., sensors and actuators): implementation of dedicated software or re-utilization of existing software (sophisticated and high fidelity simulation software might be used through the utilization of the UCB interface).

### 5.2.5 ROSS

This is in principle a closed-loop verification tool (i.e., once the on-board flight software is designed) of the on-board system. However, due to the fact that such a tool is available (one has to be taken into account that it is available but for the Hermes, Columbus and SSF scenarios, section 4.5) it might be used for the GNC/MVM design verification (same as GSP or GNCSIM).

In any case, no additional software upgrades (e.g., for a high fidelity hardware associated models for the equipments, ...) are foreseen: existing models will be used for carrying-out the performance analysis of the on-board system and only the model/algorithm parameters will be adjusted properly (either from the work performed by GMV or from the work actually underway at ESTEC). In case the algorithms selected for the ARC onboard system are different to those implemented in ROSS either they should be implemented or a different tool (e.g., GNCSIM) should be used.

### 5.2.6 GPSLAB

It is proposed that the GPSLAB test facility previously reviewed (section 4.7) will be used for performing some development tests as well as some unit tests. The facility will then be used in open loop as it is now. Existing associated general purposes software (for the simulation of the dynamics, kinematics and environment) and capabilities will be used. Some test preparatory activities will be required in order to mount the ARC GPS receivers. In addition to that the test procedures will be prepared including the values of the parameters associated to

the utilized general purposes software.

In addition to those preliminary tests, some intermediate testing (after the navigation design frozen and before the operational software development) might be planned in order to identify potential critical issues which may arise with the two receivers working at once. This intermediate testing could be performed either with the upgraded GPSLAB (i.e., with two GPS receivers in the loop) or under the GNSS TBF (depending on the ARC project planning and GNSS TBF development planning) in which the testing could be extended to the full GNC (not restricted to the navigation function).

Depending on the ARC project planning, the above mentioned unit tests might be performed with the GNSS TBF/SGSE facility (see section 5.2.11) instead then allowing the utilization of high fidelity and ARC hardware oriented models.

### 5.2.7 EPOS

It is proposed that the test facility previously reviewed (section 4.9) will be used for performing some development tests as well as some unit tests. The facility will then be used at equipment and/or open loop testing level(s). Existing associated general purposes software (for the simulation of the dynamics, kinematics and environment as well as other sensors and actuators -which in principle are not needed-) and capabilities will be used. Some test preparatory activities will be required in order to mount the ARC rendezvous sensor(s) as well as the target pattern(s). In addition to that the test procedures will be prepared including the values of the parameters associated to the utilized general purposes software.

Depending on the ARC project planning, the above mentioned unit tests might be performed with the EPOS/SGSE facility (see section 5.2.12) instead then allowing the utilization of high fidelity and hardware oriented models.

Another possibility for having high fidelity models in EPOS is to update the existing associated general purposes software by the high fidelity verified models implemented in the frame of the RV Simulator: due to the similarities between the EUROSIM environment and the EPOS one the RVD environment software developed for the RV simulator might be straightforward implemented in EPOS.

### 5.2.8 Rendezvous Simulator (RVSim)

The Rendezvous Simulator will be a high fidelity EUROSIM-shell based simulator (section 4.8) which will be used to support the required ground demonstrations with essential hardware and software in the loop prior to the in orbit demonstration. It will implement high fidelity models for the simulation of the dynamics, kinematics and environment of the chaser and target spacecraft (as well as their geometric and mass characteristics) and for the simulation of the chaser and target equipment (i.e., sensors and actuators) and will provide capabilities for running the on-board flight software and for being connected to the EGSE/SGSE for performing the required simulation.

Such a hardware associated high fidelity will be achieved by simulating the target natural environmental operational conditions relevant for the ARC mission (i.e., gravitational field, Earth atmosphere and Earth magnetic field), the proximity operations aspects relevant for the ARC mission (including gravitational forces, air drag, gravity gradient torques, magnetic torques and plume impingement forces and torques), the chaser operational characteristics, including mass characteristics (i.e., mass, center of mass and dyadic), geometric characteristics for the computation of the aerodynamic and plume impingement actions, chaser equipment gyros, star tracker, ESA RV sensor 1, ESA RV sensor 2, GPS receiver -in addition, the GPS constellation will be simulated- and cold gas system and the target operational characteristics, including mass characteristics (i.e., mass, center of mass and dyadic), geometric characteristics for the computation of the aerodynamic and plume impingement actions, target attitude control, including target attitude determination and control algorithms, target equipment gyros, star tracker, GPS receiver -in addition, the GPS constellation will be simulated- and cold gas system.

### 5.2.9 TM/TC Simulator (TMTCSim)

Based on the RV simulator, a TM/TC simulation facility shall be developed for providing appropriate and realistic TM/TC interface to the GOAS. This means that additional models have to be implemented within the RV Simulator which is based on the Eurosims simulation shell. The following functions should be developed/added to the current RV Simulator in order to implement an appropriate interface to which the GOAS should be directly connected: on-board TM/TC packeting/depacketing, effects of communications (delays/occultations), simulation of ground communications process and AMOC TM/TC data handling, and simulation of target TM.

In order to provide a modular architecture, these functions are proposed to run in a different computer (Sun/Unix computer).

It is to be noted that, as part of the TM to be managed by GOAS, not only the ESA ARC Package SW TM is needed but in general GOAS will have the capability to access all on-board TM (up to 16 kbps) and therefore, all needed data will have to be simulated to some extent. Note, however, that for some packets non realistic data could be needed at this level of verification, so some dummy packets could be used as well.

### 5.2.10 Chaser EGSE and SGSE

The EGSE and SGSE shall be based as far as possible on the design for the Astrospace/Minispas EGSE/SGSE. The ARC Chaser Electrical Ground Support Equipment (EGSE) consists of all non-flight equipment and associated firmware required to support the various phases of the ARC Chaser system integration (including NASA ARC package, if any), test and mission.

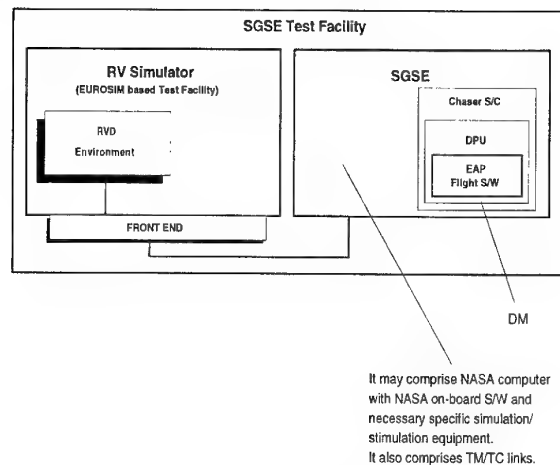


Figure 9: SGSE Test Facility.

The ARC Chaser EGSE shall consist of equipment to support: integration and test of the ARC Chaser S/C system, integration of payload (ESA and NASA ARC packages), mission simulation (together with SGSE), launch support, and mission support (in SPOC configuration). The major subsystems shall be: SSP simulator, DC-Power simulator, PSP simulator, PDI simulator, PI simulator, RCMM for Data Tape Recorder, time simulator, checkout computer, AC power distribution, intercom, Nascom interface and the necessary software packages. The individual tests performed with the EGSE are subsystem integration, functional system and subsystem tests, integrated system tests, spacecraft control during environmental tests, experiment integration tests, GNC closed-loop verification including ESA and NASA ARC packages (together with the SGSE), mission simulation with the SGSE.

The Chaser S/C Software Ground Support Equipment (SGSE) serves the purpose of software test and verification. In particular, the SGSE shall be used for closed-loop tests of the Chaser attitude control and RVD verification. For closed-loop tests, part of the Chaser hardware will be simulated by appropriate

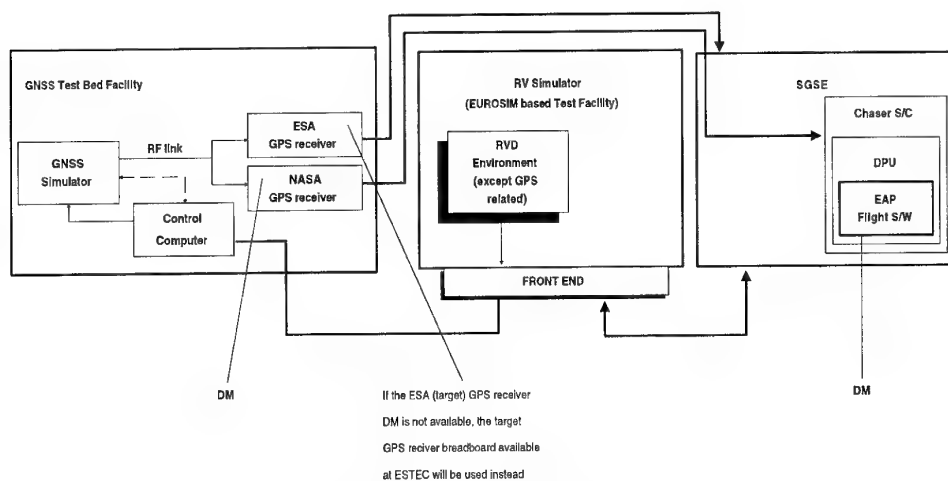


Figure 10: GNSS TBF/SGSE Test Facility.

simulation hardware being part of the SGSE and by software running on the SGSE simulation computers.

The SGSE shall consist of a re-build (or re-use) of a subset of EGSE equipment, complemented by SGSE specific interface and simulation hardware. Functions which are not relevant for the closed-loop behavior of the system shall not be realized in the SGSE, e.g. TM/TC communication will not be via RF link but rather by hardlines directly connected to the Chaser DPU.

In order to provide a commonality of models across all the tools and test facilities which shall be utilized in the frame of the ARC project, the SGSE shall incorporate the RV Simulator environment (Figure 9). This facility is taken as basic piece for the "completion" of other test facilities, namely, GNSS TBF and EPOS as it is detailed in the following.

#### 5.2.11 GNSS TBF/SGSE

The test facility proposed is a combination of SGSE and GNSS TBF (Figure 10) in order to achieve a highly realistic test environment. This facility will provide a highly flexible simulation environment: it will provide an environment with the flight software running on the DPU, GPS receivers in the loop fed by a realistic signal provided by the RF signal generator (multipath effects might be also simulated).

#### 5.2.12 EPOS/SGSE

The test facility proposed is a combination of SGSE and EPOS (Figure 11) in order to achieve a highly realistic test environment. In spite of the fact that EPOS is a highly flexible simulation environment which provides many configuration capabilities, it is proposed to use this EPOS/SGSE test facility: some variants might be used, for example, for large distances outside the operational range of EPOS (i.e., 25 m) real motion is not possible and, hence, the RVS should be stimulated.

This facility provides an environment with the flight software running on the DPU, RV sensors (both from ESA and from NASA -in order to demonstrate that the sensors can all function without interference from each other-) and associated target pattern(s) in the loop and it provides real motion and illumination conditions for the last critical phase of the RVD mission.

#### 5.2.13 DDTF

It is proposed that the test facility previously reviewed (section 4.11) will be used for performing the verification of the performances (capture and rigidisation) of the spacecraft attachment mechanism with such a mechanism (i.e., hardware) in the loop. The facility will be only used for such activities, hence, it will be used in open loop.

The facility worked properly (i.e., for the activities performed in the frame of the RVD-PDP program) for the Hermes docking berthing mechanism, however, either some upgrades of the facility or some SAM related additional activities might be required due to the characteristics (i.e., size and mass) of this ARC mechanism:

- in order to allow the use of the DDTF, a scaling procedure (already proven in the frame of the RVD-PDP program) might be required,
- an additional problem which might occur with the DDTF is that the mechanism implemented on the chaser may be too heavy for being integrated on the facility. To avoid this problem, one should foresee the development of a reduced model of the docking mechanism including only the front-end elements and not the attachment mechanism used for launch and landing,

Existing associated general purposes software (for the simulation of the dynamics, kinematics and environment as well as other sensors and actuators -which in principle are not needed-) and capabilities will be used. In addition to such upgrades, some test preparatory activities will be required in order to mount the ARC target and chaser halves of the attachment mechanism. In addition to that the test procedures will be prepared including the values of the parameters associated to the utilized general purposes software.

## 6. ACKNOWLEDGEMENTS

The work summarized in this paper was carried out by GMV under ESTEC Contract No. 10473/93/NL/JG (SC) with the European Space Agency in the frame of the ARC Preparatory Phase.

## 7. REFERENCES

1. Cosmen Schortmann, J.: "AR&C Demonstration Mission Preparation. MMS Subcontract No. 8E557.01G. Demonstration Mission Evaluation", RVD-ARCPRE-TN-GMV-06, GMVSA 2072/93, June 1993.
2. Cosmen Schortmann, J.: "AR&C Preparatory Phase. ESTEC Contract No. 10473/93/NL/JG (SC).AMOC ARC Package Functions", RVD-ARCB-TN-GMV-02, GMVSA 2137/93, December 1993.
3. Elfving, A. and Fehse, W.: "Simulation tools for the development of an Autonomous Rendezvous and Docking System", ESA Journal, Vol 11, February 1987.
4. Fehse, W. and Bentall, R.H.: "Motion Simulation for in-orbit Operations", First European In-Orbit Operations Technology Symposium, ESA SP-272, November 1987, pp 263-271.
5. Fehse, W.; Tobías, A. and Marechal, M.: "Overview of RVD simulators in Europe", ESA SP-422, February 1993.
6. Fehse, W. et al.: "The ESA-NASA Automated Rendezvous

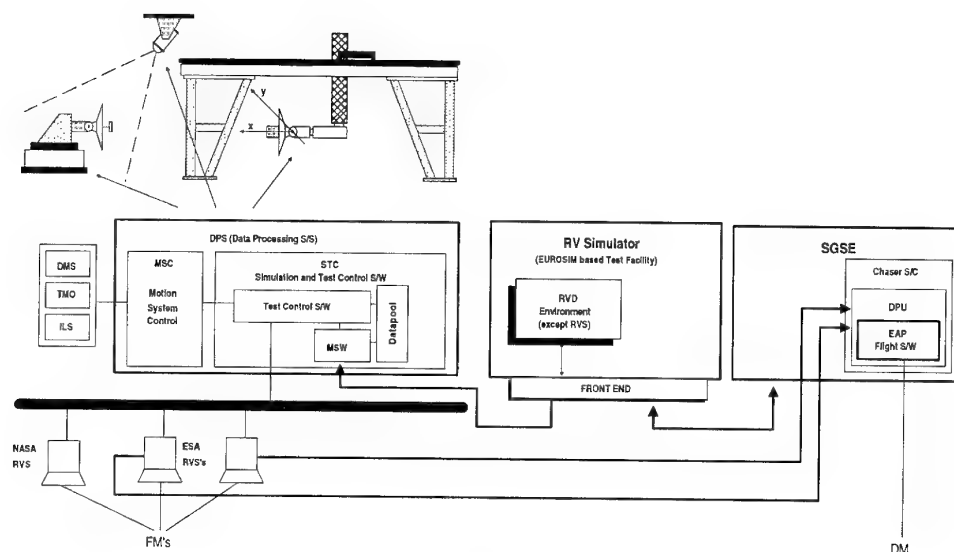


Figure 11: EPOS/SGSE Test Facility.

- and Capture ARC Mission", Third European In-Orbit Operations Technology Symposium, June 1993.
7. Grimbert, D. and Marchal, P.: "Dynamic Testing of a Docking System", First European In-Orbit Operations Technology Symposium, ESA SP-272, November 1987, pp 281-288.
  8. Heimbold, G.; Prins, JJM and Fehse, W.: "EPOS - European Proximity Operations Simulation", First European In-Orbit Operations Technology Symposium, ESA SP-272, November 1987, pp 273-279.
  9. Heimbold, G.: "EPOS. European Proximity Operations Simulator", First Workshop on Simulators for European Space Programs, October 1990.
  10. Heimbold, G.: "Phase C1 Configuration and User Access to the European Proximity Operations Simulator - EPOS", Second Workshop on Simulators for European Space Programs, November 1992.
  11. Legido, J.M.: "Testing of Two Elegant Breadboards for Space Applications. WO 4 to ESTEC FC No. 8609/89/NL/JG (SC). WP3000: Absolute Testing. Absolute Testing Report", GMVSA 2052/93, April 1993.
  12. Noirault, P. and Pairot, J.M.: "Use of the Docking Dynamics Test Facility for Rendezvous and Docking Final Approach Verification", First ESA International Conference on Spacecraft Guidance, Navigation and Control Systems, ESA SP-323, December 1991, pp 219-224.
  13. Pairot, J.M.: "RVD System Pre-Development Program. Verification and Validation Requirements for the Development of RVD", RVD-PDP-SYS-SYN-MAT-03, October 1990.
  14. Pauvert, C. et al.: "Verification Tests for a Prototype RVD GNC On-board Software", First ESA International Conference on Spacecraft Guidance, Navigation and Control Systems, ESA SP-323, December 1991, pp 203-212.
  15. Serrano Martínez, J.B.: "AR&C Demonstration Mission Preparation. MMS Subcontract No. 8E557.01G. AR&C Development and Verification Tools and Facilities", RVD-ARCPRE-TN-GMV-05, GMVSA 2058/93, June 1993.
  16. Serrano-Martínez, J.B.; Cosmen, J.; Alvarez, L.J.; Toledo, M. and de Pedro, A.: "Upgrade of RVD/GNC Algorithms and Ground Operator Assistant System (GOAS). ESA Contract No. 9982/92/NL/JG (Work Order No. 2) Final Report", RVD-URGA-FR-GMV, GMVSA 2145/93, February 1994.
  17. Serrano-Martínez, J.B. and de Miguel Asensio: "AR&C Demonstration Mission Implementation (ARCIMP). ESA Contract No. 9982/92/NL/JG (Work Order No. 3). Final Report", RVD-ARCIMP-FR-GMV, GMVSA 2143/93, February 1994.
  18. Serrano-Martínez, J.B.: "ARC Preparatory Phase. ESTEC Contract No. 10473/93/NL/JG (SC). Simulators for the ARC Project", RVD0-ARCB-TN-GMV-03, GMVSA 2021/94, February 1994.
  19. Sommer, J.: "ROSS Data Definition", RVD-PDP-ROSS-SUM-ERN-02, MBB-ERNO, June 1992.
  20. Sommer, J.: "ROSS User's Manual", RVD-PDP-ROSS-SUM-ERN-001, MBB-ERNO, August 1992.
  21. Tobías, A.; Venditti, F. and Cable, N.: "Docking Berthing Systems, Functions and Simulation", Second European In-Orbit Operations Technology Symposium, ESA SP-297, December 1989, pp 259-270.
  22. Tobías, A.: "Utilization of EUROSIM RVD Application", RVD-EUR-TN-01, October 1992.
  23. Zunker, H. and Backhaus, H.G.: "Laser Based Rendezvous Sensors in Test on the European Proximity Operations Simulator", AIAA Paper 92-4549, August 1992.

## SPACECRAFT ATTITUDE and ORBIT CONTROL SYSTEMS TESTING

F.J. Sonnenschein, M. Schoonmade & T. Zwartbol  
 National Aerospace Laboratory NLR  
 P.O. Box 90502, 1000 BM Amsterdam, the Netherlands  
 Email: sonnenschein@nlr.nl

SUMMARY

Contemporary AOCS are equipped with local Attitude Control Computers which provide sophisticated Attitude and Orbit Control functions, automatic Failure Detection and Isolation functions and extensive Telemetry and Telecommand handling functions. Generic models of the design, development and test life cycle approaches for such intelligent AOCS are emerging. Also knowledge of the activities to be performed and the generic design, development and test environments to be used during the different phases is accumulating. Lessons learned can be used to improve AOCS development life cycle approaches and to define new development and test environments which improve the efficiency of the design, development and test life cycle and quality of the product.

The SAX (Satellite per Astronomia a raggi X) satellite is equipped with a contemporary AOCS providing the above mentioned functions. In this paper the SAX AOCS software design, development and test life cycle is described as an example of AOCS software development. Lessons learned and suggestions for possible improvements are given.

The basic equipment used for SAX AOCS testing was the SAX-TSA, a further development of the MACS TSA (Test and Simulation Assembly for Modular Attitude Control Systems), the ESA standard test equipment for AOCS equipped with OBDH and MACS buses.

Currently a new generation Test and Verification Equipment (TVE) is being developed under ESA contract as successor to the Test and Simulation Assembly. It will be a modular system that can be tailored for any Attitude and Orbit Control Subsystem. The experience gained with complex AOCS for scientific missions, like ISO and SAX, has resulted in the definition of a test equipment which is not only suited for different spacecraft data handling and AOCS buses but (subsets of) which can also be used during various phases of the AOCS design and development and test life cycle. The design of the TVE is modular, based on the possible replacement of specific hardware interface processors to other spacecraft buses. The prototype TVE will interface, like the MACS-TSA, to the standard buses OBDH and MACS.

The TVE is composed of three functional parts: the External Bus Interfaces in a Front End, the Test Software and the Simulation Software. The Front End is a modular VME bus system isolating the Test Software from the spacecraft hardware buses. Abstract system bus and subsystem bus protocols have been defined, hiding the hardware details of the particular bus and the interface processor involved.

1 INTRODUCTION

Contemporary AOCS are equipped with local Attitude Control Computers which provide for sophisticated attitude and orbit control functions, automatic failure detection and isolation functions and extensive telemetry and telecommand handling functions. Generic models of the design, development and test life cycle required for such intelligent AOCS are being established. Also knowledge of the activities to be performed and the generic design, development and test environments to be used during the different phases is accumulating. Lessons learned can be used to improve AOCS development life cycle approaches and to define new development and test environments which improve the efficiency of the design, development and test life cycle and quality of the product.

The SAX AOCS software design, development and test life cycle is described in this paper as a typical example of AOCS software development.

Lessons learned and suggestions for possible improvements are given.

The basic test equipment used for SAX AOCS testing was the SAX Test and Simulation Assembly. The SAX-TSA was an improvement of the MACS TSA, the ESA standard test equipment for AOCS equipped with OBDH bus and MACS bus.

Following the development of the Modular Attitude Control System (MACS) bus in 1984 the development of a standard Test and Simulation Assembly (MACS-TSA) as a generic tool to support the design, integration and test activities of Attitude and Orbit Control Subsystems (AOCS) has been initiated (see ref. 9). The MACS-TSA has been developed under contract with the European Space Agency (ESA) and has been applied for the test and integration of the AOCS of the ESA 'Infrared Space Observatory' (ISO) and the Italian-Dutch 'Satellite per Astronomia a raggi X' (SAX).

The Front End for the SAX-TSA was a partly new design and incorporated an OBDH interface which was capable to handle the full high level (packetised) telemetry protocol of the SAX OBDH.

Currently a new generation Test and Verification Equipment (TVE) is being conceived as successor to the TSA, under ESA contract. It will be a modular system that can be tailored for any spacecraft AOCS. The experience gained with the MACS-TSA for complex AOCS for scientific missions will result in a generic test equipment, also applicable to communications satellites.

Keywords: Spacecraft Attitude and Orbit Control, Test and Verification, Real-time simulation, Hardware In the Loop, On Board Data Handling, Modular Attitude Control System, Electric Ground Support Equipment



The design of the TVE is modular, based on the possible replacement of specific hardware interface processors to other spacecraft buses. The prototype TVE, currently under development, will interface to the ESA standard buses OBDH and MACS.

The TVE is divided into three functional parts:

- The external bus interfacing.
- The basic test software.
- The simulation software.

The design of the particular bus interface processors comprises for all buses two functional levels: Low Level and High Level bus interface processors. The Low Level bus interface processors handle the hard real time requirements dictated by the physical protocol of the particular bus. A prototype will be built with the OBDH bus as system bus, the MACS bus as subsystem bus.

The TVE Test Software comprises the following main functions: Data Conversion to abstract data, Data Archiving, Data Monitoring, Automated Test Control, (interface to) Dynamic Environment and functional units Simulation, and Operator Interfacing.

The TVE Simulation Software determines the external orbital conditions, the attitude dynamics and the functional behaviour of the sensors and actuators. The design of the interface from the Simulation Software to the TVE Test Software will maximise the use of commercially available tools. In case AOCS units are absent, the MACS bus interface processors will behave as the real units on the bus. In case the hardware units are present the units are stimulated via a generic stimuli interface.

## 2 THE SAX MISSION

The Italian Space Agency (ASI), supported by the Netherlands Agency for Aerospace Programs (NIVR), is developing the SAX (Satellite per Astronomia a raggi X) satellite. Alenia Spazio (Roma) is the Prime Contractor for the SAX satellite. The mission of SAX is to perform a systematic and comprehensive observation of celestial X-ray sources in the 0.1-300 keV energy range, with particular emphasis on spectral and variability measurements. SAX is planned to be put into orbit by an ATLAS 1 launcher in the last quarter of 1995. The planned orbit is circular with an inclination of less than 5° and an initial altitude of 600 km. The nominal mission lifetime will be two years, with a design goal of four years. An early description of the SAX mission and spacecraft is given in reference 1. An overview of the design and verification approach of the SAX satellite is given in reference 2.

### 2.1 The SAX Attitude and Orbit Control Subsystem

The SAX Attitude and Orbit Control Subsystem (AOCS) is developed by Fokker Space and Systems under contract with Alenia Spazio (Prime).

The AOCS subsystem is controlled by the Attitude Control Computer (ACC). This computer is based on an 80C86 microprocessor extended with an 8087 co-processor. The ACC is fully redundant in cold stand-by.

The AOCS is equipped with a subsystem bus, the so-called 'Modular Attitude Control System bus' (MACS-bus), which is the interface between the ACC and the AOCS units. The ACC is also interfaced to the spacecraft OBDH-bus for ground communication via the spacecraft Telemetry/Telecommand link.

The AOCS is controlled by software running in the ACC. This software is divided into two parts:

- Basic Software, providing operating system services (scheduler) and basic interface services with the OBDH bus and the MACS bus.
- Application Software, providing all attitude control tasks, failure detection and isolation

tasks and the application-dependent layer of telemetry and telecommand handling tasks.

In order to meet the requirements of reliability and operational flexibility, the Application Software has been further subdivided into two parts:

- \* Basic Attitude Control (BAC) software, stored in a Read Only Memory (ROM) in the ACC, but copied to, and executed in, a Random Access Memory (RAM) when active. This part must be highly reliable and safe.
- \* Extended Attitude Control (EAC) software, stored in Random Access Memory (RAM) of the ACC and potentially (re-)loaded and/or modified on ground command.

The main functions of the Application Software are:

- Basic attitude control functions needed to acquire and keep a safe satellite attitude after separation or 'fall back' from higher modes. Sun Acquisition sensors and magnetometers are used as sensors during attitude acquisition. Quadrant sun sensors, magnetometers and gyro's are used as sensors during basic attitude control (sun-earth lock). Reaction wheels are nominally used as actuators.
- Extended attitude control laws for accurate control of the spacecraft attitude, required for pointing the X-ray instruments at celestial sources. Basically star trackers and gyro's are used as sensors for attitude determination and control and reaction wheels are used as actuators.
- Failure Detection, Isolation and Recovery (FDIR) functions, devoted to health checking and redundancy management of the AOCS units.
- Telemetry and telecommand handling functions. The telemetry software collects and formats AOCS Housekeeping Data, Event Related Data, User Selectable Data and Attitude reconstruction data. The data is sent via Basic Software services to the OBDH system. The telecommand handling checks the correctness of received telecommands.

### 2.2 SAX AOCS Software Design, Development and Testing Life Cycle

The difficulty with AOCS software development is that the software development life cycle and the development of the various test environments is coupled to, and hence must be synchronised with, the AOCS hardware development life cycle, which in turn is embedded in the spacecraft development life cycle.

The challenge of AOCS software projects is to optimize the development life cycle and to prevent that the development of the AOCS software and its test environments become the main drivers of the schedule.

Firstly, this requires that the development of the Application Software is done partly concurrently with the ongoing AOCS detailed design.

Secondly, in case an off-the-shelf operating system can not be used, Application Software and Basic Software development should be done concurrently, combined with a suitable ACC development philosophy. For the SAX AOCS it was decided to develop a Functional Model of the ACC (FUMO), prior to an Electrical Qualification Model, enabling the start of software testing in its target environment at an early moment in time.

Thirdly, the definition of the various development and test environments should be started as soon as possible. In this context it is important that at project level the use of standard development and test environments (hardware and software) to be used throughout the project is advocated.

Aspects of the above mentioned items can be found in the SAX AOCS development approach, the details of which are described in reference 3. Following reference 3, in the SAX AOCS software design, development and testing life cycle the following activities can be distinguished:

- a - Definition of (high level) AOCS software user requirements and (OBDH and MACS bus) interface specifications.
  - Development of detailed functional design specifications and execution of design simulations for verification of the design specifications. This concerns establishing the detailed functional design specifications (e.g. attitude determination and control algorithms, automatic Failure Detection, Isolation and Recovery functions) and the verification of the design by means of simulations.
  - For design verification a non-real time simulator (called SATSIM-SAX), including detailed models of the relevant AOCS units, spacecraft dynamics and environmental torques was developed. At project level it was decided to use this simulator also for the other phases of Application Software development and test, see next sections. In this way no development and qualification efforts for other locally used simulation packages would be required. Furthermore, the re-use of the simulator would enable the generation of reference simulation runs, the results of which could be used during the various stages of the verification process.
  - For the design verification simulations, a model of the Application Software was used. The model Application Software implemented the main (but not all) functionalities of the actual Application Software, as it implemented (a part of) the detailed design specifications. However, the model Application Software has a different architecture and is written in a different language (Fortran instead of C). The design of the SAX attitude control laws is also described by reference 3. The approach to automatic Failure Detection, Isolation and Recovery is described in reference 4.

- b - Development of Basic Software and Attitude Control Computer.
 

As Application Software and Basic Software had to be developed in parallel by different companies, the interface between Application Software and Basic Software was kept as simple as possible and was defined by a limited set of Service Calls, making the necessary services of the Basic Software available to the Application Software.

At project level it was decided to use identical Software Development Environments for Basic Software and Application Software development. It consists of an HP64000 work station containing a suite of CASE tools and a hardware emulator. The hardware emulator is controlled from the HP64000 master work station.

For integration tests, the Basic Software was run in the FUMO. The hardware emulator was capable to execute the Basic Software code from its local memory, but the emulator processor could also be coupled to the FUMO, replacing the FUMO 80C86 processor and executing the code located in the FUMO memory. The hardware emulator was essential for debugging the Basic Software, see reference 7.

As the Basic Software was developed in parallel with the Application Software, the actual Application Software was not yet available and hence a software test tool, capable of issuing the Service Calls available to the Application Software (Application Software simulator), was

used to test the interfaces with the Application Software.

- c - Application Software Development
 

The National Aerospace Laboratory NLR were responsible for design, coding and testing of the SAX AOCS Application Software. This development is touched upon briefly below. Further details can be found in references 5 and 6.

  - Application Software Software/Hardware Integration and Test.
 

NLR were also responsible for SAX AOCS Application Software Software/Hardware Integration and Test and the development of the main SAX AOCS test tool, the SAX Test and Simulation Assembly (SAX-TSA). The software/hardware integration and test phase comprised:

    - \* the integration of the FUMO/Basic Software with the SAX-TSA,
    - \* generation of Integrated Software from the Application Software and Basic Software and the verification of the Integrated Software running in the FUMO, through real-time closed loop tests, however without any AOCS units in the loop.

An extended version of the SAX-TSA, which was capable of controlling Unit Checkout Equipment, has been delivered by NLR to Alenia Spazio, to be used for SAX AOCS Subsystem Integration and Test, see reference 7.
- d - AOCS Subsystem Integration and Test level.
 

Alenia Spazio in Turin, Italy, were responsible, as subcontractor to Fokker Space & Systems, for integration and test of the AOCS at subsystem level. An overview and some interesting conclusions with respect to the chosen approach are given reference 7.
- e - Spacecraft System Integration and Test level.
 

Alenia Spazio as Prime contractor were responsible for the Integration and Test at spacecraft level.

### 2.3 Application Software development

The Application Software development activities have consisted of:

- Architectural Design of the Application Software,
- Detailed design, coding and module testing,
- Integration and Test of the Application Software.

At project level it was decided to use identical Software Development Environments for Basic Software and Application Software development. The Software Development Environment consists of a dedicated HP64000 development system. A suite of Computer Aided Software Engineering tools was used for requirements analysis and architectural and detailed design.

The HP64000 system is equipped with a software emulator and source code level debugger, as well as a hardware emulator, such that also native 8086/8087 machine code could be tested.

In order to test the integrated Application Software at the development station, non-real time closed loop simulations were performed using the HP64000 system. This simulation used the same SATSIM-SAX simulator as was used for AOCS design verification. The Application Software was run at the hardware emulator. Interfacing of the Application Software with the simulator was done using so-called UNIX "pipes". In this way non-real time closed loop verification of the Application Software was possible.

At the time of initial testing the Basic Software



was not yet available. Therefore a simulation of the Basic Software was used.

This simulation consisted basically of the Service Calls providing the interfaces with OBDH and MACS bus. The Basic Software simulator was also running, linked with the Application Software, in the hardware emulator.

Although, non-real-time closed loop verification of the integrated Application Software was possible, it turned out that the execution speed of the closed loop (probably because of the "pipes"), was unwieldily slow.

#### 2.4 The SAX Test and Simulation Assembly

The SAX Test and Simulation Assembly (SAX-TSA) is a further development of the MACS TSA. The MACS TSA is the standard ESA Test Equipment for AOCS which are equipped with MACS-bus and OBDH-bus. The MACS TSA can be used at different levels of AOCS integration and test.

The SAX-TSA consists of a Host computer (VAX 4000-200) and a so called Front End, interconnected by Ethernet.

The TSA Front End is equipped with a VME based, multi-processor system, which handles all communication between Host computer and the Front End MACS-bus and OBDH-bus interface boards.

The SAX-TSA provides various tools to the test engineer such as:

- send automatically series of commands to the AOCS under test via the simulated OBDH Telemetry/Telecommand link, similar to a ground station,
- monitor the Telemetry from the AOCS under test,
- monitor the traffic on the MACS-bus between ACC and AOCS units, simulated electrically on the bus,
- simulate the spacecraft attitude motion and the functional behaviour of the AOCS units,
- display test data for on-line monitoring,
- archive test data for later analysis,
- generate erroneous bus traffic.

Taking the SAX AOCS as a generic example:

The integrated software (Application Software integrated with Basic Software) being tested, runs (in real-time) in the Attitude Control Computer Functional Model (FUMO). The spacecraft attitude motion and the AOCS units, that are not present in the test set-up, are simulated in the SAX-TSA Host computer. In the SAX AOCS ACC, the Application Software is run at a cyclic basis of 2 Hz. At the start of each AOCS cycle the ACC reads the (simulated) AOCS unit data from the TSA Front End, and inputs the data to the Application Software. The Application Software then performs its attitude control task, i.e. it calculates the satellite attitude and attitude errors from the sensor readings and calculates the control torques required to bring the satellite attitude close(r) to the desired attitude. The calculated control torques are then commanded to the (simulated) AOCS actuators. Synchronized (each 0.5 s.) by the ACC, the SAX-TSA Host computer reads from the Front End the data and the commands the ACC has sent to the (simulated) AOCS units. Using the derived control torques as inputs, the SAX-TSA dynamics simulation extrapolates the satellite attitude motion over the next 0.5 s. time interval and outputs the associated sensor data to the Front End, where they are read by the ACC at the start of the next cycle. Besides the attitude motion and sensor measurement data, the SAX-TSA Host computer also simulates the AOCS Housekeeping data, such as unit on/off status, health data, and temperature data. All defined communications between the ACC and units is provided up to the level of reality required. Also different equipment failure modes can be simulated, such that the Application Software health monitoring and FDIR functions can be tested.

Via the SAX-TSA Host computer, telecommands can be given to the AOCS under test, e.g. to switch on/off units, to switch to another operational mode, etc. Via the OBDH link, the SAX-TSA receives telemetry data from the ACC, comprising Housekeeping Data and Attitude Reconstruction Data (sensor measurement data).

Furthermore, the SAX-TSA monitors the communication between ACC and AOCS units on the MACS-bus. By means of these features, not only the functioning of the software can be thoroughly tested, but also the protocol and timing of the communication on the MACS bus between ACC and the (simulated) AOCS units can be verified.

#### 2.5 Software/Hardware Integration and Test

A software/hardware integration phase is not commonly found as an explicit phase in all AOCS software development projects. The software/hardware integration and test phase was introduced in the SAX AOCS software development life cycle to test integrated Application Software and Basic Software as early as possible in its target environment, without having to deal with other AOCS units. This would protect the following AOCS subsystem Integration and Test phase from possible communication protocol problems associated with FUMO/SAX-TSA integration, possible Application Software to Basic Software interface problems and possible timing problems associated with the real-time system. It should be borne in mind that the SAX-TSA Front End and the ACC and Basic Software were newly developed for the SAX AOCS project.

During the Software/Hardware Integration and Test phase of the SAX AOCS software development life cycle the following activities took place:

- integration of the FUMO/Basic Software with the SAX-TSA. The purpose of these tests was to check out:
  - \* the low level OBDH communication protocol between SAX-TSA and ACC.
  - \* the high level Basic Software Telemetry and Telecommand handling functions which are accessible via Service Calls (e.g. dumping of simulated House Keeping Data, User Selectable Data, Event Related Data, commanding of AOCS units).
  - \* loading and dumping and verification of RAM located programs (load, dump, compare) by the TSA.
- generation of Integrated Software from Application Software and Basic Software and verification of it through real-time, closed loop tests, however without using any other AOCS hardware units in the test set-up.

The dynamics simulator used in the SAX-TSA was the same simulator as was used by Fokker Space & Systems for the design simulation, with additions to adapt the simulator to the real-time environment of the SAX-TSA and bus related data formatting.

At software/hardware integration and test level, only functional tests (contrary to performance tests) were performed. Sets of functional requirements can be tested in one test. The tests are devised by the test engineer and described in a Test Scenario document. This basically is a list of time-tagged test triggers (e.g. commands), required to test the different Application Software functions, and the expected results or events.

Test execution is automated as far as possible, under control of Test Sequences. Test Sequences are test-specific pieces of software, the translation of Test Scenario's time-tagged test triggers into computer code. The Test Sequences are executed by the Host computer and control a test and enable

monitoring of test data. For each test, specific top level Test Sequences are to be developed, re-using many lower level sequences.

In the above described way all (testable) Application Software BAC and EAC functional requirements have been tested and verified. The different steps in the test and verification process were made traceable and verifiable via associated documents (Integration and Verification Plan, Test Plan, Test Reports, Requirements Verification Control Documents).

As remarked above, the software/hardware integration and test phase was introduced in the SAX AOCS software development to protect the following AOCS subsystem Integration and Test phase from possible communication protocol problems associated with FUMO/SAX-TSA integration, possible Application Software to Basic Software interface problems and possible timing problems associated with the real-time system.

In this sense the software/hardware integration and test phase has been very useful.

During the integration of the SAX-TSA with the ACC and the verification of the Integrated Software a number of problems were detected.

The problems detected were logged in 146 (status of July 1994) Non Conformance Reports.

The non-conformances can be categorised to resulting updates as follows:

- 23% test environment, (about two third of which SAX-TSA Front End);
- 4% SATSIM-SAX simulator;
- 27% Basic Software, about one third of which were detected during integration of the FUMO with the SAX-TSA;
- 4% FUMO hardware;
- 23% design specifications;
- 8% Application Software;
- 2% development environment related (differences in compiler versions).

- Relatively many non-conformances showed up in the test environment (SAX-TSA). To a large extent this was due to the partly newly developed SAX-TSA Front End, the hardware/firmware of which had not yet stabilised at the beginning of the test phase.

- Relatively many Basic Software problems were detected. This was probably due to the fact that the (newly designed) Basic Software had not yet completed its formal test campaign, when the integration tests with the Application Software started.

- Relatively many non-conformances were due to (design) specifications. The major part of these reports can be attributed to not yet properly tuned parameter values in the FDIR functions and were easy to solve.

Another part can be attributed to FDIR functions that behaved differently from what was anticipated in the design specifications. This is probably due to the fact that not all of the FDIR functions had been verified by design simulations.

It is noted that attitude control functions also had been extensively verified by design simulations and (consequently) no attitude design non-conformances were encountered during software/hardware integration and test.

- Relatively few problems were associated with the SATSIM-SAX simulation package. This conclusion supports the decision to re-use the same SATSIM-SAX simulation at different locations in the project.

- Application Software errors were relatively few. Apparently the Computer Aided Development approach and the closed loop tests of the integrated Application Software at the (cross) development station led to high quality software.

It is noted that reference 7 reports relatively many errors in the Application Software implementing the FDIR functions, due to not properly chosen parameters values.

During software/hardware integration and test, the same software functioned according to the design specifications (sometimes after re-tuning of parameters).

The reason for the difference is, that during software/hardware integration and test simulation models of the AOCS units were used, whereas reference 7 used actual hardware in the loop. Apparently this required slightly different tuning of FDIR parameter values.

### 3 LESSONS LEARNED FROM SAX AOCS SOFTWARE DEVELOPMENT

#### 3.1 AOCS design and test environments

- The software/hardware integration and test phase was very useful, as it detected and solved many hardware and software interfacing and timing problems.
- To trace down software problems in a real-time test, it is mandatory that also at software/hardware integration and test level powerful debugging aids (e.g. hardware emulator) are available.
- Equal attention should be paid to FDIR functions as to control algorithm design, including simulations.
- The AOCS detailed design phase is performed partly concurrently with the software detailed design and coding phase. This implies that AOCS design engineers and software design engineers have to cooperate closely. For small projects this has led to the so-called "Skunkworks" approach in which one integrated team performs AOCS design as well as software design. However, also for large multi-corporate engineering projects, where complicated systems comprising hardware and software are to be developed and where large set of engineering documents and software are to be controlled, tools to allow concurrent engineering and advanced engineering data management systems are beginning to emerge, reference 8.
- The Application Software model software used for the non-real-time design simulations ideally should be programmed in the target language used to implement the actual Application Software in the ACC.
- A standard and properly validated AOCS simulation package should be used throughout the project.
- A generic test environment (subsets/supersets of) can be used throughout the development and test life cycle.

#### 3.2 Software (cross) development environments

- Computer Aided (cross) Development and the closed loop tests of the integrated Application Software (without AOCS hardware involved) can lead to high quality software.
- If parts of the AOCS software are (cross) developed concurrently by different agents, identical (cross) development environments should be used, to prevent problems during integration.
- Hardware emulators are powerful and useful debugging aids.

#### 4 THE TVE: AN APPROACH TO GENERIC AOCS TEST EQUIPMENT

To provide AOCS design engineers with tools to study the (expected) behaviour of the system to be realised, components of the spacecraft system and its environment have to be simulated. During different phases of the AOCS design, development and test life cycle, different aspects of spacecraft attitude control are studied. Therefore, different levels of detail of the simulations are required. To facilitate this, the generic simulation tool must be structured, modular and flexible to allow adaptation to various requirements of the different phases. For instance initially the total AOCS is simulated, while during subsystem integration increasingly more actual hardware is integrated in the test set up. However, the way the partly simulated and partly actual system, is being presented to the user should be as uniform as possible throughout the phases.

Analysis and experience with previous projects, like SAX, has led to the subdivision into several hardware and software layers. The simulation models of components of the system and its environment, require freedom for the user to choose his models. It is for example valid to have two models of the same component, with a different formulation of the behaviour of a component. In one stage the details are important to support the assessment of the ultimately obtainable accuracy. In another stage only the global functional behaviour is of interest in the context of the co-operation of components. The design of the test software is such that a uniform presentation to the test engineers as users can be realised. A secondary, but important, goal is the potential in reducing the costs of the design, testing and verification process as a whole. The possibility of reusing simulation models at various steps, or even from other projects has been identified. The benefit could be measured in terms of: better cross-check possibilities, early detection of errors and increased user confidence in the validated system.

The solution is called TVE: Test and Verification Equipment. A prototype is currently being built.

The test environment has to deal with the presence and the absence of flight hardware and software. The link between the flight hardware and the simulation models is formed by the TVE Front End. As parts of the equipment can be absent or present, the routing of the data between various models and real equipment must be handled, in such a way that the actual location is hidden for the respective software. The statement "the flight software must not be aware that it is operating on the ground instead of a spacecraft" is as valid as the statement "a model must not be aware whether its communication partner is another model, or a real piece of equipment".

This has led to a concept with three levels of data in the TVE. First there is the "physical (on-board bus) level", that is handled by the actually present spacecraft equipment and the TVE Front End. This level will vary from bus to bus type. The TVE Front End will be designed as modular as possible in this respect. Therefore a "protocol level data structure" has been defined as communication language between the TVE Front End and the TVE Test Software. This structure has been defined as an envelope around the possibilities of MACS, OBDH and MIL-std 1553 buses. All buses employ bus unit to bus unit communications, commands and data exchange, where the sender and receivers can be different. Further traffic health information, multi unit traffic (broadcasts) are defined. It is

the goal of the TVE to decouple the physical level from the protocol level. The protocol processor, being a reprogrammable part of a particular bus interface, will take care of the conversion in general, where the intermediate level between protocol processor and the low level bus hardware interface is hidden. The TVE test software takes care of the transformation between protocol level data format and the actually used "abstract data level" as used by the models.

Usually this is more or less identical to the data in engineering units in which the control engineer is working. By centralizing these conversions in the Test software, the TVE user (project) only once must define the conversions, and also the various parts of the software internally do not execute the various transformations on the same data more than once.

#### 5 THE AOCS DESIGN LIFE CYCLE

Again the main characteristics of various phases in the AOCS design life cycle are discussed, to identify the high level requirements for the TVE development.

Taking the above SAX AOCS design, development and test life cycle as a typical example, the following generic life cycle is considered (it is noted that phases may be partly concurrently):

- AOCS design phase,
  - \* definition of (high level) user requirements and interfaces
  - \* detailed design and verification simulations
- Development of TVE test environment
- ACC hardware and software integration
- AOCS subsystem level integration and test
- Spacecraft system level integration and test.

As a TVE will not be directly suited for AOCS software cross development, this phase will not be discussed further.

##### 5.1 AOCS Design phase

This phase of the AOCS design life cycle is a general task. However, for reasons of efficiency it should be kept in mind that software or models, developed during this initial phase, should be re-usable in later phases of the AOCS design life cycle.

At the start of this phase the AOCS is defined in concept. To be able to evaluate various options and alternative solutions the spacecraft dynamics, AOCS units and environment are modelled mathematically and implemented in a non-real-time simulation. Various AOCS units will be assessed with respect to aspects as accuracy and dynamic range, usually evaluated in simulations, but also other items like costs are important.

Control laws and on-board algorithms are conceived and parameters are chosen. The control laws and on-board algorithms are added to the non-real-time dynamics simulation.

Non-real-time simulations are run to investigate various effects and to support design choices. The main driver in this phase is a flexible but orderly way to evaluate various possibilities and options. The resulting detailed design specifications serve as inputs for the final (detailed) design of the AOCS software.

Detailed verification and validation of the total AOCS design result in reference runs to support following test and verification phases.

The design work and detailed design verification and validation work should be possible using a work

station, chosen with emphasis on available (AOCS) design tools on one hand, and on the portability of the AOCS software design to the TVE on the other hand. AOCS designs must be portable by use of well accepted design tools. Industry standards are MATRIXx, MATLAB.

Modern computer aided engineering tools for design, development and simulation of control laws and plant simulation models should support:

- interactive graphical design;
- specification of models by means of various representations like: state space, differential equations, transfer functions;
- reusable models and submodels;
- interactive simulation command and control (changing parameters, injecting errors, restarting from a known state).

The final (baseline) AOCS design will serve as input for the requirements specification for the units or components. The most important 'units' for the development of project specific items related to the TVE are the AOCS ACC emulation software and the TVE dynamics simulation software. As these are the complementary components of the closed loop, to be developed usually at disjunct locations, the missing part of the loop is needed for on-site testing and validation.

#### 5.2 Development of TVE test environment

In this intermediate phase the TVE is prepared for the next phases. Re-use of models and other software from the design study is valuable to prevent costly duplication of work. Also the validation of (sub)models is less complicated if the design information is used unchanged.

The operations have to be extended with failure mode simulation and other items usually untouched in overall design studies (e.g. thermal modelling of electric parts of units). Also realistic Input/Output for spacecraft subsystem bus and the TVE-FE environment has to be modeled. The goal of the dynamics part of this phase is to use this in later phases without further changes. The validation of the enhanced dynamics simulation, later to be run in real-time, is performed with the additional simulation of the control laws, also extended with special TVE and subsystem bus related I/O code. Pseudo-real time for debugging purposes is allowed, but the validation of the dynamics must mandatory include the proof of the real-time capability.

#### 5.3 Software and hardware integration

Once the on-board ACC control software has been produced (possibly incremental) and tested on a cross development system, it must be run in the target ACC (breadboard) hardware. It is a task of the TVE, to provide an environment hereto. The attitude control software runs, unmodified, on the flight hardware in a realistic environment with system (OBDH) and subsystem bus (MACS) connected and supplied with realistic data.

Hard real-time requirements apply for the TVE, as the ACC operates in real time and must not be aware of any differences with actual flight conditions. These requirements will vary partly from project to project, mainly depending on the frequency content of the attitude control motion. An AOCS control cycle of 20 Hz should be supported.

The high-level and low-level processors of the TVE Front End have to be designed to enhance the capabilities of the work station software in this respect. Functional simulation of unit failures is essential, as only in this phase the flight software can be confronted with gradually degrading

units. This type of simulation has to cover all possible failure types, from spurious, single bit failures to complete inoperative units.

The ground communication must be realistic in content and timing for the ACC. Both flexible operator driven testing as completely repeatable (file driven) runs are required.

Complete analysis of raw data is used for detailed low level debugging actions, while more global attitude behaviour over extended periods must be presented both graphically and numerically in engineering values. Detailed analysis and verification of the spacecraft bus timing must be supported in a user friendly way.

User friendly control of the test set-up and on-line display of major parameters is important for monitoring the evolution of tests. Automation is important for the more complex test scenario's. On the other hand, during initial integration of equipment, fast and complete access to all data is necessary.

The project specific characteristics of tests need the involvement of a "TVE project programmer", to define the project specific abstract data types, default displays, etc.

#### 5.4 Subsystem level integration and test

In this phase the subsystem is gradually built from the previous phase to a complete hardware system. Due to the earth environment, the AOCS components are assembled on a static test bench. The real hardware AOCS units, not necessarily all, are connected to the subsystem bus. Hence they are not allowed to be simulated by the Front End, but the units are stimulated by the Unit Stimulus Interface.

Health monitoring of the real AOCS hardware is now essential. Automatic actions on unsafe conditions must be supported to prevent damage. For example: gyro temperature, over-illumination of low intensity (star) sensors.

Noise and error simulation of the previous phase is absent, as the unit itself creates its errors, and it must be possible to use (breadboard) flight equipment. One of the goals of tests in this phase is to confirm the equivalent behaviour of the AOCS as a whole in comparable test scenarios. This implies that it must be verified that the real equipment behaves equivalent to the simulated equipment in the same situations.

The influence of the test set up will be compensated for, e.g. earth rotation sensed by gyroscopes, support forces (1 g) sensed by accelerometers.

#### 5.5 System level integration and test

In this phase the AOCS is assumed to be completely validated, and is integrated in the spacecraft. The system bus in use is not a simple link between the TVE Front End and the ACC, but the real hardware bus. This bus is controlled by the real Central Terminal Unit, that on its turn is controlled by some test equipment of its own. The Telemetry and Telecommands are expected to be passing through this Special Test Equipment. The Telemetry is distributed over a network to various applications, like the TVE Test Software. Also Telecommands will be routed across this path. However, the timing between Telecommand and Telemetry compared to previous phases is different.

A subset of subsystem tests is to be repeated, with possible adaptations due to the different link.

Also the stimulation of AOCS units is sometimes not possible, so that the scope of the tests must be limited.

## 6 THE TEST AND VERIFICATION EQUIPMENT

### 6.1 TVE overall concept

The TVE can be split functionally or logically and physically into modules, that have a natural overlap, but are not identical. In the ultimate implementation a number of additional modules, like communication between physical components, will be identified.

Functionally have been defined:

- External Bus Interfacing (EBI), that performs all control of the attached spacecraft buses and bus related timing, control and formatting of data: system bus interface (prototype OBDH), subsystem bus interface (prototype MACS), unit stimuli interface (prototype none);
- Test Software (TSW) containing the general basic functions for test preparation, control of test execution, automatic data analysis (monitoring), data archiving and man-machine interface (including data presentation to the test conductor and manual commanding);
- Simulation Software containing the project specific spacecraft attitude and orbit dynamics, orbital environment and functional unit simulation.

Physically there are two basic components:

- Front End (TVE-FE) containing:
  - the physical low-level spacecraft bus interface electronics,
  - associated high-level protocol processors,
  - (parts of the) simulation software and
  - the communication software to the TVE host;
- Host computer system(s) consisting of:
  - a work station containing the TVE Test Software,
  - (parts of the) simulation software and
  - the communication software to the TVE Front End.

For the relation between the functional and physical definitions other mappings are possible. The high frequency parts of the attitude dynamics simulation could be located in the Front End for performance reasons (assuming that the link between TVE host and TVE Front End is the limiting factor). Other low frequency parts of the simulation still could be located in the host. The communication between the TVE Front End and the TVE Host is called: "TVE Front End to Test Software Interface", where a generic TVE protocol level data type interface has been defined, allowing the buses to be replaced by other physical buses. The high level interface processors are in charge of the translation of the data types.

### 6.2 TVE Front End concept

The interfaces with the System and Subsystem buses have to work in the microsecond range (MACS and OBDH buses feature e.g. a word duration of 50 respectively 64  $\mu$ s). Currently available processors are able to perform a substantial amount of logic processing within such a time frame.

Taking into account the number of functions required, this calls for a design whereby the low level functions (directly interfacing with the bus

hardware), and the higher level functions (formatting, protocol processing/conversion, and communication with Test Software), are dealt with on separate processor boards.

The high level can be accommodated on standard Single Board Computers, the time frame being here in the milliseconds range.

The MACS and OBDH bus interface both feature one board accommodating the high level functions, and one or more boards for the low level functions, depending on the number of components required. The number of boards required for the stimuli bus depends on the particular bus standard selected; a number of Single Board Computers accommodate interfaces for the standard buses on the same board, which may result in only one board needed. One processor board is used for the interface with the Test Software.

### 6.3 TVE Test Software

Simulation, i.e. the modelling of the behaviour of systems and processes to represent the actual characteristics of a system, is playing an increasingly important role in several stages of design. Similarities exist with NLR's National Simulation Facility (NSF), providing a research and development facility for realistic man-in-the-loop (i.e. aircraft pilot) simulations, possibly with hardware-in-the-loop. In order to facilitate simulation of different vehicles, such as fighter aircraft or ground vehicles, a generic software tool called "Simulation Program", has been developed. The design of the Simulation Program is such that it is a generic simulation tool that can be used for design, verification, test and training of a wide range of applications, including simulators for space programmes. See reference 11.

The existence of a software simulation environment reduces the work of the future TVE programmer to the specification of models of the spacecraft dynamics and functionality of units. The communication with the TVE Front End includes the conversion from abstract data type (of the models) to the protocol data type (of the Front End). Further the existing control language is extended with Front End specific commands, to enable the user by means of scripts or by a Graphic User Interface, to set up the Front End, initialise the test scenario's and to monitor the overall process. In particular the test is controlled by sending Telecommands from scripts, as a simulation of the Ground Station.

In order to optimise working conditions and to satisfy specific requirements that must hold in each stage of design, development and testing the Simulation Program consists of two separate tools:

- the Simulation Development Software tool (SDS), and
- the Real-Time Simulator Software tool (RTS).

The Simulation Development Software tool is used to develop and test simulation models and prepare data files that are used during real-time simulation by the Real-Time Simulator. Due to the safety requirements imposed on simulations with a human-in-the-loop and/or hardware-in-the-loop, the simulation models must be tested thoroughly. For this, the Simulation Development Software tool offers a user friendly environment to develop and test software models. The Real-Time Simulator is a generic software environment for execution and control of real-time simulation runs. The Real-Time Simulator performs timing control of the simulation tasks (e.g. simulation models, communication with hardware), and user control of the complete simulation and test run using a Graphical User

Interface. Simulation tasks are executed in a sequence based on dependencies, frequencies, etc. which are defined in the schedule file. If no dependencies are defined the scheduler itself determines the proper order of execution.

The interface between the Simulation Development Software tool and the Real-Time Simulator is described by an Interface Control Document, which defines the format of all data files between the two tools. A special data file contains the structure of the "global simulator data" memory. Other data files are used to define "model parameters", "data conversion" and "mission definition", and the "schedule file" that are to be used in the Real-Time Simulator.

## 7 ACKNOWLEDGEMENT

This paper has been based on work performed under contract with the European Space Agency (ESA), the Netherlands Agency for Aerospace Programmes (NIVR), Fokker Space & Systems and Alenia Spazio. The work of Mr. B. Storni of Adelsy, Switzerland in the development of the Front End equipment for the MACS-TSA, SAX-TSA and TVE is gratefully acknowledged.

## 8 REFERENCES

1. Liroy, S. and Finocchiaro, G., SAX (X-ray) satellite design performances, IAF-88-415
2. Finocchiaro, G., Santoro, P. and Attinà P., Design and Verification of the SAX Satellite, IAF-93-Q.2.386
3. Kampen, S. and Kouwen J., Design and Development of the SAX-AOCS Control Software. 1st ESA International Conference on Spacecraft Guidance, Navigation and Control Systems, 4-7 June 1991, Noordwijk, the Netherlands.
4. Selig, A.M. and Karsten, L., Fault Detection Isolation and Recovery within the AOCS of SAX. 1st ESA International Conference on Spacecraft Guidance, Navigation and Control Systems, 4-7 June 1991, Noordwijk, the Netherlands.
5. Hameetman, G.J. and Dekker, G.J., The development procedures and tools applied for the Attitude Control Software of the Italian Satellite SAX. NLR TP 93198 L, AGARD-CP-545, Aerospace Software Engineering for Advanced Systems Architectures, 10-13 May 1993, Paris, France
6. Dekker, G.J. and Hameetman G.J., The development of flexible software for the Italian/Dutch satellite SAX. NLR TP 91288 U, AIAA conference on Computing in Aerospace 8, 21-24 October 1991 Baltimore, Maryland, USA.
7. Battistoni, G., Cassi C. and Ravazzotti M.T., SAX AOCS subsystem simulation and tests, Results evaluation and plan for future developments. 2nd ESA International Conference on Spacecraft Guidance, Navigation and Control Systems, 12-15 April 1994, Noordwijk, The Netherlands
8. Wallace, S., Accelerating engineering. BYTE, July 1994, pp 62-76.
9. Sonnenschein, F.J. and Keppel H., The MACS-TSA applied in the ISO and SAX spacecraft projects. NLR TP 92134, 1992 European Simulation Multiconference (ESM92), June 1-3, 1992, York, UK.
10. Sonnenschein, F.J., et.al., A new generation Test and Verification Equipment for Attitude Control Systems. NLR TP 94142 L, 2nd ESA International Conference on Spacecraft Guidance, Navigation and Control Systems, 12-15 April 1994, Noordwijk, The Netherlands
11. Dam, A.A. ten, Schrap P. and Brouwer W. The Simulation Program of the National simulation facility NSF. To be presented at the 3rd workshop on Simulators for European Space Programmes, november 1994, Noordwijk, The Netherlands.

## NASA TECHNOLOGY FLIGHT EXPERIMENTS PROGRAM

Stephen L. Prusha, Jet Propulsion Laboratory, California Institute of Technology

Jack Levine, NASA Headquarters

Samuel C. Russo, Hughes Aircraft Company

Mr. Jack Levine, Director, Flight Programs

NASA Headquarters, Mail Code CF

Washington, DC 20546, USA

### Summary

In addition to its scientific and life sciences experimental programs, NASA conducts flight experiments directed at development of space systems technologies. The experiments are conducted to obtain research data, to evaluate the performance or operation of experimental hardware in the space environment, or to validate components, subsystems, or systems prior to application in future spacecraft or missions.

The requirements for specific technology experiments, and the priority assigned to them, vary significantly depending on the maturity of the technology. Some of the flight experiments address technologies still in the early research stage, while others are conducted to validate technology at relatively advanced levels of maturity. This paper discusses the overall technology flight experiments program and reports in some detail on four current or recently flown experiments ranging from research to technology validation at the system prototype level.

### Introduction

Because of the cost of access to space and the cost of modern spacecraft and missions, designers and project managers cannot afford the risk of using components or subsystems incorporating untested or unvalidated technologies. Ground testing and simulation capability can often serve adequately in validating a new technology. However, there are still many instances in which the effects of microgravity, radiation, or other space environmental factors simply cannot be tested or modeled on the ground. In-space experimentation may be essential to resolving key questions of understanding, or developing a reliable design data base, or validating the performance of a component or system in the actual operational environment.

In-flight experimentation has been used in aeronautics research and development for many years. Both military and commercial aircraft have been modified for use as research aircraft or technology demonstrators. The Air Force/Calspan T-33 and C-131 in-flight simulators in the United States, the DLR VFW 614 and BO 105 aircraft and helicopter in-flight simulators in Germany, and similar vehicles in other countries have proven valuable in evaluating advanced control and other concepts prior to application in new aircraft developments. On several occasions these experimental aircraft have also been used to investigate advanced control systems being designed for space systems such as the Space Shuttle and Hermes.

Over the years, the aeronautical community has refined the process of progressing from conceptual study through computational analysis, ground testing, and simulation -- to flight testing when justified as a necessary extension to these earlier steps. Because flight experimentation may be quite costly, the necessity must be clear.

In-space experimentation is a relatively new capability. But experience in operational space flight and space environment characterization is still limited, and operational space system deployment is very expensive. For these reasons, and with increasing availability of suitable test vehicles, in-space experimentation is already a large and growing activity which is becoming a valuable tool in space systems design and development. However, because it is generally even more expensive than atmospheric flight testing, the process of selecting experiments must be even more rigorous.

Many of NASA's manned space flight, exploration, and scientific missions have themselves been experimental in nature. And considerable technology validation has been accomplished during some of the primary mission programs, either of necessity or because it was deemed more economical than experimentation prior to program initiation. This paper discusses only experimentation on technology -- technology deemed important for future space systems but not yet been specified for incorporation in a particular system development.

### Technology Flight Experiments Program

The NASA technology space flight experiments program is conducted to obtain research data, evaluate the performance or operation of experimental hardware in the space environment, or validate concepts, components, subsystems, or systems prior to application in future spacecraft or missions. The information is used to validate models, verify ground prediction, and -- most importantly -- reduce the risk of incorporating new technology in future systems.

In addition to developing technology for its own missions, NASA has responsibility for facilitating the transfer of space technology to the military, to other user agencies, and to industry. The flight experiments provide an effective mechanism for validating maturing technologies not yet adopted for incorporation in operational systems. The high cost of space access mandates that only those technology experiments which clearly require exposure to the space environment, or which are most cost-effective relative to ground testing, be selected for flight. It



also dictates that reduction of experiment cost must be a continuing and vital requirement.

A wide variety of launch vehicles and platforms may be utilized for the in-space experiments, with the choice depending on experiment requirements and cost considerations. Expendable launch vehicles (ELVs) ranging from small sounding rockets to Titans with piggyback upper stages are used when appropriate. The Shuttle Orbiter has been a particularly great asset, with experiments carried in the middeck (Figure 1), in simple "getaway special" ("GAS") cans mounted on the side wall of the cargo bay (Figure 2), or in autonomous payload packages which provide their own power, thermal, data, and telemetry capabilities. Experiments which require larger volume or weight, or may need access to Shuttle avionics, data or other services, may utilize carriers called Hitchhikers located in the Shuttle bay (Figure 3). The Columbia flight early in March 1994 carried the largest number of engineering research and technology experiments -- eleven in all -- ever flown on a single mission.

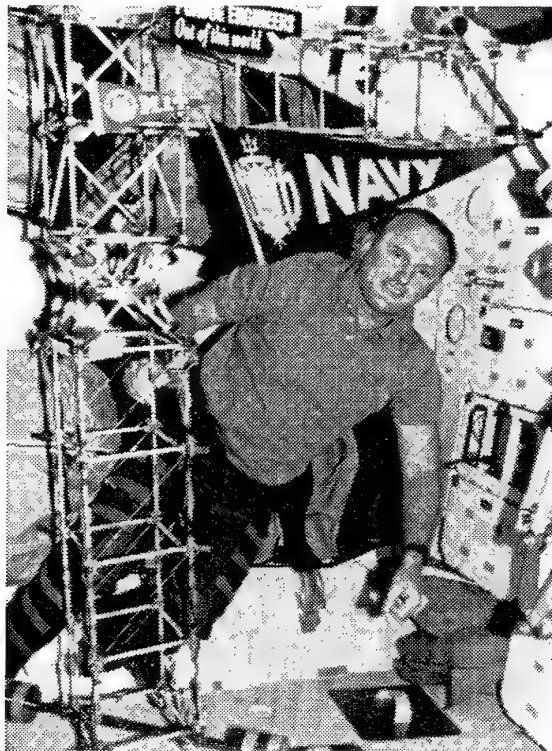


Figure 1: Middeck 0-Gravity Dynamic Experiment (MODE) performed in the Shuttle Middeck

The SPACEHAB carrier, providing additional middeck facilities in the Shuttle bay (Figure 4), has recently become operational and its two flights have already included several significant technology experiments. Free flyers placed in space by either ELVs or Shuttle (Figure 5) provide another option.

And technology experiments are now being planned to utilize the unique capabilities of International Space Station Alpha (Figure 6).

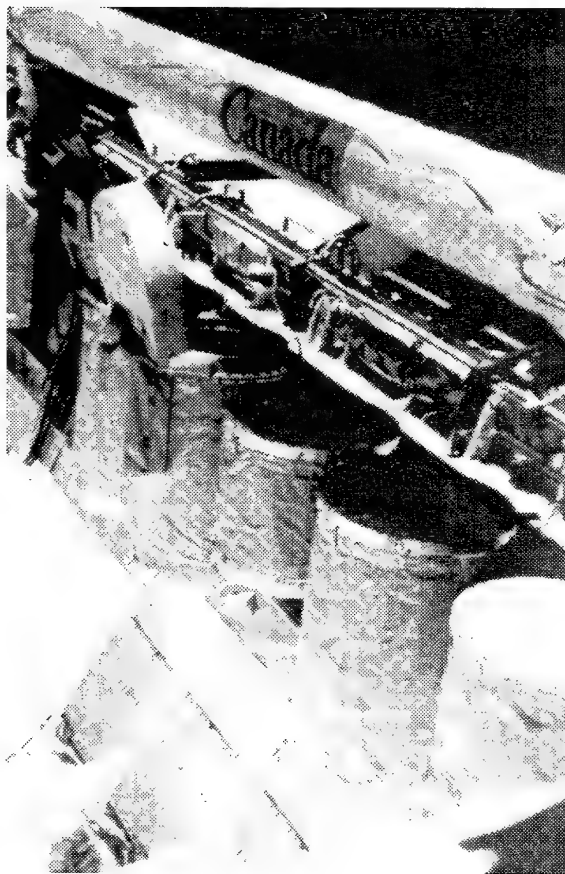


Figure 2: Get Away Special (GAS) cans in shuttle bay

The need for flight experimentation is generally based on requirements for one or more of the following issues:

- 1) Extended microgravity operation: Drop towers and suborbital rockets can be used for microgravity testing only on the order of seconds to minutes. Many experiments, however, require much more prolonged microgravity conditions -- for example, to achieve steady-state operation in experiments on fluids, to permit sample changes, or to maintain the high-quality microgravity environment necessary for crystal growth experiments.
- 2) Exposure to space environmental effects: The complex space environment is not sufficiently understood and modeled to allow duplication or simulation on the ground. Effects of atomic oxygen and other atmospheric constituents, orbital debris, exhaust plume or other contamination, and radiation on exposed payloads and/or materials are not completely known or



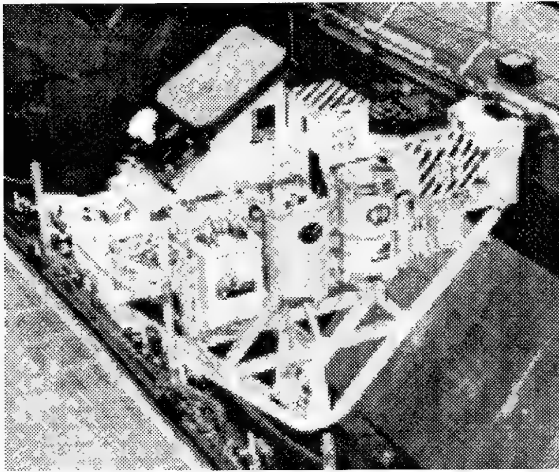


Figure 3: Experiments mounted on Hitchhiker carrier in shuttle bay

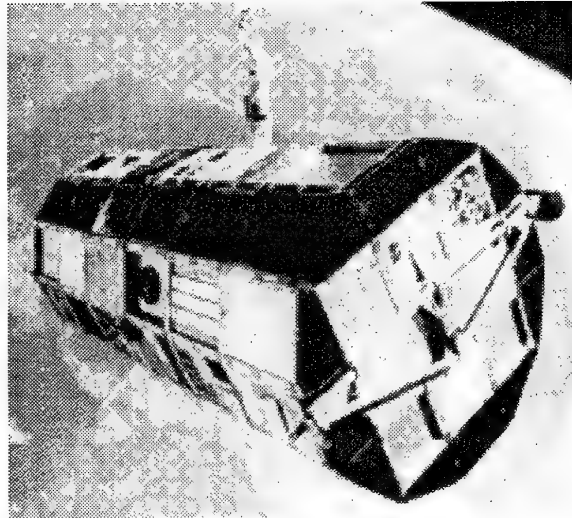


Figure 5: Long Duration Exposure Facility (LDEF)

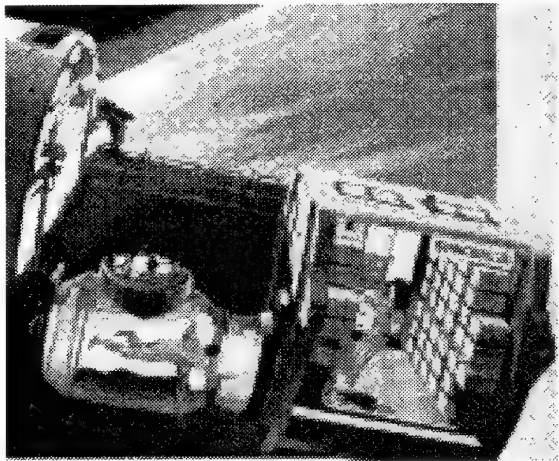


Figure 4: SPACEHAB complements middeck experiments capability

understood. The random nature of these effects, particularly the radiation effects, makes ground duplication difficult or impossible.

3) Exposure to the complex operational environment: The nature and complexity of the environment and operations in space necessitates some in-space evaluation of technology. In particular, operations requiring extravehicular activity, teleoperated robotics, or other man-in-the-loop functions are not effectively simulated on the ground.

4) Orbital "viewing" environment: Validation of technologies for optical or other sensing or communication systems depending on earth-viewing orientation may demand space experimentation. In addition, although aircraft or

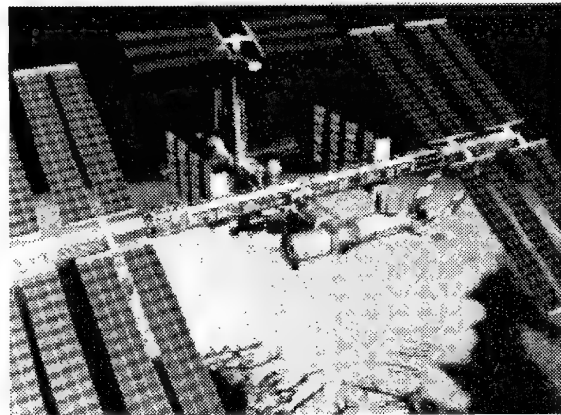


Figure 6: International Space Station Alpha (ISSA)

balloons may be adequate for some purposes depending on the spectrum and the need for radiation exposure, reliable testing of some sensing devices or subsystems may be possible only above the atmosphere.

The requirements and priority for different types of technology experiments vary significantly depending on the maturity of the technology in question. In our experiment planning, we have found it helpful to use a Technology Readiness Level (TRL) -- an incremental scale indicating the maturity of a particular technology or system. The TRL scale (Figure 7) is not meant to be a high-precision instrument or an absolute discriminator. However, it can illustrate the differences among various candidate experiments with respect to requirements and the value of anticipated returns. The TRL also serves as a basis for consideration of the evaluation, timing, benefit/cost assessment, and selection of candidate experiments.

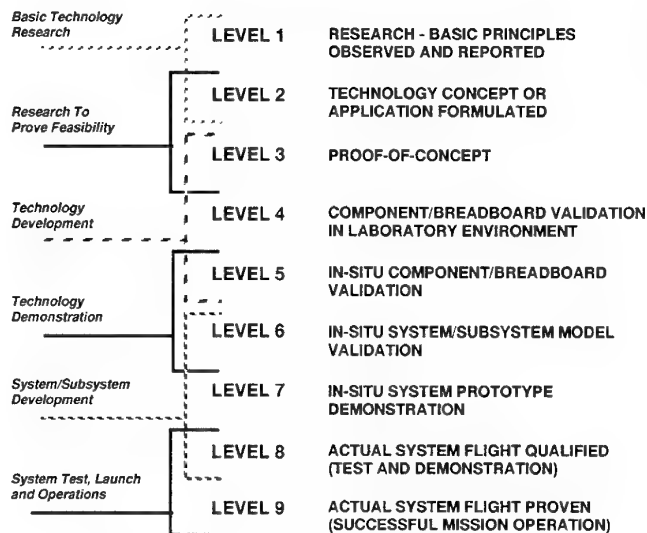


Figure 7: Technology Readiness Levels (TRL)

The nine technology readiness levels shown in the TRL scale range from the understanding of basic physical principles to the deployment of a "flight proven" system. The flight experiments primarily address technology validation at levels 5-7, but may also support research at level 1. Required testing above TRL 7 is generally considered mission- or system-specific and is conducted in development programs rather than as technology experiments. Examples of experiments at TRL 1, 5, 6, and 7 are described later in the paper.

Technology experiment requirements are defined by the "user community" -- the specialists responsible for developing the mission and spacecraft requirements for NASA's manned and unmanned science and exploration programs and for industry space systems. In the In-Space Technology Experiments Program (INSTEP), experiments are proposed in response to a NASA announcement of opportunity, and are evaluated by peer review teams which include the user community and other experts. A rigorous selection process applies strict discipline in feasibility study and cost analysis during the early (low cost) stages. Each selected experiment is subjected to a final intensive "non-advocate" review before entering the flight development phase. Because of the rigorous selection and review discipline, we have been able to maintain an extremely good record of experiment success and cost and schedule performance.

### Representative Experiments

To illustrate the program in this paper we have chosen as examples four current or recently flown experiments. They include one engineering research experiment conducted at a very early point in the technology maturation process and three system validation experiments involving technologies at different levels of maturity. A more complete

summary of current and recent experiments is included in the Appendix.

- The Experimental Investigation of Spacecraft Glow (EISG) is a research experiment developed by Lockheed Missiles and Space Company to determine the intensity and causes of spacecraft glow at various attitudes and altitudes. Experiment results will be used to develop coatings and other means to reduce the effect of surface/plasma glows on optical instruments in low earth orbit.

- The Tank Pressure Control Experiment (TPCE) is a Boeing Aerospace Company experiment, first flown in 1991, to test the effect of jet mixing of cryogenic fluids to help control pressure in cryogenic tanks. Results will be used to design lighter-weight cryogenic tanks for future space flights.

- The Heat Pipe Performance (HPP) experiment, designed by Hughes Aircraft Company, was flown in 1993 to test the microgravity performance of various types of heat pipes to be used on spinning spacecraft.

- The Cryo System Experiment (CSE), also developed by Hughes Aircraft Company, is a system-level experiment designed to validate the operation and performance of a 65 K cryogenic cooler and oxygen heat pipe in the space environment.

These four industry-proposed and fabricated experiments have all flown successfully with the exception of the CSE experiment, which is presently manifested for flight in early 1995. They are discussed with reference to the level of technology maturity and the specific driving requirements for space flight experimentation in each instance. In addition, the nature and benefits of the results are described. Results are discussed in the context of their impact on technology development and subsequent product development. The CSE is detailed as a case study to describe the role of in-flight testing in the development of a technology for an actual product development.

### Experimental Investigation of Spacecraft Glow<sup>1,2</sup>

The Experimental Investigation of Spacecraft Glow (EISG), a TRL 1 technology research experiment, was flown on Shuttle flight STS-62 in March, 1994, to study and characterize spacecraft glow (Figure 8).

Spacecraft glow is a well-known but little understood phenomenon encountered in many spacecraft including the Space Shuttle (Figure 9) and low-earth-orbit (LEO) imaging free-flying spacecraft. The glow could potentially degrade the performance of optical instruments operating in low earth orbit, especially in the far ultraviolet (FUV) region, by optically

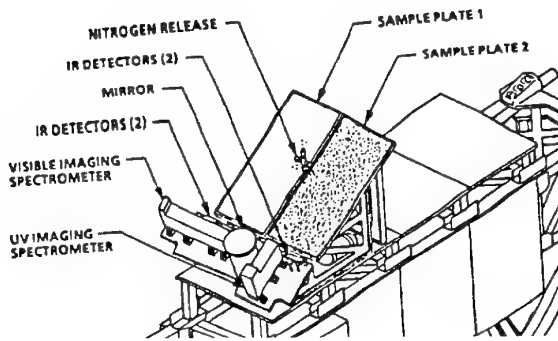


Figure 8: EISG experiment mounted on Hitchhiker (also shown in Figure 3)

contaminating the imagery. It has not been known whether the phenomenon was primarily a surface (i.e. materials) issue or a spacecraft environmental/atmospheric interaction issue. With the fundamental physics not well understood, it was not possible to develop effective countermeasures. Previous flight experiments had attempted to achieve glow characterization, but only over a very narrow spectrum and at a fixed altitude. The EISG experiment covered a large spectrum, from FUV through 5.6 micron infrared, at orbital altitudes from 105 nmi to 160 nmi, and varying spacecraft attitude.

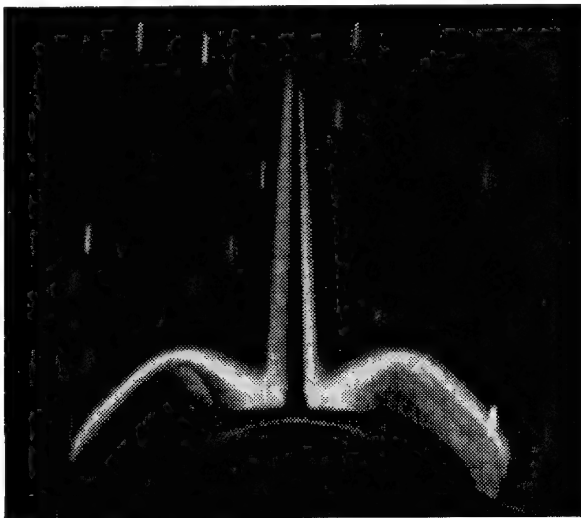


Figure 9: Obiter Glow viewed from aft flight deck

The experiment consisted of a large (1.0 x 1.0 meter) thermally-isolated sample plate, half of which was coated with a black paint typically used in instrument baffles (Z306 Chemglaze) and half with a white, insulating paint commonly used in spacecraft applications (A276 Chemglaze). The area above the sample was viewed by visible (VIS) and far ultraviolet (FUV) spectrometers, a FUV photometer and infrared (IR) radiometers to characterize spacecraft

glow under a wide variety of conditions. In addition, a US Air Force payload was used to augment the experiment and provide simultaneous observations of glow phenomena in the infrared regime. The Spacecraft Kinetic Infrared Test (SKIRT) article consisted of a cryogenically cooled infrared spectrometer dedicated to glow characterization in the 1.0 - 5.0 micron spectral wavelength region. The experiment set out to study surface and gas cloud glows over a wide range of wavelengths; to identify and characterize the atoms and molecules responsible for these emissions; and to determine how glow intensities vary as functions of material coatings, surface temperatures, orbital altitudes, and ram attitude angles. The EISG also contained a nitrogen ( $N_2$ ) gas release system to study basic chemistry with the ram atmosphere which was expected to produce glow producing compounds. Studies also addressed thruster contamination and glows associated with thruster-effluent-doped surfaces.

Data from the experiment is now providing new insights into the fundamental physics of spacecraft glow and the atmospheric chemistry which causes it. Incomplete preliminary assessment of the data verified that the glow phenomenon is primarily a surface effect and is therefore likely to be affected by material/coating selection for the optical instruments. It also validated that the black baffle paint is an effective material for FUV imaging devices and that the nitrogen release did not affect glow emissions in this region, meaning that nitrogen can be used as an effective cryogen in these instruments without fear of contamination due to nitrogen venting. Glows in the visible wavelengths were observed to change drastically with altitude, as expected, but were significantly -- and unexpectedly -- reduced during nitrogen releases.

As expected with this and other TRL 1 experiments, the results bolstered our knowledge of the physics involved and provided some insight into the nature of effective countermeasures, but did not specifically validate a technology for use in future optical systems. Follow-on experiments are being considered that would further the research by adding a mass spectrometer to characterize particular chemical species and, in addition, would validate the glow-reducing properties of selected materials and coatings.

#### The Tank Pressure Control Experiment (TPCE)<sup>3</sup>

Developed by the Boeing Company, the Tank Pressure Control Experiment (TPCE) (Figure 10) is a TRL 5 space experiment developed to meet the need for a critical aspect of cryogenic fluid management technology -- that is, control of storage tank pressures in the absence of gravity by forced-convective mixing. The experiment, first launched aboard Shuttle STS-43 in August, 1991 as a GAS payload (Figure 11), used Freon-113 at near-saturation conditions, at a constant 84% fill level, to simulate

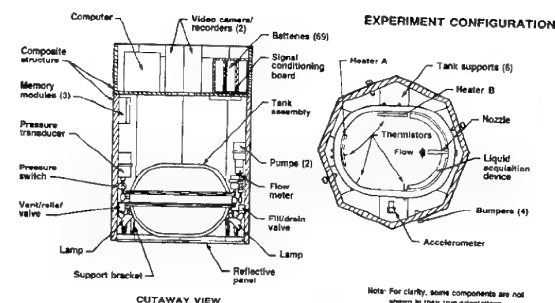


Figure 10: TPCE Experiment

the fluid dynamics and thermodynamics of cryogenic fluids in space applications. The objectives of TPCE were to characterize the fluid dynamics of axial-jet-induced mixing in low gravity, to evaluate the validity of empirical mixing models, and to provide data for use in developing and validating computational fluid dynamic models of mixing processes.

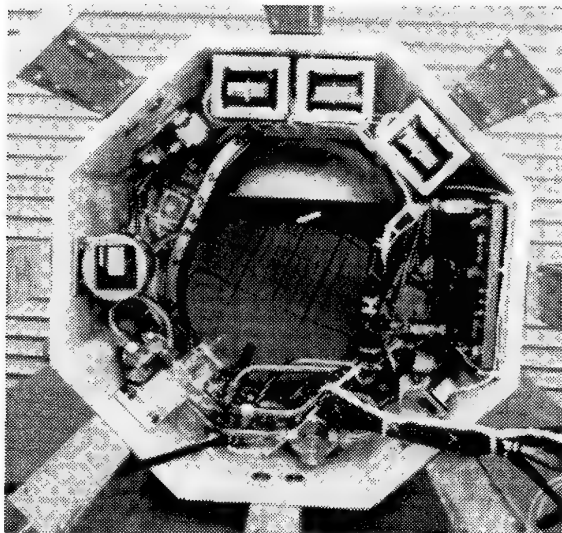


Figure 11: TPCE hardware mounted in GAS can

A reflight of the TPCE experiment was successfully completed on STS-52 in October, 1992, to examine a potentially-serious pressure spike phenomenon that was observed on the first flight. The observed pressure spikes, which are the result of sudden nucleation and flash boiling when a fluid is heated over a long period of time, could conceivably result in loss of mission if it were to occur in an operational orbiting cryogenic propellant tank. Unexpected prior to the initial TPCE flight, the phenomenon is now understood and preventive measures have been developed as a result of the second flight.

Representative results from the original flight are

shown in Figures 12 and 13 and demonstrate the efficacy of jet mixing for control of pressure and temperature. Data demonstrated that the flow patterns observed generally agreed with a prior correlation derived from drop tower tests, and several existing mixing correlations were found to provide reasonable performance predictions. Low-energy mixing jets, dissipating on the order of one percent of the kinetic energy of previous mixer designs, were found to be effective and reliable at reducing thermal non-uniformities, promoting heat and mass transfer between the phases, and reducing tank pressure. It was found that active mixing, whether continuous or periodic, offers increased reliability and predictability in space cryogenic systems, and can be accomplished with no significant boiloff penalty caused by kinetic energy dissipation.

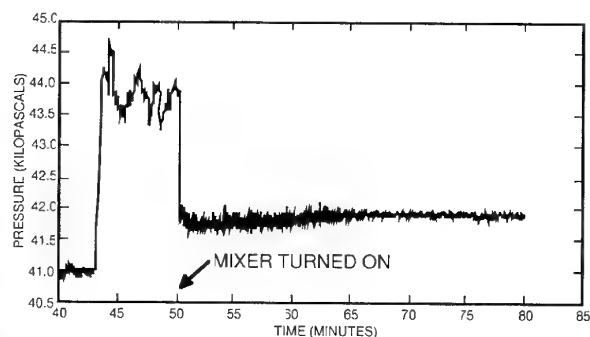


Figure 12: TPCE pressure control

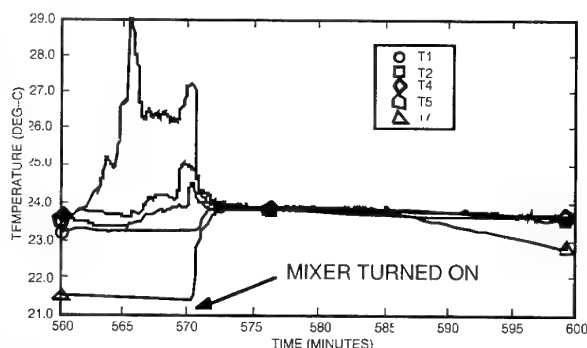


Figure 13: TPCE typical temperature measurements

This experiment demonstrated the validity of an important concept for pressure control of stored cryogenics in microgravity. It was typical of TRL 5 experiments in that completion of the experiment did not provide sufficient data for infusion of the technology in operational flight systems, and that the experiment, as designed, was fairly qualitative in the definition of its hypothesis and, hence, its data requirements (primarily video). It also provided significant insight into the physics of microgravity fluid handling and the thermodynamics of pressure control, information which has been of benefit in

understanding problems encountered with liquid-electrolyte batteries used in various space systems. The experiment is presently being prepared by student investigators for a third flight to investigate the effectiveness of jet mixing for pressure control in tanks at 40-50% fill level, a more realistic scenario in operational space systems than the 84% fill level previously flown.

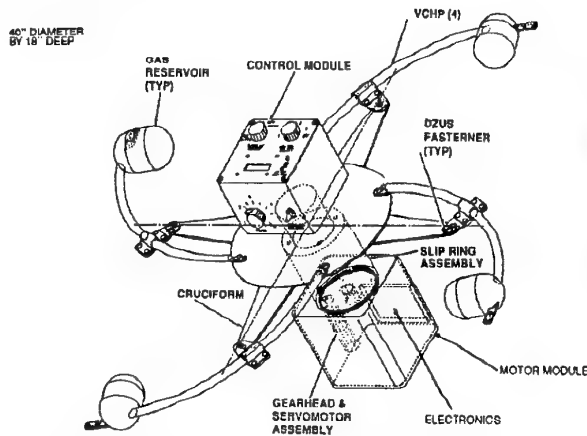


Figure 14: Heat Pipe Performance Experiment Configuration

#### The Heat Pipe Performance Experiment (HPP)<sup>4,5</sup>

The Heat Pipe Performance Experiment (HPP) is a TRL 6 experiment developed by Hughes Aircraft Company (Figures 14 and 15). It is a middeck experiment flown aboard the STS-52 mission in October 1992. HPP tested fixed conductance and variable conductance heat pipes at different rotational speeds to determine their transport capability, rewicking times, and the influence of body forces on the liquid distribution.

The primary mission objectives of the HPP were to obtain quantitative data on the thermal performance of heat pipes in a microgravity environment and to determine the performance of heat pipes as a function of the body force associated with different rotational speeds. The experiment evaluated the sensitivity of 14 state-of-the-art heat pipes to small and large accelerations by obtaining quantitative data showing spatial and temporal profiles under operational and recovery conditions. Flight test results were correlated with 1-g static test results and analytical models for both axially grooved and fibrous wick designs. Rewicking tests were also conducted to determine the time it takes for a heat pipe to reprime and operate isothermally after it has been deprimed due to excessive spin forces. As a result of the flight, a large database on the performance and behavior of heat pipe operation in microgravity was obtained. Application of HPP data will lead to improvements in current heat pipe computer modeling and predictive capabilities. Results of the experiment already

confirm that heat pipe design engineers have been too conservative in extrapolating ground performance data to zero-g. In some cases, the orbital performance was 35% to 40% better than ground performance. These results, which substantiated analytical predictions, will allow more confidence in the analytical models, leading to less conservative heat pipe design and ultimately to lighter and more efficient spacecraft. The data also enables less extensive ground testing of production axial groove heat pipes, contributing to directly lowering the cost of these activities.

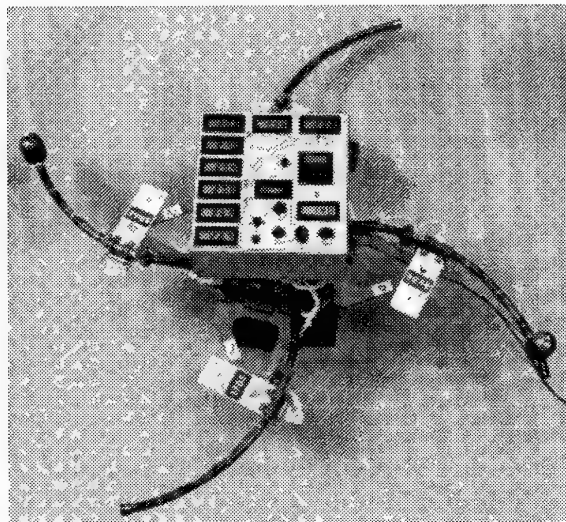


Figure 15: HPP hardware

HPP was designed to accept multiple "competing" heat pipe components or subsystems to trade off performance against other parameters (e.g. cost, manufacturability, flexibility) in an operational scenario. Inasmuch as heat pipe thermal control systems have been qualified and in fact are operational, the validation of new heat pipe configurations, materials, or working fluids at this component/subsystem level requires no system-level validation and offers a cost-effective avenue to thermal control system improvement for future space systems.

#### The Cryo System Experiment (CSE)

The Cryo System Experiment (Figure 16) is a TRL 7 space-flight experiment conducted by the Hughes Aircraft Company in a cooperative program with NASA. The overall goal of the Cryo System Experiment is to validate and characterize the on-orbit performance of two thermal management technologies that comprise a hybrid cryogenic system. These thermal management technologies consist of: 1) a new-generation long-life, low-vibration 65 K Stirling-cycle cryocooler, and 2) an oxygen diode heat pipe that thermally couples the cryocooler and an energy storage device while charging. The experiment is necessary to provide a high-confidence



CSE Flight Configuration Cryo Elements

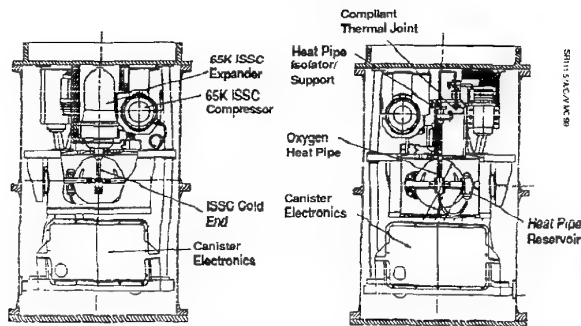


Figure 16: Cryo System Experiment

zero-g database for the design of future cryogenic systems for NASA and military space flight applications.

These technologies promise to satisfy many of the currently defined cryogenic system performance goals for planned NASA and military space programs. The Cryo System Experiment is the next step in the technology development process. Feasibility of each technology has already been demonstrated in Hughes independent R&D ground-based laboratory tests. However, questions raised by the scientific community relative to the performance of these components in a 0-g environment must be answered before these technologies can be optimized for application to flight systems. The flight experiment is configured to: (1) provide data necessary to resolve performance and design issues, (2) validate capability of the hybrid cooling system to meet future mission requirements, and (3) provide for high confidence design optimization of flight system concepts currently being considered.

During on-orbit operation, test data will be recorded to characterize performance of the technology including: (1) oxygen diode heat pipe temperature gradient and transport capacity in steady-state and transient conditions, (2) system vibration levels attributed to the active cryocooler, and (3) integrated, extended operation of the cooling system.

Before proceeding with the design of operational flight systems, an accurate correlation between 1-g and 0-g data is essential to predicting the performance of oxygen heat pipes in 0-g environment. Due to the poor capillary pumping capability of oxygen, there is serious concern in the scientific community that 1-g testing is optimistically influenced by puddle flow and therefore results cannot be extrapolated to 0-g performance. An understanding of the flight performance of these components is required to develop accurate performance models for designing flight hardware. Key issues to be addressed include unsteady heat transfer capacity and start-up behavior. Extended on-orbit operation is necessary in order to

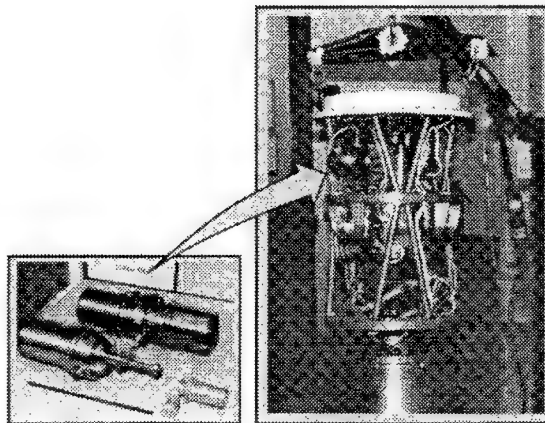


Figure 17: CSE cryocooler and GAS configuration

resolve this issue.

The cryocooler to be used for the experiment is a third generation, long-life low-vibration Stirling cycle unit (Figure 17). The cooler is a dynamically balanced unit whose expander and compressor assemblies each have an opposing moving mass counter-balance system to minimize the momentum imparted to focal plane optics of space science instruments. This technology is being developed to satisfy anticipated vibration requirements of future space-sensor systems. The cryocooler and its support structure are instrumented to record mechanical vibrations. Laboratory testing will give a good indication of the cryocooler generated disturbance. However, 1-g forces cause piston-displace offset deflections and magnetic field asymmetry that interact to alter the generated vibration. These extremely low-levels disturbances require a 0-g test. The experiment will provide the environment required to accurately perform mechanical disturbance measurements and evaluate cryocooler dynamic balance.

The flight experiment results will be significant to a number of satellites, scheduled for deployment in the late 1990s, for which cryocooler technologies are contemplated, including those in support of NASA's Mission to Planet Earth and Astrophysics Programs.

The CSE is presently undergoing payload integration and test activities at Goddard Space Flight Center in preparation for a launch in early 1995. Ground-based life testing of the cryocooler has been initiated at Hughes in support of the experiment, and will continue into next year for comparison with flight data.

The Cryo System Experiment illustrates an important type of NASA in-space flight experiment in which a relatively mature system technology is validated to provide the option for subsequent application in a near-future space system development. A successful

experiment could be followed by the use of the technology in an operational system.

### **Concluding Remarks**

NASA and in fact the entire space community are well aware of the compelling need to reduce the cost of space systems development and operation. NASA is now aggressively moving toward the direction of smaller, more focused, and cheaper missions. As an example, NASA has recently announced the Small Spacecraft Technology Initiative (SSTI), a new flight program to demonstrate technologies needed to meet that objective. Two "Smallsat" earth observation satellites will demonstrate advanced miniaturization technology for smaller, lighter spacecraft with payload fractions almost double those of today's satellites. Sensors, on-board data processing, data distribution, guidance and control, and power subsystems will also be based on advanced technologies, all directed primarily at cost reduction.

Cost reduction must be a major objective in all future new military as well as civil space systems, and success will depend heavily on the availability of new -- but proven -- technologies. The experiments conducted thus far have been very effective in proving new technologies when in-space validation is required. However, the experiments themselves are also expensive, and cost reduction is as important in the experiment programs as it is in the actual development programs. Although we are proud of the cost control we have maintained in the experiments to date, we know we must find ways to reduce cost even further.

We are reviewing a variety of cost-cutting possibilities such as increased use of common carriers, adapters, test fixtures and instrumentation, and simplification of experiment equipment to ensure that only those features necessary to achievement of the primary experiment objectives are included. Furthermore, in addition to the rigorous process of phased program planning, we are considering a requirement for a critical program review which would automatically be triggered if program cost projections indicate a ten or fifteen percent growth over the agreed-upon cost estimates. Unless the review determines that a significant cost over-run can be averted, the experiment could be subject to termination.

On the basis of our experience to date, the continuing efforts at further cost reduction may result in some valuable additional fallout. We have had several contractors tell us that our aggressive cost control measures on the flight experiments has forced them to adopt different approaches in the design and conduct of the experiments -- which in turn have been found applicable to new mainstream development programs as well. If this is true, our technology flight experiments may also be serving as an experiment on

techniques for cost reduction in design and development of major space systems.

But apart from our cost concerns and our cost-reduction focus, we are satisfied that in-space technology experimentation has proven itself as a valuable tool in preparing, validating, and reducing the risk of incorporating the technologies essential to design and development of our future space systems. The first round of IN-STEP experiments provided data needed for development and refinement of a wide range of computer models and codes. The validated computational approaches, now being used in space hardware development, reduce or eliminate costly ground testing or overly high design margins previously required for reducing technical risk. The current generation of IN-STEP flight experiments is directed at reducing the risk in specific technology areas important to development and operation of the International Space Station Alpha -- areas such as vibration isolation, materials and environment characterization, and in-space construction and maintenance. And new experiments will shortly be addressing inflatable structures and other innovative technologies that may offer still greater economies in future space systems.

We think we have good reason to believe that in-space flight experimentation has taken its place, along with computational analysis, simulation, laboratory and bench testing, and wind-tunnel or atmospheric flight testing, as another weapon in the arsenal of the space systems designer.

### **Acknowledgements**

The authors would like to thank Mr. Michael Bentz of Boeing Aerospace, Dr. Gary Swenson of Lockheed Corporation, and Mr. George Fleischman of Hughes Aerospace for their valuable input.

### **References**

- <sup>1</sup>EISG Post-Flight Mission Operations Report, Office of Advanced Concepts and Technology, NASA Headquarters, May, 1994.
- <sup>2</sup>G. Swenson, "Spacecraft Glows: Background", Lockheed Missiles and Space Company, Palo Alto, CA, July 1994.
- <sup>3</sup>M.D. Bentz, et al, "Jet Mixing in Low Gravity: Results of the Tank Pressure Control Experiment", AIAA/SAE/ASME/ASEE 28th Joint Propulsion Conference, Nashville, TN, July, 1992.
- <sup>4</sup>Heat Pipe Performance Experiment Final Report, Hughes Aircraft Co., Torrance, CA, April 1994.
- <sup>5</sup>G.L. Fleischman, et al, "Heat Pipe Performance In-Space Technology Experiment (HPP)", 6th AIAA/ASME Joint Thermophysics and Heat Transfer Conference, Colorado Springs, CO, June 1994.

# Technology Demonstration Experiments on STRV-1

Gordon L. Wrenn

Andrew J. Sims

Spacecraft Environment & Protection Section

Space Technology Division

Space & Communications Department

DRA Farnborough, Hants GU14 6TD, UK.

## 1. SUMMARY

Ariane 44LP/V64 was launched on 17 June 1994 when it placed two microsatellites, STRV-1a and STRV-1b, into Geostationary Transfer Orbit (GTO). This paper describes the technology demonstration experiments on the spacecraft, with particular emphasis on the theoretical and empirical models used for design and testing, and presents some early data as evidence that the mission objectives will be met.

## 2. INTRODUCTION

The STRV (Space Technology Research Vehicle) spacecraft were designed and built by the UK Defence Research Agency as a means of achieving in-orbit demonstration of a number of space technologies considered to be crucial to the procurement of reliable and more cost-effective spacecraft in future years.

The Ariane Structure for Auxiliary Payloads (ASAP) was utilised to inject the two 50 kg satellites, as piggy back to INTELSAT-702, into an orbit with apogee of 35953 km, perigee of 297.8 km and inclination of 7°; this orbit is relatively hostile in several environmental respects and thus ideal for proving prospective technologies during a nominal one year mission. The background to the project is described by Ryden [1] and more details of the system design and in-orbit performance are supplied by Wells [2].

Unfortunately, the failure of 44LP/V63 in January and consequent launch postponements have severely restricted the content of this report, it is possible at this time only to present a small sample of raw or provisional data as an illustration of the new results which are confidently expected.

## 3. THE PLATFORMS

The two spacecraft were built with common subsystems, this simplified construction and testing and minimised the costs and risks. Figure 1 illustrates the compactness of the equipment layout and Table 1 lists the major design features.

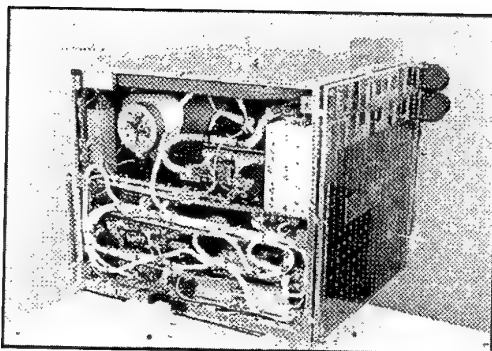


Figure 1. STRV-1b showing Internal Layout

The platform structure with the power, attitude control, on-board data handling and communications systems incorporate many advanced technologies which are *experimental* in that there is a need for proving them in the stressing launch and orbit environments. Particular interest is focused upon the performance of the carbon-PEEK structural components, a radiation-tolerant MAS 281/Mil-Std 1750 (silicon on sapphire fabrication) microprocessor and innovative solar cells.

Given the low thermal conductivity of the structural panels and the high packing density, satisfactory thermal control required some careful design. The I-DEAS [3] Finite Element

**Mass:** 50-53 kg

**Volume:** 450 x 450 x 450 mm

**Structure:** Carbon fibre/PEEK thermoplastic skinned aluminium honeycomb panels

**Power:** GaAs body mounted arrays, average output 31-33 W (BoL)

**Power Storage:** 46 Whr total (16 x NiCd cell)

**Attitude Control:** Spin at 5 rpm (provided by Ariane third stage), magnetorquer control

**Primary Computer:** GEC Plessey Mil-Std 1750 Silicon-On-Sapphire (SOS) chip set

**Primary RAM:** 128 kBytes SOS RAM

**Primary ROM:** 64 kBytes SOS ROM and 4 kBytes SOS 'boot' PROM

**Communications:** ESA TM/TC CCSDS Standard, S-band packet TM at 1 kbit/s

**Launch:** Ariane ASAP into 300 x 36000 km GTO

**Primary Ground Station:** 12 m antenna at DRA Lasham

TABLE 1. STRV Spacecraft Design Summary

Modeller was used to generate a geometrical representation of the spacecraft and the Thermal Model Generator (TMG) was used to apply boundary conditions and run analyses.

A variety of orbital configurations were modelled and the temperatures calculated for each electronics box and structural component, both steady state and transient heating conditions were studied to examine various nominal and worse cases. Figure 2 presents a typical temperature distribution produced by the mathematical model. The thermal designs of 1a and 1b were validated in the solar simulation facilities at DRA Farnborough. The thermal performance in orbit is in very good agreement with the software simulations. For nominal attitude with solar aspect angle of 90°, the internal and array temperatures are approximately 20°C, falling to about -20 °C during a 30 minute eclipse.

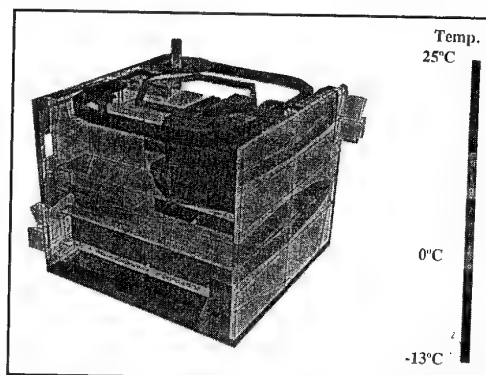


Figure 2. Temp Contours: Apogee, Long Eclipse

© British Crown Copyright 1994/DRA

Published with the permission of the Controller of Her Britannic Majesty's Stationery Office

Paper presented at the AGARD Flight Vehicle Integration Panel Symposium on "Space Systems Design and Development Testing" held in Cannes, France from 3-6 October 1994, and published in CP-561.



#### 4. THE EXPERIMENTS

The GTO orbit is challenging in several respects. Near perigee, surface materials are subject to erosion from the action of atomic oxygen; at altitudes near apogee, surface charging is a likely hazard and damaging electrostatic discharges (ESD) must be avoided; in between the spacecraft encounter the Van Allen belts of trapped high energy particles, in addition to penetrating cosmic rays, and a variety of radiation effects threaten component and system degradation. The two payloads comprise a total of fourteen experiments; these test some specific technologies and supply the environment monitoring which is central to the whole mission, see Table 2.

##### Electrostatic Charging

|                                       |    |
|---------------------------------------|----|
| Xenon Plasma Charge Neutralizer (DRA) | 1a |
| Langmuir Probe (DRA)                  | 1a |
| Cold Ion Detector (DRA/MSSL-UCL)      | 1a |
| Surface Charge Detector (DRA/SIL)     | 1a |

##### Radiation Effects

|   |    |
|---|----|
| Cosmic Ray & Dosimetry Monitor (DRA/AEA)      | 1a |
| Radiation Dose Rate Sensor (DRA/MRCS)         | 1a |
| RADIATION MONITOR (BMDO/JPL)                  | 1b |
| Radiation Environment Monitor (ESA-ESTEC/PSI) | 1b |
| CMOS Neural Network (BMDO/JPL)                | 1b |
| Novel HIP IR Sensors (BMDO/JPL)               | 1b |
| Solar Cell Technology (DRA/SSTL)              | 1b |

|                                     |    |
|-------------------------------------|----|
| Atomic Oxygen Effects (DRA/U.Soton) | 1a |
|-------------------------------------|----|

|  |    |
|--|----|
| Cryocooler Motion Suppression (BMDO/JPL) | 1b |
|--|----|

|                              |    |
|------------------------------|----|
| Battery Recharge (ESA-ESTEC) | 1a |
|------------------------------|----|

TABLE 2. STRV Experiments and Investigators

Selected features of many of these experiments are described to illustrate the test and simulation activities which are critical to design and development, the theme of this meeting.

The electrostatic charge alleviation experiment sets out to detect differential surface charging which will occur near apogee, and then to demonstrate that the build up of hazardous potentials can be prevented by the operation of a neutralizer emitting a cold xenon plasma. Measurements of surface charging are made with a novel Pockels effect device (SCD) which detects induced electric field by the change in polarisation of a laser beam passing through a uniaxial lithium niobate crystal. A cold ion analyzer (CID) characterises the ions with energy less than 1300 eV, from both plasmaspheric and onboard sources, and measures satellite potential and chart charging regimes throughout the magnetosphere. The CID employs a retarding potential-deflector energy selector with a microchannel plate detector. The neutralizer is a hollow cathode system, a modified version of a key component of the T5 ion thruster developed by DRA. Its operation on STRV is therefore a partial flight test of a much needed electric propulsion capability. The charge alleviation process will involve complex plasma/spacecraft interactions and NASA Charging Analyzer Program (NASCAP) simulations are employed as an aid to understanding the in-orbit measurements [4]. DRA has recently, under ESA contract, developed a number of refinements for NASCAP in order to improve the three dimensional modelling of surface charging in tenuous but dynamic plasma environments [5].

Figures 3 and 4 show the NASCAP model of STRV-1a with the surface elements properly characterised in the available dimensional resolution. Figure 3 shows the +z face of the satellite with the neutraliser, Langmuir probe and Cold Ion Detector clearly visible. Crucial to the charging behaviour are the semiconducting  $\pm z$  thermal blankets (carbon coated  $25\mu\text{m}$  kapton) and the body mounted solar cells ( $\pm x$  and  $\pm y$  faces) with  $200\mu\text{m}$  thick coverglasses mounted on  $25\mu\text{m}$  kapton sheet. Figure 4 shows the -z face which incorporates the surface charge detector and another thermal blanket. STRV spins at about 6 rpm which means that the dynamics of surface charging in sunlight are highly complex and have yet to be studied fully. Results presented here consider the

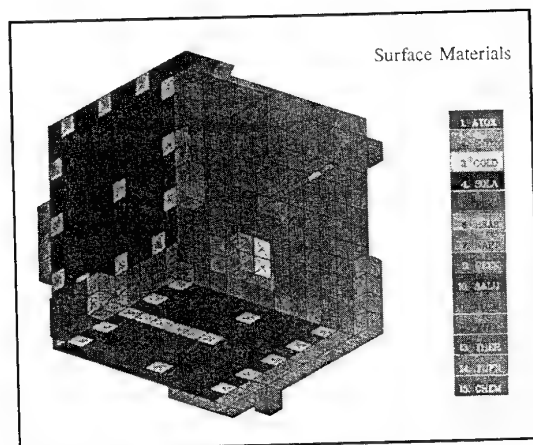


Figure 3. NASCAP model of STRV-1a, +z view

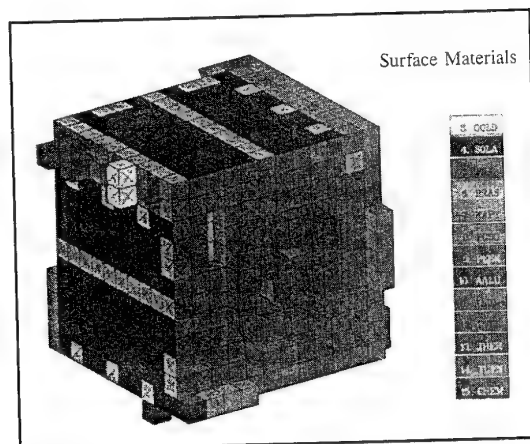


Figure 4. NASCAP model of STRV-1a, -z view

restricted (but probably worst-case) problem of charging in eclipse, near apogee when the ambient plasma is moderately active ( $n_e = n_i = 1 \text{ cm}^{-3}$ ,  $kT_e = kT_i = 5 \text{ keV}$ ). Figure 5 shows the potential history of three surface cells, one bonded to the (conducting) structure, a solar cell and a kapton patch representing the solar array insulator. Rapid vehicle charging occurs within the first second as the structure potential reaches about -1kV.

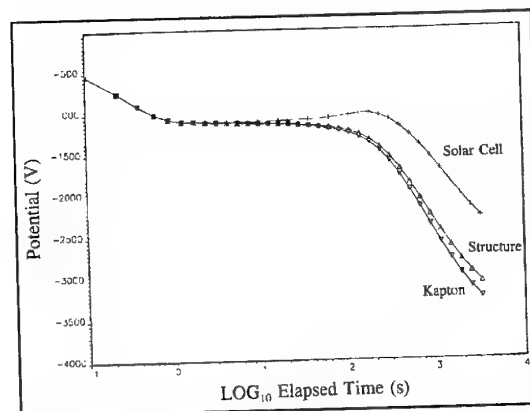


Figure 5. STRV-1a Charging in Eclipse

Figure 6 shows the net charging current to the spacecraft which is decreasing during this period as plasma electrons are repelled and the spacecraft approaches overall current balance. After about 10 seconds, the net charging current to

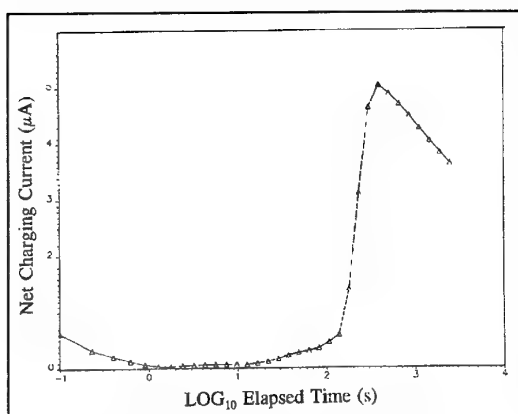


Figure 6. STRV-1a Charging in Eclipse

the satellite begins to increase, slowly at first, but rising rapidly to a maximum at about 300 seconds (figure 6). This arises from the action of potential barriers which have begun to form due to the onset of differential charging. Kapton surfaces charge more rapidly than neighbouring cover glasses and eventually a potential barrier forms above the less negative surfaces and suppresses the emission of secondary electrons. This is clearly illustrated in figure 7 which shows a potential contour plot in the x-y plane.

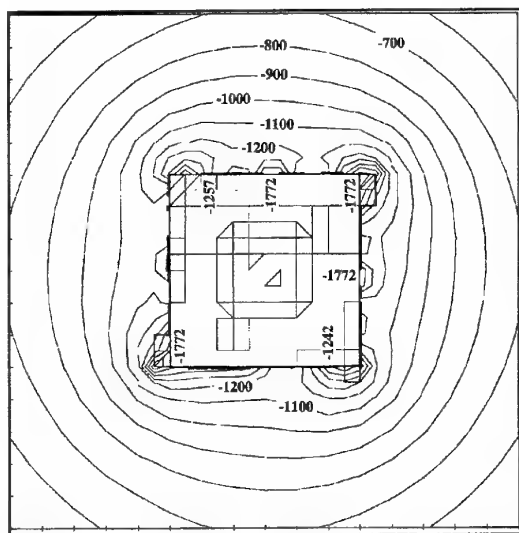


Figure 7. Contours of Potential, x-y plane

Those surface cells lying beneath a positive electric field are unable to emit secondary electrons and the overall current balance to the satellite is upset as plasma electrons once again dominate the net charging current. Figure 5 shows that this has the effect of driving surface potentials rapidly more negative (towards -2.5kV) before the barriers are overcome and the net charging current begins to decrease; the system is now heading towards equilibrium. Most importantly, differential potentials of the order of 1 kV have developed between the solar cell cover glasses and the underlying kapton; arc discharges are most likely at this stage. Internal capacitances within the satellite are such that the charging process just described occurs within one hour; approximately equal to the duration of eclipses at apogee. Furthermore, it is the action of differential charging which leads to the formation of barriers and development of hazardous potentials. The neutraliser system should be ideally suited to alleviating this situation but it will be another year before the orbit precesses such that eclipse is near apogee and the satellite is in the plasmasheet.

The radiation effects experiments depend upon accurate measurements of the fluxes of energetic particles encountered throughout the mission but they also rely upon particle transport codes which must be used to calculate received dose under the appropriate shielding. Combining UNIRAD [6], selecting AP8MAX [7] and AEMAX [8], with SHIELDOSE [9] it is possible to determine how the annual dose will vary with shielding thickness. Figure 8 presents calculations based on omnidirectional flux from  $2\pi$  steradians transmitted into a semi-infinite aluminium medium.

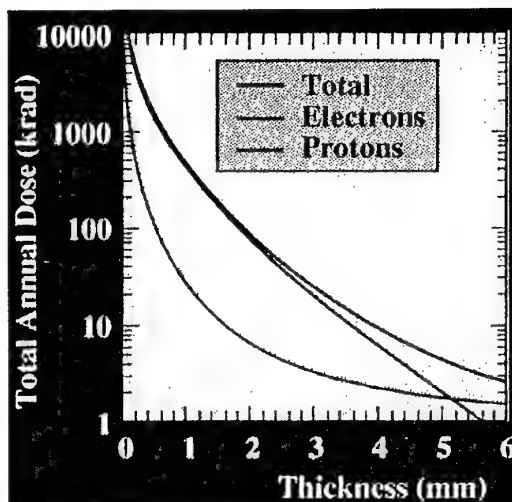


Figure 8. Effect of Shielding on Dose in GTO

The variation of dose rates around the orbit can be calculated for any particular shielding depth and figure 9 plots the predicted profiles for protons and electrons behind 2 mm of aluminium. The inner and outer belts are clearly identified.

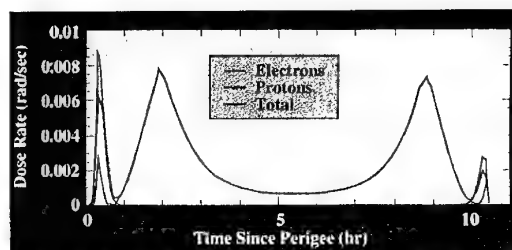


Figure 9. Dose Rates behind 2 mm Al Shield

However, it is known that the empirical model, based on 1970 data, is far removed from reality. Results from CREDO on UoSAT-3 and monitors on CRRES have already demonstrated some of the inadequacies [10,11]. CREDO on 1a employs pin diode arrays with pulse-height analysis to give energy-deposition and Linear Energy Transfer spectra and radfets, with a range of sensitivities, to give accumulated dose. Detecting coincidences between parallel arrays of diodes will give LET accurate to 40% with directional information from two orthogonal arrays; large area ( $4 \text{ cm}^2$ ) arrays for high LET (100 to  $20000 \text{ MeV g}^{-1} \text{ cm}^2$ ) and single diodes ( $1 \text{ cm}^2$ ) for low LET ( $>2 \text{ MeV g}^{-1} \text{ cm}^2$ ) at high fluxes. The occurrence rate of Single Event Upsets (SEUs) will be correlated with the flux measurements. Figure 10 summarises the main features of ESA's Radiation Environment Monitor [12] on 1b. This comprises two detectors with different areas and shielding configurations, designed for selective sensitivity to either protons or electrons.

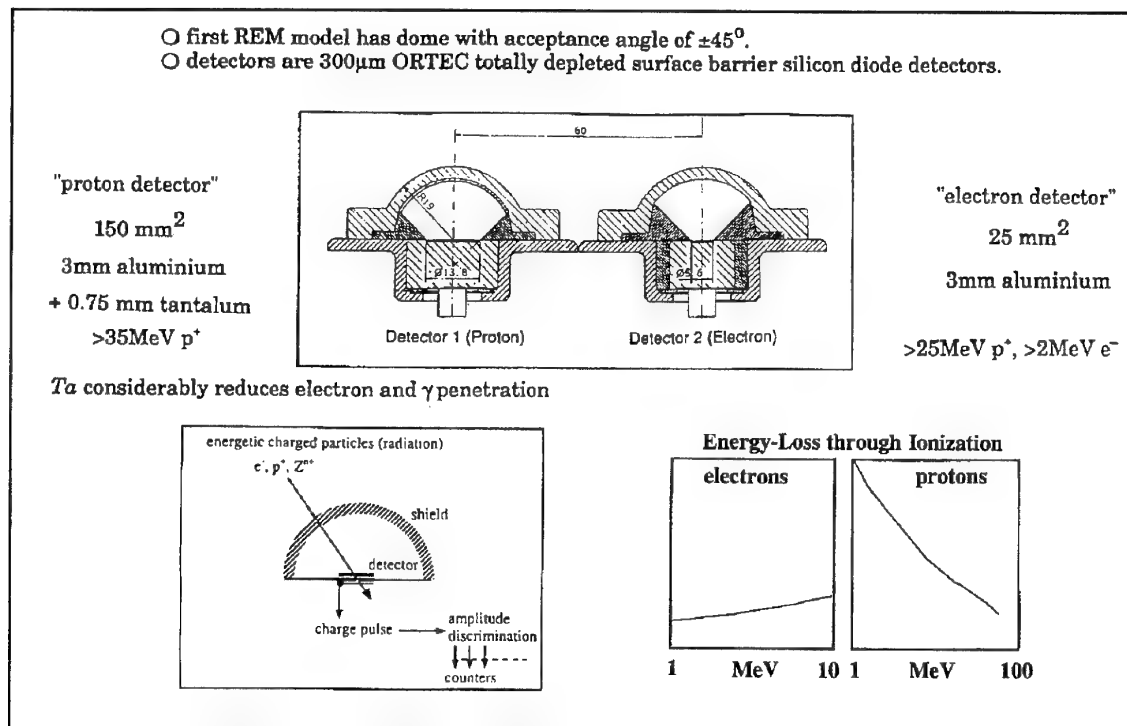


Figure 10. ESA's Radiation Environment Monitor on STRV-1b

Initial data, presented as raw count rates in figures 11 and 12, demonstrate the effectiveness of this technique and immediately establish the dynamic nature of the trapped radiation belts in the comparison of the five orbits spanning seven weeks.

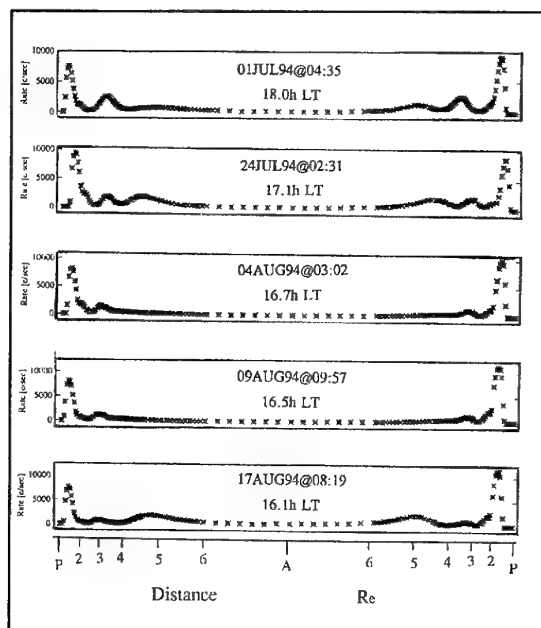


Figure 11. REM Proton Detector Data

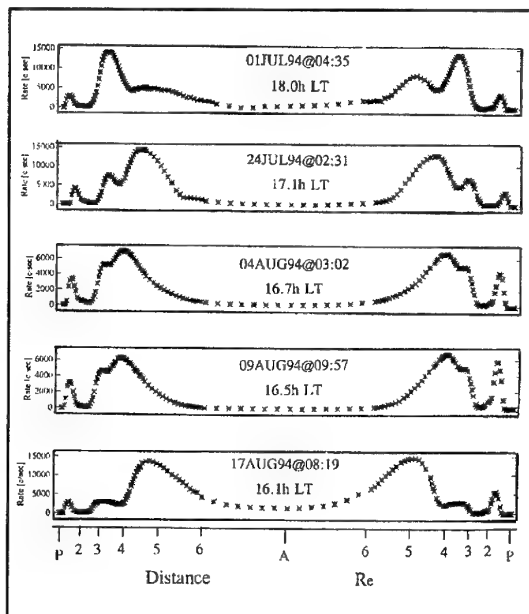


Figure 12. REM Electron Detector Data

RADMON on 1b contains sixteen 3x3 mm chips, each consisting of a 4 kbit SRAM and two p-FETs, that were fabricated using a standard 1.2  $\mu$ m CMOS process. Half are shielded by 2 mm of Aluminium, the other eight by 5.5 mm. The SRAM detects particle upsets using three bins; the first detects protons, alphas and heavy ions, the second alphas and heavy ions, the third only heavy ions. Figure 13 shows a schematic of a p-FET which detects total ionizing dose and has a sensitivity of 1.5 mV/krad.

Conversion of count rate to particle flux requires sophisticated calculation but from a qualitative comparison with figure 4, it is clear that the experiment will provide a rigorous check for the existing environment and transport models.

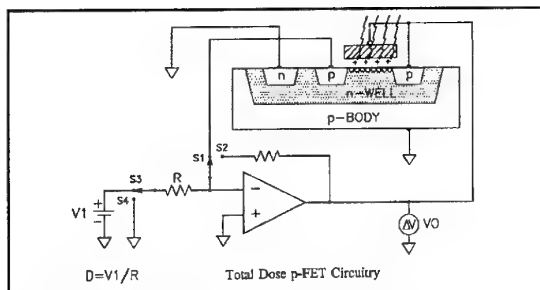


Figure 13. RADMON p-FET Schematic

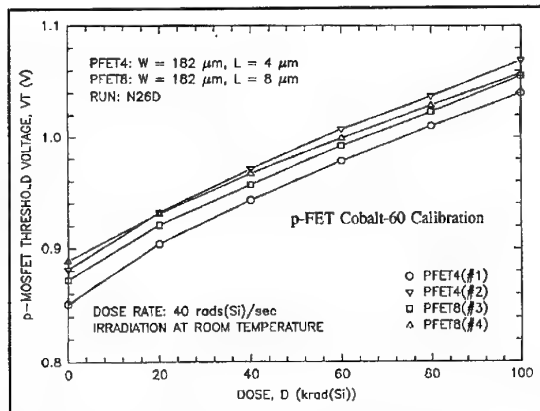


Figure 14. RADMON p-FET Calibration

The devices were calibrated in a Cobalt-60 facility and Figure 14 shows the repeatable relationship between threshold voltage and dose.

Using these calibrations, in-flight measurements are translated into dose and are plotted in Figure 15 for the first sixty days of the mission.

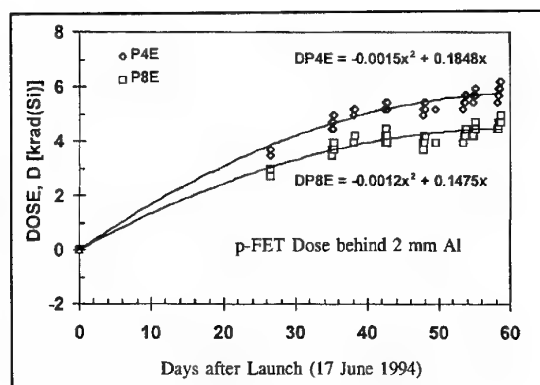


Figure 15. RADMON Measured Dose

The trend fittings are only tentative but the integrated dose, measured behind 2 mm of aluminium shield, appears to be significantly less than the models predicted. Comparing data for 2 mm and 5.5 mm shieldings also offers some suggestion that the transport models overestimate the attenuation at the larger thickness, see figure 16.

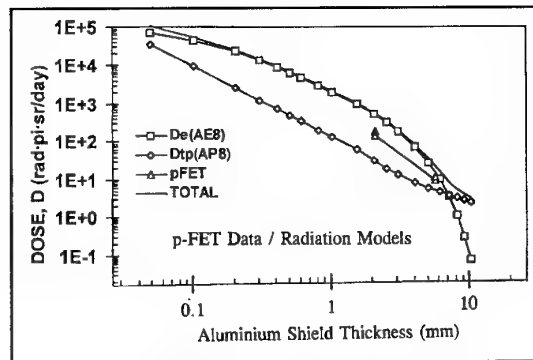


Figure 16. RADMON/Model Comparison

Knowledge of the dose behind these thicknesses of aluminium is vital to the performance assessment of two JPL technologies flown in space for the first time. Analogue neural network VLSI chips are the building blocks of a neuroprocessor technology which can have wide ranging application in future space programmes; it is essential to demonstrate that radiation will not damage the synapses and neurons within the circuits. SiGe/Si Heterojunction Internal Photoemission (HIP) diodes may offer a major advance in the technology of infra-red sensing but again it is vital to prove that their electrical characteristics, specifically the dark current noise, does not degrade with radiation exposure.

Shielding of solar cells is limited to that available from practical cover glass considerations. The solar cell technology experiment is in two parts, the flight demonstration of advanced GaAs based solar panels on 1a and 1b, and the current-voltage characteristic measurement of 47 individual solar cells on 1b. The objectives are to compare the in-orbit performance of the various cell types against ground calibration measurements and to thus achieve space qualification and acceptance of new cell types. Radiation tolerance is a crucial requirement, the test on STRV is ideal because in one year the panels should experience a dose in excess of that received in 10 years by GEO communications satellites.

## 5. MISSION STATUS

After injection on June 17th, STRV-1b was acquired and commissioned with few problems. All systems have functioned correctly and routine operations have proceeded smoothly since July. The experiment turn-ons are scheduled to meet power sharing constraints and agreed priorities; no problems have been reported, with the exception of one which presently prevents correct working of the solar cell control electronics.

By contrast the life of STRV-1a has been much more exciting and perplexing. Operations were plagued by power system and RF link problems until a favourable solar aspect angle was realised in late August. Experiment turn-ons have been few and far between, but almost all of the instrumentation has now been checked out satisfactorily and serious data gathering has commenced.

## 6. CONCLUSIONS

In the field of space technology, both ground based testing and computational models/simulations are essential for good design and development. However, there is no complete substitute for in-orbit experiment and qualification; STRV-1 is demonstrating that microsatellites can provide a relatively inexpensive means of achieving the latter. Fast turn around is a key factor, the three years from design phase to operations of STRV-1 could actually be reduced now that a mission concept and basic platform designs have been firmly established.

It is clear that results from STRV-1 will permit the refinement of existing models and provide a more realistic appraisal of the strengths and weaknesses of ground based test/calibration procedures.

## 7. ACKNOWLEDGEMENTS

STRV-1 and its success are due the skill and effort of a large number of DRA staff, contractors and collaborators. Huge pressures have continually been imposed on the project team in what was always an ambitious mission, but Nigel Wells and Neil Wallace deserve special medals for superbly coping with the operational stresses. Eamonn Daly, Alex Zehnder, Martin Buehler, Jim Kenny and Andrew Hookey are sincerely thanked for contributing previously unpublished material; the NASCAP simulations are the work of Rob Smith.

## 8. ACRONYMS

|       |   |
|-------|---|
| AEA   | Atomic Energy Authority                 |
| ASAP  | Ariane Structure for Auxiliary Payloads |
| BMDO  | Ballistic Missile Defense Organisation  |
| CID   | Cold Ion Detector                       |
| CREDO | Cosmic Ray Effects & DOSimetry          |
| DRA   | Defence Research Agency                 |
| ESA   | European Space Agency                   |
| ESD   | ElectroStatic Discharge                 |
| ESTEC | European Space & Technology Centre      |
| GTO   | Geosynchronous Transfer Orbit           |
| JPL   | Jet Propulsion Laboratory               |
| MSSL  | Mullard Space Science Laboratory        |
| OBDAH | OnBoard Data Handling                   |
| PSI   | Paul Scherrer Institute                 |
| SCD   | Surface Charge Detector                 |
| SIL   | Satellites International Ltd.           |
| SSTL  | Surrey Satellite Technology Ltd.        |
| STRV  | Space Technology Research Vehicle       |
| UCL   | University College London               |

## 8. REFERENCES

1. Ryden, K.A., "The Space Technology Research Vehicle (STRV-1)" in Proc. Royal Aeronautical Society Conf. on Small Satellites, p4.1-4.11, January 1991.
2. Wells, N.S., "The Space Technology Research Vehicles STRV-1A and 1B: First In-Orbit Results", 8th Annual AIAA/USU Conf. on Small Satellites, August 1994.
3. TMG Thermal Model Generator, a thermal analysis computer program, reference manual revision 1.1, Maya Heat Transfer Technologies Ltd.
4. Katz, I. et al., "NASCAP a three-dimensional charging analyser program for complex spacecraft", IEEE Trans. Nucl. Sci., NS-24, p2276, 1977.
5. Spacecraft/Plasma interactions and electromagnetic effects in LEO and polar orbits, Final Report on ESA Contract 7989/88/NL/PB(SC), Improvements to NASCAP, DRA/CIS(CSC3)/CR/94/06, 1994.
6. Debruyn, J.C. & Jensen, L.H., "The UNIFLUX system", ESTEC Working Paper 1308, 1983.
7. Sawyer, D.M. & Vette, J.I., "AP8 trapped proton environment for solar maximum and solar minimum", NASA NSSDC/WDC-A-R&S, 76-06, 1976.
8. Vette, J.I., "The AE8 trapped electron model environment", NSSDC Report 91-24, NASA/GSFC, 1991.
9. Seltzer, S.M., "SHIELDOSE - A computer code for space shielding radiation dose calculations", NBS Technical Note 1116, 1980.
10. Brautigam, D.H., Gussenhoven, M.S. & Mullen, E.G., "Quasi-static model of outer zone electrons", IEEE Trans. Nucl. Sci., 39, pp 1797-1803, 1992.
11. Dyer, C.S., Sims, A.J., Truscott, P.R., Farren, J. & Underwood, C., "The low Earth orbit radiation environment and its evolution from measurements using CREAM and CREDO experiments", IEEE Trans. Nucl. Sci., 40, 6, 1471-1478, 1993.
12. Daly, E.J., Adams, L., Zehnder, A. & Ljungfelt, "ESA's Radiation Environment Monitor and its Technological Role", paper IAF-92-0779, 43rd Congress of the International Astronautical Federation, Washington D.C., 1992.

-----  
 AGARD Flight Vehicle Integration Panel: "Space Systems Design and Development Testing" Symposium  
 (3-6 October 1994), Cannes, France -  
 Session V, Space Flight Experiments.

## U.S. IN-SPACE ELECTRIC PROPULSION EXPERIMENTS

**John F. Stocky**  
Manager, NSTAR  
Jet Propulsion Laboratory 126-324  
California Institute of Technology  
4800 Oak Grove Drive  
Pasadena, CA 91109 USA

**Robert Vondra**  
University of Dayton/  
Phillips Laboratory  
Albuquerque, NM, USA

**Alan M. Sutton**  
Phillips Laboratory (AFMC)  
Edwards AFB, CA, USA

### ABSTRACT

Arcjet and ion propulsion offer potentially significant reductions in the mass of propulsion systems required for Earth orbiting satellites and planetary spacecraft. For this reason, they have been the subject of validation and demonstration programs. After examining the benefits of electric propulsion, this paper discusses the technology base for the Electric propulsion Space Experiment (ESEX) arcjet demonstration experiment and the NASA SEP Technology Application Readiness (NSTAR) ion propulsion validation program. As part of the Advanced Research and Global Observation Spacecraft (ARGOS), ESEX will perform ten 15-min firings of a 30-kW ammonia arcjet.

The National Aeronautics and Space Administration's (NASA's) validation program, NSTAR, consists of two major elements: a ground-test element and an in-space experiment. The ground-test element will validate the life, integrability, and performance of low-power ion propulsion. The in-space element will demonstrate the feasibility of integrating and flying an ion propulsion system. The experiment will measure the interactions among the ion propulsion system, the host spacecraft, and the surrounding space plasma; and it will provide a quantitative assessment of the ability of ground testing to replicate the in-space performance of ion thrusters. By involving industry in NSTAR, a commercial source for this technology will be ensured. Furthermore, the successful completion of the NSTAR validation program will stimulate commercial and government (both civilian and military) uses of this technology.

### 1 INTRODUCTION

In an effort to increase the payload fraction of satellites and planetary probes, reduce the cost (i.e., size) of launch vehicles, extend the life of satellites, and reduce the duration of planetary missions, two programs have been initiated to demonstrate and validate electric propulsion. One program, sponsored by the United States Air Force Materiel Command, will demonstrate the technology associated with high-power arcjets. The other, sponsored by the United States National Aeronautics and Space Administration (NASA) will validate the technology associated with low-power (<5-kW) ion propulsion technology.

After a brief, quantitative description of the benefits derived from electric propulsion technology, this paper describes the Electric propulsion Space Experiment (ESEX) and NASA SEP Technology Application Readiness (NSTAR) validation programs.

### 2 IMPORTANCE OF ELECTRIC PROPULSION FOR MILITARY MISSIONS

#### 2.1 Military Needs

Advanced propulsion technology for military needs does not differ in kind from that for commercial and NASA spacecraft, but it does differ in degree. For any satellite, it is desirable to reduce the mass of the on-board propulsion system to increase the

functionality of the satellite. In addition, increased propellant efficiency (i.e., higher specific impulse) can be used to carry additional propellant, thereby extending satellite life or increasing the scope of work done by the propulsion system, e.g., repositioning.

If increased satellite capability were desired, using ion propulsion instead of chemical propulsion would increase the mass that could then be used for additional payload. For example, a commercial communications satellite could use this additional mass to increase the number of transponders carried by the satellite. Or a military satellite could use the increased mass to enhance communications capabilities by flying larger aperture antennas.

To reduce the cost of a space mission, it is desirable to use the smallest launch vehicle possible. Because ion propulsion can reduce the mass of the required on-board propulsion system dramatically, it may be possible in some cases to combine ion propulsion for on-board use with an ion propulsion module for low-Earth orbit (LEO)-to-geosynchronous Earth orbit (GEO) transfer and reduce the launch vehicle size required for a given spacecraft capability from a Titan to an Atlas.

#### 2.2 Benefits

##### 2.2.1 Station Keeping

Station keeping of a GEO satellite requires 49 m/sec  $\Delta V$  annually for north-south station keeping and 2 m/sec  $\Delta V$  annually for east-west station keeping. The larger the satellite and the longer it remains in orbit, the more efficient the on-board propulsion system must be in its use of propellant. The measure of this efficiency is specific impulse ( $I_{sp}$ ). Compared to on-board chemical systems, electric propulsion increases  $I_{sp}$  by factors of 2 to 4 when using arcjets and of 10 or more when ion propulsion is used.

To obtain these benefits with electric propulsion, the propulsion system dry mass must be increased. This increase in dry mass requires a propellant conditioning unit not required by a conventional chemical propulsion system. This increased dry mass means that the propulsion requirement must exceed a certain minimum before electric propulsion demonstrates a performance advantage relative to chemical propulsion (Figure 1).

##### 2.2.2 Repositioning

Repositioning refers to changing a GEO satellite's longitude so that the area on the Earth's surface can be viewed by satellite sensors and antennas. Electric propulsion can accomplish repositioning maneuvers more efficiently than chemical systems and in less time (Figure 2). Because electric propulsion uses less propellant during a satellite repositioning performed at a specified rate, electric propulsion can extend a satellite's life and reduce the wet mass required for the propulsion system. This point is made in Figure 3, in which the wet mass of the on-board propulsion system needed for station keeping and for a 90-deg, 30-day

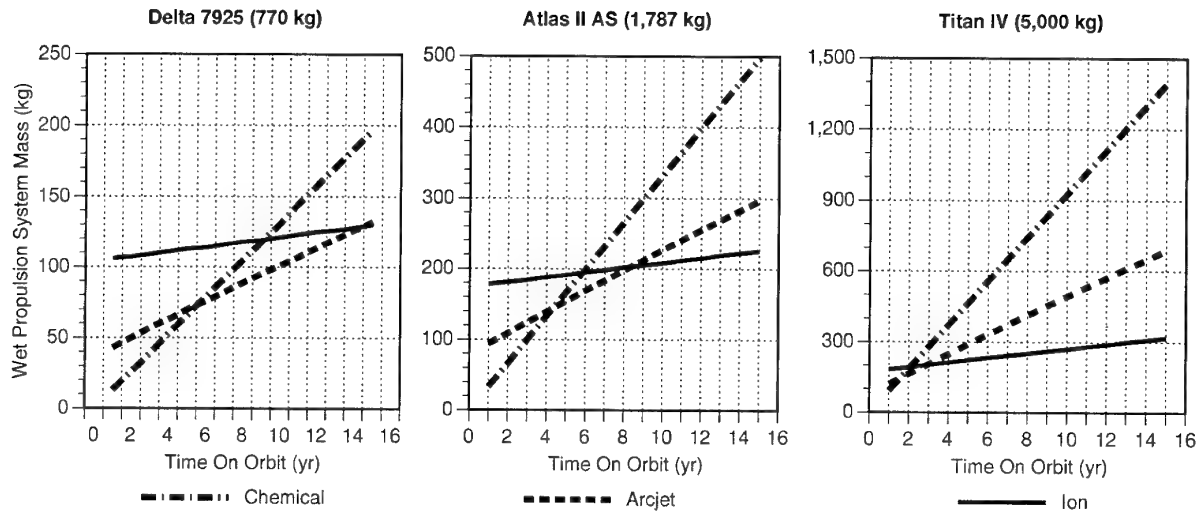


Figure 1. Comparison of station-keeping performance of chemical, arcjet, and ion propulsion.

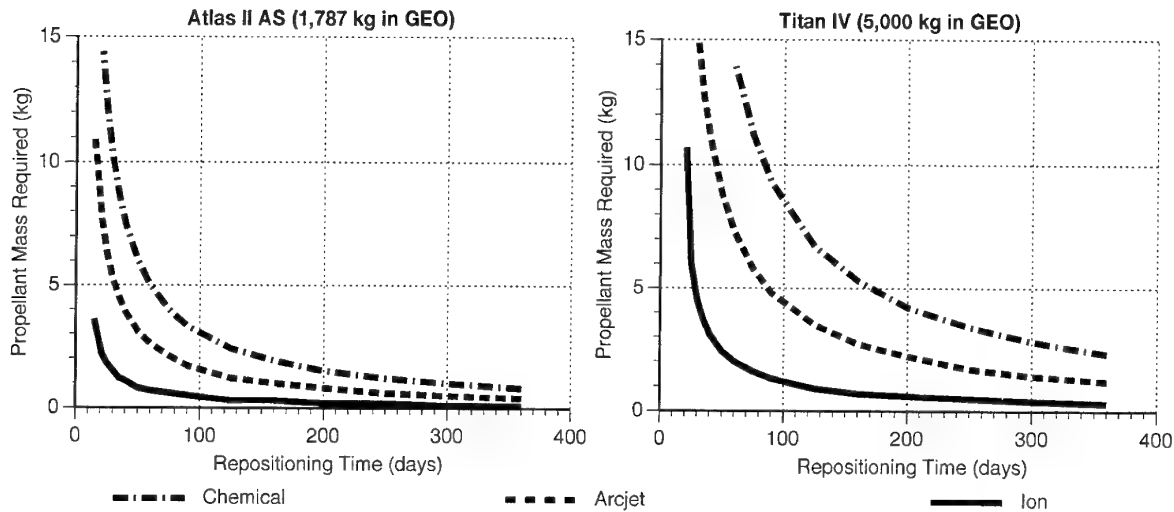


Figure 2. Propellant mass versus repositioning rate for a single 90-deg reposition.

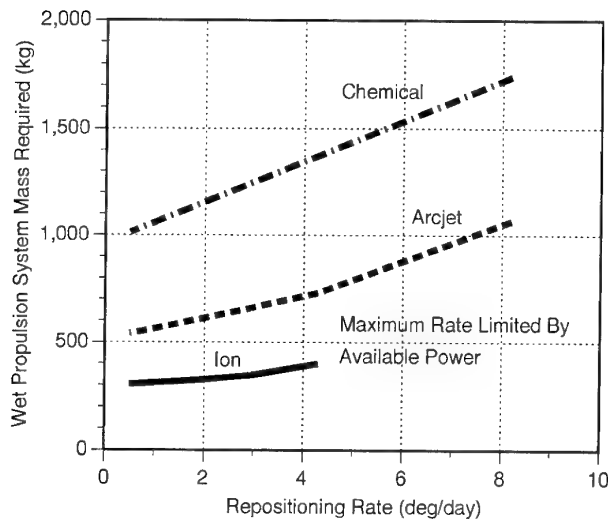


Figure 3. Repositioning performance comparison (for 10 years).

reposition of a GEO satellite with an initial mass in GEO of 5,000 kg and a life of 10 years is shown for chemical, arcjet, and ion propulsion systems. Figure 4 shows a comparison of propulsion systems calculated for Delta-, Atlas-, and Titan-class payloads as a function of on-orbit lifetime for as long as 15 years, assuming two 90-deg/30-day repositions per year. Naturally, the larger the satellite and the longer it remains in orbit, the larger the total impulse required and the more advantageous the higher specific impulse that electric propulsion systems can provide.

We assume that it is more important to increase the number of spacecraft maneuvers than it is to increase maneuver speed. This increase in maneuvers increases satellite life and operational flexibility. Currently, chemical systems nominally carry sufficient fuel for three 180-deg maneuvers. Five-deg/day maneuver rates are nominal, and 15-deg/day rates are reserved for crisis maneuvers. The mass of the chemical propulsion system (fuel and dry mass) is calculated for a range of spacecraft maneuvers at different rates. System masses for ion and arcjet systems (includ-



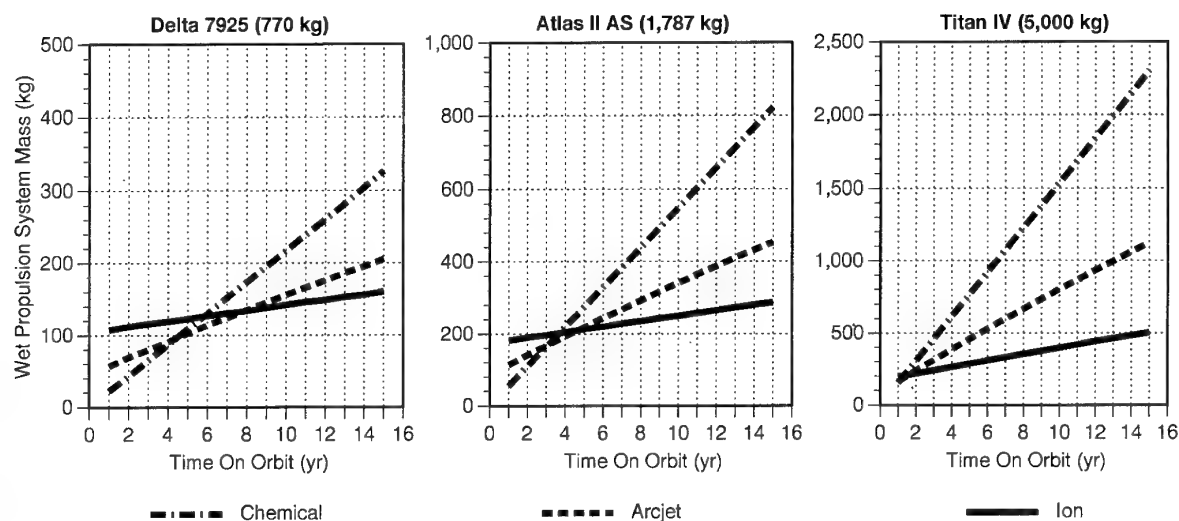


Figure 4. Station-keeping and performance comparison for chemical, arcjet, and ion propulsion.

Table 1a. Assumptions for calculations of electric propulsion performance.

| System                           | Mass, Basis | Specific Impulse, $lb_f\text{-sec}/lb_m$ | Tank Fraction, % | Efficiency, % |
|----------------------------------|-------------|--|------------------|---------------|
| Chemical Propulsion, Dry Mass    | 0 kg        | 220                                      | 10               | N/A           |
| Arcjet Propulsion, Specific Mass | 5 kg/kW     | 700                                      | 10               | 35            |
| Ion Propulsion, Specific Mass    | 10 kg/kW    | 3,500                                    | 10               | 70            |

Table 1b. Spacecraft characteristics.

| Spacecraft Mass, kg | Solar Array Specific Mass, kg/kW | Spacecraft Power, kW |
|---------------------|----------------------------------|----------------------|
| 909                 | 20                               | 1, 2, 3              |
| 2,270               | 20                               | 1, 5, 10, 30         |
| 4,550               | 20                               | 5, 10, 20, 30        |

NOTE: Maneuver = 180 deg at 5 deg/day; the number of maneuvers performed by a chemical system = 3; the electric propulsion system wet mass was set equal to that of the chemical system.

ing solar arrays) are set to equal the chemical system mass. The fuel mass component is calculated, and the number of maneuvers is found and compared to that of the chemical system.

For a given power, electric propulsion can perform a range of maneuvers dependent on fuel consumption. Maximum maneuver rate occurs at maximum fuel consumption, i.e., when the thrusters are operated continuously. Therefore, for a fixed power, the rate can be increased by increasing thruster on-time at the expense of the fuel mass per move. Also, the maneuver rate can be increased by increasing power to the thrusters, which increases the solar-array mass and decreases the total fuel that can be carried. Thus, for a given maneuver rate, there is a power level that minimizes fuel mass per move and maximizes the number of maneuvers. As an example, consider two cases in which 1) the solar array is part of the electric propulsion system and 2) the solar array is not part of the electric propulsion system. For this analysis, the assumptions shown in Table 1 (a, b) were made.

The results of these analyses are shown in Table 2, in which the power requirements for the smallest spacecraft considered are a modest 1 to 2 kW. An ion engine that carries its own power can execute two to three times the number of maneuvers than a chemical system can. If the ion propulsion system is not charged with the power mass, the number of maneuvers increases by a factor of 10 over chemical. However, 1 to 2 kW is not enough power for an ion propulsion system to execute a crisis repositioning of 15 deg/day.

For the 2,270-kg spacecraft, the power requirements are 1–5 kW. The ion engine increases the number of maneuvers by a factor of up to 10 over chemical propulsion. If the spacecraft has 10 kW of power, ion propulsion provides 15 deg/day maneuvers. The arcjet requires 5 kW.

In the case of the 4,550-kg spacecraft, the power requirements are 5–10 kW. When the ion engine carries its own power, it provides



Table 2. Power requirements for arcjet and ion propulsion systems with spacecraft masses of 909 kg, 2,270 kg, and 4,550 kg.

| Spacecraft Mass, kg | Reposition Rate, deg/day | Arcjet          |           |                 |           | Ion Propulsion  |           |                 |           | Prop. Wet Mass, kg |
|---------------------|--------------------------|-----------------|-----------|-----------------|-----------|-----------------|-----------|-----------------|-----------|--------------------|
|                     |                          | With Array      |           | No Array        |           | With Array      |           | No Array        |           |                    |
|                     |                          | Number of Moves | Power, kW | Number of Moves | Power, kW | Number of Moves | Power, kW | Number of Moves | Power, kW |                    |
| 909                 | 5                        | 3               | 1         | 7               | 1         | 9               | 1         | 26              | 1         | 39                 |
|                     | 10                       | 5               | 1         | 6               | 1         | 7               | 2         | 24              | 2         | 78                 |
|                     | 15                       | 4               | 2         | 6               | 2         | Power Limited   |           | Power Limited   |           | 117                |
| 2,270               | 5                        | 5               | 1         | 7               | 1         | 22              | 1         | 29              | 1         | 98                 |
|                     | 10                       | 3               | 5         | 6               | 5         | 7               | 5         | 24              | 5         | 196                |
|                     | 15                       | 4               | 5         | 6               | 5         | Power Limited   |           | 20              | 10        | 294                |
| 4,550               | 5                        | 3               | 5         | 7               | 5         | 8               | 5         | 26              | 5         | 197                |
|                     | 10                       | 5               | 5         | 6               | 5         | 8               | 10        | 24              | 10        | 392                |
|                     | 15                       | 4               | 10        | 6               | 10        | Power Limited   |           | 20              | 20        | 586                |

twice as many maneuvers as a chemical propulsion system. When the ion engine does not carry its own power, the number of maneuvers increases by a factor of 9 over chemical propulsion. With 20 kW of power available, the ion propulsion engine provides 15 deg/day maneuvers. The arcjet requires 10 kW.

### 2.2.3 Communications

Alternatively, the reduction in wet mass of the propulsion system can be used to increase the functional capability of the satellite. As an example, the size of an antenna that can be carried by a GEO satellite can be estimated to determine if a larger antenna can be carried. As a starting point, the non-propulsion mass of a GEO satellite having a chemical, on-board propulsion system capable of performing north-south and east-west station keeping and two 90-deg/30-day repositions per year for 15 years was calculated. This non-propulsion mass was taken to be a measure of the satellite's functional capability, its "functionality," and was held constant to ensure that the satellite's capability was not compromised. Added to this payload mass was the mass of the ion propulsion system required for the same station-keeping and repositioning functions described above for a chemical propulsion system. The difference between this sum and the mass that could be placed in GEO by the launch system was calculated for each year of the satellite's life, and the diameter of a rigid antenna having a mass equal to this difference was estimated. The results are shown in Figure 5 for Titan and Atlas launch vehicles.

The scaling equation for the antenna was

$$\text{Mass (Antenna)} = 4.747 D - 4.61 D^2 + 1.793 D^3$$

D = Antenna Diameter (m)

The results shown in Figure 5 indicate that ion propulsion would

allow a GEO satellite to carry an antenna larger than 10-m diameter (Titan launched) or 7-m diameter (Atlas launched) and still retain a long on-orbit lifetime.

### 2.2.4 Orbit Transfer

Significant savings can be realized if electric propulsion can reduce the initial mass of a GEO satellite so that it can be launched with a smaller launch vehicle without changing the functionality of the satellite. Figure 6 shows that the current performance of both ion and arcjet propulsion systems does not adequately reduce mass. The question then arises, what LEO-to-GEO transfer time would be required if, in addition to employing an on-board electric propulsion system, an electric propulsion system were used from LEO to GEO? To answer this question, we assume the following: a GEO satellite with a 15-year life requirement and an on-board ion propulsion system able to support north-south and east-west station-keeping requirements and two 90-deg/30-day repositions performed annually. The satellite also provides a functionality equivalent to that of a 15-year GEO satellite using a chemical propulsion system able to satisfy the same station-keeping and repositioning requirements.

For this scenario, the mass of solar-powered electric propulsion transfer modules was calculated. We assume the system would use either an APSA-type solar array with GaAs solar cells or a concentrator array. For the ion propulsion system, the performance being validated by NSTAR was assumed; for the arcjet system, a currently available system using ammonia was the basis for one set of calculations and an advanced system using liquid hydrogen was the basis for the other set of calculations. For each launch vehicle considered, the mass of the satellite was subtracted from the launch vehicle's lift capability to LEO. The remainder was used for the solar-powered electric propulsion system. The

Effect of On-Board Propulsion on Antenna Size

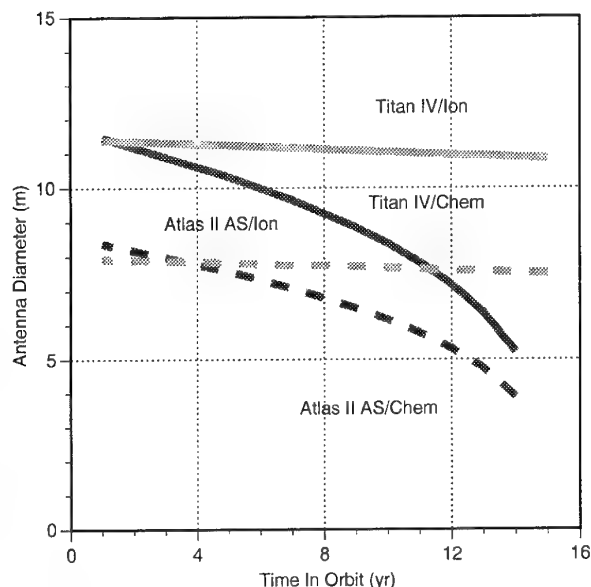


Figure 5. Antenna size is influenced by the choice of on-board propulsion technology.

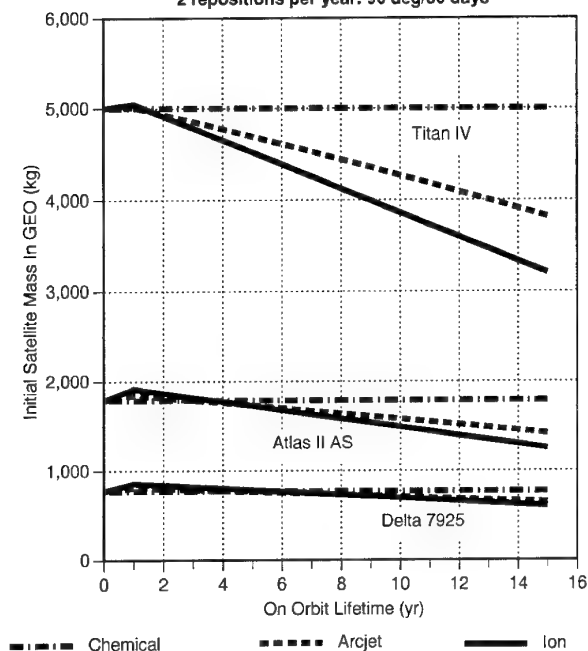
NS & EW Station Keeping  
2 repositions per year: 90 deg/30 days

Figure 6. Reductions in mass are derived from advanced on-board propulsion in GEO.

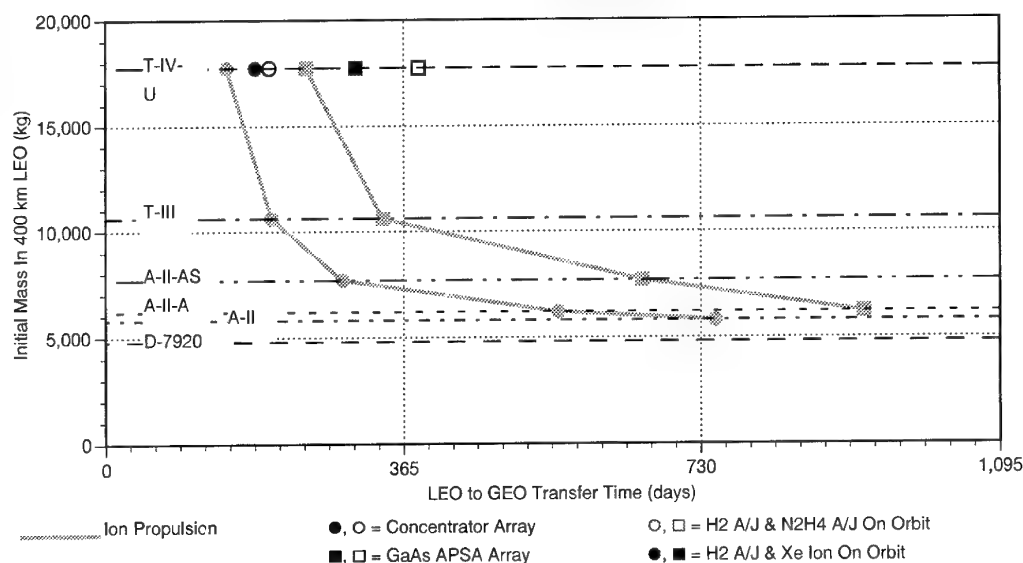
3,210-kg Satellite in GEO, Not Including Mass of Station Keeping  
or Repositioning Propulsion System

Figure 7. Initial mass in LEO versus LEO-to-GEO transfer time for constant payload mass.

larger launch vehicles would allow a higher powered electric propulsion module and would result in shorter LEO-to-GEO transfer times. The transfer times were then calculated and plotted in Figure 7; this figure shows that today's ion propulsion could be used to place a Titan-IV class payload into GEO using an Atlas or Titan-III launch vehicle with a 6-month to 2-year transfer time. According to these calculations, the size of the launch vehicle could not be reduced when using arcjet propulsion modules.

Whether the savings in launch vehicle cost and launch campaign duration outweigh the penalty of a lengthy LEO-to-GEO transfer time can only be answered in the context of a specific mission and, consequently, cannot be discussed here.

The results presented in Figure 7 assume a constant spacecraft design technology level. If we consider the advances associated with equipment and instruments made by such programs as the

Space Defense Initiative (SDI), the results shown in Figure 7 may be unduly conservative.

### 3 ESEX

#### 3.1 Arcjet Technology Background

The Phillips Laboratory has been developing arcjet technology for a number of space applications — originally for orbit raising (ESEX and Electric Insertion Transfer Experiment (ELITE)) and more recently for orbit repositioning (modified ELITE). (ESEX is a flight program that will be discussed later.) The ELITE program was canceled, but the arcjet technology and repositioning application that stemmed from it are worthy of study.

#### 3.2 Arcjet Technology Development and Testing

##### 3.2.1 30-kW Arcjet

The Phillips Laboratory began development of 30-kW ammonia arcjet technology in 1984. The Space Defense Initiative contributed to the project by funding technology development centered on endurance and performance testing of promising designs. This work was the foundation for the ESEX arcjet design. After changes were made to the cathode, constrictor, and nozzle, the best designs were endurance-tested at 30 kW. The tests ran less than 500 hours (the goal was 1,500 hours, commensurate with orbit-raising requirements). Performance testing yielded a specific impulse of 754 sec and 29% efficiency. The primary failure mechanism was cathode whisker growth that shorted the electrode gap ending operation. The cathode erosion rate seemed to support 1,500 hours of operation (Ref. 1). Rocket Research improved on this design in the ESEX program and demonstrated 815-sec specific impulse at 30% efficiency. Lifetime was not addressed.

##### 3.2.2 10-kW Arcjet

The 30-kW arcjet was throttled and performance was measured over a range of powers down to 10 kW. Operation was stable and performance was acceptable over this range. As power was reduced, specific impulse decreased and efficiency increased to >600 sec and 37%, respectively, at 10 kW, ELITE's maximum operating level. Two endurance tests were then performed, one at 10-kW continuous operation and the other a cycled on/off operation at 10 kW.

The first test ended after 1,460 hours of continuous operation. The computer shut down the test when it detected a rise in vacuum tank pressure. When examined, it was discovered that the arcjet boron nitride backplate had cracked, causing propellant to leak. The electrodes, however, were in excellent condition, and there were no signs of whiskers. The pointed portion of the cathode tip was flattened; otherwise the conical section was fully intact. The anode showed no apparent signs of erosion, and the constrictor region seemed unaffected. This demonstration represented 50% more lifetime than required for ELITE (Ref. 2).

Because the ELITE mission required 540 on/off cycles, a 10-kW cycled test was conducted with the arcjet on for one hour, off for one-half hour and repeated indefinitely. The test ended after 707 cycles because of vacuum chamber facility problems, which were believed to be caused by the arcjet. Rather than destroy evidence by turning the engine on and risking damage, the test was stopped. When the engine was disassembled, the arcjet was found to be in good condition. The thruster displayed 31% more cycles than

required for ELITE. Performance (specific impulse, 620–640 sec and thruster efficiency, 33.5–34.5%) was lower than during the continuous test, and the erosion rate (cathode loss, 0.31 g) was higher (Ref. 3).

Next, the arcjet design was modified and its performance characterized over a 3–10-kW range, which is the operational range expected on ELITE as the arrays pass through the Van Allen belt. The cathode gap was shortened (from 0.240 in. to 0.080 in.), and the constrictor diameter decreased (from 0.150 in. to 0.100 in.). The best performance design (specific impulse, 600–700 sec and efficiencies greater than 30% over 3–10 kW) was selected and tested in an integrated system that simulated the solar array–arcjet subsystem being designed for ELITE.

The integrated test-bed consisted of a solar-array simulator and peak power tracker provided by TRW, Inc., a NASA Lewis Research Center's (LeRC's) power processor unit that powered the electric thruster, and a Jet Propulsion Laboratory (JPL)-designed ammonia arcjet. The solar-array power source first turned on the arcjet. Once the arcjet was ignited, the power to the arcjet was raised to the desired level and operated at this level for a predetermined time. If the power deviated from its maximum value, it was quickly corrected by TRW's electronics. The output of the solar-array power source was then changed, and the process was repeated until the arcjet system was tested over a specified range of interest, which for ELITE was 3–10 kW.

These tests proved proper arcjet ignition and the ability of the system to operate dependably. When the operating power point was intentionally moved off its maximum value, TRW's electronics responded within a second to return it to its maximum value.

#### 3.3 ESEX Program Description

Currently, the Air Force Materiel Command's Phillips Laboratory is developing an ammonia-fueled arcjet propulsion system that will be flown as the Electric Propulsion Space Experiment. ESEX is being built by a team consisting of researchers from TRW, Inc., Olin Aerospace Corporation (OAC), and CTA (formerly DSI) (Figure 8). ESEX will be the first on-orbit demonstration of a high-power (30-kW) arcjet propulsion subsystem. After 100 hours of battery charging, ESEX will fire the arcjet propulsion subsystem 10 times each for a duration of 15 min (a total of 150 min).

##### 3.3.1 Objective

The ESEX experiment has two major objectives: The first is to develop a reliable flight arcjet system and successfully complete a test firing in space, verifying the system's performance. The second objective is to gather data on key spacecraft integration issues, verifying that a high-power arc plasma source can operate without adversely affecting a spacecraft's nominal operations (Ref. 1).

The major hardware components include a high-power arcjet, Power Conditioning Unit (PCU), and ammonia Propellant Feed Subsystem (PFS). These components were flight-qualified by vibration testing, thermal-vacuum testing, and a 150-min life test. All components were tested as an integrated system in order to gather ground-performance data (Ref. 2). These data will be compared to the flight performance data, which include thrust, specific impulse, and arcjet efficiency. Thrust will be derived by

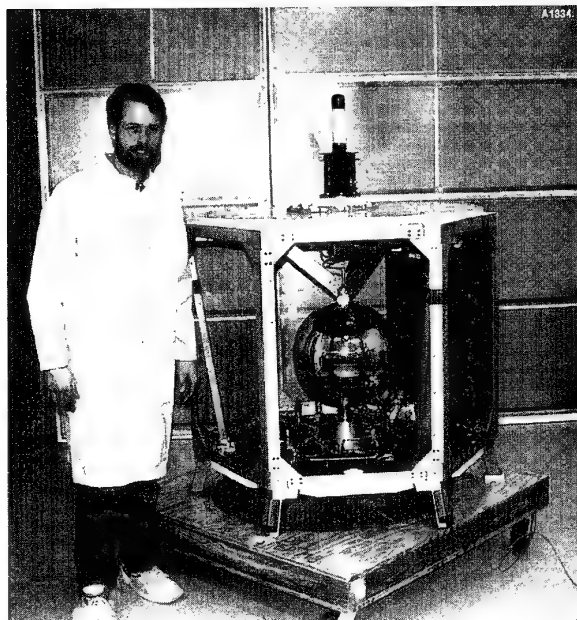


Figure 8. ESEX flight experiment.

combining the spacecraft mass with an accelerometer measurement. Specific impulse will be determined from the propellant mass flow rate and thrust. Efficiency will be derived from the voltage current product (power) and the thrust data. Because electric propulsion devices historically have been encumbered by ground-facility errors, comparable flight data are needed (Ref. 3). The electric propulsion spacecraft interactions that most concern designers are electromagnetic interference (EMI), plume contamination, and thermal radiation. However, it is difficult to measure plume contamination and EMI accurately in ground facilities because the vacuum chamber walls can greatly affect these measurements.

A high-power arcjet operating at hundreds of amperes of current is a potential source for EMI (Ref. 4). Spacecraft designers can work around EMI, but first they must characterize it. The ESEX antennas will measure EMI in the GHz-frequency range, which corresponds to satellite communication channels.

During life tests of the arcjet, it was discovered that tungsten was lost from the electrodes. Tungsten represents a serious contamination issue for solar arrays and optics. However, it is assumed that this mass is ejected away from the spacecraft at a velocity close to the arcjet exhaust velocity. ESEX will measure the deposition of tungsten and other contaminants impinging on the spacecraft to verify this assumption.

The arcjet converts approximately 30% of its energy into thrust. Therefore, about 70% of the total energy is either conducted to the spacecraft as heat or is lost into space (by radiation and frozen flow losses). Although conducted heat loss can be measured on the ground, the portion of the expelled energy that is radiated back to the spacecraft from the arcjet plume cannot easily be measured in ground tests. Radiated heat is affected by plume size and shape, which is determined by the background pressure and vacuum-chamber geometry. ESEX will be able to measure the amount of thermal radiation impinging on the spacecraft during a firing

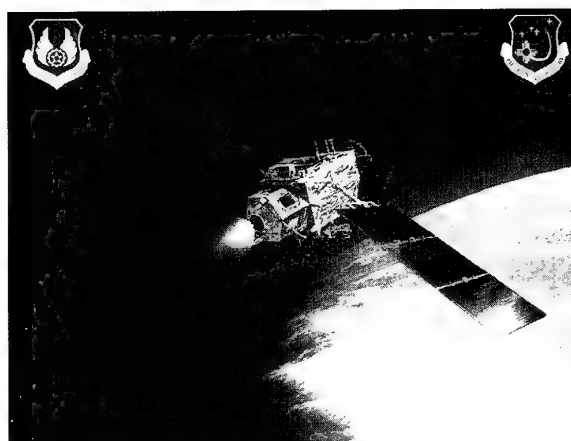


Figure 9. The ARGOS spacecraft with ESEX experiment in operation.

(Ref. 5). Additionally, measurements of the size and shape of the arcjet plume will be imaged at the Air Force Maui Optical Site (AMOS) in Hawaii.

### 3.3.2 Host Vehicle

ESEX is one of eight experiments scheduled to fly on the P91-1 spacecraft, the Advanced Research and Global Observation Satellite (ARGOS) (Figure 9) in early 1996. ARGOS is managed by the Space Test and Experiment Programs Office at the Space and Missile Systems Center (SMC). ARGOS is being built by Rockwell International and will be launched by a Delta II into a 460-nautical mile, 98.74-deg inclination orbit (Ref. 6). In addition to the measurements that will be made on board ESEX, ground controllers will be monitoring and recording the ARGOS state of health. In the event that the arcjet adversely affects ARGOS, the firing will be terminated. However, because of ARGOS' robust design and the fact that arcjet operation is not mission essential, the ESEX experiment offers little risk to the host satellite.

### 3.3.2 Schedule

In May 1994, ESEX completed component flight qualification and delivery (Figure 10a). Integration was completed in July, and harness fabrication was completed in August. System flight qualification began in September. Delivery to SMC for integration into ARGOS is scheduled for February 1995. ARGOS is currently scheduled for launch in January 1996 (Figure 10b).

## 4 THE NSTAR PROGRAM

In 1993, prompted by a request from the USAF/Phillips Laboratory (USAF/PL) to participate in the ELITE program, NASA initiated a program to validate low-power ion propulsion technology. This program, funded jointly by the NASA Office of Space Science and Office of Space Access and Technology, became the NSTAR validation program.

For NASA, two major benefits could be realized once the NSTAR program was completed. First, for small-body rendezvous and planetary flyby missions, ion propulsion would allow NASA to use Delta-class launch vehicles rather than Atlas- or Titan-class launch vehicles. With ion propulsion, the Delta-class launch vehicles could perform comparable or even enhanced missions (Figure 11).

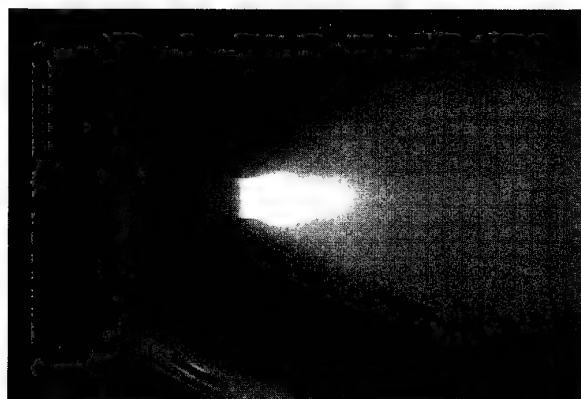


Figure 10a. 30-kW Arcjet (ESEX).

| MILESTONE                        | 1993 | 1994 | 1995 | 1996 |
|----------------------------------|------|------|------|------|
| CRITICAL DESIGN REVIEW           |      | ▽    |      |      |
| COMPONENT QUALIFICATION COMPLETE |      | ▽    |      |      |
| INTEGRATION COMPLETE             |      | ▽    |      |      |
| FLIGHT QUALIFICATION BEGINS      |      | ▽    |      |      |
| DELIVER TO ARGOS                 |      |      | ▽    |      |
| INTEGRATION WITH ARGOS           |      |      | ▽    |      |
| LAUNCH                           |      |      |      | ▽    |

Figure 10b. ESEX schedule.

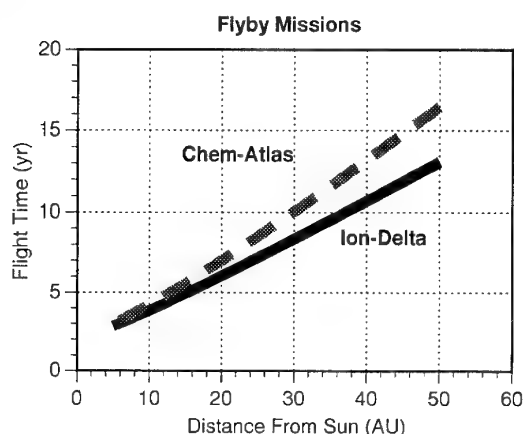
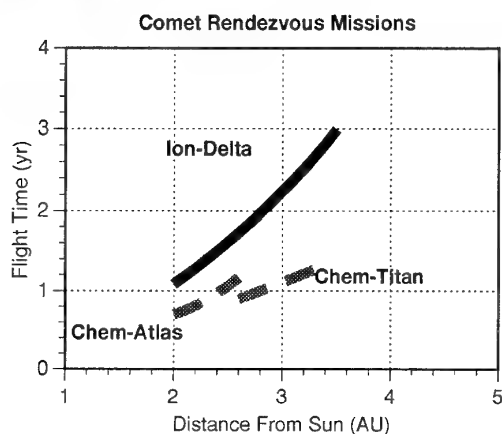


Figure 11. Comet rendezvous and planetary flyby performance comparison.

Second, using a small ion propulsion system with specific impulse ten times that of a chemical system would improve significantly the life or performance of large satellites in geosynchronous Earth orbit. For military satellites, an on-board ion propulsion system would increase the satellite's ability to reposition itself without compromising its on-orbit lifetime; it would still weigh less than the chemical system it replaced, which is sized only for station keeping of a large GEO satellite.

Studies show that for each application a single ion propulsion system is required. The system is composed of a 30-cm ion thruster, operating at a power level of 2.5 kW (input to the power processor) with a full-power lifetime of 8,000 hours, and a power processing unit with an efficiency of 92%.

An ion thruster (see Figure 12 for a schematic view) ionizes a propellant (xenon), accelerates the ions through a voltage drop (on the order of 1,000 V), and neutralizes the departing ions with electrons from a neutralizer. Like a chemical propulsion system, an ion propulsion system has a thruster and feed system and requires a power source and power processor to provide the thruster with power at the required DC voltages (Figure 13).

After years of development, the components of an ion propulsion system (ion thrusters, power processors, miniature feed system components, solar arrays, and distributed computer controls) are

ready for validation and application on a spacecraft. The development of ion propulsion technology coincides with efforts to reduce the costs of space missions. When deciding to invest in a space mission, today all costs including the costs of launch vehicles and post-launch mission operations and data analysis (MO&DA) are considered, and ways to reduce these costs are a major consideration. This focus on reducing costs has served to highlight the benefits of ion propulsion — a technology that can shorten mission duration, reduce the costs of MO&DA, and allow spacecraft to be launched with smaller launch vehicles, which would not be possible if chemical propulsion alone were used.

#### 4.1 NASA's Ion Propulsion Verification Program

##### 4.1.1 Overview

Ion propulsion offers a way to use smaller launch vehicles and still reduce trip time for a broad class of planetary missions. At the same time, ion propulsion can significantly improve the performance of large commercial and military satellites in GEO. Because of the benefits ion propulsion can offer, NASA initiated the NSTAR program to validate low-power ion propulsion technology.

##### 4.1.2 Purpose

The purpose of the NSTAR program is to obtain information that would allow a Project Manager to baseline ion propulsion for a spacecraft.

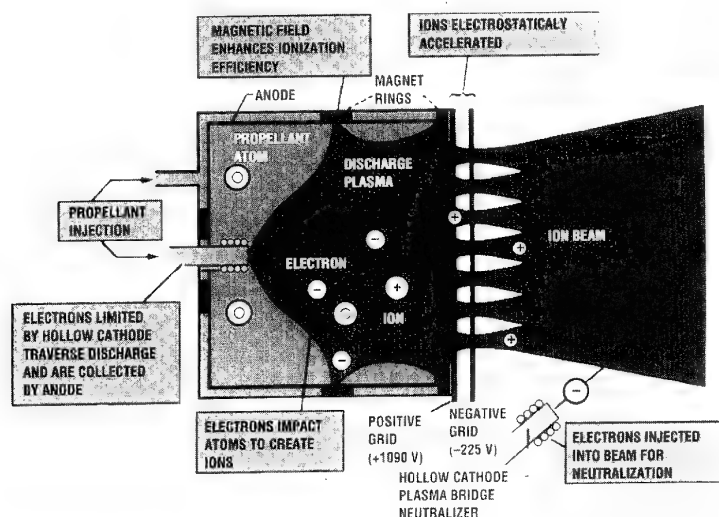


Figure 12. Operation of a gridded ion thruster.

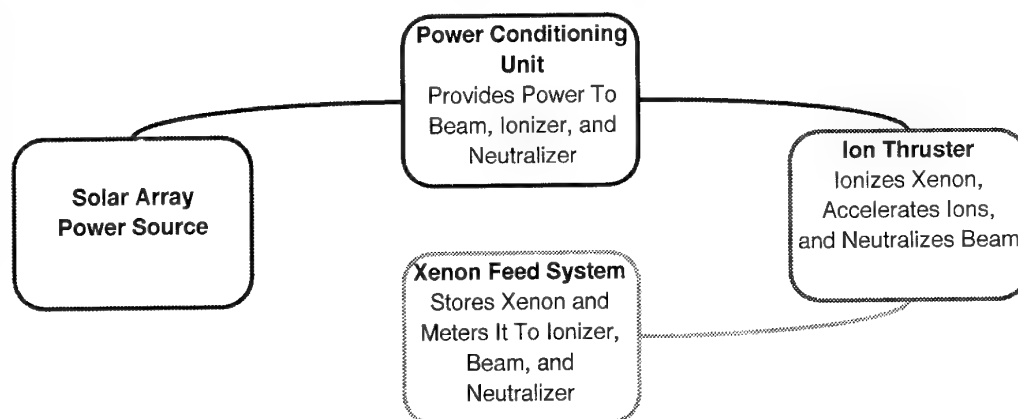


Figure 13. Conceptual block diagram of ion propulsion system.

#### 4.1.3 Objectives

The NSTAR program will accomplish the following objectives:

- Ensure that ion propulsion technology meets pertinent mission requirements by basing validation requirements on missions of interest.
- Validate life, integration, and performance in a ground-test program.
- Measure in-space interactions with the spacecraft and the surrounding space plasma by flying an ion propulsion experiment on a host spacecraft.
- Stimulate commercial sources for and uses of solar-powered ion propulsion.

## 4.2 NASA's Empirical Approach

### 4.2.1 Validation Approach

To provide the information a Project Manager needs to baseline ion propulsion on a spacecraft, it is first necessary to determine

what information is required. After this information has been identified, it is then necessary to demonstrate empirically that the hardware can satisfy the requirements.

The process for determining NSTAR requirements was accomplished in two stages. In the first stage, which continues at a low level, the user communities were surveyed to identify each community's needs. User needs were then ranked and taken as requirements (Ref. 7).

User-based requirements were then carefully apportioned to various tests and experiments that make up the NSTAR validation program. The major requirements are shown in Table 3, in which each user requirement corresponds to an NSTAR test or experiment addressing that requirement. The tests that comprise the ground-test element focus on the key issues that must be considered in any application of electric propulsion. The ground test will determine the following:

- Demonstrate service life including the modeling necessary so that the data taken during life testing can be applied to a spectrum of missions,
- Demonstrate performance (power handling, thermodynamic efficiency, specific impulse), and

- Demonstrate integrability, i.e., the ground measurement of EMI and plume effects.

The in-space experiments address key issues that can only be determined in space. The in-space experiments will accomplish the following:

- Measure direct effects (e.g., contamination, EMI) on the spacecraft and surrounding space plasma,
- Measure indirect effects that influence the cost of electric propulsion missions (e.g., guidance, navigation, and control (GN&C) and MO&DA), and
- Determine whether data taken during ground tests accurately replicate the data obtained during in-space operation.

The NSTAR program is executed jointly by the Lewis Research Center (LeRC) and the Jet Propulsion Laboratory, taking advantage of the best experience, facilities, and expertise available within NASA. LeRC is responsible for providing the ion thrusters and power processing units for the ground-test element and for the in-space experiment. JPL manages the program and is responsible for developing program requirements, the xenon feed system, and the in-space diagnostics.

The validation tests shown in Table 3 include ground-based tests that will determine ion engine life and performance and will measure plume transmissibility and EMI. The in-space experiment will measure the effects of ion propulsion on a spacecraft as

well as on the host spacecraft and the surrounding space plasma. The in-space experiment will also assess the ability of ground testing to replicate the data obtained during operation in space. In-space operation will further demonstrate the capability to integrate and operate an ion propulsion system.

#### 4.2.1.1 Schedule

Figure 14 shows a schedule for the two parallel elements: a ground-test element and an in-space experiment element.

#### 4.2.1.2 Ground-Test Element

In the ground-test element, the first parallel element, lifetime and performance of the system will be demonstrated, and data necessary for integration of the ion propulsion system will be collected for plume divergence, plume transmissibility, and EMI.

The ground-test element is composed of four main tests and several supporting test series. Three engineering model thrusters and two breadboard power processors will be used in the test program.

The first engineering model thruster will be used in a 2,000-hour test to confirm whether the life-limiting mechanisms, principally erosion of the accelerator grid by charge-exchange ions, are the same as those observed in past versions of the 30-cm ion thruster. Furthermore, this test should provide the most accurate measurement to date of the wear-out rates associated with the various wear-out mechanisms. Upon completion of the 2,000-hour test, the thruster will be refurbished and then subjected to a series of environmental qualification tests; these tests will serve as precur-

Table 3. Summary of NSTAR validation requirements.

| Requirement   | NSTAR Test Addressing Requirement                               | Planned Test/Experiment Date |
|---|---|------------------------------|
| Thruster lifetime of 8,000 hr with demonstrated margin of 50%   | Life Validation Test  | 1996–1997                    |
| Thruster cyclic life equivalent to 15-years station keeping and 2 repositions per year  | Cyclic Life Test  | 1996                         |
| Assessment of wear-out mechanisms and determination of their rates  | Cyclic Life Test<br>Life Validation Test                        | 1996<br>1996–1997            |
| Power processor efficiency of 92% at maximum power  | Cyclic Life Test<br>Life Validation Test                        | 1996<br>1996–1997            |
| Demonstration of ion propulsion system integration with host spacecraft   | System Integration  | 1998                         |
| Commercial source for ion propulsion flight experiment  | Delivery and Integration of Flight Thruster and Power Processor | 1999                         |
| Measurements of in-space performance of ion propulsion system and comparison to ground test results   | In-Space Experiment   | 1999–2000                    |
| Measurements of ion propulsion system interactions with host spacecraft and surrounding space plasma (contamination, EMI, communications, etc.) | In-Space Experiment   | 1999–2000                    |
| Assessment of impacts of ion propulsion on GN&C and MO&DA   | Post In-Space Experiment  | 2000                         |

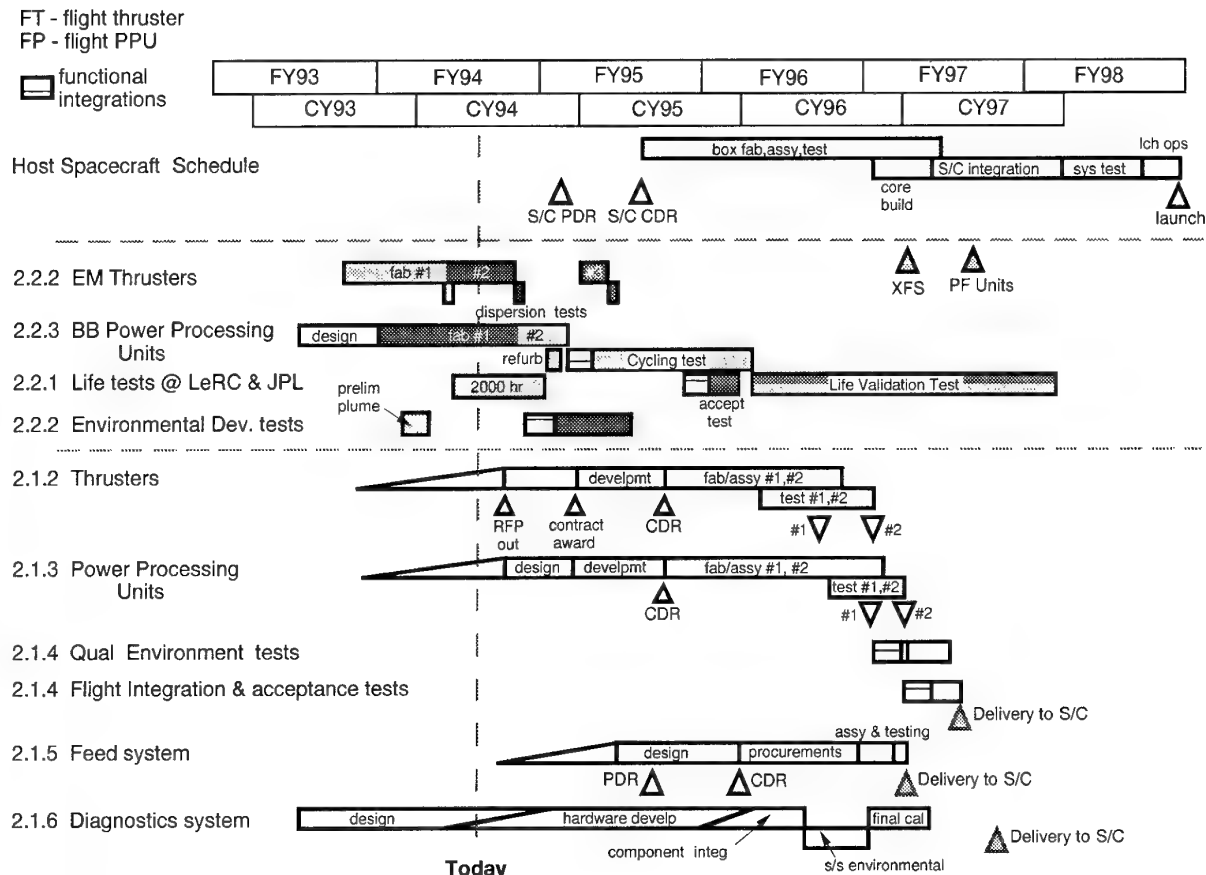


Figure 14. NSTAR activity schedule.

sors to a similar series of tests that will be conducted on a protoflight thruster.

The second engineering model thruster and the first breadboard power processor will be subjected to a test designed to simulate a thruster performing station keeping and repositioning for a satellite in geosynchronous orbit. This test will be conducted at full power for a duration of 5,700 hours and a total of 5,000 on/off cycles. At specific points during the test series, approximately once each month, the thruster's performance over its entire throttling range will be tested.

The third engineering model thruster and the second breadboard power processor will be used in the Life Validation Test, a long-duration test to validate that the service life of the system is more than 8,000 hours. This test requires a minimum of 12,000 hours that will demonstrate a 50% margin relative to the desired 8,000-hour service life. The full 2.5-kW input power will be used for the duration of the test, except when periodic measurements of performance at throttled conditions are performed, which will be approximately once per week. The validation of thruster life will be considered successful after 12,000 hours have been demonstrated. The test will continue until the thruster ceases to perform acceptably, thereby providing additional data for life assessment and failure analysis.

One of the principal objectives of these tests, besides verifying performance and demonstrating acceptable life, is identifying all

significant life-limiting processes and quantitatively measuring the pertinent rates associated with each process.

#### 4.2.1.3 In-Space Element

The second parallel element is the in-space experiment, in which the interaction of the ion propulsion system with the host spacecraft and the surrounding space plasma will be investigated and quantified. The ion propulsion experiment was designed as part of the USAF/TRW ELITE spacecraft. An artist's conception of the in-space configuration of the experiment is shown in Figure 15.

The in-space element is intended to accomplish several objectives. The first objective is to demonstrate in-space performance and capabilities of ion propulsion. The measurements taken during the course of the in-space experiment will quantify the direct effects of ion propulsion on the host spacecraft and the surrounding space plasma. Indirect impacts of ion propulsion will also be assessed. Indirect impacts include changes to spacecraft integration activities — as compared to chemical propulsion — changes in the conduct and execution of guidance, navigation, and spacecraft control, changes in the planning, training, and conduct of MO&DA, and changes in the scheduling of other spacecraft activities.

The direct measurements taken in orbit will include

- Contamination, particularly of optical and cooled surfaces,



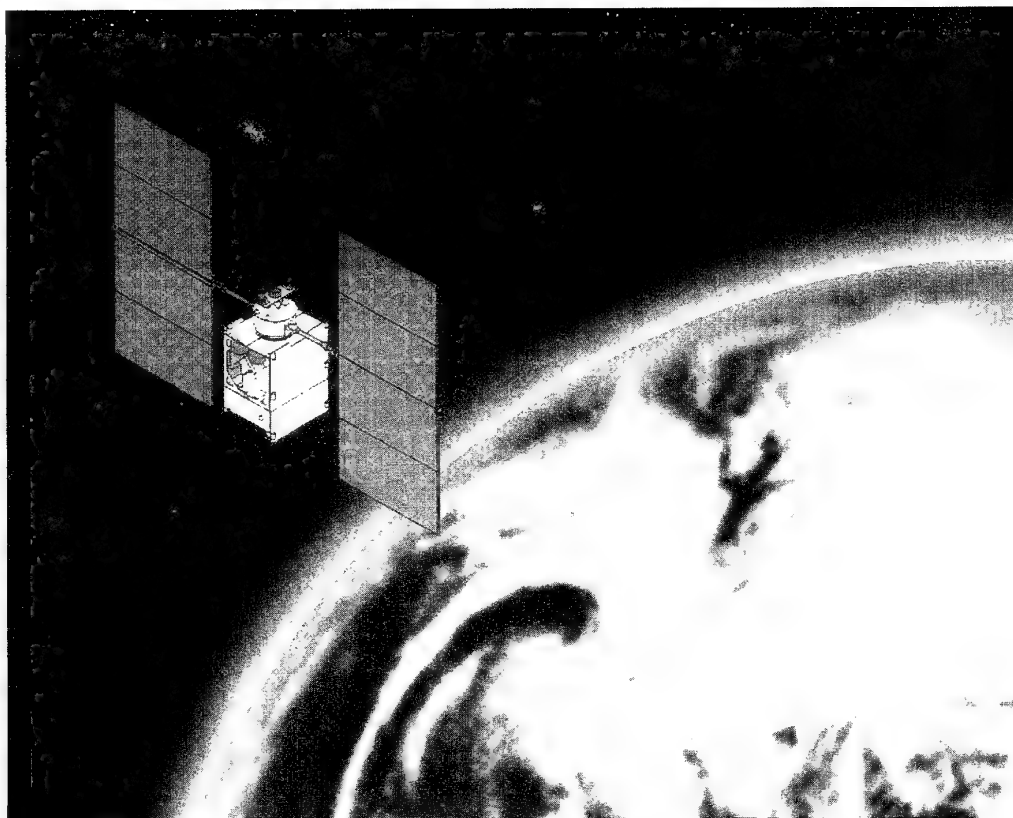


Figure 15. ELITE spacecraft with NSTAR ion propulsion experiment.

- Communications, particularly of transmission through the plume of the ion engine,
- EMI, particularly steady-state and transient-induced magnetic and electric fields, and
- Effects of the ion propulsion system on the electric and magnetic properties of the surrounding space plasma. Particular attention will be paid to obtaining data necessary to assess the effect of an ion propulsion system on interplanetary field and particles measurements.

The physical measurements that will accomplish the direct measurements are described in Table 4.

Measurements taken during operation of the ion thruster in ground testing will be compared with data obtained during in-space operation. For example, an integration of feed system pressure data combined with careful tracking of the spacecraft will enable researchers to estimate thruster performance. Power and thermal measurements will allow power conversion efficiency to be determined. Such gross measurements are important to confirm the adequacy of measurements taken during ground testing.

Also important are measurements of parameters that are supposedly influenced by the hard vacuum of space, such as accelerator grid impingement current. The behavior of these parameters as a function of thruster-operating condition and duration will be studied carefully.

After the mission, indirect impacts will be assessed by examining the change in the costs and degree of difficulty caused by incorporating ion propulsion on spacecraft integration and system test, GN&C, MO&DA, and scheduling.

The in-space element will address the program's objective to stimulate commercial sources for and uses of ion propulsion. For all government users, this objective is important for several reasons. If no commercial source of ion propulsion technology is available, then ion propulsion technology cannot be incorporated on government spacecraft. If a commercial source exists but no commercial uses of the technology are made, then the costs of this technology to the government would be significantly greater than would be the case were commercial users available.

The two flight ion thrusters and the two flight power processors will be purchased from a commercial source. We expect that the commercial source will participate in NASA's ground-test element. This participation should provide NASA's industrial partner with the knowledge and hands-on experience needed to continue the technical evolution of the ion propulsion system after NSTAR is completed. NASA would then turn its attention to the next generation of propulsion equipment, just as it did following the successful infusion of the hydrazine arcjet into the commercial space sector in 1993.

#### 4.2.1.4 Funding

The funding profile planned for the NSTAR validation program is shown in Figure 16. These funds are equally split between the ground-test portion of the program and the in-space portion and

Table 4. In-space diagnostics measurements for the NSTAR space experiment.

| Instrument                     | EMI | Plasma or Spacecraft | Plume | Communication | Contamination | Radiation |
|--------------------------------|-----|----------------------|-------|---------------|---------------|-----------|
| Electric Field Antenna         | ✓   |                      |       |               |               |           |
| Langmuir Probe                 |     | ✓                    | ✓     |               |               |           |
| Spacecraft Potential Probe     |     | ✓                    |       |               |               |           |
| Internal Discharge Monitor     | ✓   |                      |       |               |               |           |
| Solar Array Current Collectors |     | ✓                    | ✓     |               |               |           |
| Magnetometer                   | ✓   |                      |       |               |               |           |
| Mass Spectrometer              |     |                      |       |               | ✓             |           |
| SGLS Omni Antenna              |     |                      |       | ✓             |               |           |
| X-Band Transmitter/Receiver    |     |                      |       | ✓             |               |           |
| Quartz Crystal Microbalance    |     |                      |       |               | ✓             |           |
| Calorimeter                    |     |                      |       |               | ✓             |           |
| Optical Effects Monitor        |     |                      |       |               | ✓             |           |
| Solar Photovoltaics            |     |                      |       |               | ✓             | ✓         |
| Radiation Monitor              |     |                      |       |               |               | ✓         |
| Microelectronics               |     |                      |       |               |               | ✓         |

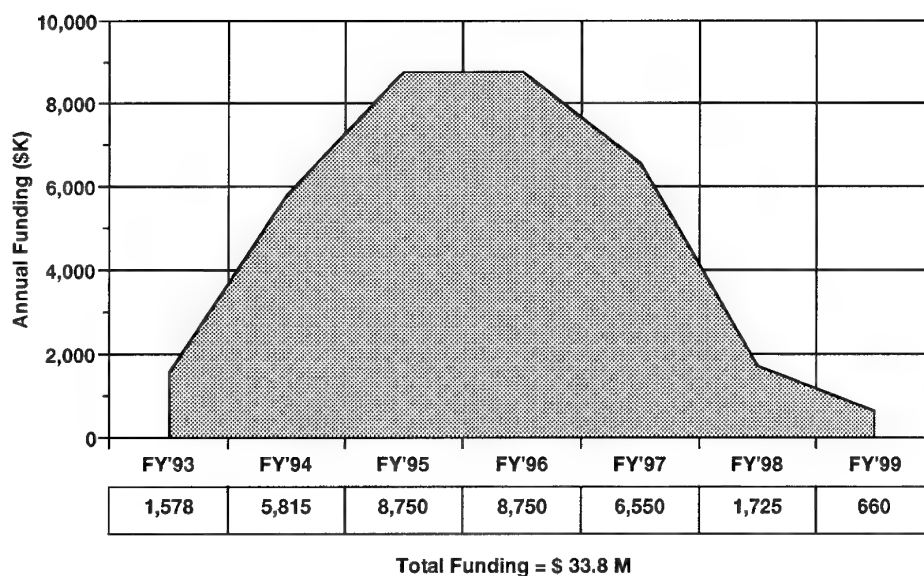


Figure 16. Funding profile.

include a nominal allowance for the integration of the NSTAR in-space experiment onto the host spacecraft. These expenditures *do not* include the cost of civil service personnel from LeRC, who support NSTAR, nor do they include the cost of the solar array, which it is assumed will be provided with the host spacecraft.

#### 4.3 Status of NSTAR Technology Validation Program

##### 4.3.1 Ground-Test Program

The ground-test element of the NSTAR validation program has been under way since late 1993, when testing of the functional

model thruster was begun. The purpose of this test was to provide data that would verify a design in which the mass of the ion thruster is reduced to 7 kg, making it more producible. These tests were successfully completed early in 1994 and served as a precursor to the subsequent fabrication and testing of the first engineering model thruster.

Figure 17 shows this 30-cm thruster installed in the test facility prior to the test. Figure 18 shows the neutralizer installed on the thruster prior to the test. The preparation of the LeRC 15-foot-diameter-by-60-foot vacuum chamber is shown in Figure 19. At

the bottom of the figure, the inlets for the diffusion pumps can be seen. Figure 20 shows a hollow cathode before it was installed on the first engineering model thruster. The high-voltage isolator used on the main cathode feed line is shown in Figure 21, and the feed system flow controllers installed outside the vacuum chamber are shown in Figure 22.

On June 23, 1994, the 2,000-hour test for the first engineering model thruster began and is continuing at the time of this meeting. During testing, a malfunction in the facility power supply resulted

in a hiatus of several weeks; this occurred after 870 hours of the test had been completed without incident. The purpose of the test was to confirm earlier work that identified wear-out mechanisms and to quantify the rates associated with those mechanisms. Preliminary examination of the data from the 2,000-hour test confirms that the principal wear-out mechanism is the erosion of the accelerator grid by charge-exchange ions, indicating that the expected life of the thruster is comfortably in excess of the 12,000 hours required to demonstrate an 8,000-hour service life.

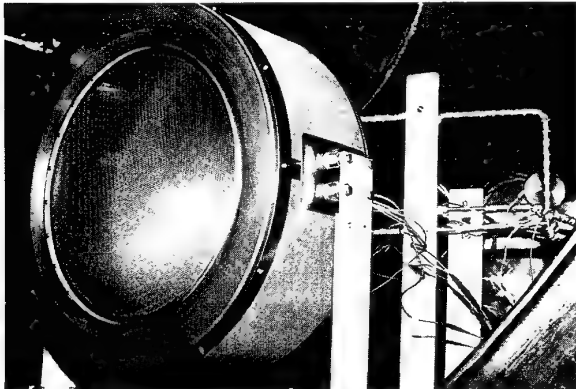


Figure 17. Engineering model thruster-1 in place for 2,000-hour wear test.

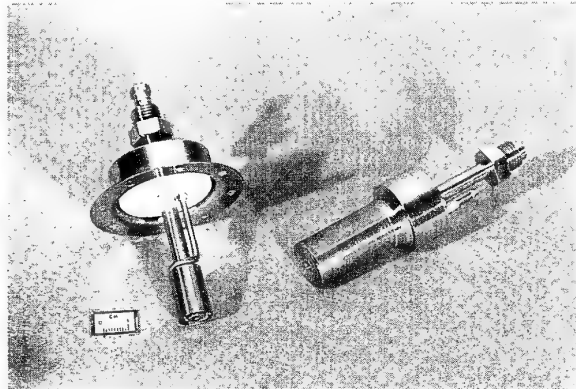


Figure 20. Hollow cathodes used for main discharge (left) and neutralizer.

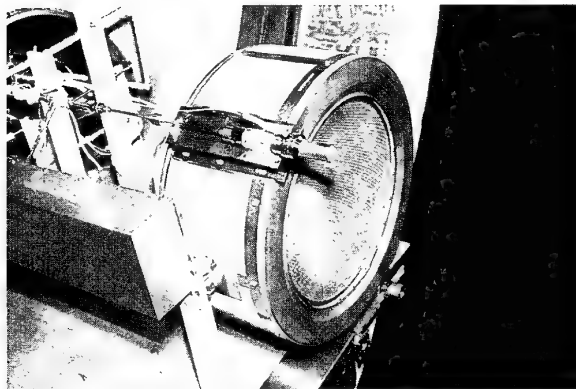


Figure 18. Engineering model thruster-2 showing neutralizer.

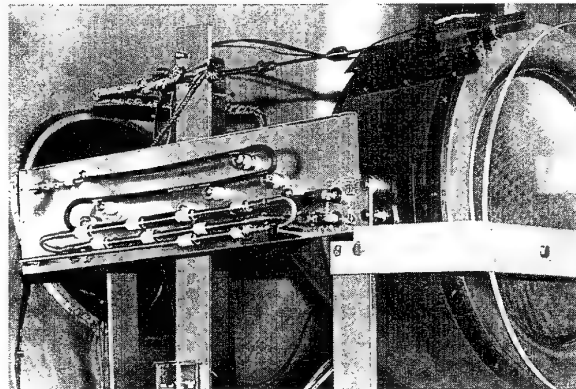


Figure 21. High-voltage isolator with metal box cover (shown in Figure 18) removed.

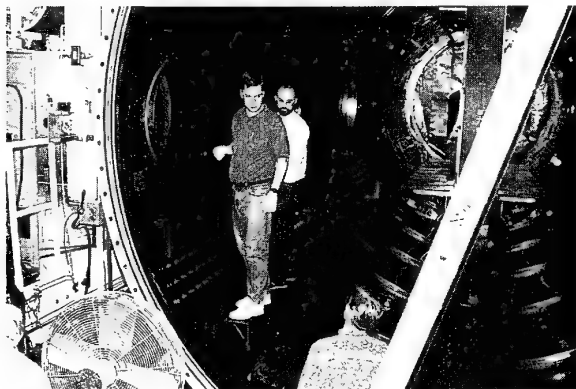


Figure 19. Vacuum test facility.

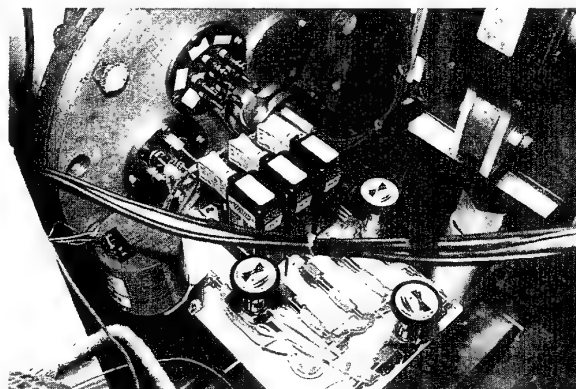


Figure 22. Facility xenon flow-control system mounted adjacent to and outside of the vacuum chamber.

The second engineering model thruster is being fabricated, and the first breadboard power processor is nearing completion and should be ready for the Thruster Cycling Test planned for April 1995. The first engineering model thruster will be refurbished and used for simulated environmental qualification tests, verifying the ability of the future flight thruster to withstand the rigors of the protoflight qualification program.

#### 4.3.2 Host Spacecraft

Early in 1994, the cooperative partnership between TRW, Inc. and the USAF/Phillips Laboratory that was to result in the ELITE program was effectively ended due to cuts in U.S. defense spending. With it, the initial impetus for the validation of ion propulsion technology using a host spacecraft for the in-space experiment element also ended. However, NASA believed the benefits of validating low-power ion propulsion technology for future government and commercial missions were significant and decided to continue the NSTAR validation program and to redouble efforts to find a host spacecraft that would support the ion propulsion experiment. As of this writing several opportunities have been identified, both with the USAF and NASA. Present planning has focused on the first or second Integrated Space Technology Flight (ISTF) planned by USAF/Phillips Laboratory.

### 5 CONCLUSIONS

- Typically, the number of arcjet spacecraft maneuvers are 1 to 2 times that of chemical propulsion, and ion engine maneuvers are 2 to 10 times the number provided by chemical propulsion for the range of spacecraft masses and powers considered here.
- Power requirements for the ion propulsion are greater than that for the arcjet, but not much greater for spacecraft maneuvers up to 10 deg/day. Therefore, ion propulsion is the best choice when the mission priority is to increase the number of spacecraft maneuvers at moderate maneuver rates.
- ESEX, a program conducted by the USAF, provides the first on-orbit validation and demonstration of the technology associated with high-power arcjets.
- NASA has initiated a program to validate low-power ion propulsion technology called NSTAR.
- The NSTAR validation program consists of two mutually dependent, interlocking parts: a series of ground-based tests and an in-space experiment.
- Successful completion of the NSTAR validation program will significantly improve the performance and life of large satel-

lites in GEO, for both civilian and military use, by reducing the mass required for on-orbit station keeping and repositioning.

- Successful completion of the NSTAR validation program will significantly improve the performance of NASA's small comet rendezvous and planetary flyby missions.
- Successful completion of the NSTAR validation program will result in the development of a commercial source for ion propulsion flight equipment.

### 6 ACKNOWLEDGMENT

The authors wish to acknowledge and thank the staff of the USAF/Phillips Laboratory's Propulsion Directorate for their contribution and assistance in the completion of this paper.

The research described in this paper was carried out by the Jet Propulsion Laboratory, California Institute of Technology, under a contract with the National Aeronautics and Space Administration and at Lewis Research Center and the USAF/Phillips Laboratory.

### 7 REFERENCES

1. Sutton, A. M., "Overview of the Air Force ESEX Flight Experiment," IEPC-93-057, 23rd IEPC, September 1993.
2. Aadland, R. S., et al., "Integrated Mission Simulation of a 26 kW Arcjet Flight Arcjet Propulsion System," AIAA 93-2395, June 1993.
3. Deininger, W. D., "30-kW Ammonia Arcjet Technology," Final Report, July 1986–December 1989.
4. Johnson, L. K., et al., "Frequency-Domain Electromagnetic Characteristics of a 26 kW Ammonia Arcjet," AIAA 93-2393, June 1993.
5. Kriebel, M. M., Stevens, N. J., "30-kW Class Arcjet Advanced Technology Transition Demonstration (ATTD) Flight Experiment Diagnostic Package," AIAA 92-3561, July 1992.
6. Turner, J. B., "The Advanced Research and Global Observation Satellite (ARGOS) Program," AIAA 94-4580, Space Programs and Technologies Conference, September 1994.
7. Kakuda, R. Y., et al., *Small Body Rendezvous Mission Using Solar Electric Ion Propulsion: Low Cost Mission Approach and Technology Requirements*, IAA International Conference on Low-Cost Planetary Missions, IAA-L-0710, April 12–15, 1994.

# Shuttle Orbiter Experiments -- Use of an Operational Vehicle for Advancement and Validation of Space Systems Design Technologies

Paul F. Holloway\* and David A. Throckmorton†

NASA Langley Research Center  
Hampton, Virginia 23681-0001  
USA

## SUMMARY

The NASA Orbiter Experiments (OEX) Program provided a mechanism for utilization of an *operational* space shuttle orbiter as a flight research vehicle, as an adjunct to its normal space transportation mission. OEX Program experiments were unique among orbiter payloads, as the research instrumentation for these experiments were carried as integral parts of the vehicle's structure, rather than being placed in the orbiter's payload bay as mission-unique cargo. On each of its first 17 flights, the Orbiter *Columbia* carried some type of research instrumentation. Various instrumentation systems were used to measure, in flight, the requisite parameters for determination of the Orbiter's aerodynamic characteristics over the entire entry flight regime, and/or the aerodynamic-heating rates imposed upon the vehicle during the hypersonic portion of atmospheric entry. The data derived from this instrumentation represent benchmark hypersonic flight data heretofore unavailable for a lifting entry vehicle. The data are being used in a continual process of validation of state-of-the-art methods, both experimental and computational, for simulating/predicting the aerodynamic and aerothermal characteristics of advanced space transportation vehicles.

This paper describes the OEX Program complement of research experiments, presents typical flight data obtained by these experiments, and demonstrates the utilization of these data for advancement and validation of vehicle aerothermodynamic-design tools. By example, the concept of instrumenting operational vehicles and/or spacecraft in order to perform advanced technology development and validation is demonstrated to be an effective and economical method for maturing space-systems design technologies.

## LIST OF SYMBOLS

|       |  |
|-------|--|
| ACIP  | Aerodynamic Coefficient Identification Package |
| AIP   | Aerothermal Instrumentation Package            |
| c. g. | center-of-gravity                              |
| CSE   | Catalytic Surface Effects                      |
| DFI   | Development Flight Instrumentation             |
| DSMC  | direct simulation Monte Carlo                  |
| GN&C  | guidance, navigation, and control              |
| HiRAP | High-Resolution Accelerometer Package          |
| IMU   | Inertial Measurement Unit                      |
| L/D   | lift-to-drag ratio                             |
| NASA  | National Aeronautics and Space Administration  |

|        |  |
|--------|--|
| OARE   | Orbital Acceleration Research Experiment     |
| OEX    | Orbiter Experiments                          |
| RCG    | reaction-cured glass                         |
| RCS    | reaction control system                      |
| SEADS  | Shuttle Entry Air Data System                |
| SILTS  | Shuttle Infrared Leeside Temperature Sensing |
| STS-xx | space shuttle mission numerical designation  |
| SUMS   | Shuttle Upper-Atmosphere Mass Spectrometer   |
| TGH    | Tile-Gap Heating                             |
| TPS    | thermal protection system                    |
| x/L    | non-dimensional vehicle length (L=32.77m)    |
| $\rho$ | density                                      |

## 1.0 INTRODUCTION

The NASA Orbiter Experiments (OEX) Program had its genesis in the early days of the design and development process of the space shuttle orbiter. The orbiter's operational requirement for repeated, controlled aerodynamic entry from low-Earth orbit to a horizontal landing at a predetermined landing site presented significant challenges to its aerothermodynamic designers. The vehicle was required to be aerodynamically controllable across the speed-regime, from Earth-orbital, hypersonic entry velocities to low-subsonic landing speeds; and the vehicle's thermal protection system (TPS) was required to protect the vehicle's structure from the extreme levels of aerodynamic heating which would accompany the hypersonic entry, yet be reusable for many additional missions.

The aerothermodynamic design process required a high degree of integration among the disciplines of aerodynamics, aeroheating, and guidance, navigation and control. The aerodynamic performance, and stability and control characteristics, of the orbiter configuration had to be adequately defined over the entire entry flight regime in order to enable design of the guidance, navigation and flight control systems. The vehicle's aerodynamic heating environment had to be adequately predicted in order to enable design of the thermal protection system and definition of the thermal flight-envelope constraints which would influence entry trajectory design.

An extensive program of ground-based testing was undertaken in order to generate the database required for aerothermodynamic design of the orbiter. This test program required tens of thousands of hours of wind-tunnel testing: including aerodynamic performance, stability and control, and aerodynamic heat-transfer testing. This expansive ground-test program notwithstanding, it was recognized that, prior to the orbiter's first flight, significant uncertainties would exist in predictions of both the vehicle's

\*Director

†Manager, Space Transportation Technology

aerodynamic characteristics and its aerodynamic-heating environment. These uncertainties resulted from inherent limitations in the ability of ground-test facilities to adequately simulate the full-scale flight environment. Additionally, since no data existed for a lifting vehicle in the actual flight environment, methodologies for extrapolation of ground-test results to the flight environment could not be validated.

The vehicle's flight control and thermal protection system designs were required to be sufficiently robust to assure fail-safe operation of the orbiter during entry in the face of these uncertainties. Systems robustness would be obtained through the application of significant factors of conservatism in the systems designs, and result in a highly-constrained aerodynamic flight envelope, severe limitations on allowable vehicle center-of-gravity variation, and most probably an overweight thermal protection system. The levels of conservatism in the orbiter's final aerothermodynamic design were anticipated to be significant, and the research community recognized the importance of eliminating such conservatism in the design of future space transportation vehicles. Members of this community also recognized the unique opportunity presented by Shuttle operations: to routinely gather hypersonic aerothermodynamic flight data with which to enhance understanding of the real-gas, hypersonic flight environment, and to enable improvement and validation of ground-to-flight data extrapolation techniques. Thus the concept of the Orbiter Experiments (OEX) Program was born.

The primary purpose of this paper is to suggest, and demonstrate by the OEX example, that the instrumentation of *operational* vehicles and/or spacecraft can provide unprecedented opportunities to further technology and validate predictive and design methodologies at a readily affordable cost. The incorporation of research instrumentation aboard an *operational* shuttle orbiter has proven to be a cost-effective method of obtaining advanced technology validation data. The data collected using this instrumentation also proved to be of substantial value to the operational shuttle system, enabling orbiter vehicle performance enhancements and incremental expansion of its flight envelope. During these current times of drastically reduced national space budgets, the authors hope that this paper will inspire others to follow the OEX example.

## 2.0 ORBITER FLIGHT RESEARCH INSTRUMENTATION

The selections of instrumentation to be implemented as part of the Orbiter Experiments Program were driven by objectives to: (1) acquire flight data of the same types as normally obtained in wind tunnels, and (2) to measure those data at accuracy levels which were equal to, or better than, those of the corresponding ground-derived data. Orbiter operational instrumentation would provide information describing the vehicle's control configuration during entry (i.e., aerodynamic control-surface positions and reaction control system jet firing activity), and orbiter flight-test instrumentation (aboard the Orbiter *Columbia*) would provide some aerodynamic surface-pressure and -temperature information. The OEX Program provided for the design, development, and integration of experiment instrumentation which augmented the existing orbiter instrumentation. OEX

experiment instrumentation focused on collection of: accurate freestream-environment and vehicle-attitude information, vehicle-motion data (for determination of aerodynamic forces and moments), and vehicle surface-temperature data (for determination of aerodynamic heat-transfer rates). The total complement of orbiter instrumentation and OEX experiments comprised a comprehensive instrumentation system for the determination of orbiter aerodynamic and aerothermal flight characteristics across the entire entry flight regime.

Several early papers (Refs. 1-3) documented the planning for utilization of the orbiter as an entry flight-research vehicle. Reference 1 provides an excellent presentation of the data requirements for orbiter aerodynamic testing, as well as descriptions of the orbiter baseline and OEX measurement systems which were to be implemented to enable orbiter aerodynamic research. A summary discussion of the more significant orbiter entry aerothermodynamic problems, and short, overview descriptions of the proposed OEX experiments are contained in Reference 2. Lastly, planned aerothermodynamic flight-research analyses, to be conducted by NASA Langley Research Center staff members, using data obtained during the Orbital Flight Test missions of the Orbiter *Columbia*, are described in Reference 3.

The following subsections contain discussions of both the orbiter baseline and OEX-unique instrumentation systems which were used to obtain orbiter entry aerothermodynamic flight-research data. Each system discussion addresses the experiment concept, its hardware implementation, and its flight operations history.

### 2.1 Freestream Environment and Vehicle Attitude Data

For shuttle orbiter *operational* purposes, inertial measurement techniques are used to infer the air-data parameters required for vehicle guidance, navigation, and control (GN&C) during hypersonic flight. The inertially-derived parameters are sufficiently accurate to enable the GN&C system to guide the vehicle to the vicinity of the landing site, where data from other sources provide updates to the vehicle state vector and enable the vehicle to be flown to a precise landing. The inertially-derived air-data parameters were *not* considered sufficiently accurate, however, for research flight data analyses. Consequently, the OEX Program provided for the development and implementation of in-situ measurement systems to enable "research-quality" determination of vehicle freestream environmental and attitude information.

**2.1.1 Shuttle Entry Air Data System (SEADS) -** The Shuttle Entry Air Data System (Refs. 4 and 5) was designed to provide "across-the-speed-range" air data from approximately 90 km altitude, when the orbiter vehicle is traveling in excess of Mach 25, through the supersonic, transonic, and subsonic portions of the entry, to landing. The SEADS system comprised a specially-designed orbiter nose-cap, which incorporated 14 pressure-orifice assemblies through which the aerodynamic surface pressure could be measured during entry (Fig. 1). Measurement of the magnitude and distribution of aerodynamic pressure acting on the orbiter's nosecap in flight, enabled accurate post-flight determination of vehicle angles-of-attack and -sideslip, as well as freestream dynamic pressure.



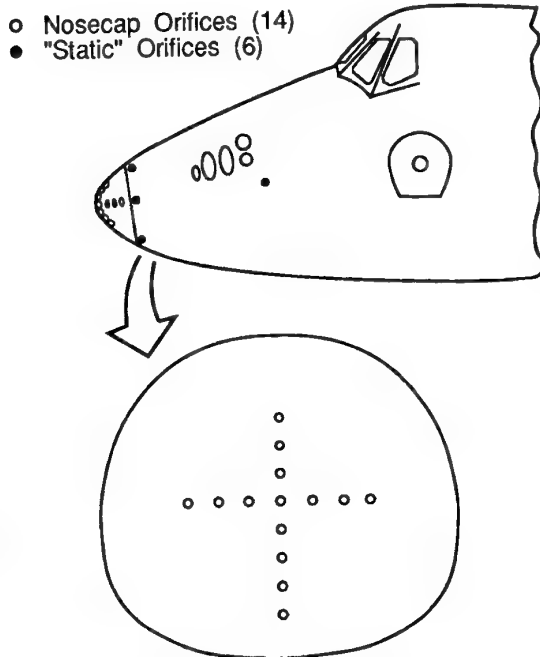


Figure 1 -- SEADS experiment system schematic.

The SEADS pressure orifices were arranged in a cruciform array (Fig. 1) with eight orifices in the plane of symmetry and six orifices in the transverse plane. The symmetry-plane orifice array contributed primarily to determination of stagnation-point location and pressure, and vehicle angle-of-attack. The transverse orifice array contributed primarily to determination of angle-of-sideslip. Each orifice assembly was connected, through internal nosecap "plumbing," to two pressure transducers -- one with a measurement range of 0-1 psia, and one with a measurement range of 0-20 psia. Dual-range measurements at each orifice assured accurate determination of pressure level for the entire altitude regime over which the system was designed to operate. Temperatures of the pressure transducer banks (of which there were two) were measured in order to account for the temperature-dependence of transducer calibrations.

The nosecap orifices were augmented by six supplementary "static" orifices located on the orbiter forebody aft of the nosecap (Fig. 1). Four of these measurements were obtained at locations around the periphery and just aft of the nosecap: two, located windward and leeward, on the plane of symmetry; and one located on either side of the fuselage. Two additional pressure orifices, located well aft of the nose, on either side of the fuselage, provided static pressure data which were of particular importance for low-supersonic and subsonic air-data parameter determination.

Air-data parameters were determined from the SEADS pressure data post-flight, by application of a unique data-processing algorithm. This algorithm incorporated a mathematical model of the pressure distribution about the orbiter forebody as a function of an "aerodynamic state vector" which had elements of total and static pressure, and angles-of-attack and -sideslip. The mathematical model was constructed based upon a combination of theoretical considerations and the

results of extensive wind-tunnel tests. The flight-observed pressures were smoothed, with respect to time, and then "fit" to the model pressures using a "digital-batch-filter" process which optimized the "aerodynamic state vector" by minimizing, in a weighted-least-squares sense, the differences between the flight-observed and model pressures.

The SEADS was installed in place of the baseline nosecap on the Orbiter *Columbia* during that orbiter's modification period in 1984-85. The SEADS was subsequently operated on five missions: STS-61C, -28, -32, -35, and -40.

**2.1.2 Shuttle Upper-Atmosphere Mass Spectrometer (SUMS)** -- The Shuttle Upper-Atmosphere Mass Spectrometer experiment (Ref. 6) was intended to supplement the SEADS by providing atmospheric density data at altitudes above 90 km. Just as SEADS would provide flight environmental information in the continuum-flow flight regime, the SUMS would provide similar data to enable aerodynamic research in the transitional and free-molecular-flow flight regimes. At these extreme altitudes, aerodynamic surface pressures are too low to be accurately sensed by conventional pressure transducers such as those used by the SEADS. The SUMS instrument, instead, utilized a mass spectrometer, operating as a pressure-sensing device, to determine orbiter stagnation-region surface pressure, and thence infer the atmospheric density in this high-altitude, rarefied-flow flight regime.

The SUMS mass spectrometer was originally spare flight equipment developed for the Viking Mars Lander. This mass spectrometer was modified to enable it to operate in the entry flight environment of the shuttle orbiter. The SUMS sampled atmospheric gases through an orifice on the orbiter's lower-surface centerline, just aft of the orbiter nosecap; this orifice was shared with the SEADS experiment. The mass spectrometer was connected to the gas-sampling orifice by a unique inlet system comprised of tubing, operation-control valves, and a pressure transducer. The SUMS instrument assembly was mounted on the forward bulkhead of the orbiter's nose wheel well (Fig. 2), with the inlet system connected to the orifice plumbing. The basic

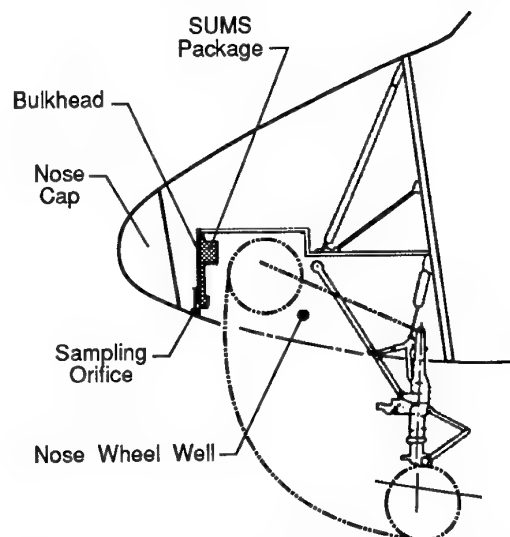


Figure 2 -- SUMS experiment installation schematic.

SUMS flight data were combined with computational modeling of the rarefied flow within both the orbiter's forebody flowfield and the inlet system, to enable determination of the freestream atmospheric density during entry.

The SUMS was initially installed aboard the Orbiter *Columbia* following its 1984-85 modification period. The experiment was subsequently flown on three missions: STS-61C, -35, and -40. SUMS flight-test results are summarized in Reference 7.

## 2.2 Aerodynamic Force and Moment Data

**2.2.1 Inertial Measurement Units (IMU)** -- The inertial measurement units are part of the orbiter's operational instrumentation system. The triply-redundant IMUs comprise all-attitude, four-gimbal, inertially-stabilized platforms, upon which are mounted two mutually-perpendicular linear accelerometers. In addition to the inertial acceleration data, primary outputs of the IMUs are vehicle velocity and attitude in the inertial reference space. Angular-rate data may be inferred from the IMU attitude outputs.

Detailed descriptions of the IMU and other orbiter operational systems can be found in Reference 8.

**2.2.2 Aerodynamic Coefficient Identification Package (ACIP)** -- Although elements of the orbiter's operational instrumentation measure each of the vehicle motion parameters required for determination of in-flight aerodynamic coefficients, these components were designed to meet only the *operational* requirements of vehicle guidance, navigation, and control. The measurement resolution and data sampling rates of these instruments are not sufficient for accurate, research-quality determination of in-flight aerodynamic stability and control characteristics. Consequently, the OEX Program implemented the Aerodynamic Coefficient Identification Package experiment, which was specifically designed to enable collection of vehicle-motion information at the data resolution and sampling rates required for accurate flight determination of the orbiter's aerodynamic characteristics. The ACIP objective was to determine aerodynamic parameters in flight at accuracy levels equivalent to, or better than, those of corresponding wind-tunnel-derived data.

The ACIP included three-axis, orthogonal sets of linear accelerometers, angular accelerometers, and rate gyros. The ACIP linear accelerometers operated over measurement ranges which enabled the ACIP to accurately measure vehicle motion data at altitudes below approximately 80 km. Thus, the ACIP experiment obtained data which was synergistic with that of the SEADS.

In addition to processing data from its own sensors, ACIP data-handling electronics also processed control-surface-position sensor information for the orbiter's four elevons and rudder, as well as operations data for a single aft reaction-control-system yaw thruster. These data were routed through the ACIP data-handling electronics to assure that they were recorded with proper time correlation, relative to the ACIP data, and at data rates which were sufficient to enable post-flight estimation of vehicle stability-and-control characteristics.

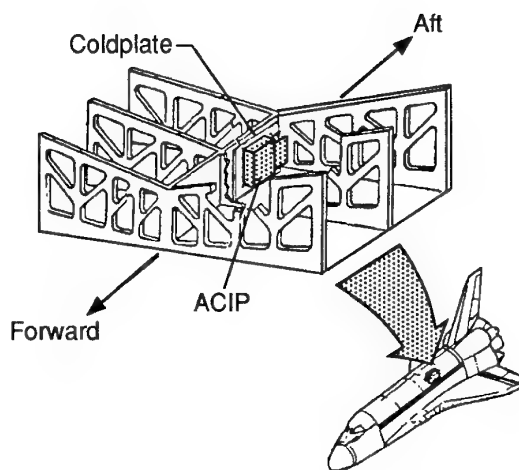


Figure 3 -- ACIP experiment installation schematic.

The ACIP was mounted on the orbiter keel (Fig. 3), in the wing carrythrough structure beneath the payload bay, at a longitudinal position of approximately 76-percent of vehicle length. This location is about 315 cm aft (10 percent of vehicle length), and 216 cm below the orbiter's entry center-of-gravity (c. g.). Proximity to the center-of-gravity minimized the significance of correction factors associated with translation of the information for reference to the vehicle c. g. The ACIP was precisely aligned with respect to the orbiter's body-axis coordinate system.

Two ACIP flight units were fabricated, for use on the Orbiters *Columbia* and *Challenger*. An ACIP has flown on every flight of these two vehicles.

**2.2.3 High-Resolution Accelerometer Package (HiRAP)** -- The High-Resolution Accelerometer Package experiment (Ref. 9) comprised a three-axis, orthogonal set of high-resolution linear accelerometers. The measurement ranges of the HiRAP accelerometers enabled it to sense aerodynamic forces acting on the orbiter from approximately 80 km to near-orbital altitudes. HiRAP data were intended to be obtained in conjunction with SUMS freestream density data, enabling direct determination (based solely upon in-situ measurements) of the aerodynamic performance characteristics of the orbiter in the rarefied-flow flight regime.

The HiRAP was located beside the ACIP in the orbiter's wing carrythrough structure, approximately 330 cm aft and 188 cm below the orbiter's c. g., and was precisely aligned with respect to the orbiter's body-axis coordinate system.

As with ACIP, two HiRAP flight units were fabricated for flight on the Orbiters *Columbia* and *Challenger*. A HiRAP unit was flown on each of *Challenger's* eight missions, and on 12 missions of *Columbia*, beginning with STS-9 and culminating with STS-65. Data from the first ten HiRAP flights are documented in Reference 10.

**2.2.4 Orbital Acceleration Research Experiment (OARE)** -- The Orbital Acceleration Research Experiment (Ref. 11) complemented the ACIP and HiRAP instruments by extending, to orbital altitudes, the



altitude range over which vehicle aerodynamic-acceleration data could be obtained. Like the HiRAP, the OARE instrument comprised a three-axis, orthogonal set of extremely-sensitive linear accelerometers. The OARE instrument could be operated over three auto-selected, or pre-programmed, measurement ranges. The least-sensitive measurement range enveloped that of the HiRAP instrument, while the most-sensitive range was almost two orders-of-magnitude more sensitive than the HiRAP. The operational-measurement range of the OARE was at such a low acceleration level that the sensors could not be accurately calibrated in the one-g ground environment. Consequently, the instrument sensors were mounted, within the OARE, on a rotary calibration table which enabled an accurate calibration to be performed on orbit, in the absence of Earth's gravity.

OARE data could be recorded on an onboard tape recorder for post-flight processing and analysis; however, because the OARE was intended to measure low-frequency, aerodynamic accelerations over long orbital time periods, the instrument also had its own internal data processing and storage capability. The internal data-processing software, which could be modified from flight-to-flight, used a "trimmed-mean-filter" algorithm to extract the "steady-state" acceleration signal.

Unlike other OEX experiments, the OARE was carried as orbiter payload. It was mounted at the bottom of the payload bay envelope, on a carrier plate attached to the orbiter's keel. This placed the instrument approximately 165 cm aft, and 137 cm below the orbiter's entry center-of-gravity. It was, of course, precisely aligned with respect to the orbiter's body axes.

OARE was flown on five *Columbia* flights: STS-40, -50, -58, -62, and -65. The OARE instrument has completed its flight program in support of OEX Program objectives; however, because of its ability to measure aerodynamic accelerations at orbital altitudes, it will continue to be used to measure and characterize the microgravity environment existing on-orbit during microgravity science missions.

## 2.3 Aerodynamic Surface Data

**2.3.1 Development Flight Instrumentation (DFI)** -- During the Orbital Flight Test missions (STS-1 thru -5), the Orbiter *Columbia* was equipped with a large complement of diagnostic instrumentation which was referred to as the Development Flight Instrumentation. DFI measurements were intended to provide the requisite data for postflight certification of orbiter subsystems designs, prior to the start of orbiter operational missions. The DFI system was comprised of over 4500 sensors, associated data handling electronics, and a data recorder.

Included among the DFI, and of particular interest to aerothermodynamic researchers, were measurements of the orbiter's aerodynamic-surface temperature at over 200 surface locations (Fig. 4). These measurements were obtained from thermocouples mounted within the thermal protection system (TPS) materials, in thermal contact with the TPS surface coatings (Ref. 12). The DFI also included temperature measurements in-depth, within the TPS materials, at some 19 locations, and along TPS tile sidewalls within the gaps between tiles at 16 locations. Aerodynamic-surface pressure measurements were also made in numbers and distribution similar to the surface-temperature measurements.

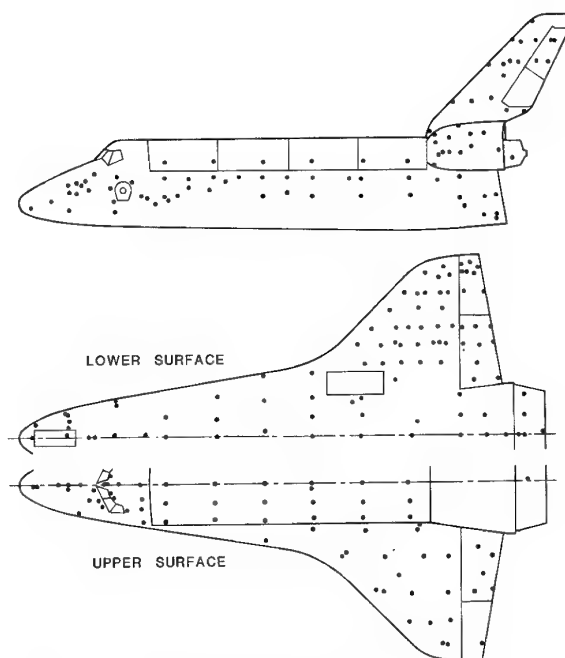


Figure 4 -- DFI surface-temperature measurement locations.

The Development Flight Instrumentation were aboard *Columbia* on missions STS-1 thru -5. However, mission unique circumstances limited the amount of hypersonic-entry temperature and pressure data collected on these flights. Pressure data were obtained over the complete entry trajectory only on missions STS-3 and -5; and temperature data were obtained over the complete entry trajectory only on missions STS-2, -3, and -5. The DFI-derived surface-temperature data from STS-2, -3, and -5 were processed to infer aerodynamic heat-transfer rates, using the methodology described in Reference 13.

**2.3.2 Aerothermal Instrumentation Package (AIP)** -- The Aerothermal Instrumentation Package comprised some 125 measurements of aerodynamic-surface temperature and pressure at locations on the leeside of the orbiter's left wing, side and upper fuselage, and vertical tail. The AIP sensors were originally elements of the Development Flight Instrumentation system, which were reactivated (prior to STS-28) through implementation of new orbiter wire harnesses and an AIP-unique data-handling system. AIP temperature sensors were intended to provide in-situ measurements which comprised both "ground-truth" and corollary information for the Shuttle Infrared Leeside Temperature Sensing (SILTS) experiment (see Section 2.3.5). The AIP pressure sensors were intended to provide data to support investigations of reaction-control-system jet interactions with the aerodynamic flowfield.

The AIP obtained data throughout the hypersonic portion of atmospheric entry on shuttle missions STS-28, -32, and -40.

**2.3.3 Catalytic Surface Effects (CSE) Experiment** -- Early arc-jet testing of orbiter thermal-protection materials indicated that the reaction-cured glass (RCG) coating of the TPS tiles was non-catalytic to the

recombination of dissociated air (specifically oxygen). Were this to be the case in flight, substantially reduced heat-transfer levels could be expected, when compared to those which would be experienced if the surface were fully catalytic. Prior to the advent of shuttle flights, however, this non-catalytic surface phenomenon had not been demonstrated to occur in the flight environment. Consequently, the shuttle TPS design was predicated on the conservative assumption that the gas chemistry at the TPS surface would be in chemical equilibrium. The Catalytic Surface Effects experiment (Ref. 14) was conceived to provide direct confirmation of the non-catalytic nature of the TPS tile surface in flight, and provide information with which to estimate, quantitatively, the catalytic efficiency of the RCG material.

The CSE experiment would provide an "inverse" demonstration of the non-catalytic nature of the baseline tile-surface material. The implementation of this experiment involved coating selected orbiter lower-surface TPS tiles (which contained DFI surface-temperature sensors) with a material which was known, based upon arc-jet tests, to be highly-catalytic to the recombination of dissociated air. By comparing the flight-measured temperatures of the coated tiles and nearby baseline tiles, the relative catalytic efficiency of the baseline tile-coating material would be demonstrated.

CSE experiment data were obtained on missions STS-2, -3, and -5 (Refs. 15 and 16). On STS-2, two individual tiles on the lower-surface centerline at 15- and 40-percent of vehicle length were coated (Fig. 5). For STS-3, individual tiles at 30- and 40-percent of vehicle length were coated. On STS-5, the catalytic coating was applied to individual tiles on the centerline at 10-, 15-, 20-, 30-, and 60-percent, and continuously along a centerline strip from 35- to 40-percent, of vehicle length. Two additional tiles, located at 76- and 82-percent of vehicle length along the 60-percent-semispan chord of the wing were also coated.

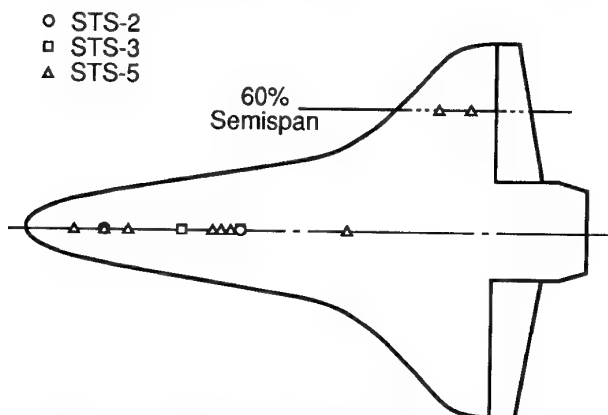


Figure 5 -- Locations of CSE-experiment coated tiles on orbiter lower surface.

#### 2.3.4 Tile-Gap Heating (TGH) Experiment --

The Tile-Gap Heating experiment (Ref. 17) was intended to obtain entry flight data with which to investigate the phenomenon of aerodynamic heating in the gaps between adjacent thermal protection system tiles. The experiment hardware consisted of a carrier panel of tiles which was

installed on the orbiter's lower surface, near the centerline, at approximately 27-percent of vehicle length. This carrier panel bolted directly to the orbiter structure and carried eleven tiles. At three locations on the array, tiles were instrumented with thermocouples in-depth, on the outer tile surface, and along the sidewalls of the tile-to-tile gaps.

The experiment tiles were fabricated and installed with exacting specifications applied to the values of tile edge radius and gap width. The experiment plan was to systematically vary these parameters over multiple flights of the experiment panel to gain an understanding of the effects of these variables on tile-gap heating, and ultimately to determine optimum values of these parameters in order to minimize gap heating.

The TGH experiment was flown only on the STS-2 mission. Results from that flight are reported in Reference 17.

#### 2.3.5 Shuttle Infrared Leeside Temperature Sensing (SILTS) Experiment --

The Shuttle Infrared Leeside Temperature Sensing experiment (Ref. 18) was designed to obtain high-spatial-resolution temperature measurements of the leeside (wing and fuselage) of the orbiter during entry. These measurements were obtained by means of an imaging, infrared radiometer (camera) located in a unique experiment pod atop the vertical tail of the Orbiter *Columbia* (Fig. 6). The SILTS camera contained a single infrared detector element and dual, rotating scanning-prisms (one horizontal and one vertical), which enabled the detector to scan the field-of-view, producing two-dimensional imagery. The experiment could be configured to view the orbiter leeside surfaces through either of two infrared-transparent windows: one of which enabled viewing of the left wing, the other enabled viewing of the fuselage.

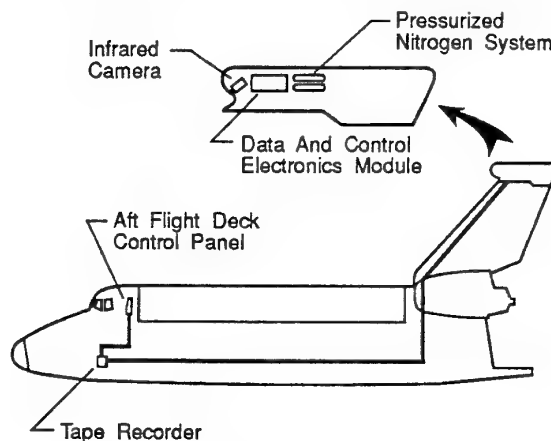


Figure 6 -- SILTS experiment system schematic.

The SILTS experiment pod also contained a data-and-control electronics module, and a pressurized nitrogen system. Window protection plugs protected the viewport windows during orbiter ground handling, launch, and orbital operations. At experiment initiation, the window protection plugs were ejected, allowing the camera to "see" the orbiter surfaces. The viewport windows were transpiration-cooled, during experiment operation, by the injection of gaseous nitrogen over the external window surfaces. Active cooling of the windows was required to prevent window temperatures

from increasing to levels at which the windows themselves would become radiators in the infrared, thus "fogging" the data images.

On a normal mission, the SILTS experiment was initiated at the time the orbiter reached the "entry-interface" altitude of 122 km, and infrared imagery were collected throughout the hypersonic portion of atmospheric entry. A data image was obtained approximately every 8.6 seconds during experiment operation.

The SILTS experiment was installed on the orbiter *Columbia* during the vehicle's 1984-85 modification period. Subsequently, the SILTS experiment was flown on five missions: STS-61C, -28, -32, -35, and -40. Experiment results obtained from those flights are presented in References 19-21.

### 3.0 OEX EXPERIMENT FLIGHT TEST RESULTS

Flights of OEX experiment instrumentation aboard the Orbiter's *Columbia* and *Challenger* provided a wealth of hypersonic aerothermodynamic flight data. These data have been, and are continuing to be, used in research analyses with the objectives of: (1) improving our understanding of the hypersonic flight environment, and (2) advancing the state-of-the-art of methodologies to be used for predicting the aerothermodynamic characteristics of advanced space-transportation vehicles. The following subsections provide a sampling (by no means an exhaustive summary) of results which have emanated from some of the research analyses performed to date, using these data.

#### 3.1 Orbiter Aerodynamic Performance -- Pitching Moment "Anomaly"

On *Columbia's* maiden flight, a significant difference was observed between the body-flap deflection required to trim the vehicle at the desired angle-of-attack in hypersonic flight, versus the deflection that was expected based upon the pre-flight-design aerodynamic database and methodology. This difference was equal to ~9-degrees of body-flap deflection, which equated to a difference in actual-versus-predicted pitching-moment coefficient of ~0.02 (Fig. 7). Several possible explanations of this pitching moment "anomaly" were originally postulated: Mach number effects (ground-based hypersonic wind-tunnel testing was conducted primarily at Mach 8), differences in flight-versus-wind-tunnel body-flap effectiveness (due to inadequate ground-

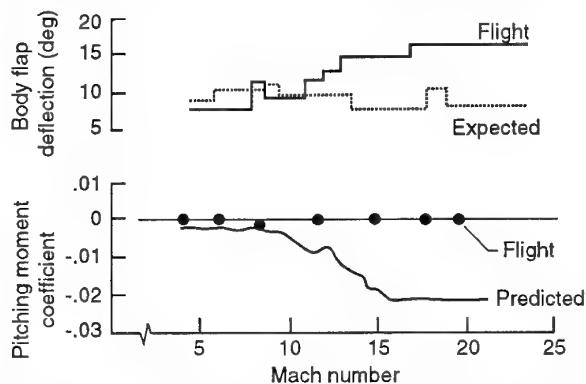


Figure 7 -- STS-1 hypersonic pitching moment "anomaly."

based Reynolds-number or viscous-interaction simulation), and/or real-gas effects (which could not be properly simulated in conventional, perfect-gas hypersonic wind tunnels).

Comparisons of the flight data with the results of computational and experimental simulations, obtained using current state-of-the-art capabilities, have identified the specific phenomenon which caused the pitching moment "anomaly," and indicated the shortcomings of the original orbiter aerodynamic-design methodology. The difference between the pitching moment predicted prior to STS-1 and that actually experienced in flight was determined to have been a "real-gas" effect, resulting directly from the inability of perfect-gas ground-based facilities to adequately simulate the flowfield which exists about the vehicle in the real-gas flight environment (Refs. 22 and 23). This work has indicated the requirement for different approaches to be applied, in both the design of a ground-based testing program and application of computational-fluid-dynamic simulations, to the aerodynamic-design process for future space-transportation vehicles.

#### 3.2 Orbiter Stability and Control

Beginning with the second shuttle flight, and continuing through 1994 on flights of *Challenger* and *Columbia*, aerodynamic maneuvers have been executed during entry specifically to obtain orbiter stability-and-control data. These maneuvers, referred to as programmed test inputs, have been designed to provide the data required for determination of specific stability-and-control parameters (Ref. 24). Execution of these maneuvers has been accomplished by direct input to the flight control system through onboard software. The amplitude and timing of control-surface motions were governed by programmed variables which generated specific control inputs at pre-designated flight conditions. Vehicle-response data were measured by the ACIP. Post-flight, the aerodynamic stability-and-control parameters were determined by analyses of the maneuvers using a "maximum-likelihood-estimation" process (Ref. 25). A typical example of flight-measured stability-and-control data (in this case, rolling moment due to sideslip) compared with preflight predictions is presented in Figure 8.

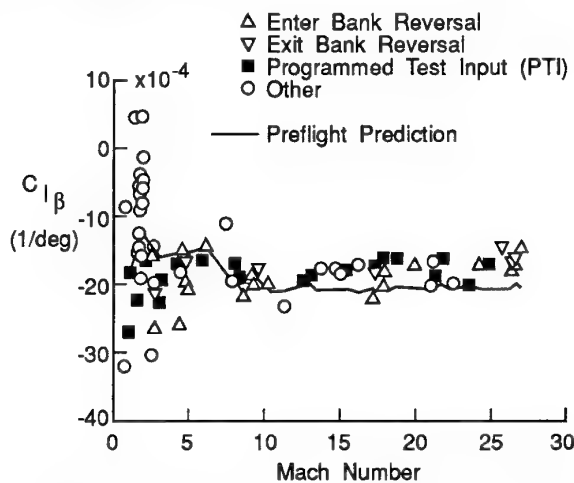


Figure 8 -- Comparison of flight-measured and preflight-predicted coefficients of rolling moment due to sideslip (adapted from Ref. 24).

### 3.3 Reaction Control System/Aerodynamic Flowfield Interactions

Due to interactions between reaction-control-system (RCS) jet plumes and the orbiter's aerodynamic flowfield, RCS jet firings during entry may *not* result in control forces and moments which are in direct proportion to the thrust of the RCS jet. The adequacy of ground-test modeling of these interactions, and the accuracy of the resultant interaction data, were of significant concern prior to the STS-1 mission. Aerodynamic stability-and-control parameters associated with RCS jet firings are determined from flight data in the same manner as described in the previous section -- firing of an RCS jet is simply treated as a control-surface input. Flight-derived RCS/aerodynamic interaction data indicated that some of the interactions were *not* well simulated in the preflight ground-based testing. As an example, Figure 9 presents a comparison of the flight-derived and preflight predicted data for rolling-moment due to yaw-jet firing.

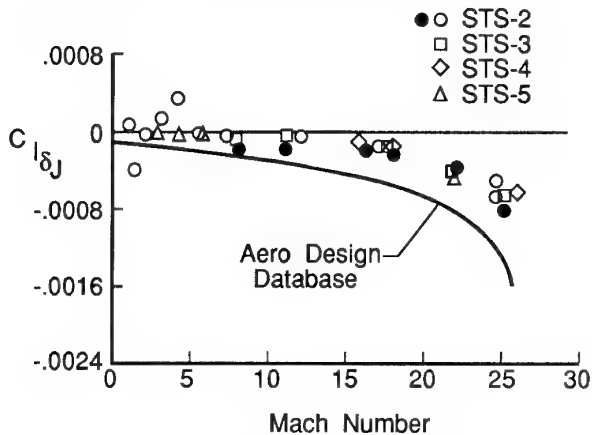


Figure 9 -- Comparison of flight-measured and preflight-predicted coefficients of rolling moment due to yaw jet (adapted from Ref. 26).

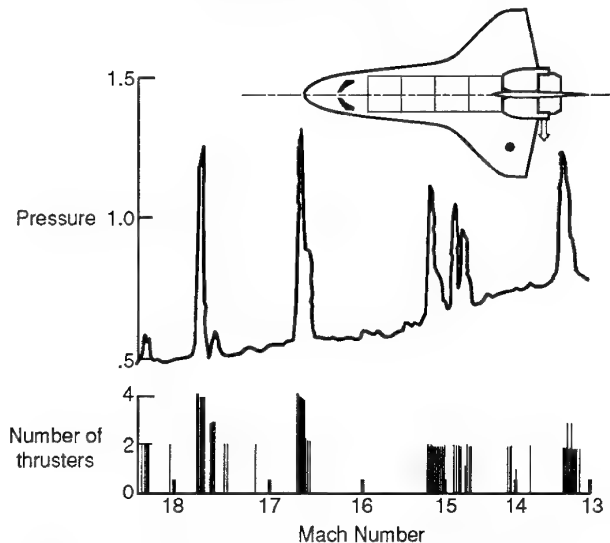


Figure 10 -- Effects of yaw-jet firing on wing upper-surface pressure (adapted from Ref. 26).

Scallion, et al (Ref. 26), demonstrated that the interaction component of the forces and moments resulting from an RCS jet firing in flight could be determined directly from measured aerodynamic-surface pressure data. The magnitude of the RCS plume/aerodynamic interaction was determined by evaluating the differences between surface pressures measured with RCS jets ON and jets OFF, and then integrating the delta-pressures over the aerodynamic surfaces (Fig. 10). Demonstration of this approach to measurement of RCS/aerodynamic interactions has led to further research focused on improved techniques for simulating these interactions in ground-based facilities.

### 3.4 Orbiter Allowable Center-of-Gravity Envelope

The pre-flight uncertainties associated with the orbiter's aerodynamic performance, and stability-and-control characteristics were reflected in a highly-constrained allowable center-of-gravity envelope for STS-1. Indeed, on STS-1, significant ballast was carried on the vehicle in order to attain the desired c. g. location. As a direct result of the determination of the orbiter's in-flight aerodynamic characteristics, using data obtained by the ACIP, the aerodynamic-uncertainty levels have been continually reduced. Reduced aerodynamic performance and control uncertainties have, in turn, resulted in significant expansion of the allowable c. g. envelope for orbiter operations. This is illustrated in Figure 11 which compares the STS-1 allowable c. g. envelope with that for STS-32. The expanded c. g. envelope affords significant flexibility in the configuration of payload-bay cargoes as the requirements for orbiter c. g. control are decreased.

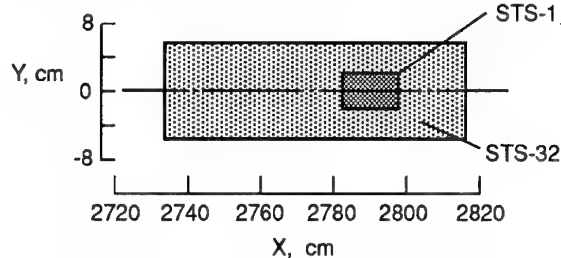


Figure 11 -- Expansion of orbiter allowable center-of-gravity envelope (courtesy of D. B. Kanipe, NASA Johnson Space Center).

### 3.5 Transitional-Flow Aerodynamic Bridging Formulas

In the absence of orbiter experimental aerodynamic data in the transitional-flow regime, an aerodynamic "bridging formula" was used to infer the aerodynamic performance of the vehicle at flight conditions where the flowfield surrounding the vehicle could *not* be considered continuum in nature. Data obtained in hypersonic wind tunnels were used to describe the vehicle's continuum-flow aerodynamic performance. Free-molecular-flow calculations were used to define aerodynamic performance at flight conditions where the free-molecular assumption was deemed appropriate (assumed for Knudsen number greater than 10). A bridging formula was then used to interpolate between these limits to define the orbiter's aerodynamic performance at the intermediate altitudes, which were assumed to represent flight conditions where the flowfield would be transitional in nature.

The pre-STS-1 bridging formula assumed a  $\sin^2$  function in Knudsen number to describe the aerodynamic-force coefficients between continuum and free-molecular "anchor points." This  $\sin^2$  functional form had its heritage in the blunt-body work of the Apollo era. Flight measurements of orbiter aerodynamic forces obtained by the HiRAP experiment, however, indicated that this bridging formula did *not* accurately predict the orbiter's aerodynamic performance characteristics in the transitional-flow regime. The blunt-body-based bridging formula was simply not appropriate for application to a lifting vehicle.

The flight-measured aerodynamic data have been used in the development of an improved bridging formula (Ref. 27), which is applicable to lifting vehicles. This new bridging formula is functionally an exponential in Knudsen number, and provides a substantially different prediction of rarefied-flow aerodynamic performance than the blunt-body-based formula (Fig. 12). Additionally, it not only compares well with the flight data (from which it was derived), but also compares well with data obtained in ground-based facilities over the Mach number range of 10-25 (Ref. 27).

### 3.6 Direct Simulation Monte Carlo (DSMC) Validation

Direct Simulation Monte Carlo is a state-of-the-art computational technique for simulating flowfields about vehicles operating in the transitional- and rarefied-flow flight regimes. Comparisons have been made between DSMC predictions and HiRAP-measured flight data, for orbiter lift-to-drag (L/D) ratio over the altitude range of 120-170 km (Ref. 28). The DSMC results and the flight data were in excellent agreement (Fig. 13). In the DSMC simulation, the molecule-surface interaction model assumed full accommodation and diffuse reflection of molecules. The agreement between the DSMC predictions and the flight data suggests that in-flight, at these altitudes, the interaction of gas molecules with the surface of the orbiter's thermal protection materials is properly characterized as fully diffuse.

### 3.7 High-Altitude Atmospheric Density Variability

Atmospheric density information for the altitude range of 60-160 km have been derived, for multiple entries, using the accelerometry data obtained by the HiRAP and IMU instruments (Ref. 29). Unlike standard atmospheric profiles which indicate atmospheric parameter variations only in the vertical, the orbiter-derived profiles were obtained over large horizontal distances. Consequently, imbedded within these profiles are data which provide insights into the latitudinal, longitudinal, and local solar time variations of atmospheric density. Typical flight-derived density data, normalized by the 1976 Standard Atmosphere values, are shown as a function of altitude in Figure 14. The flight-derived density profiles display significant wave-like variations, relative to the standard atmosphere, which appear to vary randomly from flight-to-flight. The difference between measured and standard-model densities, for any given flight and altitude, may be significant (in excess of 50 percent).

### 3.8 Orbital Atmospheric Density Variability

OARE data from the STS-50 flight (Ref. 30) have demonstrated this instrument's ability to sense the nano-g

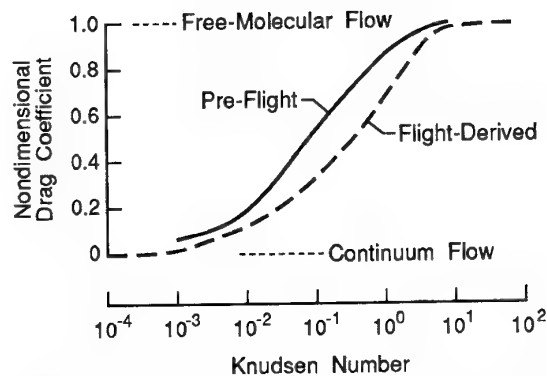


Figure 12 -- Comparison of preflight and flight-derived rarefied-flow aerodynamic bridging formulas (adapted from Ref. 27).

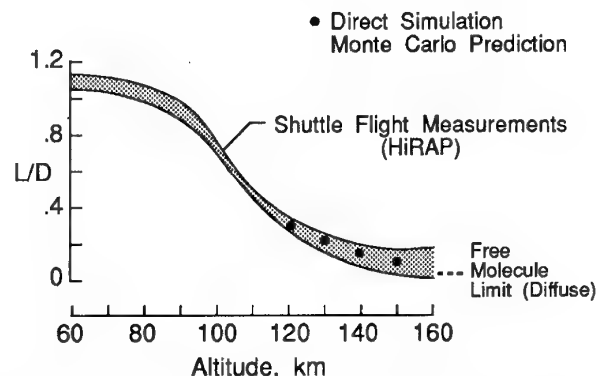


Figure 13 -- Comparison of DSMC aerodynamic predictions with flight data (adapted from Ref. 28).

accelerations resulting from aerodynamic drag of the orbiter while on orbit. Just as HiRAP data have been used to determine atmospheric-density profiles in the rarefied-flow regime during entry, OARE data may be used to infer atmospheric-density information at orbital altitudes. Figure 15 presents OARE-derived density data obtained on mission STS-58. These data were obtained over a time span of eight hours, comprising slightly more than five orbital periods.

The density data display a periodic variability about each orbit which results primarily from altitude variations inherent in the orbiter's elliptic orbit. However, additional atmospheric structure is evident in the density variation about any single orbit. The OARE results are compared with two atmospheric models: the 1976 Standard Atmosphere, and the MSIS-83 model (Ref. 31). The Standard Atmosphere model considers altitude as its only independent variable, averaging all other pertinent parameters, and thus does not capture any of the detailed structure evident in the OARE data. The MSIS-83 model, however, also includes other parameters (such as latitude, longitude, solar flux, geomagnetic flux indices, and others) as independent variables. This model displays better agreement with the OARE-derived data, as it appears to capture some of the detailed atmospheric structure evident in the flight results.

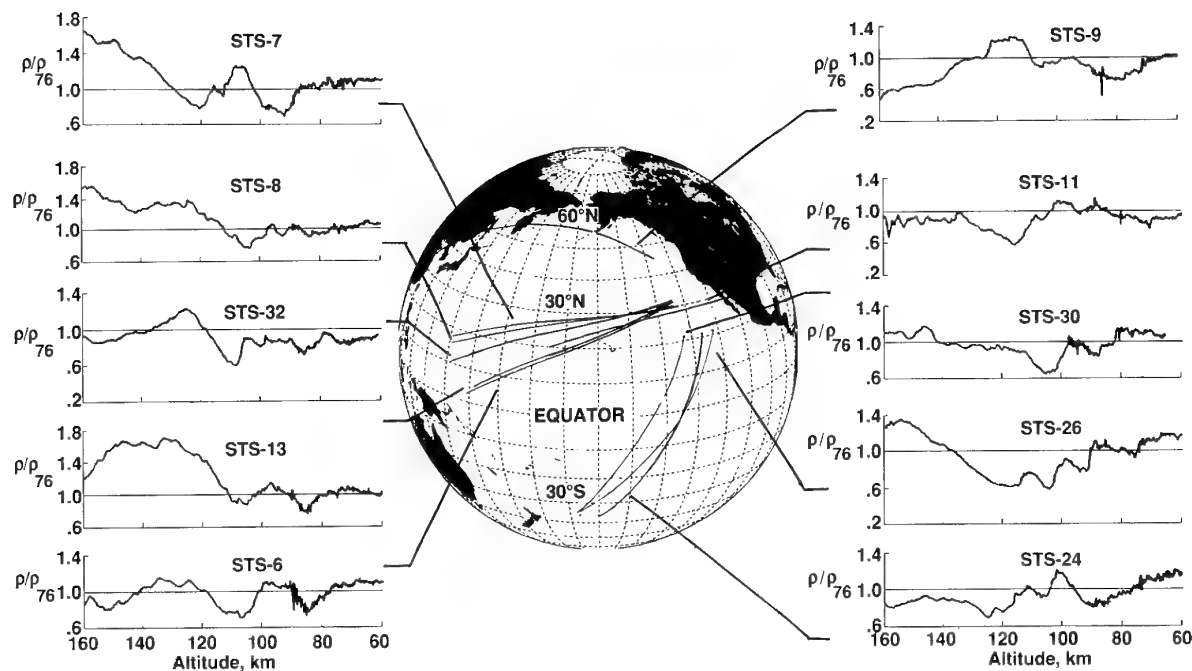


Figure 14 -- Flight-derived atmospheric-density data above 160 km (adapted from Ref. 29).

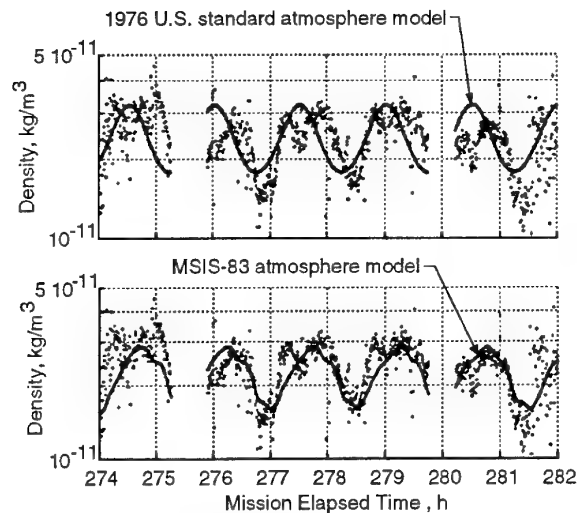


Figure 15 -- Orbital atmospheric-density variability measured by OARE on STS-58 (courtesy of R. C. Blanchard, NASA Langley Research Center).

### 3.9 Windward-Surface Boundary-Layer Transition

Temperature-time histories derived from Development Flight Instrumentation thermocouple measurements provided the basis for determination of the time, during entry, of boundary-layer transition onset and completion at each windward-surface measurement location. Hartung and Throckmorton (Ref. 32) created a database of this information and used these data to generate contour "maps" indicating the location and extent of the boundary-layer transition front, for each time at which data were recorded. These transition contour maps have been sequentially

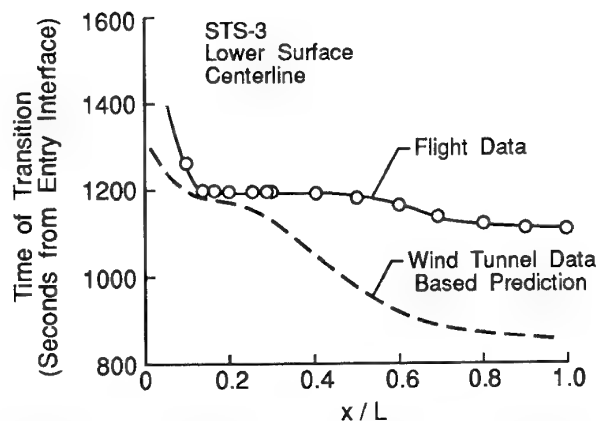


Figure 16 -- Comparison of STS-3 flight data and preflight predictions for boundary-layer transition on the windward-surface centerline (adapted from Ref. 33).

presented in a movie format to provide real-time visualization of the movement of the boundary-layer-transition front during entry. The complexity of the transition contours and the abrupt (in time) manner in which they were observed to move strongly indicated that the in-flight transition process was dominated by the effects of discrete surface-roughness elements.

Goodrich, et. al. (Ref. 33), compared the flight-observed transition along the windward centerline with pre-flight predictions derived using a methodology which was based upon wind-tunnel test results. This methodology attempted to account for the potential effects of surface roughness by comparing the wind-tunnel results obtained with both

smooth- and roughened-surface models. In flight, boundary-layer transition occurred much later than predicted over the aft 75-percent of the vehicle's centerline; while the predictions and flight results were in fairly good agreement along the forward 25-percent of the centerline (Fig. 16). The differences in predicted-versus-actual transition times, over the aft portion of the vehicle, were attributed to acceleration of the transition process in the wind tunnel as a result of tunnel noise, which is, of course, *not* present in the flight environment. The favorable agreement over the forward portion of the vehicle was attributed to surface-roughness domination of the transition process, in this region, both in the wind tunnel and in flight.

### 3.10 Leeside Shock-Layer Transition

Analysis of leeside heat-transfer data (Ref. 34) revealed the occurrence of a sudden, and unexpected, laminar-to-turbulent transition of the orbiter's leeside flowfield in flight, which was not observed in the wind tunnel. This transition was indicated by a sudden increase in surface heat-transfer observed simultaneously at multiple locations on the leeside fuselage and wing. It has been postulated (Ref. 35) that this transition occurs in the shear layer downstream of lines of flow separation that exist along the vehicle's forward fuselage and wing leading edges. Thus it is not a localized phenomenon, but rather a "global" phenomenon that, once initiated, rapidly affects the entire leeside shock-layer. Lee and Harthun (Ref. 36) noted that, in wind-tunnel tests, no differences were observed in leeside heating data obtained with or without boundary-layer trips located on the nose of orbiter models in order to induce turbulence in the leeward flowfield. They concluded that "either the turbulent flow relaminarized when it expanded to the leeward side, or the flow on the leeward side was turbulent without the trips."

Figure 17 presents typical flight heat-transfer data that illustrate the trends that are indicative of leeside shock-layer transition onset. Although not indicated in the data of

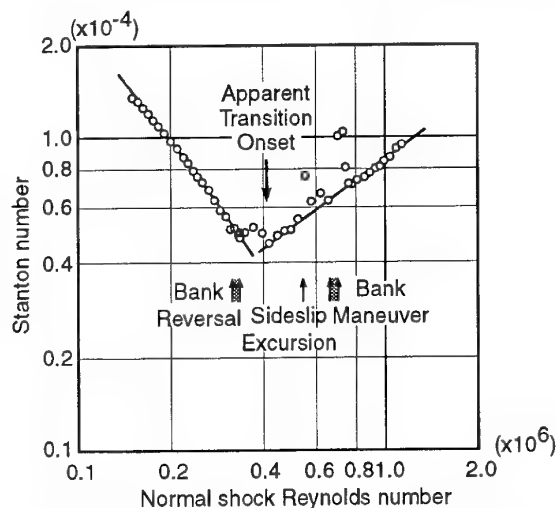


Figure 17 -- STS-28 heat transfer to leeside centerline at  $x/L = 0.70$ , angle-of-attack constant at 40 deg (adapted from Ref. 35).

Figure 17, transition of the leeside flowfield in flight is apparently "incipient" over a narrow portion of the entry flight regime and may be "tripped" as a result of disturbances to the leeside-flowfield structure that accompany small transient perturbations to the vehicle's nominal flight attitude (Ref. 35).

Since leeside shock-layer transition occurs at much higher Reynolds number conditions in flight than in the wind tunnel, leeside heat-transfer data obtained in wind tunnels *may not* accurately reflect flight heat-transfer levels at the higher-altitude, lower-Reynolds-number conditions, when the flight leeside shock-layer is laminar. Transition in the leeside flowfield is *not* related to windward-surface boundary-layer transition. The leeside phenomenon occurs at approximately Mach 16, while windward-side boundary-layer transition occurs in the Mach 8-10 range (Refs. 32 and 33).

### 3.11 TPS Surface Catalytic Efficiency

The Catalytic Surface Effects experiment successfully demonstrated that the surface of the orbiter's thermal-protection-system tiles was substantially *noncatalytic* to the recombination of dissociated oxygen atoms (Refs. 15 and 16). This result is illustrated in Figure 18.

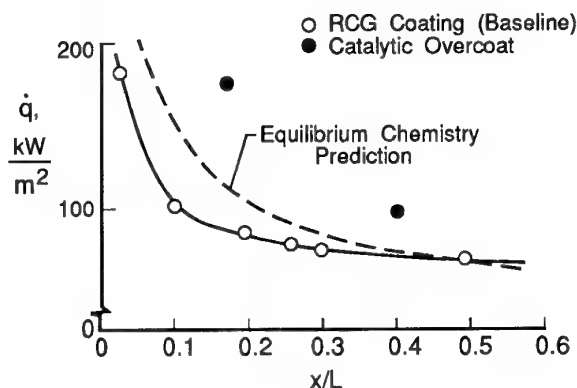


Figure 18 -- CSE experiment results confirm the noncatalytic nature of the baseline RCG tile coating (derived from STS-2 CSE experiment data at flight condition of Mach 23, 71-km altitude).

On missions STS-2 and -3, in-flight contamination of several instrumented tiles provided a further, serendipitous, demonstration of the non-catalytic nature of the baseline TPS surface (Ref. 37). On these missions, sudden "jumps" in surface temperature were observed (Fig. 19) at several measurement locations, apparently as the result of instantaneous change of the catalytic efficiency of the TPS surface. This change in surface catalytic efficiency resulted from surface deposition of highly-catalytic oxidation products from a melting, upstream sensor cover. The event apparently occurred when the stainless-steel sensor-cover's temperature reached the level at which it began to oxidize, thereby allowing contaminants to be carried downstream. As with the design of the CSE experiment, the increased heating due to the contamination confirmed the noncatalytic nature of the baseline TPS surface material.



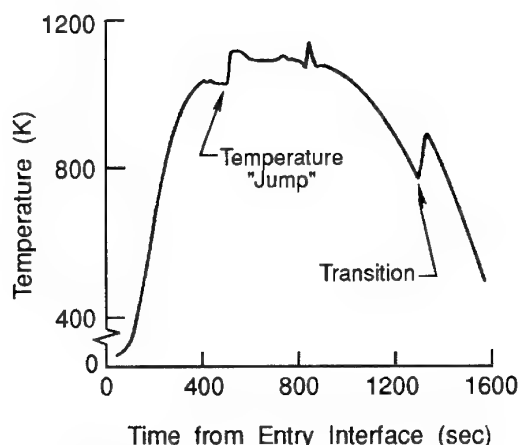


Figure 19 -- STS-2 temperature-time history for the windward centerline at  $x/L = 0.194$  (adapted from Ref. 37).

### 3.12 TPS Surface Recombination Rate Coefficients for Oxygen

The prediction of surface heat-transfer rates in a chemically-reacting flow over a surface which is *not* fully catalytic requires adequate modeling of the gas-surface interaction chemistry. For shuttle entry, the predominant surface reaction of interest is the recombination of dissociated oxygen atoms. Prior to the collection of orbiter entry flight data, the only available recombination-reaction rate data were those inferred from measurements of heat transfer to shuttle thermal-protection-system tiles in ground-based arcjet tests (Ref. 38). These experimental data were measured at wall-temperature levels ( $> 1400\text{K}$ ) significantly above the temperature range (800-1400K) actually experienced by orbiter TPS tiles during entry; consequently, their application to predictions of orbiter entry heat-transfer levels required significant extrapolation.

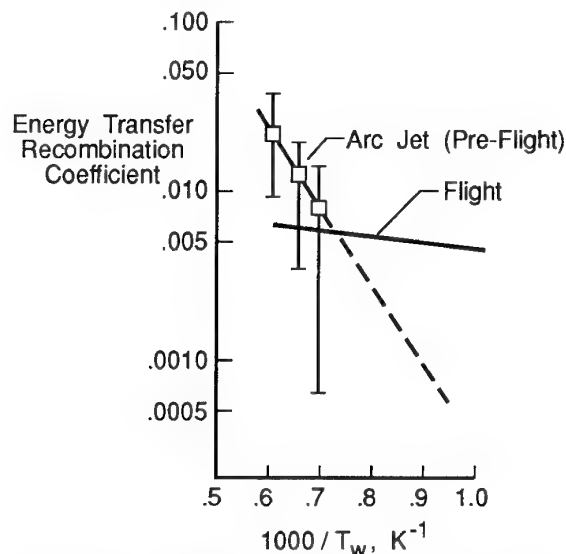


Figure 20 -- Comparison of arcjet and flight-derived energy-recombination coefficients for baseline TPS tile-surface material (adapted from Ref. 39).

Windward centerline heat-transfer data obtained over a constrained altitude range (71-78 km) on STS-2 were used as benchmarks for the determination of flight-derived surface recombination-rate data (Ref. 39). An axisymmetric viscous-shock-layer technique, capable of modeling the finite-rate reacting-gas chemistry both in the flowfield and at the body surface, was used to compute the heat transfer to the orbiter's windward centerline. In these computations, the surface reaction-rate coefficients for oxygen were treated as independent variables, and varied parametrically. Comparisons of the computational results with the STS-2 flight data allowed determination of those reaction-rate coefficients which provided the "best fit" to the measured flight data, thus defining a new expression for the temperature-dependent reaction-rate coefficients. This expression is graphically compared with the previous arc-jet data in Figure 20. Use of this recombination-rate expression for prediction of heat transfer at other flight conditions (i. e., altitudes other than the 71-78 km altitude range from which the benchmark data were obtained), and on other missions, resulted in prediction of heating rates to within approximately ten percent of the flight-measured values (Ref. 39) for the orbiter's windward centerline.

### 3.13 Computational Fluid Dynamic Technique Validation

**3.13.1 DFI Data Comparisons** -- The entry heat-transfer data derived from Development Flight Instrumentation temperature measurements constitute benchmark hypersonic flight results. These data have been used extensively for comparison with the results of various computational methods for simulating the flowfield structure about, and resulting heat transfer to, hypersonic flight vehicles. The predictive techniques have ranged from simplified engineering methods, which may only treat the vehicle windward centerline, and be limited to perfect-gas or equilibrium chemistry, to fully three-dimensional Navier-Stokes solutions, with modeling of the finite-rate, reacting-gas chemistry.

Two sets of comparisons are particularly noteworthy, as examples of the use of the flight data for validation of state-of-the-art computational-fluid-dynamic (CFD) methods. These CFD solutions were obtained for a modified orbiter geometry which provided an accurate representation of the orbiter's windward-surface geometry; however, the complex orbiter leeside geometry was replaced with a simplified shape. The modified shape of the leeside geometry had no effect on the windward-surface flowfield calculations, since both the streamwise and cross-flow components of velocity are supersonic near the leading edges.

Thompson (Ref. 40) presented surface heat-transfer predictions obtained using a three-dimensional, viscous-shock-layer technique, including consideration of the nonequilibrium flowfield chemistry and finite wall-catalytic efficiency. Figure 21 shows typical comparisons between the flight data and computed results, for the vehicle's windward centerline and spanwise at 69-percent of vehicle length.

Weilmuenster and Gnoffo (Ref. 41) presented surface heat-transfer predictions obtained using a three-dimensional Navier-Stokes code, again including consideration of the nonequilibrium flowfield chemistry and finite wall-catalytic



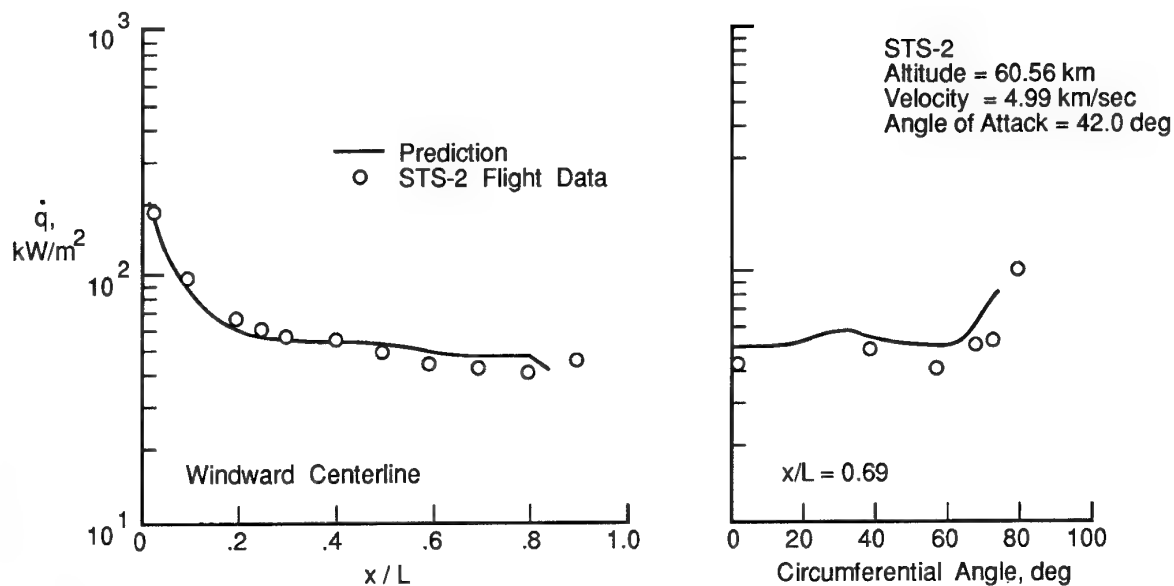


Figure 21 -- Comparison of DFI flight data with predictions of a state-of-the-art, three-dimensional, viscous-shock-layer computational technique (adapted from Ref. 40).

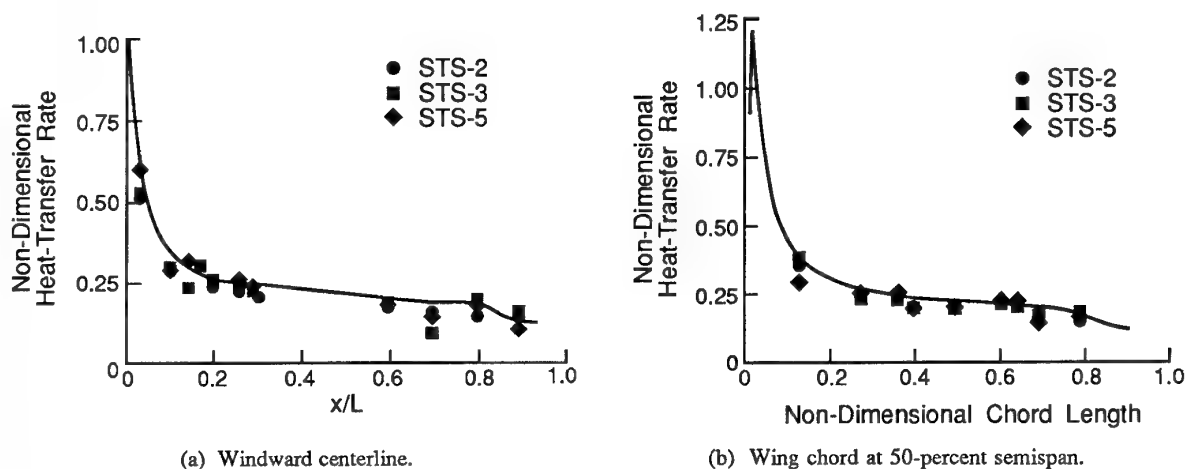


Figure 22 -- Comparison of DFI flight data with predictions of a state-of-the-art, three-dimensional, Navier-Stokes computational technique (adapted from Ref. 41).

efficiency. Figure 22 presents typical comparisons between the flight data and computed results, for the windward centerline and a wing chord at 50-percent of the vehicle semispan.

**3.13.2 SILTS Data Comparison** -- Kleb and Weilmuenster (Ref. 42) assessed the ability of a state-of-the-art computational method to accurately simulate the flowfield, and resulting heat transfer, over the leeside of the orbiter during entry. Using the same computational technique cited above in Reference 41, a solution was obtained over the complete shuttle orbiter. The computational geometry was an accurate representation of the actual shuttle orbiter, as far aft as the location of the body-flap hinge line. The only simplifications made to the

geometry definition were omission of the body flap, the shuttle main engines, and the vertical tail.

The solution results were compared with both the discrete location data obtained with DFI and AIP thermocouples as well as the full-surface, high-spatial-resolution data obtained by the SILTS experiment. A comparison among SILTS, DFI, and AIP data, obtained on five different flights, and the computational results is shown in Figure 23. The flight condition at which these comparisons are presented was chosen because (based upon approximate equality of the vehicle's attitude and velocity, and the freestream density), it was replicated at some trajectory point on each of the five flights shown. The Navier-Stokes simulation was performed for the specific flight conditions of STS-28.

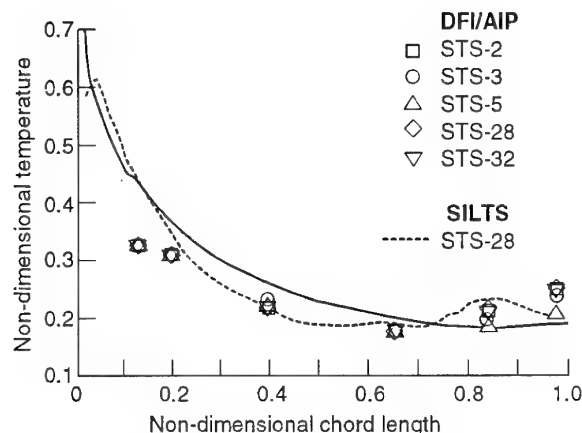


Figure 23 -- Comparison of SILTS, DFI, and AIP flight data with prediction of a state-of-the-art, three-dimensional, Navier-Stokes computational technique for wing chord at 60-percent semispan (adapted from Ref. 42).

#### 4.0 MISSED OPPORTUNITY -- HUBBLE SPACE TELESCOPE

Many spacecraft are instrumented with accelerometers and/or strain gages, for use in ground tests conducted to collect data for verification of structural math models which are subsequently employed to calculate launch loads. However, prior to integration of a complete spacecraft in preparation for its placement on orbit, it is often standard practice to simply cut the electrical leads to these sensors, as there is usually no data system aboard the operational spacecraft which could collect, process, and store or telemeter data from them. The early operational experience of the Hubble Space Telescope provides an excellent example of the potential consequences inherent in following such a procedure.

As is well known, once positioned on-orbit, the Hubble spacecraft encountered intermittent and severe structural vibrations, with resultant attitude oscillations, which coincided with its passages between sunlight to shadow. The characterization and understanding of the phenomenon which caused these vibrations, and development of spacecraft-control software to minimize the vibrations, was a time-consuming, and consequently expensive, process. No hard data were available, other than rate-gyro data, with which to determine how the structure was actually reacting to the thermal transients which were presumed to be the forcing function of the vibrations. Only through an iterative process of presuming the magnitude of the thermal transients, modeling the structure's dynamic response, assessing the expected spacecraft-attitude response, and then comparing that with the known flight gyro data, were spacecraft controllers able to characterize the phenomenon and develop a spacecraft-control-software "fix." This process may have been shortened significantly, and the cost minimized, had high-frequency structural-response data been available. The ground-test accelerometers, which had been eliminated from the flight vehicle for want of a data system, might have provided that critical data.

#### 5.0 CONCLUDING REMARKS

NASA researchers have capitalized upon the opportunity presented by recurring space shuttle operations to conduct flight research experiments to study aerothermodynamic phenomena unique to lifting entry vehicles in hypersonic flight. The Orbiter Experiments (OEX) Program enabled use of the Orbiter *Columbia* as a flight research vehicle (as an adjunct to its normal *operational* mission) through the development, implementation, and operation of unique instrumentation, specifically designed to obtain aerodynamic and aerothermal flight data during atmospheric entry. The information derived from the OEX experiments and other orbiter instrumentation, represent heretofore unavailable benchmark hypersonic flight data. These data are being used in a continual process of validation of state-of-the-art methods, both experimental and computational, for simulating and/or predicting the aerothermodynamic flight characteristics of advanced space transportation vehicles.

The flight research conducted as part of the OEX Program has resulted in significantly improved understanding of the ground-based testing and simulation requirements, both experimental and computational, which must be met for effective aerodynamic and aerothermal design of shuttle-class vehicles. The products of this research are improved, and validated, methodologies which may now be confidently applied to the designs of future space transportation vehicles.

The OEX Program was conducted for a fraction of the costs expended in comparable areas of concern during the design and development of the space shuttle orbiter. As a result of this program, the aerothermodynamic design of a next-generation space transportation system will require a significantly smaller testing, simulation, and predictive effort than was expended during shuttle orbiter development, with attendant savings of both time and money. In addition to the cost savings, the vehicle's design will display significantly less inherent uncertainty, or conservatism, than was the case for the shuttle orbiter. Similar opportunities are provided by every new vehicle or spacecraft built. The "OEX Approach" can be particularly important when applied to the first of a planned series of vehicles or spacecraft. As space program budgets decrease, this approach may represent the only practical mechanism available for collecting the type of information required to enable achievement of significant technological and validation advancements.

#### 6.0 ACKNOWLEDGMENTS

Although those individuals responsible for the OEX experiments described herein have, by and large, been recognized by reference to their published work, the authors wish to specifically recognize each of the individuals who served as Principal (or Co-) Investigators for the OEX aerothermodynamic experiments:

| Experiment | Principal Investigator(s)                         |
|------------|---|
| SEADS      | P. M. Siemers III<br>NASA Langley Research Center |

|       |  |
|-------|--|
| SUMS  | R. C. Blanchard<br>NASA Langley Research Center                                    |
| ACIP  | D. R. Cooke<br>D. B. Kanipe<br>NASA Johnson Space Center                           |
| HiRAP | R. C. Blanchard<br>NASA Langley Research Center                                    |
| OARE  | R. C. Blanchard<br>NASA Langley Research Center                                    |
| CSE   | D. A. Stewart<br>NASA Ames Research Center   |
| TGH   | W. C. Pitts<br>NASA Ames Research Center   |
| SILTS | J. C. Dunavant<br>D. A. Throckmorton<br>E. V. Zoby<br>NASA Langley Research Center |
| AIP   | D. A. Throckmorton<br>NASA Langley Research Center                                 |

No OEX experiment could have been successfully flown were it not for the untiring efforts of the personnel of the OEX Project Office at the NASA Johnson Space Center. The OEX Project Office was responsible for: overall OEX Project management, management and engineering interfaces with the Shuttle Orbiter Project, provision of an OEX data handling/recording system, assurance of OEX experiment flight operational planning and control, and integration of all OEX experiment systems aboard the orbiter. Although the numbers of people involved preclude their individual acknowledgment, the personnel of the OEX Project Office, who led the OEX Team during the 15-year lifespan of this project, are equally deserving of recognition as the experiment Principal Investigators and their hardware-support teams.

## 7.0 REFERENCES

- Siemers, P. M. III, and Larson, T. J.: "Space Shuttle Orbiter and Aerodynamic Testing," *Journal of Spacecraft and Rockets*, Vol. 16, No. 4, July-August 1979, pp. 223-231.
- Jones, J. J.: "OEX - Use of the Shuttle Orbiter as a Research Vehicle," AIAA Paper 81-2512, November 1981.
- Throckmorton, D. A.: "Research Analysis of Space Shuttle Orbiter Entry Aerothermodynamic Flight Data at the NASA Langley Research Center," AIAA Paper 81-2429, November 1981.
- Pruett, C. D., Wolf, H., Heck, M. L., and Siemers, P. M. III: "Innovative Air Data System for the Space Shuttle Orbiter," *Journal of Spacecraft and Rockets*, Vol. 20, No. 1, January-February 1983, pp. 61-69.
- Siemers, P. M. III, Wolf, H., and Henry, M. W.: "Shuttle Entry Air Data System (SEADS) -- Flight Verification of an Advanced Air Data System Concept," AIAA Paper 88-2104, May 1988.
- Blanchard, R. C., Duckett, R. J., and Hinson, E. W.: "The Shuttle Upper Atmosphere Mass Spectrometer Experiment," *Journal of Spacecraft and Rockets*, Vol. 21, No. 2, March-April 1984, pp. 202-208.
- Blanchard, R. C., Ozoroski, T. A., and Nicholson, J. Y.: "Shuttle Upper Atmosphere Mass Spectrometer Experimental Flight Results," *Journal of Thermophysics and Heat Transfer*, Vol. 31, No. 4, July-August 1994, pp. 562-568.
- Anon.: "National Space Transportation Reference," NASA TM-101,877, June 1988.
- Blanchard, R. C., and Rutherford, J. F.: "Shuttle Orbiter High-Resolution Accelerometer Package Experiment: Preliminary Flight Results," *Journal of Spacecraft and Rockets*, Vol. 22, No. 4, July-August 1985, pp. 474-480.
- Blanchard, R. C., Larman, K. T., and Barrett, M.: "The High-Resolution Accelerometer Package (HiRAP) Flight Experiment Summary for the First Ten Flights," NASA RP-1267, March 1992.
- Blanchard, R. C., Hendrix, M. K., Fox, J. C., Thomas, D. J., and Nicholson, J. Y.: "Orbital Acceleration Research Experiment," *Journal of Spacecraft and Rockets*, Vol. 24, No. 6, November-December 1987, pp. 504-507.
- Stoddard, L. W., and Draper, H. L.: "Development and Testing of Development Flight Instrumentation for the Space Shuttle Orbiter Thermal Protection System," *Proceedings of the 24th International Symposium, Instrument Society of America*, 1978.
- Throckmorton, D. A.: "Benchmark Determination of Shuttle Orbiter Entry Aerodynamic Heat-Transfer Data," *Journal of Spacecraft and Rockets*, Vol. 20, No. 3, May-June 1983, pp. 219-224.
- Stewart, D. A., Rakich, J. V., and Lanfranco, M. J.: "Catalytic Surface Effects Experiment on the Space Shuttle," *Thermophysics of Atmospheric Entry, Progress in Astronautics and Aeronautics*, Vol. 82, 1982, pp. 248-272.
- Rakich, J. V., Stewart, D. A., and Lanfranco, M. J.: "Results of a Flight Experiment on the Catalytic Efficiency of the Space Shuttle Heat Shield," AIAA Paper 82-944, June 1982.
- Stewart, D. A., Rakich, J. V., and Lanfranco, M. J.: "Catalytic Surface Effects on Space Shuttle Thermal Protection System During Earth Entry of Flights STS-2 Through STS-5," *Shuttle Performance: Lessons Learned*, NASA CP-2283, Part 2, March 1983, pp. 827-845.

17. Pitts, W. C., and Murbach, M. S.: "Flight Measurements of Tile Gap Heating on the Space Shuttle," AIAA Paper 82-0840, June 1982.
18. Throckmorton, D. A., Zoby, E. V., and Kantsios, A. G.: "The Shuttle Infrared Leeside Temperature Sensing (SILTS) Experiment," AIAA Paper 85-0328, January 1985.
19. Dunavant, J. C., Myrick, D. L., Zoby, E. V., and Throckmorton, D. A.: "Shuttle Infrared Leeside Temperature Sensing (SILTS) Experiment - STS 61-C Final Results," NASA TP-2958, December 1989.
20. Throckmorton, D. A., Zoby, E. V., Dunavant, J. C., and Myrick, D. L.: "Shuttle Infrared Leeside Temperature Sensing (SILTS) Experiment - STS-28 Preliminary Results," AIAA Paper 90-1741, June 1990.
21. Throckmorton, D. A., Zoby, E. V., Dunavant, J. C., and Myrick, D. L.: "Shuttle Infrared Leeside Temperature Sensing (SILTS) Experiment - STS-35 and STS-40 Preliminary Results," AIAA Paper 92-0126, January 1992.
22. Weilmuenster, K. J., Gnoffo, P. A., and Greene, F. A.: "Navier-Stokes Simulations of Orbiter Aerodynamic Characteristics Including Pitch Trim and Bodyflap," *Journal of Spacecraft and Rockets*, Vol. 31, No. 3, May-June 1994, pp. 355-366.
23. Brauckmann, G. J., Paulson, J. W. Jr., and Weilmuenster, K. J.: "Experimental and Computational Analysis of the Space Shuttle Orbiter Hypersonic Pitch-Up Anomaly," AIAA Paper 940632, January 1994.
24. Cooke, D. R.: "Minimum Testing of the Space Shuttle Orbiter for Stability and Control Derivatives," *Shuttle Performance: Lessons Learned*, NASA CP-2283, Part 1, 1983, pp. 447-472.
25. Iliff, K. W.: "Parameter Estimation for Flight Vehicles," *Journal of Guidance, Control, and Dynamics*, Vol. 12, No. 5, September-October 1989, pp. 609-622.
26. Scallion, W. I., Compton, H. R., Suit, W. T., Powell, R. W., Blackstock, T. A., and Bates, B. L.: "Space Shuttle Third Flight (STS-3) Entry RCS Analysis," AIAA Paper 83-0116, January 1983.
27. Blanchard, R. C., and Buck, G. M.: "Rarefied Flow Aerodynamics and Thermosphere Structure from Shuttle Flight Measurements," *Journal of Spacecraft and Rockets*, Vol. 23, No. 1, January-February 1986, pp. 18-24.
28. Bird, G. A.: "Application of the Direct Simulation Monte Carlo Method to the Full Shuttle Geometry," AIAA Paper 90-1692, June 1990.
29. Blanchard, R. C., Hinson, E. W., and Nicholson, J. Y.: "Shuttle High-Resolution Accelerometer Package Experiment Results: Atmospheric Density Measurements Between 60-160 km," *Journal of Spacecraft and Rockets*, Vol. 26, No. 3, May-June 1989, pp. 173-180.
30. Blanchard, R. C., Nicholson, J. Y., and Ritter, J. R.: "Preliminary OARE Absolute Acceleration Measurements on STS-50," NASA TM 107724, February 1993.
31. Hedin, A. E.: "A Revised Thermosphere Model Based on Mass Spectrometer and Incoherent Scatter Data: MSIS-83," *Journal of Geophysical Research*, Vol. 88, December 1983, pp. 10170-10188.
32. Hartung, L. C., and Throckmorton, D. A.: "Computer Graphic Visualization of Orbiter Lower-Surface Boundary-Layer Transition," *Journal of Spacecraft and Rockets*, Vol. 24, No. 2, March-April 1987, pp. 109-114.
33. Goodrich, W. D., Derry, S. M., and Bertin, J. J.: "Shuttle Orbiter Boundary Layer Transition at Flight and Wind Tunnel Conditions," *Shuttle Performance: Lessons Learned*, NASA CP-2283, Part 2, March 1983, pp. 753-780.
34. Throckmorton, D. A., and Zoby, E. V.: "Orbiter Entry Leeside Heat-Transfer Data Analysis," *Journal of Spacecraft and Rockets*, Vol. 20, No. 6, November-December 1983, pp. 524-530.
35. Throckmorton, D. A.: "Leeside Shock-Layer Transition and the Space Shuttle Orbiter," *Journal of Spacecraft and Rockets*, Vol. 30, No. 6, November-December 1993, pp. 774-776.
36. Lee, D. B., and Harthun, M. H.: "Aerothermodynamic Entry Environment of the Space Shuttle Orbiter," *Entry Vehicle Heating and Thermal Protection Systems: Space Shuttle, Solar Starprobe, Jupiter Galileo Probe; Progress in Astronautics and Aeronautics*, Vol. 85, 1983, pp. 3-20.
37. Throckmorton, D. A., Zoby, E. V., and Hamilton, H. H. II: "Orbiter Catalytic/Non-Catalytic Heat Transfer as Evidenced by Heating to Contaminated Surfaces on STS-2 and STS-3," NASA CP-2283, Part 2, 1983, pp. 847-864.
38. Scott, C. D.: "Catalytic Recombination of Nitrogen and Oxygen on High-Temperature Reusable Surface Insulation," *Aerothermodynamics of Planetary Entry, Progress in Astronautics and Aeronautics*, Vol. 77, 1981, pp. 192-213.
39. Zoby, E. V., Gupta, R. N., and Simmonds, A. L.: "Temperature-Dependent Reaction Rate Expressions for Oxygen Recombination," *Thermal Design of Aeroassisted Orbital Transfer Vehicles, Progress in Astronautics and Aeronautics*, Vol. 96, 1985, pp. 445-464.
40. Thompson, R. A.: "Comparison of Viscous-Shock-Layer Solutions with Shuttle Heating Measurements," *Journal of Thermophysics and Heat Transfer*, Vol. 4, No. 2, April 1990, pp. 162-169.

41. Weilmuenster, K. J., and Gnoffo, P. A.: "Solution Strategy for Three-Dimensional Configurations at Hypersonic Speeds," *Journal of Spacecraft and Rockets*, Vol. 30, No. 4, July-August 1993, pp. 385-394.
42. Kleb, W. L., and Weilmuenster, K. J.: "Characteristics of the Shuttle Orbiter Leaside Flow During a Re-Entry Condition," *Journal of Spacecraft and Rockets*, Vol. 31, No. 1, January-February 1994, pp. 8-16.

# FLIGHT TESTING VEHICLES FOR VERIFICATION AND VALIDATION OF HYPERSONICS TECHNOLOGY

Peter W. Sacher\*)  
Deutsche Aerospace AG  
D-80995 München  
Germany

## Introduction\*)

Hypersonics Technology has obtained renewed interest since various concepts for future complete reusable Space Transport Systems (STS) using airbreathing propulsion for the parts of atmospheric flight have been proposed in different countries (e.g. US, CIS, Japan, France, Germany and UK). To cover major developments in those countries, AGARD FDP has formed the Working Group 18 on "Hypersonic Experimental and Computational Capabilities - Improvement and Validation".

Of major importance for the proof of feasibility for all these concepts is the definition of an overall convincing philosophy for a "Hypersonics Technology Development and Verification Concept" using ground simulation facilities (both experimental and numerical) and flight testing vehicles.

Flying at hypersonic Machnumbers using airbreathing propulsion requires highly sophisticated design tools to provide reliable prediction of thrust minus aerodynamic drag to accelerate the vehicle during ascent. Using these design tools, existing uncertainties have to be minimized by a carefully performed code validation process. To a large degree the database required for this validation cannot be obtained on ground.

In addition thermal loads due to hypersonic flow have to be predicted accurately by aerothermodynamic flow-codes to provide the inputs needed to decide on materials and structures. Heat management for hypersonic flight vehicles is one of the "Key-Issues" for any kind of successful flight demonstration.

This paper will identify and deal with the role of flight testing during the verification and validation process of

advanced hypersonics technology needed for flight in the atmosphere with hypersonic Machnumbers using airbreathing propulsion systems both for weapons and space transport systems.

## Assessment of critical "Key-Technologies" needed for future hypersonic transportation systems based on airbreathing propulsion.

The present situation concerning payload cost to the orbit is shown in Fig. 1. In spite of very large differences in transport vehicle size, cost per kg payload to LEO is approximately 25.000 US \$. There is general consensus, that future STS in order to operate economically need a reduction of the current cost by approximately one order of magnitude. The thesis is, that reusability and aircraft-like ground operation of future STS is the "Key" to this cost reduction required.

Reusability does not necessarily mean the use of airbreathing propulsion and therefore a carefully performed trade-off is required between all-rocked driven transport systems and transport vehicles based on rocket plus airbreathing propulsion as Fig. 2 outlines schematically.

The choice of the propulsion system has a strong influence on the design philosophy of the STS. Due to aerodynamic drag, rocket-driven systems try to escape from atmosphere as soon as possible, whereas vehicles using airbreathing propulsion fly in (using) the atmosphere as long as achievable (Fig. 3).

Independent from different concepts for future space transportation systems, all countries involved in the development of hypersonics technology agree on "Key Technology Areas" as "Aerothermodynamics", "Propulsion and Propulsion Integration", "Materials and Structures" and "Systems". An assessment of the capabilities of tools for numerical (CFD) and experimental (EFD) ground simulation exhibits severe technological deficits and therefore unacceptable risks which require mandatorily extensive flight testing prior to the development of any proposed STS. One of the most important "Key-Technologies" seem to be the required suc-

\*) Manager Hypersonics Technology Programmes  
Member AIAA

cessful airbreathing engine/airframe integration. Successful means, that, according to Fig. 4, installed thrust of the engine minus drag of the vehicle remains a sufficient large positive number, so that excessive thrust can be used for the acceleration of the flight vehicle. This requires mandatorily the proof of feasibility by an in-flight demonstration.

Only flight testing may bridge the huge gap between technology today available and technology required to fly safe any type of airbreathing propelled vehicle at hypersonic speed. Fortunately, there is no need for a decision now on the question of Single-stage-to-orbit (SSTO) or Two-stage-to-orbit (TSTO) concepts both using in addition to rockets airbreathing propulsion. Both exhibit a large cut-set of advanced technologies needed for both concepts as Fig. 5 demonstrates.

Fig. 6 shows an assessment of existing aircraft and missiles characterized by size (or by GTOW or energy required) and correlated with speed. From this scenario it is clearly understood, that "Transfer-Models" have to be developed much more powerful and reliable than the old conventional scaling laws or Reynoldnumber extrapolations used in engineering design up till now to bridge the existing gap in engineering applications.

A flight experiment is therefore proposed as an adequate means to demonstrate the feasibility ("readiness") of hypersonics technology in reduced scale (and reduced cost) in realistic environment before the implementation in a full scale prototype will be realized. Risk assessment, as Fig. 8 outlines for different types of future STS, shows clearly, that the flight experiment is needed specifically for these airbreathing propelled systems where in addition to aerothermodynamics and the choice of materials and ("hot"?) structures the engine/airframe integration pose a severe engineering challenge.

#### Alternative concepts for flying testbeds to demonstrate hypersonics technologies

Airbreathing propulsion for hypersonic speed means first of all a ram propulsion system. In the range  $3.5 < M < 7$  subsonic combustion seems to be superior with respect to specific impulse in comparison with supersonic combustion (SCRAM). Both concepts could be combined with a conventional turbo-engine or rockets for lower speeds and take-off and landing. More recently the concept of liquid air cycle engine (LACE) is under discussion.

For the "Lead Concept" (SÄNGER) within the German Hypersonics Technology Programme (HTP), the TSTO concept has been chosen, having the lower stage based on combined cycle Turbo/Ram engines. The question, whether the choice of the engine type is appropriate, addresses Fig. 8.

Ground testing the most critical part of the combined cycle engine, the ram propulsion part, is obviously the first step to be taken. And therefore within the technology programme a complete engine, shown in Fig. 9 will be manufactured and tested in a free-jet mode in a large windtunnel at hypersonic speeds. Assuming that this experiment will be completed successfully in 1996, a study activity has already been initiated (see Fig. 10) to prepare a platform for the next steps in the engine validation programme : in-flight testing.

To demonstrate the feasibility of hypersonics technology specifically focussed on the combined cycle airbreathing propulsion system and the successful performed engine/airframe integration, in addition to ground testing several alternative flight test vehicle concepts have to be considered carefully. Even if the restriction is made to concentrate on the high speed branch of the flight profile for airbreathing propulsion systems, three major categories of flight test vehicles can be identified as Fig. 11 depicts.

**Category I** represents so-called "Single Purpose Demonstrators" (SPD) e.g. the engine is attached as "Passenger" on an already existing accelerator like a missile or rocket. But another example may be the a vehicle without engine to assess an aerothermodynamic database for validation of design tools. A big question-mark stands with any requirement of "Reusability" of the demonstrator vehicle. But at least the costly engine should be recovered without damage to be reused in a flight testing programme. Fig. 12 represents one example being currently under consideration, the Russian manufactured RADUGA target vehicle (drone) D2 which is launched at  $M = 1.3$  under a Tu-22M supersonic aircraft reaching a maximum speed of  $M = 6^+$ . Shown is also, attached to the vehicle, the ram engine as a "Passenger" in the same size which will be tested in the windtunnel. Such an experimental vehicle is specifically of interest because the "Passenger"- engine could be exchanged (from Ram to Scram) or improved by modifications in a step-by-step approach within a systematically processing flight testing programme.

**Category III** describes test vehicles having fully integrated demonstrator engines. This "Universal Demonstrators" need also acceleration and separation from the accelerator at a Machnumber where the installed engine ignites. The flight profile might include acceleration of the test vehicle by its own installed thrust, straight level cruise or even only deceleration during descent. These vehicles need to be recovered by a landing system and reusability due to high cost for development and manufacturing and they can meet in addition requirements from the propulsion technology also requirements from aerothermodynamics, materials/structures and systems. One potential candidate for a flying testbed is explained in Fig. 13. HYTEX (means hypersonics technology experiment) R-A<sub>3</sub> is an unmanned flight vehicle with a fully integrated (ram) propulsion system.

A compromise between Category I and III is made if in addition to the integrated engine additional integrated or external boosters provide additional thrust during operation of the hypersonic test engine. Those vehicles are understood under Category II. They fulfil requirements from all technology areas to some extent at reduced risk but not necessarily at reduced cost. GTOW for all vehicles of the category II and III is expected at 3 - 5 Mg.

#### Conclusions for future multilateral efforts to demonstrate the feasibility of hypersonics technology

Due to its technological attractiveness, these study activities within the German HTP have led already to an remarkable international cooperation. Industry, universities and research institutes from four European countries have formed the joint activity shown in Fig. 14.

The situation in France and Germany is summarized in Fig. 15. Currently in both countries hypersonic propulsion systems are developed and manufactured for ground testing in the largest test facilities available until end of 1996. The size of these engines lies in the order of magnitude required for an engine to be used for flight testing. So the most logical step seems to be to take the (hopefully successful) ground tested engines for the development of an engine built in flight-rated hardware and to demonstrate the operation of the engine in "Real-Flight" before integrating the propulsion system in a rather sophisticated flight test vehicle. This "Vision" is schematically outlined in Fig. 16.

In Fig. 17 the major steps for the development of a future European space transportation system are shown. At the end of 1996 the ground testing of major components will be accomplished and concerning the engine the components intake, combustion chamber and nozzle will be integrated and groundtested in a free jet windtunnel test facility. Then the Hypersonic Technology Flight Experiment (HYTEX) (maybe in two steps as shown) is mandatorily needed to provide confidence on the new technologies before the implementation on a future European Space Transportation System. For completeness, the general hypersonics technology development and verification concept (HTDV) based on experimental fluid dynamics (EFD), numerical fluid dynamics (CFD) and flight testing understood as three commentary tools is explained in Fig. 18.

#### Concluding remarks

In Fig. 19 the challenge of successful hypersonics vehicle design is described. In conclusion the requirements for flight testing can be summarized as :

From aerothermodynamics the improvement of the accuracy of engineering design tools with respect to

- Prediction of aerodynamic drag (Transition!)
- Prediction of heat loads
- Prediction of engine integration losses

Successful engine/airframe integration with respect to

- Achievement of (Thrust-Drag) = Maximum
- Achievement of maximum precompression of the fuselage forebody, to increase mass flux through the engine
- Achievement of optimum (SERN-) nozzle/airbody integration to balance pitching moment

In the field of materials and structures the development of

- Passively "Radiation" cooled surfaces
- reuseable "Hot" structures
- Low "Dry" mass fraction

To continue with an international cooperative activity for the demonstration of the readiness of advanced hypersonics technologies needed for a future STS, the following proposal is made :

- Step 1 : Achievement of an international consensus on selected critical hypersonics technologies to be demonstrated in flight
- Step 2 : Definition of alternative, modular concepts for test vehicles to fly with hypersonic speed using airbreathing propulsion
- Step 3 : Preparation of a proposal for future multilateral collaboration leading to the realization of a hypersonics flight test programme to demonstrate the application of the advanced technologies under real flight environment.

This fits in the overall programatics of a systematical "Step-by-Step" approach for the development of a future European Space Transportation System (Fig. 20).



| Cost (present situation) | PEGASUS   | ARIANE    | SHUTTLE   |
|--------------------------|-----------|-----------|-----------|
| per Launch               | 10 Mio\$  | 100 Mio\$ | 500 Mio\$ |
| per kg. Payload LEO      | 25.000 \$ | 20.000 \$ | 25.000 \$ |

Hypothesis :

Reuseability is the "Key" to Cost Reduction (by 1 Order of Magnitude)

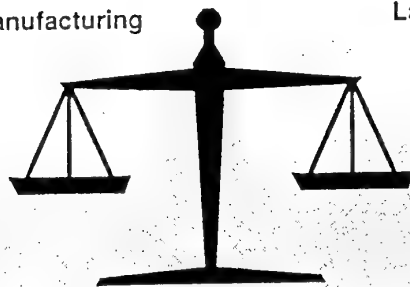


To be Achieved by Rocket or Rocket + Airbreathing Propulsion ?

FIG. 1 COST ASSESSMENT OF AVAILABLE SPACE TRANSPORT SYSTEMS  
PRESENT SITUATION

Reuseability does not mean necessarily Airbreathing Propulsion  
Trade - Off mandatorily required :  
All-Rocket vs. Rocket+Airbreathing Propelled Transport Systems

Technology Readiness  
Cost for Development & Manufacturing



Ground Operation  
Launch "Window" Flexibility  
Environmental Impact  
Launch Safety  
Mission Abort



Airbreathing Propulsion seems to be Attractive

FIG. 2 ALL-ROCKET PROPULSION VS. ROCKET + AIRBREATHING PROPULSION  
TRADE - OFF

## Why Hypersonics Technology ?

### Design Philosophy

- ☐ Rocket Propulsion :  
Atmospheric Flight as short as possible (Aerodynamic Drag)
- ☐ Airbreathing Propulsion :  
Acceleration (as much as possible) during flight in the atmosphere ("airbreathing")



Airbreathing Propulsion is the "Key-Technology"  
for Hypersonic Flight

FIG. 3 THE CHOICE OF PROPULSION FOR SPACE TRANSPORT SYSTEMS

The use of Airbreathing Propulsion Depends  
on its Capability to Accelerate the Flight Vehicle



$\text{Thrust} - \text{Drag} > 0$

#### Requires :

- ☐ Engine Thrust Enhancement
- ☐ Minimization of Engine/Airframe Integration Losses
- ☐ Aerodynamic Drag Reduction (Drag Prediction Accuracy ?)



In-Flight-Demonstration of successful Engine/Airframe Integration

FIG. 4 ENGINE/AIRFRAME INTEGRATION  
KEY PROBLEM FOR AIRBREATHING ENGINE.

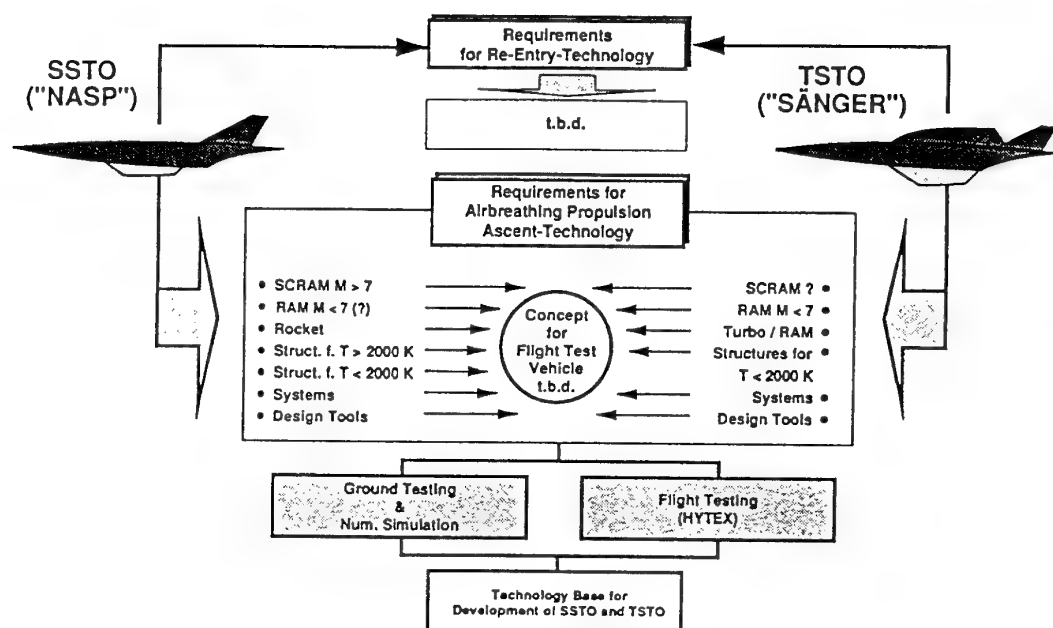


FIG. 5 SCENARIO OF TECHNOLOGICAL REQUIREMENTS FOR FUTURE STS

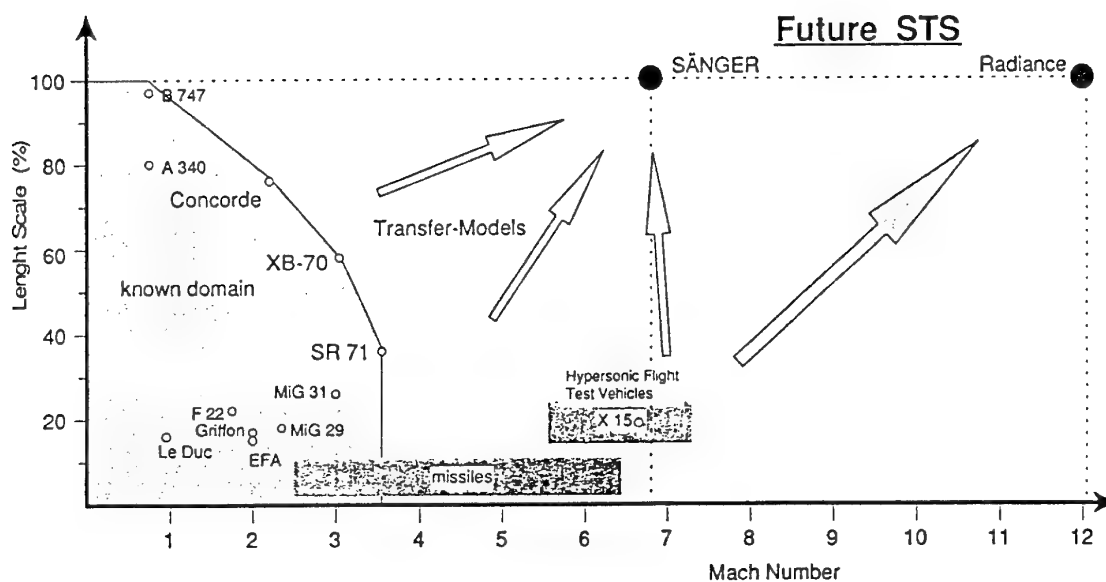
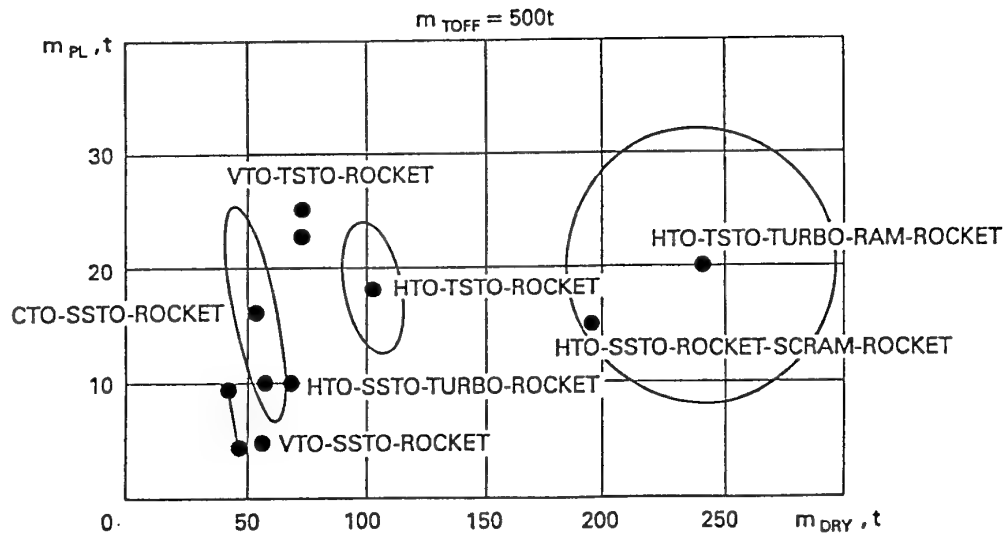


FIG. 6 THE NEED FOR FLIGHT TESTING HYPERSONICS TECHNOLOGY

- 1) Is the RAMJET the appropriate choice to accelerate TSTO
  1. Stage (e.g. SÄNGER) up to separation Machnumber = 6.8 ?  
 Answer to be given by free-jet ground test (e.g. APTU, AEDC)
- 2) Will the RAMJET operate also in real flight environment ?  
 Answer may be obtained by flight-testing  
 the engine as "Passenger" on a missile (e.g. drone D2)
- 3) Will the RAMJET work (installed thrust - drag > 0) when  
 fully integrated into an airframe ?  
 Answer to be given by flight testing (e.g. HYTEX R-A3)

FIG. 7

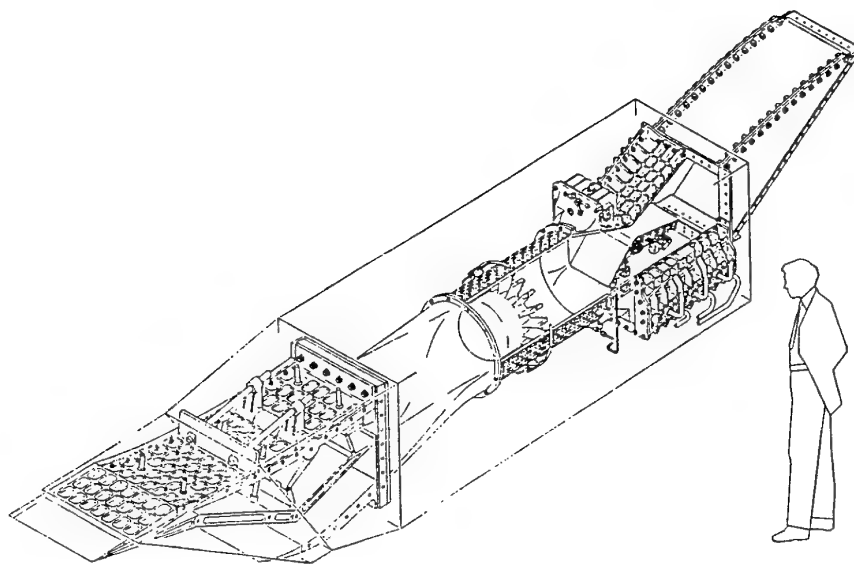
### RISK EVALUATION FOR SELECTED STS PAYLOAD MASS VS. DRY MASS CORRELATION



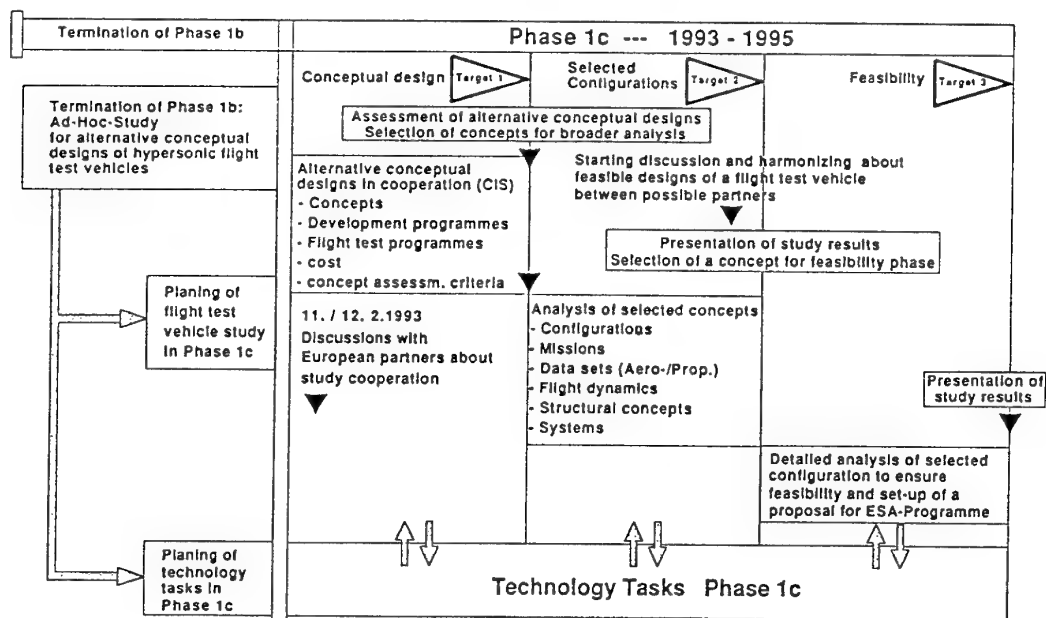
\*) L.M. Shkadov et al. / IAF-92-9865, Washington, 1992

FIG. 8

### QUESTIONS TO ANSWERED BY RAM-ENGINE TEST PROGRAMME



**FIG. 9** RAMJET ENGINE TO BE TESTED IN A FREE-JET GROUND TEST FACILITY AT HYPERSONIC SPEED ( $3.5 < M < 5.6$ )



**FIG. 10** STUDY OF ALTERNATIVE FLIGHT TEST VEHICLES SCHEDULE

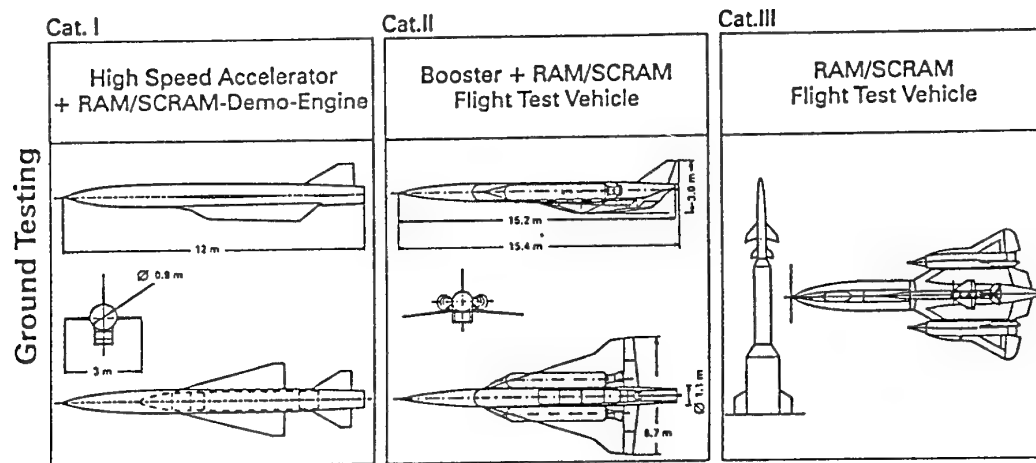


FIG. 11 CATEGORIES OF HYPERSONICS TECHNOLOGY DEMONSTRATORS  
FLYING TESTBED VEHICLES INVESTIGATED ( $3.5 < M < 7-8$ )

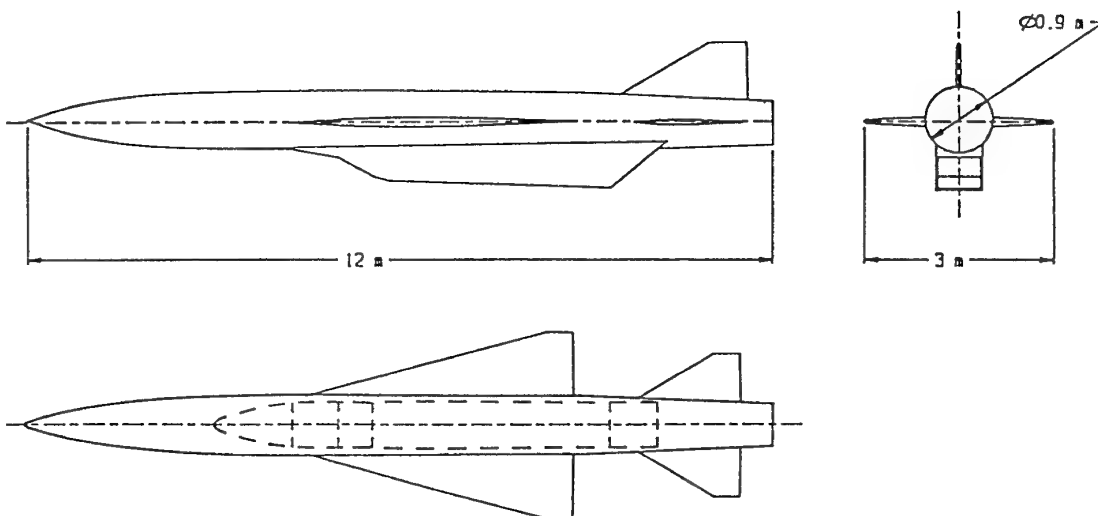


FIG. 12 HYPERSONIC FLIGHT TEST VEHICLE  
RADUGA D2 R-A<sub>3</sub>

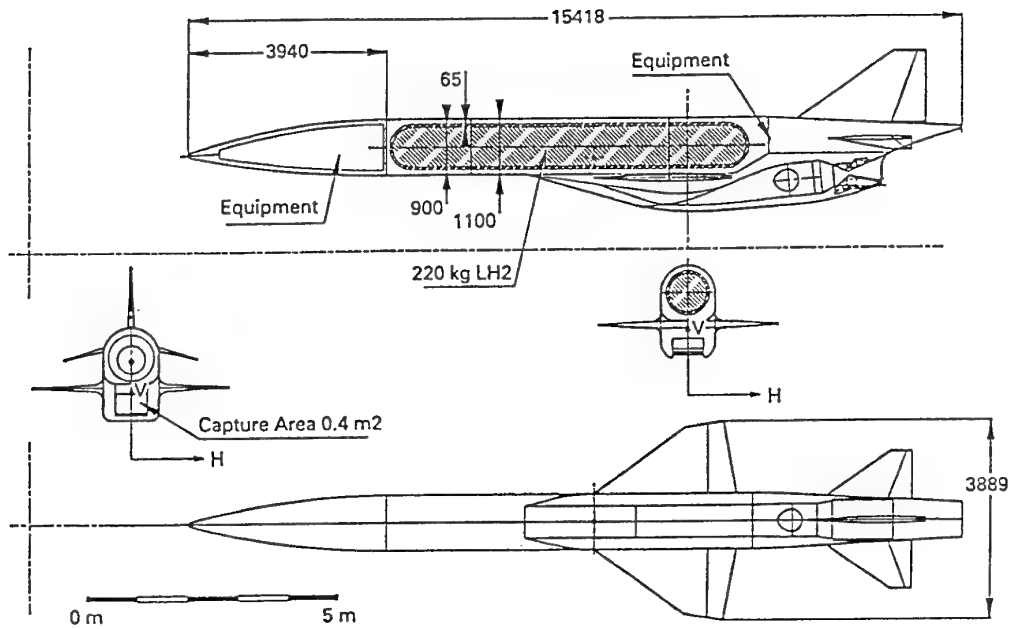


FIG. 13

### HYPERSONIC FLIGHT TEST VEHICLE HYTEX R-A<sub>3</sub>

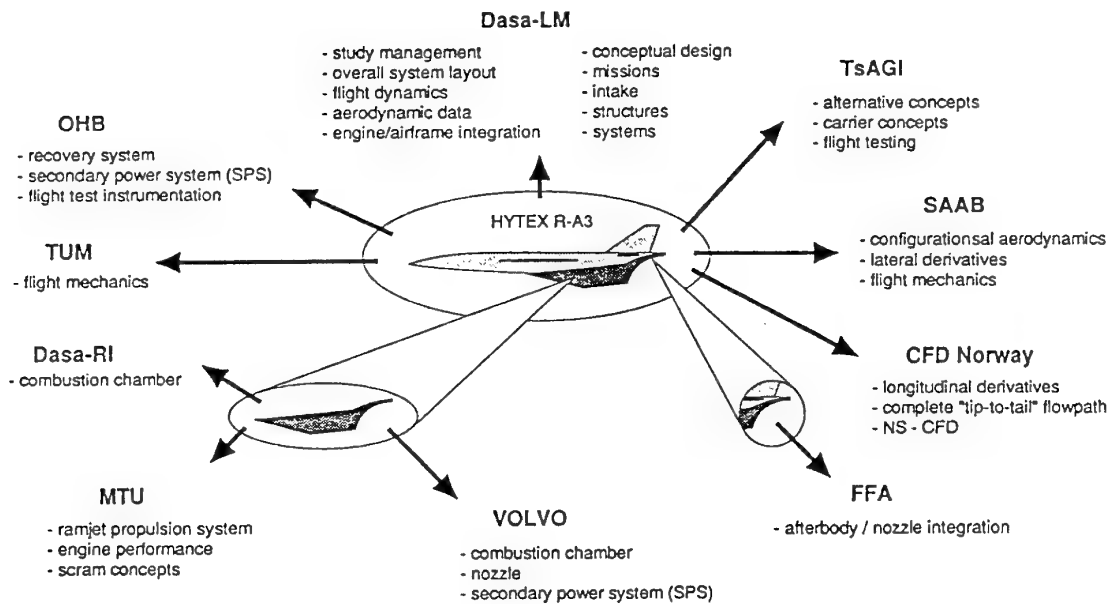


FIG. 14

### STUDY OF ALTERNATIVE CONCEPTS AND CONFIGURATIONS FOR HYPERSONIC FLIGHT TEST VEHICLES COOPERATION WITH INTERNATIONAL PARTNERS

### STATUS END 1996

- (1) National Programs are finished in France and Germany
- (2) Both countries have focussed their investigations on the airbreathing propulsion system
- (3) Both countries have tested the airbreathing engine in ground test facilities

**Flight testing the propulsion system is the logical next step**

**FIG. 15** MOTIVATION FOR A BI-LATERAL FRENCH-GERMAN COLLABORATION IN THE FIELD OF FLIGHT TESTING HYPERSONICS TECHNOLOGY

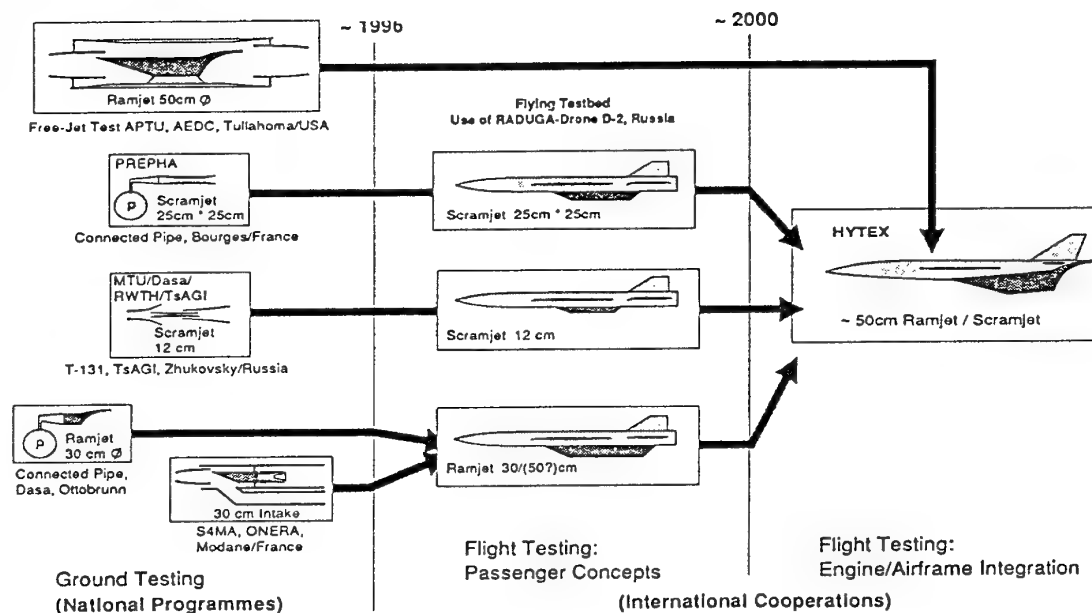


**FIG. 16** VISION OF FUTURE EUROPEAN COLLABORATION TO VERIFY ADVANCED AIRBREATHING PROPULSION TECHNOLOGY FOR HYPERSONICS



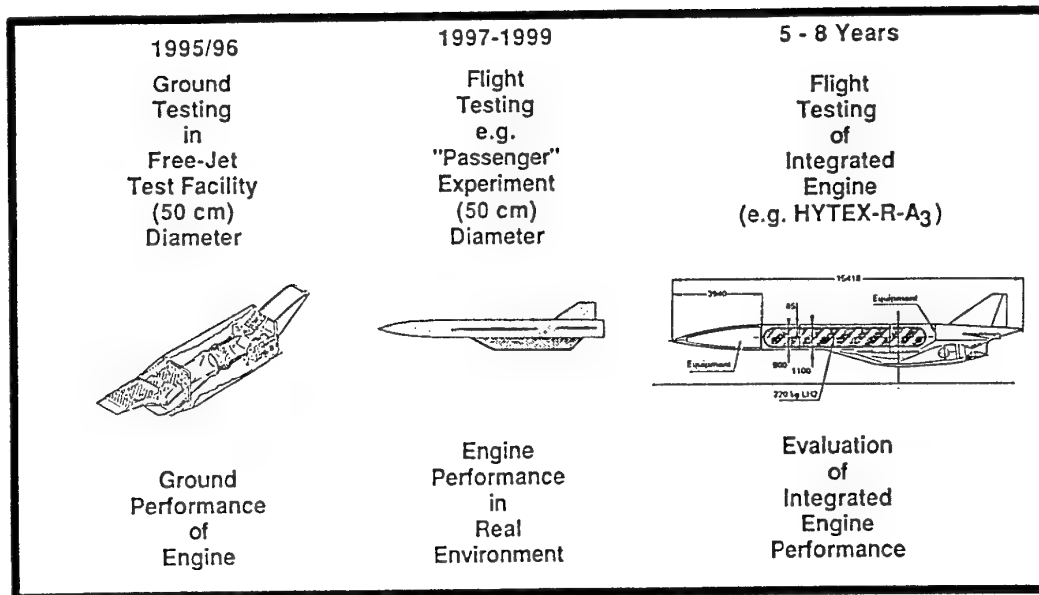


FIG. 17 STRATEGY FOR THE DEVELOPMENT OF THE AIRBREATHING PROPULSION SYSTEM AND PERFORMANCE VERIFICATION (RAM/SCRAM)

Hypersonics Technology  
Development and Verification  
Concept

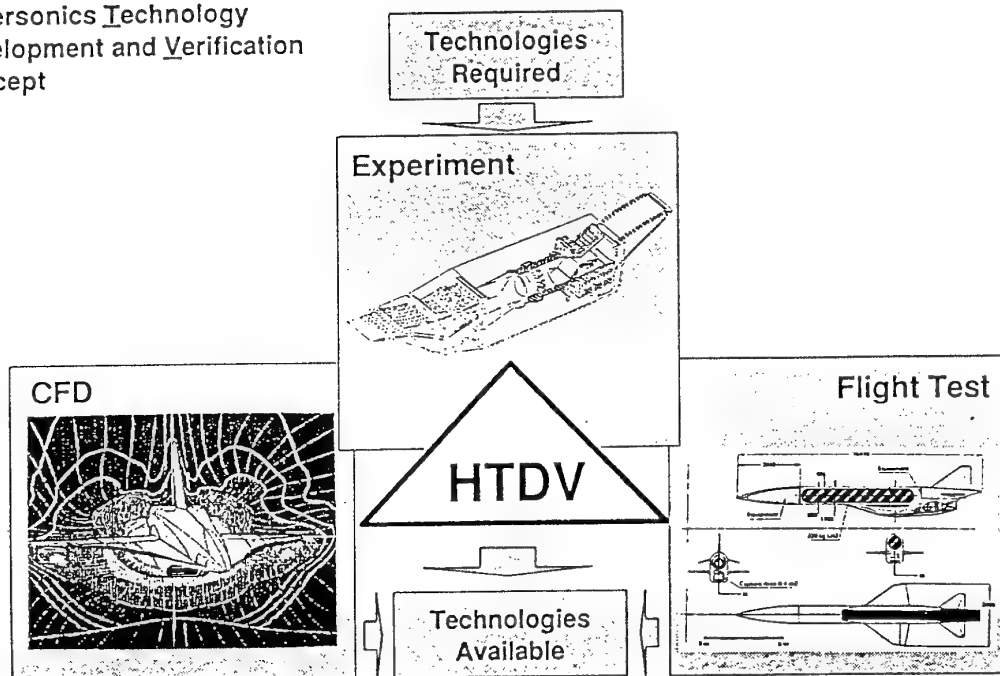


FIG. 18 HYPERSONICS TECHNOLOGY DEVELOPMENT AND VERIFICATION CONCEPT

### Conclusion

|                                    |  |
|------------------------------------|--|
| <b>Aerothermodynamics</b>          | Prediction of aerodynamic drag (Transition!)<br>Prediction of heat loads (Surface Temperature!)<br>Prediction of engine integration interference effects                                     |
| <b>Engine/Airframe Integration</b> | (Thrust-Drag) = Maximum, to achieve acceleration<br>Maximum precompression to increase mass flux through the engine<br>Optimum (SERN-) Nozzle/Airbody integration to balance pitching moment |
| <b>Materials &amp; Structures</b>  | Passively "Radiation" cooled surfaces<br>Reuseable "Hot" structures<br>Low "Dry" mass fraction   |



"Key"-Technologies Mandatorily Require  
Demonstration of Feasibility by Flight Testing

FIG. 19 THE CHALLENGE OF SUCCESSFUL HYPERSONICS VEHICLE DESIGN

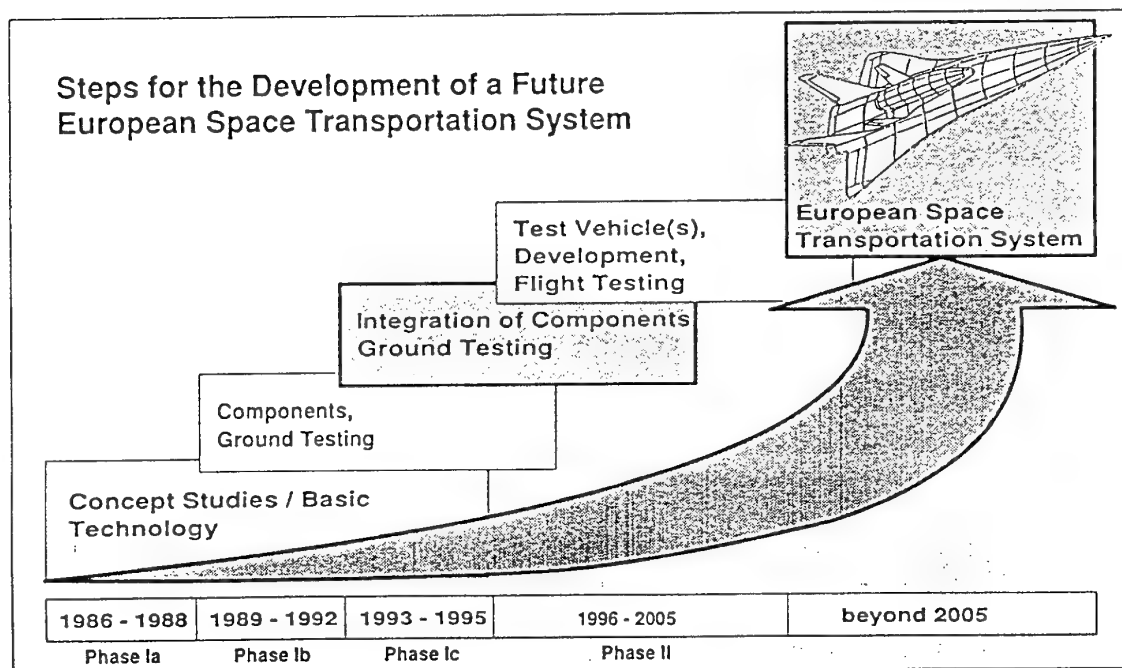


FIG. 20 STEP-BY-STEP APPROACH FOR THE DEVELOPMENT OF A FUTURE EUROPEAN SPACE TRANSPORTATION SYSTEM

## Extension of the ESA Test Centre with HYDRA, a New Tool for Mechanical Testing

Mr. Peter W. Brinkmann  
European Space Research and Technology Centre (ESTEC)  
Head Facilities & Methods Section  
ESA/ESTEC Mail Code YTF  
Keplerlaan 1  
NL-2200 AG Noordwijk  
Netherlands

### 1. SUMMARY

The introduction outlines the verification concept for programmes of the European Space Agency (ESA). The role of the Agency in coordinating the activities of major European space test centres is summarized.

Major test facilities of the environmental test centre at ESTEC, the Space Research and Technology Centre of ESA, are shown and their specific characteristics are highlighted with special emphasis on the 6-degree-of-freedom (6-DOF) hydraulic shaker. The specified performance characteristics for sine and transient tests are presented. Results of single-axis hardware tests and 6-DOF computer simulations are included.

Efforts employed to protect payloads against accidental damage in case of malfunctions of the facility are listed. Finally the operational advantages of the facility, as well as the possible use of the HYDRA control system design for future applications are indicated.

### 2. INTRODUCTION

#### 2.1 Verification Concept for Spacecraft

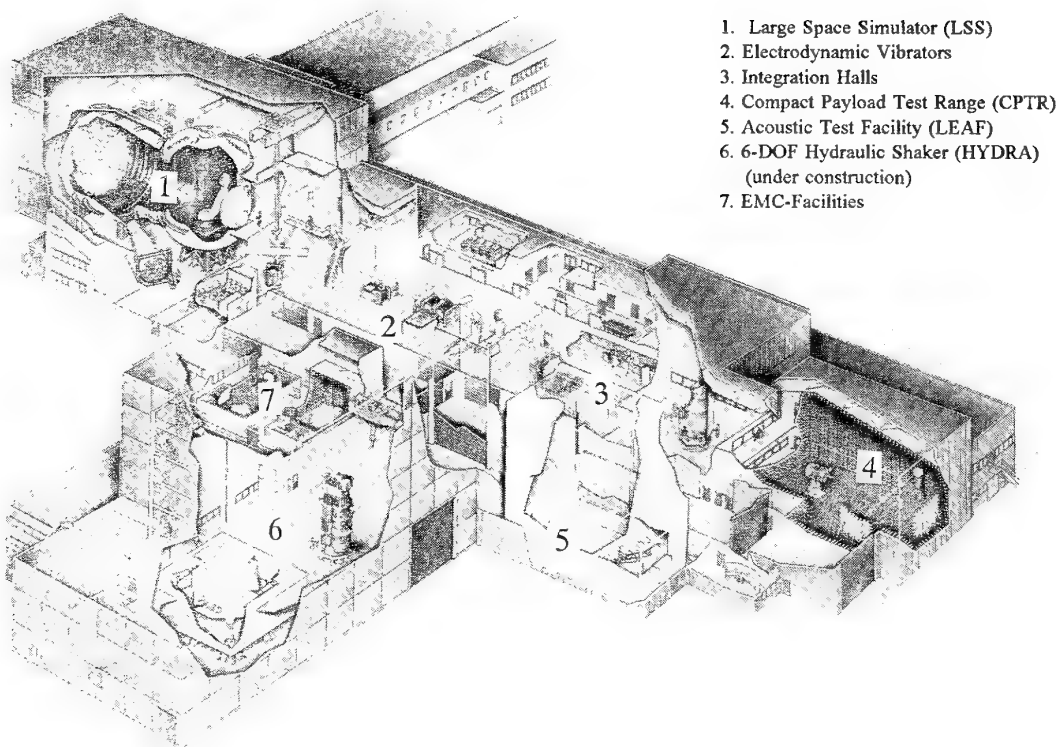
In view of the very high cost of developing and launching satellites, it is essential to ensure that the design fulfils all specified requirements and that hardware and software are free from workmanship failures before the spacecraft is placed in orbit. The verification of space systems, however, cannot be limited to a series of environmental and functional tests at the end of the development programme after the integration of the flight models. The identification of problem areas and in particular of design deficiencies at a late stage in the programme would lead to significant schedule delays and cost overruns. Efficient verification consequently needs to start with the design and must continue

throughout all project phases confirming at each phase that the programme objectives will be met. Hence the verification concept must deploy a series of verification steps including tests, which lead to satisfactory system performance without undue risks. Its purpose is to:

- o qualify the design already in the early development phase of a project;
- o permit timely selection of suitable materials and processes;
- o ensure proper functioning of components, units, subsystems before final flight model integration;
- o guarantee the integrity of system performance and identification of workmanship failures before launch.

Design verification requires the provision of computer models as well as breadboard or full scale satellite models, which are sufficiently representative with respect to the performance to be verified (e.g. structural, thermal, electrical models). Tests on satellite models are generally performed to update and qualify the corresponding mathematical models. Confidence in functional performance is built up by tests at different hardware levels, starting at component level and terminating with system performance verification. Therefore performance characteristics of the test facilities are regularly reviewed and adapted to the needs of future Agency programmes. In this context the Agency has recently decided to extend its satellite test facilities by implementing a 6-degree-of-freedom (6-DOF) hydraulic shaker until 1996.

Verification by representative tests is often time consuming and expensive and may even be impossible if the simulation of relevant parameters cannot be achieved economically.



1. Large Space Simulator (LSS)
2. Electrodynamic Vibrators
3. Integration Halls
4. Compact Payload Test Range (CPTR)
5. Acoustic Test Facility (LEAF)
6. 6-DOF Hydraulic Shaker (HYDRA)  
(under construction)
7. EMC-Facilities

Fig. 1: Cut-out View of the ESTEC Test Centre including the 6-DOF Hydraulic Shaker

Facilities for spacecraft testing usually require high investment and operational costs. Therefore complementary verification methods need to be employed such as:

- Analysis (e.g. mathematical models)
- Similarity (e.g. experience from other programmes)
- Assessment (project reviews, demonstrations, inspections).

A great deal of effort is spent in improving confidence in analytical tools and computer models in order to reduce the overall cost of spacecraft verification.

## 2.2 Facility Coordination

The European Space Agency has developed and maintains major environmental test facilities. Similarly some member states have established test centres to support their national programmes. The cut-out view in Fig. 1 illustrates the ESTEC Test Centre. The illustration already includes the test hall for the 6-DOF vibration facility, which is presently under construction. The facilities are

at the disposal of industry, scientific institutes and projects to support Agency programmes as well as space programmes of ESA member states; but these can also be made available for non-ESA projects, when not utilized for Agency purposes.

Therefore European industry and scientific institutes do not have to procure those environmental test facilities, saving not only extensive investments but also significant costs for operation and maintenance. In order to avoid duplication of facilities and subsequent underutilization of facilities in Europe, ESTEC has established a close co-operation with its partners CNES/INTESPACE (France), IABG (Germany) and CSL (Belgium). This co-operation (often referred to as the Co-ordinated European Test Facilities) is not limited to operational aspects, but also includes consultation with respect to identification of requirements of future programmes and coordination of investments for new test facilities. This improves the utilization of facilities in Europe and avoids unnecessary redundancies or over-capacities. Whilst the national test centres are equipped

for environmental tests on small and medium satellites, the ESTEC facilities are compatible with the requirements of the large spacecraft to be launched on Ariane-4 and Ariane-5. The test facilities of all centres are compliant with the stringent product assurance requirements of ESA for tests on space hardware.

### 3. THE MAIN TEST FACILITIES IN THE ESA TEST CENTRE

#### 3.1 Facilities for Thermal Tests

##### 3.1.1 Solar simulation facilities

Solar simulation facilities permit the close simulation of the main parameters encountered by satellites outside of the Earth's atmosphere. The goal of the tests is the qualification of mathematical thermal models by correlating computer calculations with results of the thermal balance tests and the proof of system performance under simulated space conditions.

During the tests the pressure inside the test chamber is reduced to levels below  $10^{-6}$  mbar with oilfree high vacuum pumps. For simulation of the deep-space heat sink, the vacuum chambers are lined with black shroud systems, which are cooled down to temperatures of about 100 K by liquid nitrogen. Simulated solar radiation is produced

by high-power xenon-arc lamps and associated optics. Motion systems make it possible to simulate the spacecraft orientation with respect to the impinging solar beam. The Large Space Simulator (LSS) at ESTEC with a solar beam diameter of 6 m is the largest solar simulator within the ESA member states with unique performance characteristics. Fig. 2 illustrates the LSS.

##### 3.1.2 Thermal vacuum facilities

Temperature cycling of space hardware under high-vacuum conditions has proven to be an excellent tool for identifying design deficiencies and workmanship failures. This test is therefore considered mandatory for qualification and acceptance at all hardware levels from components to systems. In the temperature cycling mode, the shrouds are supplied with gaseous nitrogen at variable temperatures, or the test article is heated with infrared radiators, while the shrouds are at  $LN_2$  temperatures.

A number of specific thermal vacuum facilities of different sizes are available and the solar simulation facilities at ESTEC can also be used for thermal cycling tests.

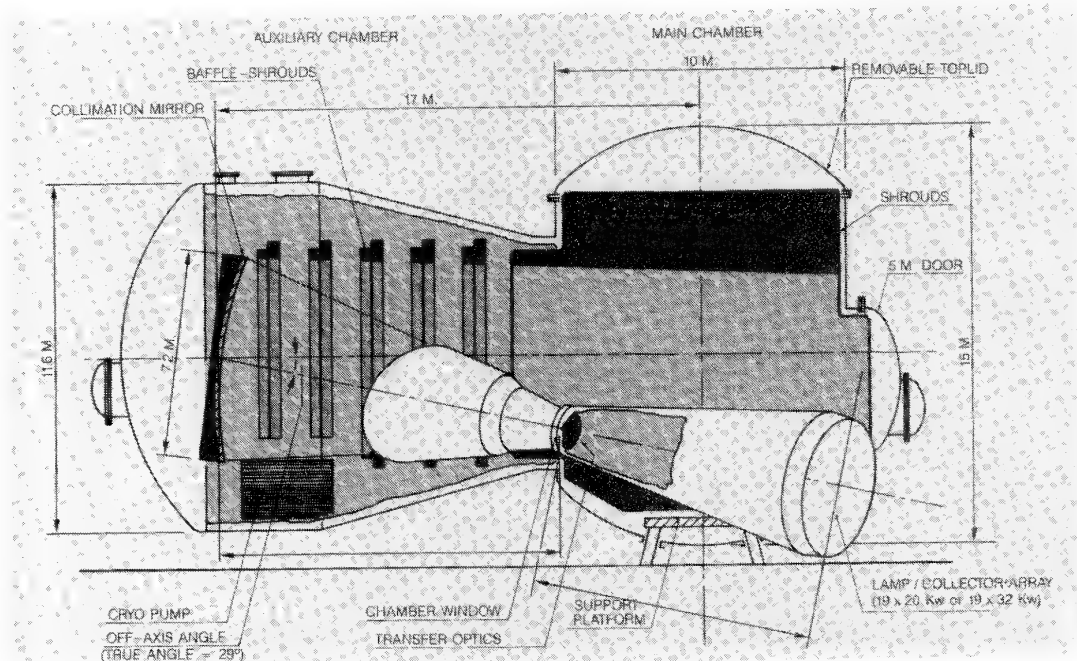


Fig. 2: Schematic of the Large Space Simulator (LSS) at ESTEC

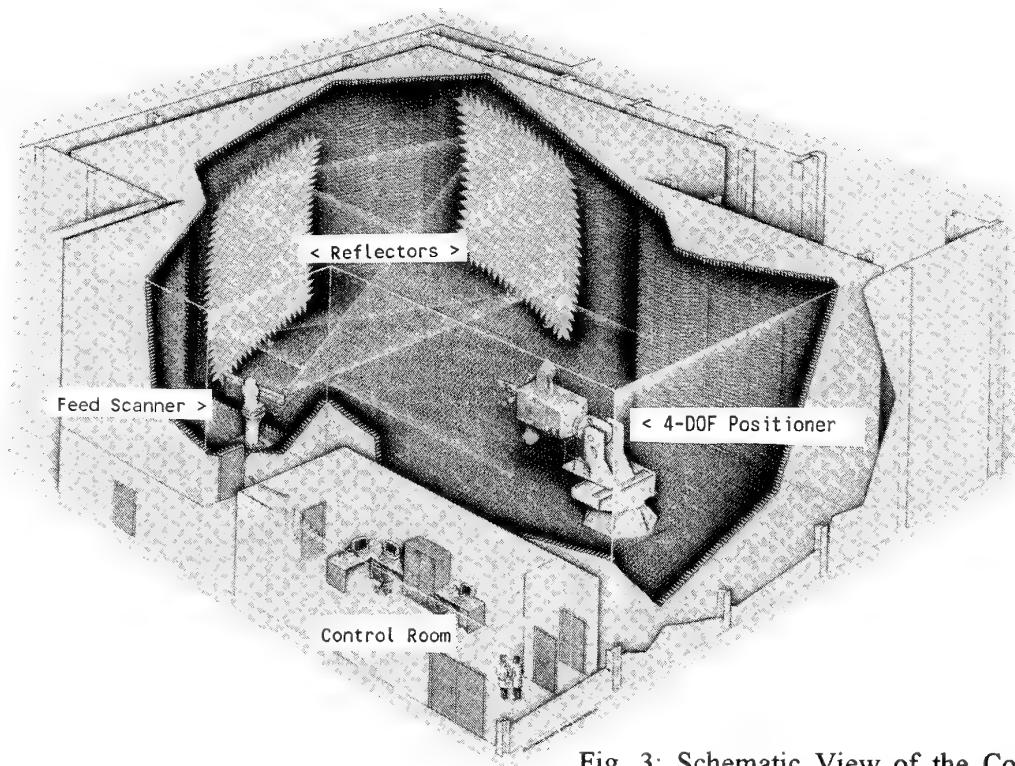


Fig. 3: Schematic View of the Compact Payload Test Range (CPTR) at ESTEC

### 3.2 Electromagnetic Test Facilities

#### 3.2.1 EMC facility

It is essential to ensure that the electronic equipment of a spacecraft functions correctly within the electro-magnetic environment created by external sources and to verify mutual compatibility of different units operating within the satellite system itself. It also needs to be confirmed that build-up of high electric potentials on satellite surfaces with subsequent electrostatic discharging is avoided. The respective tests on spacecraft or spacecraft equipment are performed in Electro-Magnetic-Compatibility (EMC) Facilities. The EMC facilities are shielded enclosures with highly conductive metal walls, floors and ceilings. The walls and ceiling are lined with an absorbent, anechoic material to attenuate reflected electro-magnetic energy.

The EMC facilities are shielded enclosures with highly conductive metal walls, floors and ceilings. The walls and ceiling are lined with an absorbent, anechoic material to attenuate reflected electro-magnetic energy.

#### 3.2.2 Compact Payload Test Range (CPTR)

The CPTR permits the testing of the links between ground stations to the satellite and even links from ground stations via satellite to another ground station or airborne terminal. The CPTR is illustrated in Fig. 3. It permits measurements of critical system parameters such as EIRP (Equivalent Isotropic

Radiated Power, PFD (Power Flux Density), beam steering, link budgets, etc. One of the facility's main features is its low cross-polar performance allowing very accurate measurements to be made of communications payloads which employ frequency re-use. Another important feature is the fact that feed horns representing ground stations can be placed at different locations in the focal plane. In a similar way, the CPTR also lends itself to measure the performance of active arrays. Here, the beam is scanned electronically by sensors in the focal plane.

### 3.3 Facilities for Mechanical Tests

#### 3.3.1 Vibration facilities

One of the risks faced by a spacecraft stems for the dynamic loads which are introduced into the structure through the interface with the launch vehicle. Spacecraft and their components are therefore tested on dynamic vibrators to verify the design and the workmanship of flight hardware. The present test philosophy is largely depending on sine sweep tests along the 3 orthogonal axes of the spacecraft. Therefore these tests require special procedures to avoid undue stresses ("notching procedures").

The test centre at ESTEC is equipped with electro-dynamic vibrators, which operate in a frequency range from 5 to 2000 Hz and can perform sinusoidal, random and shock tests sequentially along the main orthogonal axes of the specimen.

The main vibration system consists of two 140 kN shakers which can either be used individually or in multishaker configuration. In the latter configuration, the two shakers are coupled to a dual-head expander for tests in the longitudinal (vertical) axis and to a large slip table for "lateral tests". Fig. 4 illustrates the multishaker configurations.

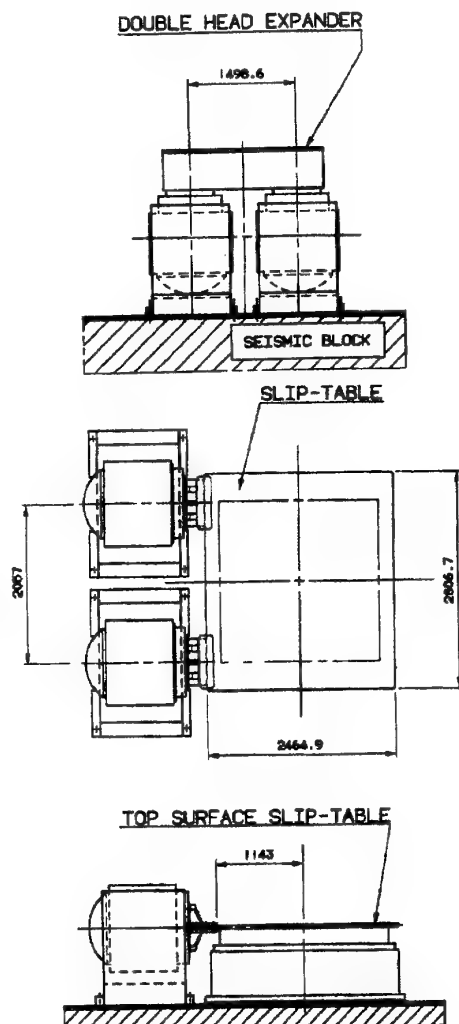


Fig. 4: The 280 kN Multi-axis Shaker in Vertical and Horizontal Configuration

### 3.3.2 Acoustic facilities

Acoustic tests are required to ensure that the noise levels generated during the launch phase do not damage spacecraft components. The noise pressure levels are caused by the launcher engines and by the air flow passing along the payload fairing during the atmospheric flight. The ESTEC facility is the largest one in Europe with a volume of approx. 1600 m<sup>3</sup>. It can produce noise levels of up 158 dB ( $P_{ref} = 2 \times 10^{-5}$  Pa).

## 4. NEW TOOL FOR STRUCTURAL QUALIFICATION (HYDRA)

Considerable effort has been expended during the last decade in studying the possibilities for improvement of dynamic structure qualification in general and for system acceptance of Ariane-4 and Ariane-5 payloads in particular. These investigations have led to the concept of the 6-DOF hydraulic shaker (HYDRA), which is distinguished by the following improved features as compared with conventional electrodynamic shakers:

- actuator force and stroke
- frequency range extended below 5 Hz
- active control of orthogonal motions
- controlled excitation in 6-DOF permitting realistic flight load testing
- improved test operations and safety

The design and engineering phase for HYDRA and the associated building has been performed during 1992/1993. The procurement, installation and acceptance phase of the building started in 1993, while the start of the shaker procurement has been delayed until August 1994 for budgetary reasons. The facility shall become operational in the second half of 1996 for tests on the structural model of the PPF/Envisat satellite (mass approx. 7000 kg). This ESA satellite is currently planned for launch in 1998 by Ariane-5.

### 4.1 Performance Characteristics

#### 4.1.1 System configuration and forces

The geometry of the table and actuator arrangements was optimised by detailed trade-offs early in the design phase. These were based upon finite element models calculating the rigid body modes and the elastic modes of the loaded and unloaded table, taking into consideration stiffness, masses and the geometric configuration of all actuators. The actuator force requirements were calculated



with a dedicated computer programme taking into account the kinematics of the loaded table. The results of the trade-offs (reported in Ref. 1) and subsequent engineering have led to an octagonal table with a span of 5.5 m and a mass of 22000 kg. The first flexible mode at 122 Hz in loaded configuration, is well above the upper operational frequency limit of the shaker, which is at 100 Hz. The table is driven by 4 actuators in the vertical direction and 2 actuators for each lateral direction. Each of the 8 actuators has a stroke of  $\pm 70$  mm, a maximum piston velocity of 0.8 m/sec and a force rating of 630 kN. The high force levels are required to accommodate the "overturning moments" created by the table and payload assembly during dynamic testing. In conventional testing with electro-dynamic shakers these need to be compensated for using bearing assemblies, i.e. passive elements. The 6-DOF hydraulic shaker counteracts these moments by the active control of the motions in all translational and rotational axes. In this way it will be possible to actively attenuate the parasitic orthogonal motions (often referred to as "cross-talk") for sine tests of large payloads. The cut-out view (Fig. 5) illustrates the PPF/Envisat satellite being tested on the HYDRA facility.

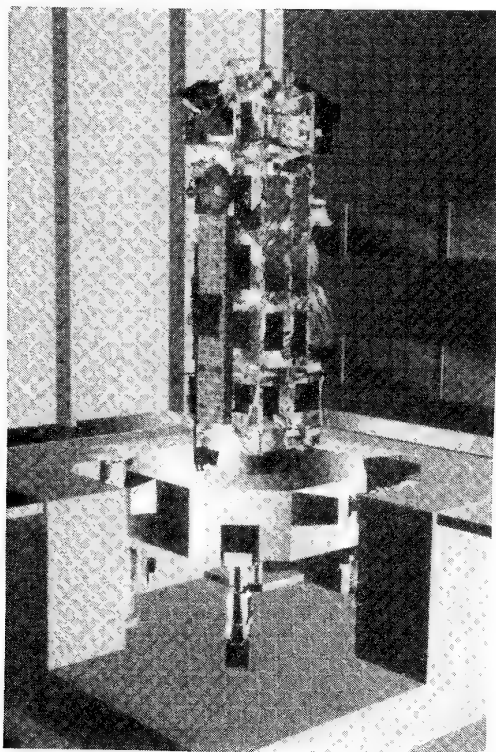


Fig. 5: HYDRA Test Configuration with the PPF/Envisat Satellite

#### 4.1.2 Operational test modes

HYDRA has been designed for sinusoidal testing along each translational axis. Besides testing at selected discrete frequencies (sine-dwell), it is possible to perform sine sweeps with sweep rates in the range of 2 to 4 octaves per minute. Furthermore transient excitation signals in 6-DOF can be generated in addition.

#### 4.1.3 Dynamic performance

The dynamic range of HYDRA is shown in Fig. 6 and Fig. 7. The upper acceleration limits of the performance diagrams are applicable for a test article mass of 7000 kg with a centre of gravity 5 m above the table surface. The acceleration limits will increase as the test article mass decreases and vice-versa. The Ariane-5 qualification levels for sinusoidal vibration tests are indicated hereafter for comparison and show the margins for payloads with higher masses.

| Ariane-5<br>(Ref. 2) | Frequency<br>range (Hz) | Qual. levels<br>(0-peak)<br>recomm. |
|----------------------|-------------------------|-------------------------------------|
|                      | 4-5<br>5-100            | 12.4mm<br>1.25g                     |
| Longitudinal         |                         |                                     |
| Lateral              | 2-5                     | 9.9mm                               |
|                      | 5-25                    | 1g                                  |
|                      | 25-100                  | 0.8g                                |
| Sweep rate           |                         | 2 oct/min.                          |

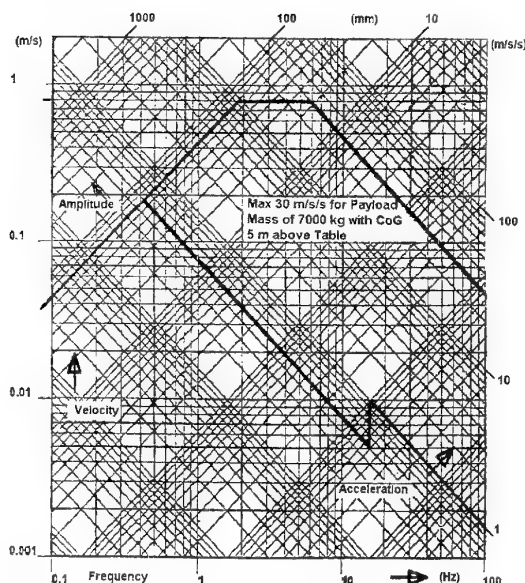


Fig. 6: HYDRA Performance for Lateral Excitation



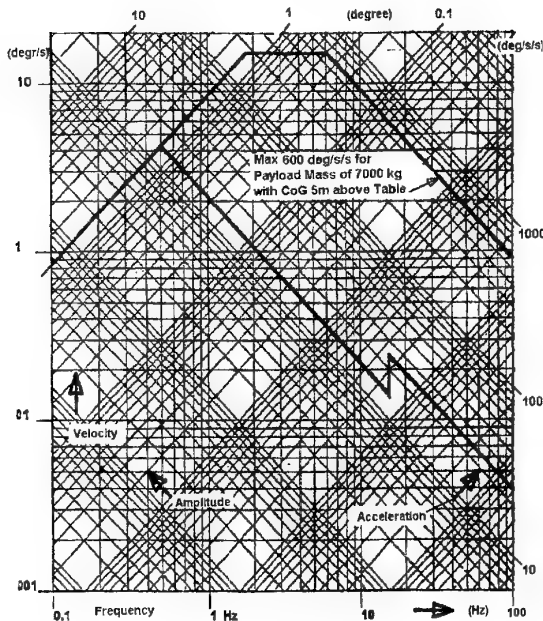


Fig. 7: HYDRA Performance for Rotational Excitation

The specified performance tolerances are as follows:

- a) Signal distortion for sine test mode (differences between measured and reference signal)

peak values:  
 $\leq 1.5$  dB  
 or  
 $\leq 0.025g$ , whichever is larger

RMS values:  
 $\leq 1.0$  dB  
 or  
 $\leq 0.025g$ , whichever is larger

- b) Parasitic cross-axis excitation in sine test mode in the unexcited orthogonal axes

$\leq 10\%$  of nominal excitation level  
 or  
 $\leq 0.025$  g, whichever is larger.

- c) Signal distortion for transient test mode (differences between measured and reference signal)

peak values (all maxima and minima):  
 $\leq 1.5$  dB  
 or  
 $\leq 10\%$  of the max. amplitude in all other degrees of freedom, whichever is larger

RMS values (difference between measured and reference signal):  
 $\leq 1.0$  dB  
 or  
 $\leq 10\%$  of the max. amplitude in all other degrees of freedom, whichever is larger

Total signal duration:  
 $\leq \pm 5\%$

#### 4.1.4 Signal quality

Hydraulic exciters cannot reproduce acceleration signals free from distortion, mainly because of non-linearities of the hydrodynamics in servovalves and actuators (Ref. 3). An example of this phenomenon is shown in Fig. 8. The graph shows the distorted acceleration at the table centre during a sine test at 4 Hz with an existing 6-DOF hydraulic shaker.

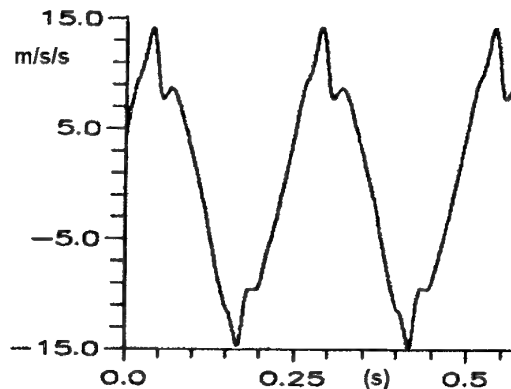


Fig. 8: Acceleration Time History with 4 Hz Sinusoidal Input of an Existing 6-DOF Earth Quake Simulator

In order to reduce these distortions to an acceptable level, special effort has been put into the careful design of servovalves, actuators, and bearings and particularly into the actuator control system of HYDRA. The digital control system (Ref. 4) uses detailed mathematical models of the shaker system with the following features:

- non-linear control algorithms for servovalve/actuator
- on-line prediction of actuator motions
- on-line prediction of system kinematics

The functioning of the actuator control algorithm was verified by tests with an available actuator and a simplified control system. A typical result of these tests is shown in Fig. 9.

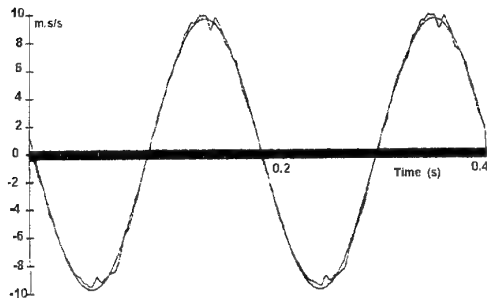


Fig. 9: Acceleration Time History Measured with Single Axis Test Rig Using a Simplified HYDRA Control (Input 5 Hz Superimposed)

Subsequently a 6-DOF computer model was set up, and initial investigations were performed at discrete frequencies from 0.5 Hz up to 100 Hz without yet employing table acceleration feedback and oil pressure feedback of the servovalves.

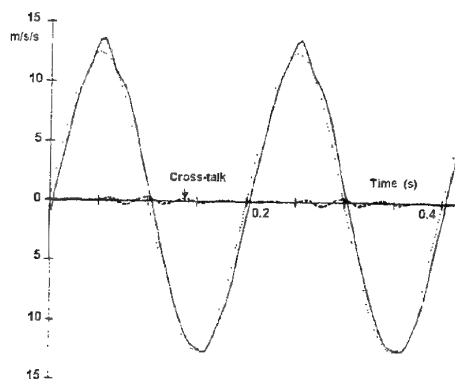


Fig. 10: Acceleration Time History Simulated with the 6-DOF HYDRA Computer Model without Feedback Loops (Input 5Hz Superimposed)

Fig. 10 illustrates a typical result of these simulations, which shows good coincidence between the nominal and actual waveform; it also shows that the orthogonal motions ("cross-talk") are well below 10% of the nominal excitation. The 6-DOF simulations will be continued in order to perform sensitivity analyses and to test various feedback options for the final optimisation of the control software. Due to the delayed start of the implementation phase of the project, these results cannot be presented in this publication.

#### 4.2 Transient Testing

The introduction of a test method that reflects a more realistic representation of the space flight environment has been a major objective for the development of HYDRA. In preceding studies it has been concluded that the simulation of the multi-directional transients at the interface of launcher and spacecraft produces more realistic structural responses. In contrast, traditional sine tests lead to unrealistic responses and therefore involve an inherent risk of over- or under-testing (Ref. 5, 6, 7). Multi-degree-of-freedom hydraulic shakers designed for earthquake simulation have been used in the past to demonstrate that the reproduction of transients is feasible after several iterations (Ref. 8). Recent advances in computer technology permit the control system of HYDRA to simulate transients in 6-DOF without iteration. Fig. 11 shows the simulation results of a representative transient for Ariane-5 at lift-off. The quasistatic portion of the transient signal as well as its frequency contents above 100 Hz has been filtered out.

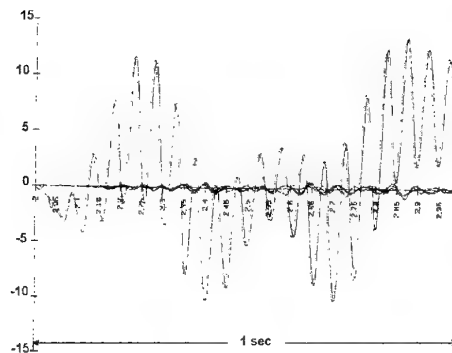


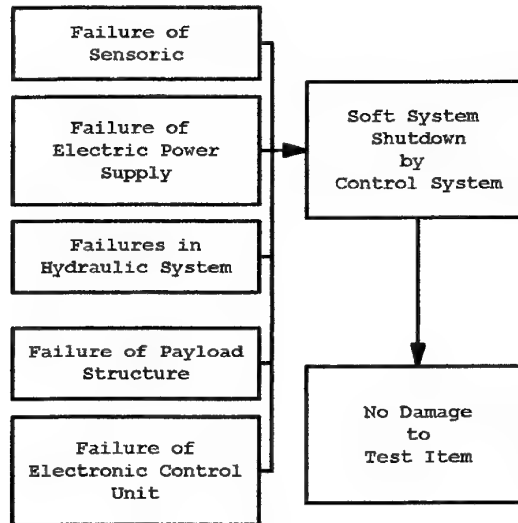
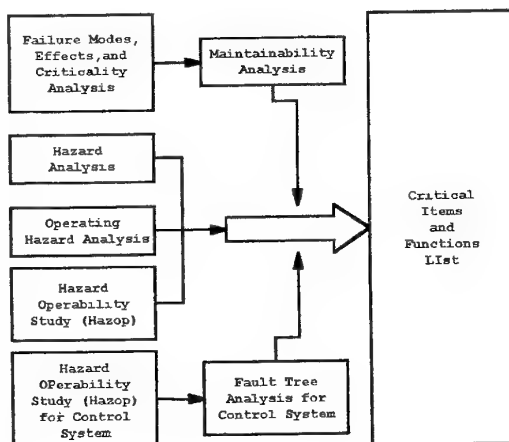
Fig. 11: A Transient Simulated with a HYDRA Mathematical Model (Input Superimposed)

### 4.3 Operational Aspects

The 6-DOF hydraulic shaker allows the specimen to be tested along both the vertical and the lateral axes with one single test setup. It is therefore no longer necessary to dismount, relocate and re-instrument the payload for the different excitation directions. This not only reduces the effort involved in handling and instrumentation, with consequent reductions in test durations and risk, but it also provides flexibility in the sequencing of tests. In particular, x-, y- and z-signature tests can be performed without particular effort before and after each single-axis test run.

The large octagonal test table is flush with the test floor. It facilitates the mounting of heavy and/or geometrically large specimens (e.g. appendages such as solar arrays). Due to the wide span of the table the complexity and mass of the adaptors can be kept low. All shaker equipment and supplies are located in the basement of the building, mechanically isolated from the clean test area (class 100.000 Fed.Std. 209). The gap between the aluminium test table and the test floor is closed by a flexible seal. This provides mechanical separation of the clean test area from the hydraulic equipment located below the table.

Detailed reliability and safety analyses were made during HYDRA's design, as outlined in the following diagrams. The control system has been designed in such a way that the failure events identified in the various analyses will not lead to a hazardous situation for facility or payload, because it will trigger a "soft facility shutdown" in time.



### 5. CONCLUDING REMARKS

The installation of the hydraulic shaker will ensure that the ESA test centre at ESTEC, Noordwijk, remains compliant with the testing requirements evolving from the ongoing launcher developments, which lead to larger satellites with higher masses.

However, the new facility will not only extend the performance for applying traditional test methods, it will also provide ESA with the tool to verify the advanced test method of "transient testing" after more than one decade of intense theoretical study work and subsequently apply this method for the qualification of satellite structures.

The control system design, once verified in practical application, will certainly have the potential to improve the performance characteristics of other machines and simulators driven by hydraulic actuators. In fact, the control algorithm for the HYDRA hydraulic system has already been successfully used for the control of the horizontal moving system of the 6-DOF driving simulator at Daimler-Benz, Berlin, Germany. Both the acceleration control accuracy and the time behaviour could be improved drastically compared to the previous analogue feedback control.

**6. REFERENCES**

1. Brinkmann, P.W. , Kretz, D, 1992  
The Design Concept of the 6-Degree-of-Freedom Hydraulic Shaker at ESTEC,  
NASA Publication 3181
2. Arianespace, 1994  
Ariane-5 User's Manual, Issue 2,  
May 1994.
3. Lachenmayr, G, Krautwald W.,  
Development of High-Precision  
Computer Models of a Multi-Axis  
Vibration Test Facility and Usage for  
Control System Design and Test  
Prediction,  
ESA WPP-066, October 1993
4. Kretz, D., Grimm, A.,  
Design and Performance Characteristics  
and Control and Safety System of the  
Hydraulic Shaker at ESTEC,  
ESA WPP-066, October 1993
5. Brunner, O., Stavrinides C., Klein, M.,  
Transient Vibration Testing of  
Satellites,  
ESA SP-304, September 1990
6. Ams, A., Wedig, W.,  
Identification and Variation of  
Transients - A New Test Procedure for  
Space Structures,  
ESA WPP-066, October 1993.
7. Erben, E., Beig, H-G., Lachenmayr, G.  
A Transient Test Method Applicable  
for Spacecraft Structure Qualification,  
ESA WPP-066, October 1993.
8. Füllekrug, U., Sinapius, M.,  
Simulation of Multi-Axis Vibration in  
the Qualification Process of Space  
Structures,  
ESA WPP-066, October 1993

# ESSAIS DE PROPULSEURS A PLASMA STATIONNAIRE

## EN AMBIANCE SPATIALE SIMULEE

**Mr. Dominique Valentian**  
**Expert-conseil — S.E.P.**  
**Groupe Petite Propulsion & Équipement**  
**Aérodrome de Melun/Villaroche**  
**77550 Moissy-Cramayel**  
**France**

### 1. RESUME

La SEP (Société Européenne de Propulsion) a développé une installation d'essai permettant d'effectuer les essais de recette des propulseurs SPT 100 et les essais de développement d'un propulseur de deuxième génération le SPT MK II.

Cette installation résulte de la modification d'une chambre à vide existante. Elle est munie d'une pompe cryogénique de grande capacité permettant de pomper efficacement le Xénon, d'une balance de mesure de poussée et d'un système de conduite automatique d'essai. Les résultats obtenus se comparent favorablement à ceux enregistrés sur des installations plus volumineuses aux USA et en Russie.

### 2. INTRODUCTION

La SEP (Société Européenne de Propulsion) a conclu un agrément avec K.B. FAKEL et Space System Loral dans le cadre d'un joint venture nommé ISTI (International Space Technology Inc.) dans le but de proposer en Europe des sous systèmes de propulsion électrique utilisant le SPT 100 et de développer une version avancée du SPT appelée SPT MK II.

Le SPT fournit une poussée plus élevée (80 mN) que les propulseurs ioniques bombardement conventionnels.

Cet avantage se traduit par un débit masse de Xénon (5 mg/s) qui est au delà de la capacité de pompage des chambres à vide poussée. Il faut donc repenser le moyen de pompage.

Une autre particularité du SPT est la distribution relativement large de l'énergie des ions ; il en résulte qu'on ne peut déduire la poussée des paramètres électriques, comme dans un moteur ionique conventionnel, il faut donc mesurer la poussée.

Les modifications nécessaires pour permettre les essais du SPT dans notre installation ont porté sur quatre points :

- Introduction d'une pompe cryogénique puissante permettant de garantir une pression de service de  $3.10^{-5}$  mbar
- Montage d'une balance de mesure de poussée,
- Système d'alimentation en Xénon de haute pureté,
- Dispositifs d'analyse du faisceau (sondes passives, coupes de Faraday et sondes d'analyse à potentiel retardé (R.P.A)).

Le principe du SPT est passé en revue. L'état initial de l'installation d'essai est décrit, montrant les améliorations nécessaires pour permettre l'essai du SPT. Les spécifications de chaque nouvel équipement sont analysées et comparées aux performances réellement obtenues.

Quelques exemples pertinents de résultat d'essais sont présentés et comparés à ceux obtenus aux USA et en Russie.

### 3. DESCRIPTION DU SPT

Le SPT (Stationary Plasma Thruster) a été développé il y a 25 ans par le Pr MOROZOV en Russie [1]. Le SPT appartient à la famille des propulseurs à dérive fermée d'électrons. Les SPT sont utilisés d'une manière opérationnelle dans

l'espace depuis 1972 sur les satellites METEOR, METEOR-PRIRODA, GORIZONT, EKRA et récemment GALS [2].

Le schéma de principe du SPT (Figure 2.1) repose sur l'accélération des ions dans un plasma neutre à l'aide d'un champ électrique formé entre une anode et une cathode creuse. L'accélération des ions dans un plasma neutre élimine les effets de charge d'espace, la densité de courant d'ions peut être alors très élevée. A titre d'exemple la poussée du SPT 100 est de 80 mN pour un potentiel du SPT 100 de décharge de 300 V et un courant d'ion de 3 A pour un diamètre de faisceau de 100 mm.

Un moteur ionique de même diamètre fournit une poussée inférieure à 25 mN pour une tension d'accélération de 1100 V.

Dans le but d'obtenir un rendement élevé, il faut minimiser le courant d'électrons remontant dans le canal, pour cela un champ magnétique radial est appliqué dans le canal.

Le champ magnétique doit obéir à d'autres contraintes : afin de garantir un fonctionnement stable, il doit être maximal dans le plan de sortie du propulseur.

Afin de bien situer l'origine des spécifications de l'installation d'essais, il convient de situer les valeurs des paramètres physiques caractérisant le propulseur.

La densité de neutres en amont de la zone d'ionisation est de  $5.10^{13} \text{ cm}^{-3}$ , en aval de cette zone, elle diminue d'un ordre de grandeur ( $5.10^{12} \text{ cm}^{-3}$ ). La densité ambiante à l'intérieur de la chambre à vide doit donc être inférieure à cette valeur pour simuler l'environnement du propulseur dans l'espace. En effet quand la densité à l'intérieur de la chambre à vide est voisine de celle régnant dans le canal d'accélération, il y a réingestion de neutres de Xénon et augmentation artificielle de la poussée. La pression correspondant à une densité de  $5.10^{12} \text{ cm}^{-3}$  est  $2.10^{-4} \text{ mbar}$  pour le Xénon à 300 K.

Le tableau 3.1 indique les caractéristiques principales du SPT 100.

Tableau 3.1

|                                 |            |
|---------------------------------|------------|
| Poussée nominale                | 80 mN      |
| Impulsion spécifique            | 1560 s     |
| Débit nominal (Xénon)           | 5,4 mg/s   |
| Tension de décharge             | 4,5 A      |
| Courant de décharge             | 300 V      |
| Puissance électrique            | 1350 W     |
| Puissance cinétique du faisceau | 375 W      |
| Induction magnétique maximale   | 0,02 Tesla |
| Diamètre du canal               | 100 mm     |
| Masse                           | 5,5 kg     |

La répartition de l'induction magnétique est l'un des paramètres de fonctionnement important du moteur. L'installation d'essai ne doit donc pas générer d'induction parasite au delà de  $10^{-4}$  Tesla.

#### SPT MK II

Le Pr MOROZOV a remarqué que les caractéristiques du plasma peuvent être améliorées par un réaménagement du profil des lignes de champ magnétique [3] et du dessin du canal d'accélération. Ainsi, il est possible d'obtenir une fonction de répartition des électrons plus favorable ce qui conduit à obtenir des équipotentielles plus proches des lignes de champ [4] donc à une divergence réduite, une diminution de l'érosion ionique (durée de vie augmentée), et une augmentation de l'impulsion spécifique par suppression des ions basse énergie (figure 3.2).

De plus l'amélioration des caractéristiques du plasma permet d'augmenter le potentiel de décharge sans augmentation proportionnelle des pertes thermiques. Il est aussi possible d'augmenter à la fois le rendement et l'impulsion spécifique.

Le tableau 3.2 résume les caractéristiques du modèle de laboratoire conçu selon ce principe.

Tableau 3.2

|                      |          |
|----------------------|----------|
| Poussée nominale     | 80 mN    |
| Débit nominal        | 4,6 ms/s |
| Tension de décharge  | 350 V    |
| Puissance électrique | 1480 N   |
| Diamètre du faisceau | 70 mm    |

#### 4. DESCRIPTION DE L'INSTALLATION NON MODIFIEE

Cette installation a été utilisée pour le développement de propulseur à émission de champ FEED [5] et de propulseurs ioniques bombardement.

La figure 4.1 montre une coupe de l'installation. Le propulseur à émission de champ fonctionne uniquement avec du Césium très pur à l'état liquide. Il est donc nécessaire d'atteindre un vide très poussée ( $10^{-7}$ ,  $10^{-8}$  mbar) en particulier lors du démarrage, cependant il n'est pas utile de disposer de vitesses de pompage importantes.

Le propulseur ionique bombardement consomme de 0,05 à 0,1 mg/s de Xénon. Une vitesse de pompage de 2500 dm<sup>3</sup>/s est suffisante pour maintenir une pression de  $10^{-5}$  à  $2 \cdot 10^{-5}$  mbar.

L'installation utilise une pompe à diffusion de 12000 l/s munie d'une baffle à azote liquide.

Une cible refroidie à l'azote liquide élimine les traces d'huile résiduelles.

La vitesse de pompage utile est de 5000 dm<sup>3</sup>/s pour l'azote de 2400 dm<sup>3</sup>/s pour le Xénon.

Avant tir, le propulseur était maintenu dans un sas de diamètre utile 600 mm évacué par une cryopompe RPK 1500.

Cette disposition autorisait une pression de service de  $5 \cdot 10^{-8}$  mbar dans le sas,  $10^{-7}$  mbar dans la chambre principale (propulseur arrêté) et  $10^{-5}$  mbar en tir avec un débit de Xénon de 0,2 mg/s.

Le jet du propulseur était analysé par un ensemble de 9 sondes de Faraday placées à 1 m du moteur sur un bras en arc de cercle et courant un arc de  $\pm 30^\circ$ . Le bras était mobile en azimut sur  $\pm 30^\circ$ .

Cette installation a été utilisée pour effectuer les essais d'endurance du propulseur à émission de champ (FEED). Pour assurer un fonctionnement automatisé (essais 24 h/24 sans surveillance nocturne), l'ensemble de l'installation a été contrôlée par un calculateur HP 16 relié à deux centrales de mesures HP 3497 dont l'une était isolée de la masse par montage dans une baie à isolation galvanique.

Le HP 16 a été ultérieurement remplacé par un calculateur HP 320 plus puissant.

Il était clair que pour essayer le SPT, il fallait entreprendre des modifications importantes :

- changer la pompe à vide et multiplier la vitesse de pompage par un facteur au moins égal à 10,
- monter une balance de mesure de poussée,
- prévoir de nouvelles alimentations stabilisées adaptées aux caractéristiques du SPT,
- réaliser un nouveau câblage,
- réécrire le logiciel de contrôle.

#### 5. SPECIFICATION DE L'INSTALLATION

##### Pression de fonctionnement

La spécification de pression de fonctionnement est fixée par deux critères :

- la densité de neutres dans la chambre à vide doit être au moins 5 fois plus basse que dans le plan de sortie du propulseur. Cela correspond à  $10^{12}$  cm<sup>-3</sup> soit  $4 \cdot 10^{-5}$  mbar pour le Xénon.

- le libre parcours moyen doit être plus élevé que la distance propulseur/coupes de Faraday de manière à limiter la déformation du faisceau d'ions par les collisions.

La pression correspondant à un libre parcours moyen de 1 m est de  $3,5 \cdot 10^{-5}$  mbar pour le Xénon.

##### Vitesse de pompage

La vitesse de pompage se déduit des exigences de pression de fonctionnement et de contraintes de débit masse liées au propulseur.

Pour un débit masse de 5,4 mg/s (0,96 nccs) la vitesse de pompage doit être :

$$s = \frac{0,96}{3 \cdot 10^{-5}} = 32\,000 \text{ dm}^3/\text{s}$$

pour garantir une pression de  $3 \cdot 10^{-5}$  mbar cela correspond à 68500 dm<sup>3</sup>/s pour l'azote ce qui est au delà de la capacité des pompes commerciales.

##### Capacité d'absorption de la pompe

Les exigences de vide propre conduisent à utiliser des pompes cryogéniques qui ont par définition des capacités d'absorption limitées.

La durée de fonctionnement sans régénération a été fixée à un minimum de 100 heures, cela correspond à une masse de Xénon de 1,94 kg.

### Qualité du vide

L'expérience obtenue en Russie a montré que les remontées d'huile de pompe à diffusion perturbaient d'une manière importante les caractéristiques de la décharge. Il est donc important d'opérer en vide propre. Les pompes turbo moléculaires ayant des vitesses de pompage trop faible, il faut faire appel à des pompes cryogéniques.

### Balance de mesure de poussée

Pour une poussée nominale de 80 mN, il faut pouvoir explorer une plage de poussée de 40 à 120 mN. De plus, afin de pouvoir essayer dans le futur des propulseurs de plus forte poussée, il a été prévu d'étendre la capacité de mesure à 200 mN mais avec une précision moindre.

Pour l'étendue de mesure nominale, la précision de la balance a été spécifiée à  $\pm 2\%$  la répétabilité étant  $\pm 1\%$ .

Ces exigences sont en pratique très sévères car une variation de 1 mN correspond à un centmillième du poids de l'ensemble propulseur + balance ( $\sim 100$  N). Ces balances sont sensibles aux dérives thermiques (y compris les forces parasites générées par le câblage), il est donc essentiel de pouvoir calibrer la balance sous vide.

### Analyse du faisceau d'ions

Le faisceau d'ions est analysé à l'aide de coupes de Faraday et de sondes à potentiel retardé. Ces dernières permettent d'établir la répartition énergétique des ions. Il est alors possible d'effectuer les calculs précis d'érosion ionique due au faisceau. Cela permet aussi de vérifier indirectement les mesures de poussée.

Compte tenu de la puissance importante dissipée par le faisceau, le temps de balayage du bras porte sonde doit être minimisé.

Il a donc été spécifié que les mesures sur les 9 coupes de Faraday devaient être effectuées par acquisition numérique en un seul passage.

### Interface propulseur

L'installation doit être capable d'essayer indifféremment un SPT MK II ou un SPT 100 dont les interfaces mécaniques et électriques sont différentes.

### Contrôle et commande de l'installation

Les alimentations stabilisées ont été définies pour ouvrir des besoins plus larges que ceux du SPT 100 et du SPT MK II.

Les spécifications de ces alimentations sont résumées dans le tableau 5.1

Tableau 5.1

| Fonction            | Tension (V) | Courant (A) |
|---------------------|-------------|-------------|
| Décharge            | $\geq 500$  | $\geq 8$    |
| Courant de bobine 1 | $\geq 10$   | $\geq 10$ A |
| Courant de bobine 2 | $\geq 10$   | $\geq 10$   |
| Courant de bobine 3 | $\geq 10$   | $\geq 10$   |
| Chauffage cathode   | $\geq 15$   | $\geq 15$   |

Il est nécessaire de remplacer le calculateur par un modèle plus puissant pour permettre un pré dépouillement en temps réel et une gestion des nombreuses sécurités à prendre en compte.

## **6. DESCRIPTION DE L'INSTALLATION**

### **6.1 Système de pompage**

Dans tout système à vide poussé, il faut non seulement absorber le gaz émis par le dispositif essayé mais aussi les gaz résiduels (vapeur d'eau, oxygène, azote) et leurs produits de décomposition par le bombardement ionique et électronique (radicaux, ions OH<sup>-</sup>, hydrogène). A cette fin, il faut généralement recourir à plusieurs types de pompes.

Pour éliminer les "gaz permanents" et la vapeur d'eau, deux cryopompes standard RPK 1500 sont utilisées. Elles sont mises en service avant la pompe à Xénon.

Compte tenu de la vitesse de pompage très importante, le diamètre de la pompe Xénon est pratiquement égal à celui de la chambre à vide. Il n'est donc pas possible d'isoler cette pompe par une vanne. Lorsqu'il faut la régénérer, le propulseur est reculé dans le sas et isolé par la vanne tiroir du sas.

Les pompes cryogéniques classiques fonctionnent à 20 K. Pour maintenir un panneau de diamètre 1,4 m à 20 K il faut une puissance réfrigérante (électrique) considérable. On peut diminuer considérablement la taille du cryoréfrigérateur en maintenant l'écran en dessous de 50 K.

La température du baffle est soigneusement régulée afin d'une part de limiter le rayonnement de la chambre sur la paroi à 50 K, d'autre part d'éviter la condensation du Xénon au niveau du baffle ce qui



empêche l'action de la paroi à 50 K mais conduit à une pression de Xénon de quelques  $10^{-3}$  mbar.

Les pompes cryogéniques ne pompent pas l'hydrogène, pour cela un dépôt de titane actif est utilisé. Il n'est pas pour autant nécessaire d'utiliser une pompe à sublimation de titane. Une partie de la cible érodée par les ions est constituée de titane : sous l'effet du bombardement ionique elle fournit le dépôt de titane assurant le pompage de l'hydrogène.

Le schéma des pompes est présenté sur la figure 6.1.

Les pompes sont contrôlées par un automate programmable. Elles peuvent fonctionner jour et nuit sans présence humaine. La conception, la réalisation et l'intégration du système de pompage a été réalisée par Leybold S.A.

#### Description de la chambre à vide

La longueur de la chambre à vide a été augmentée de 30 cm pour introduire la section comportant le baffle refroidi. Il y a une distance de 2,6 m entre le propulseur et le baffle (figure 6.2).

La chambre a subi d'autres modifications mineures : modifications des lignes de pompage primaire et des pompes interjoints.

La pression est mesurée à l'aide de jauges Pirani et Bayard Alpert. Le sas est muni d'un spectromètre de masse quadripolaire BALZERS QMG 64 qui permet de mesurer la composition des gaz résiduels et de détecter une éventuelle contamination du Xénon.

L'installation est placée dans un local climatisé de classe 100 000. Il est ainsi possible d'effectuer des essais de recette sur du matériel de vol sans risque de pollution.

#### Commande et contrôle

Le schéma du sous système de contrôle et commande est présenté figure 6.3.

Le contrôle est assuré par un ordinateur HP 360. Les tableaux et les courbes sont édités par une imprimante laser.

Les centrales de mesure sont des HP 3852 dont une est référencée à la masse, l'autre au potentiel de la cathode.

Un rack de distribution de mesures assure l'ensemble des connexions électriques avec les alimentations électriques, le propulseur et les

centrales de mesure. Ce rack contient aussi le circuit d'amorçage de la décharge et le filtre L.C.R qui assure le découplage entre le propulseur et l'alimentation de décharge.

Les oscillations du courant de décharge sont étudiées à l'aide d'un analyseur de spectre HP 35665A.

#### Balance

Il existe différents concepts permettant de réaliser une balance à faible poussée :

- balance de torsion,
- pendule,
- bras articulé (connu aussi sous le nom de "door hinge"),
- plateau suspendu,
- plate-forme flottante (sur bain de Gallium),
- suspension à paliers magnétiques.

Ces concepts ont pratiquement tous fait l'objet d'applications.

Pour chaque concept précisé, il existe deux variantes :

- balance libre,
- balance asservie en position par un moteur force ou un moteur couple (méthode de zéro).

Les critères de sélection du concept se déduisent aisément des spécifications :

- précision,
- répétabilité,
- possibilité de tirer différents propulseurs sans réglages fastidieux (c'est à dire balance insensible à la position du centre de gravité de l'équipage mobile),
- faible sensibilité à la raideur (et à sa variation) des canalisations de Xénon et du circuit électriques,
- possibilité de calibration sous vide,
- faible sensibilité aux vibrations de l'installation (pompes cryogéniques),
- faible rapport coût/performances.

L'étude de sélection de concept a retenu la balance à plateau suspendu asservie en position.

Cette solution offre la meilleure combinaison de simplicité et de précision. Elle répond à deux des principaux critères de sélection :

- la suspension du plateau le rend insensible à la position du centre de gravité,
- l'asservissement de position permet de s'affranchir des effets de raideur (variable en fonction de la température et de la pression de Xénon) due aux câblages électriques et à l'alimentation en Xénon.

La balance a été étudiée et réalisée par la société Prévention Technologies.

Au cours de la phase d'étude, il a fallu s'attacher à diminuer l'influence des bruits sismiques.

Ces derniers sont essentiellement générés par les moteurs électriques et les pompes cryogéniques. Les fréquences correspondantes sont :

2, 10, 48 et 50 Hz et leur harmoniques. Il fallait éviter une résonance entre ces fréquences et l'une des fréquences propres de la balance ; à cette fin un modèle dynamique de la balance a été établi (figure 6.4) et la balance a été dimensionnée afin d'éliminer toute résonance nuisible.

L'électronique de contrôle est munie d'une sélection de gain qui permet de couvrir trois gammes de mesure :

- 0,40, 0-120, 0-200 mN

Un moteur électrique sous vide permet un réglage fin de l'horizontalité de la balance, ce qui permet d'ajuster le zéro en position de tir sous vide (la mise en station et la mise sous vide engendrent une déformation des supports).

Afin de limiter les dérives thermiques, la balance est protégée par une superisolation multicouches et les matériaux sont appariés en dilatation.

#### Alimentation en Xénon

Le circuit d'alimentation en Xénon a été conçu pour permettre aussi bien l'alimentation du SPT 100 (entrée de Xénon unique et asservissement de débit interne) que le SPT MK II (entrées de Xénon séparées cathode et chambre, régulation de débit par l'installation).

En outre, le circuit d'alimentation doit fournir du Xénon ultrapur. Ceci est particulièrement

important pour la cathode creuse qui est particulièrement sensible à la contamination [6].

Afin d'aboutir à cet objectif, le circuit d'alimentation est entièrement métallique, les vannes sont munies de soufflets et l'ensemble du circuit est vérifié à l'aide d'un détecteur de fuite à hélium.

Le circuit peut être mis sous vide à l'aide d'une pompe primaire munie d'un piège à tamis moléculaire et purgé par circulation d'azote.

Le débit de Xénon est mesuré par deux débitmètres massiques. La figure 6.5 présente le schéma du circuit.

## **7. RESULTATS D'ESSAIS**

### **7.1 Essais de recette de l'installation à vide**

La vitesse de pompage, déduite du rapport du signal de gauge Bayard Alpert corrigé pour le Xénon et du débit masse de Xénon, a pour valeur :

$$S = 29\,000 \text{ l/s}$$

Ceci est en bon accord avec la vitesse calculée au niveau de la pompe (45000 l/s) et de la conductance de la chambre à vide (64000 l/s) ce qui donne une vitesse théorique de 26400 l/s légèrement inférieure à la spécification. La vitesse réelle est très proche de la spécification.

### **7.2 Essais des propulseurs**

Un SPT 100 a été essayé pendant 260 h au régime nominal sans aucun incident. On a pu ainsi vérifier que la pompe pouvait fonctionner sans arrêt ni saturation pendant plus de 100 h et que l'installation pouvait fonctionner sans surveillance durant la nuit.

Les mesures de pousser ont été comparées à celles obtenues au JPL [7] et à la recette effectuée par FAKEL sur ce moteur [8]. Ces essais ont été effectués dans des installations plus vastes et avec des balances de construction différentes. Les vitesses de pompage étant comparables dans les trois cas, les pressions de fonctionnement étaient similaires. Les courbes de la figure 7.1 permettent de constater l'excellent accord entre les résultats.

La figure 7.2 représente un spectre de fréquence des oscillations de courant du SPT 100 et la figure 7.3 une reconstitution tridimensionnelle de la forme du faisceau d'ions après traitement des données fournies par les sondes de Faraday.

La divergence du faisceau calculée à partir de ces données est en bon agrément avec les résultats du JPL et de FAKEL.

La figure 7.4 montre la distribution d'énergie des ions obtenue par le SPT 100 et par le SPT MK II. On remarque que la distribution d'énergie du SPT MK II est plus étroite ce qui reflète l'amélioration de comportement du plasma.

## 8. CONCLUSION

L'installation destinée à effectuer les essais de développement et les essais de recette des propulseurs SPT a atteint les objectifs fixés malgré la difficulté associée aux différentes spécifications dans le domaine du vide, de la précision de mesure de poussée et du contrôle automatique.

Cela montre qu'il est possible d'effectuer des essais représentatifs dans une chambre à vide de dimensions modérées et avec un investissement limité.

Cette installation est utilisée pour les essais de développement du SPT MK II et les essais système du SPT 100. Elle sera utilisée pour les essais des modèles d'ingénierie et de qualification du SPT MK II puis pour les essais de recette des modèles de vol.

## REFERENCES

- [1] Morozov A.L  
Doklady Akademii Nauk SSSR  
1965, 163 N° 6 P1313-1366
- [2] Artsimovitch L.A et Al  
Kosmicheskoe Issledovanie,  
1974, 12 N° 3, p451, 468
- [3] IEPC 93.101 Stationary Plasma Thruster  
(SPT) développement steps and future  
perspective  
A.I MOROZOV  
23 rd International Electric Propulsion  
Conference Seattle - Sept 13-16 1993
- [4] IEPC 93-223 - Development status of the SPT  
MK II thruster  
D. Valentian  
23rd International Electric Propulsion  
Conference Seattle, Sept 13,16 1993
- [5] IAF 84.382 : Endurance Testing of Field  
Emission Thruster  
D.Valentian, J.P.Bugeat, J.Macaigne,  
C.Bartoli  
34th IAF Congress Lausanne Oct 1984
- [6] IEPC 93.020 - Extended test of a xenon  
hollow cathode for a Space Plasma Contactor  
T.R. Sarver - Verhey  
23rd International Electric Propulsion  
Conference Seattle, Sept 13,16 1993
- [7] AIAA 94.2856 - Cyclic Endurance Test of a  
SPT 100  
Stationary Plasma Thruster  
C. Garner, J. Polk and J. Brophy  
30 th Joint Propulsion Conference - July 1994  
Indianapolis
- [8] AIAA 94.2854 - SPT 100 Module Lifetime  
tests results  
B. Arkhipov, R. Gnizdor, V. Kim,  
K. Kozubsky, N. Maslennikov, T. Randolph,  
W. Rogers and M. Day  
30 th Joint Propulsion Conference - July 1994  
Indianapolis

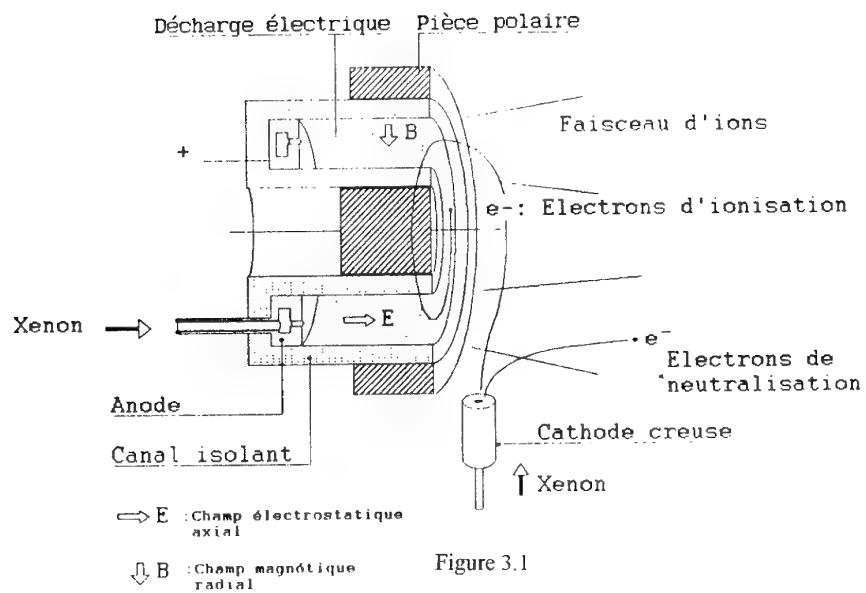


Figure 3.1

Schéma de principe du SPT

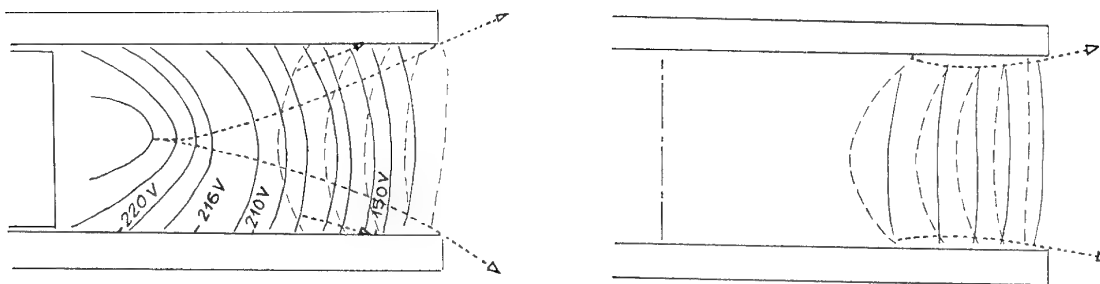


Figure 3.2

Comparaison des équipotentiels SPT - SPT MK II

- Equipotentielle
- - - Lignes de force magnétique
- ..... Trajectoires des ions

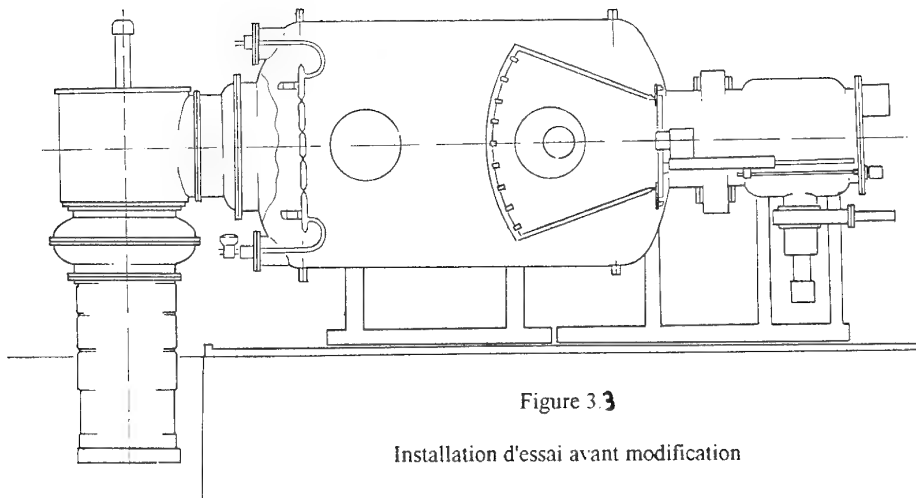


Figure 3.3

Installation d'essai avant modification

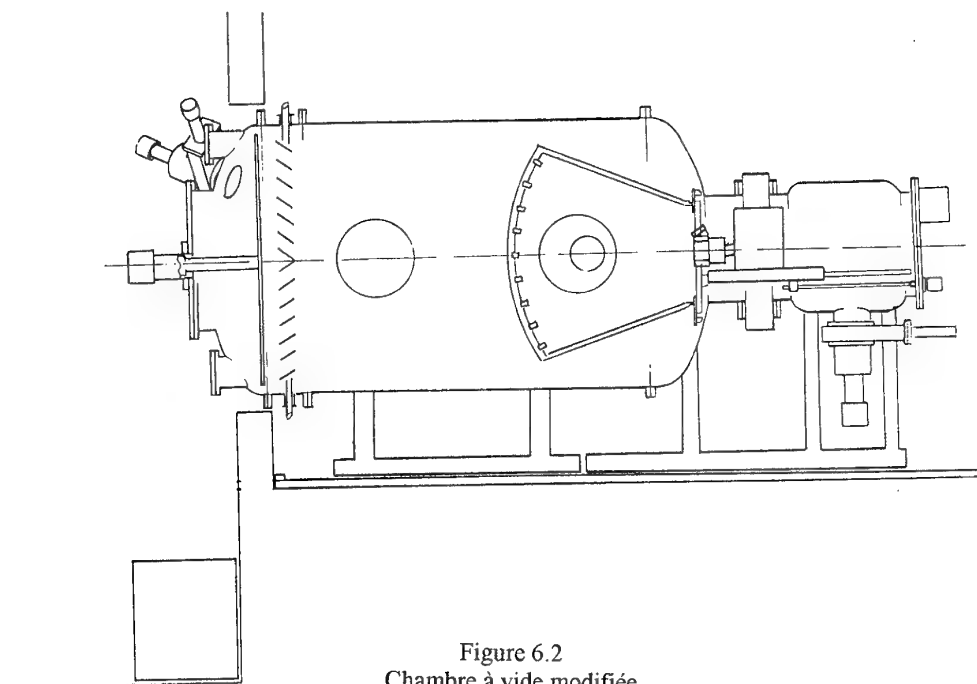


Figure 6.2  
Chambre à vide modifiée

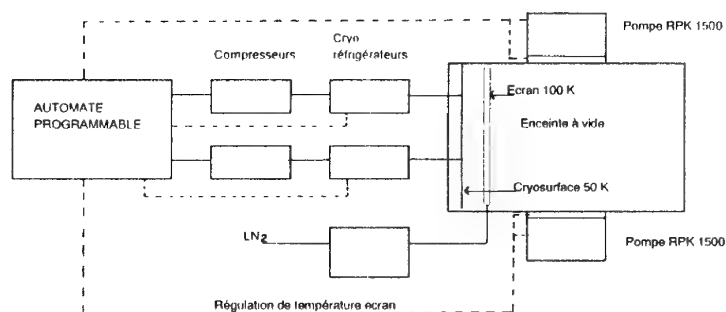


Figure 6.1  
Schéma des pompes cryogéniques

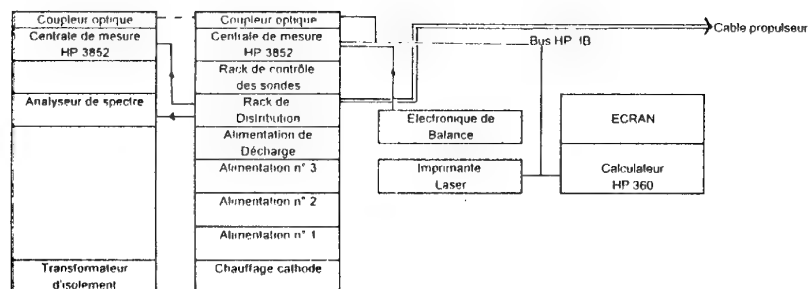


Figure 6.3  
Système de contrôle et de commande

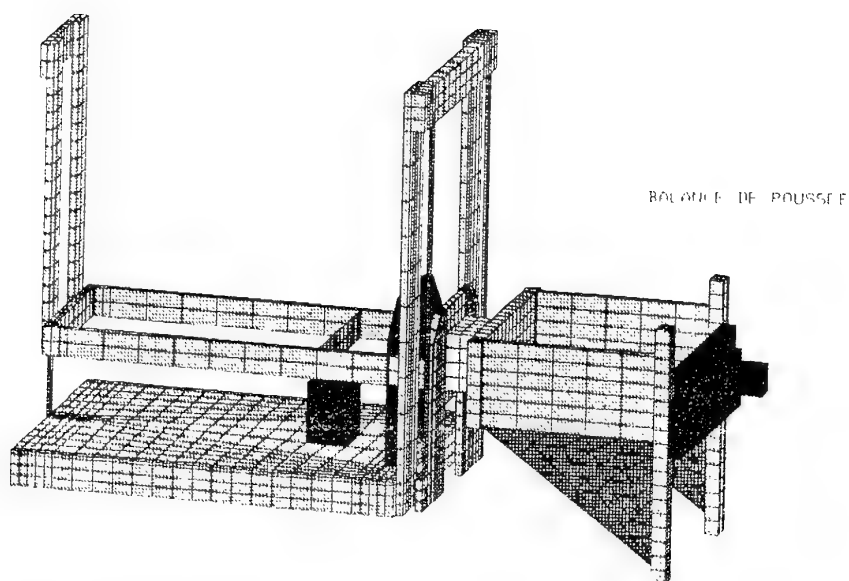


Figure 6.4  
Modèle dynamique de la balance

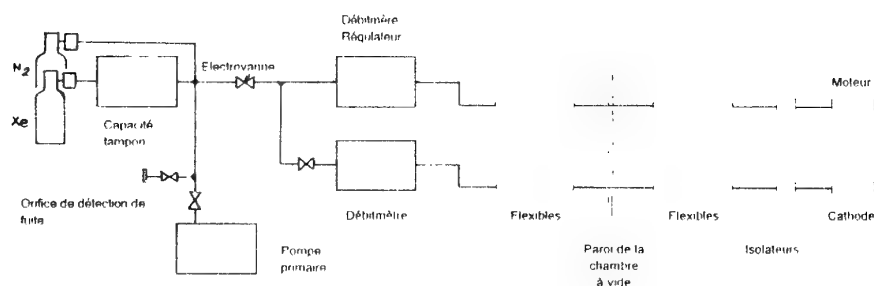
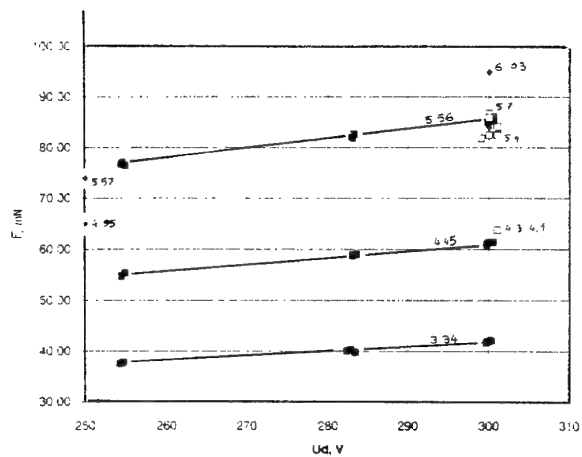


FIGURE 6.5  
SCHEMA BLOC CIRCUIT D'ALIMENTATION EN XENON

FIGURE 7.1  
POUSSEE DU SPT EN FONCTION DE LA TENSION  
D'ACCELERATION ET DU DEBIT



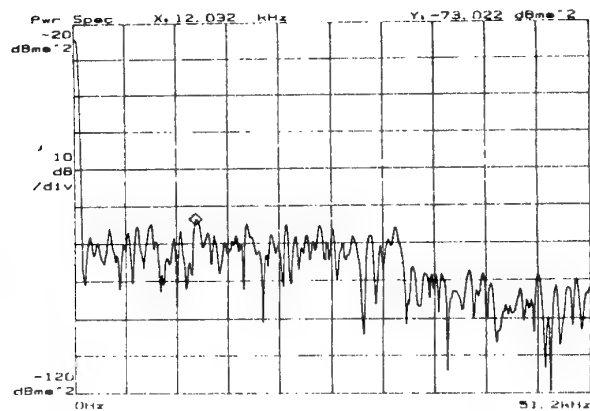


FIGURE 7.2  
ANALYSE EN FREQUENCE DES OSCILLATIONS  
DU COURANT DE DECHARGE

SPT 100  $U_d=300$  V Debit = 5 mg/s

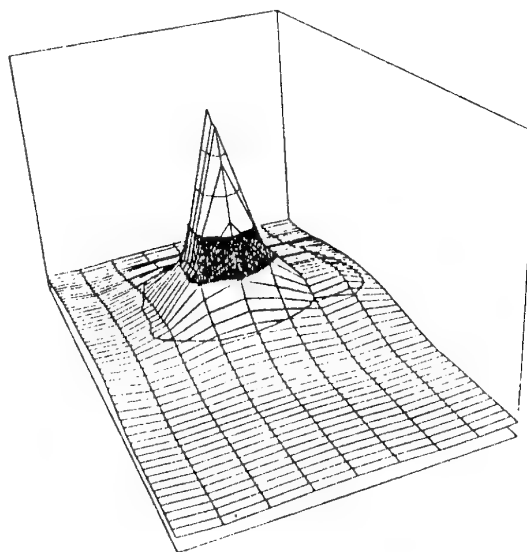
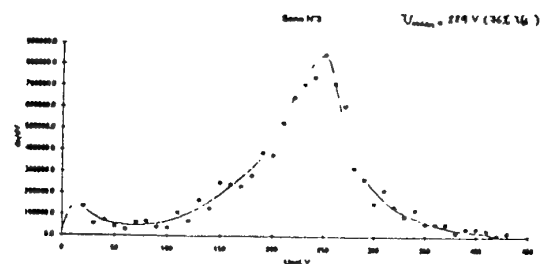


FIGURE 7.3  
DIVERGENCE DU FAISCEAU DU SPT 1000

SPT 100



MARK 2

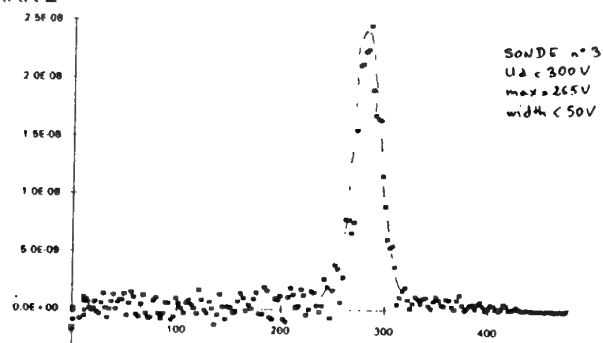


FIGURE 7.4  
DISTRIBUTION D'ENERGIE DES IONS

# Development of a Modal Testing Support System for Space-Based Radar Satellite Structures

D. J. McTavish

Dynacon Enterprises Ltd.  
5050 Dufferin St., Suite 222,  
Downsview, Ontario,  
Canada M3H 5T5

G. B. Sincarsin

University of Toronto  
Institute for Aerospace Studies  
4925 Dufferin St.,  
Downsview, Ontario,  
Canada M3H 5T6

Y. Soucy

Canadian Space Agency  
6767 route de l'Aéroport,  
St-Hubert, Québec,  
Canada J3Y 8Y9

## Summary

The development of a modal testing support system (MTSS) for the Canadian Department of National Defence (DND) is described. The MTSS consists of both hardware and software elements which will augment existing testing facilities of the Canadian Space Agency. A critical capability of the MTSS is the ability to deal methodically with structures so large and flexible that they are unable to properly support their own weight in a 1-g environment. The structures of the envisioned space-based radar (SBR) satellites fall into this class. The performance of such a surveillance system depends upon satisfactory structural dynamic response of the spacecraft, among other factors. The output of the modal testing process is an experimentally validated structural model which becomes a valuable tool for predicting dynamic behavior. To support the validation of this system, a number of test structures are being produced which will emulate the structural behavior of a generic SBR mechanical system.

## 1 INTRODUCTION

### 1.1 Project Overview

As part of the Canadian Department of National Defence's Space-Based Radar Project, a technique for ground-based structural dynamics testing of large flexible space structures is being investigated. This investigation includes the construction of a proof-of-principle demonstration of a facility capable of performing such tests. The contributions to that facility, constructed and validated under this contract, are referred to as the Modal Test Support System or MTSS. The MTSS will be integrated with the existing systems at the Canadian Space Agency's David Florida Laboratory (DFL) to provide the facility.

The prime contractor for this project is Dynacon Enterprises Ltd. of Toronto, Canada. Dynacon is producing the software segment of the MTSS along with collection of test-article structures which will be used as a testbed to validate the system. Spar Aerospace Ltd. of Canada, through its Systems AIT Operations in Ottawa, is providing the hardware segment of the MTSS as a subcontractor to Dynacon. The David Florida Laboratory is located just outside Ottawa, Canada.

### 1.2 Project Status

At the time of writing this paper, the MTSS project has entered its *Fabrication and Coding Phase*, following a Critical Design Review in July 1994. During this time, all elements of the system will be produced. A Final Design Review will mark the end of the fabrication phase, and will be followed by an extensive testing program scheduled to begin around January 1995.

tered its *Fabrication and Coding Phase*, following a Critical Design Review in July 1994. During this time, all elements of the system will be produced. A Final Design Review will mark the end of the fabrication phase, and will be followed by an extensive testing program scheduled to begin around January 1995.

### 1.3 Challenges of Flexible Structures Testing

Ground-based dynamics testing of large space structures (LSS) is a difficult problem, as many of these structures are so flexible (i.e., large *flexible* space structures, or LFSS) that they cannot support their own weight in the Earth's gravitational field (1-g) without severely distorting, buckling, yielding or even breaking. For SBR testing, owing to size alone (see Figure 1) which may be several tens of meters, conventional testing of the entire system in its deployed state becomes impractical. The MTSS is a testing tool which addresses these problems.

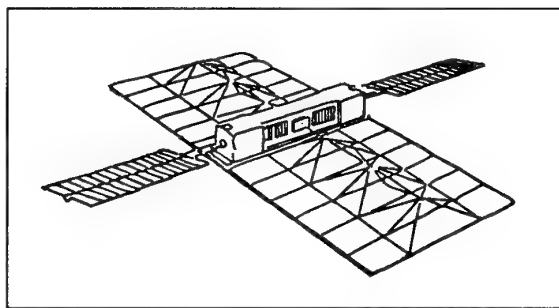


Figure 1: Corporate-Fed SBR Satellite Concept

Testing separate satellite substructures where required is part of the MTSS methodology. The structural performance of the entire satellite is then predicted by a model that is an assemblage of test-validated substructure models. Another feature of the MTSS is the utilization of the multiple boundary-condition testing (MBCT) approach (see next section) wherein the self-support problem inherent in LFSS is handled by the introduction of hard support points to normally unrestrained locations on the test article. Together with existing DFL systems the MTSS will provide all the hardware and software components necessary to conduct comprehensive LFSS dynamics testing.



### 1.4 Multiple Boundary-Condition Testing (MBCT)

The MTSS System is a comprehensive application of the multiple boundary-condition testing (MBCT) approach developed by Wada et al. [1] during the 1980's at the Jet Propulsion Laboratory as a practical approach to ground-based dynamics testing of large flexible space structures. The justification for the MBCT approach is, briefly, as follows.

The near-zero gravity conditions of orbiting space systems, allow the operation of large mechanical structures ranging from antenna reflectors and solar arrays to the radar surfaces of space-based radar. Mass and size restrictions related to launch lead to very lightweight, deployable structural subsystems which are exceptionally flexible. Such structures will often be unable to support their own weight in terrestrial gravity (according to their nominal on-orbit boundary conditions) to the extent that they may collapse or be sufficiently pre-stressed and/or deformed that their dynamic behavior will be too far removed from the domain of zero-gravity conditions and the modeling thereof.

Conventional modal testing generally attempts to maintain the structure under test in a single simple configuration, usually emulating the operational configuration. Thus, stowed spacecraft systems are often fixed to a solid-base which may be 'driven' to represent launch conditions, while deployed substructures may be held cantilevered either attached to the spacecraft bus or separately. As an alternative, some substructures may be supported by special means in a simulation of 'free-free' boundary conditions. In the latter case, some means of physical support is certainly required, while the inability to support self-weight must be compensated for in the case of cantilevered substructures. Especially when the exercise is one of finite-element model verification or updating, the provision of support while maintaining freedom of motion can be difficult. Efforts in this regard include both active and passive means of low-frequency overhead suspension, air-bearings (constrained motion), and so on. Inevitably, there is dynamic coupling between these moving support systems and the structure under test. Generally, as the test article becomes larger, more flexible and more needing of weight relief, such efforts become increasingly costly and overly intrusive in the test environment.

In the MBCT approach, the structure under test is deliberately restrained at a number of points. For highly flexible structures, these points serve also as needed support points. The structure is then modal-tested over some of its area, generally only a subarea of the whole. A number of these modal tests are performed with the structure supported in various support configurations and with different areas of the structure excited. The restraint (or ground) points may be designed such that they are effectively immobile, can be considered as such, and hence do not unduly interfere with the behavior of the test article.

The MBCT is inherently a *model-based* procedure. The data acquired from the separate tests performed on various configurations of the structure are compared against a *common* model (manipulated appropriately for each configuration). It is assumed here that a complete finite-element model of the test article is used, and that the boundary conditions of each

tested configuration are easily obtained in the model through simple coordinate restraints. The test data, then, may be used as a verification of the model, or, as in case of the MTSS, be used to update the model. In the end, the product of the MBCT exercise is an improved structural model which can be used to characterize the general behavior of the structure, or can be integrated with other models to predict ultimately the dynamics of the complete spacecraft system.

The practical advantages of this approach include:

- Fragile structures are less likely damaged—collapse under self-weight is avoided and the possibility of test-load induced failure is lessened.
- Self-weight is supported—preloading due to self-weight is reduced to levels more similar to those on-orbit.
- Structure boundary-conditions are well understood—questionable soft-support systems (often expensive) are avoided.
- Test-frequency bandwidth is raised—often makes the use of conventional facilities (data acquisition, accelerometers, etc.) more applicable for these otherwise very low-frequency structures.

Some key disadvantages of MBCT are that the structure is not necessarily tested in its nominal on-orbit configuration (which is desirable) and the frequency ranges of structural responses will be generally higher than on-orbit raising the concerns that nonlinear, or rate-dependent mechanical processes may be activated differently. The approach is intended, however, for those structures where traditional methods are impractical or impossible for ground-based testing. The use of MBCT testing obviously does not preclude other tests from being performed.

In principle, the modal data collected during MBCT testing could be augmented by data from static stiffness tests and even mass properties tests, and processed *en masse* to verify and/or update a structural model. While this is a good idea, the scope of the current MTSS project is limited to the processing of modal data only.

## 2 MTSS SYSTEM DESCRIPTION

### 2.1 Overview

The MTSS includes both the mechanical and software elements which when integrated with existing DFL apparatus and other general analysis software provide the capability to perform modal testing of highly flexible structures and the generation of accurate finite-element models [2]. This capability will be demonstrated via a Proof of Principle (PoP) demonstration utilizing Large Space Structure Test Articles (LSS-TAs) which emulate the self-support and dynamic characteristics expected with the large structures of SBR satellites. Figure 2 provides a conceptual overview of the MTSS and associated systems, with major subsystems and interfaces identified.

The MTSS *system* consists of both a hardware segment and a software segment. These are the *Test-Articles Support Fixtures* subsystem and the *MTSS Software* subsystem respectively, as highlighted in Figure 3. These subsystems are described in the following sections.

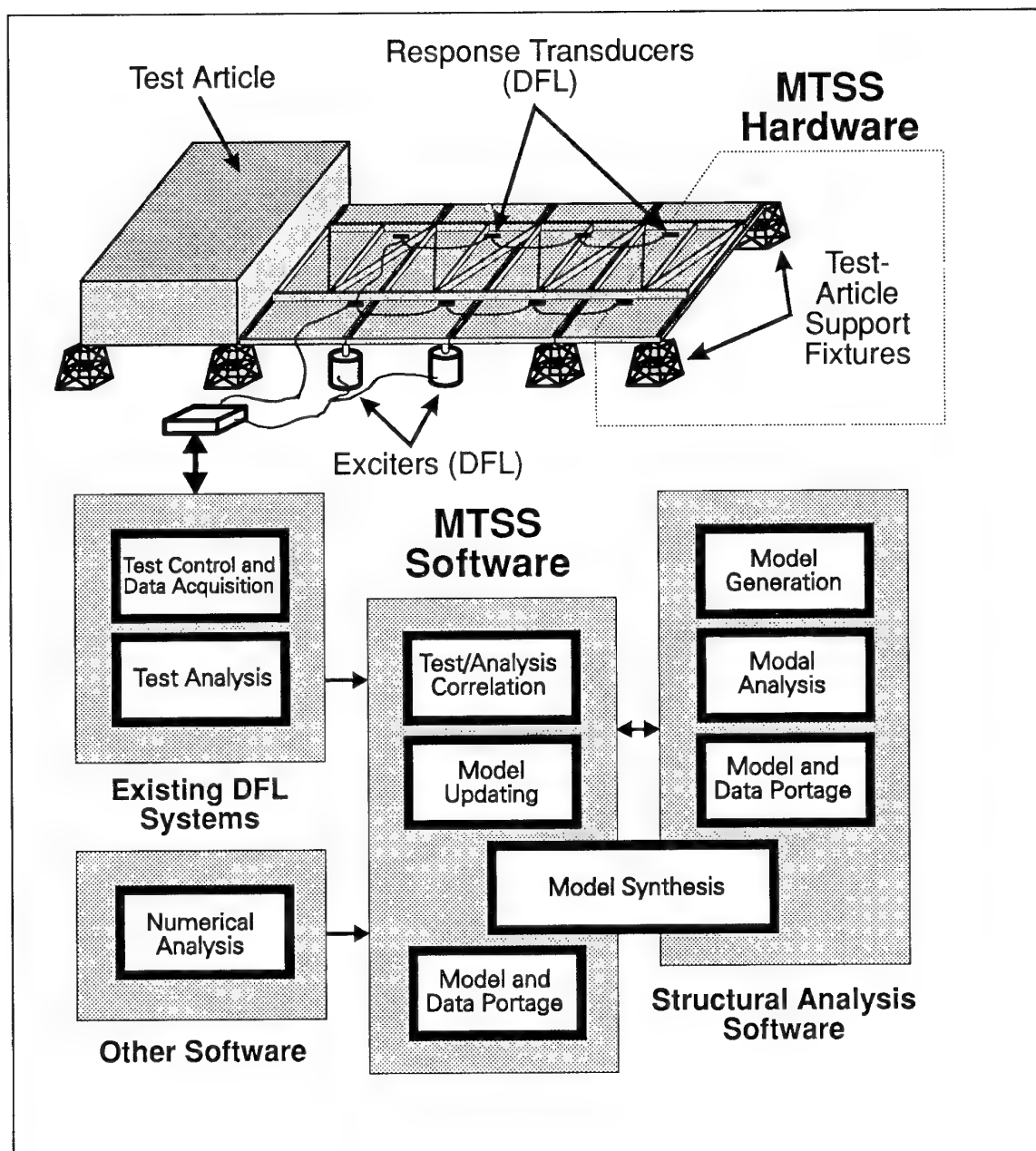


Figure 2: MTSS and Associated Systems Overview

## 2.2 Test-Article Support Fixtures

The hardware segment of the MTSS consists of a system for providing physical support to flexible structures undergoing dynamics testing. In particular, the MTSS Hardware is designed for use with the *LSS Test Articles* testbed developed expressly for the MTSS project. The hardware design is relatively general and modular so that it can be used with other spacecraft structures.

The fixtures consist of a series of modular structures that support the test articles from below. The heights of these fixtures are dependent upon the need for adequate access below the TAs for personnel and for the modal exciters. The modules are based upon an incremental height of 12" (0.305 m) with

the test articles to be nominally held at 36" (0.91 m) off the floor.

The Support Fixture subsystem consists of sets of three different components as follows:

- A *Tapered Frame* component constructed from welded steel square tube (See Figure 4), which is bolted on top of the *Extension Frame* component. The top of the tapered frame incorporates a connection point for the test article. The tapered frame can also attach directly to the Base Rails.
- An *Extension Frame* component constructed from welded steel tubing (see Figure 5), which is bolted on

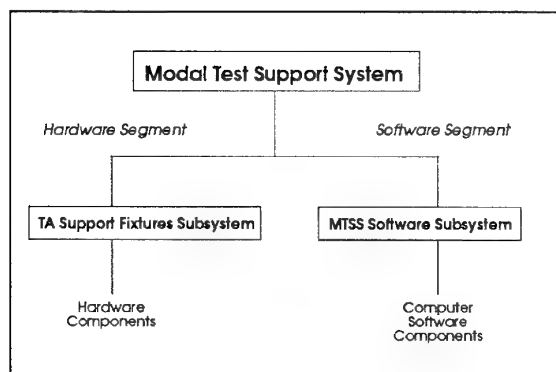


**Figure 3:** The MTSS System

to the Base Rail components. The extension frames also allow attachment to each other when stacked.

- A *Base Rail* component which forms the interface between the frame components and the seismic mass modal platform of the DFL facility. Each piece is composed of two identical aluminum-alloy, slotted, rectangular members for direct attachment to the seismic block. (See Figure 6.)

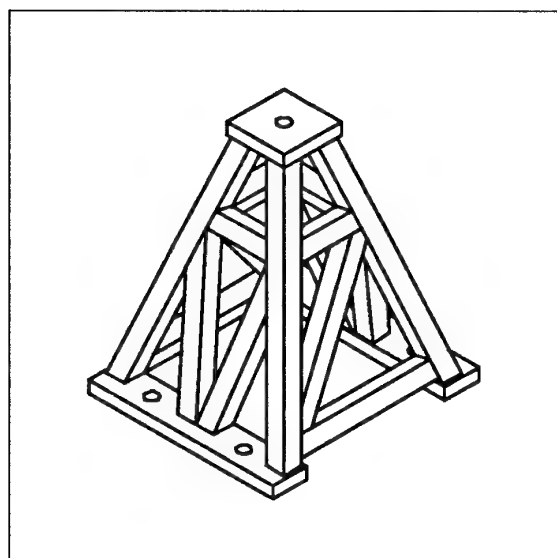


**Figure 4:** Support Fixture Tapered-Frame Module

A nominal configuration consists of a tapered frame mounted atop an extension frame for a height of 36" (0.91 m). Figure 7 is an illustration of a test article mounted on the support fixtures (not an actual test configuration). The Support Fixtures are extremely stiff and quite heavy—the noted nominal configuration weighs 165 lb (mass 75 kg). The unloaded natural frequencies and translational flexibility of this Support Fixture configuration are provided in Tables 1 and 2.

### 2.3 Model-Processing Software

The MTSS Software is a sophisticated menu-driven computer program with a variety of features for MBCT data management, finite-element model enhancement (updating), and eigen-

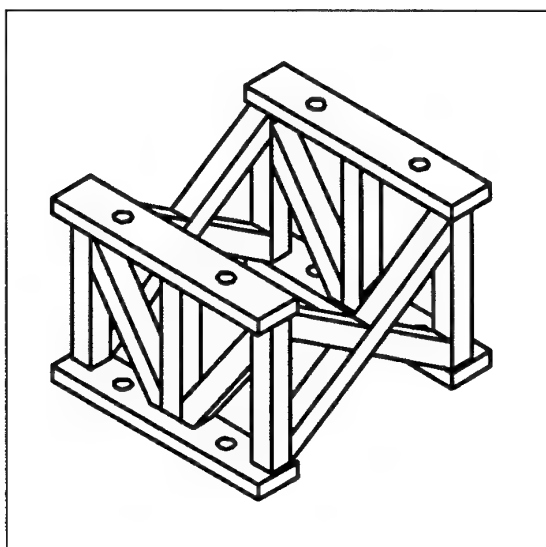


**Figure 5:** Support Fixture Extension-Frame Module

**Table 1:** Natural Frequencies with No Vertical Load

| Mode | Frequency (Hz) |
|------|----------------|
| 1st  | 296.0          |
| 2nd  | 393.6          |
| 3rd  | 588.5          |
| 4th  | 715.0          |
| 5th  | 744.9          |

analysis including model and mode-shape plotting. The conceptual architecture for the MTSS Software is shown in Figure 8. The various software components are organized in groups:

- *Control Software* which governs the interaction between the graphical user-interface and the rest of the MTSS software.
- *Interface Software* which maintains data transfer between the MTSS software and external systems.
- *Task Software* which are the core computational routines of the software, that process data and perform numerical algorithms.
- *GUI (Graphical User Interface) Software* which is a library of routines which control the terminal display and

**Table 2:** Translational Flexibility — Deflection with 1 lb Force Applied in Sequence Along +X, +Y and -Z (vertical) Axes

| Deflection        | Force Direction          |                        |                         |
|-------------------|--------------------------|------------------------|-------------------------|
|                   | +X                       | +Y                     | +Z                      |
| $\delta_x$ [in.]  | $4.435 \times 10^{-6}$   | $1.852 \times 10^{-7}$ | 0                       |
| $\delta_y$ [in.]  | $1.852 \times 10^{-7}$   | $2.623 \times 10^{-6}$ | 0                       |
| $\delta_z$ [in.]  | 0                        | 0                      | $-3.747 \times 10^{-7}$ |
| $\theta_x$ [deg.] | $1.389 \times 10^{-6}$   | $3.193 \times 10^{-6}$ | 0                       |
| $\theta_y$ [deg.] | $-6.972 \times 10^{-8}$  | $6.352 \times 10^{-7}$ | 0                       |
| $\theta_z$ [deg.] | $-2.941 \times 10^{-12}$ | 0                      | $4.166 \times 10^{-7}$  |

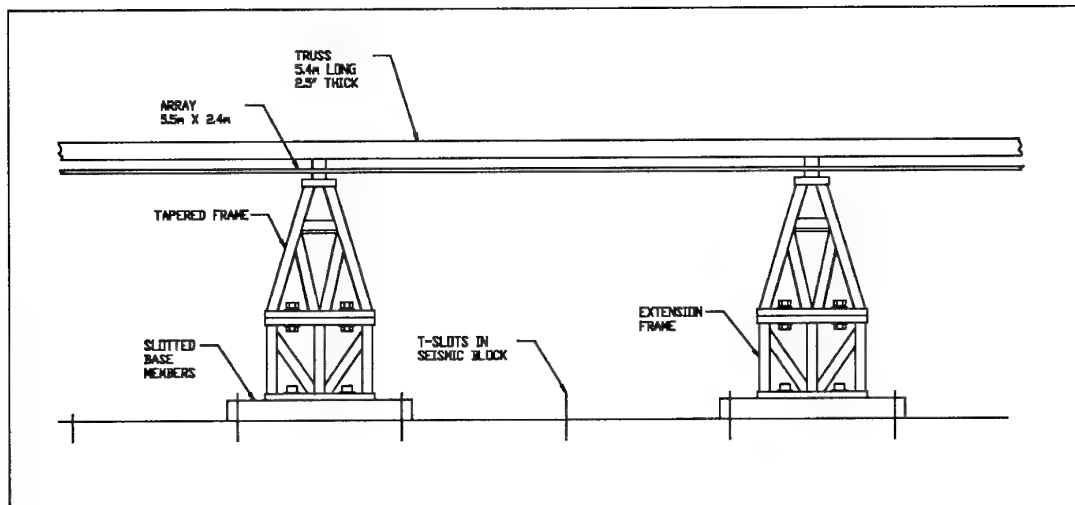


Figure 7: Test Article Support Concept (TA-3 Truss-Array combination shown)

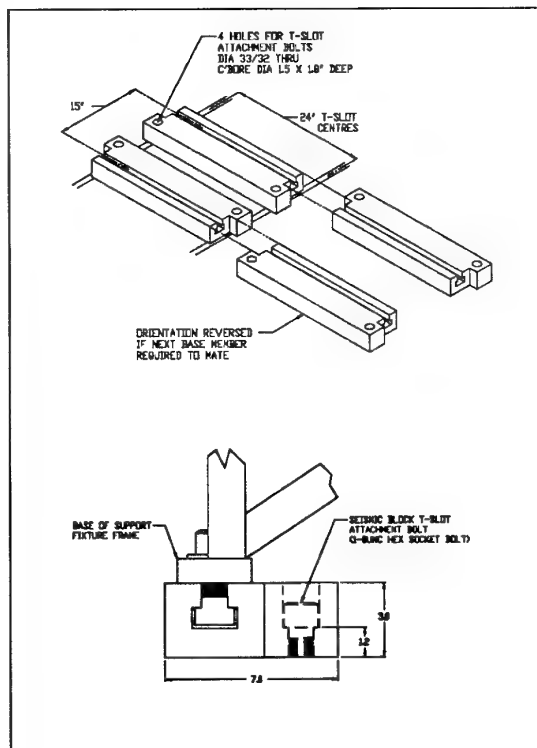


Figure 6: Support Fixture Base

handle user I/O.

Please refer to the Appendix A for nomenclature and information on structural modeling, modal analysis and model synthesis relevant to the methods of MBCT and the MTSS Software.

### 2.3.1 Environment and User Interface

The MTSS Software makes use of a menu-driven graphical user-interface (developed by Dynacon) which is a package of driver routines for the popular X-Windows "X-11" display-graphics library. The entire MTSS Software is intended to

work within the UNIX operating system, with the aforementioned X-Windows library available, presumably installed on an engineering computer workstation. The eventual platform for the MTSS Software is a Hewlett-Packard Series 9000 computer workstation which resides at the David Florida Laboratory (DFL).

### 2.3.2 External Interfaces

As indicated in Figure 2, the MTSS System, the software in particular, must rely on external systems to provide and/or receive data. The following external systems are of key importance:

- *Test Control, Data Acquisition and Analysis.*

The existing modal-test/analysis facilities at DFL will be used to conduct the MBCT tests and process single-configuration test data.

- *Structural Analysis Software.*

Established finite-element software will be used to provide the initial structural models for the test articles as well as to perform the synthesis of post-updated models.

The MTSS Software post-processes modal-test and model data, and thus does not require any real-time or on-line connection with the noted external systems. For maximum portability and simplicity then, ASCII-format *neutral files* are to buffer data between the MTSS and other systems. Such data files are easily moved over network connections or by floppy disk.

The primary system in place at DFL for modal-test/analysis is a "CADA-X" system from LMS (Leuven Measurement Systems). For each test configuration of a particular test article studied, this system is used to conduct the test and then process the test data (generally frequency-response functions) to obtain modal parameter estimates, namely frequencies, damping and mode shapes. This data then must be provided to the MTSS software. The resident "Universal File" (ASCII format) export capability of the LMS CADA-X system is used to this end.

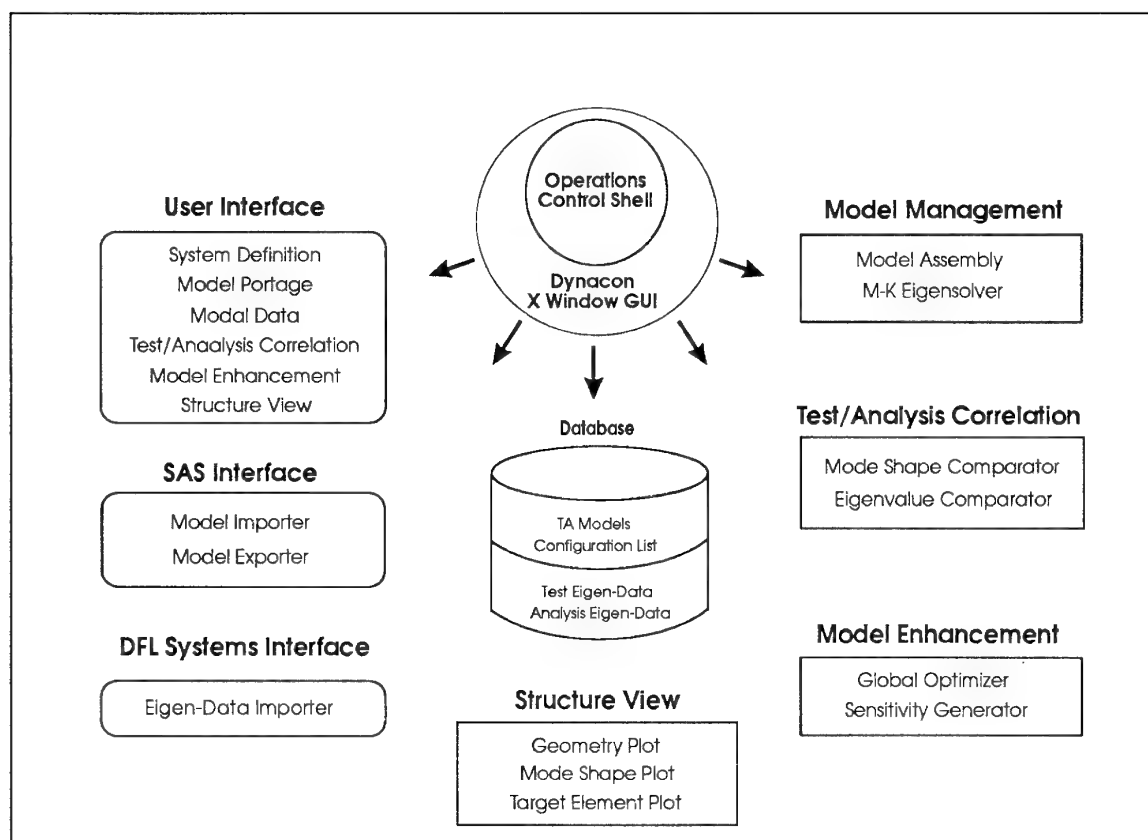


Figure 8: MTSS Software Architecture

Structural-model information including grid-point information, element connectivity, and element matrices are imported into the MTSS Software through ASCII files of a predefined neutral format. This allows the MTSS user to employ the structural modeling/analysis software of his choice so long as model output capability is present. For the current project, MSC/NASTRAN is being used to develop finite-element models. Through NASTRAN's "DMAP" capability, model information is output to a binary-format file. A post-processing program (using subroutines provided by MSC) is then used to decode the NASTRAN output file and to create the portable ASCII file required by the MTSS.

### 2.3.3 Model Definition and Optimization

The MTSS Software accepts the test-article structural model as a collection of individual element mass ( $\mathbf{M}_i^e$ ) and stiffness ( $\mathbf{K}_i^e$ ) contributions (subscripted for the  $i$ -th element):

$$\mathbf{M} = \sum_i \mathbf{M}_i^e \quad \mathbf{K} = \sum_i \mathbf{K}_i^e \quad (1)$$

A parameter is then associated with each of these element matrices as a scale factor:

$$\mathbf{M} = \sum_i m_i \mathbf{M}_i^e \quad \mathbf{K} = \sum_i k_i \mathbf{K}_i^e \quad (2)$$

where, initially these element parameters are all set to unity ( $m_i = k_i = 1$ ). This defines the *initial model* for the test article.

Traditionally, model updating is accomplished through the adjustment of certain model parameters from their initial values. Two extremes in this regard, representing a trade-off between mathematical efficiency and realism, are:

- The arbitrary modification of the global mass and/or stiffness matrix entries after finite-element model assembly, and
- The adjustment of physical structural and material properties (e.g., plate thickness, Poisson's ratio, etc.) prior to model assembly.

See the discussion in Appendix A for more information. The MTSS Software takes an intermediate approach to model updating. The element scaling parameters  $\{m_i, k_i\}$  (or, more precisely, user-defined combinations of them) are taken as the adjustable model parameters:

- The use of element-scaling parameters preserves the algebraic structure of the mass and stiffness matrices describing the test-article, consistent with the objective of retaining physical-correctness through the MBCT-based updating process and in the final updated finite-element model (see Appendix A).
- Macro element* parameters, denoted  $\alpha_j$  and  $\beta_j$  for macro mass and stiffness parameters respectively, are employed which allows the user to group element-scaling parameter changes together (nonexclusively). In this way, the

contributions of similar elements can be subject to adjustment simultaneously.

- The matrix-eigensystem perturbations remain linear with respect to parameter changes for algorithmic convenience.

The initial modeling of the test article is assumed to be 'correct' with respect to element definition and connectivity, and 'adequate' with respect to grid-point quantity and arrangement. The purpose of the MTSS model updating process is to *enhance* a finite-element model rather than to correct an improperly formulated one. If an initial finite-element model is indeed seriously flawed, the exercise of MBCT and the MTSS-updating process may help to indicate and localize the problem, but should not be expected to fix it. In such cases, the model should be reformulated, correcting deficiencies, and then resubmitted to the updating process.

An apparent disadvantage to the element-scaling approach, is the fact that many structural finite-elements combine, in a single element matrix, different elastic behaviors. For example, a typical three-dimensional beam element will combine lateral flexure and longitudinal torsion. These two behaviors involve different material moduli and section properties. Varying these properties simultaneously may be both unrealistic and counter-productive. In cases where the separation of stiffness characteristics, which would normally be packaged in a single element-matrix, is desirable, it is suggested that overlaid 'subelements' be used that isolate the targeted behaviors one at a time. These subelements then would appear as separate scaleable elements to the MTSS Software.

The model updating is driven by reducing the difference between model-predicted and test-observed *modal* parameters on a configuration-by-configuration basis following the MBCT approach. These modal parameters include both frequencies and mode shapes. The user selects which test modes correspond to which model modes. Their correlation is then optimized during the model updating process. The proposed objective function, subject to minimization, is defined to be

$$F = \sum_i [-\omega_i^2(\alpha, \beta) - \lambda_i^2]^H [-\omega_i^2(\alpha, \beta) - \lambda_i^2] w_{\omega^2 i} + \sum_i [S_i e_i(\alpha, \beta) - \phi_i]^H [S_i e_i(\alpha, \beta) - \phi_i] w_{e i} + \alpha^T W_\alpha \alpha + \beta^T W_\beta \beta \quad (3)$$

where  $\alpha$  and  $\beta$  are vectors of the model macro-parameters and the  $\{\omega_i, e_i, \lambda_i, \phi_i\}$  are the predicted and test-observed modal parameters as described in Appendix A. The superscript 'H' denotes conjugate transpose of a matrix. The  $S_i$  are selection matrices which reduce the generally larger-dimension predicted mode-shape down to the test-recorded mode-shape coordinates assumed to be a subset of the former. The  $w_{\omega^2 i}$  and  $w_{e i}$  are scalar weights associated with the user's confidence in the modal parameter correlations.  $W_\alpha$  and  $W_\beta$  are diagonal weighting matrices reflecting the user's confidence in the associated structural parameters.

The following points are noted:

- The modal parameter summations in Equation 3 include relevant modes from all MBCT test configurations.

- The MTSS manipulates mass and stiffness matrices only, performing "normal modes" analysis (see Appendix A). Consequently, the modal parameters produced involve pure frequencies  $\omega_i$  and real-valued mode-shapes  $e_i$ .
- The test-data is free to be complex-valued (damping) as produced by whatever modal parameter estimation technique is employed.
- Comparable physical scaling is assumed for both the predicted and test-observed mode shapes.
- Inclusion of the structural model parameter changes is based on the premise that the initial model does not contain serious errors which would lead to bias through the updating cycle.
- Any of the weights may be set to zero, effectively eliminating constraints on the solution process.

The analytically-produced modal parameters are a nonlinear function of the set of selected macro element parameters, thus the function  $F$  defined in Equation 3 is a nonlinear function. A solution algorithm developed by Davison and Wong [3] is used to perform the optimization. This algorithm is of the "conjugate-gradient" type offering greater robustness through multi-direction searching (through parameter space) than the simpler single-direction search procedures such as the "steepest descent" method.

### 3 TESTBED DESCRIPTION

#### 3.1 Test-Article Structures

Four Test-Article Structures (TASs) are being built which are representative of the substructures of an SBR satellite, with respect to self-supportability and modal characteristics [4]. They are identified by the letters A-D, illustrated in Figure 9, and described briefly here.

##### Structure A: Array Support Truss

This is a beam-like truss structure. Physically, the structure represents a stiffening support-structure which would form the backbone of a corporate-fed radar array. The overall dimensions are approximately  $5.5 \times 1.0$  m. This structure is designed to operate in both a linear and nonlinear configuration through the incorporation of a controllable gap in one of its joints.

##### Structure B: Planar Array

This structure is a planar array-like structure with an aspect ratio low enough that it can be classed as two-dimensional. Size is approximately  $5.5 \times 2.5$  m. Structure B is intended to represent the antenna surface of a corporate-fed SBR spacecraft.

Structures A and B are designed to be mated as structural *components* to form a "truss-array" resembling the radar-array assembly of a corporate-fed SBR spacecraft (see next section for illustration).

##### Structure C: Bus

In contrast to Structures A and B, this structure is quite stiff. Structure C is intended to represent a spacecraft

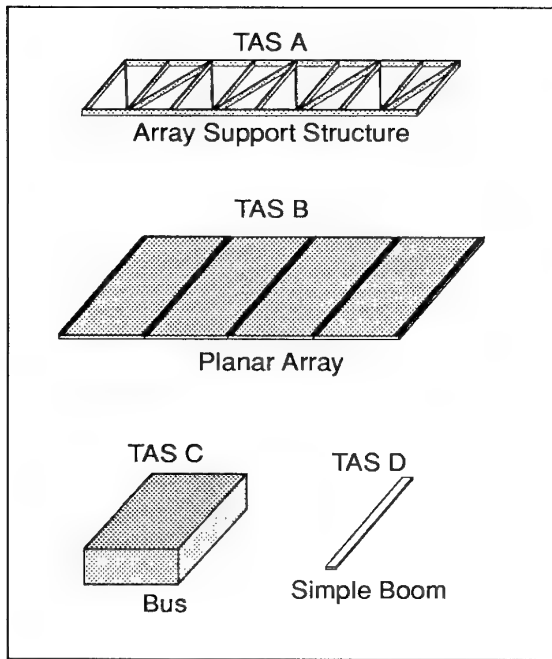


Figure 9: Test-Article Structures

bus. The outside dimensions of this box-like structure are 2.5 by 1.5 × 0.6 m.

#### Structure D: Simple Boom Appendage

This boom-like structure serves a dual role. First, the simple form of this structure will allow for *high-confidence* validation of basic MTSS operation. Second, this structure is used to emulate a simple spacecraft appendage. The length of this structure is about 2.7 m.

Three of these structures (A, B and D) are *highly* flexible. While these are scaled-down in size from their SBR counterparts, their capacity for self-support (in 1 *g*) and their modal characteristics are designed to represent those of large flexible space structures. Table 3 summarizes the degree to which these characteristics are realized in the design. The information is based on cantilever restraint, nominal orientation, and linear finite-element analysis with no self-weight preloading for natural frequencies.

Table 3: Characteristics of Test-Article Structures

| Structure         | Maximum Deflection /Length    | Lowest Natural Frequency |
|-------------------|-------------------------------|--------------------------|
| Truss (A)         | 38% (3×yield)                 | 0.43 Hz                  |
| Array (B)         | 1750% (≫ yield)               | 0.063 Hz                 |
| Truss-Array (A+B) | 10% (2×yield)                 | 0.84 Hz                  |
| Bus (C)           | (negligible)                  | 79 Hz                    |
| Boom (D)          | 22% ( $\frac{1}{3}$ of yield) | 0.85 Hz                  |

### 3.2 Test-Article Combinations

The four Test-Article Structures are designed to be configured into seven different Test Articles which involve either the individual structures or selected assemblies of the structures—six of these test articles are shown in Figures 10 and 11. (TA-4, which is the rigid Bus structure, is not shown.)

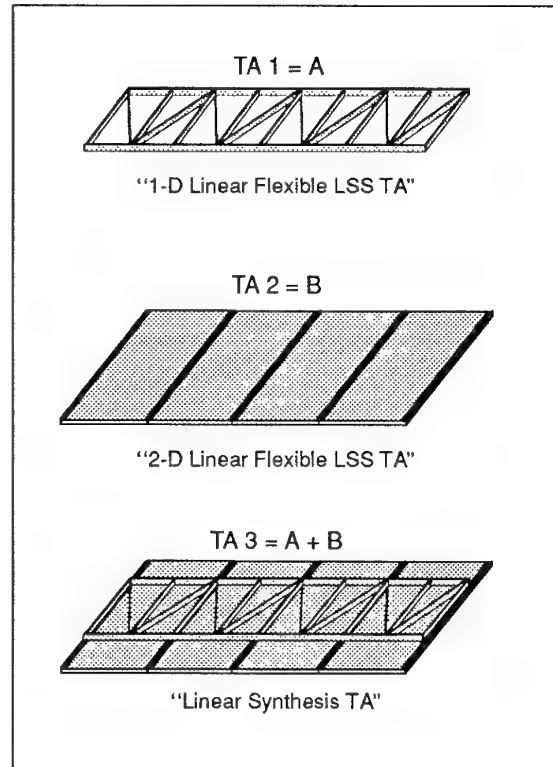


Figure 10: Test Articles 1, 2 and 3

## 4 THE MTSS VALIDATION TEST PROGRAM

### 4.1 Testing Objectives

Validation testing of the MTSS System [5] is intended to address the following high-level project objectives:

- To demonstrate the methods and operation of the MTSS System consisting of both Software and Hardware sub-systems.

In particular, for the Software...

- To update flexible structure models in order to produce improved predictive capability for the purposes of:
  - unrestrained dynamics (0-*g*);
  - integration with other structures (model synthesis); and,
  - other restraint configurations typical of LFSS.

In particular, for the Hardware...

- To show that the support of the structure in a 1-*g* environment does not unduly corrupt test article modal behavior with respect to the idealized boundary conditions the supports are supposed to provide.

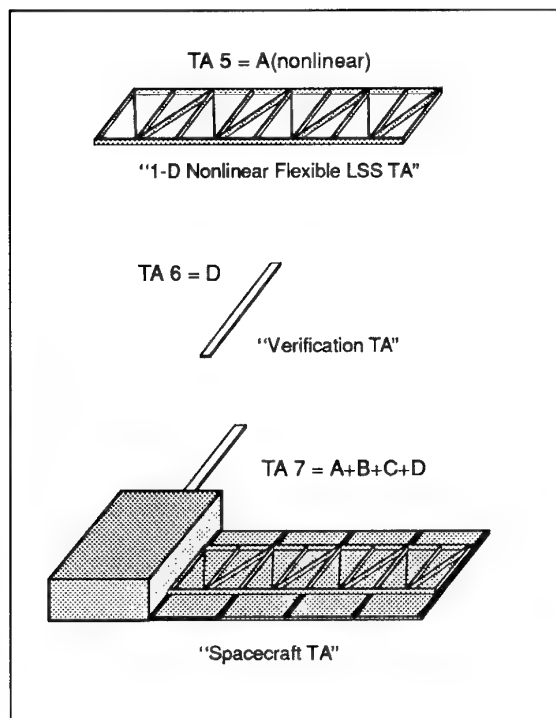


Figure 11: Test Articles 5, 6 and 7

And, regarding the testbed...

- To use the LSS Test Articles developed for the project as well-understood structures having certain dynamic and self-support properties typical of SBR spacecraft, in particular, and LFSS, in general.

#### 4.2 Bases for Assessment

Two types of comparison will be utilized for assessing system performance.

##### • Test-to-Test Validation

The first "test" refers to a comprehensive Multiple Boundary-Condition Test (MBCT) suite, the modal data from which is processed by the MTSS Software to produce an enhanced, or updated, model of the TA. This model is then available for predicting structural behavior in other testing situations.

Two options exist within test-to-test validation:

- MBCT-to-CMT:** Comparison of MBCT/MTSS prediction to the results of a Conventional Modal Test (CMT). Here, CMT refers to the type of modal test which would conventionally be performed on a structure—a single restraint-condition which is either simulated 'free-free' or some other simple restraint which usually represents an operational configuration.
- MBCT-to-SBCT:** Comparison of MBCT/MTSS prediction to the results of a *Selected* Boundary-Condition Test (SBCT). In some cases, it will be impractical to conduct a conventional modal test for the highly flexible TAs. Instead, the TA can be

tested in one or more selected restraint configurations, which will generally be different from those used for the MTSS/MBCT tests.

##### • Test-to-Model Validation

The LSS Test Articles have been designed to be both highly modelable and linear [4], with the exception of one 'nonlinear' TA. It is expected, therefore, that comparison with finite-element models will serve as useful validation standards in most or all situations.

For each TA there will exist a *good* model based on careful analysis and data from prior TA components testing. For demonstrating the performance of the model enhancement capabilities of the MTSS, a good FE model can be deliberately corrupted and then provided to the MTSS Software as an *initial* model to be subjected to updating, based on the test data. The MBCT-based MTSS-enhanced model can be compared against both the 'good' and the 'initial' models, either to predict real or hypothetical modal behavior, as well as by direct inspection of the model parameters targetted in the model updating process.

Please refer to Figure 12 for a diagrammatic description of the validation process. Table 4 summarizes the modal tests planned for the MTSS Validation testing.

Table 4: Modal Tests for MTSS Validation

| TA No. | MBCT+ME | SBCT | CMT |
|--------|---------|------|-----|
| 1      | •       | —    | •   |
| 2      | •       | •    | —   |
| 3      | —       | •    | —   |
| 4      | —       | —    | —   |
| 5      | •       | —    | •   |
| 6      | —       | —    | •   |
| 7      | —       | •    | —   |

##### Legend:

- MBCT - Multiple Boundary-Condition Test
- ME - Model Enhancement via MTSS
- SBCT - Selected Boundary-Condition Test(s)
- CMT - Conventional Modal Test

#### Acknowledgements

The MTSS project is funded by the Canadian Department of National Defence, with technical support provided by the Canadian Space Agency. System testing at the David Florida Laboratory has been made available at subsidized facility rates.

#### References

- Wada, B.K., Kuo, C.P. and Glaser, R.J., "Extension of Ground-Based Testing for Large Space Structures", *Journal of Spacecraft and Rockets*, Vol. 23, No. 2, March-April 1986, pp. 184-188.
- McTavish, D.J., Hosking, R., Sincarsin, W.G. and Golla D.F., "MTSS Detailed Design", Contract No. SSC



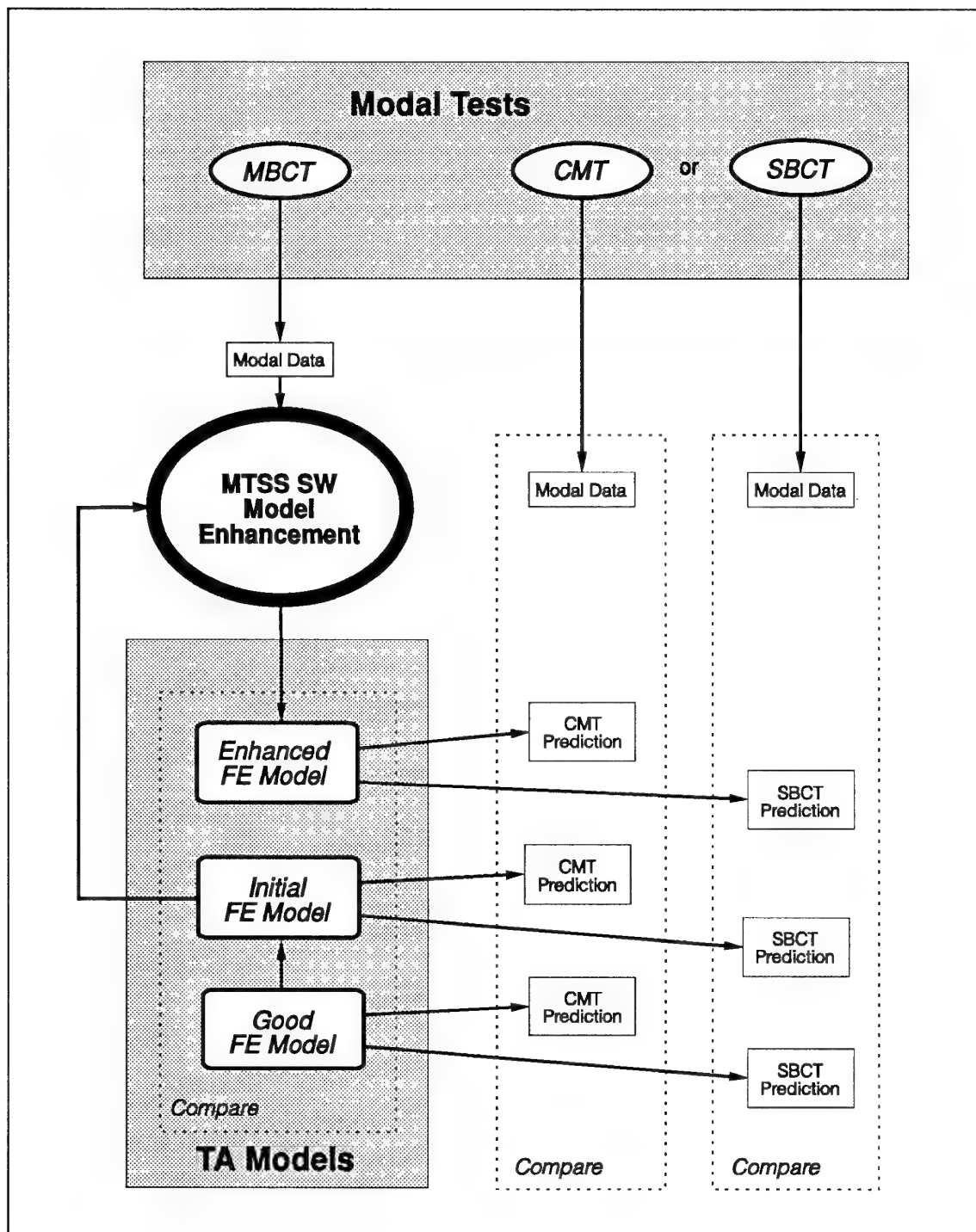


Figure 12: MTSS Validation with Linear Flexible Test Articles

- W8477-2-TD01/01-SV, Dynacon Report 29-212/0910 (Draft), June 1994.
3. Davison, E.J. and Wong, P., "A Robust Conjugate-Gradient Algorithm which Minimizes L-Functions", *Automatica*, Vol. 11, pp 297-308.
  4. Piggott, S.R., Sincarsin, W.G. and McTavish, D.J., "TA Detailed Design", Contract No. SSC W8477-2-TD01/01-SV, Dynacon Report 29-212/0909 (Draft), June 1994.
  5. McTavish, D.J., and Sincarsin, W.G., "MTSS Validation Test Plan", Contract No. SSC W8477-2-TD01/01-SV, Dynacon Report 29-212/0911 (Draft), May 1994.

## A STRUCTURAL MODELING, MODAL ANALYSIS AND MODEL UPDATING

In general, model-updating is implemented through the adjustment of some set of model parameters with the goal of improving the model's performance against certain predefined criteria. To appreciate some of the implications of this practice, it is useful to review certain aspects of finite-element modeling and modal analysis.

### A.1 Finite-Element Models

A typical finite-element model takes the form

$$\mathbf{M}\ddot{\mathbf{q}}(t) + \mathbf{K}\mathbf{q}(t) = \mathbf{f}(t) \quad (4)$$

where  $\mathbf{q}$  is a vector of physical displacement coordinates, and  $\mathbf{f}$  is a vector of corresponding applied forces. The square matrices  $\mathbf{M}$  and  $\mathbf{K}$  are the structure mass and stiffness matrices respectively. These *global* matrices can be written as summations of the *element* mass and stiffness matrices (denoted  $\mathbf{M}^e$  and  $\mathbf{K}^e$ ) representing the finite structural elements of the model.

$$\mathbf{M} = \sum_i \mathbf{M}_i^e \quad \mathbf{K} = \sum_i \mathbf{K}_i^e \quad (5)$$

The model represented in Equation 4 implicitly assumes pure linear-elastic material behavior with no damping present in the system. The linear-elastic assumption is one of practical convenience, which, for many engineering materials, is a good approximation. Nonlinear stiffness can be significant in structures, usually associated with structural interfaces (i.e., *joints*) where small relative motion between substructures exists. Such nonlinear joint behavior usually goes unmodeled and, moreover, the model coordinates  $\mathbf{q}$  generally do not include the degrees of freedom required to do so—relative joint motion is explicitly zero. Damping is normally excluded as the nature of this behavior is unknown and/or the tools to model it are unavailable. This does leave, however, Equation 4 as that of a *perpetual-motion* machine which must be applied with appropriate discretion. In some situations, the structural motion equation will be written with a " $\mathbf{D}\dot{\mathbf{q}}$ " term included. This *viscous* damping has a comfortable mathematical form but is an unjustified, usually incorrect, presumption of material behavior which is best not made. As with stiffness, overall structure damping will have contributions from both internal material damping and relative-motion effects at the joints (mechanical friction). Unlike the stiffness however, the damping may be dominated by the joint action which is likely far from linear—deployable space structures often have many loose joints.

### A.2 Modal Analysis

In modal analysis, a structure is characterized by its *natural* modes of vibration—the possible states of motion when there is no external force acting on it. The finite-element model (4) predicts the shapes and vibration frequencies of these modes via the matrix eigenvalue problem:

$$-\omega^2 \mathbf{M}\mathbf{e} + \mathbf{K}\mathbf{e} = \mathbf{0} \quad (6)$$

which yields a number of discrete solutions  $\{\omega_i, \mathbf{e}_i\}$  for the modes. These pure frequencies  $\omega_i$  (perpetual motion) and

real-valued eigenvectors  $\mathbf{e}_i$  (uni-phase motion) provided by the undamped-linear model are called the *normal modes* solution.

The estimation of modal parameters from test-data obtained from a real structure by most modern methods assumes much less than the finite-element model of the same. Typically these assumptions include linearity, reciprocity, and compatibility with second-order (temporal) behavior—no assumptions of damping behavior are made outside of the previous restrictions. As a result, the natural modes of vibration extracted from test include decay rates along with frequency, and relative phase characteristics in the modes shapes. These are represented by complex numbers (and conjugates) as  $\{\lambda_i, \phi_i\}$ ; for example  $\lambda_i = -\sigma_i + j\omega_i$  where  $\omega_i$  is the frequency, and  $\sigma_i$  is the exponential decay rate for the  $i$ -th mode.

For modal-parameter-based model-updating these experimental data have to be reconciled with their normal-mode counterparts from the finite-element model (FEM):

|                             | FEM                 | Test-Data   |
|-----------------------------|---------------------|---|
| Eigenvalue<br>(Frequency)   | $j\omega_i$         | $\longleftrightarrow \lambda_i = -\sigma_i + j\omega_i$ |
| Eigenvector<br>(Mode Shape) | $\mathbf{e}$ (real) | $\longleftrightarrow \phi_i$ (complex)                  |

'Quick' modal parameter estimation techniques sometimes force some assumptions regarding the structural response (uni-phase (normal) modes, for example). Such assumptions are usually made for computational expediency and may or may not be valid. Frequency-domain procedures may require the user to select a viscous or *hysteretic* damping model to estimate the "modal damping".

Modal damping (i.e., a  $\sigma_i$  value obtained from test or otherwise) is sometimes 'tacked on' to modal models derived from normal-modes solutions when it is required to estimate structural responses to force inputs (A perpetual-motion model just won't do here!). A coordinate associated with each mode, based on this modal damping, is given the characteristic of a viscously damped harmonic oscillator. This procedure should be used only when the structure is studied all by itself in exactly the same configuration that gave rise to the modal damping factors used. In particular, added normal-mode viscous damping should not be used when different structural models are integrated together or when the original structure is constrained differently. While the mode shapes may make good *shape functions* for extrapolating structural response, and likewise the natural frequencies, which are based upon relatively well-known mass and stiffness properties, can be trusted; a modal damping factor has validity only for predicting the decay of the corresponding mode for the original natural frequency at which the modal damping was originally defined. *Simple modal damping, once imbedded in a model, cannot be extrapolated to differing configurations of the structure.*

### A.3 Model Updating

Traditionally, model updating is accomplished through the adjustment of some set of model parameters from their initial values. Two extremes in this regard are:

- (a) The arbitrary modification of the global mass and/or stiffness matrix entries after finite-element model assembly, and
- (b) The adjustment of physical structural and material properties prior to model assembly.

These approaches are now briefly discussed.

The first of these—arbitrary modification of global matrices—is essentially a “black-box model” approach. The physical significance of the initial finite-element model becomes lost once updating has been done. Such models will generally reproduce the objective output characteristics the updating was based on; but having lost the internal structure required of a physical model (representing load paths, inertial coupling, etc.), should not be expected to extrapolate reliably to other configurations of the structure.

Any updating strategy which disregards the physical structure of the test article and/or the corresponding algebraic structure of a (correctly) formulated finite-element model is not suitable for any procedure which extrapolates dynamic behavior from one configuration of the structure to another. MBCT and model synthesis are procedures which explicitly rely on such extrapolation, and as such must generally be based on physically-correct structural modeling.

The second extreme listed above is an approach which holds much promise. Disadvantages of this approach include the implementation overhead of having to provide ground-up finite-element assembly in the update cycle, and a very large parameter space often containing redundancies.

A premise of most model-updating implementations is that the structure is modeled *correctly*. Specifically, poor performance of the finite-element model is taken to be due to parameter uncertainty. Correct modeling—including grid-point quantity, suitable element selection, adequate detail near interfaces, and so on—is taken for granted or not appreciated. Practical experience suggests that poor modeling is frequently predominant over parameter uncertainty. While, updating may *appear* to compensate for model incorrectness, the underlying structure of the model remains fundamentally flawed and, as with a black-box model, extrapolation to other configurations becomes unadvisable.

#### A.4 MBCT and Model Synthesis

As model-based procedures, both MBCT and model synthesis are best restricted to physically-correct models. Moreover, these models should be restricted to those aspects of the model where reasonable confidence can be expected—damping, for example, should not be propagated through these processes. For MBCT and model-updating, it remains the responsibility of the user to collect test-data and specify the model parameters in a manner appropriate to maintaining a physically sensible model.

# A Preliminary Study of the Air Data Sensing Problem on a Re-entry Vehicle

Mr. E. Hettena  
Institut supérieur des affaires,  
Groupe HEC  
Bâtiment B1 — Chambre 76  
1, rue de la Libération  
78351 Jouy-en-Josas, France

## ABSTRACT

A brief review of different measurement techniques for speed, pressure and temperature on a re-entry vehicle is given in order to evaluate their applicability and limitations to the design of an air data system. A pressure-sensors based air data system is then assumed and an engineering aerodynamic model is used to investigate the influence of the measurement errors on the relevant air data parameters necessary for flight guidance and control.

## 1. INTRODUCTION

The knowledge of air speed, pressure altitude, Mach number and flow direction angles is necessary to control the flight of any civil or military vehicle. A basic conventional Air Data System (ADS), based on pitot-static concept, normally includes the following sensors [1]:

- i) a total pressure sensor or "pitot probe";
- ii) an ambient pressure sensor or "static probe";
- iii) a total air temperature sensor;
- iv) flow direction sensors in form of vanes or differential pressure probes.

Other air data are obtained from these "sensed" quantities, either directly from the transducers or from the air data computer, and are supplied to the vehicle Flight Control System (FCS) :

- baroaltitude from (ii);
- calibrated airspeed from ambient pressure supplied by (ii) and from pitot pressure;
- vertical speed from the rate of change of static pressure with the time;
- total and ambient temperatures from (iii)
- Mach number from (i) and (ii)

This concept has been adapted for use on a wide variety of airplanes and is normally implemented on civil or military aircraft flying up to supersonic speed.

The flight envelope of a re-entry vehicle involves the Mach number ranging from 0.2 to 27, the angle of attack from 0° to more than 40° and stagnation temperatures up to 1800°K. The severe thermal environment, experienced during the hypersonic phase of a re-entry, prevents the straight extension of the classical ADS concept and sensors to hypersonic vehicles,

then the determination of the air data necessary to control the flight must be carefully studied. A solution, adopted for the early flights of the U.S.Orbiter [2], is to estimate some air data from the Inertial Navigation System (INS), while a conventional ADS is deployed at supersonic speed and used up to the landing. The vehicle controllability at high speed, however, is not completely assured since the INS-derived data can be affected by the imprecise knowledge of vehicle aerodynamics, non-zero wind velocity, INS errors or failure. The availability of measured air data is then recommended.

This paper focuses on aerodynamic problems, measurement techniques and simple error modeling concerning the preliminary design of an air data system for a re-entry vehicle. The basic air data parameters, needed for flight control purposes, are discussed first, the air dissociation effects are briefly reviewed through the study of the flow along the stagnation streamline. A short review of different methods to evaluate the Mach number then follows and, finally, a simple error estimation, based on engineering methods, is carried out in order to evaluate the effects of aerodynamics on Mach and static and dynamic pressures.

## 2. BASIC PARAMETERS

A winged re-entry vehicle is controlled by means of both aerosurfaces and reaction control jets (RCS). Aerodynamic drag is used to decelerate the vehicle through controlled dissipation of its energy. The control of energy dissipation is exerted by following an angle of attack profile, compatible with thermal and structural load limits. A roll angle scheduling is used to satisfy the range requirements.

The vehicle aerodynamics is usually expressed in terms of forces and moment coefficients, their derivatives and the contributions of the control devices. FCS control parameters are normally scheduled to match the vehicle aerodynamics as a function of air data as incidence, static and dynamic pressure and Mach number; incidence and yaw angles are primary feedback signals to provide closed loop optimum control of the vehicle trajectory. All these parameters must be made available to the FCS during flight.

The characteristic flow regimes along a very general

Earth entry trajectory are shown in fig.1. The first re-entry phase develops in the rarefied gas region. Here the pressure is very low and the measurement of air data is not meaningful. The vehicle control relies on air data generated by the INS. The trajectory

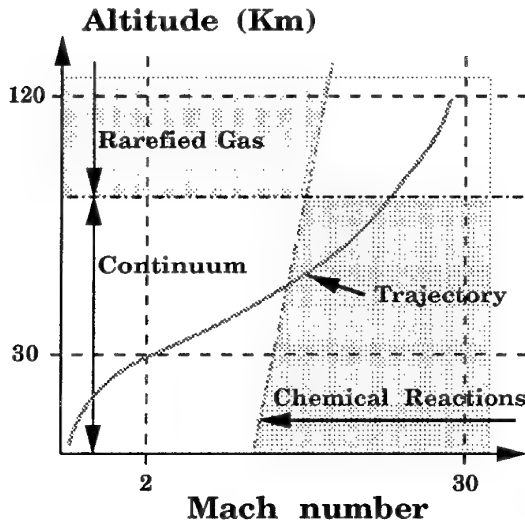


Figure 1: General Earth re-entry trajectory

then enters into the continuum gas region. In this region the speed reduces progressively from hypersonic to subsonic before the final approach. Although the very high temperature prevents the use of conventional Pitot probes, the pressure can be measured by sensors mounted on the vehicle surface. An example of this approach is the SEADS [2, 3, 4] developed for the U.S.Orbiter whose nose is instrumented with a pressure sensors system. Total and static pressures, incidence and yaw are reconstructed by fitting the measured pressures to an aerodynamic model of the Shuttle forebody. The Mach number is obtained by the normal shock relation.

Incidence and sideslip can also be determined by the differential pressure that correlates the "apparent" angles to true  $\alpha$  and  $\beta$ . The correlation can be established by wind tunnel tests and by theoretical models. Alternatively, or additionally,  $\alpha$  and  $\beta$  can be obtained by the INS.

At supersonic ( $M_\infty \leq 4$ ) and subsonic speeds a conventional ADS probe can be used to increase the accuracy of air data, even if both mechanical problems (deployment mechanisms) and spurious aerodynamic and thermal interference (local skin deformations, local heating radiated from the vehicle) can arise.

At speed/altitude combinations at which the air behaves like an ideal gas<sup>1</sup>, well assessed calibration procedures exist [1, 5] that allow to obtain the air data with good precision. At hypersonic speeds the usual

relationships between sensed static pressure and ambient pressure, break down due to the departure of air from the ideal gas behaviour. The evaluation of Mach number and of the ambient temperature is more critical as it will be shown respectively in sections 4. and 4.3.

### 3. REAL GAS EFFECTS

Among the various phenomena apperaring at hypersonic speeds, the most important are the so-called "Real gas" effects. When the air particles cross the bow shock at hypersonic speeds, part of their kinetic energy is converted to thermal energy. The resulting higher temperature causes vibrational molecular motion that changes the specific heats  $C_v$ ,  $C_p$  and their ratio  $\gamma$  and, depending upon the thermal energy level, a partial chemical dissociation of air can occur. In these conditions, pressure, temperature and the ratio of specific heats become interdependent, and no closed formulas between the air parameters are known. Moreover, depending on the ratio of the flow velocity and the chemical reaction velocity, two gas states can be obtained :

- if the gas is in thermal equilibrium, its reaction rate is very high compared to the flow velocity, then its chemical composition is a unique function of the local pressure and temperature. In this case it is possible to use some gas tables to obtain the gas status.
- If non-equilibrium dissociation of air occurs, the reaction rate is comparable to the flow velocity, now the chemical composition of the gas is not a unique function of pressure and temperature then it is not possible to know the local gas status.

Some indications of the air behaviour at hypersonic speeds can be obtained from the flow properties along the streamline ending at the stagnation point. Assuming the steady, one-dimensional Euler equation model (1) across the shock,

$$\begin{aligned} \rho_\infty u_\infty &= \rho_1 u_1 \\ p_\infty + \rho_\infty u_\infty^2 &= p_1 + \rho_1 u_1^2 \\ h_\infty + \frac{1}{2} u_\infty^2 &= h_1 + \frac{1}{2} u_1^2 \end{aligned} \quad (1)$$

followed by an isentropic deceleration up to the stagnation point and using a model of air in thermal equilibrium (for example [6]), the flow properties behind a normal shock (subscript 1) and at the stagnation point (subscript 2) can be obtained and compared to the same obtained by using the perfect gas relations. The comparison is presented in figures 2-4 at fixed altitude of 40Km and for Mach numbers ranging from 4 to 24. While large differences (fig.2) in the total to static temperature ratio  $T_{t2}/t_\infty$  are visible, the increment in the pressure coefficient  $C_p$  (fig.3) is not so large ( $\approx 5\%$ ).

<sup>1</sup>An ideal gas is calorically and thermally perfect. The specific heat capacities are constant and the thermal equation of state  $p = \rho RT$  holds.

The behaviour of total-to-static pressure ratio  $P_t/p_\infty$  (fig.4) is similar to the one of the pressure coefficient, but it shows smaller differences between perfect and thermal equilibrium gas.

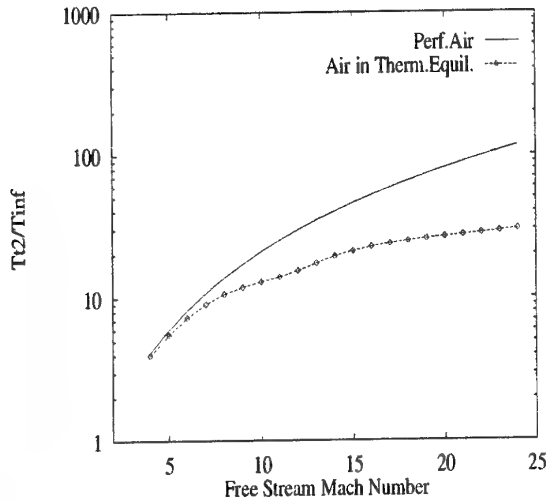


Figure 2: Total to free stream temperature ratio

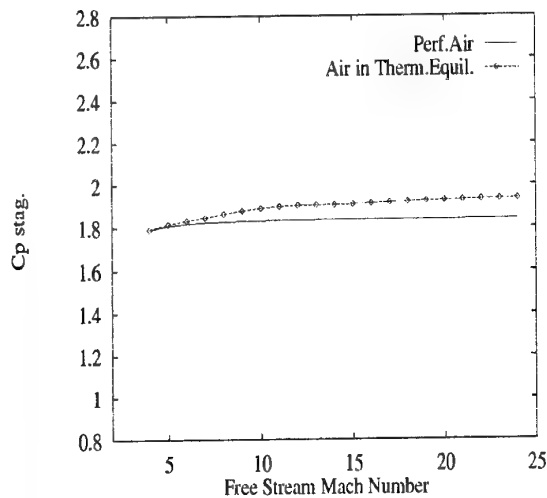


Figure 3: Stagnation pressure coefficient

#### 4. EVALUATION OF MACH NUMBER

Reference [7] reports various systems and methods for determining the Mach number in flight. Some are briefly resumed herein:

- Measurement of total pressure and total temperature by surface mounted sensors and use of normal shock relationships and gas tables (see [8]) to obtain the Mach number.
- Direct measurement of true airspeed (TAS) from light scattering generated by particles of atmospheric dust crossing Laser beams. The Mach number is then evaluated from the mea-

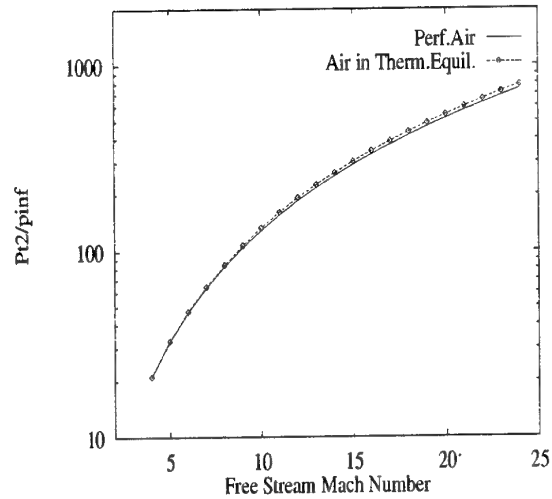


Figure 4: Total to free stream static pressure ratio

sured speed and from the ambient temperature obtained from another source (e.g. meteorological satellites and balloons).

- TAS derived from the ground speed output by the inertial navigation system and from the local wind speed and direction obtained from meteorological sources [9]. The Mach number is then evaluated by combining the speed value with the air temperature data obtained as in the previous case.

The main limitation of the last two methods is the uncertainty in the determination of the meteorological data at any particular point and time of the trajectory that, together with their variability in time, can introduce significant errors into the evaluation of Mach number. Another limitation of a method requiring information supplied from an external source, is the blackout in the communications due to the gas ionization at high speed and altitude. Additional problems, especially concerning the determination of the temperature, are discussed in the following sections.

##### 4.1 Use of Local Pressure Information

At supersonic regimes, since the body is blunt, the static or ambient pressure is related to the total pressure by the normal shock relation that, assuming ideal gas conditions, is :

$$\frac{P_t}{p_\infty} = \left[ \frac{(\gamma + 1)M_\infty^2}{2} \right]^{\frac{\gamma}{\gamma-1}} \left[ \frac{\gamma + 1}{2\gamma M_\infty^2 - (\gamma - 1)} \right]^{\frac{1}{\gamma-1}} \quad (2)$$

This formula, also known as Rayleigh pitot formula, is valid for  $M_\infty \geq 1$  or  $P_t/P_\infty > 1.89$ . In subsonic flow ( $P_t/p_\infty \leq 1.89$ ) the isentropic relation can be used:

$$\frac{P_t}{p_\infty} = \left[ 1 + \frac{\gamma - 1}{2} M_\infty^2 \right]^{\frac{\gamma}{\gamma - 1}} \quad (3)$$

The adoption of the SEADS approach allows to determine the total-to-free stream static pressure ratio  $P_t/p_\infty$  by fitting the measured pressures to an aerodynamic model of the vehicle forebody. If the ideal gas behaviour is assumed ( $\gamma = 1.4$ ), the Mach number can be directly computed by solving either equation (2) or equation (3). A direct approximate solution of eq.(2) is also presented in [1] in order to avoid iteration.

Even if the ideal gas assumption is justified by the fact that real gas effects are small on  $P_t/p_\infty$ , as it has been shown previously, the resulting Mach will be affected by an error depending on altitude and speed. At an altitude of 40 Km and assuming thermal equilibrium, this error is lower than 1% up to  $M_\infty \approx 8$  then increases up to nearly 3% at higher speed. Non-equilibrium chemistry can introduce another source of errors due to increased non-uniformity of air behaviour on the vehicle surface.

When the static pressure and Mach number are available, the dynamic pressure  $q_\infty$  can be computed from  $q_\infty = (\gamma/2)p_\infty M_\infty^2$ .

#### 4.2 TAS Measurement by LASER

The true airspeed can be accurately measured by a Laser velocimeter. The motion of a spherical particle in a fluid flow has been reviewed and summarized by Hinze [10]. The results show that, given the particle diameter, specific gravity and the local flow conditions, the particle response to sinusoidal velocity fluctuations of the surrounding fluid can be estimated from:

$$\left( \frac{d^2 \rho_p}{18 \mu_f} \right) \left( \frac{d V_p}{dt} \right) - (V_f - V_p) = 0 \quad (4)$$

where the subscript  $p$  refers to the particle quantities while the subscript  $f$  refers to the flow. The analysis, which assumes Stoke's drag with the Cunningham correction, gives the particle response to turbulent fluctuations in the moving frame of reference of the particle. Equation (4) may be transformed to:

$$\frac{V_p(S)}{V_f(S)} = \frac{1}{(T_p S + 1)} \quad (5)$$

where  $S$  is a differential operator and  $T_p$  is the time constant defined as:

$$T_p = \left( \frac{d^2 \rho_p}{18 \mu_f} \right) \quad (6)$$

Equation (5) can be used to study the particle response in the frequency domain. The time constant (6) must be corrected for the low density and

static temperature environments associated with hypersonic regime. In particular the Stoke's drag coefficient must be modified so to extend its range of application to flows where the Knudsen number is significant. The form used in ref. [11] results in a modified time constant which may be written as :

$$T_p = \left( \frac{\rho_d d_p^2}{18 \mu_f} \right) \left( 1 + k \frac{\lambda}{d_p} \right) \quad (7)$$

where  $k$  is the Cunningham constant,  $d_p$  is the particle diameter and  $\lambda$  is the particle mean free path. Equation (7) shows that relative seed particle response is proportional to the product of the square of the particle diameter and to a parameter inversely proportional to the seeding density. The *natural seeding* decreases with increasing altitude, leading very rapidly to unacceptable increase of the time constant  $T_p$ . It is estimated [7] that, above 33 Km approx., a Laser-based measurement device has an acquisition time too long for practical applications.

#### 4.3 Temperature Measurement

The necessity to know the ambient temperature depends on the method used to determine the Mach number. In particular, the ambient temperature is necessary to compute the Mach number if the TAS is obtained directly from INS or from laser velocimetry. The ambient temperature can normally be obtained from the measured total temperature, provided that the flight Mach number is lower than  $\approx 5$ , so that the real gas effects are negligible, and the total temperature probe is not influenced by local heat sources.

At hypersonic flight regimes these conditions can not be realized since it is not possible to use probes, the surface local temperature depends on the equilibrium between the aerodynamic and radiative heat fluxes and these fluxes are dependent on the local gas and surface properties. As an example of the importance of these effects, the total temperature at  $M_\infty = 25$ ,  $z = 75 \text{ Km}$  exceeds  $25000^\circ \text{K}$  if air is considered an ideal gas, it results  $\approx 5700^\circ \text{K}$  if equilibrium chemistry is assumed and it reduces to about 1/4 of this value if surface radiation and laminar flow are taken into account.

The gas status depends on local pressure, temperature (see section 3.) and, if non-equilibrium dissociation is present, on the reaction rate and vehicle dimensions. If the flow is in non-equilibrium dissociation, the cataliticity of the vehicle surface can influence the aerodynamic heating. Its effect is to accelerate the recombination process of the dissociated air locally. Heat is released during this process then the local temperature increases. A direct consequence of the phenomenon is that the correction of the errors in determining the total temperature can become impossible.

Some correlation between ambient temperature and total temperature measured on the vehicle surface can be established by numerical flow simulations (an example is shown in fig.5-6), but the errors due to limited modelling capability and, more important, to local changes in the surface properties can make the correlation meaningless.

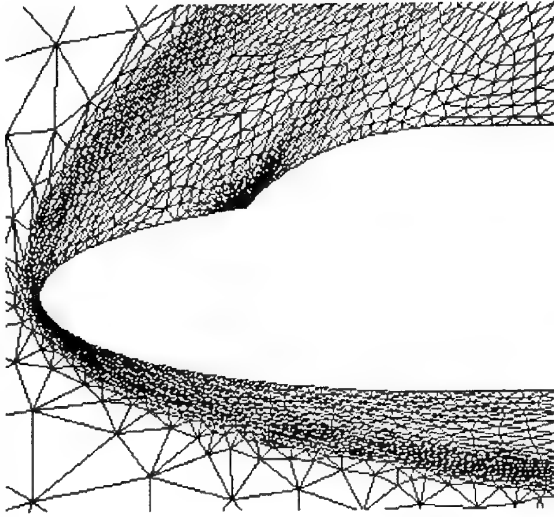


Figure 5: Computational grid around a 2D forebody



Figure 6: Computed temperature field assuming equilibrium chemistry at  $M_\infty = 25$ ,  $z = 75 \text{ Km}$

The ambient temperature can be determined with a certain level of accuracy at supersonic and subsonic speeds. However, the re-entry time is generally short then the vehicle temperature will depends on the thermal transient, leading to relevant radiated heat fluxes also at these speeds. The adoption of an extractable total temperature probe will then require adequate radiation shields to surround the temperature sensing element in order to minimize the sensing error.

In conclusion, the temperature measurement on the

vehicle surface is certainly one of the techniques for determining the heat load on the thermal protection system, but, at hypersonic speeds, it can not be used as a method to determine the ambient temperature. At lower speeds, care must be taken in designing the probes so to minimize the errors due to the heat radiated by the vehicle.

## 5. ERROR ESTIMATION

The influence of some aerodynamic effects on the characteristics of the hypersonic flow surrounding the spacecraft has been discussed in the previous sections. It can also be shown that, apart some exotic measurement technique, the only alternative way, to the INS, to obtain the air data during a large part of the re-entry trajectory is the adoption of a pressure sensor system. A preliminary assessment of the error levels produced by aerodynamic and geometric factors on static and dynamic pressures, can be carried out, in hypersonic flow, by using the Modified Newtonian Flow model.

This theory is based on the assumption that the free stream Mach number is so high that the speed and direction of the gas particles in the free stream remain unchanged until they impact the body surfaces exposed to the flow and the shock layer becomes very thin [12]. In these conditions, the normal component of momentum of the impinging fluid particle is lost while the tangential component of momentum is conserved. A very simple relation holds among the pressure coefficient  $C_p$ , its value at the stagnation point  $C_{p,stag}$  and the local angle between the body normal  $\vec{n}$  and the free stream velocity vector  $\vec{V}_\infty$ :

$$\frac{C_p}{C_{p,stag}} = \frac{\vec{V}_\infty \cdot \vec{n}}{||\vec{V}_\infty|| ||\vec{n}||} = \cos^2 \phi \quad (8)$$

The attractiveness of the Modified Newtonian Flow theory is the possibility to determine the local pressure, with a reasonable accuracy, based only on the knowledge of the body geometric quantities and of the free stream velocity direction. In the simplest case of a pressure sensor placed on the vehicle symmetry plane, naming  $\theta$  the local surface inclination (positive counterclockwise), the outward body normal  $\vec{n}$  is expressed as:

$$\vec{n} = -\sin \theta \vec{i} + \cos \theta \vec{k}$$

$$\vec{V} = U_\infty (\cos \alpha \cos \beta \vec{i} + \sin \beta \vec{j} + \sin \alpha \cos \beta \vec{k}) \quad (9)$$

$$\cos \phi = -\cos \alpha \sin \theta + \sin \alpha \cos \theta$$

A correlation between the local stagnation and static pressures  $P_t, p_L$  and the free stream static pressure can be obtained from the definition of pressure coefficient:

$$\frac{C_p}{C_{p,stag}} = \frac{p_L - p_\infty}{P_t - p_\infty} \quad (10)$$



then, from (8) and (10) and being  $R$  the ratio  $P_t/p_\infty$ , the free stream static pressure is obtained:

$$p_\infty = \frac{p_L}{(R-1)\cos^2\phi + 1} \quad (11)$$

The influence of the sensor position and of the incidence and yaw are embedded in  $\phi$ , while real gas effects have an impact on  $p_L, R$ . The Mach number has a direct impact on  $q_\infty$  since  $q_\infty = (\gamma/2)p_\infty M_\infty^2$ . A sensitivity study can be carried out in order to estimate the errors arising by incidence calculation, sensors precision, local body geometry and air behaviour.

### 5.1 Reference Conditions

The super-hypersonic regime of a very general entry trajectory (fig.7) is considered<sup>2</sup>. Along it, five points have been chosen for the error checking.

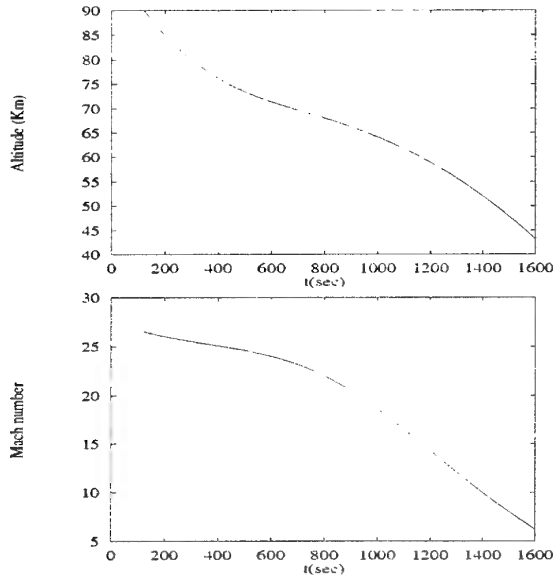


Figure 7: Mach and altitude profiles

The points are summarized in table 1, the  $R$  values have been computed by using a real gas model for air in thermodynamic equilibrium.

| Altitude (Km) | $M_\infty$ | $R_{realgas}$ |
|---------------|------------|---------------|
| 75.85         | 25.00      | 851.83589     |
| 65.80         | 20.11      | 548.80307     |
| 60.07         | 15.22      | 311.87401     |
| 52.00         | 10.00      | 134.07053     |
| 43.17         | 6.25       | 51.35123      |

Table 1: Check points for error estimations

The following error sources have been considered in the reconstruction of  $p_\infty, M_\infty, q_\infty$ :

- i) Incidence and Yaw angles:  $\Delta\alpha = \pm 1^\circ$ ,
- ii) Sensor position (local body inclination):  $\Delta\theta = \pm 1^\circ$ ,
- iii) Sensor accuracy:  $\Delta p_L = \pm 5\%$
- iv) Real gas effects and method for determining  $R$ :  $\Delta R = \pm 5\%$ .

### 5.2 Mach Number

The starting point is the availability of the ratio  $R = P_t/p_\infty$  that is assumed to be obtained from pressure measurement. The Mach number is computed from equation (2) for an ideal gas ( $\gamma = 1.4$ ). The error with respect to the nominal Mach number is shown in fig.8 along the entry trajectory.

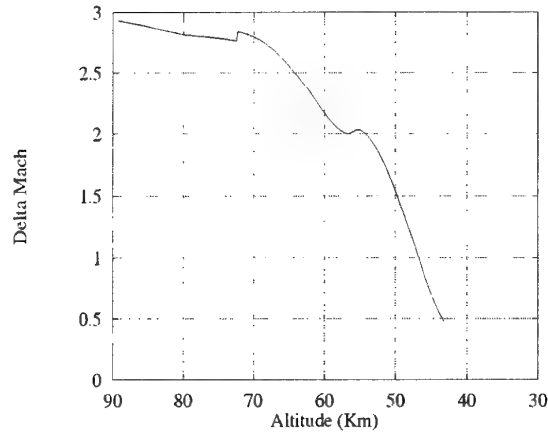


Figure 8:  $\Delta Mach = \frac{(M_{from eq.(2)} - M_\infty)}{M_\infty} \times 100$

Its maximum value is about 3% and tends to zero while the flight Mach number and altitude decrease. A 5 % increase of  $R$  (indicated as  $R^+$ ) leads to additional overshoot of the computed Mach, while a decrease ( $R^-$ ) is favorable at high Mach numbers, and it leads to underestimation at low Mach. The errors, in terms of  $\Delta M/M_\infty \times 100$ ,  $\Delta M = M_{computed} - M_\infty$ , are reported in table 2.

| $M_\infty$ | $M_{eq.(2)}$ | $\frac{\Delta M}{M_\infty} \%$ | $\left(\frac{\Delta M}{M_\infty}\right)_{R^+}$ | $\left(\frac{\Delta M}{M_\infty}\right)_{R^-}$ |
|------------|--------------|--------------------------------|--|--|
| 25.00      | 25.70        | 2.812                          | 5.350  | 0.210  |
| 20.11      | 20.64        | 2.635                          | 5.173  | 0.032  |
| 15.22      | 15.55        | 2.219                          | 4.748  | -0.373   |
| 10.00      | 10.19        | 1.874                          | 4.399  | -0.715   |
| 6.25       | 6.29         | 0.645                          | 3.153  | -1.927   |

Table 2: Errors due to real gas effects and pressure measures

### 5.3 Static Pressure

The reconstruction of the static pressure is carried out by assuming eq. (11) as aerodynamic model. The analysis has been carried out assuming a constant incidence range  $20^\circ \leq \alpha \leq 40^\circ$  for all the check points and error sources selected in the previous section. Fig. 9-upper shows the error behaviour with

<sup>2</sup>This trajectory is used as a pure example and it is not referred to any existing vehicle or project

$\Delta\alpha = +1^\circ$  and with  $R = R_{\text{real gas}} \times 0.95$  while fig. 9-lower presents the error analysis along the trajectory with a fixed incidence  $\alpha = 35^\circ$ . The error is defined as:

$$\text{error} = \frac{p_\infty - p_{\infty \text{ computed}}}{p_\infty} \times 100 \quad (12)$$

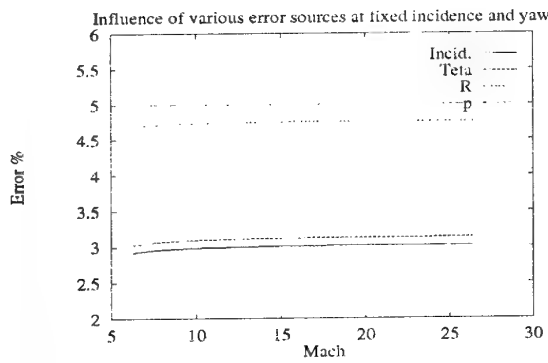
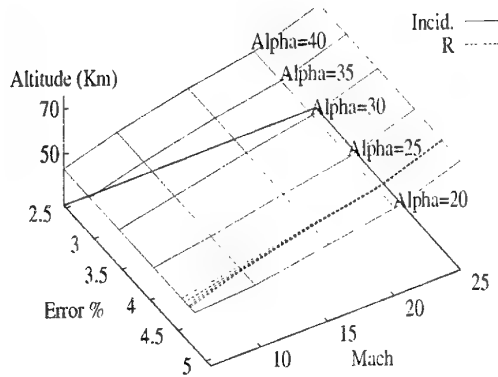


Figure 9: Static pressure reconstruction

The error is not linear with incidence only because its source is not a linear percentage of the nominal value (5 % at  $20^\circ$ , 2.5 % at  $40^\circ$ ), while it is almost constant at constant incidence with the Mach number. Table 3 reports the errors (%) computed assuming  $\alpha = \alpha_{\text{nominal}} + 1^\circ$  versus  $\alpha_{\text{nominal}}$ .

| $M_\infty$ | $\alpha = 20^\circ$ | $\alpha = 25^\circ$ | $\alpha = 30^\circ$ | $\alpha = 35^\circ$ |
|------------|---------------------|---------------------|---------------------|---------------------|
| 25.00      | 5.08                | 4.25                | 3.58                | 3.02                |
| 20.11      | 5.07                | 4.25                | 3.57                | 3.01                |
| 15.22      | 5.05                | 4.23                | 3.56                | 3.01                |
| 10.00      | 4.98                | 4.19                | 3.53                | 2.98                |
| 6.25       | 4.80                | 4.06                | 3.45                | 2.92                |

Table 3: Errors due to  $\Delta\alpha = +1^\circ$

A quite similar behaviour is shown by the error due to sensor positioning. This error is evaluated assuming a fixed  $\theta = -20^\circ$  (sensor placed on the vehicle windward side) and an error  $\Delta\theta = +1$  degree. The incidence and yaw are maintained at their nominal values. The errors are reported in table 4.

| $M_\infty$ | $\alpha = 20^\circ$ | $\alpha = 25^\circ$ | $\alpha = 30^\circ$ | $\alpha = 35^\circ$ |
|------------|---------------------|---------------------|---------------------|---------------------|
| 25.00      | 5.19                | 4.36                | 3.69                | 3.13                |
| 20.11      | 5.18                | 4.37                | 3.69                | 3.12                |
| 15.22      | 5.16                | 4.34                | 3.68                | 3.12                |
| 10.00      | 5.09                | 4.30                | 3.64                | 3.09                |
| 6.25       | 4.90                | 4.17                | 3.56                | 3.03                |

Table 4: Errors due to  $\Delta\theta = +1^\circ$

The error due to sensor accuracy is linear in eq. (11), so if the static pressure is sensed with 5% of error, the same will result for  $p_\infty$ . It is important to notice the range of variation of the pressure along the re-entry trajectory (from nearly zero up to more than 100 KPa). Since the effect of the sensing error on  $p_\infty$  is direct, it can be convenient to adopt two sensors with different sensitivity. Fig. 10 shows the stagnation pressure along the trajectory predicted by eq.(1) with thermal equilibrium assumption. It can be noted that, down to about 60 Km, the stagnation pressure is lower than 1 psi ( $\approx 6.89 \text{ KPa}$ ), then an appropriate sensor has to be selected.

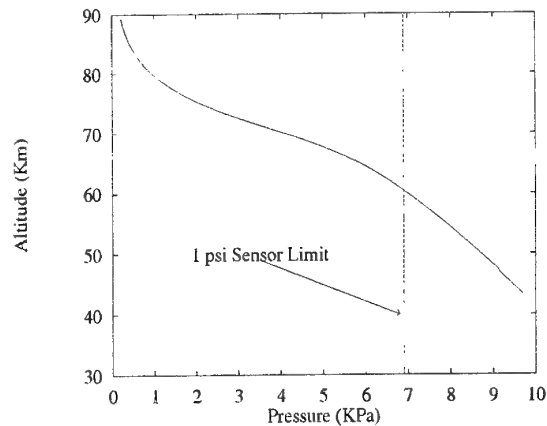


Figure 10: Stagnation pressures along the trajectory

Finally the +5 % error of  $R$  is considered. The error is almost constant with incidence and it leads to a quasi-constant error ( $4.75\% \leq \Delta p/p_\infty \leq 4.56\%$ ) over the considered Mach range ( $25 \leq M_\infty \leq 6.25$ ).

#### 5.4 Dynamic Pressure

The dynamic pressure is affected by the pressure errors and by the error in the calculation of the Mach number. In fact, if the nominal  $M_\infty$  is assumed, the same % errors reported in tables 3 and 4 are applicable to  $q_\infty$ . More interesting is the error variation along the reference trajectory shown in fig.11. Incidence and yaw are fixed at their nominal values and the three curves show the effects of  $\Delta\alpha = +1^\circ$  (Incid), a -5 % applied to  $R$  (R) and the assumption of ideal gas in evaluating the Mach number (Mach). This last error source is obtained by computing the  $M_\infty$  with eq. (2). The resulting  $\Delta q/q_\infty$  is always

lower than 0.06 along the trajectory.

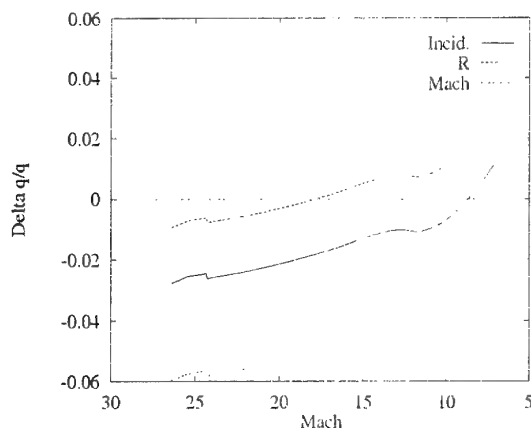


Figure 11: Dynamic pressure reconstruction

## 6. CONCLUSIONS

A preliminary study of the air data sensing problem for hypersonic flows has been carried out. A brief review of some of the key problems related to hypersonic flows has been presented. A simple sensitivity study has been carried out, by using an engineering tool, in order to estimate the influence of the measurement errors on the relevant air data parameters necessary for flight guidance and control.

However, the extreme conditions of hypersonic flight, in terms of high temperature and low pressure, must always be considered in the choice of the system components and layout. In particular, if an air data system based on pressure sensors mounted on the vehicle surface is selected, some additional keypoints must be taken into account :

- transition and separation zones should be avoided in the choice of pressure sensors location, since their effects on the sensed pressure can become important at high angle of attack.
- Care must be taken in the creation of the vehicle aerodynamic model.
- Fast hardware can be required for the onboard computer, depending on the complexity of the calculations needed to obtain the air data parameters.

Nevertheless, air data sensors can be used to record data for post flight analysis without restriction, but the use of measured information for guidance and control is linked to a lot of technological problems that can be partially overcome by the use of an inertial system.

## REFERENCES

- [1] ESDU (1986) *Introduction to Air Data System Parameters, Errors and Calibration Laws* - ESDU International. Data Item 86031.
- [2] Pruett, C.D., Wolf, H., Heck, M.L. and Siemers, P.M. III (1983) *Innovative Air Data System for the Space Shuttle Orbiter* - J.Spacecraft and Rockets, Vol. 20, No.1, pp 61-69
- [3] Cunningham, J.A., Rochelle, W.C., Norman, I., Ting, P.C., Gallegos, J.J. (1987) *Shuttle Entry Air Data System Preflight Testing and Analysis* - J.Spacecraft and Rockets, Vol. 24, No. 1, pp 33-39.
- [4] Siemers, P.M. III, Wolf, H., Henry, M.W. (1988) *Shuttle Entry Air Data System (SEADS) - Flight Verification of an Air Data System Concept* - AIAA 4th Flight Test Conference, Paper 88-2104
- [5] ESDU (1983) *The correction of flight test anemometric data* - ESDU International. Data Item 83029.
- [6] Srinivasan, S., Tannehill, J.C., Weilmuenster, K.J. (1987) *Simplified Curve Fits for the Thermodynamic Properties of Equilibrium Air* - NASA RP 1181
- [7] Brailsford, E.N. (1992) *In-flight evaluation of Mach number at hypersonic speeds* - Aeronautical J., pp 152-156.
- [8] ESDU (1989) *Derivation of primary air data parameters for hypersonic flight* - ESDU International. Data Item 88025.
- [9] Haerings, E.A.Jr. (1992) *Airdata Calibration Techniques for Measuring Atmospheric Wind Profiles* - J. of Aircraft, Vol. 29, No. 4, pp 632-639.
- [10] Hinze, J.D. (1959) *Turbulence, An Introduction to its Mechanism and Theory* - McGraw Hill
- [11] Yanta, W.J., Gates, D.F. (1971) *The Use of a Laser Doppler Velocimeter in Supersonic Flows* - AIAA Paper 71-287
- [12] Hayes, W.D., Probstein, R.F. (1966) *Hypersonic Flow Theory, Volume I: Inviscid Flows* - Academic Press, New-York.

## HYPERSONIC AERODYNAMIC/AEROTHERMAL TEST FACILITIES AVAILABLE IN EUROPE TO SUPPORT SPACE VEHICLE DESIGN

D. Vennemann\*  
ESA/CNES MSTP Team  
Centre Spatiale de Toulouse  
18, Av. Edouard Belin  
31055 Toulouse Cedex, France

### SUMMARY

The paper gives an overview of the major hypersonic wind-tunnels available in Europe for the determination of aerodynamic characteristics, like forces and moments, or for the measurement of heat transfer rates and heat transfer distributions of space vehicle configurations. The following facilities are presented:

- the blow-down wind-tunnel S4 of ONERA at Modane, France,
- the longshot facility of the Von Karman Institute at Rhode-Saint-Genèse, Belgium,
- the shock tunnel TH2 of the Aachen Technische Hochschule RWTH, Germany,
- the piston-driven wind-tunnel HEG of DLR at Göttingen, Germany,
- the hot shot test facility F4 of ONERA at Le Fauga, France.

The operating principle of each of these facilities is being described, the performance characteristics given and the main features of their construction high-lighted. This is followed by a short presentation of some advanced optical measurement techniques available for use in the facilities like the electron beam technique, the laser induced fluorescence technique LIF, the tunable IR laser diode, and holographic interferometry.

### 1. INTRODUCTION

In any aerospace project ground testing in wind-tunnels plays an important role throughout all phases by providing detailed inputs to the designer on performance and flight qualities of the configuration under development. In order to be able to make this important contribution, wind-tunnels must simulate as closely as possible on reduced scale models what happens during the flight of the real air- or spaceplane. The quality of such simulation is governed by so-called "similarity" laws containing similarity parameters like MACH Number and REYNOLDS Number to name the most commonly known. A wind-tunnel test on the model of a conventional aircraft is "correct" if the ground simulation is performed at the Mach and Reynolds Number of the full scale version. In the case of Reynolds Number which is defined as the ratio of the product of air density times a characteristic length of the body (for example wing chord) and the air viscosity, the wind-tunnel test must compensate the much smaller model wing chord by an increase of density, by a decrease of viscosity or a combination of both, so that

the ground test and the flight happen at the same value of Reynolds number.

A spaceplane, when re-entering into earth atmosphere, passes through several different flow regimes, each of them governed by different similarity laws and therefore often requiring specialized test facilities for representative simulation.

In the following, after a brief description of the different flow regimes encountered during re-entry, we will focus on the simulation requirements for the "hot phase" of re-entry and then we will present the operating principle and the main features of the five major wind-tunnels which are available or under development in Europe to cover these particular simulation needs. An associated effort concerning the parallel development of measurement techniques for these facilities is described and a few examples are presented.

### 2. FLOW SIMULATION REQUIREMENTS

Space vehicles encounter largely different flow conditions during their flight as depicted in **Figure 1**, taken from reference 5. In case of a re-entry vehicle for example they are varying from highly rarefied flow at high altitudes where the atmosphere is "thin" (low density) to the classical Mach-Reynolds flow regime nearer to ground.

Coming down initially through a zone of low ambient air density using jet control, the vehicle experiences increasing density. This flow is characterized by a thick boundary-layer which interacts with the inviscid external flow. Usually we call this flow regime the "viscous interaction regime". Viscous interaction can have important effects on the surface pressure distribution and hence affecting lift, drag and stability. In addition skin friction and heat transfer are increased.

Next, at further increasing densities, the space vehicle decelerates rapidly and traverses a zone where the nitrogen and oxygen molecules of the air are dissociated behind the bow shock caused by the vehicle. This is the period where heat load is highest. The flow regime is sometimes called the "hypervelocity regime". The dissociation of the flow and the associated potential recombination of molecules are called high temperature effects.

---

\* seconded into MSTP Team by DLR Cologne, Germany

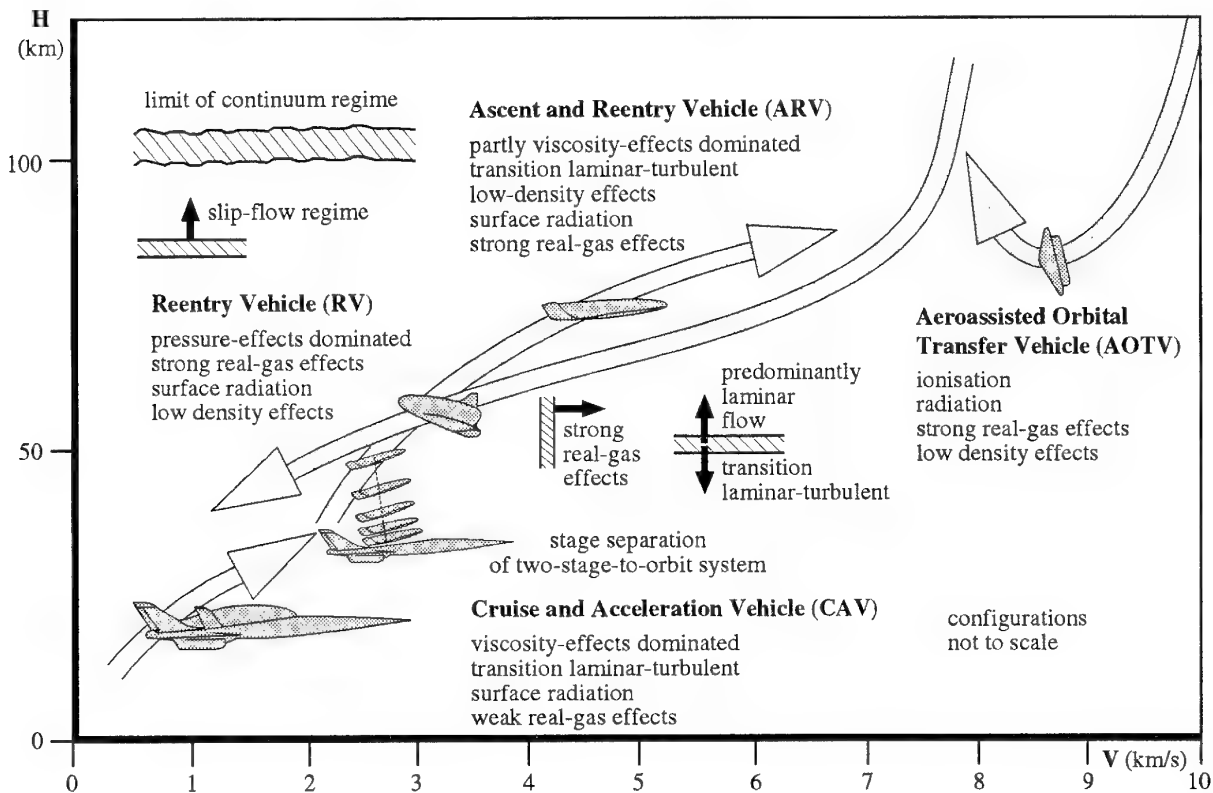


Figure 1. Flow Phenomena and different categories of hypersonic vehicles

Then we approach a flight situation where classical Mach-Reynolds effects occur. The flight speed is already significantly reduced and the vehicle moves in the denser atmosphere close to ground. This flow is dominated by the state of the boundary-layer (laminar, transitional, turbulent), the wall temperature ratio having significant influence. The physical laws governing the flow behavior are relatively well known.

Ground simulation in the hypervelocity regime is particularly important because it is here that the heat loads on the vehicle surface are highest and therefore need to be known accurately in order to allow an adapted design of the thermal protection. As indicated above, dissociation and recombination of oxygen and nitrogen are the predominant mechanisms in this flow regime. The test facility must therefore use air as a test gas flowing at speeds between 3 and 8 km/s. In addition, the simulation of high-speed chemically reacting flows with dissociation and recombination occurring requires the duplication of the number of intermolecular collisions necessary to dissociate a molecule or to recombine two atoms. Investigations have shown that dissociation is a result of collisions between two partners and therefore dissociation simulation is governed by the so-called binary scaling parameter which is the product of density and linear size ( $\rho \times L$ ) of the flow field looked at.

To simulate correctly recombination effects three-body collisions are required which make it necessary to

duplicate the product of density squared times linear size ( $\rho^2 \times L$ ) in addition to speed. Thus, in a given ground experiment with a reduced scale model, binary and three-body collisions can not be simulated at the same time.

A test set-up for binary scaling will have the three-body reactions proceeding relatively too fast.

The complexity of the technical challenges presented by hypersonic systems, the lack of adequate ground test facilities, the cost and the risk of flight testing, and the advent of more and more powerful hard- and software for computation and simulation of physical phenomena enforces (and makes possible) an integrated and coordinated use of the "triad" [4] of ground testing, flight testing and computation and simulation. The widely adopted strategy consists of

- testing in dedicated facilities chosen according to the flight regime of interest,
- calculating the conditions and results of experiments to validate the codes,
- cross-checking these codes with flight results,
- applying the codes to real case re-entry.

The following chapter will first describe briefly the role of ground testing within the 'triad'. Then more information regarding test or simulation requirements for hypersonic flight will be provided. And finally the major difficulties associated with hypersonic test facilities will be mentioned.

### 3. HYPERSONIC GROUND TEST REQUIREMENTS

Following the needs of the development process for a space vehicle, two different classes of ground test facilities can be distinguished. The 'Research and Development Test Facilities' are used in the early phases of a project to help the understanding of the basic physical phenomena and to aid in the development and validation of computer codes. Therefore it is important to have well defined flows and to provide for non-intrusive high-resolution diagnostics of the flow properties. Typically these facilities can be small and do not need long testing times.

'Engineering Development Facilities' become necessary in later phases of a project to validate the design by evaluation of system durability and operability. Large or full-scale hardware must be tested in adequately defined flow conditions. But global measurements are usually sufficient.

Figure 2, reproduced from reference [4], represents the ground test simulation requirements for hypersonic flight. The list shows the basic types of test, the corresponding test and simulation requirements and the necessary test times.

For R & D type testing these requirements most often can be met with some difficulties, but as soon as engineering development is concerned, the test engineer faces a major challenge. He undertakes to provide adequate measurements for test analysis and code comparison while trying to achieve simultaneously the correct velocity in the correct gas, at sufficient scale and adequate run times.

Most of the inadequacies of hypersonic facilities arise from the need to provide very high temperatures and pressures for simulation. Therefore the devices to add energy to the flow are a key issue and several new concepts are under investigation.

In the following chapter a description of the major hypersonic facilities available in Europe for 'aerodynamic/ aerothermal' type testing is given. These facilities were selected by the European Space Agency ESA to perform work related to 'Hypersonic ground testing comprehension and use for design'. The aim of this program is on the one hand to improve the understanding of hypersonic nozzle flow over a wide range of parameters and on the other hand to test generic models in these then well known flows to provide data for code validation. The program provides also for some improvement of the facilities.

| TYPE OF TEST   | REQUIREMENTS   | SIMULATION   |                                | TEST TIME REQUIRED |
|--|--|--|--------------------------------|--------------------|
|  |  | DUPLICATE  | RELAX                          |                    |
| <b>AERODYNAMIC</b><br>• Classical<br><br>• Real gas chemical effects | • Reproduce force coefficient, pressure, & heating distributions                                     | • Mach   | • Temperature<br>• Reynolds N° | Milliseconds       |
|  | • Evaluate effects of dissociated flows on aerodynamics measurements                                 | • Gas composition<br>• Temperature<br>• Density X Length<br>• Mach N°                  | Run time                       | Milliseconds       |
| <b>AEROTHERMAL</b>   | • Duplicate heating rates and aero-shear, full size hardware   | • Total temp.<br>• Surface pressure  | Mach N°                        | Minutes            |
| <b>AEROPROPULSION</b>  | • Conditions for proper chemical reactions, mixing, boundary layers & shocks<br>• Full-size hardware | • Gas composition<br>• Pressure<br>• Temperature<br>• Mach N°<br>• Velocity<br>• Scale |                                | Minutes            |
| <b>STRUCTURE AND MATERIALS</b>                                       | • Combined loads (mechanical, thermal, acoustics)<br>• Temperature gradients                         | • Loads<br>• Temperature<br>• Heating rates  | Flow vel.                      | Minutes            |
| <b>IMPACT</b>  | • Target interaction<br>• Debris propagation   | • Relative velocity<br>• Mass  |                                | Microseconds       |

Figure 2. Test and Simulation Requirements for Hypersonic Flight

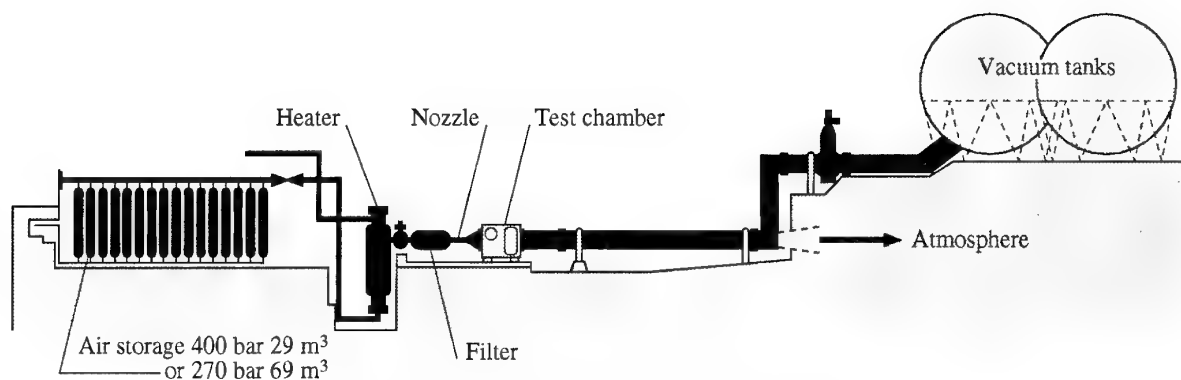


Figure 3. Blow down Wind-Tunnel S4 of ONERA

#### 4. TEST FACILITIES IN EUROPE

In the following we want to concentrate on the major test facilities available in Europe for 'Aerodynamic' and 'Aerothermal' types of test. First their operating principle will be explained and then their basic layout will be described.

##### 4.1 Blow-Down Wind-tunnel S4 of ONERA [6]

###### 4.1.1 Facility Operating Principle and Layout

In a typical blow-down wind-tunnel cycle air is compressed to high temperature, dried, and then stored in large tanks. In parallel a large mass of ceramic pebbles is heated to high temperatures by a gas-fired burner. A run is initiated by opening a throttling valve, which allows high pressure air from the storage tank to flow through the pebble bed, heating up there, and then expanding this heated gas through a convergent-divergent nozzle to the desired hypersonic Mach number. Typically tunnels employing this operating principle allow settling chamber temperatures just high enough to avoid liquefaction of the test gas in the test section.

The S4 facility (Figure 3) uses the 29 m<sup>3</sup> storage tank of the ONERA Modane test center which allows pressures up to 400 bar. The pebble bed heater of 2 m diameter and a height of 10 m contains 12 tons of aluminum pebbles which can be heated up to a maximum temperature of 1850 K by combustion of propane. The air leaving the heater passes through a 10 micron filter

to retain the dust particles originating from the pebbles. Three hypersonic nozzles are available. The Mach 6.4 nozzle is 3.6 m long, has a throat diameter of 75 mm and an exit diameter of 685 mm. The Mach 10 and the Mach 12 nozzles employ the same hypersonic exit section with an exit diameter of 994 mm. The interchangeable throat section has a diameter of 36 mm in the Mach 10 case and of 21.5 mm in the Mach 12 case. Both nozzles are about 7 m long. The cubic test section of 3 m side length houses the model support which provides an incidence range of  $\pm 15$  degrees at 2 to 5.5 degrees/second and a side slip range of  $\pm 50$  degrees at 2.8 to 11 degrees/second. A rapid injection device allows to inject the model into position once the flow in the nozzle is fully established, thus avoiding the heavy loads caused by the flow starting process. The model can also be retracted rapidly before the flow stops. Downstream of the test section the flow is recollected in a diffuser and either blown to atmosphere or collected in vacuum vessels of 3000 or 4000 m<sup>3</sup> volume.

##### 4.2 Longshot Facility of VKI

###### 4.2.1 Facility Operating Principle and Layout

This facility, fully described in [7] and sketched in Figure 4, is a heavy piston gun tunnel, consisting of a 12.5 cm bore, 6 m long driver tube (initially pressurized with dry nitrogen to 300 bar at room temperature) and of a 7.5 cm bore, 27 m long driven tube (initially

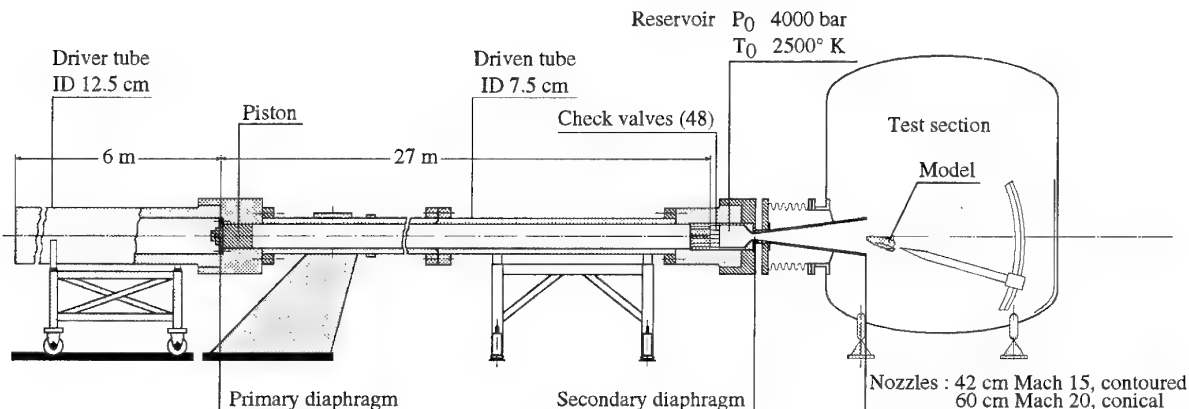


Figure 4. Longshot Facility of VKI

pressurized with dry nitrogen to about 1 bar at room temperature). These two parts are separated by a heavy piston with a mass of 1.8 to 9 kg, which is held at its initial position by an aluminum diaphragm. Rupture of this diaphragm releases the piston, which is shot down the driven tube, thereby compressing the nitrogen gas in front of it into a 320 cm<sup>3</sup> reservoir, where pressures as high as 4000 bar and temperatures up to 2500 K may be attained. The compressed gas is trapped in the reservoir by the automatic closure of 48 poppet valves. The subsequent bursting of a secondary copper diaphragm located in the converging part of the contoured hypersonic nozzle allows the test gas to expand to Mach 14 into a 16 m<sup>3</sup> test section, depressurized to a high vacuum (5 mm Hg) before the test. The diameter of the nozzle exit is 42.7 cm, and that of the core of uniform Mach number is 24 cm. Due to the small reservoir volume, the useful duration of a test is limited to about 10 to 15 ms, and the test conditions continually evolve with time.

To define the test conditions, the reservoir pressure and the pitot pressure in the test section are measured. The reservoir temperature is derived from a measurement of the heat transfer rate at the stagnation point of a spherical probe located in the test section.

The test model is sting-mounted in the test core. Two different stings are available, a 1.2 m long one, supported on a circular sector mount, and a shorter one (0.5 m long), supported on the upper platform of a 5-degrees of freedom orientation mechanism.

### 4.3. Shock Tunnel TH2 of RWTH Aachen [8]

#### 4.3.1 Shock Tunnel Operating Principles

A shock tunnel consists of a driver, driven section, nozzle, and dump tank with test section. **Figure 5** shows schematically the set-up of the Shock Tunnel TH 2.

Driver and driven section are separated by the main diaphragm. The driver section is filled with the so-called driver gas, usually helium. The driven section contains the test gas, usually air.

Typical driver pressures are between 100 and 1500 bar and driven gas pressure between 0.1 and 10 bar. Before the test starts the dump tank is evacuated. Driven

section and receiver tank are separated by another, thin diaphragm to avoid the inflow of the test gas into the dump tank before the test starts.

To initiate a run the diaphragm is burst by a simple mechanical device. A shock wave propagates into the test gas compressing it to higher pressure and increasing its temperature. A few milliseconds after the bursting of the diaphragm the incident shock wave arrives at the end wall of the driven section. The shock tunnel at Aachen operates in the reflected mode, i.e., the incident shock wave is reflected at the end wall and thereafter propagates upstream. During this reflection process the second diaphragm between driven section and nozzle bursts and the nozzle flow starts. The flow velocity behind the reflected shock is zero to a first approximation if the outflow from the nozzle is neglected. The complete kinetic energy of the shock heated gas is thus converted to high temperature and pressure behind the reflected shock. The compressed test gas having a temperature of a few thousand degrees centigrade expands subsequently through the nozzle. The high stagnation enthalpy is thus converted to a high free stream velocity in the test section.

After a short time the reflected shock interacts with the contact surface. During this interaction usually new waves are generated which are propagating again downstream towards the end wall while the reflected shock moves with changed velocity further upstream. In the case of a special combination of the initial parameters the reflected shock penetrates the contact surface without generating waves of finite amplitudes, the so-called tailored interface case. In the tailored interface case the nozzle reservoir pressure and temperature produced by the initial reflection of the incident shock at the endwall persists for a relatively long time.

In the undertailored case the incident shock Mach number is lower than for the tailored case. In this case an expansion wave is generated when the reflected shock and the contact surface interact. In the overtailored case the incident shock Mach number is higher than in the tailored case. This leads to a secondary reflected shock and a transmitted shock which are generated by the interaction of the initial

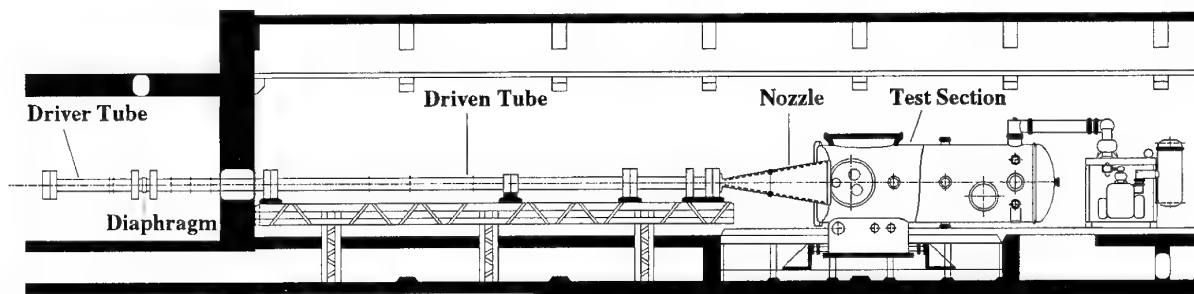


**Figure 5.** Shock tunnel of RTWH Aachen



reflected shock and the contact surface. The secondary reflected shock again reflects at the end wall and in this way a region of multiple reflections develops which leads to an equilibrium nozzle reservoir pressure. The Shock Tunnel TH 2 is operated in the tailored and over-tailored interface mode but undertailored operation is also possible.

#### 4.3.2 TH2 Facility Layout

The shock tube of the Aachen shock tunnel has an inner diameter of 140 mm with a wall thickness of 80 mm. The lengths of the driver and driven section are 6 m and 15.4 m. The building which houses the shock tunnel was built especially for the use of such tunnels. A 800 mm steel-enforced concrete wall which separates the rooms for driver and driven section serves as a protecting wall but is also used for supporting the recoil absorbing system of the tunnel. There is a gliding joint between the driven section and the nozzle. The nozzle and dump tank form one unit which is also fixed by a recoil damping system to the foundation. The model support has an independent foundation. Thus even if the receiver tank may move the model support is fixed to the laboratory foundation.

Driver and driven section are separated by a double-diaphragm chamber which at maximum pressures utilizes two 10 mm thick stainless steel plates as diaphragms scored in the form of a cross by a milling cutter. Another diaphragm of brass or copper sheet is located between the driven section and the nozzle entrance. The maximum operating (steady) pressure of the complete tube is 1500 bar. The driver can electrically be heated to a maximum temperature of 600 K. The exit diameter of the conical nozzle amounts to 572 mm. Two other truncated cones allow nozzle exit diameters of 1 m and 2 m. The nozzle throat diameter and therefore the test section Mach number can also be changed by inserting different throat pieces. Furthermore a contoured nozzle of 586 mm exit diameter and a nominal Mach Number of 7 is available.

### 4.4 The High Enthalpy Facility (HEG) [11, 12]

#### 4.4.1 Free piston driver technique

The HEG operates according to the shock tunnel

principle also but the designers aimed at much higher enthalpies than in the Aachen facility. To generate the desired level of reservoir enthalpies, shock speeds of the order of 5 km/s are needed. For this level of shock speeds the driver gas must be heated also. Typically, if helium is chosen as driver gas, its temperature must be of the order of 4000 K. This can only be achieved by a short duration method, and the technique chosen for HEG is the adiabatic compression of the driver gas with a piston.

Details of the free-piston driver technique, its performance and limitations, are described by Stalker [14].

#### 4.4.2 HEG Facility Layout

A schematic view of the High Enthalpy facility in Göttingen is presented in **Figure 6**. The free piston shock tunnel arrangement consists of three main sections: the "driver", consisting of an air buffer and a compression tube, the shock tube and the nozzle with a large test section downstream.

The facility operation proceeds as follows: First, high pressure air in the air buffer is used to accelerate a heavy piston down the compression tube thereby heating the driver gas adiabatically. Usually, pure helium is used as driver gas. When the desired pressure is reached, a diaphragm at the downstream end of the compression tube ruptures, causing a shock wave to propagate down the shock tube. This shock wave reflects at the end of the shock tube leaving behind a region of gas at high temperature and pressure, the reservoir conditions, which are maintained "constant" for about 1 millisecond. From these reservoir conditions the gas expands through a convergent-divergent contoured nozzle into the test section where the models to be investigated will be mounted.

The driver consists of a 0.55 m inner diameter tube of 33 m length in which the piston can move freely. The air buffer is "wrapped" around to reduce the required building length and has a volume of 5 m<sup>3</sup>. A steel diaphragm separates the compression tube (driver) from the shock tube. 500, 1000, 1500 and 2000 bar were selected as rupture pressures. With a compression ratio of 60 the desired density range can be obtained. In order to be able to operate "tuned" piston condition at these four different pressure levels, four pistons of different

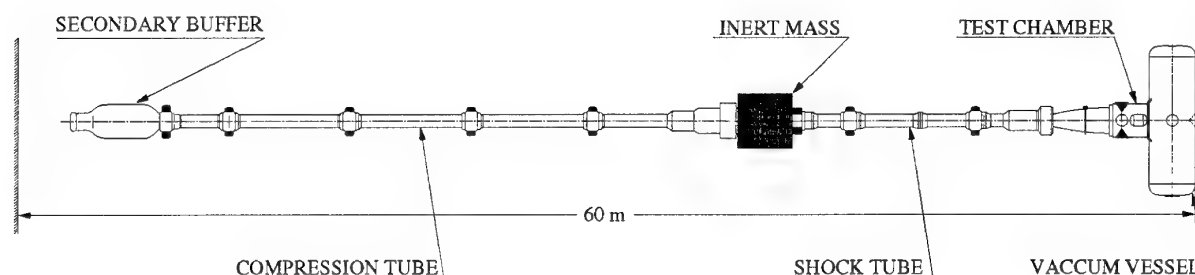


**Figure 6. High Enthalpy Facility of DLR**

mass are planned. With that, it will be possible to maintain the driver pressure constant for at least 1 ms. The shock tube with its internal diameter of 0.15 m has a length of 17 m. In order to get some flexibility to optimize the driver operation, an interchangeable orifice is mounted at the inlet of the shock tube controlling the driver gas pressure by restricting the flow rate into the shock tube.

At the downstream end of the shock tube the reservoir condition will exist for about 1 ms. This is a region of very high loading because here maximum pressures of around 2000 bar and temperatures of up to 14000 K will occur.

The nozzle is contoured and was designed for operation at Mach 7-8 giving the required air speed and density at the location of the model. With a throat diameter of 22 mm and an outlet diameter of 880 mm the useful core of the flow is large enough to accommodate HERMES models of 30 to 40 cm length. The overall length of the nozzle is 3.75 m.

The test section with a diameter of 1.5 m is equipped with a model support allowing a variation of the angle of attack of the models. Eight viewing ports give optical access to the model flow field.

#### 4.5 F4 Hot Shot Facility [9, 11]

This chapter explains the hot-shot driver technique used to create the necessary reservoir conditions for the F4 facility which is followed by a description of the wind-tunnel lay-out.

##### 4.5.1 Hot-shot driver technique.

The hot-shot driver technique uses a true reservoir with a volume of several liters. This volume is initially filled with the test gas, air in our case, at pressures selected according to the final pressure level desired. The air is heated up and further compressed with an electric arc ignited between two electrodes integrated in the wall of the arc chamber surrounding the volume of air. The duration of the arc can be varied so that more or less energy can be transferred to the gas according to the desired reservoir conditions.

##### 4.5.2 F4 Facility Layout

A schematic view of the F4 facility at ONERA, Le Fauga is presented in **Figure 7**. The hot-shot wind-tunnel arrangement consists of the following main elements:

- the impulse machine (not shown)
- the arc chamber
- the convergent-divergent nozzle
- the test section where the model can be mounted
- the diffuser
- the vacuum tank

The facility operation proceeds as follows: First the alternator of the impulse generator, acting as a motor accelerates the fly wheel to its nominal speed. Then the alternator in generator mode decelerates the fly wheel thus providing the electric energy to the arc chamber which has previously been filled with pressurized air.

The electric arc between the arc chamber electrodes heats and further pressurizes the air until a high reservoir pressure is reached. Then a plug placed in the throat of the nozzle which is connected to the arc chamber is exploded and the hot gas can expand from the volume through the convergent-divergent nozzle to the test section where the model will be mounted. Downstream of the model the gas is recollected, decelerated and flows into the vacuum tank from where it will be exhausted after the test.

The impulse machine consists of a fly wheel with a mass of 15 tons which is coupled to an alternator of 150 MW. Functioning as synchronous motor with variable frequency the alternator accelerates the fly-wheel to 6000 RPM which represents an energy storage of 400 MW. The motive electric circuit is then disconnected and the rotor is excited for generator action supplying DC current to the electrodes of the arc chamber via rectifiers and high speed switches.

The arc chamber is a cylindrical container designed for pressures up to 2000 bar. At each end of the cylinder electrode holders close the volume. These holders can be set in different positions that the volume can be

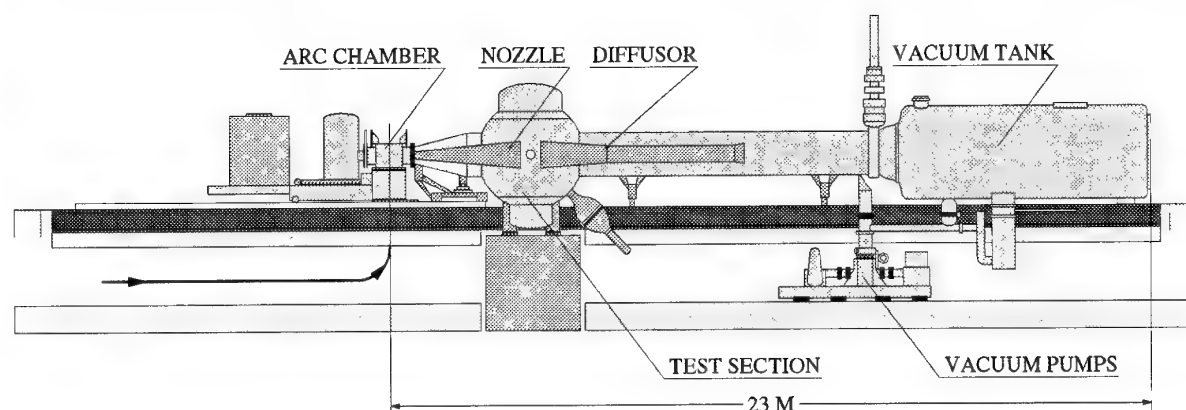


Figure 7. Hot Shot Facility F4 of ONERA

chosen between 4 to 15 liters according to the run duration desired. The electrodes have spiral form and by that create a magnetic field which makes the electric arc rotate in order to reduce the erosion rate of the electrodes. The arc is initiated with the help of an electric wire and is usually maintained for about 30 to 90 ms. The set reservoir pressure, when the plug in the nozzle throat is exploded, is reached just before the arc is switched off. The arc chamber can be quickly evacuated into a dump tank when the projected test time (20 to 100 ms) is over in order to avoid too much pollution of the test section by the remaining gas having been in contact with isolation materials for the longest time.

Four different nozzles are available to cover the specified flow regimes with exit diameters ranging from 430 to 860 mm. For the first tests an existing nozzle (no.1) was used with a design point at Mach 16. It has a 6.3 mm copper-tungsten throat and a contoured supersonic part out of steel near the throat, and out of fiberglass near its exit of 670 mm diameter. Nozzle no.2 is identical with no. 1 with the exception of the throat which has 10 mm diameter. Nozzle no.3 with an outlet diameter of 430 mm will provide the highest values of the binary scaling parameter ( $\rho \times L$ ). The nozzle no.4 with an exit diameter of 860 mm will be available for viscous interaction simulation. According to these nozzle sizes Hermes models of 1/45th to 1/50th scale could be mounted and tested in the test section.

The test section is equipped with an adjustable or with an actuated model support which can change the angle of attack of the model by 20 degrees in 50 ms. Due to the relatively lower energy level of F4 with respect to HEG testing times can be longer in F4 and with 20 to 100 ms they are long enough that force measurements with balances in the model can be made.

## 5. SIMULATION CAPABILITY OF FACILITIES

The principal characteristics of the five test facilities described above are summarized in **Figure 8**. As can be seen from the nozzle exit dimensions none of these facilities can be counted among the 'Engineering Development Facilities', although F4 and HEG are among the largest facilities of their kind in the world.

For the purpose of presenting the simulation capabilities of our facilities versus simulation requirements, the HERMES re-entry trajectory is used because of two reasons:

- The S4, the TH2 and the Longshot facilities were modified for their use in the HERMES program and the F4 and the HEG facilities were newly constructed.

- The trajectory is that of a low L/D vehicle and therefore can be regarded as roughly representative of the vehicle configurations actually under consideration at the European Space Agency.

| NAME OF FACILITY           | OPERATOR    | COUNTRY | TEST GAS  | MACH N°   | NOZZLE EXIT DIAMETER (m) | MAX. TOTAL PRESSURE (MPa) | MAX. TOTAL TEMPERATURE (K) | RUN TIME (s)  |
|----------------------------|-------------|---------|-----------|-----------|--------------------------|---------------------------|----------------------------|---------------|
| BLOW-DOWN FACILITY S4      | ONERA       | FRANCE  | AIR       | 6, 10, 12 | 0.7, 1.0                 | 15                        | 1100 (1500)                | 30 - 100      |
| LONGSHOT FACILITY          | VKI         | BELGIUM | N2, (CO2) | 14, 20    | 0.43, 0.60               | 400                       | 2500                       | 0.005 - 0.01  |
| SHOCK TUNNEL TH2           | RWTH AACHEN | GERMANY | AIR, N2   | 7, 6 - 12 | 0.6, 1.1, 2.0            | 63                        | 4700                       | 0.002 - 0.009 |
| HIGH ENTHALPY FACILITY HEG | DLR         | GERMANY | AIR, N2   | 7         | 0.8                      | 180                       | 10000                      | 0.001         |
| HOT SHOT FACILITY F4       | ONERA       | FRANCE  | AIR, N2   | 9 - 18    | 0.43, 0.67, 0.93         | 200                       | 5500                       | 0.02 - 0.1    |

**Figure 8. Principal characteristics of hypersonic test facilities**

**Figure 9** places the performance envelopes of the five facilities on a Reynolds-Mach number map. The Reynolds numbers of each facility are calculated for the model length L of a typical model that can be tested in the particular test facility. The re-entry path representing the simulation requirements is calculated for a length L=15.5m. Model scales vary between 1/60 for the smallest facility to 1/40 for the largest. The graph also shows lines of constant rarefaction

parameter (dashed) and of constant viscous interaction parameter (solid). Furthermore a boundary between 'strong' and 'weak' viscous interaction (reciprocal influencing between boundary layer and outer inviscid flow field) is shown. As viscous interaction can have important effects on the surface pressure distribution over the vehicle and through that can affect lift, drag and stability, it is important to be capable to test on both sides of this boundary.

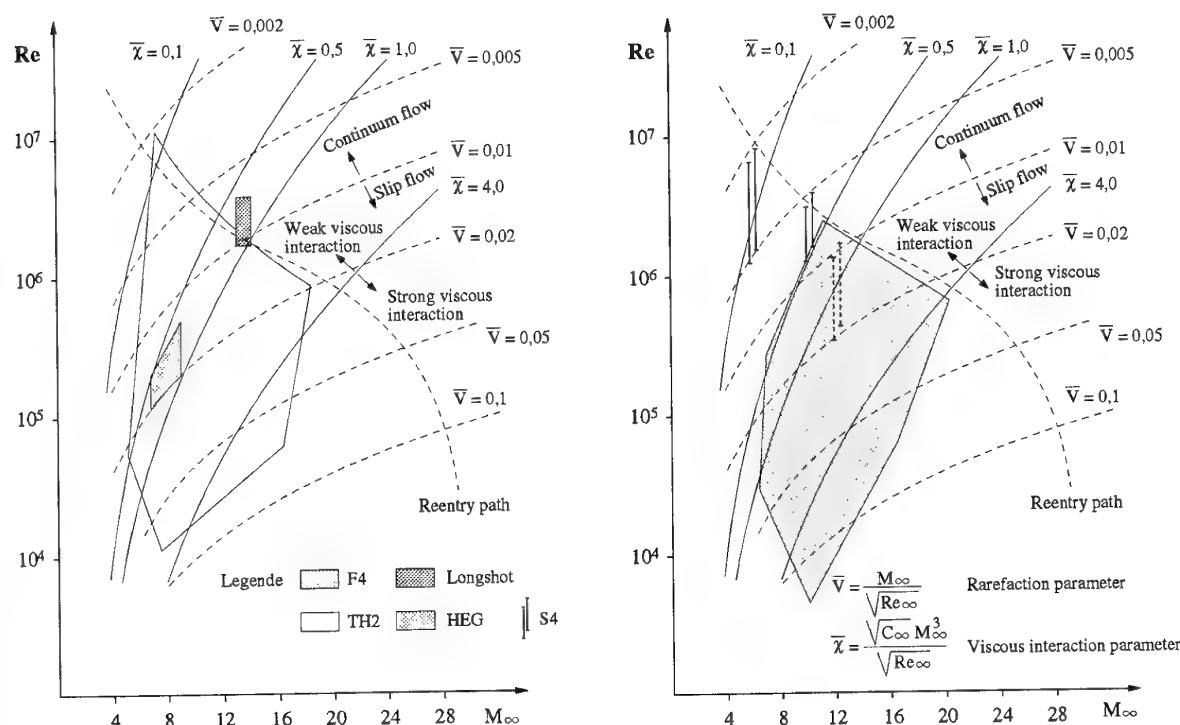


Figure 9. Performance Envelopes of TH2, HEG, S4, F4 and the Longshot

Figure 10 shows the simulation capability of our facilities with respect to the binary scaling factor  $\rho \times L$  (free stream gas density times length of the body). Here again  $L=15.5m$  was taken as reference length for the reentry trajectory and typical model lengths for the different facilities.

The very high kinetic energy and the correspondingly high temperatures of hypersonic flight cause vibrational excitation or dissociate the diatomic components of the air. Thus the gas can not be regarded as 'ideal' anymore. The binary scaling factor is an often scaling factor for the simulation of real gas effects, which can significantly change the flow around the space vehicle.

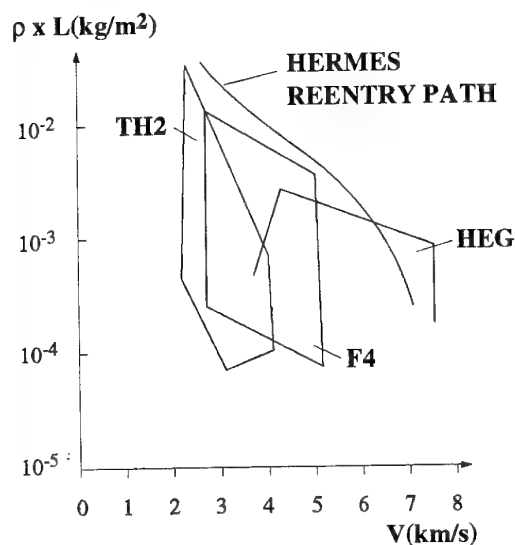


Figure 10. Binary Scaling performance

As can be seen from the simulation capability of TH2 and from the projected capabilities of F4 and HEG duplication of  $\rho \times L$  is nearly possible over the full range of oxygen and nitrogen dissociation. For this simulation the other two facilities are not used.

The simulation capabilities presented above determine the role of each facility within our research effort related to 'Hypersonic ground testing comprehension and use for design': The blow-down facility S4 serves as 'cold' hypersonic reference case. Viscous interaction effects are mainly studied in the hot shot facility F4 and real gas effects are studied in the High Enthalpy Facility HEG and in F4 (using the appropriate nozzle). The shock tunnel TH2 can be described as a go-between. It allows viscous interaction studies on the one hand and enlarges the range of simulation for real gas effects on the other hand. The longshot facility plays a particular role in that it is used for 'variable gamma' testing to study deviations from ideal gas behavior.

One more test facility is participating in the effort: the hypersonic wind-tunnel TCM2 of the Université de Provence at Marseille, France [13]. Being a free piston driven facility like HEG but of much smaller size it was not included in this presentation.

Our effort is to be seen within the 'triad' of ground testing, flight testing and computation mentioned in chapter 2. The aim is to provide a thorough characterization of the flow in these wind-tunnels over their full operating range- in the TH2 we even participate in the extension of its operating range by adding a detonation driver [10] - and to choose standard operating conditions.

We add instrumentation and enhance our testing and measurement capabilities. This goes hand in hand with a computational reconstruction of the nozzle flow, the results of which then can be used as input for flow computation over wind-tunnel models. A blunted cone 'ELECTRE' was chosen as standard model to undergo

testing in all facilities. **Figure 11** shows the basic geometry of this model. Flight test data are available for comparison. Other generic models like spheres or a hyperbolic flare the geometry of which is also shown in Figure 11, will be tested.

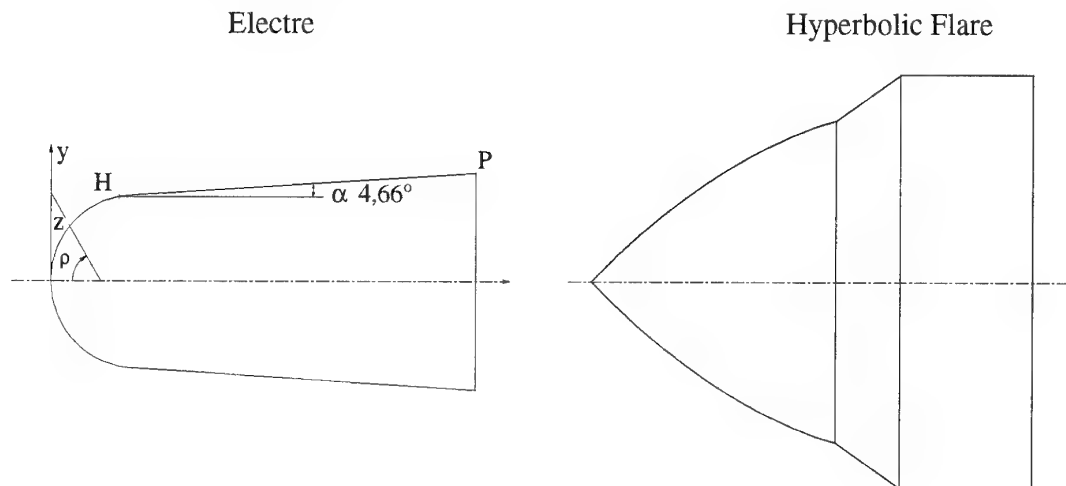


**Figure 11.** Standard model geometries

## 6. MEASUREMENT TECHNIQUES

The five test facilities are well equipped with the usual pressure, and heat transfer gauges to probe the oncoming flow. Acceleration compensated sting mounted balances are available in the S4, the F4, the TH2 [23] and the Longshot facility [16] for force measurements. An effort is being made to develop a mass flow probe in the TH2 facility. IR thermography [21] can be used for heat flux measurements.

In general, there is an intense exchange of experience and new developments, although being done in a particular wind-tunnel, are always developed in view of their application in the other tunnels.

Special attention was and is given to the development and use of non-intrusive optical techniques. Besides being non-intrusive several of these techniques are capable of providing locally detailed information on temperatures or number densities. Flow velocities can be probed as well. The major methods being worked on are

- Electron Beam Fluorescence
- Laser Induced Fluorescence
- Raman Spectroscopy
- Tunable IR Laser Diode
- Holographic Interferometry

The first three methods provide local information whereas the latter two give information integrated along the light path. Work on the application of Raman Spectroscopy is the least advanced the other methods are more or less operational. They will be highlighted in the following.

### 6.1 The Electron Beam Technique

This technique [15] is widely used in hypersonic experimental aerodynamics to measure species concentrations and temperatures. A high-energy electron beam (20 to 50 keV) is passed through the flow to be probed. The electrons of this beam excite the molecules of the gas flow from their basic electronic energy level to a higher but unstable level. From this elevated level the molecules fall back to a stable energy state by spontaneously emitting light. Within given limits, the intensity of the emitted light is proportional to the gas density. Spectroscopic analysis of the light gives access to the vibrational and rotational energy states, and thus allows one to measure vibrational and rotational temperatures which, as noted previously, differ from one another in the hypervelocity regime because the internal degrees of freedom of the molecules are not in equilibrium.

**Figure 12** is a schematic of the electron beam apparatus setup in F4 [19]. The electron gun is directed perpendicular to the flow and can be moved along the flow axis in front of a model in the wind tunnel. For density measurements or flow visualization, the beam can be shifted periodically along the flow axis, exciting a two-dimensional plane. This light is focussed via a lens system on a CCD camera, from which the data can be stored on magnetic tape.

For temperature measurements on the nitrogen molecules in the flow, the light from the static beam is focussed via a lens system into a spectrometer, which registers the light intensity emitted as a function of

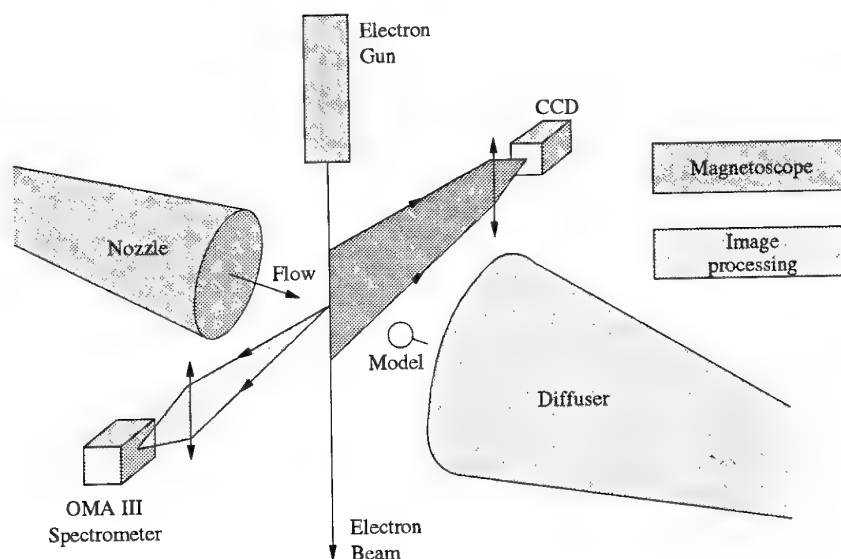


Figure 12. Electron Beam Setup

wavelength. At a moderate wavelength resolution, the relative intensities of two suitable vibrational lines give access to the vibrational temperature of nitrogen. By further resolving one such vibrational line, the rotational fine structure of the nitrogen molecule becomes accessible and, via its analysis, the rotational temperature can be deduced.

The electron-beam technique is basically a low-density technique and so cannot be reasonably employed at densities above 0.001 kg/m<sup>3</sup>. It therefore covers only the low pressure operating range of the F4 facility. Outside this range, other methods are being used.

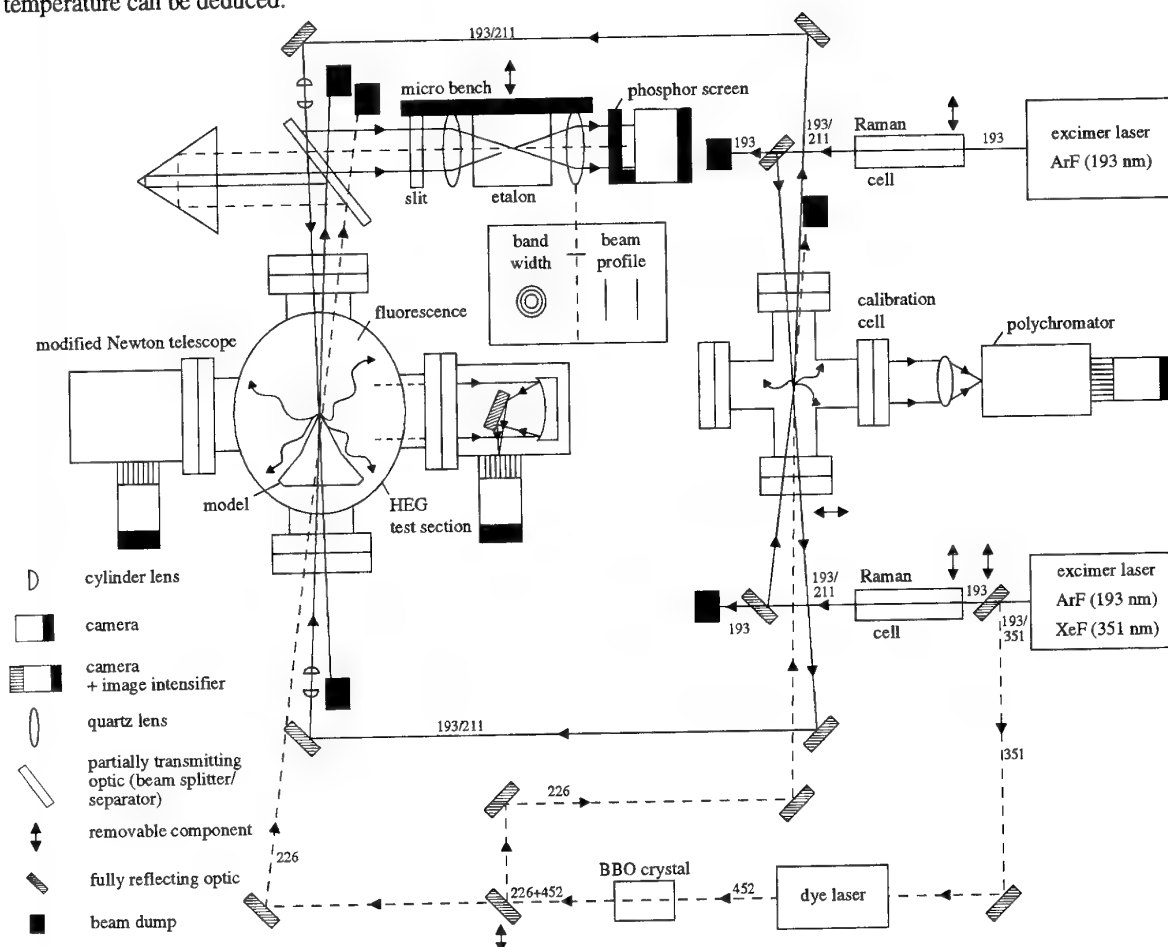


Figure 13. Laser Induced Fluorescence Setup

## 6.2 Laser Induced Fluorescence

The Laser Induced Fluorescence Method, in contrast to the electron beam technique, is capable of selectively exciting particular molecular states. The resulting emission of light can be spectrally analyzed and gives information on the internal energy state of the selected molecule. A Laser Induced Fluorescence apparatus capable of local measurements of species concentrations and temperatures in the free stream and in model flow fields placed in this flow is being developed for the High Enthalpy Facility HEG [18].

A schematic of the LIF apparatus is given in **Figure 13**. For NO measurement (2D), the beams of the two excimer lasers are formed to sheets and crossed in front of the model in the HEG test section. The emitted fluorescence is captured by an image-intensified, gated camera system via a modified Newton telescope with a large light gathering power. The lasers are fired sequentially (time separation  $< 1 \mu\text{s}$ ) so that the fluorescence arising from one laser beam is captured only by its corresponding signal capturing system. Hereby one obtains a "quasi-instantaneous" determination of NO density and temperature. The short run times ( $< 1 \text{ ms}$ ) dictate the use of two separate lasers in this application.

Both beams also pass through a heated calibration cell with an attached monochromator and intensified camera (operating as an OMA), enabling the tuning of the laser to be checked easily. A small percentage of both beams is deflected via a beam splitter to another camera which records both beam profiles during a run - this allows for corrections due to beam fluctuations to be made. This setup also incorporates an etalon, which allows the laser bandwidths to be checked before a run. Raman cells are included to widen the accessible pumping range of the ArF lasers to near 211 nm (i.e. 210-211 nm).

In order to compensate, at least in part, for the complexity of the timing and control events of the laser system (gate widths and delays can be as small as 5 ns), it has been fully automated and can run remotely under computer (PC) control.

## 6.3 Tunable IR Laser Diode

Absorption spectroscopy with laser diodes is a non intrusive technique which allows the determination of rotational temperatures and concentrations of minor species in hypersonic flow fields. The Doppler shift of the absorption lines gives access to one flow velocity component along the line of sight of the instrument.

**Figure 14** shows a principal setup of the technique as it was used in development tests for the hot shot facility F4 of ONERA [22]. The laser is housed in a diode laser mount which provides cooling at low temperature with a stability better than  $10^{-3}$ . The laser diode operates near  $5 \mu\text{m}$ . The laser light passes through the test section and is projected onto a monochromator at the outlet of which it is split and passed through a Fabry-Pérot with small fringe spacing for precise frequency calibration. The other beam passes through a reference cell onto a liquid nitrogen cooled HgCdTe detector.

Currently the instrument can detect an absorption of a few  $10^{-3}$  along the line of sight. Integrated NO densities of a few  $10^{15} \text{ cm}^{-3}$  near room temperature can be detected in the flow. Spectra are recorded at a rate 1 per millisecond. Velocity measurements are obtained by monitoring the Doppler shift of the absorption line with respect to the position of this line in a gas at rest. Static temperature is determined from the Doppler width of an absorption line.

As the instrument integrates along the line of sight, its principal application will be for the analysis of the free stream. The instrument is conceived transportable and shall be used in other facilities as well.

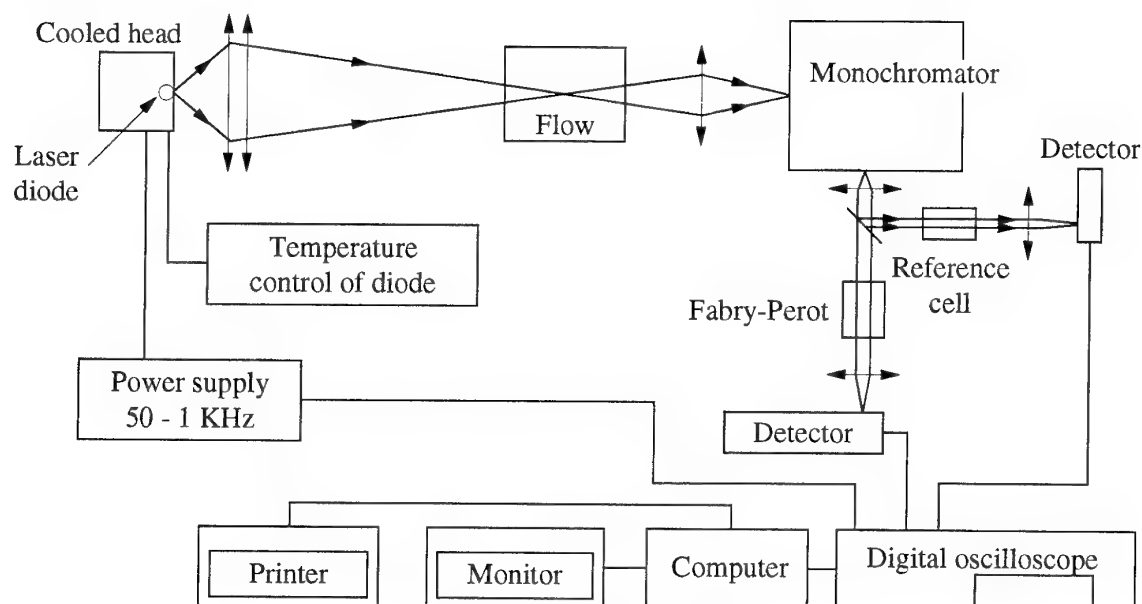


**Figure 14. Laser Diode Setup**

### 6.4 Holographic Interferometry

Holographic interferometry is an optical method for studying density variations in the optically transparent flow around a model installed in a wind tunnel. It is based on the ability to record and re-construct wavefront shapes by the use of diffraction grids. The information recorded is a two-dimensional representation of the (optically integrated) density of the gas in the model flow field. It is the same information as obtained by other interferometers like the Mach-Zehnder or Michelson, except that in the holographic interferometer the two wavefront shapes that are compared are obtained at different times along the same propagation path, rather than at the same time along different propagation paths. Figure 15 shows the set-up of the method in HEG.

The no-flow picture is recorded on a holographic, high-resolution, optically sensitive plate as an interference pattern between the object beam propagating through the test section and the reference beam propagating around it. This interference pattern serves as a diffraction grid when illuminated with a reconstruction beam. When the re-construction beam is identical to the original reference beam, the first-order diffraction behind the recorded hologram will be identical to the object beam.

The hologram with the flow is recorded in an identical manner on the same holographic plate. When the developed double-exposed hologram is reconstructed by illuminating it with the reconstruction beam(s), the interference pattern between the two first order waves behind the holographic plate is caused by changes of density in the test section between the two recordings, and is made visible as a series of dark and bright lines representing lines of constant density in the flow field. This interferogram can then be further analyzed or used as an illustration of the flow field directly.

The reconstructed interferogram is recorded on a CCD camera connected to a computer on which the data can be processed.

### 7. ACKNOWLEDGEMENT

The author gratefully acknowledges the collaboration and assistance by the different wind-tunnel groups. He would like to mention particularly G. François of ONERA, J.-M. Charbonnier of VKI, G. Eitelberg of DLR and last but not least H. Olivier of RWTH Aachen.

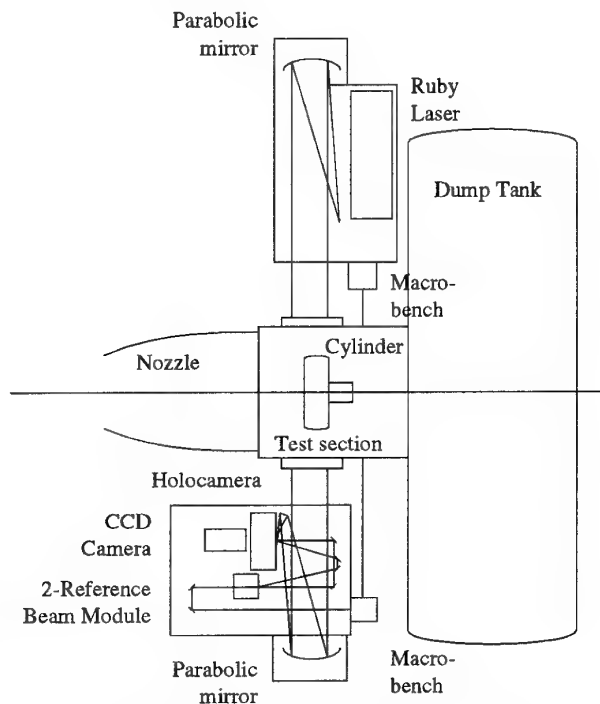


Figure 15. HEG Holographic Interferometer

### 8. REFERENCES

#### References on the general subject

1. Wendt, J. F., "European Hypersonic Wind Tunnels." paper presented at the AGARD Symposium on Aerodynamics of Hypersonic Lifting Vehicles at Bristol, U.K., April 1987.
2. Watson, A. and Wake, A.J., "Ground Facilities for Hypersonic Simulation", paper presented at the International Conference on Hypersonic Aerodynamics, University of Manchester, U.K. 4-6 September 1989.
3. Muylaert, J. et al., "Review of the European Hypersonic Wind Tunnel Performance and Simulation Requirements", ESA SP 318, p. 559 - 574.
4. "Methodology of Hypersonic Testing", VKI/AEDC Special Course, Lecture Series 1993-03, von Karman Institute for Fluid Dynamics, Rhode Saint Genèse, February 22-26, 1993.

5. Hirschel, E.H., "Hypersonic Aerodynamics", paper presented at the Space Course in Munich, Germany, October 1993.

#### References on the different facilities

6. Laverre, J., "Amélioration de la soufflerie S4MA pour les essais Hermès", Office National d'Etudes et de Recherches Aérospatiales, ONERA TP nr. 1987-60, 1987.
7. Simeonides, G. "The VKI Hypersonic Wind Tunnels and associated Measurement Techniques", Technical Memorandum 46 of the von Karman Institute, Rhode Saint Genèse, November 1990.
8. Anonymous, "Description of the Aachen Shock Tunnel TH2", Shock Wave Laboratory of Rheinisch-Westfälische Technische Hochschule (RWTH) Aachen, Germany, January 1991.



9. Chanetz, B. et al. "Nouveaux moyens d'essais hypersoniques à l'ONERA - Les souffleries R5 et F4.", paper presented at the AGARD Symposium on Theoretical and Experimental Methods in Hypersonic Flows, Turin, Italy, May 4-8, 1992.
10. Yu, H.-r., Esser, B., Lenartz, M. and Grönig H., "Gaseous Detonation Driver", Shock Waves 2, p. 245-254, 1992.
11. Vennemann, D., Eitelberg, G. and Francois, G., "Simulation of hypersonic flight - A concerted European effort." ESA Bulletin, no. 74, May 1993, p. 62-69.
12. Eitelberg, G., "First Results of Calibration and Use of the HEG", AIAA 94-2525, 18th AIAA Aerospace Ground Testing Conference, Colorado Springs, CO, USA, June 20 -23, 1994.
13. Dumitrescu, M.-P., "Mise au point et fonctionnement de TCM2- Soufflerie Hypersonique a piston libre de Marseille.", Thèse de Doctorat, Laboratoire des Systèmes Energétiques et Transferts Thermiques URA CNRS 1168, Université de Provence, Aix-Marseille, France, Juillet 1994.
14. Stalker, R.J., "A study of the Free-piston Shock Tunnel", AIAA Journal, Vol. 5, 1967.
18. Beck, W.H., Koch, U. and Müller, M., "Spectroscopic Diagnostic Techniques for the High Enthalpy Shock Tunnel in Göttingen (HEG): Preparatory LIF Studies in other facilities", NATO Advanced Research Workshop on "New trends in instrumentation for hypersonic research", ONERA Le Fauga-Mauzac, France, April 27 - May 1, 1992.
19. Mohamed, A.K., "Electron Beam Velocimetry", NATO Advanced Research Workshop on New trends in instrumentation for hypersonic research", ONERA Le Fauga-Mauzac, France, April 27 - May 1, 1992.
20. Consigny, H., Le Sant, Y., Bouvier, F., Baumann, P. and Merienne, M.C., "Heat transfer Measurement Techniques used or in Development at ONERA Chalais-Meudon". NATO Advanced Research Workshop on New trends in instrumentation for hypersonic research", ONERA Le Fauga-Mauzac, France, April 27 - May 1, 1992.
21. Barbé, S. et al., "Infrared Thermography for Hot-Shot Wind Tunnel." NATO Advanced Research Workshop on New trends in instrumentation for hypersonic research", ONERA Le Fauga-Mauzac, France, April 27 - May 1, 1992.
22. Rosier, B., Mohamed, A.K., Henry, D. and Juville, S., "Mesures par spectroscopie d'absorption diode laser à la soufflerie F4", Office National d'Etudes et de Recherche Aérospatiales, ONERA Contractor Report nr. 8/4383 PY, February 1993.
23. Jessen, C. and Grönig, H., "Six component force measurement in the Aachen shock tunnel.", paper presented at the 19th International Symposium on Shock Waves, Marseille, France, July 26 - 30 , 1993.

#### References on Measurement Techniques

15. Bütetisch, K.A. and Vennemann, D., "The Electron Beam Technique in Hypersonic Rarefied Gas Dynamics", Progress in Aerospace Science, Volume 15, p. 217 ff., 1974.
16. Carbonaro, M., "Aerodynamic Force Measurements in the VKI Longshot Hypersonic Facility", NATO Advanced Research Workshop on "New trends in instrumentation for hypersonic research", ONERA Le Fauga-Mauzac, France, April 27 - May 1, 1992.
17. Surget, J. and Dunet, G., "Multipass Holographic Interferometer for the high enthalpy hypersonic wind tunnel F4", NATO Advanced Research Workshop on "New trends in instrumentation for hypersonic research", ONERA Le Fauga-Mauzac, France, April 27 - May 1, 1992.

# Ground Testing and Simulation Assessment of Space Environment Hazards

**Manola Roméro, Jacques Bourrieau**  
 CERT-ONERA/DERTS (Department of Space Technology)  
 BP 4025 31055 Toulouse Cédex  
 France

## 1. INTRODUCTION

For military and civilian needs, satellites are becoming more and more autonomous, smart (i.e., including high integration devices) and capable (i.e. processing large quantities of broad bandwidth data). The technologies used to achieve such goals are sensitive to both noise and steady-state damage produced by the space environment.

The purpose of this presentation is to describe some aspects of the problem, aiming at predicting overall system behavior in space. Indeed such a ground check of environmental hardness can be a daunting task considering the complexity of the space threat and the understandable reluctance of project managers to subject all or large portions of their systems to extensive possibly destructive testing.

## 2. SPACE ENVIRONMENT AND ITS CONSEQUENCES

Space is an aggressive environment affecting most of spacecraft functions. The components of space environment that are of importance for the behavior of spacecraft are:

- vacuum with influence on mechanical functions (outgassing of material can affect the dimensional stability, tribology is thus more difficult), optics (through re-deposition), thermics (enhancement of temperature field), electrics (beware of Pashen effect).
- Neutral particle such as:
  - . oxygen atoms of the upper layers of the atmosphere, able to damage mechanical, thermal and optical function through erosion processes and luminescence,
  - . self contamination (see vacuum effect),
  - . cosmic dust and debris.
- Electro-magnetic radiation
  - . solar spectrum with an UV component producing changes in optical and mechanical properties of thermal coatings
  - . earth albedo
  - . earth IR emission
- Plasmas
  - . cold plasmas in the ionosphere and plasmasphere, generating coupling effects with voltages, particle and field measurements, RF communications

. hot plasmas around geostationary orbit, due to magnetospheric substorm and producing voltage building ending by ESD with effects such as false commands and service disruptions.

- High energy charged particles, generating cumulative radiation damages on electronics, optics and materials, noises on electronics, EMC effects on systems, and coming from:

- . radiation belts
- . solar eruption particles
- . cosmic rays.

Such a quick look over various effects of space environment emphasizes the difficulty to ensure proper system function, reliability and lifetime of spacecraft. The main problems arising are the following.

### A. How can we identify which effects are to be taken into account?

The interaction of space environment with spacecraft depends strongly of which missions and technologies are concerned. For instance, atox was a well known problem for rockets, it has been forgotten and discovered again when some trouble arose during Shuttle flights. Changes in orbits, materials, sensitivity of experiments, scale of spacecraft can switch a phenomenon from harmless to noscious.

An other example of damage strongly related to technology is cosmic rays interactions with electronics which produces damages only on large scale integrated components where signals are written as low quantities of charges, whereas old technology components are not sensitive.

### B. How can be taken into account the effects having impacts at system level?

Very often a whole system cannot be tested thoroughly. The usual development approach of such a problem is: specification, numerical simulation, test on sample to provide input, test on system to provide some cases of validation, conception rules, exploitation rules. Sometimes the problem is more difficult due to the fact that numerical simulation is not possible.

For systems under space environment, it is basically the same approach but with some specific aspects. Many are the cases in which there is no continuity between stresses achievable through testing of samples, testing of systems, and furthermore the one that will be really undergone in space. The confidence thus obtained is less

where as space system will be used in such conditions that most of time any repair will be forbidden, and with few vehicle being built.

To make things worse, the specification of the space environment constraints is often poorly known, when no perturbed by the spacecraft itself.

An example of such situation is observed with the occurrence of ESD and the subsequent troubles resulting from the interferences thus created being interpreted as orders.

### **C. How can be taken into account the effects due to synergistic effects of various components of space environment?**

Usually each environmental factor is treated separately. This approach is more and more subject to conflict. More comprehensive hardware and software dedicated to aid in system level design trade studies have to be developed. One example of technology on which such approach has to be adopted is thermal coating, exposed to each aspect of space environment and having strong requirements when their thermo-optical and electrical properties are concerned.

## **3. THREE EXAMPLES OF SPACE ENVIRONMENT RELATED PROBLEMS**

### **3.1 Cosmic rays effects on electronic components**

An important consideration in the miniaturization of electronic components in the phenomenon of SEEs - Single Event Effects (upset, latch-up...). They are a current problem for high integration devices and will become increasingly important because of the trend to smaller components and more complex circuitry with more and more bits of memory.

During the process involved in SEE production, charges formed along the track are collected at the sensitive zone level and mistaken for a signal. The factors expressing the creation of charge - or the loss of energy - of the heavy ion in the component is the Let (Linear Energy Transfer) usually in  $\text{MeV}/\text{mm}/\text{cm}^2$ . The sensitivity of the component is expressed as a SEE cross section, the curve (cross section versus LET) describing the behaviour of the component. For practical matter, the description of the curve is often reduced to two values: the LET threshold and the cross section at saturation.

These values are obtained through various means such as radioactive sources and accelerators delivering a range of LET as close as possible to those observed in space. But the energy of particles used from sources is far lower than that obtained in space, with consequence that their depth of penetration is much thinner and many components, even unshielded, cannot be tested with such a cheap and easy mean. Fast ion accelerators are heavy and costly hardware used for most of test. Nevertheless, they do not reach as high energies as those observed in space, and do not reproduce adequately isotropic flux and combined cosmic ray and cumulated dose effects.

In addition, generally the testing procedures of circuits do not adequately reflect the future spaceborne applications. Therefore, the rough knowledge of the particle fluxes added to the critical nature of ground testing data may dramatically impact the Single Event Effects (SEE) rate prediction.

Hence the interest to perform some on-board experiments in order to check whether the ground testing is correct or not.

For instance, it was the purpose of the EXEQ experiment developed in the framework of the French-Russian space cooperation program and supported by CNES. It was flown on the MIR orbital stations from July 92 to January 94.

EXEQ is based on a specific computer developed with a MC68020 microprocessor from Motorola connected to a static RAM array from MATRA MHS (twelve 32K8 parts, see Figure 1) and a controller including the interface with the MIR station (power and dating) and a special watchdog designed to check program flow. (Ref. 1)

Figure 2 presents the geographical distribution of the event observed, emphasizing the correlation of their occurrence with fast protons in the South Atlantic Anomaly. Fast protons do not create directly SEE. They induce nuclear reactions whose products are fast ions generating SEE. Hence the necessity either of performing specific tests with proton accelerators or to develop numerical simulation for the whole process, using heavy ions test results as input.

Table 1 (hereafter) summarizes the results obtained (proton induced events represent about 14% of the whole).

A simple model with the supposed environment and the cross sections measured give a rather good agreement with the on-board measurements for cosmic rays, and a questionable one for protons.

A more sophisticated one (CREME), taking into account the spatial distribution of impinging fluxes in space, leads to a worse evaluation.

The experiment will flow again in 94, to contribute to a better understanding of what really happens in space.

Some of the features of this example are quite general when problem A is concerned:

- On-flight experiments are very precious in order to identify problems and validate models.

- They give isolated results, meaning that the characteristics of the environment thus explore cannot be varied easily in a reproducible form, and even is more of the time not well known. As consequence, they must not be used as qualification tests, and no mission having

survived is a proof that the following will endure successfully its environment.

No result issued from sophisticated numerical simulations must be taken for granted as long as they are not validated by experiment!

### 3.2 Voltage building and discharges - Plasmas

It has become well known that dielectric material used as satellite external coatings can be differentially charged by the ambient environment at geosynchronous orbits.

The current understanding is to associate the possibility of such charging with the development of geomagnetic substorms which affect the electron and ion populations in a given section (midnight-to-dawn) of the geosynchronous orbit. This theory is supported by the numerous anomalies that a lot of satellites undergo precisely in this orbit section when geomagnetic activity is high.

Nevertheless, the anomalies distribution is not always so clear, and many other satellites present a different pattern. Not always correlation is found with the satellite location, nor with geomagnetic activity. These cases may be due to triggered discharges activating, high energy penetrating electrons, or special configurations such as floating metallisations.

For instance, the spacecraft TELECOM 1A, launched in 1984, has undergone service disruptions due to electrostatic discharges, with a chronogram of event (Figure 3, Ref 2) very different of the "classic" MARECS-A distribution.

The night-side environment is considered since the earliest investigations on spacecraft charging as a worst environment because it corresponds to the highest fluxes of electrons of energy less than 50 keV, able to build voltages on spacecraft coatings.

But some parts of the spacecraft are highly insulating. We have tested such an element that is likely to be used as a strut to ensure mechanical fixations of thermal shields.

We have found that very little intensity beam was necessary to charge it. It could be considered as a pure capacitor, a piece of material (fiber glass material held above the structure of the satellite). The value of the leakage current for such an element was lower than  $5 \text{ pA/cm}^2$ . The capacitor value was less than  $5 \text{ pF/cm}^2$ .

The surface potential was built during a test with two monoenergetic beams of values  $E1 = 4 \text{ keV}$  and  $E2 = 20 \text{ keV}$ . The ratio between the two associated intensities  $I1$  and  $I2$  constant =  $0.1 \text{ nA/cm}^2$ . The result was a variation of the mean incoming energy and an increasing surface potential with the energy.

The strut was covered with metallized kapton which was found to exhibit arcing not grounded.

So, there is at least one category of elements for which day-side environment constitutes the worst case, we could call them: "pure thick dielectrics in the shadow". (Ref. 3).

The day-side environment will constitute the worst case environment for pure dielectrics (if they do exist at the surface of the satellite). Additional conditions to propose them as good candidates for being sources of arcing and anomalies are that they are in the shadow, thick enough to stop incoming electrons, and that they do effectively arc when charged by the environment. Another condition is that their capacity with respect to the structure should be very low (this should be the case for thick materials).

A global approach of the ESD problem has been started at mid seventies with the NASA-DOD technological satellite SCATHA and the development by Scubed of NASCAP, a software able to predict what would be the limit voltages that would be reached on spacecraft if no discharge were to occur, the threshold of discharge occurrence remaining within the experimental competence. With consequences such as definition of worst case midnight environments, availability of NASCAP, general rules of conception, this effort gave strong means to cope with ESD at system level.

Nevertheless, if ESD effects have been greatly reduced 10 years after they were present in most of space vehicles, as exemplified by the case described here above. Studies concerning "scale factors" role of absolute and differential voltages in providing charges to the arcing were then performed and lead to more detailed rules of conception.

Now that we are in the mid nineties (20 years after SCATHA) another NASA DOD satellite (CRRES) with part of its payload dedicated to that problem has been launched, some events still happen mainly due to penetrating charge, with the new aspect of microsystems using technologies sensitive to voltage building and strong concern for interference with plasmas, due to the low earth orbit environment and to ionic thruster.

What that example of ESD shows is that when problem B (impact at system level) is concerned one can assert that a very large, long and comprehensive program of research and development must be started to cope correctly with it..

The second aspect shown concerns quality approach. Rules of conception are not enough. They must be not only known, but also understood so that to be adopted to any change of scale, for instance that is relevant.

### 3-3 Thermal coating

In order to control spacecraft temperature within acceptable limits, it is desirable to obtain data for the thermal control coating property changes during orbital life. Such data will allow to select materials according to their resistance to radiation and to decide corrective actions to be taken concerning the variations that are likely to occur in orbit. The ultraviolet (UV) radiation and the particle fluxes (electrons and protons) constitutes

the environment factors which are prevailing in damaging the thermo-optical properties of surfaces in geosynchronous Earth orbit (GEO); at low Earth orbits (LEO), the action of UV radiation (cumulated to particle irradiation in the particular case of polar orbits) has to be considered together with that of oxygen atoms. The solar absorptance changes induced in thermal control coating have presently to be known for very long lasting space missions: ten to fifteen years for application satellites in GEO, twenty to thirty years for space stations in LEO. Irradiation conditions which simulate the exposure to the space environment must be fulfilled on an accelerated time scale.

As the operational life of satellites tends to become longer, the requirements for the test facility become more severe. Typical laboratory conditions call for a 20 to 45 days exposure duration in order to simulate one complete year in space environment. It was proving extremely difficult to ensure the reliability of the complex test facility of the CERT/DERTS for such tests needing operation of irradiation by electrons, protons, UV and subsequent measurement without breaking the vacuum for long test periods.

Figure 4 presents a synoptic view of this experimental array, dedicated to the study of evolution under space environment of both the thermo-optical properties of coatings (chamber "SEMIRAMIS") and the mechanical properties of structural materials (chamber "MIRASITU").

Figure 5 (Ref. 4)) presents recent results obtained on white paint, showing how the solar reflectance is damaged by ultraviolets and when ionizing radiation are added (zone 1), and when ionizing radiation then air, are added (zone 2). In such cases each factor of space environment cannot be coped with separately, however more expensive could appear the experimental array and its running.

#### 4. CONCLUSION

Space systems usually include few models and those who are flown are supposed to perform well at first and without any repair after launching.

Space environment can affect in many ways the behavior of modern, smart, long duration spacecraft. The problem can be coped with using the usual project management approach but with some rather worrying specific features.

Space environment is composed of many factors. Some undergo considerable fluctuations and many are not well

known, so that the specification of constraint is sometimes difficult.

The identification of which part of the environment has to be considered depends on the technologies used and on the mission and performances aimed at. In order to identify problem and validate models, on-board experiments are irreplaceable. Due to the singularity of the environment thus explored, but for scarce cases, they must not be used for qualification purpose.

Usually, space environment interaction with spacecraft is treated at sample level. In those cases in which the effects are produced at system level, many difficulties arise and only a long and thorough research and development program can relieve. Rules of design and of use are tedious concern. Twenty five years after the first steps of a men on the moon, it is only now that an international set of normalization for space matters is being processed in the frame of the ISO Organisation, one of the five working groups being dedicated to space environment.

The financial effort to support such research programs and to implement and run some sophisticated experimental arrays may appears deterrent. The still numerous troubles observed in orbit should remind to project managers that very often spending some money early enough in a space program is saving money on the whole.

Ref.1 D. Falguère, S. Duzellier (Cert-Onéra), R. Ecoffet (Cnes), "SEE in-flight measurements on the MIR orbital station", 1994 IEEE NSREC, Tucson (July 1994)

Ref. 2 J.P. Catani (Cnes) "Anomalies en vol : cas des décharges électrostatiques", Cours de Technologie Spatiale sur l'Environnement Spatial", Cépadues Edition, Toulouse (novembre 1990)

Ref. 3 L. Lévy, D. Sarraïl, J.P. Philippon (Cert-Onéra), J.P. Catani (Cnes), J.M. Fourquet (Matra), "Occurrence of differential voltages on day-side in GEO", 1986 Agard Conference, La Haye (June 1986)

Ref. 4 J. Marco, A. Paillous (Cert-Onéra), G. Gourmelon (Esa), "Thermal control coatings : simulated LEO degradation under UV and particle radiation (September 1994)

|         | Total number of events during flight | On-flight SEU rates | Predicted SEU rates simple model | Predicted SEU rates CREME | Predicted proton induced SEU |
|---------|--------------------------------------|---------------------|----------------------------------|---------------------------|------------------------------|
| HM65756 | > 600                                | 0.06-0.3            | 0.1-0.4                          | 0.2-1.2                   | 0.07                         |
| MC68020 | < 10                                 | 0.008               | 0.0009                           | 0.002                     | 0.008                        |

Table 1 -Flight predicted rates comparison (SEU/part-day)

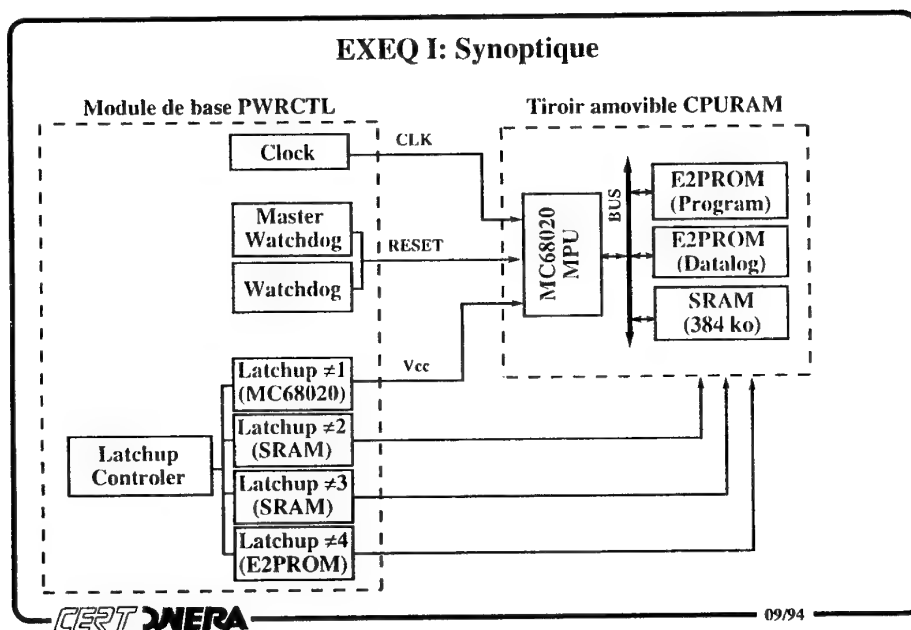


Figure 1 - Diagram of the EXEQ experiment. The left part including the housekeeping functions (clocks, controller, connections with power and tests ...) remains on the station. The right part (microprocessor, main memory and samples memories) is taken back to Earth.

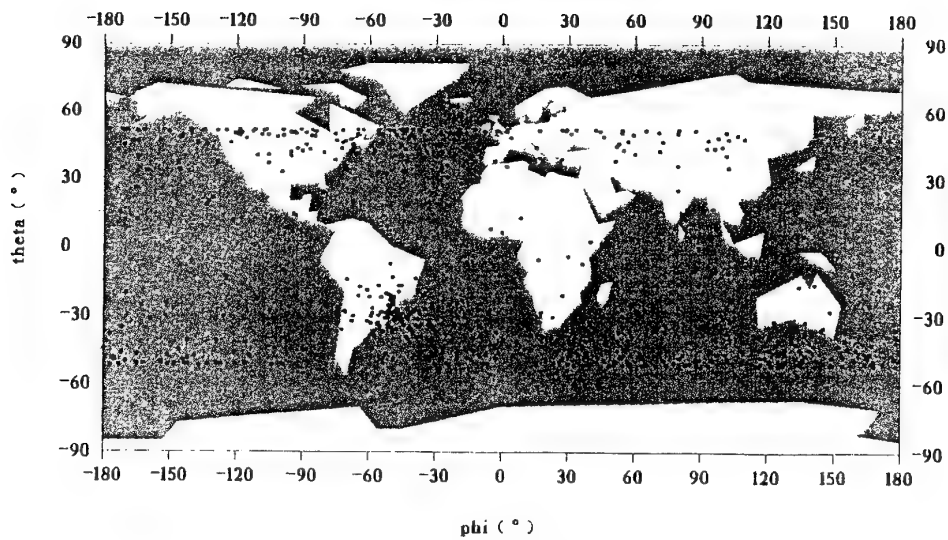


Figure 2 - Geographical distribution of events as observed by EXEQ 1

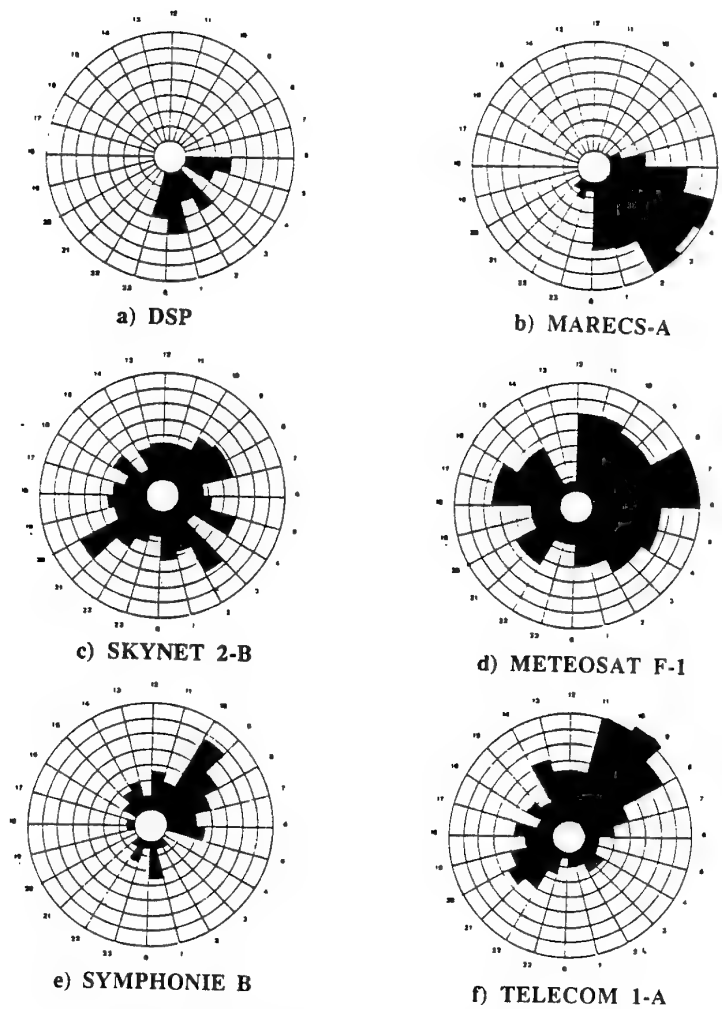


Figure 3 - Chronograms of events/local time for various satellites (after Ref. 2)

## SEMIRAMIS

- Vacuum chambers :
- 1- Safe-keeping and optical measurements
  - 2- Optical system
  - 3- Combined irradiations
  - 4- Miscellaneous (Contamination, Cryogenic screening)

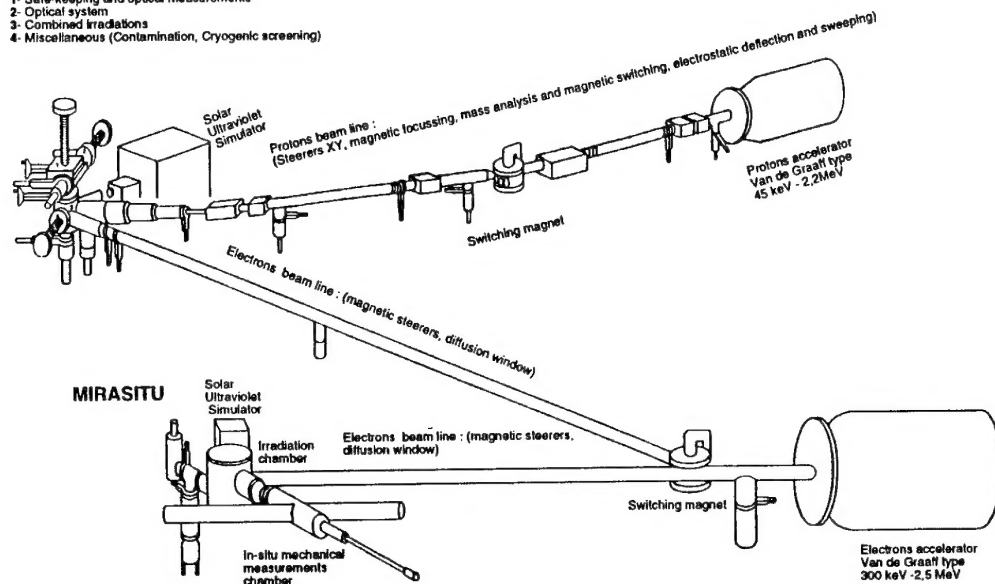


Figure 4 - Synoptic of the implementation of the combined irradiation array "SEMIRAMIS"

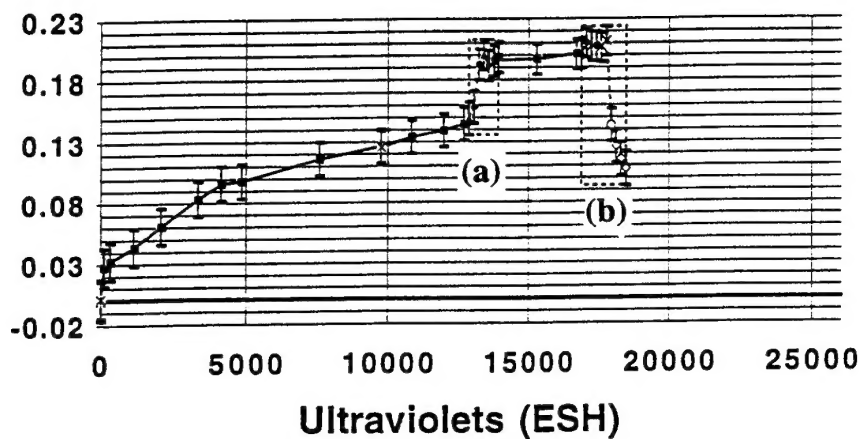


Figure 5 - Synergistic effect : irradiation of white paint SG120FD-MAP - Evolution of absolute solar absorptance as a function of UV exposure with electron and proton irradiations (A) and air annealing (B)



## REPORT DOCUMENTATION PAGE

|  |  |   |   |              |            |                |                        |                  |                 |                     |       |               |            |                   |           |        |                  |
|--|--|---|---|--------------|------------|----------------|------------------------|------------------|-----------------|---------------------|-------|---------------|------------|-------------------|-----------|--------|------------------|
| <b>1. Recipient's Reference</b>  | <b>2. Originator's Reference</b><br>AGARD-CP-561 | <b>3. Further Reference</b><br>ISBN 92-836-0014-2 | <b>4. Security Classification of Document</b><br>UNCLASSIFIED/<br>UNLIMITED |              |            |                |                        |                  |                 |                     |       |               |            |                   |           |        |                  |
| <b>5. Originator</b> Advisory Group for Aerospace Research and Development<br>North Atlantic Treaty Organization<br>7 rue Ancelle, 92200 Neuilly-sur-Seine, France   |  |   |   |              |            |                |                        |                  |                 |                     |       |               |            |                   |           |        |                  |
| <b>6. Title</b><br>Space Systems Design and Development Testing  |  |   |   |              |            |                |                        |                  |                 |                     |       |               |            |                   |           |        |                  |
| <b>7. Presented at/sponsored by</b><br>The Flight Vehicle Integration Panel Symposium,<br>held in Cannes, France from 3-6 October 1994   |  |   |   |              |            |                |                        |                  |                 |                     |       |               |            |                   |           |        |                  |
| <b>8. Author(s)/Editor(s)</b><br>Various   |  |   | <b>9. Date</b><br>March 1995  |              |            |                |                        |                  |                 |                     |       |               |            |                   |           |        |                  |
| <b>10. Author's/Editor's Address</b><br>Various  |  |   | <b>11. Pages</b><br>328   |              |            |                |                        |                  |                 |                     |       |               |            |                   |           |        |                  |
| <b>12. Distribution Statement</b><br><br>Information about the availability of this and other AGARD unclassified publications is given on the back cover.  |  |   |   |              |            |                |                        |                  |                 |                     |       |               |            |                   |           |        |                  |
| <b>13. Keywords/Descriptors</b><br><table><tr><td>Space flight</td><td>Simulation</td></tr><tr><td>Space vehicles</td><td>Flight characteristics</td></tr><tr><td>Space structures</td><td>Test facilities</td></tr><tr><td>Flexible structures</td><td>Tests</td></tr><tr><td>Space systems</td><td>Evaluation</td></tr><tr><td>Hypersonic flight</td><td>Standards</td></tr><tr><td>Design</td><td>Lifting vehicles</td></tr></table>  |  |   |   | Space flight | Simulation | Space vehicles | Flight characteristics | Space structures | Test facilities | Flexible structures | Tests | Space systems | Evaluation | Hypersonic flight | Standards | Design | Lifting vehicles |
| Space flight   | Simulation                                       |   |   |              |            |                |                        |                  |                 |                     |       |               |            |                   |           |        |                  |
| Space vehicles   | Flight characteristics                           |   |   |              |            |                |                        |                  |                 |                     |       |               |            |                   |           |        |                  |
| Space structures   | Test facilities                                  |   |   |              |            |                |                        |                  |                 |                     |       |               |            |                   |           |        |                  |
| Flexible structures  | Tests  |   |   |              |            |                |                        |                  |                 |                     |       |               |            |                   |           |        |                  |
| Space systems  | Evaluation                                       |   |   |              |            |                |                        |                  |                 |                     |       |               |            |                   |           |        |                  |
| Hypersonic flight  | Standards  |   |   |              |            |                |                        |                  |                 |                     |       |               |            |                   |           |        |                  |
| Design   | Lifting vehicles                                 |   |   |              |            |                |                        |                  |                 |                     |       |               |            |                   |           |        |                  |
| <b>14. Abstract</b> <p>In view of the importance of space capability to the fulfillment of future NATO requirements, the Flight Vehicle Integration Panel of AGARD has placed increased emphasis on space technology. The goal of the symposium reported in this document was to permit information exchange and discussion on the test aspects of space systems design and development with the emphasis on systems related to anticipated future capabilities and the importance of adequate testing, and continued with six sessions comprising 28 technical papers in all. These sessions focused on: Testing Requirements and Practices; Flight Dynamics and Flexible/Deployable Structures; Systems Development and Evaluation; Simulation; Space Flight Experiments; and Test Facilities and Support.</p> <p>Two keynote speakers introduced the forum, clearly establishing the importance of the topic, and its relevance to NATO's requirements.</p> <p>A Technical Evaluation Report on the Symposium is also included.</p> <p>Copies of papers presented at the Flight Vehicle Integration Panel Symposium held in Cannes, France, 3-6 October 1994.</p> |  |   |   |              |            |                |                        |                  |                 |                     |       |               |            |                   |           |        |                  |

Aucun stock de publications n'a existé à AGARD. A partir de 1993, AGARD détiendra un stock limité des publications associées aux cycles de conférences et cours spéciaux ainsi que les AGARDographies et les rapports des groupes de travail, organisés et publiés à partir de 1993 inclus. Les demandes de renseignements doivent être adressées à AGARD par lettre ou par fax à l'adresse indiquée ci-dessus. *Veuillez ne pas téléphoner.* La diffusion initiale de toutes les publications de l'AGARD est effectuée auprès des pays membres de l'OTAN par l'intermédiaire des centres de distribution nationaux indiqués ci-dessous. Des exemplaires supplémentaires peuvent parfois être obtenus auprès de ces centres (à l'exception des Etats-Unis). Si vous souhaitez recevoir toutes les publications de l'AGARD, ou simplement celles qui concernent certains Panels, vous pouvez demander à être inclu sur la liste d'envoi de l'un de ces centres. Les publications de l'AGARD sont en vente auprès des agences indiquées ci-dessous, sous forme de photocopie ou de microfiche.

CENTRES DE DIFFUSION NATIONAUX

**ALLEMAGNE**

Fachinformationszentrum,  
Karlsruhe  
D-76344 Eggenstein-Leopoldshafen 2

**BELGIQUE**

Coordonnateur AGARD-VSL  
Etat-major de la Force aérienne  
Quartier Reine Elisabeth  
Rue d'Evere, 1140 Bruxelles

**CANADA**

Directeur, Services d'information scientifique  
Ministère de la Défense nationale  
Ottawa, Ontario K1A 0K2

**DANEMARK**

Danish Defence Research Establishment  
Ryvangs Allé 1  
P.O. Box 2715  
DK-2100 Copenhagen Ø

**ESPAGNE**

INTA (AGARD Publications)  
Pintor Rosales 34  
28008 Madrid

**ETATS-UNIS**

NASA Headquarters  
Code JOB-1  
Washington, D.C. 20546

**FRANCE**

O.N.E.R.A. (Direction)  
29, Avenue de la Division Leclerc  
92322 Châtillon Cedex

**GRECE**

Hellenic Air Force  
Air War College  
Scientific and Technical Library  
Dekelia Air Force Base  
Dekelia, Athens TGA 1010

**ISLANDE**

Director of Aviation  
c/o Flugrad  
Reykjavik

**ITALIE**

Aeronautica Militare  
Ufficio del Delegato Nazionale all'AGARD  
Aeroporto Pratica di Mare  
00040 Pomezia (Roma)

**LUXEMBOURG**

Voir Belgique

**NORVEGE**

Norwegian Defence Research Establishment  
Attn: Biblioteket  
P.O. Box 25  
N-2007 Kjeller

**PAYS-BAS**

Netherlands Delegation to AGARD  
National Aerospace Laboratory NLR  
P.O. Box 90502  
1006 BM Amsterdam

**PORTUGAL**

Força Aérea Portuguesa  
Centro de Documentação e Informação  
Alfragide  
2700 Amadora

**ROYAUME-UNI**

Defence Research Information Centre  
Kentigern House  
65 Brown Street  
Glasgow G2 8EX

**TURQUIE**

Millî Savunma Başkanlığı (MSB)  
ARGE Dairesi Başkanlığı (MSB)  
06650 Bakanlıklar-Ankara

**Le centre de distribution national des Etats-Unis ne détient PAS de stocks des publications de l'AGARD.**

D'éventuelles demandes de photocopies doivent être formulées directement auprès du NASA Center for AeroSpace Information (CASI) à l'adresse ci-dessous. Toute notification de changement d'adresse doit être fait également auprès de CASI.

AGENCES DE VENTE

NASA Center for  
AeroSpace Information (CASI)  
800 Elkridge Landing Road  
Linthicum Heights, MD 21090-2934  
Etats-Unis

ESA/Information Retrieval Service  
European Space Agency  
10, rue Mario Nikis  
75015 Paris  
France

The British Library  
Document Supply Division  
Boston Spa, Wetherby  
West Yorkshire LS23 7BQ  
Royaume-Uni

Les demandes de microfiches ou de photocopies de documents AGARD (y compris les demandes faites auprès du CASI) doivent comporter la dénomination AGARD, ainsi que le numéro de série d'AGARD (par exemple AGARD-AG-315). Des informations analogues, telles que le titre et la date de publication sont souhaitables. Veuillez noter qu'il y a lieu de spécifier AGARD-R-nnn et AGARD-AR-nnn lors de la commande des rapports AGARD et des rapports consultatifs AGARD respectivement. Des références bibliographiques complètes ainsi que des résumés des publications AGARD figurent dans les journaux suivants:

Scientific and Technical Aerospace Reports (STAR)  
publié par la NASA Scientific and Technical  
Information Division  
NASA Headquarters (JTT)  
Washington D.C. 20546  
Etats-Unis

Government Reports Announcements and Index (GRA&I)  
publié par le National Technical Information Service  
Springfield  
Virginia 22161  
Etats-Unis  
(accessible également en mode interactif dans la base de  
données bibliographiques en ligne du NTIS, et sur CD-ROM)



AGARD holds limited quantities of the publications that accompanied Lecture Series and Special Courses held in 1993 or later, and of AGARDographs and Working Group reports published from 1993 onward. For details, write or send a telefax to the address given above. *Please do not telephone.*

AGARD does not hold stocks of publications that accompanied earlier Lecture Series or Courses or of any other publications. Initial distribution of all AGARD publications is made to NATO nations through the National Distribution Centres listed below. Further copies are sometimes available from these centres (except in the United States). If you have a need to receive all AGARD publications, or just those relating to one or more specific AGARD Panels, they may be willing to include you (or your organisation) on their distribution list. AGARD publications may be purchased from the Sales Agencies listed below, in photocopy or microfiche form.

NATIONAL DISTRIBUTION CENTRES

## BELGIUM

Coordonnateur AGARD — VSL  
Etat-major de la Force aérienne  
Quartier Reine Elisabeth  
Rue d'Evere, 1140 Bruxelles

## CANADA

Director Scientific Information Services  
Dept of National Defence  
Ottawa, Ontario K1A 0K2

## DENMARK

Danish Defence Research Establishment  
Ryvangs Allé 1  
P.O. Box 2715  
DK-2100 Copenhagen Ø

## FRANCE

O.N.E.R.A. (Direction)  
29 Avenue de la Division Leclerc  
92322 Châtillon Cedex

## GERMANY

Fachinformationszentrum  
Karlsruhe  
D-76344 Eggenstein-Leopoldshafen 2

## GREECE

Hellenic Air Force  
Air War College  
Scientific and Technical Library  
Dekelia Air Force Base  
Dekelia, Athens TGA 1010

## ICELAND

Director of Aviation  
c/o Flugrad  
Reykjavik

## ITALY

Aeronautica Militare  
Ufficio del Delegato Nazionale all'AGARD  
Aeroporto Pratica di Mare  
00040 Pomezia (Roma)

## LUXEMBOURG

See Belgium

## NETHERLANDS

Netherlands Delegation to AGARD  
National Aerospace Laboratory, NLR  
P.O. Box 90502  
1006 BM Amsterdam

## NORWAY

Norwegian Defence Research Establishment  
Attn: Biblioteket  
P.O. Box 25  
N-2007 Kjeller

## PORTUGAL

Força Aérea Portuguesa  
Centro de Documentação e Informação  
Alfragide  
2700 Amadora

## SPAIN

INTA (AGARD Publications)  
Pintor Rosales 34  
28008 Madrid

## TURKEY

Millî Savunma Başkanlığı (MSB)  
ARGE Dairesi Başkanlığı (MSB)  
06650 Bakanlıklar-Ankara

## UNITED KINGDOM

Defence Research Information Centre  
Kentigern House  
65 Brown Street  
Glasgow G2 8EX

## UNITED STATES

NASA Headquarters  
Code JOB-1  
Washington, D.C. 20546

**The United States National Distribution Centre does NOT hold stocks of AGARD publications.**

Applications for copies should be made direct to the NASA Center for AeroSpace Information (CASI) at the address below.

Change of address requests should also go to CASI.

SALES AGENCIES

NASA Center for  
AeroSpace Information (CASI)  
800 Elkridge Landing Road  
Linthicum Heights, MD 21090-2934  
United States

ESA/Information Retrieval Service  
European Space Agency  
10, rue Mario Nikis  
75015 Paris  
France

The British Library  
Document Supply Centre  
Boston Spa, Wetherby  
West Yorkshire LS23 7BQ  
United Kingdom

Requests for microfiches or photocopies of AGARD documents (including requests to CASI) should include the word 'AGARD' and the AGARD serial number (for example AGARD-AG-315). Collateral information such as title and publication date is desirable. Note that AGARD Reports and Advisory Reports should be specified as AGARD-R-nnn and AGARD-AR-nnn, respectively. Full bibliographical references and abstracts of AGARD publications are given in the following journals:

Scientific and Technical Aerospace Reports (STAR)  
published by NASA Scientific and Technical  
Information Division  
NASA Headquarters (JTT)  
Washington D.C. 20546  
United States

Government Reports Announcements and Index (GRA&I)  
published by the National Technical Information Service  
Springfield  
Virginia 22161  
United States  
(also available online in the NTIS Bibliographic  
Database or on CD-ROM)



Printed by Canada Communication Group  
45 Sacré-Cœur Blvd., Hull (Québec), Canada K1A 0S7